Journal of the Arkansas Academy of Science

Volume 48 Article 1

1994

Proceedings of the Arkansas Academy of Science - Volume 48 1994

Academy Editors

Proceedings of the

CODEN: AKASO
ISBN: 0097-4374

ARKANSAS ACADEMY OF SCIENCE

VOLUME 48
1994

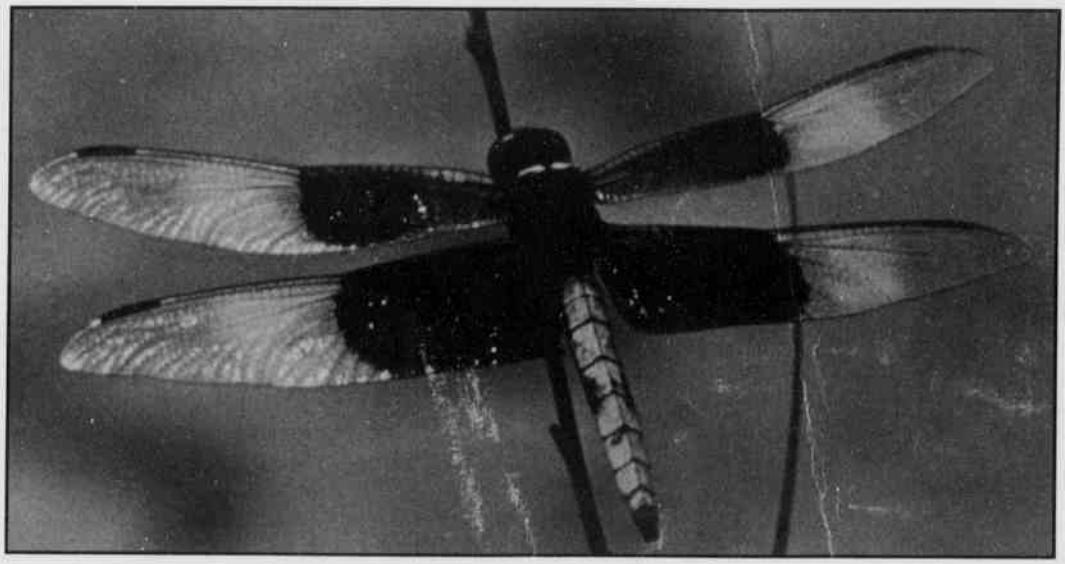

ARKANSAS ACADEMY OF SCIENCE
DEPT. OF NATURAL SCIENCE
MONTICELLO, ARKANSAS 71655

Library Rate

Arkansas Academy of Science, Dept. of Natural Science, University of Arkansas at Monticello
Monticello, Arkansas 71655

PAST PRESIDENTS OF THE ARKANSAS ACADEMCY OF SCIENCE

Charles Brookover, 1917
Dwight M. Moore, 1932-33, 64
Flora Haas, 1934
H. H. Hyman, 1935
L. B. Ham, 1936
W. C. Munn, 1937
M. J. McHenry, 1938
T. L. Smith, 1939
P. G. Horton, 1940
I. A. Willis, 1941-42
L. B. Roberts, 1943-44
Jeff Banks, 1945
H. L. Winburn, 1946-47
E. A. Provine, 1948
G. V. Robinette, 1949
John R. Totter, 1950
R. H. Austin, 1951
E. A. Spessard, 1952
Delbert Swartz, 1953
Z. V. Harvalik, 1954
M. Ruth Armstrong, 1955
W. W. Nedrow, 1956
Jack W. Sears, 1957
J. R. Mundie, 1958
C. E. Hoffman, 1959
N. D. Buffaloe, 1960
H. L. Bogan, 1961
Trumann McEver, 1962
Robert Shideler, 1963
L. F. Bailey, 1965
James H. Fribourgh, 1966
Howard Moore, 1967
John J. Chapman, 1968
Arthur Fry, 1969
M. L. Lawson, 1970
R. T. Kirkwood, 1971
George E. Templeton, 1972
E. B. Wittlake, 1973
Clark McCarty, 1974
Edward Dale, 1975
Joe Guenter, 1976
Jewel Moore, 1977
Joe Nix, 1978
P. Max Johnston, 1979
E. Leon Richards, 1980
Henry W. Robison, 1981
John K. Beadles, 1982
Robbin C. Anderson, 1983
Paul Sharrah, 1984
William L. Evans, 1985
Gary Heidt, 1986
Edmond Bacon, 1987
Gary Tucker, 1988
David Chittenden, 1989
Richard K. Speairs, Jr. 1990
Robert Watson, 1991
Michael W. Rapp, 1992
Arthur A. Johnson, 1993
George Harp, 1994

INSTITUTIONAL MEMBERS

The Arkansas Academy of Science recognizes the support of the following institutions through their Institutional Membership in the Academy.

ARKANSAS STATE UNIVERSITY, State University
ARKANSAS TECH UNIVERSTIY, Russellville
HARDING UNIVERSITY, Searcy
HENDERSON STATE UNIVERSITY, Arkadelphia
HENDRIX COLLEGE, Conway
JOHN BROWN UNIVERSITY, Siloam Springs
MISSISSIPPI COUNTY COMMUNITY COLLEGE, Blytheville
OUACHITA BAPTIST UNIVERSITY, Arkadelphia
SOUTHERN ARKANSAS UNIVERSITY, Magnolia
UNIVERSITY OF ARKANSAS AT FAYETTEVILLE
UNIVERSITY OF ARKANSAS AT LITTLE ROCK
UNIVERSITY OF ARKANSAS FOR MEDICAL SCIENCES, Little Rock
UNIVERSITY OF ARKANSAS AT MONTICELLO
UNIVERSITY OF ARKANSAS AT PINE BLUFF
UNIVERSITY OF CENTRAL ARKANSAS, Conway
UNIVERSITY OF THE OZARKS, Clarksville

EDITORIAL STAFF

COVER: Male widow skimmer (*Libellula luctuosa* Burmeister). Photo by John Rickett

ARKANSAS ACADEMY OF SCIENCE 1994

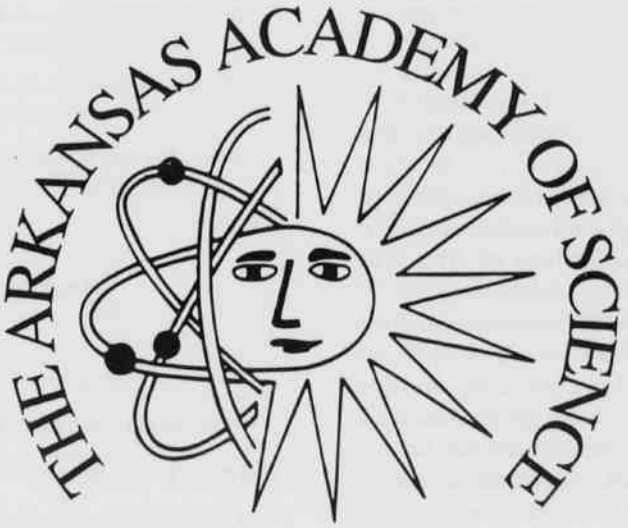

APRIL 8-9, 1994
78th ANNUAL MEETING

JONESBORO

ARKANSAS ACADEMY OF SCIENCE

ANNUAL FINANCIAL STATEMENT

(1 JANUARY 1993 TO 31 DECEMBER 1993)

ANNUAL MEETING 8-9 APRIL 1994
ARKANSAS STATE UNIVERSITY, JONESBORO, AR

George Harp President	**James Peck** President-Elect	**John D. Rickett** Secretary
Robert Wiley Treasurer	NAAS Delegate	**Henry Robison** Historian

Secretary's Report

FIRST BUSINESS MEETING

Members present: 28

President George Harp called the meeting to order at 1137 hrs.

1. Harp recognized Lynita Cooksey to make announcements concerning the meeting (mixer location, banquet ticket availability, Sigma Xi breakfast location and time, and ASU personnel who are available to help with problems). Cooksey also introduced Dr. Richard McGhee, Dean of the College of Arts and Sciences, who extended the official welcome.
2. Harp recognized John Rickett, Secretary, who presented copies of minutes from the two 1993 Annual Business Meetings and asked for comments and/or corrections in writing before the second business meeting. Rickett moved (2nd: Tom Palko) the acceptance of the minutes. Rickett also reported on membership categories and asked for advice regarding retention of arrears members. Stan Trauth suggested the Secretary send a reminder letter to arrears members.
3. Harp recognized Henry Robison, Historian, for a historical report. This is the 78th annual meeting, and the sixth time at Arkansas State University. Other meetings here occurred in 1952, 1967, 1973, 1980, 1990.

FUNDS

Balance on 1 January 1993		22,634.54
Total Income (Page 2)	12,442.37	
Total Expenses (Page 3)	-12,202.67	
Balance for the Year	$239.70	239.70
TOTAL FUNDS AS OF 31 DECEMBER 1993		**$22,874.24**

DISTRIBUTION OF ACCOUNTS

Interest Bearing Checking Account (Union Bank and Trust Co., Monticello, AR)	5,211.97
Certificates of Deposit	
Dwight Moore Endowment (Heritage Bank - A Federal Savings Bank - Monticello - No. 506334.1 - 3.55% Int.)	2,232.43
Life Membership Endowment (Heritage Bank - A Federal Savings Bank - Monticello - No. 508910 - 3.55% Int.)	9,562.72
AAS Endowment (Heritage Bank - A Federal Savings Bank - Monticello - No. 509173 - 3.55% Int.)	5,867.12
TOTAL	**$22,874.24**

Respectfully Submitted

Robert W. Wiley, AAS Treasurer

FINANCIAL STATEMENT, ARKANSAS ACADEMY OF SCIENCE

INCOME: 1 January 1993 to 31 December 1993

1. INDIVIDUAL MEMBERSHIPS		
a. Regular	2,685.00	
b. Sustaining	400.00	
c. Sponsoring	60.00	
d. Life	150.00	
e. Associate	80.00	
	3,375.00	3,375.00
2. INSTITUTIONAL MEMBERSHIPS		2,200.00
3. PROCEEDINGS, LIBRARY SUBSCRIPTIONS		326.50
4. PROCEEDINGS, MISC. SALES (UAF)		2,141.37
5. PROCEEDINGS, PAGE CHARGES		2,562.50
6. ANNUAL MEETING		653.58
7. INTEREST		
a. Interest Bearing Checking Account	111.24	
b. Dwight Moore Endowment	91.73	
c. Life Membership Endowment	330.94	
d. AAS Endowment	199.40	
e. AAS General CD's	75.11	
	808.42	808.42
8. MISCELLANEOUS		55.00
9. ENDOWMENT DONATIONS		
a. Dwight Moore Endowment	120.00	
b. AAS Endowment	200.00	
	320.00	320.00
TOTAL INCOME		**$12,442.37**

FINANCIAL STATEMENT, ARKANSAS ACADEMY OF SCIENCE

EXPENSES: 1 January 1993 to 31 December 1993

1.	AWARDS		
	a. Arkansas Science Fair Association (#604)	400.00	
	b. Arkansas Junior Academy of Science (#605)	250.00	
	c. Robert Cowherd (#606)	50.00	
	d. Michael Eckles (#607)	25.00	
	e. Connie Baber (#608)	25.00	
	f. E. E. Ward (#609)	50.00	
	g. Mandy Prosser (#610)	25.00	
	h. Edward Boone (#611)	25.00	
	i. Anthony Holt (#612)	50.00	
	j. John Peck, Plaques - Arkansas Science Talent Search (#613)	165.08	
		1,065.08	1,065.08
2.	PROCEEDINGS		
	a. Linda Lee, Editorial Consultant Vol. 46 (#602)	500.00	
	b. Phillip's Litho (Vol. 46) (#614)	7,810.80	
	c. Joy Trauth, Editorial Consultant Vol. 47 (#618)	500.00	
	d. Federal Express (#619)	22.00	
	e. Multigraphics - Reprint 54 copies Vol. 46 (#623)	1,667.76	
		10,500.56	10,500.56
3.	OFFICE EXPENSES		
	a. Secretary's Office, John Rickett (#620)	415.06	
		415.06	415.06
4.	ANNUAL MEETING EXPENSES (HSU)		
	a. George Harp, Plaques (#603)	81.22	
	b. HSU Motor Pool (#617)	10.00	
		91.22	91.22
5.	NEWSLETTERS		
	a. UAM Department of Forest Resources (#600)	40.07	
	b. UAM Department of Forest Resources (#624)	38.18	
		78.25	78.25
6.	DUES		
	a. National Association of Academies of Science (#601)		52.50
TOTAL EXPENSES			$12,202.67

4. Harp recognized Robert Wiley, Treasurer, for a financial report. Wiley referred to available copies of the report, briefly summarized its categories of income and expenses, and invited questions or comments. Wiley moved (2nd: Henry Robison) the approval of the financial report.

5. Harp recognized Stan Trauth, *Proceedings* Editor, for a report. The quality and price have increased, and Trauth hopes the membership will approve. Trauth moved (2nd: Robert Watson) the appropriation of $500 plus $200 for editorial assistance be made to support his office. Trauth also requested paper section chairs collect and transfer to him any manuscripts being submitted for publication.

6. Harp announced, in connection with the higher quality and higher price of the *Proceedings*, the Executive Committee will consider raising membership dues.

7. Harp recognized Richard Kluender, *Newsletter* Editor, for a report. He referred to available copies of his report. Kluender also summarized the subsidization of *Newsletter* production by his department and that this support may be lost when a new editor is elected. He moved (2nd: Art Johnson) the Academy appropriate $1500 to support the *Newsletter's* production during next year.

8. Harp recognized Robert Watson, Chair of Nominations Committee, for a report. Other committee members were Walt Godwin and Dennis McMasters. Richard Kluender and Tom Palko were nominated to the office of Vice President, David Saugey for *Newsletter* Editor, and John Rickett for Secretary. Harp opened the floor to additional nominations. None came, and Harp declared nominations closed and the work of the Nominations Committee are accepted.

9. Harp called for a report from the Science Education Committee, but none came.

10. Harp recognized Mark Draganjac, Chair of Auditing Committee. Other committee members are Robert Engelken, Larry Mink, and Tina Teague.

11. Harp recognized Jimmy Bragg, Chair of Resolutions Committee. Other committee members are Dan Marsh and Mark Karnes.

12. Harp recognized the Constitution Committee; Jim Peck, Chair, Peggy Rae Dorris, and John Rickett. Rickett called attention to copies of the three motions the committee is placing before the membership (Appendix A), briefly explained the justifications, and asked for comments or questions. Rickett moved (2nd: Tom Palko) the approval of these three motions for constitutional revision, and Harp stated that the Executive Committee recommends a "do pass."

13. Harp recognized Tom Palko, Director of Junior Science and Humanities Symposium, for a report (see Appendix B). JSHS is very active and just completed an excellent meeting. Recognition should be given to all winners for their achievements.

14. Harp reported, for Robert Skinner, that the Junior Academy is meeting this weekend, and that Skinner is requesting continued support of $250 from the Academy. John Peck moved (2nd: Tom Palko) that the support be approved.

15. Harp recognized Robert Wiley to report, on behalf of Mike Rapp, on the Arkansas Science Fair Association. It is also being held this weekend. Rapp requests continued support of $400 from the Academy. Moved by Art Johnson, (2nd: John Peck).

16. Harp recognized John Peck, Director, Arkansas Science Talent Search, for a report. The 43rd Annual Arkansas Science Talent Search was held in conjunction with the 53rd Westinghouse Science Talent Search. Winners were:

First Place: Lisa Anne Turner
Route 5, Box 348
Sheridan, AR 72150
"The formation of 4-vinyl guaiacol as a result of yeast contamination in sealed frozen orange juice"
Sheridan High School; sponsored by Mr. Jim Gunnell

Second Place: Eric Evan Chen
1411 Stonehenge Pl.
Little Rock, AR 72212
"Separation of polycyclic aromatic hydrocarbons by charge-transfer chromatography"
Central High School; sponsored by Ms. Jacqueline Dyer

Third Place: Jennifer G. Baquial
1205 Glenda Drive
Little Rock, AR 72202
"Modulation of nitric oxide synthase may account for the anticonvuland and analgesic activities of Cu(II)2(3,5-diisopropylsalicylate)4"
Central High School; sponsored by Mr. Dennis Brant

Peck also requested continued support of $200 from the Academy (2nd: Henry Robison).

17. John Peck also reported that an *ad hoc* committee, which he chairs, is seeking to consider appropriate ways the annual meetings might be diversified and enhanced. He asked for ideas via a questionnaire to be returned to him.

18. Presidential announcements:
    a. Doug James (UAF) will chair the Biota Survey Committee, with James Peck and Henry Robison cooperating and, respectively, representing the botanical and zoological interests. James is in the process of computerizing Leo Paulissen's records, and the University of Arkansas Press is interested in publishing the material. The committee will meet at 1700 hrs. today.
    b. The Development Committee has been chosen and charged to generate ideas for Academy advancement. Ed Griffin, Chair, Ed Bacon, and Dick Kluender comprise the committee and will welcome any ideas.

19. Harp called for any old business. None came.

20. Harp announced future meetings:
    a. University of Arkansas at Pine Bluff has officially invited the Academy to meet on their campus in 1995. Motion to accept by Tom Palko (2nd: Henry Robison).
    b. WestArk Junior College is interested in hosting the meeting in 1996, and the Oklahoma Academy of Science is interested in meeting jointly with the Arkansas Academy at that time.

21. Harp: final announcements:
    a. Sigma Xi breakfast Saturday at the Holiday Inn.
    b. Reminded section chairs to collect manuscripts being submitted for publication.

22. Motion to adjourn by Tom Palko (2nd: Robert Watson). Meeting adjourned at 1225 hrs.

SECOND BUSINESS MEETING

Members present: 56

President George Harp called the meeting to order at 1200 hrs.

1. Harp recognized Secretary Rickett to revisit the minutes of the 1993 business meetings. Having no comments or corrections, the minutes were approved by voice vote.

2. Harp recognized Doug James for a report on the activities of the Biota Committee. The committee will continue assembling lists, will work toward computerizing existing lists, and approach the University of Arkansas Press for publication.

3. Harp recognized Treasurer Wiley to revisit the financial report. Wiley asked for comments; none came. The Auditing Committee reported the following:

   The Auditing Committee, after careful examination, found the financial records of the Academy as prepared by Treasurer Bob Wiley to be accurate and in good order. The committee would suggest, if possible, that in future reports, all transactions involving certificates of deposit be listed on a separate summary sheet (submitted by M. Draganjac, Chair).

   A motion to accept the committee's report passed, and voice vote accepted the Treasurer's report.

4. Harp asked Rickett to represent the requests for continued funding, as follows:

   $ 700 for the *Proceedings* Editor's office

1500 for the *Newsletter* Editor's office
250 for the Junior Academy
400 for the Science Fair Association
200 for the Science Talent Search

Rickett asked for comments and moved (2nd: Walt Godwin) the approval of these requests as a block. Passed.

5. Harp asked all new members to stand and be recognized, then all life members to do likewise.

6. Harp asked Robert Watson to review the slate of nominations (Dick Kluender and Tom Palko for Vice-President, David Saugey for *Newsletter* Editor, and John Rickett for Secretary). Harp then asked for nominations from the floor. None came, and Bob Wiley moved (2nd: Ed Bacon) that nominations cease. Passed. Robert Watson moved that the two unopposed candidates be accepted by acclamation. Passed.

   Written ballots elected Richard Kluender to the office of Vice-President.

7. Harp recognized Jimmy Bragg for a report from the Resolutions Committee (Appendix C). Resolutions were accepted and approved.

8. Harp reminded the audience of the motion from the First Business Meeting to accept the invitation from UAPB for the 1995 meeting.

9. Harp then recognized David Meeks, who formally invited the Academy to meet on the WestArk Campus in 1996 and to formally approach the Oklahoma Academy of Science for a joint meeting. Motion to accept their invitation was made by Palko and passed.

10. Harp recognized Phoebe Harp for announcement of paper award winners (see Appendix D).

11. Harp recognized Lynita Cooksey for a report on the meeting involvement. There were 258 registrations, 140 banquet participants, and 133 papers presented, of which 62 were student papers.

12. Harp reminded attendees to pick up unclaimed *Proceedings* and return them to their respective campuses, as appropriate.

13. New business:
    a. Harp reannounced John Peck's survey and invited members to respond with suggestions and comments.
    b. Harp announced that a graduate assistantship to study freshwater mussels is available.
    c. Harp recognized Joe Stoeckel (ATU) who gave a brief report on the activities of the new Arkansas River Conservation Committee and invited broader participation.
    d. Harp recognized Rickett, who reviewed the three motions to amend the Constitution proposed by the Constitution Committee. Motions passed as a group without discussion.

14. Harp extended appreciation to all who helped his office during the past year and the local arrangements committee for the current meeting. He then called Dick Kluender to the front and presented a plaque to him of appreciation as outgoing *Newsletter* Editor.

15. Harp then called Jim Peck to the front and passed the gavel to him as the new president. Peck then presented Harp with a plaque of appreciation for his year as president.

16. President Peck cited the Academy's growth as a healthy trend and invited everyone to the 1995 meeting. Peck also introduced the new President-Elect, Peggy Rae Dorris.

17. Peck entertained a motion by Walt Godwin to adjourn (several seconds). Meeting adjourned at 1252 hrs.

--- Respectfully submitted,
John Rickett, Secretary

APPENDIX A

TO: ARKANSAS ACADEMY OF SCIENCE EXECUTIVE COMMITTEE AND MEMBERSHIP
DATE: 8 APRIL 1994
FROM: CONSTITUTION COMMITTEE (JAMES PECK, PEGGY RAE DORRIS, AND JOHN RICKETT)

MOTIONS FOR CONSTITUTIONAL REVISION

MOTION 1: The insertion of the following item into the By-laws as item 9:

9. In the event an officer, except President, Past-President, President-Elect, and Vice-President, is unable to complete a term, the Executive Committee shall appoint a successor to complete that term, or open a new 5-year term with an election at the next general meeting.

COMMENTARY ON MOTION 1: The recent resigning

of Harvey Barton from the office of *Proceedings* Editor before expiration of his elected term caused considerable debate within the Executive Committee regarding how to get a new Editor. This motion would give the Executive Committee some guidance and reduce the time spent debating the mechanism.

MOTION 2: The following revision of Appendix A (CONSTITUTIONAL AND STANDING COMMITTEES OF THE ACADEMY):

APPENDIX B

(NOTE: proposed additions are bold-faced; deletions are *italicized*)

AAS CONSTITUTIONAL COMMITTEES

1. EXECUTIVE COMMITTEE: The Executive Committee shall consist of the President, Past President, President-Elect, Vice President, Historian, *Proceedings* Editor, *Newsletter* Editor, Secretary, and Treasurer. The Executive Committee shall make recommendations concerning the policies and activities of the Academy in accordance with the Constitution and By-laws of the Academy. The committee shall meet prior to the first annual business meeting to discuss any motions to be presented at the annual business meeting or any other matters that pertain to the Academy.

AAS STANDING COMMITTEES ESTABLISHED BY THE BY-LAWS

1. AUDITING COMMITTEE: The Auditing Committee shall consist of a Chairperson and three additional members. The President shall appoint the Committee prior to or at the first annual business meeting, and it shall function only for that annual meeting. The Committee shall examine the financial records of the Academy, provided by the Treasurer, and report its findings to the Academy at the second business meeting.

2. AWARDS COMMITTEE: The Awards Committee shall be named by the Local Arrangements Committee for the upcoming annual meeting. The Awards Committee shall consist of a Chairperson and two as many additional members as the Chair and/or Local Arrangements Committee deem necessary. The Awards Committee shall review evaluate undergraduate and graduate papers presented paper presentations during the annual meeting and make recommendations for the various undergraduate awards established by the Executive Committee.

3. BIOTA COMMITTEE: The Biota Committee shall consist of a Chairperson and five additional members, and shall be appointed by the President for undefined terms of service. A term of service may be terminated by either the President or the committee Chair or member. The Biota Committee shall collect, organize, and disseminate taxonomic information on the flora and fauna of Arkansas. Reports shall be made available to the members of the Academy and any other interested party when sufficient information exists.

4. CONSTITUTION COMMITTEE: The Constitution Committee shall be appointed by the President whenever a need for constitutional examination exists and consist of the President-elect, Vice President, and one additional member. The President-elect shall serve as the Chairperson. The Committee shall make recommendations on changes in the Constitution and By-laws whenever such changes shall be are deemed necessary.

5. DEVELOPMENT COMMITTEE: The Development Committee shall consist of a Chairperson and two additional members and be appointed by the President to undefined terms. Either the President or the committee Chair or member may terminate an appointment. The Development Committee shall promote the growth and development of the Academy by contacting private industries to secure endowment funding to support activities of the Academy.

6. LOCAL ARRANGEMENTS COMMITTEE: The Local Arrangements Committee shall consist of a Chair, appointed by the President, and a minimum of two additional members, selected by the Chair. The Local Arrangements Committee shall make the arrangements necessary to host the annual meeting in accordance with the established guidelines for hosting a meeting adopted by the Executive Committee.

7. NOMINATIONS COMMITTEE: The Nominations Committee shall consist of a Chairperson and two additional members. The Nominations Committee shall be appointed by the President prior to the annual meeting and shall recommend candidates for office to the members of the Academy for election. Two candidates shall be proposed for Vice President, and one candidate shall be proposed for each of the other offices (Treasurer, Secretary, Historian, and Editors) as their terms expire.

8. PUBLICATIONS COMMITTEE: The Publications Committee shall consist of the Editor of the *Proceedings*, who serves as Chair, and two additional

members. The two additional members shall be appointed by the President for undefined terms, and either the President or the committee member may terminate an appointment. The Chair may select as many associate editors as deemed necessary. The *Publications Committee* Editor and associate editors shall review papers submitted for publication in the *Proceedings* and any other publications deemed necessary by the Executive Committee. Papers submitted for publication in the *Proceedings* shall may be forwarded to selected reviewers, and the Committee has jurisdiction over all matters concerning acceptance, rejection, or modification revision of scientific papers.

9. PUBLICITY COMMITTEE: The Publicity Committee shall consist of a Chairperson and two additional members. The Committee shall be appointed by the President for undefined terms, and either the President or the committee Chair or member may terminate an appointment. The Publicity Committee shall promote the public image of the Academy with news releases on activities and accomplishments of the Academy. All news releases shall be reviewed and approved by the Executive Committee prior to release to the news media.

10. RESOLUTIONS COMMITTEE: The Resolutions Committee shall consist of a Chairperson and two additional members. The Committee shall be appointed by the President prior to or at the first annual business meeting and serve only for that meeting. The Resolutions Committee shall present an appropriate resolution expressing the appreciation of the Academy to all individuals and organizations involved in activities sponsored by the Academy during the year.

11. SCIENCE EDUCATION COMMITTEE: The Science Education Committee shall consist of a Chairperson and additional members as deemed necessary by the Chairperson of the Committee. The President shall appoint the Chair and, in consultation with the Chair, additional members for undetermined terms. Either the President or the committee Chair or member may terminate an appointment. The Science Education Committee shall provide information to the Academy on current programs and activities in science education in the state, promote programs, including the Junior Academy, Science/Engineering Fairs, and Science Talent Search(es), and cooperate with state agencies and other educational organizations in the study and development of innovative ideas or activities to improve science education at all levels in the state.

COMMENTARY ON MOTION 2: This proposed revision simply clarifies and adds information regarding the make-up, who appoints, and terms of members of the various standing committees.

MOTION 3: The addition of the following item as Appendix B to the Academy Constitution:

DUTIES OF ELECTED OFFICERS

a. *President* --
i. Calls to order and presides over all Executive and General Business Meetings.
ii. Handles official Academy correspondence as pertains to the Office of President, and/or delegates correspondence pertaining to other offices to those officers, as appropriate
iii. Asks any other officers and directors of subunits, as appropriate, for advice and assistance

b. *President-Elect*--
i. Serves in the capacity of President should the President be unable to perform his/her duties
ii. Assists and advises the President when called on to do so

c. *Vice President*--
Assists and advises the President and/or President-Elect when called on to do so

d. *Past President*--
By virtue of his/her service and experience, the Past President assists and advises the President when called on to do so

e. *Treasurer*--
i. Keeps all financial records of the Academy
ii. Receives payments of dues, *Proceedings* subscriptions, and any other source of income
iii. Manages investments of the Academy with the approval of the Executive Committee
iv. Disburses funds for payment of Academy operating expenses and gifts awarded

f. *Secretary*--
i. Keeps all clerical records of the Academy: memberships by approved categories, *Proceedings* subscription, exchange, and abstracting service lists, and other records as deemed necessary and appropriate by the Executive Committee
ii. Sends out copies of the *Proceedings* to members (as needed) and as requested by subscription, exchange, and abstracting service lists
iii. Corresponds with members and libraries as appropriate regarding payment of dues and payment of invoices for *Proceedings*

iv. Furnishes mailing labels to other Executive Committee members as requested and appropriate
v. Furnishes membership information, as appropriate, to anyone requesting
vi. Corresponds with AAAS (American Association of Academies of Science) to receive or provide information as needed and appropriate

g. *Proceedings Editor*--
i. Receives manuscripts submitted for publication and cooperates with Associate Editors in the review, revision, and acceptance process
ii. Prepares the next issue of the *Proceedings* by assembling the final copies of manuscripts accepted for publication
iii. Works with the Publisher in the technical preparation of the *Proceedings*
iv. Arranges for the distribution of copies of the *Proceedings* at the next annual meeting

h. *Newsletter Editor*--
i. Receives and compiles news items regarding Academy operations, Executive Committee decisions, and general Academy activities and involvements
ii. Prepares two issues of the *Newsletter* per year, the contents of which are subject to approval and revision by the Executive Committee--
a. the "Fall" issue shall contain general news about Academy activities and general information about the next annual meeting
b. the "Spring" issue shall contain more specific information about the next annual meeting, an abstract form, meeting reservation/registration form(s), and specific news about achievements of Academy members
iii. Distributes copies to all Academy members and prospective members, as directed by the Executive Committee

i. *Historian*--
i. Keeps historical records of Academy meetings and other activities
ii. Reports on past activities at the annual meeting, as the presiding officer directs, and as the Executive Committee requests

COMMENTARY ON MOTION 3: In the past, we have been comfortable with the officers' titles sufficiently conveying their duties. Anticipating the possibility of problems or misunderstandings, we probably should document the major duties or expected functions of each elected officer.

IMPLEMENTATION--
These items will be presented for discussion at the First Business Meeting on 8 April 1994 and (possibly) further discussed and voted on during the Second Business Meeting on 9 April 1994. The approval and implementation of Motion 1 will cause items in the By-laws currently numbered 9 through 14 to be renumbered 10 through 15.

APPENDIX B

ARKANSAS JUNIOR SCIENCE AND HUMANITIES SYMPOSIUM TOM PALKO, DIRECTOR

The 28th Arkansas Junior Science and Humanities Symposium was held on the Arkansas Tech University campus on March 18-20, 1994. There were 119 students and 25 teachers in attendance, representing all regions of Arkansas. Activities during the symposium included talks by scientists about their research, seminars, tours, a field trip for the student delegates, and a workshop for teachers. The delegates were entertained with two one-act plays performed by the ATU Theater Department. They also enjoyed a keyboard concert with selections performed on the harpsichord, piano, and pipe organ.

The main event of the meeting occurred Saturday morning when 15 students were given the opportunity to present their research papers. Four of the presenters won a full freshman scholarship at ATU. Six won a trip to the National JSHS which will be held the last week in April at NCSU and Triangle Research Center, Raleigh, NC. Anna Terry was selected as the outstanding presenter, and she will compete at the National JSHS meeting for a free two-week tour of London, England. The title of her paper was, "The Fractal Geometry of Landforms: A Report on a Mathematical Investigation." Anna is a 15-year-old sophomore at Southside High School, Fort Smith, Arkansas.

APPENDIX C

RESOLUTIONS

BE IT RESOLVED, that we, the members of the Arkansas Academy of Science, offer our sincere thanks to Arkansas State University at Jonesboro for hosting the 1994 meeting of the Arkansas Academy of Science. In particular, we thank the local arrangements committee for an outstanding job of organizing the meeting: Lynita Cooksey, Chairperson; Phoebe Harp; Julia Bollinger; Jim Bednarz; Marty Huss; Susan Cady; J. D. Wilhide; and Larry Mink. Appreciation is expressed for the use of ASU's excellent facilities and the hospitality shown us by all ASU personnel. The banquet was excellent, as was Dr. Ken Paige and his dynamic presentation, "Plant-Animal Interactions and the Dynamic Nature of Plants."

The Academy recognizes the important role played

by the various section chairpersons and expresses appreciation to: Jerry Darsey, Susan Cady, and Edward Bennett (Chemistry); Leon Richards and Dennis McMasters (Botany); Lawrence Hinck and William Willingham (Biomedical); Betty Cochran (Herpetology); Robert Watson (Invertebrate Zoology); William Braithewaite and Robert Engleken (Physics, Computers, Energy, Geology); Roland McDaniel and Alan Price (Aquatic Biology); Andrew Sustich (Geology, Astronomy, Physics); Ronald Johnson and David Gilmore (Microbiology, Cellular Biology); Alan D. Christian (Science Education, Toxicology, Water Quality); Michael Harvey and Renn Tumlison (Ecology, Conservation); Todd Wiebers and David Saugey (Birds, Mammals).

A special thanks is owed the individuals who devoted considerable time and energy to judging student papers: Anthony Holt and Earl Hanebrink (Undergraduate Life Sciences); Roger Buchanan and Julia Bollinger (Graduate Life Sciences); David Chittenden and Ed Gran (Undergraduate Physical Sciences); Norman Trautwein and Andy Sustich (Graduate Physical Sciences).

We express gratitude to the various directors of the science and youth activities which are supported by the Academy: Tom Lynch (Chairperson, Science Education Committee); Mike Rapp (President, Arkansas State Science Fair Association); Tom Palko (Director, Junior Science and Humanities Symposium); John Peck (Director, Science Talent Search); and Robert and Raynell Skinner (Co-Directors, Arkansas Junior Academy of Science).

We wish to thank all those individuals who served as directors at science fairs and Junior Academy meetings: Kathryn Shinn and Marian Douglas (Central Region); Veryl Board and Kathy Campbell (Northcentral Region); Larry Minck and Ron Johnson (Northeast Region); John Hehr (Northwest Region); Wayne Everett (Southcentral Region); Guy Nelson and Deborah Phillips (Southeast Region); Tim Daniels (Southwest Region); Mike Rapp, Robert and Raynell Skinner (State Meeting, UCA, Conway).

The continued success of the Academy is due to its strong leadership. We offer sincere thanks to our officers for another excellent year: George Harp (President), James Peck (President-Elect), Peggy Dorris (Vice President), John Rickett (Secretary), Robert Wiley (Treasurer), Art Johnson (Past President), Stan Trauth (*Proceedings* Editor), Richard Kluender (*Newsletter* Editor), and Henry Robison (Historian). In addition, the Academy expresses appreciation to all those individuals who have contributed their time and efforts on various committees of the Academy.

Finally, we congratulate all those who presented papers at this meeting. Student participants are especially recognized, since their continued efforts will be directly responsible for the future success of the Academy, and the continuation of science education and research in Arkansas.

Resolutions Committee
J. D. Bragg, Chair
Daniel L. Marsh
Mark Karnes

APPENDIX D

PAPER PRESENTATION AWARDS

Life Sciences - undergraduate:

First -- Reproductive structures of adult cottonwood borer beetles *Plectrodera scalator*). **Jason A. Kilgore,** Hendrix College, Conway, AR, and Steven K. Goldsmith, Tulsa University, Tulsa OK.

Second-- Species packing in a North Carolina creek. **James J. English** and Alvan A. Karlin, University of Arkansas at Little Rock, and Laurie D. Lacer, Biotechnical Services, Inc., North Little Rock , AR.

Third-- Nectar production in *Lobelia puberula:* Undergraduate research on native plants and their pollinators. **Michael J. Boyd,** Lachi R. Kishen, and William H. Baltosser, University of Arkansas at Little Rock, AR.

Life Sciences -- graduate:

First-- Water quality of an Ozark stream receiving urban point and non-point pollution: Physicochemical parameters. **Phillip B. Drope** and James J. Daly, University of Arkansas for Medical Sciences, Little Rock, AR.

Second-- Selected community characteristics of freshwater mussels (Unionacea) in the Cache River, Arkansas. **Alan D. Christian,** John L. Harris, William R. Posey, and George L. Harp, Arkansas State University, State University, AR.

Third-- A comparison of macrophytes of two small northwest Arkansas reservoirs. **John J. Sullivan** and A. V. Brown, University of Arkansas at Fayetteville, AR.

Physical Sciences -- undergraduate:

First-- Tetraethylene glycol-based electrolytes for high temperature electrochemical deposition of compound semiconductors. **Chris Poole,** Robert D. Engelken, Brandon Kemp, and Jason Brannen, Arkansas State University, State University, AR.

Second-- Storm dominated channel sequences on a shallow marine shelf: Middle Morrowan of northwestern Arkansas. **Kimberly R. Jones,**

University of Arkansas at Fayetteville, AR.

Third-- Studies of Copper(II) 2-hydroxy-5-N, N-diethylsulfonamide benzoate. **Elsie Williams,** Shaheen Khan, Israt J. Chowdhurry, and William M. Willingham, University of Arkansas at Pine Bluff, AR.

Physical Sciences -- graduate:

First-- Evaluation of photodiode arrays in rocket plume monitoring and diagnostics. **D. H. Snider,** M. K. Hudson, R. B. Shanks, and R. Cole, University of Arkansas at Little Rock, AR.

Second-- Multisite microprobes for electrochemical recordings in biological dynamics. **G. Screenivas,** S. S. Ang, R. M. Ranade, A. S. Salian, and W. D. Brown, University of Arkansas at Fayetteville, AR.

Third-- An integrated data acquisition and data analysis system for high energy physics. **Charles A. Byrd,** Christine A. Byrd, and W. J. Braithwaite, University of Arkansas at Little Rock, AR.

APPENDIX E

STATE SCIENCE FAIR AND JUNIOR ACADEMY OF SCIENCE 1994 ANNUAL REPORT

Below are shown the numbers of students who participated in the Arkansas science fairs that are affiliated with Science Service and the numbers of students who participated in the State Junior Academy of Science meeting for 1994 (see below for the locations of the fairs). The senior division is for students in grades 9-12, and the junior division is for students in grades 8 and below. Since statewide competition is not allowed for students before high school, there are no "junior divisions" for the state fair or junior academy.

	Cent	NCen	N.E.	N.W.	SCen	S.E.	S.W.	State	JrAcad
Senior	134	65	120	100	140	156	92	256*	63*
Junior	120	68	123	105	131	93	526	n/a	n/a

*54 schools

For 1994, the locations and dates for the events and the individuals serving as directors were:

		Science Fair	Junior Academy
Central Region	UAMS	Kathryn Shinn	Marian Douglas
Saturday, March 5		Lonoke H.S.	U.A.L.R.
North Central	Batesville	Veryl Board	Kathy Campbell
Friday, March 25		Arkansas College	Newark H.S.
North East	Jonesboro	Larry Mink	Ron Johnson
Friday, Saturday, March 4, 5		Ark. State U.	Ark. State U.
North West	Fayetteville	John Hehr	
Friday, March 18		Univ. of Ark.	
South Central	Arkadelphia	Wayne Everett	Wayne Everett
Friday, March 8 (sic)		Ouach. Bap. U.	Ouach. Bap. U.
South East	Monticello	Guy Nelson	Deborah Phillips
Friday, March 11		U of A-Mont.	DeWitt H.S.
South West	Camden	Tim Daniels	
Friday, March 11		SAU-Tech Station	
State	Conway	Mike Rapp	M/M Bob Skinner
Friday, Saturday, April 8, 9		Univ. Cen. Ark.	U.A.M.S.

MEMBERS 1994

LAST NAME	FIRST MI	INSTITUTION
Adams	Al	Univ. of Arkansas at Little Rock
Addison	Stephen R.	University of Central Arkansas
Al-Khayri	Jameel M.	University of Arkansas/Fayetteville
Bacon	Robert	University of Arkansas at Fayetteville
Bailey	Claudia	University of Arkansas at Fayetteville
Baker	Max L.	University of Arkansas/Medical Sciences
Ball	Kenneth M.	El Dorado Public Schools
Baltosser	William H.	University of Arkansas at Little Rock
Barber	Gwen	
Basford	Adelphia M.	Henderson State University
Bass	Ralva	University of Central Arkansas
Bates	Vernon	
Battles	Les	Arkansas State University
Beadles	John Kenneth	Arkansas State University -- retired
Bennett	J. Edward	Arkansas State University
Benson	Ann Marie	University of Arkansas/Medical Sciences
Bickle	Elaine	Univ. of Arkansas at Little Rock
Bowman	Leo H.	Arkansas Tech University
Bragg	Jimmy D.	Henderson State University
Bragg	Ann T.	Garland County Community College
Breen	David	Mississippi County Community College
Brown	Art	University of Arkansas
Brown	William D.	University of Arkansas at Fayetteville
Buchanan	Roger A.	Arkansas State University
Burnside	Gaylen	University of Arkansas at Little Rock
Cady	Susan	Arkansas State University
Cartwright	Michael E.	Arkansas Game & Fish Commission
Chapman	Stanley L.	University of Arkansas at Fayetteville
Chowdhury	Aslam H.	University of Arkansas at Pine Bluff
Cisar	Cindy	University of Arkansas at Fayetteville
Clayton	Frances E.	University of Arkansas at Fayetteville
Cloud	Gary	University of Arkansas
Cochran	Betty S.	U.S. Forest Service
Cole	David	Harding University
Collins	Joseph T.	University of Kansas
Cooksey	Lynita	Arkansas State University
Cordova	Robert M.	Cordco Consulting
Crisp, Jr.	Robert M.	University of Arkansas at Fayetteville
Culwell	Donald	University of Central Arkansas
Dalske	Fred	University of Central Arkansas
Daly	James J.	University of Arkansas/Medical Sciences
Daniels	James T.	Southern Arkansas University/Tech Br.
Daster	Robert H.	Arkansas Highway & Transp. Dept.
David	Stanley N.	Arkansas State University
Davis	Jerry W.	USDA, Forest Service
Demarest	Jeffery R.	University of Arkansas at Fayetteville
Desrochers	Patrick	Univ. of Central Arkansas
Doran	Ronald H.	Harding University
Dorris	Peggy Rae	Henderson State University
Doster	Robert H.	Ark. Highway &Transp. Dept.
Douglas	Marian	University of Arkansas at Little Rock
Duhart	Benjamin T.	University of Arkansas at Pine Bluff
Dunn	Jane	Henderson State University
Dussourd	David	University of Central Arkansas
Edwards	Richmond	
Eichenberger	Rudolph J.	Southern Arkansas University
Eldridge	Hudson B.	University of Central Arkansas
Engelken	Robert	Arkansas State University
England	Don	Harding University
Epperson	Claude E.	University of Arkansas/Medical Sciences
Fifer	E. Kim	University of Arkansas/Medical Sciences
Fijan	Nikola	Univ. of Arkansas at Pine Bluff
Fletcher	M. Doug	Riceland Foods Inc. (ASU)
Floyd	E. P. (Perk)	U.S. Public Health Service
Foti	Thomas L.	Natural Heritage Commission
Freiley	Kenneth	University of Central Arkansas
Fuller	Gary	University of Arkansas at Little Rock
Gagen	Charlie	Arkansas Tech University
Gaiser	Jack	University of Central Arkansas
Gentry	Joe P.	Arkansas Science & Technology Authority
Gildseth	Wayne	Southern Arkansas University
Gilmore	David F.	Arkansas State University
Gilmour	John T.	University of Arkansas at Fayetteville
Goforth	Calvin	Univ. of Arkansas at Fayetteville
Goforth	R. R.	University of Arkansas at Fayetteville
Gooch	Jan W.	Georgia Institute of Technology
Gray	Wayne L.	University of Arkansas/Medical Sciences
Green	Reid	U.S. Geological Survey
Griffin	Edmond E.	University of Central Arkansas
Griggs	Gaston	John Brown University

Secretary's Report

LAST NAME	FIRST MI	INSTITUTION
Hanebrink	Earl L.	Arkansas State University -- retired
Harris	John L.	Arkansas Highway & Transportation Dept.
Harvey	Michael J.	Tennessee Tech University
Hawk	Roger M.	University of Arkansas at Little Rock
Hemmati	Mustfa	Arkansas Tech University
Henson	Stanley	Arkansas Tech University
Hilburn	Larry R.	Black River Technical College
Hinck	Larry	Arkansas State University
Hirschi	Dean	University of Central Arkansas
Hite	Maxine R.	
Hodges	Howard	University of Arkansas at Little Rock
Holt	Anthony	Arkansas State University
Hood	William G.	University of Arkansas at Little Rock
Huang	Feng Hou	University of Arkansas at Fayetteville
Hudson	M. Keith	University of Arkansas at Little Rock
Huey	Jim	University of Arkansas at Monticello
Huffman	Jannie	Arkansas State University
Huggins	Julie A.	East Arkansas Community College
Hughes	Charles A.	Arkansas State University
Hurlburt	Barry K.	Univ. of Arkansas for Medical Sciences
Huss	Martin	Arkansas State University
Hyatt	Philip E.	Savannah River Forest Station
Igietseme	Joseph U.	University of Arkansas/Medical Sciences
Ison	Celia	
Jalaluddin	M. D.	University of Arkansas at Pine Bluff
Jamieson	David	Ark. St. Univ.-Beebe/Newport
Jansma	Harriet	University of Arkansas at Fayetteville
Jeffries	Douglas L.	University of the Ozarks
Jenness	Jeff	Arkansas State University
Jimerson	David	Arkansas State University
Johnson	Ronald	Arkansas State University
Johnson	Michael I.	Nettleton High School
Johnson	Hugh	Southern Arkansas University
Johnson	George P.	Arkansas Tech University
Jones	Suzanne M.	Arkansas State University
Justice	Jay	Ark. Dept. Pollution Control & Ecology
Kane	Cynthia J.M.	Univ. of Arkansas for Medical Sciences
Kaplan	Arnold	
Karlin	Alvan A.	University of Arkansas at Little Rock
Kehler	Philip L.	University of Arkansas at Little Rock
Kennedy	Bud	Arkansas State University
Khan	Shaheen	University of Arkansas at Pine Bluff
Kleve	Maurice G.	University of Arkansas at Little Rock
Kluender	Richard	University of Arkansas at Monticello
Knight	Frank M.	University of the Ozarks
Knighten	Pat	Arkansas Game & Fish Commission
Koeppe	Roger E., III	University of Arkansas at Fayetteville
Komoroski	Richard A.	University of Arkansas/Medical Sciences
Kopper	Randall A.	Hendrix College
Kral	Timothy	University of Arkansas at Fayetteville
Krause	Paul	University of Central Arkansas
Lane	Forrest E.	University of Arkansas at Fayetteville
Lanza	Janet	Univ. of Arkansas at Little Rock
Lavers	Norman	Arkansas State University
LeJeune	J. K.	Red River Technical College
Lee	Linda A.	Pocahontas Middle School
Lewis	Carolyn	Arkansas Tech University
Lindquist	David	University of Arkansas at Little Rock
Linnstaedter	Jerry L.	Arkansas State University
Lockhart	J. Mitchell	University of Arkansas at Fayetteville
Lockhart	Brian	University of Arkansas at Monticello
Lockley	Judy	Marked Tree Public Schools
Lortz	David	Univ. of Arkansas at Monticello
Lynch	Thomas J.	University of Arkansas at Little Rock
Mackey	James	Harding University
Malasri	Siripong	Christian Brothers University
Manion	Jerry	University of Central Arkansas
Matthews	H. Michael	Henderson State University
Mazumder	M. K.	University of Arkansas at Little Rock
McAllister	Chris T.	Veterans Affairs Medical Center
McAllister	Russell B.	Ark. Dept. Pollution Control & Ecology
McCarty	Clark W.	Ouachita Baptist University (retired)
McDaniel	V. Rick	Arkansas State University
McLemore	John A.	USDA, Forest Service
McMasters	Dennis W.	Henderson State University
Meeks	David	Westark Community College
Mehta	Rahul	University of Central Arkansas
Mink	Lawrence A.	Arkansas State University
Mitchell	Richard S.	Arkansas State University
Mittelstaedt	Roberta A.	National Center for Tox. Research
Mittelstaedt	James S.	
Montague	Warren	
Moody	Bonnie	Henderson State University
Moore	Phillip	Arkansas Highway & Transportation Dept.
Moore	Jewel	University of Central Arkansas
Morgans	Leland F.	University of Arkansas at Little Rock
Moss	Linda	
Murphy	Michael	Arkansas State University
Mwasi	Lawrence M.	Univ. of Arkansas at Pine Bluff
Nagappa	H. Y.	Univ. of Arkansas at Pine Bluff
Nave	Paul	Arkansas State University
Neal	Joseph C.	U. S. Forest Service
Nehus	Nathaniel	Ark. Dept. Pollution Control & Ecology
Nelson	Thomas	Arkansas Tech University
Nordeen	Russell	University of Arkansas at Monticello
O'Brien	Timothy J.	University of Arkansas/Medical Sciences
Oosterhuis	Derrick M.	University of Arkansas at Fayetteville
Orr	Clifton	University of Arkansas/Pine Bluff
Owen	Wilbur	University of Central Arkansas
Owens	Don R.	University of Arkansas/Little Rock
Palmer	Bryan D.	Henderson State University
Parsons	Barbara	Univ. of Arkansas at Little Rock
Paulissen	Leo J.	University of Arkansas at Fayetteville
Paulissen	Mark A.	McNeese State University
Peck	John D.	University of Central Arkansas
Pennington	Carlos H.	USAE Waterways Experiment Station
Peterson	Charlotte A.	Veterans Admin. Hospital
Piper	Ed	University of Arkansas
Plummer	Michael V.	Harding University
Pray	Harold	University of Central Arkansas
Price	Mazo	University of Arkansas at Pine Bluff
Prince	Denver L.	University of Central Arkansas
Quartucci	Gregory M.	Burns & McDonnell
Rasmussen	James A.	Southern Arkansas University
Reynolds	Ruby S.	University of the Ozarks, retired
Richards	Edward L.	Arkansas State University
Rodgers	Michael R.	Ark. Dept. Pollution Control & Ecology
Roe	Amy L.	Nat. Center for Toxicological Research
Roop	Marty	University of Arkansas/Medical Sciences
Rowe	Marsha	Stamps High School
Runge	Steven W.	University of Central Arkansas
Sanders	Terry A.	Taylor High School
Sealander	John A.	University of Arkansas at Fayetteville
Setliff	Frank L.	University of Arkansas at Little Rock
Shade	Elwood B.	University of Arkansas at Monticello
Shaikh	Ali U.	University of Arkansas at Little Rock
Sharp	J. Craig	Univ. of Central Arkansas
Shepherd	William H.	Arkansas Natural Heritage Comm.
Siegel	Samuel	University of Arkansas at Fayetteville
Sifford	Dewey H.	Arkansas State University
Simpson	Kim	Arkansas Children's Hospital
Skinner	Robert	
Smith	Edwin B.	University of Arkansas at Fayetteville
Smith	Kimberly G.	University of Arkansas at Fayetteville
Smith, Jr.	Roy J.	U. S. D. A./Univ. of Arkansas
Snow	L. Dale	Louisiana Tech University
Snyder	David G.	University of Arkansas at Monticello
Spiegel	Frederick W.	University of Arkansas at Fayetteville
Standage	Richard W.	U. S. Forest Service
Steward	T. W.	Union University
Stoeckel	Joseph N.	Arkansas Tech University
Sundell	Eric	University of Arkansas at Monticello
Sutherland	Mark	Hendrix College
Sutton	Keith	Hendrix College
Swindell	Robert T.	University of Arkansas at Little Rock
Tappe	Phil	University of Arkansas at Monticello
Taylor	William S.	University of Central Arkansas
TeBeest	David O.	University of Arkansas at Fayetteville
Thompson	Lyell	University of Arkansas at Fayetteville
Thurmond	John T.	University of Arkansas at Little Rock
Timmerman	Dan	Arkansas State University
Timmerman	Lorraine	Van-Cove High School
Timmerman	Rudy	Rich Mountain Community College
Trauth	Stanley E.	Arkansas State University
Trautwein	Norman	Arkansas State University
Tull	Dalena	University of Central Arkansas
Tumilson	Renn	Henderson State University
Vere	Victor K.	Arkansas Tech University
Walker	Richard B.	University of Arkansas at Pine Bluff
Walker	Stephen A.	Eastern Kentucky University
Weaver	K. Casey	University of Central Arkansas
Webb	Jerry	University of Arkansas at Monticello
Weidemann	G. J.	University of Arkansas at Fayetteville
Wennerstrom	David	University of Arkansas/Medical Sciences
Wennerstrom	Delores	Pulaski Academy
Wiebers	Todd	Henderson State University

LAST NAME	FIRST MI	INSTITUTION
Wilhide	J. D.	Arkansas State University
Williams	Richard A.	University of Arkansas/Monticello
Willis	Rebecca L.	Southern Arkansas University
Wilson, Jr.	Edmond W.	Harding University
Wold	Donald C.	University of Arkansas at Little Rock
Wolf	Duane C.	University of Arkansas at Fayetteville
Woolverton	Heather L.	University of Central Arkansas
Wright	Robert D.	University of Central Arkansas
Wyatt	Bill	Arkansas State University
Yang	Chia C.	Arkansas Tech University
Yang	Dominic T.	University of Arkansas at Little Rock
York	J. Lyndal	University of Arkansas/Medical Sciences
Young	David A.	Fayetteville Public Schools
Zachry	Doy L.	University of Arkansas/Fayetteville
Zimmer	Steven W.	Arkansas Tech University

SPONSORING MEMBERS

Bean	Judith A.	Harmony Grove High School
Bradley	Richard	Univ. of Arkansas at Little Rock
Braithwaite	Wilfred J.	University of Arkansas at Little Rock
Davies	David L.	University of Arkansas/Medical Sciences
England-Whaley	Lawana	Arkansas State University
Hardin	Joyce M.	Hendrix College
Howick	Lester C.	University of Arkansas at Fayetteville
Sharrah	Paul C.	University of Arkansas at Fayetteville

SUSTAINING MEMBERS

Barton	Harvey E.	Arkansas State University
Board	Veryl	Arkansas College
Bollinger	Julia Reed	Arkansas State University
Cleaveland	Malcolm K.	University of Arkansas at Fayetteville
Dale, Jr.	Edward E.	University of Arkansas at Fayetteville
Darsey	Jerry A.	University of Arkansas at Little Rock
Farris	Jerry L.	Arkansas State University
Gandy	Lisa C.	FTN Associates
Glover	Mattie	University of Arkansas at Pine Bluff
Johnston	Perry Max	University of Arkansas at Fayetteville
Karnes	Mark	The Ross Foundation
Marsh	Daniel L.	Henderson State University
McConnell	Rose	University of Arkansas at Monticello
Meyer	Richard	University of Arkansas at Fayetteville
Nisbet	Alex R.	Ouachita Baptist University
Peacock	Lance	The Arkansas Nature Conservancy
Price	Alan D.	Ark. Dept. Pollution Control & Ecology
Rothrock, III	Perry C.	University of Arkansas/Medical Sciences
Sustich	Andrew T.	Arkansas State University
Tendeku	Felix K.	University of Arkansas at Pine Bluff
Watson	Robert L.	University of Arkansas at Little Rock
Wear	James O.	Veterans Admin., No. Little Rock Div.
Willingham	William M.	University of Arkansas at Pine Bluff

LIFE MEMBERS

Anderson	Robbin C.	University of Arkansas at Fayetteville
Bacon	Edmond J.	University of Arkansas at Monticello
Chittenden	David	Arkansas State University
Cotton	Calvin	Geographics Silk Screening Co.
Davis	Leo Carson	Southern Arkansas University
Dilday	Robert H.	University of Arkansas at Fayetteville
Draganjac	Mark	Arkansas State University
Edson	Jim	University of Arkansas at Monticello
England	Daniel R.	Southern Arkansas University
Evans	William L.	University of Arkansas at Fayetteville
Fribourgh	James H.	University of Arkansas at Little Rock
Fry	Arthur	University of Arkansas at Fayetteville
Geren	Collis R.	University of Arkansas at Fayetteville
Giese	John	Ark. Dept. of Pollution Control & Ecol.
Godwin	Walter E.	University of Arkansas at Monticello
Guenter	Joe M.	University of Arkansas at Monticello
Harp	George L.	Arkansas State University
Harp	Phoebe A.	Arkansas State University
Heidt	Gary A.	University of Arkansas at Little Rock
Helms	Ronnie	University of Arkansas at Fayetteville
Jacobs	Carol A.	
James	Douglas	University of Arkansas at Fayetteville
Johnson	Arthur A.	Hendrix College
Mattison	Donald R.	University of Pittsburgh
McDaniel	Roland E.	FTN Associates, Ltd.
Moore	Clementine	
Northrop	Gaylord M.	University of Arkansas at Little Rock
Palko	Tom	Arkansas Tech University
Peck	James H.	University of Arkansas at Little Rock
Rapp	Michael W.	University of Central Arkansas
Rickett	John D.	University of Arkansas at Little Rock
Robison	Henry W.	Southern Arkansas University
Saugey	David A.	U. S. Forest Service
Sewell	Stephen A.	University of Mississippi
Spears	Betty M.	Ouachita Mtns. Biological Station
Spears	Richard K.	Ouachita Mtns. Biological Station
Templeton	George E.	University of Arkansas at Fayetteville
Tucker	Gary	FTN Associates
Wickliff	James L.	University of Arkansas at Fayetteville
Wiley	Robert W.	University of Arkansas at Monticello

STUDENT MEMBERS

Adair	Robert E.	University of Arkansas/Fayetteville
Allen	Michelle	University of Arkansas at Little Rock
Ashburn	Charles	University of Arkansas at Little Rock
Baber	Connie	Henderson State University
Bean	Ashley	Hendrix College
Bearden	Stacy Lee	Arkansas State University
Bray, Jr.	James R.	Henderson State University
Caster	Paul	Univ. of Arkansas at Little Rock
Clark	Mark	Henderson State University
Clark	Murray R.	University of Arkansas at Little Rock
Davis	Angela Wynette	University of Arkansas at Pine Bluff
Dukes	Rebecca	
Ekworomadu	Charles	University of Arkansas for Medical Sciences
Elder	Ginger	Arkansas State University
Eller	David	Henderson State University
Everett	William R.	University of Arkansas at Fayetteville
Fletcher, III	Thomas M.	University of Arkansas/Medical Sciences
Freeman	Leah	Arkansas State University
Garner	Heath	Arkansas State University
George	Steven G.	Northeast Louisiana University
Gillum	Russell	University of Arkansas at Little Rock
Haider	Neena	Arkansas State University
Hansen	Debra	
Harris	Kristi	Arkansas State University
Heckathorn, Jr.	Walter	University of Arkansas
House	Kelly L.	Garland Co. Comm. Coll./H.S.U.
Huskins	Mark W.	Arkansas Tech University
Isenberg	Seth B.	University of Arkansas at Fayetteville
Jiles	Denise	Arkansas State University
Jones	Kimberly Rhae	University of Arkansas at Fayetteville
Khan	Imran	Arkansas State University
King	Chris	University of Arkansas
Martin	Randy	University of Arkansas at Little Rock
Mayes	Eric	Arkansas State University
Metcalf	Chris	Northeast Louisiana University
Mooney	Donna	University of Arkansas/Little Rock
Murray	Susan	Arkansas Natural Heritage Comm.
Persons	Cecil C.	University of Arkansas at Little Rock
Posey	William R., II	Arkansas State University
Pringle	John	University of the Ozarks
Russell	William A., Jr.	University of Arkansas at Little Rock
Ryan	John M.	University of Arkansas/Fayetteville
Sims	Jay	University of Arkansas/Little Rock
Smith	Jerome V.	University of Arkansas at Little Rock
Smith	Anna	Henderson State University
Snider	D. H.	University of Arkansas at Little Rock
Stickel	Sara	Arkansas State University
Townsend	Teddy L.	University of Central Arkansas
Whitehead	Greg A.	Henderson State University
Wilkins	Phillip K.	Arkansas State University
Williams	Michelle	University of Arkansas/Little Rock
Williams	Gregg R.	Arkansas State University
Withgott	James H.	University of Arkansas at Fayetteville
Yang	Zibin	University of Arkansas at Little Rock

PROGRAM
Arkansas Academy of Science

Seventy-Eighth Annual Meeting
April 8-9, 1994
Arkansas State University

SCHEDULE OF EVENTS

Friday, 8 April 1994

10:00 - 14:00	Registration	LS Lobby
09:00 - 11:00	Executive Committee	LS 441
11:00 - 17:00	Exhibits	LS 433
11:30 - 12:30	First Business Meeting	LS 219
15:00 - 15:30	Refreshments	LS 441
11:30 - 17:00	Slide Preview	LS 442
	PAPER SESSIONS	
13:30 - 17:15	Chemistry	LS 203
13:30 - 17:00	Botany	LS 204
13:30 - 16:45	Biomedical	LS 205
13:30 - 15:00	Herpetology	LS 206
15:45 - 17:00	Invertebrate Zoology	LS 206
13:30 - 17:15	Physics/Computers/ Energy/Geology	LS 207
13:30 - 17:15	Aquatic Biology	LS 444
17:30 - 18:15	Tours**	See page 2
17:30 - 18:30	Mixer	Alumni Lounge
18:30	Banquet	Ball Room Reng Center
19:45	Speaker:	

Dr. Ken N. Paige - University of Illinois
"Plant - Animal Interactions and the Dynamic Nature of Plants"

Saturday, 9 April 1994

07:45 - 11:00	Slide Preview	LS 442
08:00 - 10:00	Registration	LS Lobby
08:00 - 13:00	Exhibits	LS 433
07:45 - 08:15; 09:45 - 10:00	Refreshments	LS 441
12:00 - 13:00	Second Business Meeting/ Awards	LS 219
14:00	Biology Department Chairs Meeting	TBA
	PAPER SESSIONS	
08:15 - 10:30	Chemistry	LS 203
08:15 - 11:15	Geology/Astronomy/Physics	LS 204
08:15 - 10:30	Microbiology/Cell Biology	LS 205
08:15 - 11:45	Ecology/Conservation	LS 344
08:30 - 09:30	Science Education Toxicology/Water Quality	LS 207
08:15 - 11:45	Birds/Mammals	LS 444

****FRIDAY TOURS**

Aquatic Ecotoxicology Research Facility	Meet in LS Lobby
Aquatic Macro-Invertebrate Laboratory & Museum	LSE 304
Cell Biology Laboratory	LSW 545
Electron Microscopy Laboratory	LSW 109
GIS Laboratory	LSW 443
Herbarium	LSE 406
Herpetology Museum	LSW 440
Mammal Range	LSW 439
Physiology Research Laboratory	LSE 302
Toxicology Research Laboratory	LSW 544

For tours at different times than scheduled, contact Phoebe A. Harp.

SECTION PROGRAMS

***Undergrad **Grad Students**

Friday, April 8, 1994 LS 203

CHEMISTRY

Chair: Dr. Jerry A. Darsey, University of Arkansas at Little Rock.

*Substituted Nitrophenylfurans: Chemistry and Mutagenicities. E. Kim Fifer, Kevin S. Robertson, Robert M. Freeze, University of Arkansas for Medical Sciences at Little Rock, AR, Ali U. Shaikh, University of Arkansas at Little Rock, AR, and J.P. Freeman, National Center for Toxicological Research, Jefferson, AR.

*Conformational Studies of Mehyl, Dimethyl and Chloro Derivatives of Dantrolene Using *AB Initio* SCF-MO Procedures. Amber D. Climer, Lori L. Rayburn and Jerry A. Darsey, University of Arkansas at Little Rock, AR.

*Conformational studies of *Ortho* and *Meta*-Nitro Isomers of Dantrolene Using *AB Initio* SCF-MO Procedures. Lori L. Rayburn, Amber D. Climer and Jerry A. Darsey. University of Arkansas at Little Rock, AR.

*Studies of Copper (II) 2-Hydroxy-5N, N-Diethylsufonamide Benzoate. Elsie Williams, Shaheen Khan, Israt J. Chowdhury and William M. Willingham, University of Arkansas at Pine Bluff, AR.

*Evidence for Copper Complexation of an Oxazolidine Formed From (-) Ephedrine and Salicylaldehyde. Antonie Rice, Lawrence D. Fitz, Gordon L. Eggleton and Richard B. Walker, University of Arkansas at Pine Bluff, AR.

*The Reaction of $CpRu(PPh_3)2^+$ with Cyclothioethers. M. Draganjac, Mark Green, Yanjing Jiang, Arkansas State University, State University, AR, and A. W. Cordes, University of Arkansas at Fayetteville, AR.

*Proton-Coupled Electron Transfer Reactions of Ruthenium Pyrazole Complexes. Kevin Stanfield, Sharon Ezell, Spencer Slattery and Kenneth Gloldsby. University of Arkansas at Pine Bluff, AR, and Florida State University, Tallahassee, FL.

Break

Chair: Dr. Susan G. Cady, Arkansas State University

*Hammett Correlations of Half-Wave Reduction Potentials in a Series of N-(ARYL Substituted)-Dichloro Nicotinamides. Cecil C. Persons, Ali U. Shaikh, Julie Shiflett and Frank L. Setiff, University of Arkansas at Little Rock, AR.

*Analysis of Ammunition by X-Ray Fluorescence. Michael W. Rapp and Teddy Townsend. University of Central Arkansas, Conway, AR.

Use of a Cyclodextrin Chromatography Column to Confirm the Resolution of Several D, L. Tryptophan Analogs. Susan Cady, Arkansas State University, State University, AR.

Determination of The Pesticide, 2,4-DP by Room Temperature Phosphorimetry. Lorrie Jenkins and Norman Trautwein, Arkansas State University, State University, AR.

High Surface Area Covalent Metallophosphate Gels. D. A. Linquist, S. M. Poindexter, S. S. Rooke, D. R. Stockdale, A. L. Smoot, W. E. Young and K. B. Babb, University of Arkansas at Little Rock, AR.

**Ultrasound Assisted Reactions with Sodium Percarbonate. Y. Cao, A. Toland and D. T. C. Yang, University of Arkansas at Little Rock, AR.

Synthesis and Characterization of Trispyrazolylborate Complexes of Nickel (III). P. J. Desrochers, J. C. Sharp, University of Central Arkansas, Conway, AR.

Friday, April 8, 1994 LS 204

BOTANY

Chair: Dr. E. Leon Richards, Arkansas State University.

Noteworthy Collections: Arkansas. Phillip E. Hyatt, Savannah River Forest Station, New Ellenton, SC.

Notes on Bryophytes and Pteridophytes of Southern Arkansas. James R. Bray, Greg A. Whitehead, Daniel L. Marsh, Dennis W. McMasters and Winfred D. Crank, Henderson State University, Arkadelphia, AR.

The Shumard Oak Complex in Arkansas. George P. Johnson, Arkansas Tech University, Russellville, AR.

A Comparison of Soil pH and Vegetation for Maple-Leaved Oak Habitat. David W. Rouw and George P. Johnson, Arkansas Tech University, Russellville, AR.

Comparative Gas-Exchange in Leaves of Intact and Clipped, Natural and Planted Cherrybark Oak (*Quercus Pagoda* Raf.) Seedlings. Brian R. Lockhart, University of Arkansas at Monticello, AR, and John D. Hodges, Mississippi State University, Mississippi State, MS.

Detection of *Septoria nodorum* on Wheat Leaves with an Antibody-based Serological Kit. Rebecca Dukes. University of Arkansas at Little Rock, AR, and Gary L. Cloud, University of Arkansas, Cooperative Extension Service, Little Rock, AR.

Distance of interference of Red Rice (*Oryza sativa*) in Rice (*O. sativa*). Roy J. Smith Jr., Sam L. Kwon, Agricultural Research Service, U.S.D.A., Stuttgart, AR, and Ronald E. Talbert, University of Arkansas at Fayetteville, AR.

Break

Chair: Dr. Dennis W. McMasters, Henderson State University.

*Variability in Nectar Characteristics of *Impatiens capensis*. Marti Terrell and Janet Lanza, University of Arkansas at Little Rock, AR.

*Nectar Production in *Lobelia puberula*: Undergraduate Research on Native Plants and their Pollinators. Michael J. Boyd. Lachi R. Kishen and William H. Baltosser, University of Arkansas at Little Rock, AR.

A New Candidate Species, *Chaetomium elatum*, for Wood Rot Via Lignin Biodegradation. Wilson H. Howe, University of Arkansas at Little Rock, AR, and Joyce M. Hardin, Hendrix College, Conway, AR.

Biosystematic Studies of Arkansas Lycopsids. James R. Bray, Greg A. Whitehead, Dennis W. McMaters and Daniel L. Marsh, Henderson State University, Arkadelphia, AR.

Evidence for Genetic Homogeneity among Populations of *Lycoperdon pyriforme* Based on Paterns of Isozymic Variation. Martin J. Huss, Arkansas State University, State University, AR.

An investigation of the Failure of Traditional Economic Incentives in Regenerating Arkansas' Non-Industrial Private Forest: A Historical Perspective. James R. Jolley, University of Arkansas at Monticello, AR.

Friday, April 8, 1994 LS 205

BIOMEDICAL

Chair: Dr. Lawrence W. Hinck, Arkansas State University.

*The Distribution and Morphology of Nitric Oxide Producing Neurons in the Rate Brain Septum. Jeff Marotte, Hendrix College, Conway, AR, and Kevin Phelan, University of Arkansas for Medical Sciences, Little Rock, AR.

*Development of Anti-Peptide Antibodies Targeted Against Specific Regions of the Rat Cannabinoid Receptor. Christopher E. Collins, Hendrix College, Conway, AR, Elizabeth M. Laurenzana, University of Arkansas for Medical Sciences, Little Rock, AR Billy R. Martin, Medical College of Virginia, Richmond, VA, and S. Michael Owens, University of Arkansas for Medical Sciences, Little Rock, AR.

*Decreased Sensitivity of Human Multiple Transitional Cell Carcinoma Cells (252J) to 5-Fluorouracil by Anguidine. Jacqueline A. Potter, Sederick C. Rice, Chandreas S. Mosley, Mattie M. Glover, and Clifton Orr, University of Arkansas at Pine Bluff, AR.

*Effects of Ethanol on Cultured Microglial Cells. Annisha C. Hickman, University of Arkansas at Pine Bluff, AR, G. C. Mays and D. L. Davies, University of Arkansas for Medical Sciences, Little Rock, AR.

*Regulation of the Extracellular Signal Regulated Kinase 2 (ERK2) by Phorbol Esters and Fetal Calf Serum in Human Melanoma Cells. Miram Glass, University of Arkansas at Pine Bluff, AR, Fan Yang and Estela E. Medrano, University of Cincinnati, Cincinnati, OH.

*Transforming Growth Factor-Beta (TGFß) Controls Astrocyte Expression of Growth Factors and Extracellular Matrix. Laura Bogan. Hendrix College, Conway, AR, and Cynthia Kane, University of Arkansas for Medical Sciences. Little Rock, AR.

**The Complexity of Fetal Movement Detection Using a Single Doppler Ultrasound Transducer. William A. Russell, Jr., University of Arkansas at Little Rock, AR, Curtis L. Lowery, MD, Patrick J. Baggot, MD, University of Arkansas for Medical Sciences, Little Rock, AR, James D. Wilson, University of Arkansas at Little Rock, AR, Robert Walls, Ph.D., University of Arkansas for Medical Sciences, Little Rock, AR, Roger M. Hawk, Ph.D., University of Arkansas at Little Rock, AR, and Lynn Bentz, RN, University of Arkansas for Medical Sciences, Little Rock, AR.

Break

Chair: Dr. William M. Willingham, University of Arkansas at Pine Bluff.

Lipids Changes in Nude Mice Implanted Subcutaneously with Cells of Human Prostate Adenocarcinoma Grade IV. Lawrence M. Mwasi, University of Arkansas at Pine Bluff, AR.

UV-Induced Chromosomal Breaks and the DNA Replication Fork. Daniel M. Yoder, Jason M. Hiles and Gaston Griggs, John Brown University, Siloam Springs, AR.

Computational Fluid Dynamics in Small Airway Models of the Human Lung. Galen Burnside, University of Arkansas at Little Rock, AR, Dr. Jeff Hammersley, University of Arkansas for Medical Sciences at Little Rock, AR, Dr. Rama Reddy, University of Arkansas at Little Rock, AR, and Dr. Boyd Gatlin, Mississippi State University, Mississippi State, MS.

*Physicochemical and Biological Parameters of Ephedrine Prodrugs. Lance M. Williams, Lawrence D. Fitz and Richard B. Walder, University of Arkansas at Pine Bluff, AR.

*Partition Coefficients of Essential Metalloelement Complexes. Israt J. Chowdhury, Tim Henderson, Lawanda Jones, Shawndra Thompson, Richard B. Walker and William M. Willingham, University of Arkansas at Pine Bluff, AR.

Friday, April 8, 1994 LS 206

HERPETOLOGY

Chair: Betty G. Cochran, USDA Forest Service, Ouachita National Forest.

Pleistocene Amphibians of the Jones Local Fauna, Meade County, Kansas. Leo Carson Davis, Southern Arkansas University, Magnolia, AR.

Riparian Association of Montane Cottonmouths in SW Arkansas. Seth White, C. Metcalf, K. Casico, Northeast Louisiana University, Monroe, LA, B. Cochran, USDA Forest Service, Ouachita National Forest, Glenwood, AR, and F. Pezold, Northeast Louisiana University, Monroe, LA.

Female Reproductive Traits in Selected Arkansas Snakes. Stanley E. Trauth, Arkansas State University, State University, AR, Robert L. Cox, (deceased), Walter E. Meshaka, Archbold Biological Station, Lake Placid, FL, Brian P. Butterfield, Auburn University, Auburn AL, and Anthony Holt, Arkansas State University, State University, AR.

Reproductive Cycles in Two Arkansas Skinks in the Genus *Eumeces* (Sauria: Scincidae). Stanley E. Trauth, Arkansas State University, State University, AR.

Ultrastructure of *Myxidium serotinum* (Protozoa: Myxozoa) from the Gallbladder of *Bufo speciosus* (Amphibia: Anura). Chris T. McAllister, Dept. Veterans Affairs Medical Center, Dallas, TX, B. L. J. Delvinquier, University of the Witwatersrand, Johannesburg, South Africa, and Stanley E. Trauth, Arkansas State University, State University, AR.

Parasites of the Graybelly Salamander, *Eurycea multiplicata griseogaster* (Caudata: Plethodontidae), from Arkansas. Chris T. McAllister, Dept. Veterans Affairs Medical Center, Dallas, TX, Stanley E. Trauth, Arkansas State University, State University, AR, Charles R. Bursey, Pennsylvania State University-Shenango Campus, Sharon, PA, Steve J. Upton, Kansas State University, Manhattan, KS.

Friday, April 8, 1994 LS 206

INVERTEBRATE ZOOLOGY

Chair: Dr. Robert L. Watson, University of Arkansas at Little Rock.

Burying Bettle (Coleoptera: Silphidae, *Nicrophorus*) Surveys on Poteau Ranger District, Ouachita NF. Joseph C. Neal and M. Earl Stewart, Poteau Ranger District, USDA Forest Service, Waldron, AR.

A Larval Mosquito Survey in Northeastern Arkansas including a New Record for *Aedes albopictus*. David H. Jamieson, Arkansas State University-Beebe, Beebe, AR, Larry A. Olson and J. D. Wilhide, Arkansas State University, State University, AR.

*Reproductive Structures of Adult Cottonwood Borer Beetles (*Plectrodera scalator*). Jason A. Kilgore, Hendrix College, Conway, AR, and Steven K. Goldsmith, Tulsa University, Tulsa, OK.

Genetic Variability in Developing Periodical Cicadas. Eric Stout, Lance T. Adams, Lisa R. Duke, James J. English, and Alvan A. Karlin, University of Arkansas at Little Rock, AR.

Occurrence of Massospora from Non-Emergent Periodical Cicada. Lisa R. Duke, Daniel White, James J. English, Lance T. Adams, Eric Stout, Alvan A. Karlin and Maurice G. Kleve, University of Arkansas at Little Rock, AR.

Friday, April 8, 1994 LS 207

PHYSICS/COMPUTERS/ENERGY/GEOLOGY
Chair: Dr. William J. Braithwaite, University of Arkansas at Little Rock.

Calculation of Energy Levels in a Linear Potential Well. H. E. McCloud, Arkansas State University, State University, AR.

**Using the Cern Program-Library Graphics and Interactive Data Display. Morgan T. Burks, Christine A. Byrd and W. J. Braithwaite, University of Arkansas at Little Rock, AR.

**An Integrated Data Acquisition and Data Analysis System for High Energy Physics. Charles A. Byrd, Christine A. Byrd and W. J. Braithwaite, University of Arkansas at Little Rock, AR.

**Application of Machine Learning Principles to Modeling of Nonlinear Dynamic Systems. Murry R. Clark, University of Arkansas at Little Rock, AR.

Structural Design by Evolution. S. Malasri, D. A. Halijan and M. L. Keough, Christian Brothers University, Memphis, TN.

Construction of a Reliable, Inexpensive Cryofixation Device. L. A. Mink and R. A. Buchanan, Arkansas State University, State University, AR.

**Solid State NMR of Hydrogen in Thin Film Synthetic Diamond. Galen Burnside and Roger M. Hawk, University of Arkansas at Little Rock, AR.

Break

Chair: Dr. Robert D. Engelken, Arkansas State University.

**Polishing and Planarizing of CVD-Diamond for MCM Application. S. Raju, A. P. Malshe, W. D. Brown and H. A. Naseem, University of Arkansas at Fayetteville, AR.

A Trace Element Soil Analysis of the Sloan Site: A 10,500 Year Old Cemetery in Northeast Arkansas. D. Glen Akridge and David Chittenden III, Arkansas State University, State University, AR.

Pleistocene and Holocene Remains from the Red River, Southwest Arkansas. Terry A. Sanders, Taylor High School, Taylor, AR.

Development of a Model Undergraduate Laboratory Course Sequence in Semiconductor Materials through the NSF ILI and NASA JOVE Programs. Dr. Robert K. Engelken, Arkansas State University, State University, AR.

Analogy of Stability in the Lasers with Saturable Absorbers and Human Mind. Mansour Mortazavi and S. P. Singh, University of Arkansas at Pine Bluff, AR.

*Tetraethylene Glycol-Based Electrolytes for High Temperature Electrochemical Deposition of Compound Semiconductors. Chris Poole, Dr. Robert D. Engelken, Brandon Kemp and Jason Brannen, Arkansas State University, State University, AR.

*Storm Dominated Channel Sequences on a Shallow Marine Shelf: Middle Morrowan of Northwestern Arkansas. Kimberly R. Jones, University of Arkansas at Fayetteville, AR.

Friday, April 8, 1994 LS 444

AQUATIC BIOLOGY
Chair: Roland McDaniel, FTN & Associates
Water Resource Consultants.

Peltodytes (Halipidae: Coleoptera) in Arkansas. George L. Harp, Arkansas State University, State University, AR.

First Record of *Leptodora kindti* (Crustacea: Cladocera) in Dardanelle Reservoir and Review of Other Recent Additions to the Faunal Community. John D. Rickett and Robert L. Watson, University of Arkansas at Little Rock, AR.

A 24-Year Study of the Benthic Community in Dardanelle Reservoir. John D. Rickett and Robert L. Watson, University of Arkansas at Little Rock, AR.

Benthic Macroninvertebrate Densities in an Oligotrphic Headwater Creek. Flaherty R. Wheeler, Northeast Louisiana University, Monroe, LA, B. Cochran, USDA Forest Service, Ouachita National Forest, Glenwood, AR, F. Pezold, Northeast Louisiana University, Monroe, LA.

A Recent Record of the Plains Minnow, *Hybognathus placitus* Girard, from Arkansas. Thomas M. Buchanan, Westark Community College, Fort Smith, AR, and Henry W. Robison, Southern Arkansas University, Magnolia, AR.

First Record of the Channel Shiner, *Notropis wickliffi* Trautman, in Arkansas and comments on the Current River Population of *Nortropis volucellus* (Cope). Henry W. Robison, Southern Arkansas University, Magnolia, AR.

Break

Chair: Alan Price, Arkansas Dept. of Pollution Control & Ecology.

**Age and Growth of the Largemouth Bass, *Microptenus salmoides*, of Lake Ashbaugh. Rosalyne M. Davis and Ronald L. Johnson, Arkansas State University, State University, AR.

A Noninvasive Method of Estimating Populations of Yellow Grub (*Clinostomum marginatum*) in Stream Black Bass and Farm-Raised Channel Catfish. James J. Daly, University of Arkansas for Medical Sciences, Little Rock, AR, and Jeurel Singleton, University of Arkansas at Fayetteville, AR.

Food Habits of Introduced Rainbow Trout (*Oncorhynchus mykiss*) in the Upper Little Missouri River Drainage of Arkansas. Chris Metcalf, Northeast Louisiana University, Monroe, LA. b. Cochran, USDA Forest Service, Ouachita National Forest, Glenwood, AR, and F. Pezold, Northeast Louisiana University, Monroe, LA.

Spawning Habitat of the Paleback Darter in the Ouachita Mountains, AR. Mitzi G. Pardew, USDA Forest Service, Womble Ranger District, Mt. Ida, AR, and Dean Heckathorn, U.S. Fish and Wildlife Service, Portland, OR.

Pre-spawning Migration of Channel Catfish into Three Warmwater Tributaries--effects of a Cold Tailwater. Gary L. Siegwarth, Iowa Dept. Natural Resources, Manchester, IA, and James E. Johnson, Arkansas Cooperative Fish and Wildlife Research Unit, University of Arkansas at Fayetteville, AR.

**Selected Community Characteristics of Freshwater Mussels (Unionacea) in the Cache River, Arkansas. Alan D. Christian, John L. Harris, William R. Posey and George L. Harp, Arkansas State University, State University, AR.

*Status of The Zebra Mussell (*Dreissena polymorpha*) in the Arkansas River System. Jeffrey L. Herod and Joseph N. Stoeckel, Arkansas Tech University, Russellville, AR.

Saturday, April 9, 1994 LS 203

CHEMISTRY
Chair: Dr. J. Edward Bennett, Arkansas State University.

Preparation and Assay of New Pepstatin Analogs. Rose McConnell. University of Arkansas at Monticello, AR.

Thermal Decomposition Studies of Selected Transition Metal Polysulfide Complexes. II. Effect of Atmosphere on Decomposition. Benjamin Rougeau and M. Draganjac, Arkansas State University, State University, AR.

Differential Thermal and Gravimetric Analysis of the Cr-O-H_2O System. J. Edwatd Bennett, M. Draganjac and Eric Barnett, Arkansas State University, State University, AR.

New Organometallic Oligomer. Reaction of Titanocene Dichloride with Acetylenedicarboxylate. Tanya L. Hagler, M. Draganjac, Paul Nave, J. Edward Bennett, Farooq Khan, Robert Engelken, Gerard Williams, Chris Poole, Kwok Fai Yu, Arkansas State University, State University, AR.

Chemical Kinetics of Phospholipid Hydrolysis Catalyzed by the Venom of the Brown Recluse Spider (*Loxosceles reclusa*) as Followed by P-31 NMR. Michael Merchant. James Hinton and Collis Geren, University of Arkansas at Fayetteville, AR.

*Cross-Linkable Conduction Polymers. Tito Viswanathan and Sterling Rook, University of Arkansas at Little Rock, AR.

Break

Chair: Dr. J. Edward Bennett, Arkansas State University.

Coherent Mixing of Scattered Laser Light, Aslam H. Chowdhury, University of Arkansas at Pine Bluff, AR.

*Determining the Growth Rate of Bacteria in Antibiotic Using Laser. Stephanie Johnson, William Willingham, Shelton Fitzpatrick and Aslam H. Chowdhury, University of Arkansas at Pine Bluff, AR.

Saturday, April 9, 1994 LS 204

GEOLOGY/ASTRONOMY/PHYSICS
Chair: Dr. Andrew T. Sustich, Arkansas State University

Tree-Ring Evidence of New madrid Seismic Activity 1321-1991. M. K. Cleaveland, D. W. Stahle, University of Arkansas at Fayetteville, AR, and R. B. VanArsdale, Memphis State University, Memphis, TN.

**Monte Carlo Simulations of a NASA Scintillating Optical Fiber Calorimeter for 10- to 1,000-MEV Gamma Rays. R. Gillum, A. Yang and D. Wold, University of Arkansas at Little Rock, AR.

**Monte Carlo Simulations of a NASA Scintillating Optical Fiber Calorimeter-for 0.5- to 1.5-TEV Gamma Rays. Z. Yang, R. Gillum and d. Wold, University of Arkansas at Little Rock, AR.

*Gamma Ray Emissions From Binary Pulsar Systems. Tony A. Hall and Andrew T. Sustich, Arkansas State University, State University, AR.

A Method for Determining Atmospheric Aerosol Optical Depth Using Solar Transmission Measurements. Felix Tendeku, University of Arkansas at Pine Bluff, AR.

**Evaluation of Photodiode Arrays in Rocket Plume Monitoring and Diagnostics. D. H. Snider, M. K. Hudson, R. B. Shanks and R. Cole, University of Arkansas at Little Rock, AR.

Break

Chair: Dr. William J. Braithwaite, University of Arkansas at Little Rock.

*Energetic Photon Scattering From Electrons: In Advanced Laboratory. Christine A. Byrd, Morgan T. Burks, and W. J. Braithwaite, University of Arkansas at Little Rock, AR.

Summary of M-Shell Ionization by Light Incident Ions. Rahul Mehta, University of Central Arkansas, Conway, AR.

**Multisite Microprobes for Electrochemical Recordings in Biological Dynamics. G. Screenivas, S. S. Ang, R. M. Ranade, A. S. Salian and W. D. Brown, University of Arkansas in Fayetteville, AR.

**A comparison of High-Temperature Superconductors in Multi-Chip Module Applications. D. E. Ford, S. S. Scott, S. S. Ang, and W. D. Brown, University of Arkansas at Fayetteville, AR.

**Geologic Site Evaluation for Assessing Non-Point Source Pollution in the St. Francis Sunken Lands, Northeast Arkansas. Jonathan Q. Miller and M. J. Guiccione, University of Arkansas at Fayetteville, AR.

Saturday, April 9, 1994 LS 205

MICROBIOLOGY/CELLULAR BIOLOGY
Chair: Dr. Ronald L. Johnson, Arkansas State University.

Dietary Levels of Starch Affects Intestinal Flow of Total and Bacterial Calcium, Copper, and Manganese in Ruminants. D. W. Kennedy, Arkansas State University, State University, AR, and L. D. Bunting, Louisiana State University, Baton Rouge, LA.

The isolation of *Borrelia burgdorferi* from infected Laboratory Mice. Lawrence W. Hinck, Arkansas State University, State University, AR.

*Determination of Tumor Necrosis Factor Levels in Genital Tracts of Guinea Pigs Infected with Chlamydia. L. R. Kishen, University of Arkansas at Little Rock, AR, T. Darville, K. Simpson, Children's Hospital, Little Rock, AR, and R. G. Rank, University of Arkansas for Medical Sciences, Little Rock, AR.

*Utilization of Object-Oriented Database Design for the Complete Analysis of Data from the Human Genome Project. Chris Bennett and Alvan A. Karlin, University of Arkansas at Little Rock, AR.

DNA Sequence and Genetic Organization of the Inverted Repeat Region of the Simian Varicella Virus Genome. Nanette J. Gusick and Wayne L. Gray, University of Arkansas for Medical Sciences, Little Rock, AR.

Chain Termination Sequencing of DNA Using Silver Staining Technique. Ronald L. Johnson, Arkansas State University, State University, AR.

Break

Chair: Dr. David F. Gilmore, Arkansas State University.

Analysis of Anti-Chlamydial Mechanism of T Cells in the Polarized Epithelial-Lymphocyte Culture System. J. U. Igietseme, University of Arkansas for Medical Sciences, Little Rock, AR, P. B. Wyrick, D. Goyeau, University of North Carolina School of Medicine, Chapel Hill, NC, and R. G. Rank, University of Arkansas for Medical Sciences, Little Rock, AR.

Enzymatic Degradation of Biodegradable Plastic by Myxobacteria. David F. Gilmore, Arkansas State University, State University, State University, AR, and R. Clinton Guller, University of Massachusetts, Amherst, MA.

Saturday, April 9, 1994 LS 207

SCIENCE EDUCATION/TOXICOLOGY/WATER QUALITY

Chair: Dr. James J. Daly, University of Arkansas for Medical Sciences.

*Survey of Southwest Arkansas Students' Attitudes Toward Science. Anna Smith, Connie Baber and Renn Tumlison, Henderson State University, Arkadelphia, AR.

**Water Quality of an Ozark Stream Receiving Urban Point and Non-Point Pollution: Total Coliform and Total Bacterial Counts. Claude Rector, W. David Holcomb and James J. Daly, University of Arkansas for Medical Sciences, Little Rock, AR.

**Water Quality of an Ozark Stream Receiving Urban Point and Non-Point Pollution: Physics-Chemical Parameters. Phillip B. Drope and James J. Daly, University of Arkansas for Medical Sciences, Little Rock, AR.

**Effect of Pesticides for Mosquito Control on Target and Non-Target Organisms. Cristin D. Milam, Jerry L. Farris, J. D. Wilhide and Larry A. Olson, Arkansas State University, State University, AR.

Saturday, April 9, 1994 LS 344

ECOLOGY/CONSERVATION

Chair: Dr. Michael J. Harvey, Tennessee Technological University.

**A Comparison of Macrophytes of Two Small Northwest Arkansas Reservoir. John J. Sullivan and A. V. Brown, University of Arkansas at Fayetteville, AR.

Status of Endangered Gray Bat (*Myotis grisescens*) Hibernating Populations in Arkansas. Michael J. Harvey, Tennessee Technological University, Cookeville, TN.

Herpetofaunal Responses to Even-Aged and Selective Timber Harvesting in the Ouachita Mountains, Arkansas. Doyle L. Crosswhite, Stanley Fox and Ronald E. Thill. Oklahoma State University, Stillwater, OK.

Renewal and Recovery: The Red-Cockaded Woodpecker and Shortleaf Pine/Bluesterm Grass Ecosystem on the Ouachita National Forest. George A. Bukenhofer, Joseph C. Neal and Warren G. Montague, Poteau Ranger District, USDA Forest Service, Waldron, AR.

*Does Simulated Herbivory of *Passiflora incaarnata* Cause an Increase in Ant Attendance? James Bryant and Janet Lanza, University of Arkansas at Little Rock, AR.

*Species Packing in a North Carolina Creek. James J. English. Alvan A. Karlan, University of Arkansas at Little Rock, AR, and Laurie D. Lacer, Biotechnical Services, Inc., North Little Rock, AR.

Break

Chair: Dr. C. Renn Tumlison, Henderson State University.

*A Preliminary Assessment of the Effect of Supplemental Feeding on Movement of Three-Toed Box Turtles (*Terrapene carolina triunguis*). Jeffrey P. Demuth and Michael V. Plummer, Harding University, Searcy, AR.

*The Effects of Timber Management on Small Mammal Populations in Southwestern Arkansas. David Eller and Renn Tumilson, Henderson State University, Arkadelphia, AR.

*Plant and Animal Recovery after Coal Mine Reclamation. John Pringle and Randy Groves. University of the Ozarks, Clarksville, AR.

Cavity Protection Techniques for Red-Cockaded Woodpeckers. Warren Montague. Poteau Ranger District, USDA Forest Service, Waldron, AR.

The Effects of Forest Management on the Densities and Population Biology of Neotropical Migrant Birds in West-Central Idaho: A Preliminary Study. James C. Bednarz. Arkansas State University, State University, AR.

Sex Ratio and Success, An Assessment of *Lindera melissifolia* in Arkansas. Robert D. Wright, Conway, AR.

A Classification System for the Natural Vegetation of Arkansas. Thomas Foti, Arkansas Natural Heritage Commission, Little Rock, AR, Ziaojun Li, University of Arkansas at Fayetteville, AR, Martin Blaney, Arkansas Game and Fish Commission, Little Rock, AR, And Kimberly G. Smith, University of Arkansas at Fayetteville, AR.

Saturday, April 9, 1994 LS 444

BIRDS/MAMMALS

Chair: Dr. Todd Wiebers, Henderson State University.

Species of Birds New to the State Recorded in Arkansas Since the Mid 1980s. Douglas A. James, Max Parker, Charles Mills, Joseph C. Neal, University of Arkansas at Fayetteville, AR.

Long Range Dispersal of a Red-Cockaded Woodpecker. Warren Montague and George Bukenhofer, Poteau Ranger District, USDA Forest Service, Waldron, AR.

Food Habits of Barn Owls From a Nest Site in Southwestern Arkansas. Jonathan Westmoreland and Renn Tumlison, Henderson State University, Arkadelphia, AR.

Weight Estimates for Arkansas White Tailed Deer From Field Measurements. J. D. Wilhide, Jeffrey W. Jenness, Arkansas State University, State University, AR, and Michael E. Cartwright, Arkansas Game and Fish Commission, Calico Rock, AR.

Notes on the Natural History of *Lasiurus borealis* (Chiropter: Vespertillonidae) in Arkansas. David A. Saugey, USDA Forest Service, Jessieville, AR, Betty G. Cochran, USDA Forest Service, Glenwood, AR, and Gary A. Heidt, University of Arkansas at Little Rock, AR.

Use of Visual and Tactile Behaviors by Rate (*Rattus norvegicus*) in an Object Discrimination Swimming Task. Todd Wiebers. Henderson State University, Arkadelphia, AR.

Break

Chair: David A. Saugey, USDA Forest Service, Jessieville, AR.

New Records for the Badger (*Taxidea taxus*) in Arkansas. Michael Cartwright, Arkansas Game and Fish Commission, Calico Rock, AR, and Gary Heidt, University of Arkansas at Little Rock, AR.

Nonendangered Mammals of Questionable Status in Arkansas. Gary A. Heidt, University of Arkansas at Little Rock, AR, and V. Rick McDaniel, Arkansas State University, State University, AR.

*Food Habits of the Common Barn Owl in Western Arkansas. Rhonda M. Huston and Thomas A. Nelson, Arkansas Tech University, Russellville, AR.

*Heavy Metal Concentrations in the Kidneys of White-Tailed Deer on Fort Chaffee, Arkansas. Greg Humphreys, Thomas Nelson and Timothy Sherwood, Arkansas Tech University, Russellville, AR.

*Faunal Use of Nest Boxes in the Ouachita Mountains of Central Arkansas. Paul T. Caster, Gary A. Heidt and Karen D. Stone, University of Arkansas at Little Rock, AR.

*Comparison of Structure of White Winter Fur and Brown Summer Fur of Northern Mammals. John E. Russell and Renn Tumlison, Henderson State University, Arkadelphia, AR.

Compton Scattering of γ-Rays from Electrons in Advanced Laboratory

Christine A. Byrd, Morgan T. Burks, Lawrence A. Yates, and W.J. Braithwaite
Department of Physics and Astronomy
University of Arkansas at Little Rock
Little Rock, AR 72204

Abstract

A kinematically-complete 2-body final state measurement of Compton scattering of 662-keV photons is presened, where both scattered photon energy and electron recoil energy are measured versus photon scattering angle, $\theta\gamma'$. Passive collimation of the photon beam is avoided; each recoiling electron triggers a photon-scattering event providing active beam collimation. Recoiling electrons have low energies at small $\theta\gamma'$, impairing electron detection efficiency. Examining the recoiling-electron energy spectra in coincidence with high-resolution gammas indicates a 1"x1"NaI detector is superior to a 1"x1" NE-102 plastic scintillator as the active scattering material, for efficient recoil-electron detection. Electron efficiencies versus $\theta\gamma'$ are measured by comparing e-γ' coincident yield with the relativistically-correct Klein-Nishina predictions, indicating the detection-efficiency for recoil-electrons is near 100% at $\theta\gamma' \geq 30$ degrees. Scattered-photon energy pulses and recoil-electron energy pulses are summed electronically to produce an invariant peak at 662 keV, reducing systematic errors in coincident-yield extraction, In addition, $E\gamma'$ spectra are taken at several $\theta\gamma'$ to provide an experimental value for electron mass; an easier measurement than the Millikan oil drop experiment, but with similar predictive consequences.

Introduction

Students in the physical sciences are introduced to 4-momentum conservation (or momentum-energy conservation) with special relativity, usually in first-year physics. Compton scattering of energetic photons from electrons (Compton, 1923) provides a graphic example of this principle, while establishing the photon with tangible particle properties in the mind of each student (possibly supporting laboratory work by the student on the photoelectric effect which also shows photons have particle properties).

As seen below, both scattered photon energy $E\gamma'$ and recoiling electron kinetic energy T_e (and electron-recoil angle ϕ) are predicted as a function of outgoing photon angle $\theta\gamma'$ in this two-body final state. Little energy variation is predicted for soft X-ray photon scattering in contrast to the strong $\theta\gamma'$ dependence seen for incident photon energies ≈511 keV ($m_e c^2$). In the present work 662-keV photons from a ^{137}Cs source were scattered from electrons.

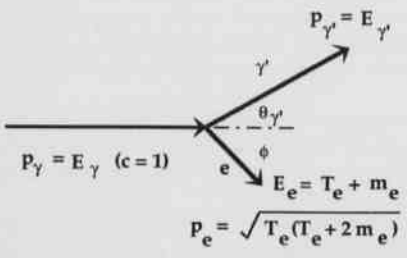

Energy Conservation

$E_\gamma = E_{\gamma'} + T_e = 662$ keV

Momentum Conservation

$E_\gamma = E_{\gamma'} \cos\theta_{\gamma'} + p_e \cos\phi$

$0 = E_{\gamma'} \sin\theta_{\gamma'} + p_e \sin\phi$

Eliminating p_e and ϕ from equations above gives: $\frac{1}{E\gamma'} - \frac{1}{E\gamma} = \frac{1}{m_e}(1 - \cos\theta\gamma')$, where m_e is the electron mass (in energy units). This expression predicts a plot of the photon scattering data as $\frac{1}{E\gamma'}$ versus $(1 - \cos\theta\gamma')$ will result in a straight line whose slope is $\frac{1}{m_e}$ (Melissinos, 1973). Thus, the mass of the electron may be extracted from a least-squares fit to this straight line, providing an experimental value for m_e.

Measuring the mass of the electron by Compton Scattering is easier than measuring the electronic charge in the Millikan Oil Drop Experiment. Either measurement is historically interesting, even at the few percent level, as electromagnetic measurements only provide e/m_e and m_e/m_p ratios. With m_e (or e) measured, the charge of the electron (or its mass m_e) and the mass of the proton m_p may be extracted, as well as Avogadro's Number ($1/m_p$ in grams).

Laboratory measurements of $E\gamma'$ versus $\theta\gamma'$ are complicated by the finite geometry of the detectors. Students are introduced to "kinematic line broadening," an experimental condition seen in particle scattering, in the rapid variation of $E\gamma'$ with $\theta\gamma'$. In developing student experimental design skills, predictions of line widths at several detector positions may be carried out and tested.

The TELTRON Company offers a laboratory series on X-rays, with the Compton Effect listed as Physics Experiment D.21 (TELTRON, 1994). The development of

this experiment has not been completed as yet. A soft X-ray experiment could serve as an introductory experiment where scattering yield measurements should compare fairly well with predictions from classical electromagnetic theory (Thompson, 1907; Evans, 1955b).

The 662-keV gamma rays in the present experiment bombard electrons at energies comparable to the electron rest mass, recoiling them in rough analogy to billiard balls, providing results in agreement with relativistic momentum-energy conservation, and allowing the extraction of m_e. For students who completed a soft-X-ray scattering experiment, this value of m_e may be compared with the m_e value extracted from soft-X-ray scattering using a curved crystal spectrometer. Since these students found the Thompson yield predictions satisfactory for soft-X-ray scattering, and since all photons move a the speed of light, students are likely to expect Thompson predictions to correctly provide scattering yields for gamma-ray photons as well.

The failure of the Thompson yield predictions for photon scattering in the energy regime $E\gamma \approx m_e c^2 = 511$ keV may induce student interest in measuring the yield versus scattering angle at fairly high precision to investigate this conundrum. Klein and Nishina (1929) applied Dirac Theory to the relativistic scattering of electrons. Agreement with data provided early confirmation of Dirac Theory, initially suspect because of its prediction of negative energy states for the electron (the "positron").

In this experiment students may be introduced to the relativistic Klein-Nishina formulation of photon scattering probability as a function of $\theta\gamma$ (Evans, 1955). Comparing measured photon scattering probability versus $\theta\gamma$ allows Klein-Nishina predictions to be used to extract the recoiling-electron efficiency as a function of $\theta\gamma$. This establishes a region (e.g., $\theta\gamma \geq 30°$) where the electron-recoil detection efficiency is flat (near 100%), allowing centroid to be extracted reliably from the $E\gamma$ peaks, in order to measure the mass of the electron.

Materials and Methods

A 3" X 3" NaI detector was used to measure the energy of the scattered γ-ray photon and a vertically-mounted cylindrical 1" by 1" NaI detector was used as the active scattering material, taken in coincidence with each scattered photon, allowing the simultaneous measurement of each scattered photon energy ($E\gamma$) with each recoil-electron kinetic energy (T_e). Figure 1 is an electronics diagram, showing the electron-gamma coincidence scheme using these two NaI detectors. Summing the two energy pulses, $E\gamma + T_e$, provides an invariant peak in the Multi-Channel Analyzer (MCA) spectrum equal to the incident photon energy. Figure 2 shows this sum peak at 662 keV at 35 different scattering angles. Gain matching between the two NaI detectors was accomplished by triggering the linear gate, in turn, with the output of each timing SCA. A similar circuit is discussed in some detail in an earlier publication (Braithwaite, 1990).

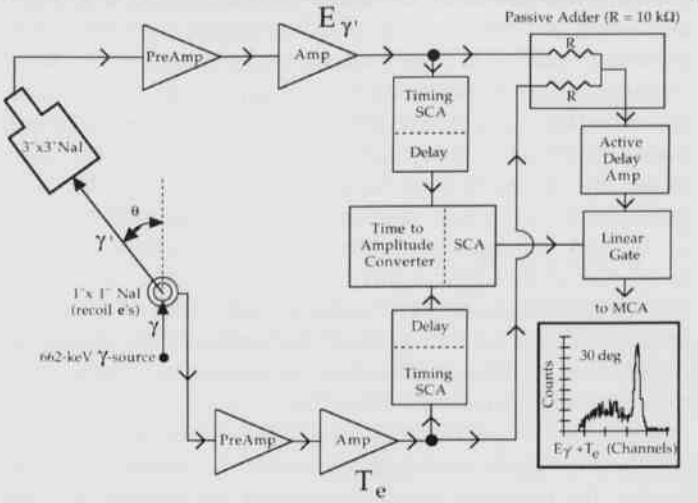

Fig. 1. Electronics diagram for electron-gamma coincidence using small NaI detectors. SCA (single channel analyzer) MCA (multi channel analyzer).

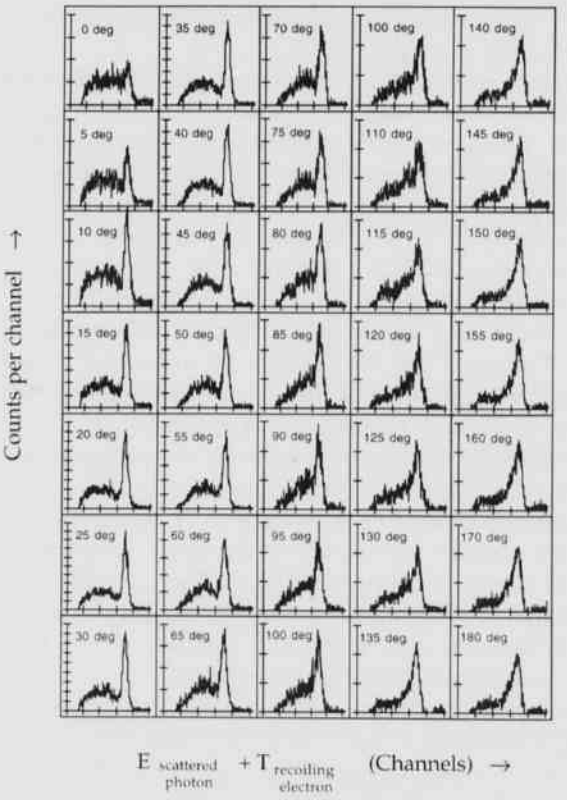

Fig. 2. Coincident photon yields at different photon scattering angles, versus total deposited energy.

Finite geometrical acceptance in both the 3" by 3" NaI detector and the 1" by 1" NaI detector results in broad peaking in both photon and electron distributions, each varying as a function of photon scattering angle θ. The precision of yield extraction is reduced by systematic errors, when taken at a variety of different energy positions and different peak widths, under variable background conditions. However, increased precision in yield extraction may be obtained by adding energy signals from γ and e [$E\gamma + T_e = 662$ keV] to provide a spectral peak whose position is independent of $\theta\gamma$ and narrower than either the individual gamma-ray or electron peaks. The peak width in the sum spectrum is fairly insensitive to $\theta\gamma$, as the NaI detector have comparable resolutions (with 3" by 3" NaI resolution slightly better than the 1" by 1" NaI resolution). Even so, Fig. 2 suggests some difficulty in peak extraction due to the varying background conditions at different scattering angles, despite constancy in peak position and near-constancy in width.

Detection of each scattered photon is triggered in coincidence by each recoiling electron. At forward photon angles, the recoiling electron has very low energy, and the student must examine its detection efficiency. A high-resolution Intrinsic Germanium detector was used to detect each scattered photon at 14.4 degrees in the laboratory, triggered by its recoiling electron in a 1" by 1" NaI detector, for three different angular acceptances: $\Delta\theta = \pm 2.1, \pm 3.2$ and ± 6.4 degrees.

Figure 3 shows three sets of paired coincidence spectra at these three angular acceptances. The left spectrum in each of the three paired spectra is a Germanium detector gamma ray spectrum taken in coincidence with the recoil-electron spectrum (from a 1" by 1" NaI detector), and vice versa. For the 1" by 1" NaI spectra with the smallest angular acceptance of ± 2.1 degrees, the coincident electron yield drops into the noise above the lower-discriminator level, indicating detection efficiency is approximately 100%. For the 1" by 1" NaI spectra with the ± 3.2 degree acceptance, some loss to the lower-discriminator is seen, with even greater losses seen at the ± 6.4 degree acceptance. The electron-recoil spectrum shows significant losses (roughly 1/3) at the ± 6.4 degree acceptance. The geometrical acceptance (± 6.4 degrees) is about the same as the total angular acceptance of the detector geometry for the NaI detectors shown in Fig. 1. The 1/3 efficiency loss which may be estimated roughly from Fig. 3 is approximately the same size as the 28% efficiency drop from the Klein Nishina prediction seen in Fig. 4.

The greatest efficiency loss seen on the right-hand side of Fig. 3 is for the 1" by 1" NE-102 plastic scintillator spectrum at the smallest angular acceptance of ± 2.1 degrees, shown at the top right. This means the plastic scintillator is unreliable for either centroid or yield extraction for a wider range of angles.

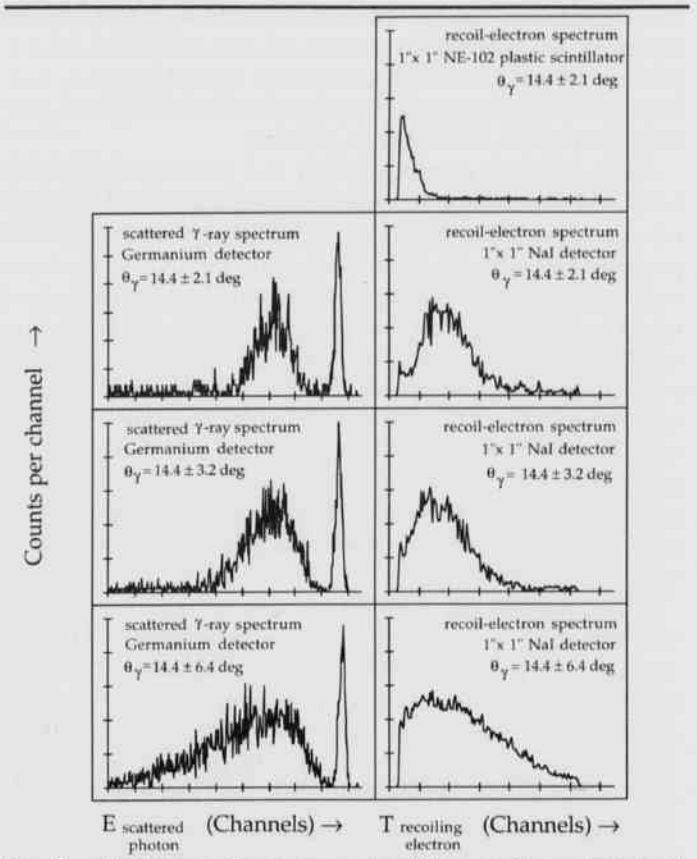

Fig. 3. Scattered-photon spectra (Germanium detector) are compared to corresponding recoil-electron spectra (1" by 1" NaI detector): $\Delta\theta = \pm 2.1, \pm 3.2$ and ± 6.4 deg.

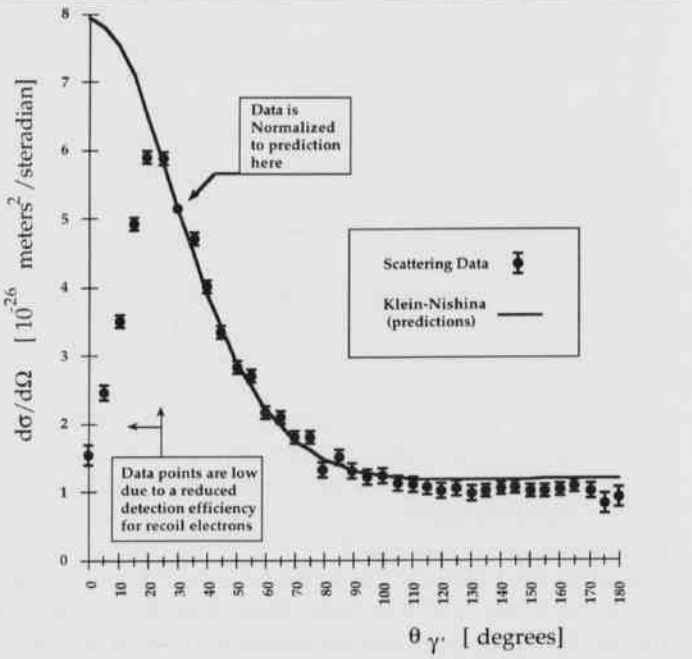

Fig. 4. Yield versus photon angle for photon scattering from electrons: Data and Klein-Nishina predictions.

A 1" by 1" NE-102 plastic scintillator will have a smaller multiple-photon scattering probability than will a 1" by 1" NaI detector, a possible concern for the lower photon energies at the backward scattering angles. However, the fair agreement seen in Fig. 4 between the coincident scattering data and the Klein-Nishina predictions indicates multiple-photon scattering is negligible for 662-keV photon scattering by electrons in a 1" by 1" NaI detector. Also, estimates of recoiling-electron ranges associated with back-angle photon scattering within the 1" by 1" NaI indicates ≥97% of the recoil electron energy is deposited within the NaI (averaged over scattering events). γ-detection efficiency in the 3" by 3" NaI detector is determined for each scattering energy as a product of detection efficiency times photopeak fraction (Marian and Young, 1968).

Figure 4 compares data and prediction for photon yield versus photon scattering angle, for an incident photon energy of 662 keV. Fair agreement is obtained except at the most forward angles, where the data is significantly lower than the Klein-Nishina predictions.

These data points are lower than prediction, due to a reduced detection efficiency for recoil electrons at the forward angles where electron kinetic energies are quite low. This attribution may be tested by changing the effective electron discriminator, by changing either the amplifier gain or the discriminator level. Lowering the effective discriminator level results in obtaining 100% efficiency at the smaller scattering angles, whereas increasing this level results in an efficiency reduction at even larger angles than 30 degrees.

Results and Discussion

The present work presents a kinematically-complete 2-body final state measurement of Compton scattering of 662-keV γ-ray, avoiding passive collimation of the incident γ-rays, as each recoiling electron triggers a γ-ray-scattering event. Systematic errors are reduced in coincident-yield extraction by summing electronic pulses associated with each scattered γ-ray energy and electron recoil energy, at each scattering angel, $\theta\gamma$, producing spectrally invariant peaks at 662 keV, as seen in Fig. 2.

Detection efficiency was examined at small $\theta\gamma$ for recoiling electrons, where they have low energies. Examining the recoiling-electron energy spectra, taken in coincidence with high-resolution gammas, indicates a 1" by 1" NaI detector is superior to a 1" by 1" NE-102 plastic scintillator as the active scattering material, for efficient recoil-electron detection.

A second method examined recoil-electron efficiency versus $\theta\gamma$ by comparing the e-γ coincident yield with the relativistically-correct Klein-Nishina predictions. This work indicated the detection-efficiency for recoil-electrons is essentially 100% for $\theta\gamma \geq 30$ degrees. Thus a region (e.g., $\theta\gamma \geq 30°$) is established where the electron-recoil detection efficiency is essentially 100%, allowing centroid to be extracted reliably from the Eγ spectral peaks, in order to measure the mass of the electron.

Centroid measurements are less sensitive than coincident-yield measurements to varying peak widths and varying background conditions, which is fortunate, as the centroid of the gamma-ray peak $E\gamma(\theta)$ versus $\theta\gamma$ was measured in order to test momentum-energy conservation, and to provide the basic data for extracting a value for the electron mass, m_e. Eγ spectra, taken at several $\theta\gamma$ are shown in Fig. 5, provide experimental values needed to extract electron mass. Figure 6 is a plot of photon scattering data as $\frac{1}{E\gamma}$ versus $(1 - \cos\theta\gamma)$. The straight line in Fig. 6 is a linear fit to this data, where $\frac{1}{m_e}$ is obtained from the slope of this straight line. Measuring electron mass to a few percent is an easier than carrying out the Millikan oil drop experiment, but either allows an unlocking of the charge/mass ratios from electromagnetic measurements, providing e, m_e, proton mass m_p (and Avogadro's number = $1/m_p$).

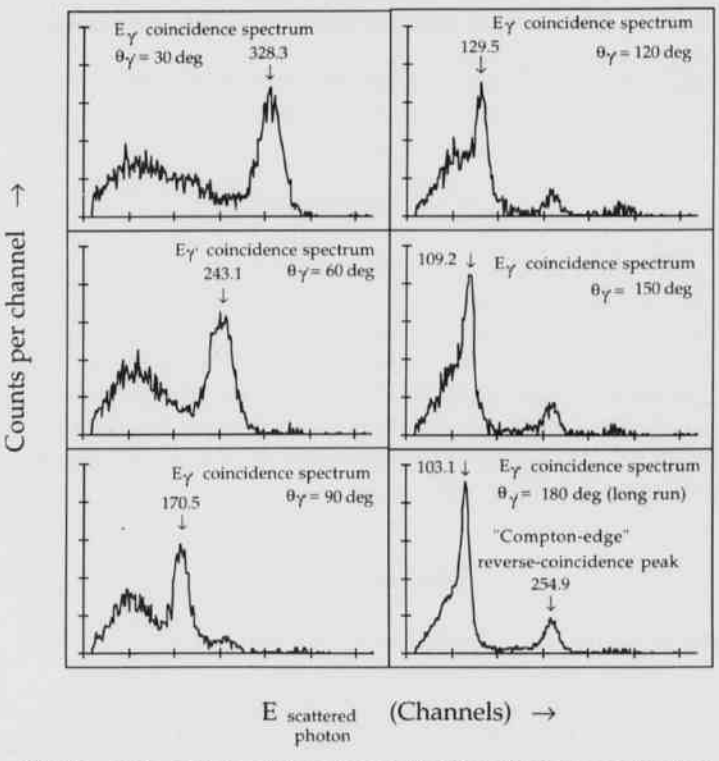

Fig. 5. Eγ peak position versus $\theta\gamma$ for photon scattering from electrons.

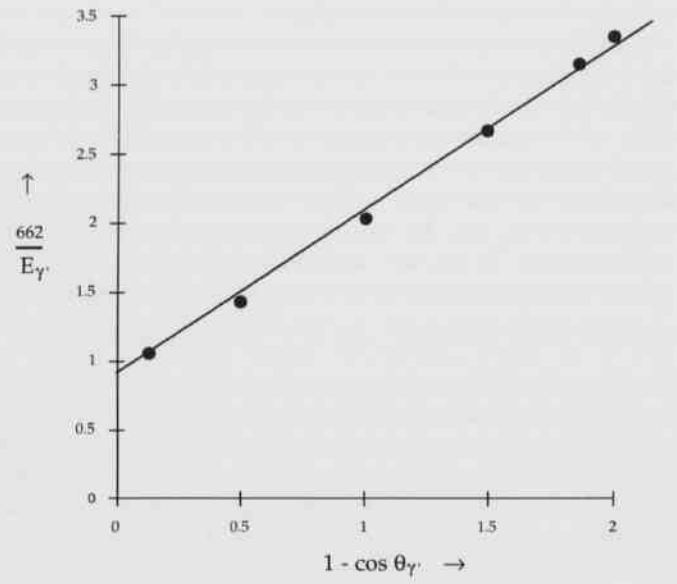

Fig. 6. Plot of photon scattering data as $\frac{1}{E\gamma'}$ versus (1 - cos θγ'). The straight line is a linear fit to this data, where $\frac{1}{me}$ is obtained from the slope of this straight line.

Acknowledgements

The first author acknowledges financial support from the UALR Donaghey Scholars Program. The first and second authors acknowledge support from the U.S. Department of Energy and the Arkansas Science and Technology Authority. All the authors would like to thank Dr. Richard Prior for his pioneering work in the development of the Compton experiment at the University of Arkansas at Little Rock.

Literature Cited

Braithwaite, W. J. 1990. Rotational symmetries of nuclear states: spin determinations in advanced laboratory. Proc. Arkansas Acad. of Sci. 44:19-22.

Compton, A.H. 1923. Physical Review 21:483 and Physical Review 21:715.

Evans, R.D. 1955. The atomic nucleus. McGraw-Hill Book Co., New York, 972 pp.

Evans, R.D. 1955b. The atomic nucleus. McGraw-Hill Book Co., New York, Chapter 1 (Section 2) and Appendix A.

Klein, O. and **Y. Nishina.** 1929. Z. Physik 52:853.

Marian, J.B. and **F.C. Young.** 1968. Nuclear Reaction Analysis Graphs, and Tables. (North Holland, Amsterdam) p. 10 and pp. 48-53.

Melissinos, Adrian C. 1973. Experiments in modern physics. (Academic Press, New York) 252-265 pp.

TELTRON. 1994. Student Enquiry Series D the production properties and uses of X-rays. Part 2: Experimental Manual. PHYSICS D.21 The Compton Effect, A Quantitative Measurement.

Thompson, J.J. 1907. The corpuscular theory of matter. Constable and Company, Ltd., London.

Using the CERN Program-Library Graphics and Interactive Data Display

Morgan T. Burks, Wilson Howe, Christine A. Byrd and W.J. Braithwaite
Department of Physics and Astronomy and
Department of Electronics and Instrumentation
University of Arkansas at Little Rock
Little Rock, AR 72204

Abstract

Small scale Monte Carlo programming is growing rapidly due to the ease with which complex problems may be formulated by any programmer. These programmers may choose to exploit graphics and interactive displays available in the program library developed and maintained by CERN (the Center for European Nuclear Research). This paper outlines the use of graphics and interactive data display features of the CERN program library, developed for visualizing simulated data events in particle detectors. One example uses GEANT, CERN's Monte Carlo modeling program, to simulate 300 MeV/c protons incident on a silicon slab. Display packages for GEANT are available both on-line and off-line for 3-D tracking of particles through any detector system. On-line displays provide the user a qualitative sense of the inner workings of various detector components. On-line displays may be updated for each particle track in the detector system, so any design change in detector geometry or component material may have its consequences visualized immediately. This visualization is useful for repeatedly making gross changes in the detector system. CERN has been very generous in making its program library available to any institution tied to groups working on experiments at CERN, however peripherally.

Introduction

GEANT (1994) is a powerful Monte Carlo modeling software package widely used in the high-energy physics community. It is capable of modeling sophisticated particle detectors by simulating their response to secondary events following a relativistic nuclear collision with a fixed target nucleus, or their response to central collisions of gold on gold in a colliding beam environment. GEANT is available to researchers at the University of Arkansas at Little Rock (UALR) because of the participation of our research group in experiments at CERN, the Center for European Nuclear Research in Geneva, Switzerland.

Until recently, only large institutions and national labs such as CERN used GEANT due to the complexity of the software and the extent of the computer resources required. However, with the growing availability of high-powered computing, more and more universities are beginning to use GEANT and its associated software packages. Since GEANT has traditionally been run by the sophisticated user, its complicated structure and lack of documentation is daunting to the beginner. To help fill this gap, two papers were published (Byrd et al., 1993; Roetzel et al., 1993) explaining the main features of GEANT and their uses. This paper expands on the previous two by describing the details of a simulation run by UALR students. Furthermore, the visualization capabilities of the CERN program library were not addressed previously; this paper describes the routines needed to implement the visualization of the detector and its response to particle events.

GEANT is a software package consisting of hundreds of FORTRAN subroutines. Each subroutine performs a specific task. Together these subroutines are used to model a particle detector by simulating its response to known incoming particles. A few subroutines, called user subroutines, have a special function. User subroutines are written entirely by the user for the purpose of customizing the simulation. Only CERN routines and user routines needed to implement visualization will be discussed, since non-graphic GEANT routines have been discussed extensively elsewhere (Roetzel et al., 1993).

For this simulation, a simple detector design was chosen, consisting of a silicon slab set in a vacuum. The event was chosen to be a stream of protons incident on the slab at 90°. The silicon slab represents an adequate model of a silicon drift detector (Gatti, 1989) in its interaction with charged particles. The simulation was done with the purpose of studying the energy deposition characteristics of protons while traveling through the silicon slab.

Materials and Methods

Detector Design and Event Definition.--The detector geometry consisted of a silicon slab and a mother volume. The silicon slab had dimensions of 300 m in the z (beam axis) direction and 6 by 7 cm in the x and y directions respectively. The mother volume is a large box surrounding the silicon slab. The mother volume defines the area

of the vacuum.

Each proton was given an initial momentum of 300 MeV/c, entirely in the z-direction. Figure 1 shows the vertex (the proton source position) set 2 cm upstream (left) from the silicon slab with the protons incident on the silicon at 90°.

Based on the geometry defined, GEANT created a three dimensional, scaled representation of the slab of silicon and mother volume. GEANT then triggered the particles one by one and tracked them through the detector geometry in minute detail. To obtain high statistical accuracy, one million protons were triggered through the detector, requiring about one hour on a DEC 5000 workstation.

User Subroutines.--UGEOM is the routine where the user designs the specific shapes and material composition of each detector component and its spatial relation to the other components. GEANT uses this information for many purposes including drawing the detector on the screen. A call to GSVOLU defines a volume shape (for example: box, cylinder or sphere). GSPOS positions each volume with respect to the origin. GSROTM defines the viewing angle of the master coordinate system. GSATT is used to set attributes such as color and appearance.

GUKINE is the routine where the user defines the components of momentum and initial position of the event particles. For the present simulation, the protons were given an initial z-component momentum of 300 MeV/c from a source position located 2-cm upstream from the silicon detector.

GUTRAK calls the GEANT routine GTRACK. GTRACK initializes the physics processes. These processes may include electromagnetic interactions, hadron collisions, nuclear fission, bremsstrahlung, etc. GTRACK then begins with a single particle and determines the trajectory of that particle by creating a series of many small steps. Each step is determined by considering which physics processes have occurred during the previous step. The trajectory may also be influenced by bending from a magnetic field or decay of the particle into secondaries.

GUSTEP is one of the most important user subroutines for visualization of particle trajectories. It takes control after each step in GUTRAK. In GUSTEP the user can determine which physics information is to be stored, such as energy loss, secondary particles and detector hits. GUSTEP is called repeatedly for each particle at every step. GUSTEP also determines when to abandon tracking of a particular particle. To implement the visualization it is necessary to make three additional GEANT calls: 1) to store the position coordinates of the particle currently being tracked into the data structure, JXYZ, with a call to GSXYZ, 2) to store the momentum components and the time of flight information with a call to GSKING, and 3) to plot the tracks on the screen as they are created by GTRACK by calling GDCXYZ.

Results and Discussion

This simulation had several advantages over simulations done in the past and demonstrated some of GEANT's powerful visualization features. For example, while the present simulation consisted of only a simple silicon slab, much more complex designs may be made. Thus, any mistakes made when initially designing the detector geometry can be observed immediately. Without visualization, errors in detector geometry are difficult to find. These errors may only be found by carefully analyzing data taken in a batch run. The non-visual approach to error detection is difficult and time consuming and not always successful. Second, the tracking of particles can be done interactively. This allows the user to observe such features as angular distribution and back scattering.

Figure 1 shows the display of the silicon slab with the proton and secondary particle trajectories. As expected, most of the protons went through the silicon and left the mother volume on the right side. However, a few particles scattered at large angles and a few "back scattered". Also, different types of particles such as electrons and photons can be seen, represented by the dotted lines.

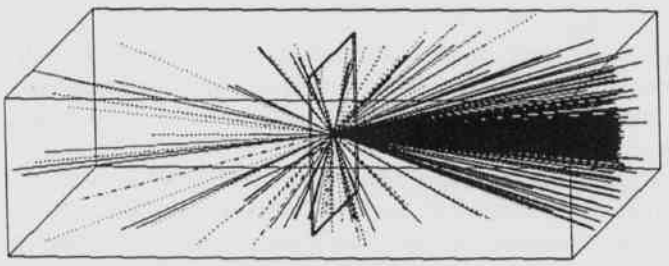

Fig. 1. Scaled diagram of the detector showing outgoing secondary particles (including protons). This figure represents 10% of this multiplicity.

Figure 2 shows the energy loss for all particles passing through the silicon. The GEANT prediction for peak energy loss is over 1000 keV. Based on predictions from other models (Williamson et al., 1966; STAR, 1992), a peak between 700 and 800 keV was expected. The value obtained was close enough to suggest that the GEANT modeling was reasonable. However, work is presently being done to determine if a more accurate value can be obtained and what the mechanisms determining the discrepancy might be.

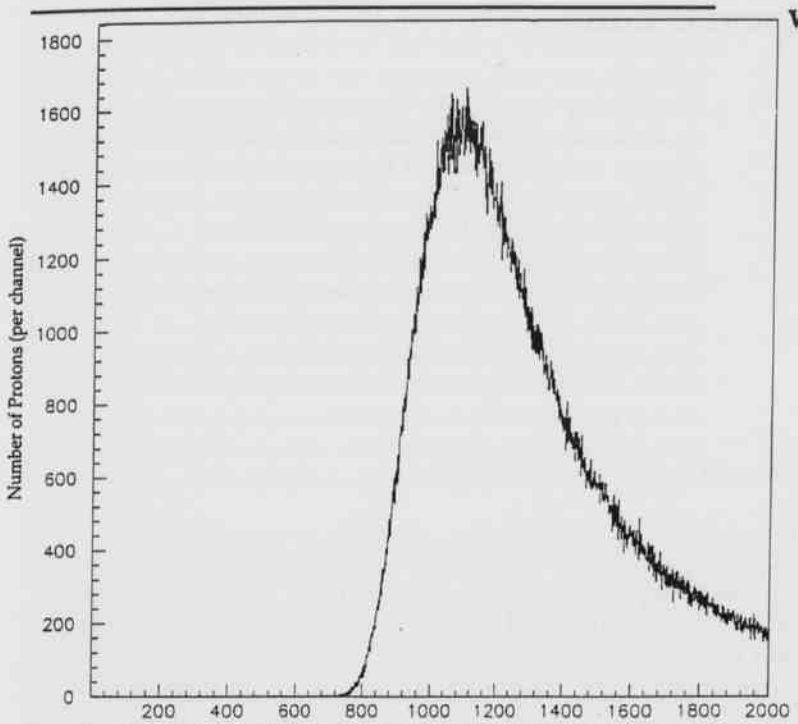

Fig. 2. Energy loss of incident protons on a 300 micron silicon slab.

Acknowledgements

This work was supported by the U.S. Department of Energy, the Arkansas Science and Technology Authority, and the UALR Donaghey Scholars Program. The authors would also like to thank Charles Byrd for his helpful advice.

Literature Cited

Byrd, C.A., C.M. Byrd and W.J. Braithwaite. 1993. Monte Carlo Detector Modeling and Display, Using the CERN library. Proc. Arkansas Acad. Sci. 47:26.

Gatti, E., P. Rehak and M. Sempietro. 1989. Double Particle Resolution in Semiconductor Drift Detectors. Nuclear Instruments and Methods, Vol. A274. p. 469.

GEANT. 1994. Detector Description and Simulation Tool. Geant user's guide. CERN internal report.

Roetzel, D.L. and W.J. Braithwaite. 1993. User-Interface Coding for the CERN/GEANT Nuclear Physics Program. Pro. Arkansas Acad. Sci. 47:98.

STAR collaboration. 1992. dE/dx distribution for various particles. Conceptual Design Report for the Solenoidal Tracker At RHIC., Section 4H, p. 27.

Williamson, C.F., J.P. Boujot and J. Picard. 1966. Tables of Range and Stopping Power of Chemical Elements for Charged Particles of Energy 0.05 to 500 MeV. Atomic Energy Commission Report CEA - R3042, Center for Nuclear Studies, Paris, France.

Computational Fluid Dynamics in Small Airway Models of the Human Lung

G. Burnside
University of Arkansas at Little Rock
Department of Electronics and Instrumentation
2801 S. University Ave.
Little Rock, AR 72204

R.N. Reddy
University of Arkansas at Little Rock
Department of Computer and Information Science
2801 S. University Ave.
Little Rock, AR 72204

J. R. Hammersley
University of Arkansas School for Medical Sciences
Department of Pulmonary Medicine
4301 West Markham Ave.
Little Rock, AR 72205

B. Gatlin
NSF Engineering Research Center
Mississippi State University
P.O. Box 6176
Mississippi State University, MS 39762

Abstract

The promise of gene replacement therapy for cystic fibrosis, the administration of drugs via inhalation therapy, and the deposition location of man-made airborne particulates all involve a more complete understanding of the fluid dynamics in the human lung. Flow in the larger airways may be measured through life-sized models directly, but the airways in the peripheral lung are too small and the flows are too complex to be studied in this manner. Computational models can be developed which will accurately represent both the geometric nature of the central airways and the fluid dynamics within them.

Two-dimensional and three-dimensional models of central lung airway bifurcations were developed based on morphometry. These models were used as the spatial basis upon which the differential equations that describe incompressible flow, the Navier Stokes equations, are solved. Flow solutions have been computed at Reynolds numbers from 1000 down to 100. Solutions for single and double bifurcations agree with the experimental data for flow in a branching tube. These studies are being extended to multiple bifurcations in three dimensions.

Introduction

Scientific investigation of fluid flow within the human lung is important in the understanding of the transportation of particulates in gasses. The human lung is comprised of a series of 16 Y-shaped branches which divide the flow into ever smaller branches terminating in the aveolei. Because the lung does not have an 'outlet', there is no flow at the aveolei. The necessary exchange of oxygen and carbon dioxide at the terminus of the lung is driven solely by diffusion, so the geometry produced mixing of gasses within the lung is of utmost importance. The geometry of the lung consists of a single symmetric primary branch while the remaining branches (bifurcations) are asymmetric. A generalized symmetrical and asymmetrical model has been developed from morphometry of samples of small human airways and is the geometry used in this study (Hammersley and Olsen, 1992).

Physical models can be used only to investigate the flow of simple geometries since complex three dimensional models are difficult to manufacture, and the transduction elements actually interfere with the slow flows found in the central airways. Grid generation techniques are more suitable to model complex geometries of multiple bifurcations and accurately represent the flows found in them.

Materials and Methods

Numerical Simulation.--Numerical simulation of physical phenomenon can be performed by many methodologies. One of the oldest methods involves the use of the iterative solution of governing partial differential equations (PDEs) expressed in an appropriate coordinate system. For example, the Navier-Stokes equations may be cast in the different form in cylindrical coordinates and used to determine the steady-state flow of a fluid in a cylinder. The geometry thus obtained is a 'grid' of points described by a points axial and radial values as well as some angular indicia. Boundary values, initial conditions, the present value of neighboring points and the last iterated values of the point in question are all applied at a point on the geometry to solve the difference equation at

that point. The solution then marches to another point until solutions at all points of the entire volume are generated. The solutions of the previous iteration are then used in subsequent interations until some predefined minimum between previous and present solutions in reached, this limit is known as the convergence criteria for the solution. Convergence criteria may be also based on the first or even the second derivatives of solutions differences. Solutions to partial differential equations by this method are useful for simple geometries, but are not applicable to more interesting and practical problems. The generation of complex geometrical grids may be performed by developing a boundary-conforming coordinate system. The boundary-conforming coordinate system may then be transformed with transformational matrices into a cubic computational grid where the PDE system is more readily solved.

Small Airway Grid Generation.--The generation of internal geometry points (field values) for a boundary-conforming coordinate system can be obtained by interpolation between the boundaries or by solving the boundary value problem. Algebraic interpolation produces a grid which reduces computational time, but the grid can have non-uniform variations in first and second order spatial derivatives, which can cause the solution to diverge. Solution of the boundary-conforming coordinate system that has smooth variations in spatial derivatives by maximizing grid surface orthogonality (Thompson, et. al. 1982).

An elliptic boundary-conforming coordinate system grid generation program developed for the U.S. Air Force known as EAGLE (Eglin Arbitrary Geometry Implicit Euler) has been used to develop the small airway models for this project (Thompson, 1988; Thompson and Gatlin 1988a, b). The program requires the boundary values of the geometry in question to be input in the form of points used to generate space curves, which are in turn linked to produce surfaces, which are assembled to produce grid volumes. Since solution of the flow equation is calculated on a computational cube, the grid volumes (blocks) generated must have a total of six four-sided surfaces. The complex geometry of the airway models is divided into multiple blocks which reduces the grid generation time as well as reducing the size of the computational matrices for the solution (Thompson, 1986; Steinbernner and Chawner, 1988). Continuity for the solution is provided between blocks by overlapping the blocks along mutual faces by a point in depth, this allows a derivative to be calculated between the blocks which aids in the solution convergence.

Flow Solution.--The form of the Navier-Stokes equations used to obtain the results in this research is an implicit incompressible algorithm described by Taylor and Whitfield (1991).Finite-volume mass conservation maintains accuracy while an artificial compressibility term (Chorin, 1967) added to the mass conservation term couples pressure and velocity. The resulting algorithm allows the incompressible equations to be solved as time-marching compressible equations. The viscous diffusion terms are center differenced while the convection terms are upwind differenced. The code is written to allow almost any arrangement of arbitrarily sized blocks (Arabshahi, 1989). This allows the flow solver to operate on the complex geometrics created by the boundary-conforming coordinate system.

Results and Discussion

Two Dimensional Solutions.--The two dimensional symmetrical and asymmetrical single bifurcation multiblock grids produced using the EAGLE grid generation program appear in Fig. 1. From the figure, it may be seen that the grids possess a high degree of orthogonality at the coordinate boundaries. Additionally, a tight grid spacing is maintained at the boundary while the spacing in the interior is larger. This aids in solution convergence, and yields more information at the flow boundaries where the pressure and velocity derivatives are larger, while reducing the amount of computation in the interior. The blocking structure for the single asymmetric bifurcation is shown in Fig. 2. The inset in Fig. 2 shows a small radius at the flow divider (carina) which simulates the structure of the airway in that region.

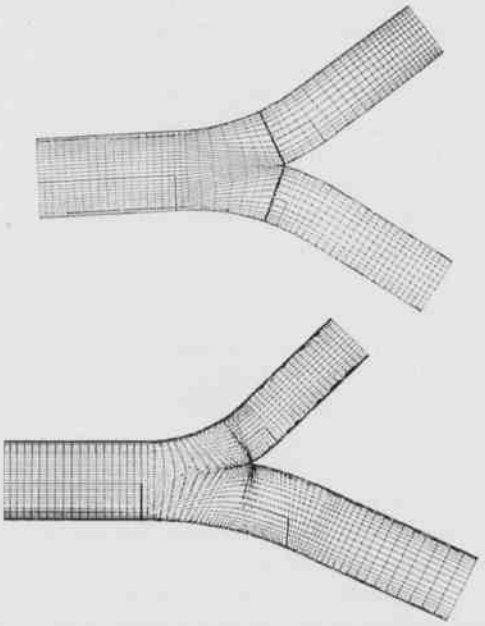

Fig. 1. Two dimensional symmetric and asymmetric double outlet lung bifurcation grid.

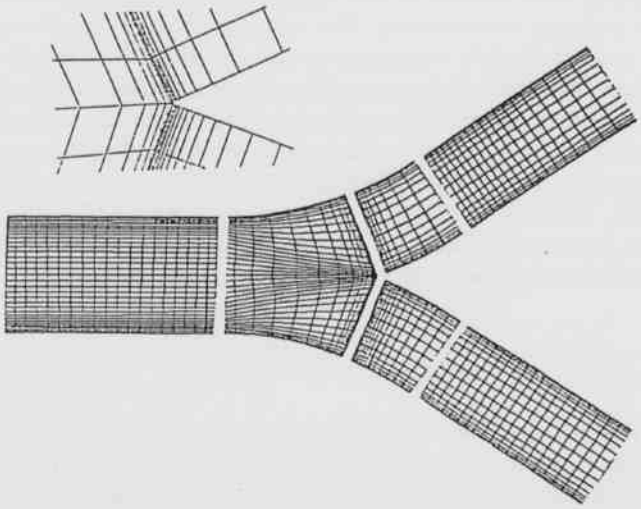

Fig. 2. Blocking structure for two dimensional symmetric model. Inset is grid at flow divider.

Velocity vectors which are normalized with the central inlet velocity are shown in Fig. 3. Flat inlet profile is seen which develops into a parabolic profile as the flow proceeds down the inlet tube. At the carina, the flow divides equally but the maximum velocity vectors are shifted towards the proximal surfaces of the bifurcation which thins the boundary layer at the flow divider. This is due to the momentum of the flow which resists the change in direction as the two daughter tubes sweep away from each other. Velocity vectors on the distal surfaces just past the carina are slightly negative indicating flow separation at that location, flow solutions at higher Reynolds numbers indicate a greater degree of separation at higher Reynolds numbers. For the asymmetrical bifurcation, the majority of the flow divides into the larger branch, but the smaller branch shows a strong skew from parabolic flow towards the proximal surface. Clinically the surfaces just past the carina are the major sites of inhaled particle deposition, in spite of the high velocities found there. Figure 4 shows a two dimensional asymmetric double – outlet bifurcation produced by dimensional scaling, translation and radial point reduction of the original single bifurcation. Radial point reduction matches the inlet points of the second (daughter) bifurcation with the outlet of the first (parent) bifurcation. For the four outlet bifurcations the majority of the flow is concentrated along the bifurcations which parallel the parent tube. The flow is not equally divided at the outlet as was thought by pulmonary researchers. Flow separation in these two dimensional models does not agree with closed form solutions for simple flow dividers and are now being compared with 3D solutions.

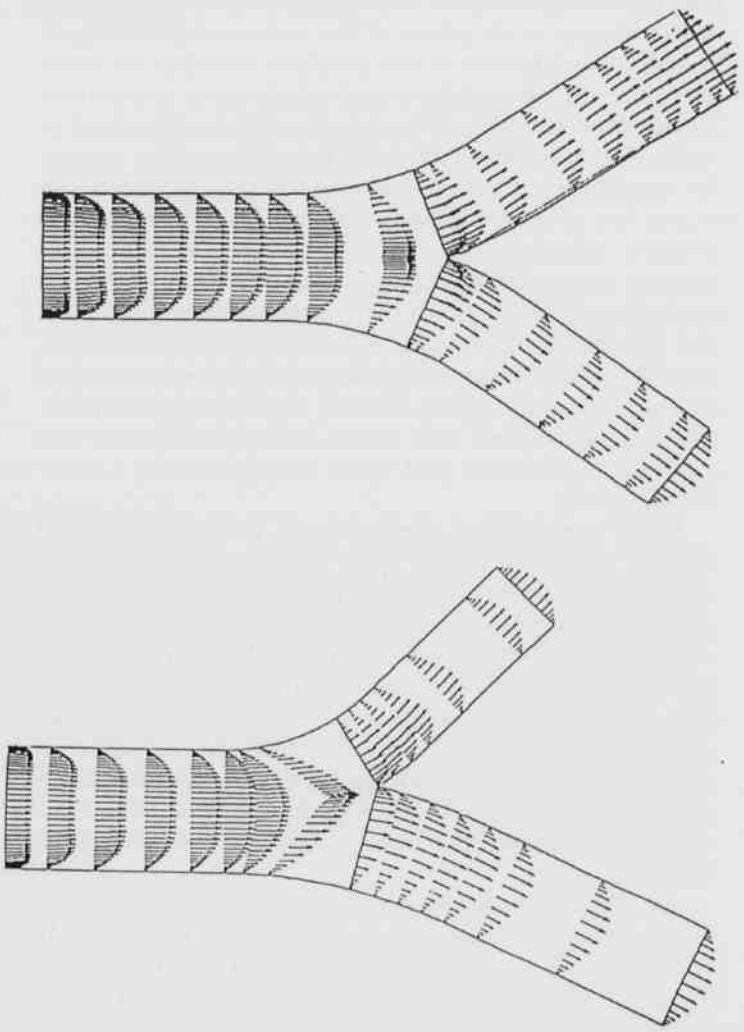

Fig. 3. Velocity vectors for double outlet grid. Flow is skewed towards flow divider.

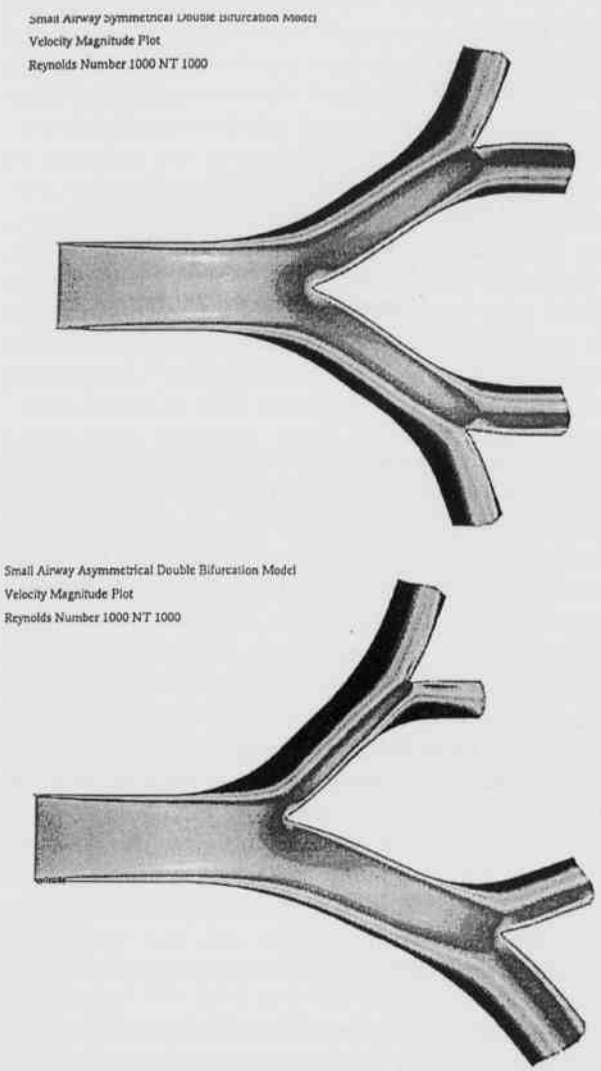

Fig. 4. Velocity magnitude for four outlet grids. Negative values indicate flow separation.

Literature Cited

Arabshahi, A. 1989. A Dynamic Multi-block Approach to Solving the Unsteady Euler Equations about Complex Configurations, Ph.D. Dissertation, Mississippi State University.

Chorin, A.J. 1967. A Numerical Method forSolving Incompressible Viscous Flow Problems, Journal of Computational Physics, Vol. 2., p.12.

Hammersley, J.R., D.E. Olsen. 1992. Physical Models of the Smaller Pulmonary Airways, J. Applied Physiology. 72:2402-2414.

Steinbernner, J.P., J.R. Chawner, Generation of Multiple Block Grids for Arbitrary 3D Geometries, Recent Progresses, AGARD-AG No. 309, AGARD, NATO.

Taylor, L.K. and **D.L. Whitfield,** 1991. Unsteady Three-Dimensional Incompressible Euler and Navier-Stokes Solver for Stationary and Dynamic Grids, AIAA-91-1650.

Thompson, J.F. 1988. A Composite Grid Generation Code for General 3D Regions-the EAGLE Code, AIAA Journal, Vol.26, No3 p.271.

Thompson, J.F. 1986. A Survey of Composite Grid Generation for Generalized Three-Dimensional Regions, in Numerical Methods for Engine Airframe Integration, Murthy and Paynter, G.C., S.N.B.AIAA.

Thompson, J.F. and **B. Gatlin.** 1988a. Program EAGLE User Manual, Volume II-Surface Generation Code, USAF Armament Laboratory Technical Report, AFATL-TR-88-117.

Thompson, J.F. and **B. Gatlin.** 1988b. Program EAGLE User Manual, Volume III-Grid Generation Code, USAF Armament Laboratory Technical Report, AFATL-TR-88-117.

Thompson, J.F., Z.U.A. Warsi and **C.W. Mastin.** 1982. Boundary-Fitted-Coordinate System for Numerical Solution of Partial Differential Equations-A Review, Journal of Computational Physics, Vol. 47, p.1.

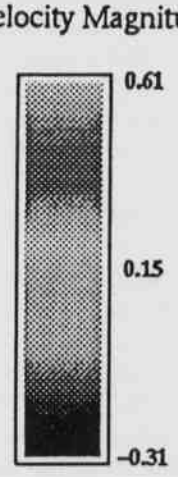

Fig. 4. (continued).

Solid State NMR of Hydrogen in Thin Film Synthetic Diamond

G. Burnside, R.M. Hawk
University of Arkansas at Little Rock
Department of Electronics and Instrumentation
2801 S. University Ave.
Little Rock, AR 72204

R. Komoroski
NMR Lab
University of Arkansas School for Medical Sciences
4301 West Markham Ave. Mail Slot 582
Little Rock, AR 72205

W.D. Brown
Department of Electrical Engineering
3217 Bell Engineering Center
University of Arkansas
Fayetteville, AR 72701

Abstract

Thin film synthetic diamond promises to be the next semiconductor material, if the manufacturing processes which produce it can be controlled. Solid state nuclear magnetic resonance (NMR) using magic angle spinning (MAS) is used to measure the content of hydrogen in diamond which controls the resistivity of the diamond thin films. Spectral results are presented for proton NMR of thin film synthetic diamond. Experimental calibration techniques using BaF_2 as the hydrogen standard will be discussed, as well as acquisition times, pulsing sequences, spinning rates, and rotor composition.

Introduction

Solid State Effects.--In a magnetic field, atomic nuclei which poses a magnetic moment will interact with the magnetic component of r.f. irradiation, elucidating information about nuclear spin interactions, Such interactions, in turn, yield information about the composition and structure of the sample. For a spin 1/2 nucleus such as ^1H, in a uniform field, these interactions can be described by the total Hamiltonian (K.M. McNamara and K.K. Gleaason, 1992):

$$H_{tot}=H_z+H_{d,ii}+H_{d,is}+H_{cs,is}+H_{rf(t)}+R(t) \qquad (1)$$

where H_z is the Zeeman interaction between the observed nucleus and the external magnetic field; $H_{d,ii}$ is the interaction between the observed nucleus and the magnetic field generated by neighboring nuclei of the same species (homonuclear dipolar coupling); $H_{d,is}$ the interaction between the observed nucleus and the magnetic field generated by neighboring nuclei of the different species (heteronuclear dipolar coupling); $H_{cs,is}$ the interaction between the observed nucleus and nearby bonding electrons (chemical shift interaction); $H_{rf(t)}$ is the experimentally controlled Hamiltonian produced by the magnetic component of r.f. irradiation; and R(t) is the coupling of observed nuclei to fluctuating magnetic fields in the lattice, primarily a result of phonon (thermal) modes or due to paramagnetic centers. This last component represents the process by which the spin system comes to equilibrium with the external field and is known as spin-lattice relaxation.

The Zeeman interaction is the dominant term in the total Hamiltonian, and the other terms are treated as perturbations on the Zeeman term. The effects of this term can be eliminated from (1) by changing the reference frame to one rotating at the resonant frequency of the observed nucleus. In addition, manipulation of $H_{rf(t)}$ allows selective suppression of the remaining Hamiltonians, simplifying the interpretation of the resulting spectra.

The homonuclear and heteronuclear dipolar couplings, $H_{d,ii}$ and $H_{d,is}$, between NMR active nuclei are responsible for a significant portion of the line broadening observed in the NMR spectra of solids. For diamond films with low hydrogen concentrations, the homonuclear coupling term $H_{d,ii}$ is small, and only the hetertonuclear term will be important. The dipolar coupling between ^1H nuclei is a strong function of internuclear spacing and depends on the angle between the internuclear vector and the direction of the applied magnetic field. The dipolar decoupling term, D, (Komoroski, 1986) of the Hamiltonian $H_{d,is}$ may be expressed as:

$$D=h\gamma_c\gamma_H(3\cos^2\theta-1)/2\pi r^3 \qquad (2)$$

where γ_c and γ_H are the carbon and proton gyromagnetic ratios which are proportional to the magnetic moments of the nuclei; θ is the angle that the C-H vector makes with the external field; h is Plank's constant; and r is the distance between the nuclei. From this formula, it is seen

that the heteronuclear dipolar decoupling term is a strong function of internuclear distances. The polycrystalline nature of diamond films produces C-H vectors of all possible orientations, and their individual contributions inhomogeneously broaden the normal spectra toward a Gaussian shape. In solutions, the effects of dipolar coupling are removed by very rapid rotational and transnational motions which average the angle dependent term to zero. Weak dipolar decoupling interactions of a solid sample may be reduced by mechanically spinning the sample at 54.74°, which is known as the magic angle. Rotation at this angle at speeds greater than the dipolar linewidth, called magic angle spinning (MAS) (Komoroski, 1986), reduces the $3\cos^2\theta - 1$ term to zero.

The chemical shift interaction, $H_{cs,is}$, arises from the surrounding electrons which shield the nuclei from the external magnetic field. The chemical shift is directionally dependent, as the electronic shielding varies in a molecule. Once again, rapid molecular reorientation in liquids reduces these contributions of the anisotropic chemical shift to an isotopic average. For solids, the chemical shift anisotropy (CSA) will cause individual peaks to overlap and can reduce the spectrum to a featureless mound. MAS at or above half the width of the CSA pattern will reduce the anisotropy to its isotopic average, but also produces rotationally dependent sidebands which appear about the central peak at distances equal to the spinning speed.

Materials and Methods

Sample Preparation.--Two 600 mg samples of diamond film labeled TD 1114 and TD 1117 were obtained from Norton Diamond Films. The samples were gently broken with an agate mortar and pestle so that they would fit into the 9.5 mm sample rotor. The NMR used for the experiments is a GE GN300 with a Chemagnetics CMP 300 VTH solid state probe with MAS capability. A Chemagnetics Kel-F rotor was used to spin the sample within the probe assembly. The Kel-F (polychlorotrifluoroethylene) rotor produces little NMR signal due to its large dipolar coupling which broadens the signal beyond high-resolution detection (Komoroski, 1986).

Before the samples could be used in an experiment, background hydrogen signals from airborne water vapor and contamination of the probe surfaces due to handling must be removed. The rotor and the samples were cleaned and soaked in a 120°C oven for 18 hours prior to the experiments to drive off any physi-sorbed water in them.

A simple one pulse experiment with a 5-second delay between signal averages was used to obtain proton spectra for the rotor only, for the rotor and the barium fluoride packing material, and for the rotor will barium fluoride packed around the TD1117 diamond film slivers. Additionally, the drive pressure of the MAS unit was varied to produce a static spectrum and spectra at two different speeds. The barium fluoride packing material was chosen due to its low proton content. Levy and Gleason (1993) extrapolated that a 0.45 g sample of barium fluoride contains ~3.5×10^{16} hydrogen atoms, which is the lowest published hydrogen detection level from a solids NMR experiment. The probe ninety degree pulse width was determined with a quadropolar doped (Cu_2SO_4) water sample in a peak inversion experiment. The experiment was allowed to run 4096 scans.

Results and Discussion

The TD1117 sample was chosen for the experiment because the included analysis indicated that it possessed the largest percentage of impurities (including hydrogen), and thus, a proton spectra could more easily be obtained (Beera, 1993). The rotor only experiment showed a flat response when scaled to the same intensity scale as the rest of the experiments. Similarly, the barium fluoride spectrum Fig. 1 indicated several unresolved Gaussian shaped peaks at from 0-2000 Hz. The static TD1117 diamond in the BaF_2 experiment (Fig. 2), shows a Lorentzian peak with a Gaussian base. This is expected for a static sample since the dipolar coupling and CSA broadening effects are present. Half-width at half-height measurements indicate a line width of 6000 Hz. MAS results for the TD1117 diamond film (Fig. 3 and 4), show a marked decrease in the line width to 35 Hz. Also present in the spectra are spinning sidebands from the CSA frequency mixing. In Fig. 3, three sets of spinning sidebands are evident; the sidebands at 3050 Hz and -1900 Hz are due to first order frequency mixing and indicate a spinning speed of 2500 Hz. The sidebands which occur within the primary sidebands are due to frequency folding because of the limited spectral width (10000 Hz) of the experiment. The spectrum in Fig. 4 shows only the primary Lorentzian peak with a small Gaussian component. The sidebands are evident at 3708 Hz and -2493 Hz which suggest a MAS speed of 3089 Hz. Also evident in theses spectra are the BaF_2 undifferentiated peak at 1500 Hz and perhaps a secondary peak downfield from the main 587 Hz diamond peak at 480 Hz. The relative height of the central diamond peak to the barium fluoride peak indicates that the diamond sample has many times more hydrogen than the barium fluoride sample. Future experiments will quantify the barium fluoride hydrogen, as well as the diamond hydrogen for the various chemical environments of the hydrogen in the samples.

Fig. 1. MAS proton spectra of barium fluoride. A small Gaussian peak extends from 2000-0 Hz, with an unresolved Lorentzian component at 1500 Hz. Intensity on all graphs is the same.

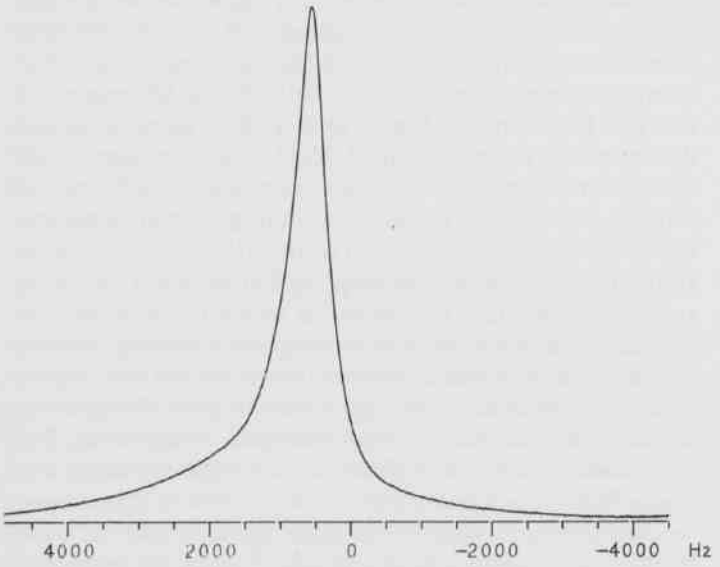

Fig. 2. Static proton NMR spectrum of TD1117 synthetic diamond thin film. The spectrum is broad due to the anisotropic effects of dipolar coupling and chemical shift anisotropy.

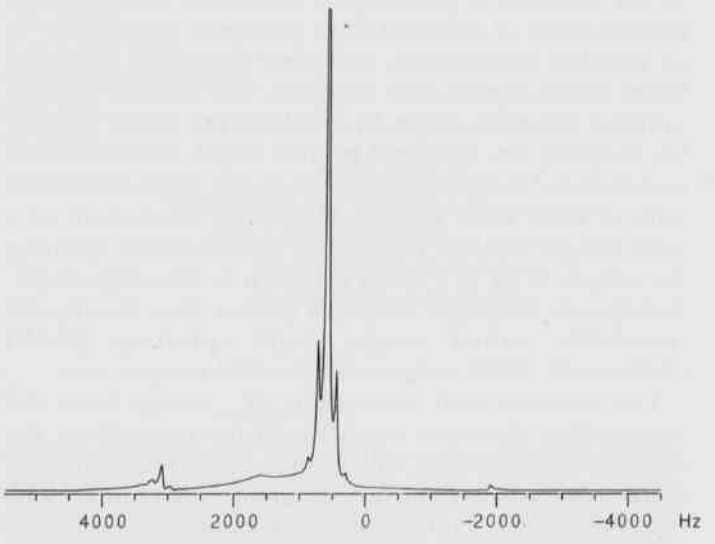

Fig. 3. MAS proton spectrum of TD1117 diamond film. Symmetrical peaks around larger central diamond peak are from spinning sidebands. The smaller peaks within the primary sidebands at 3750 and -2500 Hz are due to spectral width induced frequency folding. Primary sidebands indicate a MAS spinning speed of -2600 Hz. The small barium fluoride peak is evident at 1700 Hz.

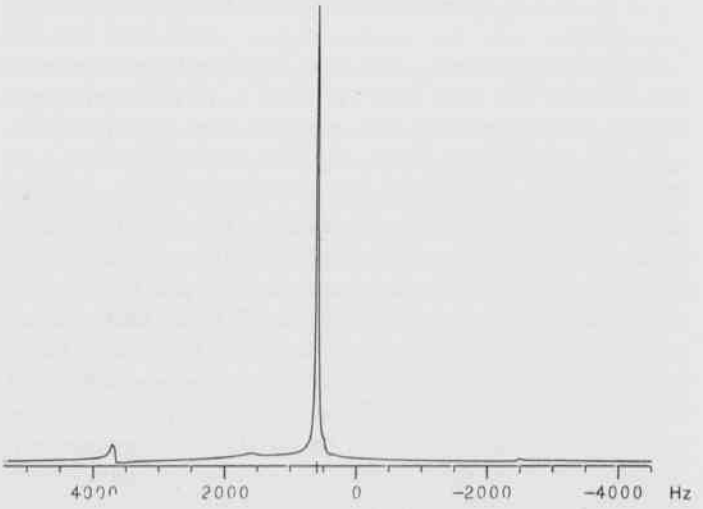

Fig. 4. MAS proton spectrum of TD1117 diamond film. Primary sidebands indicate a MAS spinning speed of ~3080 Hz. The small barium fluoride peak is again evident at 1700 Hz. A small peak on the right shoulder of the central peak can be seen possible indicating a secondary proton environment.

Literature Cited

Beera, R.A. 1993. Characterization of Diamond Samples, Internal Document.

Komorowski, R.A. 1986. High Resolution NMR Spectroscopy of Synthetic Polymers in Bulk, VCH, 16-61.

Levy, D.H. and **K.K. Gleason.** 1993. Nuclear Magnetic Resonance Probe for Low Level Hydrogen Detection, J. Vac. Sci. Technol., Vol 11(1): 195-198.

McNamar, K.M. and **K.K. Gleason.** 1992. Selectively ^{13}C-Enriched Diamond Films Studied by Nuclear Magnetic Resonance, J. Appl. Phys., 71(6): 2884-2889.

Application of Machine Learning Principles to Modeling of Nonlinear Dynamic Systems

Murray R. Clark
Department of Electronics and Instrumentation
University of Arkansas in Little Rock
2801 S. University ETAS 575
Little Rock, AR 72204

Abstract

A method for the development of mathematical models for dynamic systems with arbitrary nonlinearities from measured data is described. The method involves the use of neural networks as embedded processors in dynamic system simulation models. The technique is demonstrated through generation of models for anharmonic oscillators described by the Duffing Equation and the Van der Pol Equation from measured input/output data. It is shown that high quality models of these systems can be developed using this technique which are efficient in terms of model size. Using neural networks as embedded processors, accurate models of the Duffing Oscillator and the Van der Pol Oscillator were generated which contained eighteen parameters in each case. The architecture used requires that the neural networks perform only function fitting, a task to which they are well suited while integrators handle the modeling of energy storage by the system. This allows model parameter count to remain low, averting the undesirable high parameter counts sometimes associated with neural network based models. Model architecture, test problem specification, model optimization techniques used, quality of the models produced, practical applications and future work are discussed.

Introduction

The development of accurate models for systems exhibiting both nonlinear and dynamic behavior is a topic of considerable interest to professionals in a broad spectrum of fields, including signal processing, control, structural science, and ecology. The use of modern computing tools and algorithms such as neural networks and conjugate gradient learning have allowed the iterative solution of problems previously prohibitive in size and defiant of analytical solution. Linear dynamic systems, on the other hand, are well understood, with numerous tools available for their identification. This paper explores the use of neural networks as function fitting modules embedded in differential-equation-based models of nonlinear dynamic systems.

In the evaluation of a new modeling technique, simple systems offer an opportunity for such evaluation to be carried out with maximum comprehensibility of the results. The Duffing and Van der Pol Oscillators are singe-degree-of freedom (SDOF), second order, nonlinear processes which have been used as test problems for nonlinear system identification method evaluation previously (Masri, 1979), (Masri, 1993). For these reasons, the identification of these systems was chosen as the test problem set here.

In order to extend an SDOF linear model of a constant mass mechanical system to include nonlinearity, accomodation must be made for two possible sources of nonlinear behavior: nonlinear spring characteristics and nonlinear damper characteristics. A single neural network can be used to provide a function mapping capable of representing a spring-damper combination of arbitrary characteristic (Masters, 1993). This method has been demonstrated previously (Masri, 1993) in the successful development of a neural network based model for the Duffing Oscillator. In this work, it is demonstrated that the embedded network architecture gives much flexibility as the Duffing and Van der Pol Oscillators are here modeled using identical topology (only the parameters are changed); furthermore, accurate models can be constructed using very small neural networks, resulting in compact, high-quality system models. Usage of a few terms essential to the discussion will be clarified before proceeding further: A Linear System is one possessing the properties of additivity and homogeneity as commonly referred to in system theory. A Dynamic System is a history dependent system; for mechanical systems, this implies energy storage. Those processes which do not store energy will be referred to as static systems. A Time Invariant System is a process whose transfer function does not change with time. The work presented here will focus on the identification of systems representable as a mass-spring-damper combination, where the mass is constant, and the spring-damper combination may possess arbitrary characteristics. A schematic representation of such a system is shown in Fig. 1. The type of systems to be identified here are therefore nonlinear, dynamic, and

time invariant.

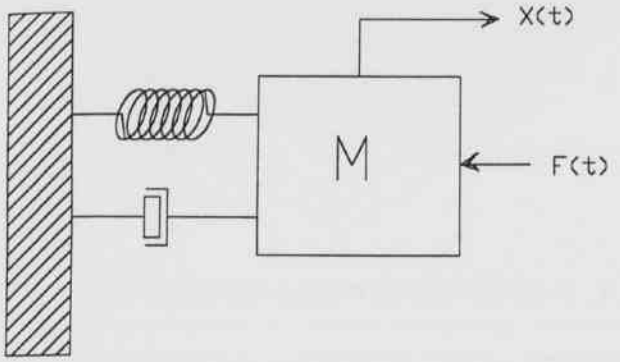

Fig. 1. Schematic representation of mass-spring-damper system.

Materials and Methods

Architecture of the Model.--The modeling method to be demonstrated is based on the well-known analog computer simulation architecture shown in Fig. 2. Here, integrators, adders and linear amplifiers are used to numerically solve the describing differential equation for a mass-spring-damper system:

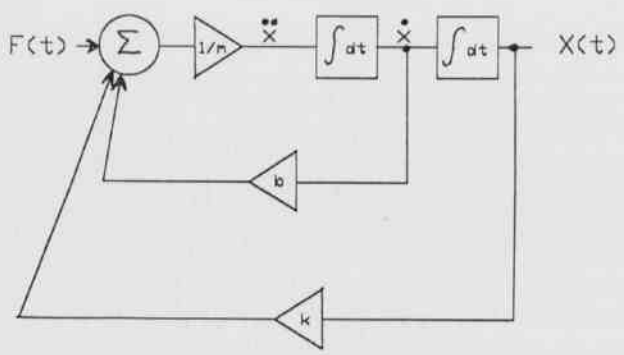

Fig. 2. Simulation architecture for a linear, second order, single degree of freedom system.

$F(t) = m\ddot{x} + b\dot{x} + kx$
where:
F(t) is the force input to the system (N),
x(t) is the position output (m),
m is the mass (kg),
b is the damping constant (N-s/m),
k is the spring constant (N/m).

In order to extend this model to accomodate systems with nonlinear spring and damper characteristics, the force terms $b\dot{x}$ and kx must be replaced by an appropriate nonlinear function of velocity and position. This mapping of position and velocity can be accomplished using a feedforward neural network as shown in Fig. 3.

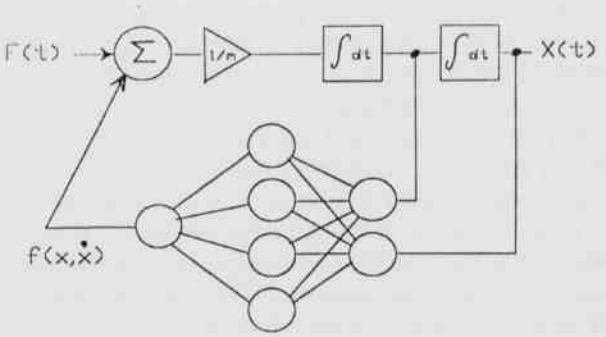

Fig. 3. Simulation model with embedded neural network for calculation of force function of nonlinear spring-damper combination.

Specification of the Test Problems.--In order to demonstrate the modeling technique, input and output data were generated through numerical solution of two well known nonlinear differential equations: the Duffing equation and the Van der Pol equation, listed below.

Duffing Equation
$F(t) = m\ddot{x} + b\dot{x} = k_1x + k_2x^3$
in the present study, this equation was modified to include a coupling term, resulting in a spring-damper characteristic that is nonlinear in both position and velocity, and thus a more challenging function fitting problem for the network.

$F(t) = m\ddot{x} + b\dot{x} + k_1x + k_2x^3 + a\dot{x}x^2$
where: m=500e-9, b=0.001, k_1=1.0, k_2=0.015, a=5e-6
These values were chosen to give an interesting amplitude and frequency response.

Van der Pol Equation
$F(t) = m\ddot{x} - a\dot{x}(1 - x^2) + x$

where: m=0.2, a=0.2
This is nonlinear in position and velocity. Parameter values were chosen to give an interesting amplitude and frequency response.

Model Optimization Techniques.--The method of training the networks to accurately map position and velocity to force for each oscillator to be identified is now described. If the force is due to a spring and damper of arbitrary characteristics is denoted as $f(x,\dot{x})$, the differential equation governing the motion of a constant mass system containing them becomes $F(t) = m\ddot{x} + f(x,\dot{x})$. Solving for this force gives $f(x,\dot{x}) = F(t) - m\ddot{x}$.

By recording many data points representing $F(t)$ and $x(t)$ and then numerically estimating the first and second time derivatives of $x(t)$ at each point, an array of data $x,\dot{x},f(x,\dot{x})$ can be found for each data point. A subset (400 well-spaced points) of this list of inputs (position and velocity) and resulting output (force due to spring-damper combination) are used in the training of a feed-forward neural network that the network may learn an accurate mapping of the force function $f(x,\dot{x})$ of the system to be modeled. If the mass of the system is known or measurable, the model is completed. In the present study, the conjugate gradient algorithm (Masters, 1993) was used for training of the networks.

Probing Signals for Identification.--For each nonlinear oscillator to be identified, the training data was generated through excitation of the equation based simulation model with an amplitude modulated swept sine signal. This gave efficient coverage of the input space of the force function $f(x,\dot{x})$.

Results

Duffing Oscillator.--The force function $f(x,\dot{x})$ measured from the Duffing oscillator simulation is graphically depicted in Fig. 4. The effect of the cubic term in the nonlinear spring is clearly visible as an increasing nonlinearity in x. Note that for a linear system, the force function will be planar. The time domain output of the neural-network-based model of the Duffing oscillator is compared with that of the equation-based reference system in Fig. 5.

Van der Pol Oscillator.--The force function $f(x,\dot{x})$ measured from the Van der Pol oscillator simulation is graphically depiced in Fig. 6. The effect of the coupling between the spring and damper is clearly visible. The time domain output of the neural-network-based model of the Van der Pol oscillator is compared with that of the equation-based reference system in Fig. 7.

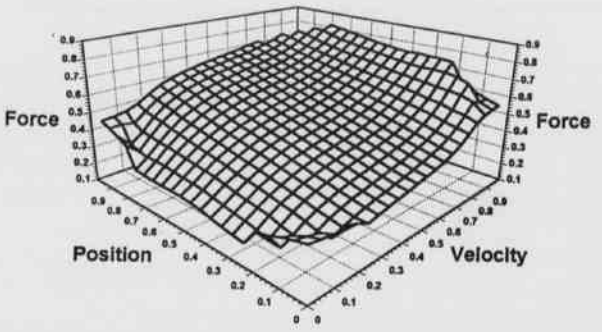

Fig. 4. Force function of Duffing Oscillator

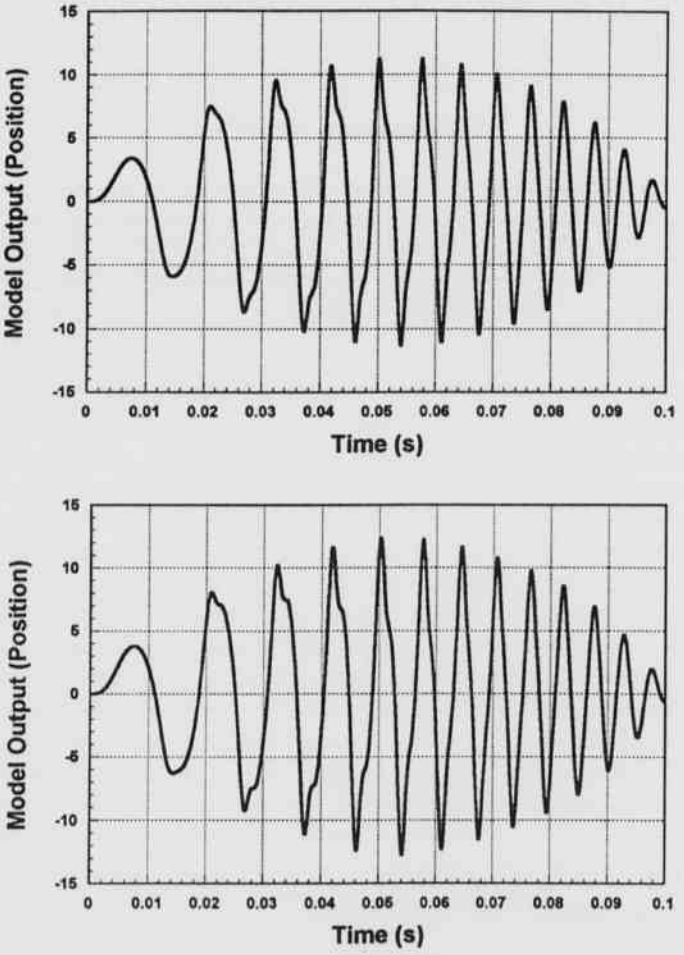

Fig. 5. Comparison of time domain response of reference system based on Duffing equation (top) with that of neural network based model (bottom).

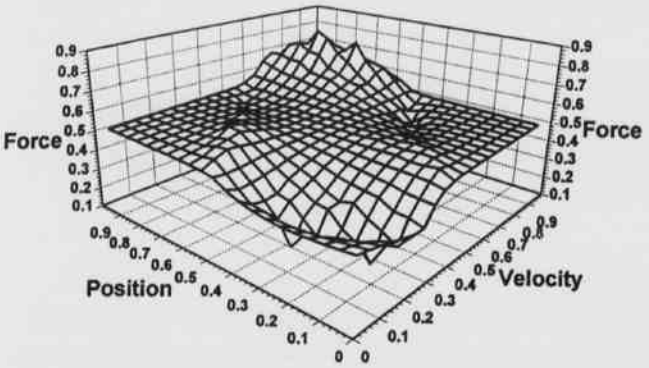

Fig. 6. Force function of Van der Pol Oscillator.

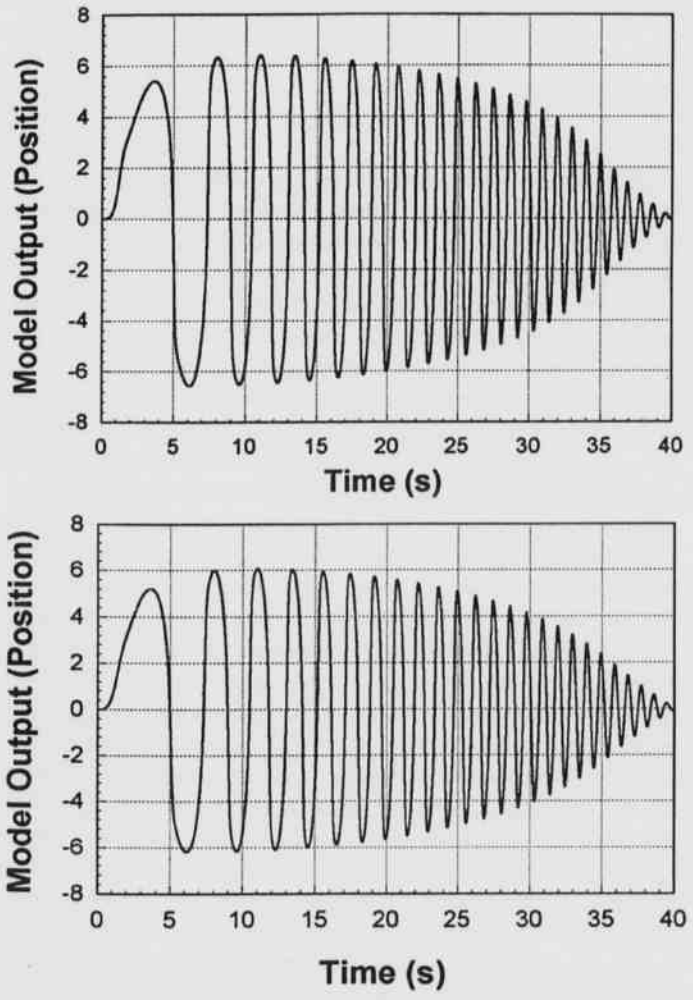

Fig. 7. Comparison of time domain response of reference system based on Van der Pol Equation (top) with that of neural network based model (bottom).

Discussion

Quality of the Models Produced.--As can be seen from Fig. 5, the time domain output of the neural-network-based Duffing oscillator model is very comparable to that of the equation-based reference model. In each case the input is an amplitude modulated swept sine signal. The output error can be seen to be small at all points. Similarly, good agreement is seen in Fig. 7 between the neural-network-based model of the Van der Pol oscillator and the equation-based reference model.

Complexity of the Models Produced.--In the Duffing oscillator model, the neural network employed contained two inputs, five hidden neurons, and one output neuron. This corresponds to seventeen network parameters (weights) in each model. This is slightly more complex than the orthogonal-polynomial-expansion-based model reported in (Masri, 1979), which used eight, but less complex than the normal network based model reported in (Masri, 1993) which contained 216. In the Van der Pol oscillator model, the neural network again employed seventeen network parameters (weights). This is less complex than the orthogonal-polynomial-expansion-based model reported in (Masri, 1979), which used 64. No precedent for comparison is found in the literature for a neural network based Van der Pol oscillator model. The low complexity of the model is most likely attributable to the assignment of tasks within it; feedforward neural networks perform static nonlinear mappings well, and an integrator is perhaps the most basic example of an energy storing device. Since these are the tasks here assigned, each component is utilized efficiently.

Complexity of Implementation of the Modeling Method.--The method was found to be easy to implement by the author, largely due to the fact that the architecture did not need to be changed from one problem to the next (only the network weights were changed), and because the training of these networks requires no special mathematical aptitude.

Applications of the Modeling Method.--Perhaps the most interesting application of nonlinear dynamic system modeling from measured data is the identification of a poorly understood process for the purposes of behavioral prediction or control. Possession of an accurate system model allows estimation of the response of the reference system to a hypothetical input, as well as offering benefit in the design of a controller for the reference system.

Future Work.--The next step in this work will be the development of a method for on-line optimization (as opposed to the training of the force function mapping network off-line as in the present work). Greater accuracy, as well as accommodation of time variance in the reference system could result. With on-line training, new training data can be incorporated into the training data

set as the reference system is observed, allowing the model to "track" gradual changes in the behavior of the reference system. The application of the modeling method to the development of controllers for nonlinear dynamic systems is an area of possible future work also.

Literature Cited

Masri, S.F. 1979. A nonparametric identification technique for nonlinear dynamic problems. J. Appl. Mech. 46:433-447.

Masri, S.F. 1993. Identification of nonlinear dynamic systems using neural networks. J. Appl. Mech. 60:123-133.

Masters, T. 1993. Practical neural network recipes in C++. Academic Press, London.

Spatial Distributions of Three Species of *Desmognathus* in a North Carolina Stream

James J. English
Department of Biology
University of Arkansas at Little Rock
Little Rock, AR 72204

Alvan A. Karlin
Department of Biology
University of Arkansas at Little Rock
Little Rock, AR 72204
Author for all correspondence

Laurie D. Lacer
Biotechnical Services, Inc.
4700 W. Commercial Dr.
North Little Rock, AR 72116

Abstract

Salamanders of the family Plethodontidae comprise the most common salamanders in eastern North America. It is not uncommon for more than 10 plethodontid species to occur syntopically in one creek. The purpose of this research was to determine whether the spatial distribution of one species affected the spatial distribution of other species. Geographic Information System technology and nearest-neighbor analyses were used to determine the spatial distributions of three species of the salamander genus *Desmognathus*. The analysis demonstrates that *D. ochrophaeus* and *D. monticola* change their spatial use from a random distribution during the day to a clumped distribution during evening hours. The data also suggest the *D. monticola* moves into the creek during evening hours.

Introduction

Over the past 40 years, salamander communities have provided excellent experimental systems for ecological experimentation on community organization (Hairston, 1949, 1986; Kleeberger, 1984; Roudebush and Taylor, 1987; Formanowicz and Brodie, 1993) because they provide the researcher long-lived animals with stable populations. Furthermore, salamander communities conform to many of the assumptions necessary for the theories of community organization and of evolution under the influence in interspecific interactions.

The plethodontid salamander genus *Desmognathus* consists of a series of species whose ecological preferences range from aquatic to semi-terrestrial. Concomitant with the particular species' ecological preference are morphologies, size ranges, and behaviors (Dunn, 1926; Hairston, 1949; Formanowicz and Brodie, 1993). In the southern Appalachian Mountains of eastern North America, communities of salamanders usually contain four to seven species of *Desmognathus* in addition to salamanders of three to five other plethodontid genera. Generally, the most terrestrial species is smallest, most brightly colored, and possesses the least keeled tail, whereas the most aquatic species is the largest, most heavily pigmented, and possesses the most fish-like tail. Species inhabiting intermediate ecological positions generally possess intermediate characteristics (Dunn, 1926).

In this study the relative positions of individuals of three species of *Desmognathus* in a North Carolina creek were analyzed. We investigated the following three species: (1) *D. quadramaculatus*, the largest and most aquatic salamander in the community; (2) *D. monticola*, an intermediate-sized species preferring aquatic environments (Roudebush and Taylor, 1987); and (3) *D. ochrophaeus*, a small, semi-terrestrial species. Specifically, our goal was to determine the feasibility of using Geographic Information System (GIS) technology to determine the following: (1) the spatial distribution of individuals of these three species; (2) whether diurnal spatial distribution could be differentiated from nocturnal spatial distribution; and (3) whether differential species' movements could be determined.

Methods and Materials

Field methods.--During the spring of 1993 (20 - 28 May), the Advanced Field Biology class from the University of Arkansas - Little Rock conducted the field experiment in Kinsey Creek, Deep Gap Vista, Macon Co., North Carolina. The headwaters of the creek form from a series of seepage areas that coalesce into a permanently flowing creek. A position approximately 50 m downstream from the seepage areas was selected. At this location the creek was clearly identifiable. A 90-m transect through the center of the creek served as a baseline to establish study plots. Each study plot was 10 m in length (along the creek) and 3 m wide (perpendicular to the axis of the creek.) Nine continuous 3 m by 10 m "creek-plots" were determined in this manner. Numbered surveyor's flags were used to demarcate the corners of each study plot.

Teams of students systematically searched plots by carefully observing the surface and by gently turning over and replacing rocks and debris. When a salamander was found, it was identified by species, and its position was marked by a color-coded surveyor's flag. Different colored flags were used for daytime and nighttime positions so

that a field map could be constructed for the study area. Ninety square meters of the total transect were searched each day (once diurnally and once nocturnally) for three consecutive days, for a total of 270 m² of study area.

Analytical Methods.--Geographic Information System ARC/INFO (ESRI, 1989) was used to digitize field maps into the computer. Once digitized, the data were translated into a planar coordinate system and scaled. Relative coordinates for salamander locations were used to construct analytical maps. Those coordinates were extracted and used for statistical analysis. Study maps were plotted using the animals' coordinates in the creek as points. A grid of 1 m² was superimposed on the study map. Each 1 m² was considered a sample unit for statistical analysis.

Statistical analysis involved two general analytical protocols. First, to determine the spatial distribution of the animals in the study area, their observed distribution was compared to a Poisson and a Negative Binomial distribution; Chi-square was used as the test statistic (Ludwig and Reynolds, 1988). Second, to determine the relationships between the positions of individuals with respect to other individuals or to the boulder centroids, nearest-neighbor analysis (Cressie, 1991) was used. To compare daytime nearest-neighbor distributions with nighttime nearest-neighbor distributions, the degrees of freedom were adjusted for non-independence, and analysis of variance (Legendre, 1993) served as the test statistic.

Results

During the three-day study period, a total of 346 salamander observations were recorded from the 270 m² of creek sampled. Because the study did not involve the removal of individuals, the number of unique salamander sightings was not determined. Nighttime observations accounted for 63% of all observations, whereas daytime observations accounted for 37% of the total. Although the number of *D. quadramaculatus* observations did not differ significantly between day and night (35 daytime: 43 nighttime; Chi-square = 0.82, ns), the number of *D. monticola* (31:103; Chi-square = 77.9, $P < 0.05$) and the number of *D. ochrophaeus* (54:79; Chi-square = 4.68, P , 0.05) sightings indicated significantly more nighttime observations were made.

The distribution of boulder centroids and salamanders was compared to a Poisson distribution. As the variance/mean ratio (= index of dispersion) was very close to 1, $|\underline{d}|$ (= the index of dispersion) was less than 1.96, and Chi-square value was not significant (Table 1), therefore the hypothesis that the boulders follow a Poisson distribution (=random) in the study area can not be rejected. Similarly, on an individual basis, each species is randomly distributed (i.e., variance/mean ratios are near unity, $|\underline{d}|$ less than 1.96, and not significant Chi-square values) during the daytime (Table 1). However, the observed distributions for *D. monticola* and *D. ochrophaeus* indicate a significant (variance/mean ration greater than 1, $|\underline{d}| > 1.97$, Chi-square, $P<0.05$) departure from expected values during the nighttime (Table 1). The direction of the departure suggests a clumped pattern, as indicated by the variance/mean ratios being greater than 1.0. Therefore, a comparison of these two distributions to a negative binomial was made. Chi-square values for *D. monticola* (Chi-square = 3.30, df = 2) and *D. ochrophaeus* (Chi-square = 4.59; df = 2) evening observations do not permit us to reject a departure from the negative binomial distribution.

Table 1. Spatial distribution of three species of *Desmognathus* in a North Carolina creek, May, 1993 compared to a Poisson distribution.

	Chi-Square[1]	d[2]	Variance: Mean ratio
Boulders	1.59 ns	0.609	1.05
Desmognathus monticola			
day (31)	0.07 ns	1.07	1.09
night (104)	10.56*	4.84	1.45
Desmognathus ochrophaeus			
day (54)	0.09 ns	1.15	1.10
night (79)	8.77*	7.36	1.72
Desmognathus quadramaculatus			
day (43)	0.09 ns	0.90	1.07
night (35)	0.01 ns	0.11	0.98

1- minimum of 5 observations per cell, df varied with case.
2- index of dispersion
* $P < 0.05$, ns = not significant

The results of the nearest-neighbor analysis indicate that the distances recorded at night and those recorded during the day between *D. quadramaculatus* and boulder centroids do not differ significantly (Table 2). Similarly, the nearest-neighbor distances between *D. quadramaculatus* and *D. ochrophaeus* do not change night vs. day. However, the nearest-neighbor distances between *D. quadramaculatus* and *D. monticola* are significantly smaller ($F_{1:38} = 23.29$, $P < 0.05$) at night (Table 2), as are the nearest-neighbor distances between *D. monticola* and *D. ochrophaeus* ($F_{1:66} = 16.22$, $P < 0.05$). To account for the difference in number of sightings (day vs. night), 20 inter-individual distances were randomly selected and the data reanalyzed. For each case there were no qualitative difference between the random sample and the entire data set.

Table 2. Nearest neighbor distances for three species of *Desmognathus* in Kinsey Creek, North Carolina.

Species	*Desmognathus monticola*	*Desmognathus ochrophaeus*	*Desmognathus quadramaculatus*
Boulders			
day	1.26	1.33	1.12
night	1.15 ns	1.08 ns	1.17 ns
Desmognathus monticola			
day (31)	1.36	2.30	2.51
night (104)	0.48 *	0.72 *	0.77 *
Desmognathus ochrophaeus			
day (54)		0.71	1.38
night (79)		0.72 ns	1.54 ns
Desmognathus quadramaculatus			
day (43)			1.02
night (35)			1.65 ns

*$P < 0.05$, ns = not significant

Discussion

Theories of community organization based on competition and niche partitioning (Hutchenson, 1959) have been challenged on several grounds (Simberloff, 1980; Hairston, 1986). The discussion of eco-evolutionary factors influencing desmognathine community structure and evolution began with Dunn's (1926) hypothesis linking *D. quadramaculatus*, by virtue of it's creek-bed habitat, to the prototypical *Desmognathus*. In Dunn's phylogeny, terrestrialism evolved as a response to competition pressure for optimum mid-creek habitat. Thus Dunn (1926) interpreted competition to be the single force that molded both evolution and community structure. Later, Hairston (1949) and Organ (1961) investigated desmognathine salamander communities and followed Dunn's interpretations.

However, Hairston (1980) re-evaluated his earlier conclustions concerning community structure resulting from competition in light of the assumptions for the competition models and the absence of experimental data. Hairston constructed a series of nine predictions based on the competition model. Of these, only three were confirmed. Competition appeared to be inadequate to explain or to describe the *Desmognathus* community. In this analysis, Hairston (1980) could produce no evidence for competition and invoked predation as the only eco-evolutionary force in desmognathine communities.

In a later paper, Hairston (1986) presented the results of four years of his experimental field removal studies. He constructed several specific hypotheses that could differentiate between competition and predation. Hairston (1986) demonstrated that both *D. monticola* and *D. quadramaculatus* were predators of *D. ochrophaeus*. This led him to suggest and demonstrate that if *D. ochrophaeus* were removed, *D. monticola* and *D. quadramaculatus* would compete. He concluded that both competition and predation occur within this apparently well-defined guild and warned of the danger of a casual interpretation of ecological observations.

Although the data from this study do not directly address either predation or competition, they do provide further evidence that the community spatial structure changes on a daily basis. Unlike the data presented from field enclosures (Southerland, 1986a; b), these observations were made in an unrestricted environment. Furthermore, although the data in this study do not differentiate between adult and juvenile individuals, all larvae (individuals under 3 cm snout-vent length) were excluded from our analyses.

It appears that the distribution of *D. quadramaculatus* in the creek is not influenced by other species' distributions. It's distribution with relation to the optimal boulder habitat (Roudebush and Taylor, 1987) did not change. However, the distributions of both *D. monticola* and *D. ochrophaeus* were observed to be clumped and individuals of both species appeared significantly closer to each other (Table 2) at night. Although the change in the distribution does not indicate a cause, several hypotheses can be constructed and tested. The purpose of this study was to determine the feasibility of using GIS to investigate the distributional aspects of community ecology and this has been accomplished.

The changes in distribution observed are consistent with the direction of change observed by Southerland (1986b) for enclosed *D. monticola* trials. It is suggested that *D. monticola* move from the forest floor into the creek at night. However, there was no observation of a concomitant decrease in the number of *D. quadramaculatus* or a shift in the position of *D. quadramaculatus*, as was suggested by Southerland (1986b). In fact, the number, position, and random distribution of *D. quadramaculatus* did not change, so no inference about either competition or predation can be made to account for the movements of *D. monticola*. Again, to eliminate competition or predation, specific removal experiments will need to be performed. If, for example, the removal of *D. monticola* results in *D. quadramaculatus* venturing further from the center of the creek (as determined by differences between day and night distances from boulder centroids), then competition is involved in generating the observed spatial distribution.

Similarly, if the removal of *D. ochrophaeus* intensifies the competition between *D. monticola* and *D. quadramaculatus* (as determined by increased clumpedness), then well defined patches of these species should be apparent in the creek. These and other experiments are currently in the planning stage.

Finally, the observations of this study were directed at only the 90 by 3 m area contained within the creek bed. Hairston (1949, 1980, 1986) and others included the forest floor up to 15 m from the creek and measured average distances from the creek. Incorporation of these additional habitats may provide additional insights into the diurnal and nocturnal dynamics and specific interactions in this community.

Acknowledgements

We thank the UALR 1993 Advanced Field Biology class, Drs. W. Baltosser and G. Heidt, G. Baltosser, T. LeCroy, and K. Stone, for their field assistance. We also thank the U.S. Department of Agriculture - Wayah District for their cooperation in this study.

Literature Cited

Cressie, N.A.C. 1991. Statistics for spatial data. John Wiley and Sons. New York.

Dunn, E.R. 1926. Salamanders of the family Plethodontidae. Smith College Fiftieth Anniversary Publ. Northampton, Mass.

ESRI. 1989. ARC/INFO: The Geographic Information System Software. Redlands, California.

Formanowicz, D.R. and **E.D. Brodie.** 1993. Size-mediated predation pressure in a salamander community. Herpetologica 49:265-270.

Hairston, N.G. 1949. The local distribution and ecology of the plethodontid salamanders of the southern Appalachians. Ecol. Monogr. 19:47-73.

Hairston, N.G. 1980. Species packing in the salamander genus *Desmognathus:* what are the interspecific interactions involved? Am. Nat. 115:354-366.

Hairston, N.G. 1986. Species packing in *Desmognathus* salamanders: Experimental demonstration of predation and competition. Am. Nat. 127:266-291.

Hutcheson, G.E. 1959. Homage to Santa Rosalia; or, why are there so many kinds of animals. Am. Nat. 93:145-159.

Kleeberger, S.R. 1984. A test of competition in two sympatric populations of desmognathine salamanders. Ecology 65: 1846-1856.

Legendre, P. 1993. Spatial autocorrelation: trouble or new paradigm. Ecology 74:1659-1673.

Ludwig, J.A. and **J.F. Reynolds.** 1988. Statistical ecology, A primer on methods and computing. John Wiley and Sons, Inc. New York.

Organ, J.A. 1961. Studies of the local distribution, life history, and population dynamics of the salamander genus *Desmognathus* in Virginia. Ecol. Monogr. 31:189-220.

Roudebush, R.E. and **D.H. Taylor.** 1987. Behavioral interactions between two desmognathine salamander species: Importance of competition and predation. Ecology 68:1453-1458.

Simberloff, D. 1980. A succession of paradigms in ecology: essentialism to materialism and probabilism. Synthese 43:3-39.

Southerland, M.T. 1986a. Behavioral interactions among four species of the salamander genus *Desmognathus.* Ecology 67:175-181.

Southerland, M.T. 1986b. Coexistence of three congeneric salamanders: The importance of habitat and body size. Ecology 67:721-728.

A Comparison of High-Temperature Superconductors in Multi-Chip Module Applications

D.E. Ford, S.S. Scott, S.S. Ang and W.D. Brown
High-Density Electronics Center (HiDEC)
Department of Electrical Engineering
University of Arkansas
Fayetteville, AR 72701

Abstract

In the application of high-temperature superconductors (HTSCs) in multi-chip module (MCM) technology, it is first necessary to investigate the advantages and disadvantages of the various HTSC compounds. The standard criteria for comparing the suitability of HTSCs in electronics applications has been critical temperature (T_c) and critical current density (J_c). It is also necessary to consider the physical properties of HTSCs in relation to the various processing techniques required in fabrication of MCMs. These techniques can be grouped into four main areas: deposition, patterning, packaging, and characterization. The four main HTSC materials, Y-Ba-Cu-O, Bi-Sr-Ca-Cu-O, Tl,Ba-Ca-Cu-O and Hg-Ba-Ca-Cu-O, will be compared to determine which is most suitable for MCM application.

Introduction

In the decades since the popular advent of the transistor in the 1960s, there has been continual and steady improvement in both the performance and cost of electronics equipment through miniaturization. This effort has given us the multi-chip module (MCM) as the latest and most promising technique to be introduced. MCM technology improves the speed at which devices can operate and decreases the power lost by eliminating as much length as possible from the interconnection between the individual devices. With this new technology some new barriers to increased speed and performance have arisen. By concentrating all of the devices in one area, the problems due to Joulean heating (I^2R losses) and electromigration are increased. Also, the lack of recent improvements may indicate that the upper limit of the speeds that can be expected from current semiconductor devices using conventional interconnects have been reached.

All of these problems can be addressed by combining high-temperature superconductors (HTSCs) with MCMs. Some of the interconnecting lines may typically carry 50 - 100 mA of current. Therefore, they account for a major portion of the heat generated (Burns et al., 1993). Replacing the lines with zero resistance HTSCs eliminates these I^2R losses. This means less heat and less power consumed. The refrigeration required for HTSC operation further limits the overall heat production to less than that produced by the individual devices. All of this allows for an even greater decrease in the interconnection lengths which, in turn, maximizes the operating speed of the MCM.

HTSC devices have been shown to be more than 2.5 times faster than their semiconductor counterparts, use three orders of magnitude less power, and do not suffer from electromigration problems (Van Duzer and Tuner, 1981). Their use in MCMs should produce the next quantum jump in performance. A cross-sectional schematic of an MCM is shown in Figure 1.

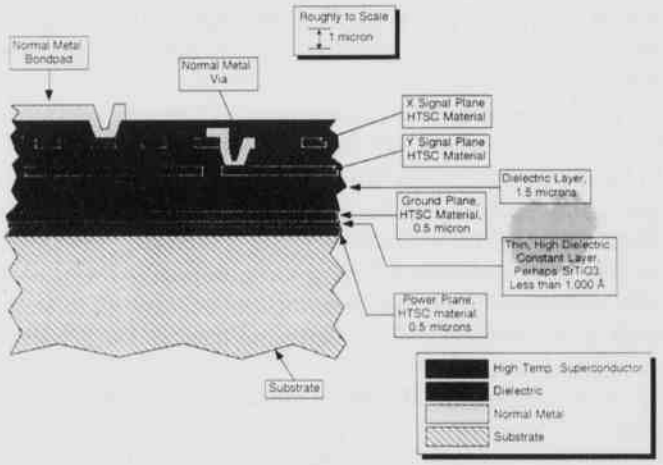

Fig. 1. Cross-sectional Schematic of a Superconducting Multi-Chip Module.

But, which HTSC offers the best overall prospects for MCM applications? This is the first question to be answered in the search for a viable superconducting MCM. When comparing HTSCs, the standard for suitability in electronics applications has been the materials critical temperature, (T_c), and critical current density, (J_c). It is

also necessary to consider the additional requirements and effects due to the different fabrication steps such as material deposition, patterning, packaging and characterization. This paper is the result of our research in each of these areas.

Using the initial criterion of T_c, a great number of HTSCs can be eliminated. The cost of cooling below liquid nitrogen temperature (77K) tends to preclude using HTSCs with T_c's any lower. The currently viable HTSC materials with T_c's above liquid nitrogen temperature can be separated in to four groups: yttrium-based, bismuth-based, thallium-based, and mercury-based. These four groups will be dealt with in this paper.

Yttrium

There are at least three variations to the yttrium-based HTSCs with the only significant differences being the T_cs (40K, 80K, 90K) and the ease of production. Fortunately, the highest T_c (90K) belongs to the phase of yttrium material that is the easiest to produce. $YBa_2Cu_2O_x$, known commonly as either YBCO or 123, was the first material discovered to superconduct above liquid nitrogen temperature (Wu et al., 1989). This fact and the relatively low toxicity of the component materials seem to be the only really good characteristics that YBCO possesses.

An ongoing study by our group at the University of Arkansas indicates that to achieve an effective current density, a given HTSC must be held to 10 - 20% below its T_c (Ulrich, 1994). While this is better than the 30% or $T_c/2$ values commonly accepted in the scientific community (Doss, 1989), it still puts YBCO at the very borderline for use with liquid nitrogen.

Most of the drawbacks encountered in the production of YBCO thin films can be tied to one problem. Due to critical mismatches in lattice parameters, it is difficult to get good epitaxial growth for YBCO on the viable low dielectric substrates in use today (Werder, 1991). This means that, no matter how good a deposition technique, YBCO films will tend to be comparatively rough in texture and have a limited J_c due to internal flaws in the achievable crystalline structure.

The deposition of YBCO on a substrate has typically been accomplished using off-axis sputter deposition. While this method can produce usable thin films, it is often necessary to anneal these films in an oxygen ambient at approximately 450°C after deposition in order to correct for oxygen depletion and to achieve an acceptable T_c. Fortunately, an on-axis method has been demonstrated that produces thin films with T_cs of 88K and J_cs of greater than 10^6 A/cm^2 with no post annealing required (Blue and Boolchand, 1991). It should be noted however, that the current density for this material is only 10^4 A/cm^2 at 77K just as for most YBCO films (Jin et al., 1988).

Another successful method for the deposition of YBCO has been demonstrated using metalorganic chemical vapor deposition (MOCVD) combined with rapid isothermal processing (RIP) (Singh et al., 1991). With T_cs of 89K and J_cs of 1.5 x 10^6 A/cm^6 at 77K, this is by far the best method for producing YBCO films seen to date.

Pulsed laser deposition has also been used successfully to cover small areas, but this technique has proven to be a very costly and a difficult process to control (Burns et al., 1993). Laser deposition does seem to be an excellent choice for spot deposition of YBCO in applications such as individual connections between layers commonly called vias.

In the areas of patterning, packaging and characterization, there is another major drawback. YBCO has a very high affinity for water. When exposed to moisture, the properties of YBCO tend to degrade. This process is accelerated by flaws in the crystalline structure so common to current processing techniques. Another aspect of this fault is that YBCO tends to form an oxide skin layer. This means an added difficulty for any patterning process. Also, this creates a problem in making direct contact to YBCO films as is necessary for multilayer applications, metalization for packaging purposes, or just testing the material. With some small difficulty, this can be dealt with using a procedure consisting of a solution of bromine in methanol that will remove the skin layer (Vasquez et al., 1988). A non-superconducting surface layer can also be removed by brief exposure to a low-energy cleaning ion bombardment.

Yttrium-based HTSCs have been successfully etched using weak acidic solutions such as phosphoric, nitric and hydrochloric acids. However, YBCO's reactivity with the various substrates, while not notably greater than for other HTSCs, when combined with the noted skin effect creates a scum layer between the substrate and the YBCO thin film that seems impervious to these enchants.

Yttrium-based HTSCs can also be dry etched using either a reactive process with a halogen such as chlorine, or by argon ion milling. Both of these methods suffer from the same structural distortions found in deposition techniques. For the reactive process, it is necessary to either post-etch anneal or use a mask that can keep oxygen from escaping during the etching process. In argon ion milling, the problem can be solved by cooling the sample during the etching process, preferably with liquid nitrogen. But, since photoresist are often used for masking in both dry etching processes, the problem with moisture is still present.

Bismuth

There are several different bismuth based HTSCs, with

the highest T_c being ~114K for $Bi_2Sr_2Ca_2Cu_3O_x$, but it is very difficult to produce the higher T_c phase of this compound (Bi 2223). This is due to the intergrowth of the Bi 2212 phase which has a T_c of 85K. Many attempts to enhance growth of the 2223 phase have been made with varied results (Endo et al., 1988; 1989; Tarascon et al., 1988; Huang et al., 1990). One procedure produces good thin films, but requires a heating period of one week (Sleight, 1988). The most promising method seems to be the addition of lead in the form $Bi_{2-y}Pb_ySr_2Ca_2Cu_3O_x$ to stabilize the Tc. This method has produced T_cs in the usable range of 104 - 112K (Xin and Sheng, 1991). This is the most commonly encountered form of the bismuth compound and can be deposited using the same methods as described for YBCO. Most of the information gathered about the bismuth-based system has been for this lead mixed form. As other easily produced phases of the bismuth compound have lower T_cs than YBCO, they are of little interest to the MCM field.

The addition of lead to bismuth HTSCs defeats one of the bismuth compound's major benefits. That is, the relatively low toxicity of the elements used. While the lead can be incorporated easily, it will still require special handling like the thallium and mercury compounds.

Most reports of J_cs are somewhere above 10^4 A/cm² at 77K which is similar to YBCO (Doss, 1989). This is probably due, in part, to the difficulty in producing a pure phase of this material. The lattice parameters of the bismuth compounds, though not exact, are better matched to the low dielectric substrates than YBCO's. This would indicate better epitaxial growth and better J_cs. Comparison of the thermal power properties also indicates this conclusion (Xin et al., 1992). Indeed, a 110K sample with a J_c of 3.4 x 10^6 Z/cm² at 77K has been reported (Grenwald, 1991), but it should be noted that this sample did not contain lead and is not easily reproduced.

Bismuth-based HTSCs can be etched with the same methods as YBCO and slow none of the problems due to YBCO's affinity for moisture. Most forms of this compound appear to be fairly stable and much less brittle than YBCO. It should be noted that bismuth compounds require the same precautions for dry etching methods as YBCO, and although the etching damage is generally of a lesser extent, bismuth compounds can easily be destroyed during any annealing process.

Bismuth compounds have shown a tendency to flake in layers similar to mica (Doss, 1989). This could cause some slight problems in packaging, but should not prove to be a major concern.

The only problems with the characterization of bismuth based HTSCs are directly related to the ability to produce a pure phase material.

Thallium

Like bismuth, thallium-based HTSCs exist in many different phases. Unlike bismuth, however, the highest T_c (125K) phase is relatively easy to produce. $Tl_2Ba_2Ca_2Cu_3O_x$, commonly referred to as Tl2223, has one major drawback. Thallium is a very toxic substance that can be absorbed through the skin. It can be absorbed over a period of time and is not normally purged from the body. Therefore, proper precautions must be taken when dealing with this material. Special precautions should be taken when working with lead or mercury. However, the precautions required for working with these materials are only slightly more than those normally observed in a conscientious production facility (Chelton et al., 1991). As these facilities are already dealing with arsenide, cyanides, and many other toxic compounds, the addition of thallium should present no insurmountable problems.

Excellent quality thin films of the 2223 phase have been deposited by several methods such as spin coating, spray pyrolysis, sputtering, thermal evaporation, electron beam, laser ablation, and MOCVD (Shih and Qiu, 1988; Ichikawa et al., 1988; Ginely et al., 1989; Hammond et al., 1990; Collins et al., 1991; Liu et al., 1991; Malandrino et al., 1991), but the method of choice seems to be the post deposition annealing technique. First, a precursor layer of BaCaCuO of the desired stoichiometry is sputter deposited onto a substrate. Then the film is annealed in thallium vapor which drives the thallium into the matrix forming the actual HTSC. While a one step sputter deposition is possible, the two step method consistently provides better results with average T_cs of 125K and J_cs typically above 10^6 A/cm² at 77K (Grenwald, 1991). This includes the best quality samples to date with a J_c of over 10^7 A/cm² at 77K (Chu et al., 1991). The two step method may also have a hidden benefit in that it isolates thallium contamination to the furnace used for the drive-in procedure.

The lattice parameters for the 2223 phase are much closer to those of the low dielectric substrates with as little as 0.75% mismatch for CeO_2 (Holstien et al., 1992). This means better epitaxial growth and smoother films than possible with either YBCO or bismuth (Lee et al., 1992).

Thallium-based HTSCs can be etched using the same methods as yttrium-based and bismuth-based compounds, but because of the greater stability, require less attention to reactivity and oxygen loss. The preliminary results from a wet etch process our group is currently investigating indicates that the extra strength and consistency of 2223 films makes the etching process much easier to control.

Other than the special precautions for dealing with thallium 2223 makes no special demands on packaging or characterization. Indeed, the additional strength can only serve to make these processes easier. A comparison of T_c curves for Yttrium, Bismuth and Thallium superconduc-

tors is shown in Fig. 2.

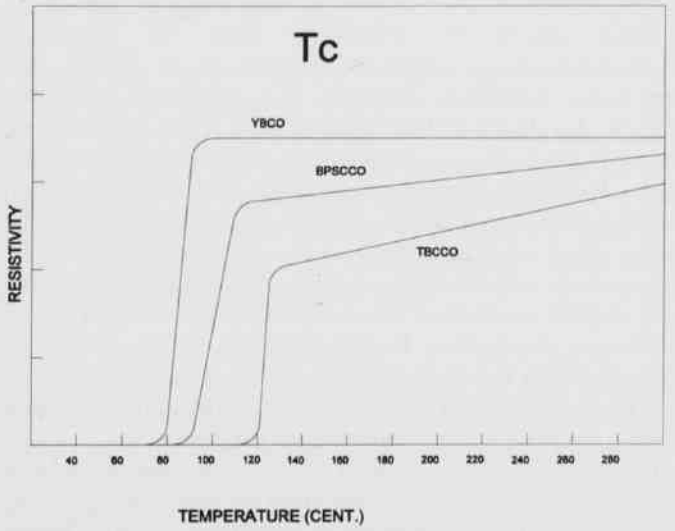

Fig. 2. Comparison of Typical T_c Curves.

Mercury

The recent discovery of mercury based HTSCs with possible T_cs above the 145K boiling point of Freon™ is truly exciting. But, as of yet, little is known of the characteristics of the mercury-based compounds. The $HgBa_2Ca_2Cu_3O_x$ phase (Hg 1223) with the highest T_c of 135K at ambient pressure has been shown to increase to a T_c of over 150K under hydrostatic pressure (Chu et al., 1993). However, 1223 is not produced without some amount of effort. 1223 thin films have currently been produced only by post deposition annealing under special pressure controlled conditions. With the additional cost due to current government efforts to ban the use of Freon™, the added effort necessary to produce the material and then maintain the hydrostatic pressure, means that practical Freon™-cooled HTSCs are still far in the future. Indeed, the added effort required just to achieve an additional 10K increase in T_c from thallium's 125K to 135K seems to serve no purpose, but improvements could be just over the horizon.

The reported lattice parameters combined with the initial troubles in separating out the different phases, tend to indicate that 1223 will have a J_c somewhat less than the thallium-based HTSCs (Huang et al., 1993), but this remains to be confirmed. The bottom line with mercury-based HTSCs is that we just don't know yet. A comparison of the J_c's of the four materials is shown in table 1.

Table 1. Critical Current Density (J_c) in A/cm².

	YBCO	BSCCO	TBCCO	HBCCO
TYPICAL	10^4	10^4	10^6	?
MAXIMUM	1.5×10^6	3.4×10^6	2.8×10^7	?

Summary and Conclusion

Yttrium base HTSCs, while having several drawbacks, have only one advantage. The comparatively low toxicity of the component materials. While, bismuth-based HTSCs have much more to offer than the yttrium based compounds, the current production of viable bismuth thin films requires the additional of lead. This tends to nullify any benefits relative to thallium-based HTSCs. Most processes used in MCM production have been demonstrated for thallium HTSVs with significantly better results than any other material. Mercury-based materials have shown some prospects and raised some new questions, but until they can be produced with more ease and characterized more definitively, they offer no apparent advantages. However, they definitely warrant more research.

While the evidence does not totally rule out any of the candidate HTSCs, the majority of the information indicates that thallium-based HTSCs should be the HTSC of choice in MCM applications.

Acknowledgements

This research was funded by E-Systems, Melpar Division.

Literature Cited

Blue, C. and **P. Boolchand,** 1991, Appl. Phys, Lett., vol. 58,p. 2036-2038.

Burns, M.J., K. Char, B.F. Cole, W.S. Ruby and **S.A. Sachtjen.** 1993. Appl. Phys. Lett., vol. 62, p. 1435.

Chelton, C.F., M. Glowatz and **J.A. Mosovsky.** 1991. IEEE Trans. on Educ., vol. 34, p. 269-288.

Chu, M.L., H.L. Chang, C. Wang, J.Y. Juang, T.M. Uen and **Y.S. Gou.** 1991. Appl. Phys. Lett., vol. 59, p. 1123-1125.

Chu, C.W., L. Gao, F. Chen, Z.J. Huang, R.L. Meng and **Y.Y. Xue.** 1993. Nature.

Collins, B.T., J.A. Ladd and **J.R. Matey.** 1991. J. Appl. Phys., vol. 70, p. 2458.

Doss, J.D. 1989. *Engineer's Guide to High-Temperature Superconductivity,* John Wiley and Sons, New York.

Endo, U., S. Koyama and **T. Kawai.** 1988. Jpn. J. Appl. Phys., vol. 27, p. L1467.

Endo, U., S. Koyama and **T. Kawai.** 1989. Jpn. J. Appl. Phys., vol. 28, p. L190.

Ginely, D.S., J.F. Kwak, E.L. Venturini, B. Morosin and **R. J. Baughman.** 1989. Physics C., vol. 160, p. 42.

Grenwald, A.C. 1991. Microelec. Manuf. Tech., p. 25.

Hammond, R.B., G.V. Negrete, L.C. Bourne, D.D. Strother, H. Cardona and **M.M. Eddy.** 1990. Appl. Phys. Lett., vol. 57, p. 825.

Holstien, W.L., L.A. Parisi and **D.W. Face.** 1992. Appl. Phys. Lett., vol. 61, p. 982-984.

Huang, Y.T., C.Y. Shei, W.N. Wang, C.K. Chiang and **W.H. Lee.** 1990. Physics C, vol. 76, p. 169.

Huang, Z.J., R.L. Meg, X.D. Qiu, Y.Y. Sun, J. Kulick Y.Y. Xue and **C.W. Chu.** 1993. Physics C.

Ichikawa, Y., H. Adachi, K. Setsune, S. Hatta, K. Hirochi and **K. Wasa.** 1988. Appl. Phys. Lett., vol. 53, p. 919.

Jin, S., T.H. Tiefel, R.C. Sherwood, R.B. van Dover, M.E. Davis, G.W. Kammlott and **R.A. Fastnacht.** 1988. Phys. B, vol. 37, p. 7850-7853.

Lee, W.Y., S.M. Garrison, M.Kawasaki, E.L. Venturini, B.T. Ahn, R. Boyers, J. Salem, R. Savoy and **J. Vazquez.** 1992. Appl. Phys. Lett., vol. 60, p. 772-774.

Liu, R.S., J.L. Tallon and **P.P. Edwards.** 1991. Physics C, vol. 182, p. 119.

Malandrino, G., D.S. Richeson, T.J. Marks, D.C. Degroot, J.L. Schindler, C.R. Kannewurf. 1991. Appl. Phys. Lett., vol. 58, p. 182.

Shih, I. and **C.X. Qiu.** 1988. Appl. Phys. Lett., vol. 53, p. 523.

Singh, R., S. Sinha, N.J. Hsu, J.T.C. Ng, P. Chou and **R.P.S. Thakur.** 1991. J. Vac. Sci. Technol., vol. A-9, p. 401-404.

Sleight, A.W. 1988. Science, vol. 242, p. 1519-1527.

Tarascon, J.M., W.R. McKinnon, P. Barboux, D.M. Hwang, B.G. Bagley, L.G. Greene, G.W. Hull, Y. LePage, N. Stoffel and **M. Giroud.** 1988. Phys. Rev. B, vol. 38, p. 8885.

Ulrich, R. 1994. Private communication, Chemical Engineering Dept. University of Arkansas.

Van Duzer, T. and **C.W. Turner.** 1981. *Principles of Superconductive Devices and Circuits,* Elsevier, New York.

Vasquez, R.P., B.D. Hunt and **M.C. Foote.** 1988. Appl. Phys. Lett., vol. 53, p. 2692-2694.

Werder, D.J. 1991. Physics C, vol. 179, p. 430-436.

Wu, M.K., J.R. Ashburn, C.J. Torng, P.H. Hor, R.L. Meng, L. Gao, Z.J. Huang, Y.Q. Wang and **C.W. Chu.** 1989. Phys. Rev. Lett., vol. 58, p. 908-910.

Xin, Y. and **Z.Z. Sheng.** 1991. Physics C, vol. 176, p. 179-188.

Xin, Y., D. Ford and **Z.Z. Sheng.** 1992. Rev. Sci. Instrum., vol. 63, p. 2263-2267.

A Classification System for the Natural Vegetation of Arkansas

Thomas Foti
Arkansas Natural Heritage Commission
Suite 1500, Tower Building
Little Rock, AR 72201
Xiaojun Li
Department of Biological Sciences
University of Arkansas
Fayetteville, AR 72701

Martin Blaney
Arkansas Game and Fish Commission
2 Natural Resources Drive
Little Rock, AR 72205
Kimberly G. Smith
Department of Biological Sciences
Univeristy of Arkansas
Fayetteville, AR 72701

Abstract

We present a hierarchical classification system for existing natural vegetation of Arkansas based on the United Nations Educational, Scientific and Cultural Organization (UNESCO) system. It incorporates aspects of systems in use by the Nature Conservancy, Arkansas Natural Heritage Commission, Arkansas Game and Fish Commission, Society of American Foresters, and United States Forest Service, as well as data on potential vegetation from maps by E.E. Dale and A.W. Kuchler. A total of 18 physiognomic cover types are recognized for natural terrestrial cover, 6 for palustrine cover, and 4 each for lacustrine cover and riverine cover. Over 200 community types are recognized, grouped into 57 cover types and 90 intermediate groupings. This system is appropriate for use with remotely sensed data and the level of detail dealt with can be rationally adjusted by working at a higher or lower level of the hierarchy. We suggest that this system form the basis for future vegetation analyses and research within Arkansas.

Introduction

The Arkansas Gap Analysis Project (see Scott et al., 1993 for a complete discussion of Gap Analysis), being conducted by the University of Arkansas in cooperation with several other academic institutions, state and federal agencies, and private organizations, will produce a map of existing vegetation and potential vertebrate distribution within Arkansas. The map will be created from satellite imagery, GIS maps of geology, topography, soil and other physical features, and databases of species occurrence and habitat characteristics.

The vegetation units mapped will be those that can be distinguished on satellite imagery and GIS data layers. It is expected, based on results in other states, that approximately 50 vegetation units will be mapped. It is desirable for maximum utility of the map that these map units be related to an overall classification of Arkansas vegetation. Therefore one of the initial priorities of the Arkansas GAP was to produce such a vegetation classification for Arkansas.

Several plant community classifications exist for Arkansas (AGFC, 1948; Moore, 1959; Foti, 1974; Pell, 1981; Dale, 1986; and unpublished classifications used by several agencies cooperating in this project). A valuable published classification exists for Missouri (Nelson, 1985). Several national classifications have applicability within Arkansas (Eyre, 1980; Kuchler, 1964). However, since plant communities are not discrete entities, each classification is a reflection of the philosophy of the creator and the philosophies vary.

None of these classifications met the needs of all agencies cooperating in the Arkansas GAP. Most were too general for GAP purposes; several (Foti, 1974; Pell, 1981; Nelson, 1985) combine physical and biological diagnostic features, e.g. Dry-Mesic Oak-Hickory Forest. Including both physical and biological features simplifies a classification in that, using the above example, it is not necessary to distinguish the various combinations of *Quercus alba, Q. falcata, Q. velutina, Carya tomentosa, C. texana* and other species that may dominate such sites. However, such simplification of biological communities inevitably results in loss of information.

The technology being used in the Arkansas GAP, GIS and remote sensing, allows physical features of sites to be characterized using digital elevation models, geology, and soil layers while vegetation or land cover can be independently classified based on satellite or other imagery.

In addition to ecosystemic classifications which classify physical features to indirectly classify vegetation (such as those classifications discussed above) two general approaches focus strictly on vegetation: physiognomic and floristic (Whittaker, 1978).

Physiognomic classification depends on morphological characteristics (structure) of vegetation, and it is primarily determined by growth-form and life-form of the dominant or codominant plants. Physiognomic classification is extensively used to characterize vegetation over large geographical areas because it can be visually recognized and distinguished and does not require much floristic detail

about the vegetation.

The floristic approach focuses on analysis and synthesis of the floristic composition of communities. The diagnostic species, which occupy ecological niches of different dimensions, are used to characterize the basic unit (association) as well as higher units of the classification hierarchy.

Arkansas Vegetation Classification System Assumptions and Methods

For the reasons stated above, it was decided that the Arkansas vegetation classification would be based strictly on biological features of the community.

Further, it was desired that the product of this effort be a hierarchical framework to allow the level of detail to vary for different users and, since GAP is a national effort, that the vegetation units recognized here should be as compatible as possible with those of other states.

Three assumptions are made for the vegetation classification system of Arkansas (based on recommendations from National GAP): 1) This system is used to describe actual or existing vegetation rather than potential or climax vegetation; 2) It does not include transition zones of vegetation (the level of detail at the lowest level is high enough that some units considered by others to be transition zones are recognized as units); and 3) It is open-ended in that categories may be added to any of the hierarchical levels as long as the additions are truly an equivalent category within the given classification level. Furthermore, it is reasonably easy to combine units recognized here and produce a classification that can be readily correlated to this one.

Based on the approach adopted for the National Gap Analysis Project (Scott et al., 1993), the vegetation classification system of Arkansas presented here follows the UNESCO (United Nations Educational, Scientific, and Cultural Organization) (1973) format with modification of the lower two levels (Jennings, 1993). This classification scheme offers a widely accepted and useful hierarchical grouping that is based primarily on 1) the physiognomic or structural expression of plant cover relative to environment at higher levels of the scheme, and 2) the floristic composition at lower levels.

There are six levels in this vegetation classification system: class, subclass, group, formation, cover type, and community type. The first four levels are physiognomic and the latter two are floristic (to the extent of defining dominant, diagnostic, or indicator species).

The following definitions of the levels of the hierarchy follow the definitions of National Gap Analysis project (Jennings, 1993) with slight modifications by us. The criteria used to define classification categories (e.g., woodland = tree canopy cover of 26-60%) are general. They are meant to be a means for grouping and discussing discrete cover types from coarse categories to finer categories. The growth-form and the life-form used in this classification system follow the growth-form categorization of Rubel (1930) and the life-form classification of Raunkier (1934), respectively.

Class.--There are six primary classes. The first five of these represent vegetation cover; the sixth represents substantial bare ground. The distinctions between classes representing vegetation are based on the spacing and height of dominant vegetation growth form.

1. *Forest:* Forests are dominated by trees with a total canopy cover of 61% or more and tree crowns usually interlocking.
2. *Woodland:* Woodlands are dominated by trees with a total canopy cover of 26-60%, most tree crowns not touching each other. A herbaceous or shrub understory, or both, are usually present. They are open stands of trees, sometimes called "open forest".
3. *Dwarf shrubland:* These are comprised of shrubs rarely exceeding 0.5 m in height at maturity. The type probably does not occur in Arkansas.
4. *Shrubland:* These are areas dominated by shrubs that generally range from 0.5 m to 5 m in height when mature, with a total canopy cover of 26% or more. A tree canopy cover of 26% or less may be present.
5. *Herbaceous:* These are areas dominated by grass, grass-like, or forb vegetation with a tree or shrub component not exceeding 25% cover.
6. *Barren/sparesely vegetated:* These are areas where vegetation cover is less than 5%. This type includes mud flats, sandy areas, and bare rock.

Note that such widely-used (but often inconsistently defined terms as "savanna", "prairie", "glade" and "barrens" are not used here. This is meant to reduce confusion in terminology. Some of these traditional terms, however, are used as common names in the classification or in descriptions of the units.

Subclass.--Subclasses are categories within each class comprised of areas in which the main vegetation is morphologically similar. For the classes of forest, woodlands, dwarf shrublands and shrublands the similarities are based on these factors:

1. evergreen;
2. deciduous or mixed.

For the class of herbaceous the similarities are based on:

1. tall grasses, more than 1.0 m in height;
2. medium-tall grasses, from 0.5 to 1.0 m in height;
3. short grasses, less than 0.5 m in height;
4. forbs.

Group.--Groups are categories within each subclass which may be based on any of the following:

For forests, woodlands, and shrublands:

1. climate, e.g., tropical, temperature, subpolar;

2. morphology, e.g., broad-leaved, sclerophylous, needle-leaved.

Formation.--Formations are categories within each group comprised of areas in which the vegetation similarities are based on any of the following criteria.

Tree size and crown shape:

Non-giant forests are those 5-50 m in height having

1. rounded crowns, e.g., *Pinus echinata*
2. conical crowns, e.g., *Juniperus virginiana*

Life zone:

1. temperate lowland
2. montane
3. alpine

Substrate:

1. alluvial
2. serpentine

Kinds of associated vegetation, e.g., broad-leaved forest with or without evergreen needle-leaved trees, or with or without succulents.

Amount and kind of understory.

Cover type.--Cover type is a group of plant community types having the same primary dominant species and similar physiognomy; an aggregation of plant community types.

Community type.--The community type is an assemblage of plant species that interact at the same time and place and have defined species composition and physiognomy, regardless of seral stage; usually named by the names of the species that dominate the canopy layer.

A modification of the national model was made to allow users to more easily find wetland community types: at the highest level we distinguished Terrestrial, Palustrine, Riverine and Lacustrine systems (following Cowardin, 1979). In the national model these have been incorporated lower in the hierarchy (at the formation level). However, there are enough wetland types in the Arkansas classification that such an approach adds to confusion by users. If a user desires, it should be straightforward to place these groups at the formation level. In either event it should be understood that these units are a classification of the emergent vegetation of wetland communities, not a classification of the physical wetland communities.

By agreement of the review committee, as well as National GAP guidance, community types that are the result of human activity, e.g., urband and agricultural areas, are not included in this scheme, but widespread successional communities that may result from previous human disturbance are included.

The first draft of the vegetation classification system was generated by correlating several of the existing classification systems that are in use within Arkansas. These included the vegetation classification of Arkansas developed by Dale (1986); the system used by the Society of American Foresters (Eyre, 1980) and that developed by Kuchler (1964), the unpublished classifications used by the U.S. Forest Service and the Arkansas Natural Heritage Commission (based on Pell, 1981), and the unpublished vegetation cover types used by the Arkansas Game and Fish Commission. We also referred to other sources, such as the unpublished southeast and midwest regional ecological community classification systems of The Nature Conservancy, and the draft ecological community classification system for Tennessee GAP Project.

These cross-correlated units were placed into the appropriate levels (either cover type or community type) of the modified UNESCO system, and revised several times based on review by the GAP vegetation classification committee.

Results and Conclusions

The final vegetation classification system of Arkansas contains approximately 215 community types (Table 1). Approximately 75 of the community types are within the wetland systems, while the remainder are within the terrestrial system.

Of the higher levels in the hierarchy, 32 physiognomic types are recognized at the formation level and 57 floristic types at the cover type level. The authors were concerned about the dramatic increase in units from 57 at the cover type level to 215 at the community type level, so an intermediate level comprising 94 units was created to provide an intermediate level of detail.

In order to add to the objectivity and usefulness of the classification, the committee will develop a list of type stands or example stands that will be documented with vegetation data and will be available for further review and research. The near-term documentation will be used in classifying satellite imagery to produce the GAP vegetation map.

Review and revision of this classification by a large and diverse committee has demonstrated that it is easily compressed to provide fewer units or extended to provide more detail, and is therefore highly flexible. Furthermore, its emphasis on plant community composition and structure makes it well adapted for use with satellite and aerial imagery. The U.S. Forest Service is presently developing a site classification system which will complement this vegetation-centered approach.

Because of the flexibility, clear focus and suitability of this system for use with remote sensing data, we suggest tits use in future vegetation and habitat studies in Arkansas.

Acknowledgements

Besides the authors, the GAP Vegetation Classification

Committee included Belinda Ederington and Chris Ware from Arkansas Game and Fish Commission, Carl Minehart from Ozark National Forest, Bill Pell from Ouachita National Forest, Lance Peacock from Arkansas Chapter, Nature Conservancy, Philip Tappe from University of Arkansas at Monticello, Bob Bennett from Arkansas State University, and Jim Grant from the Arkansas Forestry Commission. Edward E. Dale also offered comments on an earlier draft. This research was supported by the National Biological Survey through the Arkansas Gap Project.

Literature Cited

Arkansas State Game and Fish Commission. 1948. Wildlife and Cover Map of Arkansas.

Cowardin, L.M., V. Carter, F.C. Golet and **E.T. LaRoe.** 1979. Classification of wetlands and deepwater habitats of the United States. USDI Fish and Wildlife Service, Washington, 103 pp.

Dale, E.E. 1986. The vegetation of Arkansas (text and map). Arkansas Natural 4(5) :6-27.

Eyre, F.H. (ed.) 1980. Forest cover types of the United States and Canada. Society of American Foresters. Washington, 148 pp.

Foti, T.L. 1974. Natural divisions of Arkansas. Pp. 11-34 *In* Arkansas Natural Area Plan. Arkansas Department of Planning. Little Rock, Arkansas. 248 pp.

Jennings, D.M. 1993. Natural Terrestrial Cover Classification: Assumptions and Definitions. GAP Analysis Technical Bulletin 2. U.S. Fish and Wildlife Service, Idaho Cooperative Fish and Wildlife Research Unit, Univ. of Idaho, Moscow, Idaho, 28 pp.

Kuchler, A.W. 1964. Potential natural vegetation of the conterminous United States. Amer. Geog. Soc. Spec. Pub. 36. 156 pp.

Moore, D.M. 1959. Trees of Arkansas. Arkansas Forestry Commission. Little Rock, 142 pp.

Nelson, P.W. 1985. The terrestrial natural communities of Missouri. Missouri Dept. Nat. Res., Missouri Dept. Cons., Missouri Nat. Areas Comm., Jefferson City, 197 pp.

Pell, W.F. 1981. Classification and protection status of remnant natural plant communities in Arkansas. Proc. Arkansas Acad. Sci. 35:55-59.

Raunkier, C. 1934. The Life Forms of Plants and Statistical Plant Geography. Oxford: Clarendon.

Ruble, E. 1930. Pflanzengesellschaften der Erde. Bern/Berlin: Huber.

Scott, J.M., F. Davis, B. Csuti, R. Noss, B. Butterfield, C. Groves, H. Anderson, S. Caicco, F. D'Erchia, T.C. Edwards, Jr., J. Ulliman and R.G. Wright. 1993. Gap analysis: A geographic approach to protection of biological diversity. Wildlife Monographs No. 123:1-41.

United Nations Educational, Scientific and **Cultural Organization.** 1973. International classification and mapping of vegetation. Paris. 35 pp.

Whittaker, R.H. 1978. Classification of Plant Communities. Dr. W. Junk Publishers, The Hague: Netherlands, 408 pp.

Table 1. Natural Vegetation Classification System of Arkansas. Hierarchy is explained in text. (I)=indicator species.

Terrestrial

1. Forest (61-100% tree cover; trees > 5m tall)

1.A. Mainly evergreen forest (>75% evergreen)

1.A.9. Temperate evergreen needle-leaved forest

1.A.9.b. Temperate evergreen needle-leaved forest with rounded crowns

I. 1.a. Pinus echinata, Probably even-aged, resulting from disturbance, NW and Coastal Plain.

II. 2.a. Pinus taeda, Probably even-aged, resulting from disturbance, Primarily SE.

III. 3.a. Pinus echinata - Pinus taeda - Carya spp, Dry-mesic to dry sites, principally Coastal Plain.

1.A.9.c. Temperate evergreen needle-leaved upland forest with conical crowns

I. 1.a. Juniperus virginiana, Often high pH sites, sometimes rock, unburned.

1.B. Mainly deciduous or mixed forest (25%-75% evergreen)

1.B.2. Cold-deciduous forest, with evergreen broad-leaved trees and climbers (25%-75% evergreen)

1.B.2.a. Cold-deciduous forest with evergreen broad-leaved trees and climbers

I. 1.a. Fagus grandifolia - Ilex opaca (I), In Coastal Plain on sandy branch bottoms.

1.B.3. Cold-deciduous forest with evergreen needle-leaved trees (25%-75% evergreen)

1.B.3.a. Cold-deciduous broad-leaved upland forest with evergreen needle-leaved trees

I. Quercus stellata, marilandica - Pinus echinata - Carya spp.

1.a. Pinus echinata - Quercus stellata - Carya texana, Mesic to dry sites, NW and Coastal Plain.
b. Pinus echinata - Quercus stellata - Juniperus virginiana, Dry, open sites resulting from disturbance, NW and Coastal Plain.
c. Quercus stellata - Pinus echinata - Quercus marilandica (I), Dry or very dry sites, mostly NW and Coastal Plain.
d. Quercus stellata - Quercus marilandica - Juniperus virginiana, like 2a., but out of range of pines; higher pH.

II. Quercus spp.(alba, rubra) - Pinus echinata - Carya spp.

2.a. Quercus rubra - Pinus echinata - Quercus stellata, Dry sites, principally NW.
b. Quercus rubra - Pinus echinata - Carya texana, Dry sites, principally NW.
c. Pinus echinata - Quercus rubra - Quercus velutina, Mesic to xeric sites, NW.
d. Pinus echinata - Quercus rubra - Carya tomentosa, Dry to xeric sites, NW.

3.a. Quercus alba - Quercus rubra - Pinus echinata, Dry-mesic to dry sites, principally west half.
b. Quercus alba - Pinus echinata - Quercus (velutina, falcata) Dry-mesic to dry sites, principally west half.
c. Pinus echinata - Quercus alba - Carya tomentosa, Mesic to dry sites, NW and Coastal Plain.

III. Pinus taeda - Pinus echinata - Quercus spp.

4.a. Pinus echinata - Pinus taeda - Quercus spp. (stellata, alba, falcata), Dry to dry-mesic sites, principally Coastal Plain, probably deserves more detailed classification, but few natural stands remain.
5.a. Pinus taeda - Quercus stellata - Quercus falcata, Mesic to dry sites, principally Coastal Plain. Moister sites than 4.
b. Pinus taeda - Quercus (phellos, nigra, stellata), On occasionally flooded to dry sites, usually Coastal Plain.
6.a. Pinus taeda - Liquidambar styraciflua, Successional on old fields.

IV. Juniperus virginiana

7.a. Juniperus virginiana - Quercus muehlenbergii - Fraxinus quadrangulata, High pH sites or out of range of pine.
b. Juniperus virginiana - Rhus spp. - Diospyros, Old fields.

1.B.4.a. Temperate lowland and submontane broad-leaved cold-deciduous forest

I. Fagus grandifolia

1.a. Fagus grandifolia - Magnolia tripetala (I), Principally northwest on mesic sites.
b. Fagus grandifolia - Acer saccharum - Quercus spp. (alba, muehlenbergii, rubra), Mixed mesic forest (see David Graney, RNA nomination, Dismal Hollow), primarily Ozarks. Tilia americana may also occur, Acer is seldom in the community with Fagus.
c. Fagus grandifolia - Acer spp. (rubrum, saccharum) - Liriodendron tulipifera (I), Mixed mesophytic forest, Crowley's Ridge.

II. Quercus alba - mixed hardwoods

2.a. Liriodendron tulipifera - Quercus alba, On Crowley's Ridge, typically dry sites.
3.a. Acer saccharum - Quercus spp. (alba, rubra) - Carya spp. (ovata, tomentosa, cordiformis), Most common community for A. saccharum in Arkansas. Ozarks, Coastal Plain.
4.a. Quercus alba - Carya spp. (ovata, tomentosa), Dry-mesic to mesic sites throughout state on uplands.
b. Quercus alba - Liquidambar styraciflua - Carya tomentosa, Mesic to dry-mesic sites throughout state on uplands.
c. Quercus alba - Quercus velutina - Quercus falcata, Mesic to dry-mesic communities throughout state on uplands, Quercus velutina most characteristic of southern Ozarks; Liquidambar styraciflua is common.
5.a. Quercus alba - Quercus stellata, Dry to dry-mesic sites in uplands throughout state.
b. Quercus phellos - Quercus alba - Quercus falcata var. pagodifolia, Moist uplands, Arkansas River Valley, also with Liquidambar styraciflua.

III. Quercus rubra - Quercus spp.

6.a. Quercus rubra - Quercus alba, Mesic, north-facing slopes.
b. Quercus rubra - Quercus alba - Quercus velutina

IV. Quercus falcata - Quercus spp.

7.a. Quercus shumardii - Quercus falcata, Dry-mesic sites, particularly in southwestern Arkansas, Ouachitas and Coastal Plain. Sometimes bottomlands.
b. Quercus falcata - Quercus alba - Quercus velutina, Dry to dry-mesic sites; perhaps same community as 4c, but probably drier sites.

V. Quercus stellata

8.a. Quercus rubra - Quercus stellata - Quercus marilandica, Dry to xeric sites, northwest. Quercus rubra appears to have bimodal distribution: mesic and xeric.
b. Quercus stellata - Quercus (alba, velutina) - Carya texana, Dry sites, mostly northwest.

VI. 9.a. Liquidambar styraciflua, Old fields.

1.B.4.b. Montane cold-deciduous forest

I 1.a. Quercus alba (stunted), Forest at high elevations in Ouachitas. Ice and wind are key physical factors. May have full canopy cover, but trees are less than 15 feet tall.

2. Woodland (26%-60% cover; trees over 5m tall)

2.A. Mainly evergreen woodland

2.A.2 Evergreen needle-leaved woodland

2.A.2.b. Evergreen needle-leaved woodland with conical crowns

I. Juniperus virginiana - Quercus spp.

1.a. Juniperus virginiana - Quercus muehlenbergii, Throughout state, primarily on high pH, thin soils, unburned.
b. Juniperus virginiana - Quercus stellata, Throughout state, primarily on high pH, thin soils, unburned.
c. Juniperus virginiana - Quercus stellata - Fraxinus quadrangulata, Throughout state, primarily on high pH, thin soils, unburned, mostly dolomite.
2.a. Juniperus virginiana - Liquidambar styraciflua, Old fields.

2.B. Mainly deciduous or mixed woodland (25%-75% evergreen)

2.B.3 . Cold-deciduous woodland with evergreen needle-leaved trees

2.B.3.a. Mixed upland woodland, evergreens with rounded crowns

I. Pinus echinata - Quercus spp.

1.a. Pinus echinata - Quercus stellata - Quercus marilandica (I), Xeric sites in northwest, Coastal Plain. Q. marilandica often var. ashei = Quercus X bushii.
b. Pinus echinata - Quercus alba - Quercus falcata, NW, Coastal Plain, Fire maintained.
2.a. Pinus echinata - Quercus incana - Quercus arkansana, Sandhills of Coastal Plain.

II. Juniperus ashei - Quercus spp.

3.a. Juniperus ashei, Ozarks (dolomite outcrops) and Coastal Plain (chalk).
b. Juniperus ashei - Quercus sinuata (=durandii), Coastal Plain (White Cliffs, Little River County) on chalk.
c. Juniperus ashei - Quercus muehlenbergii - Fraxinus quadrangulata, Dolomite outcrops in Ozarks.

2.B.4. Cold-deciduous woodland (<25% evergreen)

2.B.4.a. Cold-deciduous upland deciduous woodland

I. Quercus spp. - Carya texana

1.a. Quercus alba - Quercus stellata, Xeric sites in northwest, occasionally elsewhere.
b. Quercus stellata - Quercus marilandica - Carya texana, Xeric sites in northwest, occasionally elsewhere. Sometimes stunted. Q. marilandica often var. ashei = Quercus X bushii.
2.a. Quercus arkansana - Quercus incana, Sandhills of Coastal Plain.

4. Shrubland (shrubs <5m >25% cover; trees >5m <10% cover)

4.A. Mainly evergreen shrubland

4.A.2.a. Evergreen needle-leaved shrubland

I. Juniperus spp. - Quercus spp.

1.a. Juniperus virginiana - Quercus muehlenbergii - Fraxinus quadrangulata, Rock outcrops of northwest.
b. Juniperus ashei - Quercus muehlenbergii - Fraxinus quadrangulata, Rock outcrops of northwest.

4.B.3.a. Temperate deciduous shrubland

I. 1a. Quercus alba - Quercus stellata, In northwest, often at high elevation in Ouachitas.

II. Mixed shrub species

2.a. Vaccinium spp. (arboreum, stamineum, pallidum), Usually on thin soils or rock outcrops, glades in northwest.
b. Crataegus spp. (marshallii, crus-galli), Thicket.

5. Herbaceous

5.A. Tall Grassland

5.A.1 Tall Grassland consisting mainly of sod grasses

5.A.1.a. Tall dense upland grassland

I. Mesic Prairie

1a. Tripsacum dactyloides, In moist to wet areas of prairies throughout state.
1b. Panicum virgatum, In moist areas of prairies throughout state, particularly Grand Prairie of MAP.
1c. Andropogon gerardii - Sorghastrum avenaceum, Mesic areas of prairies throughout state.

1d. Andropogon virginicus, Old fields.

5.B. Medium tall grassland

5.B.1. Medium tall grassland consisting mainly of sod grasses

5.B.1.a. Medium tall upland dense grassland

I. Dry Prairie

1.a. Schizachyrium scoparium - In dry areas of prairies.
b. Sporobolus asper - Especially in Ozarks.
c. Bouteloua curtipendula - On very dry, thin soils.

5.C. Grasslands with a tree layer

5.C.1. Tall Grasslands with a tree layer

5.C.1.a. Evergreen needle-leaved tree layer

I. Schizachyrium - Andropogon - Pinus

1.a. Schizachyrium scoparium - Pinus echinata - Quercus stellata, NW, fire and thin soils, savanna/barrens, glades. Andropogon gerdardii common.
1.b. Andropogon virginicus - Juniperus virginiana, Old fields.

5.C.1.b. Mainly deciduous or mixed tree layer

I. 1.a. Schizachyrium scoparium - Quercus spp. (stellata, shumardii, muehlenbergii), Oak savanna on thin soils, burned.

II. Dry Shrubby Grassland

1.a. Bouteloua curtipendula - Quercus stellata - Juniperus virginiana, On thin soils and rock outcrops in northwest and Coastal Plain.
b. Schizachyrium scoparium - Ilex decidua - Fraxinus pennsylvanica, Blackland prairies of Coastal Plain.
c. Andropogon virginicus - Sassafras albidum, Old fields.

5.C.3. Short grassland with a tree layer

6.C.3.b. Deciduous tree layer

I. 1.a. Aristida spp. - Quercus stellata, On saline soils.

6. Barren/sparsely vegetated

I. Sparsely vegetated area

1.a. Bare rock, In northwest and Coastal Plain, glades.
b. Lichen covered rock, In NW, glades.
c. Talus, In northwest, particularly Ouachitas.
d. Chasmophytic vegetation (Juniperus spp. on rock), In northwest and Coastal Plain, glades.
2.a. Eroding slopes, Throughout the state, particularly along streams.
2.b. Bare Soil.

II. Fern - Moss

3.a. Nonvascular plants - Fern (moist) or Moss (dry).
b. Shaded cliff (mosses, fern), In NW and Coastal Plain.

Palustrine

(These are distinguished at lower levels in the national classifications; that change can be made, but if so it will be harder to find the wetland communities.)

1.B.3.c. Cold deciduous alluvial forest

I. Quercus lyrata

1.a. Quercus lyrata - Carya aquatica, In bottomlands flooded less than 50% (ca. 20%-40%). Throughout except Ozarks and Crowley's Ridge.
b. Quercus lyrata - Carya aquatica - Fraxinus spp., In bottomlands flooded less than 50% (ca. 20%-40%), Throughout except Ozarks, and Crowley's Ridge.
c. Quercus lyrata - Carya aquatica - Quercus nuttallii (=texana), In bottomlands flooded less than 50% (ca. 20%-40%), Throughout the state except Ozarks, and Crowley's Ridge.
2.a. Quercus lyrata - Quercus phellos, Poorly drained bottomlands subject to long-duration flooding, Primarily Coastal Plain, MAP.
b. Quercus lyrata - Quercus phellos - Carya ovata, Poorly drained bottomlands subject to long-duration flooding, Primarily Coastal Plain, MAP.
c. Quercus lyrata - Quercus phellos - Quercus nuttallii (=texana), Poorly drained bottomlands subject to long-duration flooding, Primarily Coastal Plain, MAP.
d. Quercus lyrata - Quercus phellos - Liquidambar styraciflua, Poorly drained bottomlands subject to long-duration flooding, Primarily Coastal Plain, MAP.
3.a. Quercus lyrata - Celtis laevigata - Carya aquatica, Primarily MAP.
b. Quercus lyrata - Celtis laevigata - Fraxinus pennsylvanica, Primarily MAP.
c. Quercus lyrata - Gleditsia aquatica - Celtis laevigata, Primarily MAP.
4.a. Quercus lyrata - Quercus nuttallii (=texana) - Liquidambar styraciflua, In better-drained low bottoms, mostly southeast.
b. Quercus lyrata - Quercus nuttallii (=texana) - Quercus phellos, In better-drained low bottoms, mostly southeast.

II. Carya aquatica

5.a. Carya aquatica, Primarily MAP.
b. Carya aquatica - Fraxinus pennsylvanica - Quercus lyrata, Primarily MAP.

III. Quercus falcata var. pagodifolia

6.a. Quercus falcata var. pagodifolia - Quercus phellos - Liquidambar styraciflua, In bottomlands not subject to long duration flooding.
b. Quercus falcata var. pagodifolia - Quercus alba - Quercus stellata, In bottomlands not subject to long duration flooding.
c. Quercus falcata var. pagodifolia - Quercus michauxii - Quercus phellos, In bottomlands not subject to long duration flooding.
7.a. Quercus falcata var. pagodifolia - Quercus nuttallii (=texana), In bottomlands subject to moderate duration flooding.

IV. Celtis laevigata

8.a. Celtis laevigata - Carya aquatica, In poorly drained bottomlands, MAP.
b. Celtis laevigata - Fraxinus pennsylvanica - Carya illinoensis, Generally sandy, poorly drained bottomlands.
9.a. Celtis laevigata - Fraxinus pennsylvanica - Ulmus americana, In poorly drained bottomlands, MAP.
b. Celtis laevigata - Ulmus crassifolia - Fraxinus spp., In poorly drained bottomlands, MAP.

V. Quercus nuttallii (=texana)

10.a. Quercus nuttallii (=texana) - Quercus lyrata - Quercus phellos, In bottomlands subject to medium to long duration flooding, mostly southeast.
b. Quercus nuttallii (=texana) - Quercus lyrata - Liquidambar styraciflua, In bottomlands subject to medium to long duration flooding, mostly southeast.
c. Quercus nuttallii (=texana) - Quercus lyrata - Carya aquatica, In bottomlands subject to medium to long duration flooding, mostly southeast.
d. Quercus nuttallii (=texana) - Quercus lyrata - Fraxinus spp., In bottomlands subject to medium to long duration flooding, mostly southeast.
11.a. Quercus nuttallii (=texana) - Celtis laevigata - Fraxinus pennsylvanica.
b. Quercus nuttallii (=texana) - Celtis laevigata - Ulmus spp.

VI. Quercus palustris

12.a. Quercus palustris - Quercus lyrata - Carya laciniosa.
b. Quercus palustris - Fraxinus pennsylvanica - Quercus phellos.
c. Quercus palustris - Quercus phellos - Quercus lyrata.
d. Quercus palustris - Quercus phellos - Liquidambar styraciflua.

VII. Quercus phellos

13.a. Quercus phellos.
14.a. Quercus phellos - Quercus palustris - Carya aquatica.
b. Quercus phellos - Quercus palustris - Quercus lyrata.
c. Quercus phellos - Quercus laurifolia.
d. Quercus phellos - Quercus nigra.
15.a. Quercus phellos - Quercus lyrata.

1.B.3.d. Cold-deciduous swamp forest

I. Taxodium distichum - mixed hardwood

1.a. Taxodium distichum, In long-duration swamps, throughout except Ozarks and Crowley's Ridge.
b. Taxodium distichum - Nyssa aquatica, In long-duration swamps, throughout except Ozarks and Crowley's Ridge.
2.a. Taxodium distichum - Quercus lyrata, In bottomlands flooded ca. 50% of the year throughout state.
b. Taxodium distichum - Quercus lyrata - Fraxinus spp.

II. Nyssa

3.a. Nyssa aquatica.
b. Nyssa aquatica - Nyssa biflora - Taxodium distichum.
4.a. Magnolia virginiana - Nyssa (aquatica, sylvatica), Seeps

and occasionally streamsides in Coastal Plain.

4.B.3.c. Deciduous alluvial shrubland

I. Cornus amomum

1.a. Cornus amomum, Stream floodplains, northwest.

II. Mixed shrub

2.a. Planera aquatica, Bottomlands subject to long-term inundation, mostly southeast.
3.a. Forestiera acuminata, Bottomlands subject to moderate to long-term inundation, mostly southeast.
4.a. Cephalanthus occidentalis, On areas subject to long-term inundation throughout the state.

5.A.4.a. Tall grass

I. Tall grass

1.a. Tripsacum dactyloides, Moist prairies.
2.a. Panicum virgatum, Moist to wet prairies.

5.A.4.b. Tall grass consisting mainly of bunch grasses

I. Tall grass

1.a. Schizachyrium scoparium - Panicum virgatum, Wet sites, occasionally flooded, usually in prairies throughout.

II. Typha - Zizaniopsis Marsh

2.a. Typha latifolia, Open areas subject to long-term inundation, throughout.
3.a. Zizaniopsis milinacea, South, swamps and marshes.

III. 4.a. Arundinaria gigantea, Common understory, becomes dominant when overstory is removed, e.g., by fire or cutting.

5.B.2.c. Medium tall vegetation with deciduous shrub layer

I. Fen

1.a. Parnassia grandifolia - Carex lurida, Fen - high pH ground water seepage.

II. Sedge - rush

2.a Scirpus spp. - Juncus spp.
3.a. Carex spp. - Osmunda spp. - Sphagnum spp., Acid seeps.

Riverine

1.B.3.c. Forest

I. Populus - mixed hardwood

1.a. Acer negundo - Carya illinoensis - Populus deltoides, Also Acer rubrum, Platanus occidentalis. Riverfronts.
2.a. Populus deltoides, Riverfronts, usually sandy, throughout the state.
b. Populus deltoides - Quercus lyrata - Quercus nuttallii, Riverfronts, usually sandy, throughout the state.

c. Populus deltoides - Salix nigra - Celtis laevigata, Riverfronts, usually sandy, throughout the state.
3.a. Salix nigra, In poorly drained riverfronts.

II. Betula - Platanus - Acer Riverfront

4.a. Betula nigra - Platanus occidentalis, On well-drained riverfronts, primarily NW.
5.a. Acer saccharinum - Ulmus americana, In infrequently flooded bottomlands, primarily northwest.

4.B.3.c. Shrub

I. Shrub willow

1.a. Salix caroliniana, Gravel, sand bars in northwest.
2.a. Salix exigua, Gravel, sand bars, ditchbanks, throughout the state.

5.A.1.c. Herbaceous with woody layer broad-leaved deciduous

I. 1.a. Xanthium strumarium - Cynodon dactylon (alien) - Populus deltoides, Sandbars.

6. Barren

I. Bare

1.a. Sand bar
1.b. Gravel bar
2.a. Mud flat
3.a. Eroding bank

Lacustrine

1.B.3.d. Forest

I. 1.a. Taxodium distichum - Nyssa aquatica, Shallow lakes and margins of others, mostly southeast.

4.B.3.c. Shrub

I. 1.a. Cephalanthus occidentalis, Shallow lakes and margins of others, mostly southeast.

5.D.2.a. Herbaceous

I. Marsh

1.a. Nuphar lutea, Shallow to medium depth lakes, mostly southeast.
2.a. Typha latifolia, Open shallow edges, throughout.
3.a. Scirpus spp. - Juncus spp., Open shallow edges, throughout.

6. Barren

I. 1.a. Mud flat

Reaction of Titanocene Dichloride with Acetylenedicarboxylate

Tanya L. Hagler, M. Draganjac, Paul Nave, J. Ed Bennett and Farooq Kahn
Department of Chemistry and Biochemistry
Arkansas State University
State University, AR 72467
R. Engelken, Gerard Williams, Chris Poole and Kwok Fai Yu
Department of Engineering
Arkansas State University
State University, AR 72467

Abstract

The reaction of Cp_2TiCl_2 with either the mono- or dipotassium salt of acetylenedicarboxylic acid (ADC) gives high yields of an insoluble orange product. The insoluble compound shows potential semiconductor behavior, as evidenced by an apparent bandgap in the orange region of the visible spectrum. Under N_2, the compound decomposes at 238° C, eventually losing approximately 46% total mass up to 1350° C. The exothermic decomposition in air, beginning at 235° C, results in the formation of titanium oxides.

Introduction

Electron transfer between metal centers is important in many industrial and biological catalyst systems. To model these catalysts, Stephan and coworkers have prepared several early-late heterobimetallic (ELHB) compounds, with S and/or P atoms bridging the two metals (Stephan, 1989). Titanocene dichloride is often used as the electron deficient metal in these complexes. The challenge lies in finding new and diverse ligands that would make suitable candidates for the synthesis of novel multimetal complexes. Either acetylene dicarboxylic acid (ADC), or acetylene dicarboxylic acid, monopotassium salt (KADC) meet these requirements. The structure of these ligands affords the potential for bridging two metal centers. Herein is reported the reaction of titanocene dichloride and potassium salts of acetylene dicarboxylic acid.

Materials and Methods

Reactions were carried out in air at ambient conditions. The dipotassium salt of ADC was prepared as described by Carraher (Williams, et al., 1989). All other reagents were used as purchased without further purification. Infrared spectra were obtained on a Nicolet 5PC FT-IR Spectrophotometer using KBr pellets or Nujol mulls on NaCl plates. X-ray diffraction patterns were acquired on a Rigaku D/MAX-B unit. Bandgap measurements were taken on a Perkin-Elmer Lambda 19 UV/VIS/NIR Spectrophotometer. For the bandgap measurements, the sample was prepared by suspending the orange powder in acetone and brushing it onto a glass slide. An apparatus consisting of a Hewlett Packard 712B voltage supply, a Keithley 177 Digital Multimeter (DMM), and JDR Instruments DMM-300 Multimeter, was used to procure resistivity-conductivity measurements. Thermal gravimetric analyses were obtained on a Seiko TG/DTA 320 instrument. Elemental analysis was performed by Galbraith Laboratories, Inc., Knoxville, TN.

Reaction of Cp_2TiCl_2 with KADC

A 0.10 g (0.40 mmol) sample of Cp_2TiCl_2, 0.06 g (0.39 mmol) KADC and 20 mL H_2O was stirred for several hours. The orange product began to precipitate out of the slurry after approximately 30 min. The reaction was considered complete when there was no longer any Cp_2TiCl_2 visible in the mixture. The orange powder, *1*, was filtered by suction filtration and washed with several protions of CH_3OH and water. Yield = 0.1086 g. Anal. found C, 56.41; H,3.43; Ti, 15.60%. IR: 1635.84 (s), 1442.94 (m), 1298.26 (s), 1018.54 (m), 769.70 (m), 621.15 (m) cm^{-1}. X-ray Diffraction (d-spacings) (Å): 6.328 (s), 5.805 (vs), 4.683 (m), 4.089 (w), 3.942 (m), 3.540 (w), 2.860 (w), 2.620 (w), 2.272 (w), 2.029 (vw), 1.789 (vw), 1.544 (vw).

Reaction of Cp_2TiCl_2 with K_2ADC

Method A. A 0.14 g (1.2 mmol) sample of ADC and a 0.14 g (2.4 mmol) sample of KOH were dissolved in 30 mL of H_2O to yield a clear colorless solution of K_2ADC. A 0.31 g (1.2 mmol) sample of Cp_2TiCl_2 was dissolved in 30 mL of $CHCl_3$ in a separate flask. The contents of the two flasks were combined and allowed to react by rapid stirring.

Method B. A 0.14 g (1.2 mmol) sample of ADC and a 0.14 g (2.4 mmol) sample of KOH were dissolved in 30 mL of H_2O to yield a clear colorless solution of K_2ADC. A 0.31 g (1.2 mmol) sample of Cp_2TiCl_2 was dissolved in 30 mL of $CHCl_3$ in a separate flask. The contents of the two flasks were combined and allowed to react by a much slower process of magnetic stirring. The resulting solution was allowed to stir for 10 minutes followed by diffusion of the layers for several days.

In both cases, the product (a yellow-orange powder) was recovered by suction filtration and washed with water and chloroform. IR: 1624.22 (s), 1442.94 (m), 1296.33 (s), 1033.98 (m), 769.70 (m), 623.45 (m) cm^{-1}. X-ray Diffraction (d-spacings) (Å): 6.308 (m), 5.804 (s), 4.680 (m), 4.090 (w), 3.931 (m), 3.532 (w), 2.851 (w), 2.622 (w), 2.261 (w), 2.045 (vw), 1.782 (vw), 1.536 (vw).

Results and Discussion

The orange product from the reaction of Cp_2TiCl_2 and KADC is easily obtained. The two reagents are allowed to stir in water in air at room temperature, and the powder is recovered by suction filtration. A slight excess of Cp_2TiCl_2 was used to insure complete reaction of KADC. This necessitated several washings with CH_3OH to remove excess Cp_2TiCl_2. The product was also washed with water to remove any KCl.

An alternate method for the synthesis of the orange product is similar to reactions of Carraher (Williams et al., 1989). In this method, K_2ADC, the dipotassium salt of the acid, is employed. The acid in the aqueous phase is allowed to come in contact with the organic phase containing the titanocene dichloride. This contact is accomplished either by stirring the layers with a rapid stirrer or stirring the layers for 5-10 minutes with a magnetic stirrer, then allowing the reaction to remain covered, undisturbed for several days. When chloroform is used as the organic solvent of Cp_2TiCl_2, a microcrystalline product is obtainable. Further attempts to grow larger crystals suitable for single crystal x-ray diffraction have been unsuccessful.

The reported time required for rapid stir techniques is on the order of sixty seconds (Williams et al., 1989). Rapid stir techniques for the reaction of Cp_2TiCl_2 and K_2ADC require considerably longer times for completion, often taking 15-30 minutes. Possible differences in reaction times may be due to the lower nucleophilicity of ADC ions or to solution pH. Carraher alters the pH of the carboxylic acid with additional base to a slightly basic solution (Williams et al., 1989). No attempts were made to control pH in any of our reactions. Fig. 1 shows the pH of the solution as a function of time for an aqueous reaction of 0.3 g Cp_2TiCl_2 with 0.18 g KADC in 30 mL of H_2O. The pH of the solution drops rapidly with the addition of KADC and continues to drop exponentially with time.

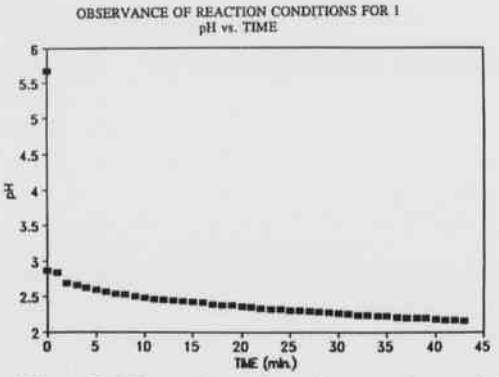

Fig. 1. Plot of pH vs. time for the reaction of Cp_2TiCl_2 with KADC.

The orange products from either method are not soluble in any common solvent or solvent systems. The products react with N,N-dimethylformamide (DMF), pyridine, and hydrochloric acid. Characterization of the products obtained from the reactions with DMF and pyridine are still underway. The addition of HCl to the orange powder reforms the starting material, Cp_2TiCl_2. The insolubility of the adc compounds precludes molecular weight determination. Carraher and Lee (1975) have reported the formation of polymers from the reaction of Cp_2TiCl_2 with salts of diacids. Some of their products were also insoluble and could not be further characterized. The soluble polyesters had average molecular weights of 3×10^5 g/mol. These results suggest that the orange products formed from Cp_2TiCl_2 and ADC salts are also insoluble polyesters. The IR data indicates a chelated ester stretch at 1625-1635 cm^{-1}. R.N. Kapoor et al., (1987) have reported the structure of a titanocene complex in which the titanium atom has two chelated esters as ligands.

Because the two products from the two separate synthetic methods had observably different orange colors they were analyzed to see if the two methods gave dissimilar products. The decomposition points of the materials using a Mel-temp apparatus are 235° C for the reaction with KADC and 190° C for the reaction with K_2ADC. Singly, this indicates two distinct products. However, X-ray diffraction patterns (Fig. 2) and infrared spectra show conclusively that the two products are identical in structure. The difference in color and decomposition point suggests a difference in chain length of a polymer.

A thermal gravimetric analysis (TGA) of the Cp_2TiCl_2/KADC product under N_2 shows a small mass loss at approximately 70° C (Fig. 3). The compound

begins rapid decomposition at 238° C. This initial 14% mass loss is associated with a large exotherm. Calculations based on mass loss indicate possible loss of one CO_2 per acetylenedicarboxylate ligand. The TGA exhibited almost continual loss of material up to 1350° C, losing a total of 46% of its mass. The TGA of the Cp_2TiCl_2/KADC product in air (Fig. 4) shows a small mass gain before decomposition at 235° C. A second mass increase of 1.2% occurs before the burning off of the organic fragments to a final total mass loss of 69.8%. This percentage remaining would be consistent with the formation of TiO_2.

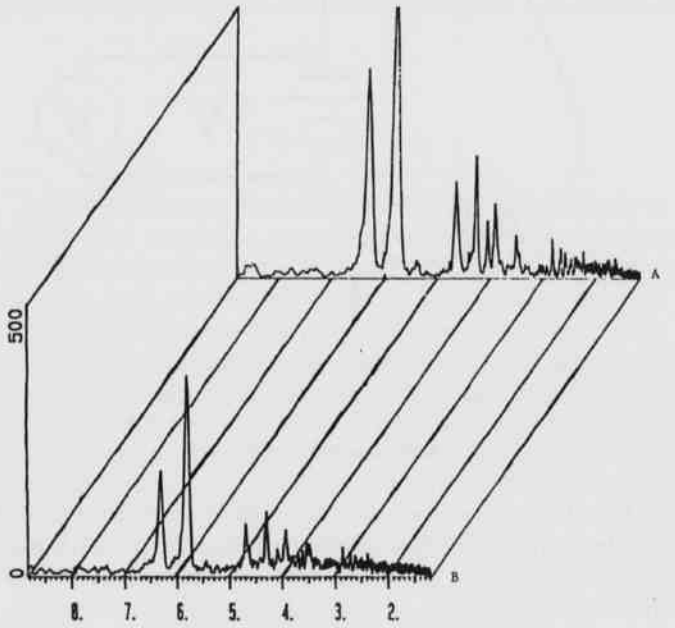

Fig. 2. X-ray diffraction patterns for A) Cp_2TiCl_2/ KADC product and B) Cp_2TiCl_2/ K_2ADC product.

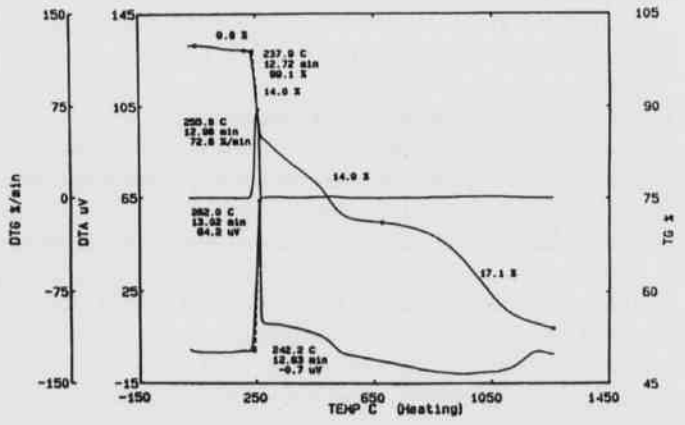

Fig. 3. Thermal gravimetric analysis in N_2 of the orange product from the reaction of Cp_2TiCl_2 with KADC.

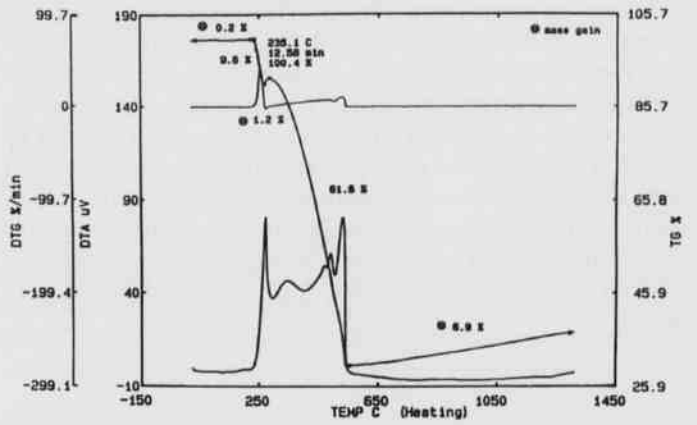

Fig. 4. Thermal gravimetric analysis in air of the orange product from the reaction of Cp_2TiCl_2 with KADC.

An X-ray diffraction pattern of Cp_2TiCl_2/KADC sample after thermal decomposition in air was computer matched to several different titanium oxide phases. While none of the phases were exact matches, most were close enough to indicate the decomposed material is a titanium oxide of unknown stoichiometry.

An optical absorbance vs. wavelength spectrum of the Cp_2TiCl_2/KADC product is shown in Fig. 5. The data indicated a transmittance window from 875-600 nm. The rapid increase in absorbance near 600 nm results from electron transitions from the valence band to the conduction band as photons are absorbed. Absorbance spectra of this type are typical of semiconducting materials. The spectrum indicated a bandgap of approximately 2.1 eV. Considering the narrow transmittance window, a possible application of *1* may be as an optical bandpass filter. The absorption in the portion of the spectrum from 3200-875 nm results from a combination of bond-resonance and intraband free carrier absorption. It is possible to observe the bond-resonance absorptions because these wavelengths make up the near-infrared (NIR) portion of the spectrum.

The electrical resistivity was determined through straightforward electrical resistance measurements for pressed pellets of diameter 28 mm and thickness approximately 3 mm. Resistance was determined by application of voltage up to a maximum of 500 V DC between silver ink contacts applied to the faces of the pellets, measurement of current through the pellets via a standard ammeter and use of Ohm's Law:

$$R = V/I \text{ and } \rho = RA/l = 1/\sigma, \text{ where}$$

ρ is the resistivity in ohm-cm, R the resistance in ohms, A the cross sectional area of the face, l the thickness, and σ the conductivity in $(\text{ohm-cm})^{-1}$. Resistivity measurements

yielded a linear relationship between current and voltage. This can be seen from Fig. 6. The resistivity, ρ, of the orange K_2ADC/Cp_2TiCl_2 product, *1*, is approximated by ρ = Vwt/I1. The symbols w, t, and 1 are dimensions of the sample. Voltage and current are denoted by V and I, respectively. A diagram of this apparatus is presented in Fig. 7. The resistivity of *1* is 2.86×10^7 ohm-cm. Although very simple, this measurement scheme was rapid, convenient, and satisfactory for "order-of magnitude" estimates as required in this preliminary study. Further research is needed to explore all possible applications of this material.

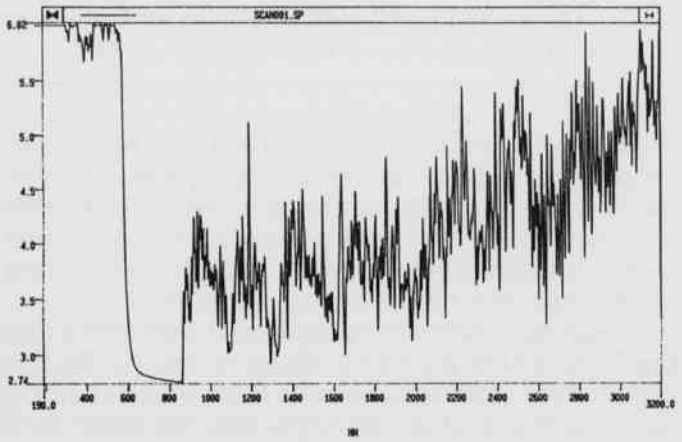

Fig. 5. Optical absorbance spectrum of the orange product from the reaction of Cp_2TiCl_2 with KADC.

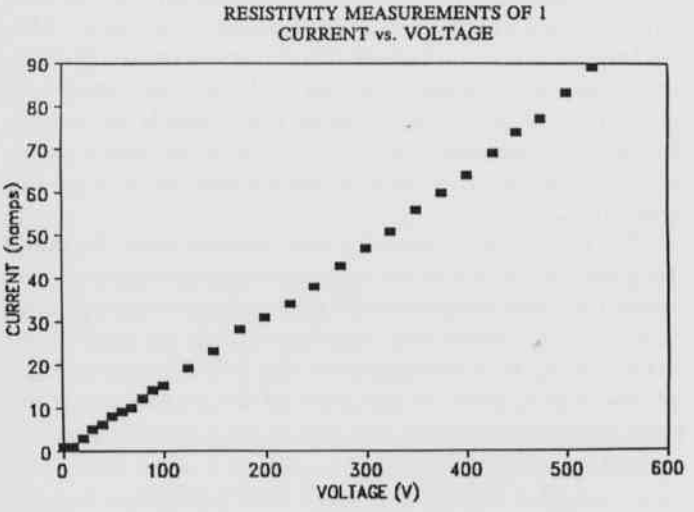

Fig. 6. Resistivity measurements of the orange product form the reaction of Cp_2TiCl_2 with KADC.

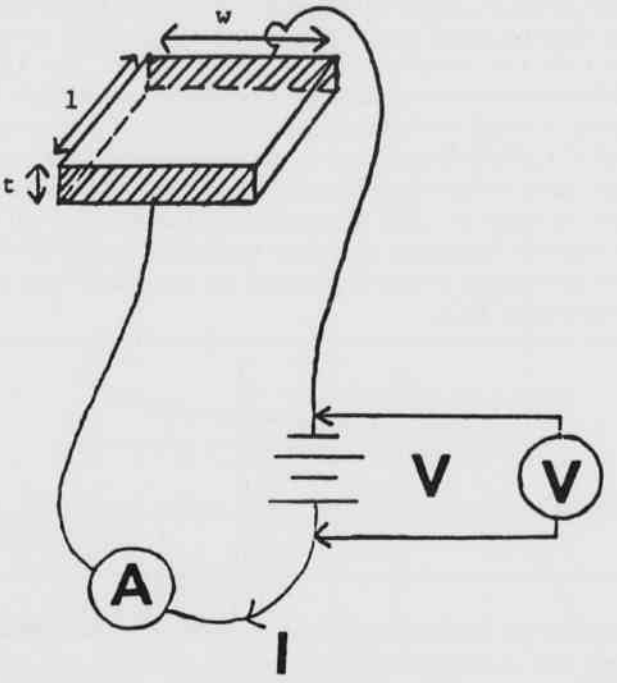

Fig. 7. Diagram of the resistivity apparatus.

Acknowledgements

Funding provided by the Arkansas Science and Technology Authority, Arkansas Department of Energy EPSCoR, and the National Science Foundation (Grant #DUE-9351560).

Literacture Cited

Carraher, C.E. and **J.L. Lee.** 1975. Tentative identification of the reactive species in the reaction of Cp_2TiCl_2 with salts of diacids. J. Macromol. Sci.-Chem. A9:191-198.

Kapoor, R.N., S.C. Dixit and **R. Sharan.** 1987. Heterocarboxylates of dichlorobis (cyclopentadienyl) - zirconium (IV) and dichlorobis (cyclopentadienyl) titanium (IV). Inorg. Chim. Acta. 133:251-254.

Stephan, D.W. 1989. Early-late heterobimetallics. Coord. Chem. Rev. 95:42-107 and references therein.

Williams, M., C. Carraher, Jr., F. Medina and **M. Aloi.** 1989. Synthesis and structural characterization of the condensation product of squaric acid and bis(cyclopentadienyl) titanium dichloride. American Chemical Society, Division of Polymeric Materials Science and Engineering. 61:227-231.

Gamma Ray Emissions From Binary Pulsar Systems

Tony A. Hall and Andrew T. Sustich
Arkansas State University
Department of Physics
State University, AR 72467

Abstract

A method is developed for estimating the gamma ray flux impinging upon the earth from production in binary pulsar systems. We calculate production of the 6.13 MeV gamma ray line characteristic of ^{16}O. These are produced by protons emitted by the pulsar interacting with ^{16}O atoms at the surface of the companion. We examine different types of companion stars and estimate the gamma ray flux at the earth as a function of proton emission from the pulsar and distance from the earth. Prospects for detection from earth are discussed.

Introduction

A binary star system consists of two gravitationally bound stars, orbiting a common center of mass. A pulsar is a rapidly rotating neutron star, which, due to its intense magnetic field, emits a wide energy spectrum of charged particles and electromagnetic waves into narrow cones about each of its magnetic poles. In binary pulsar systems in which at least one of the stars is a pulsar, protons emitted from the pulsar can strike the surface of the companion star, where they interact to produce nuclear excitations (see Zeilik et al., 1992). Gamma rays are emitted in the de-excitation process, and theses gamma rays travel outward from the system until they may ultimately be detected at the earth.

In spectra from solar flare bursts, the most prominent gamma ray lines are the 4.43 MeV line from ^{12}C followed by the 6.13 MeV line from ^{16}O (Chupp et al., 1984). Since others have already focused on the 4.43 MeV line from ^{12}C in previous solar flare work (Lang et al., 1987; Werntz et al., 1990), we study the 6.13 MeV line from ^{16}O in this article.

Model and Methods

Gamma rays are produced when a proton scatters inelastically off a target ^{16}O nucleus. The ^{16}O nucleus is left in an excited state and emits a gamma ray upon de-excitation,

$$p + {}^{16}O \rightarrow p' + {}^{16}O^*$$

$$^{16}O^* \rightarrow {}^{16}O + \gamma\,(6.13\ \text{MeV}). \qquad (1)$$

The probability that a proton of energy E'_p, in traversing a thickness dx of the target at distance x into the target, will excite an ^{16}O nucleus to the appropriate excitation level is given by

$$dP(x) = \sigma(E'_p)\, n_a(x)\, dx\,. \qquad (2)$$

where $\sigma(E'_p)$ is the production cross section for the gamma ray line in question and $n_a(x)$ is the number density of target nuclei (^{16}O).

In most laboratory experiments, the target number density n_a is constant, and the target is so thin that the proton does not lose any appreciable amount of energy in traversing the target. In this case, an integration over the thickness t of the target yields the thin-target approximation for the probability of interaction (and production of a gamma ray),

$$P(E'_p) = \sigma(E'_p)\, n_a\, t\,. \qquad (3)$$

In our situation, the protons continually lose energy as they penetrate into the companion star and we must employ a thick-target approximation. The probability of interaction in a thickness dx at a distance x into the companion is

$$dP(x) = \sigma(E_p(x,E'_p))\, n_a(x)\, dx\,, \qquad (4)$$

where E(p) is the energy of the proton of initial energy E'_p after traversing the distance x. We change to an integration over initial proton energy

$$dx = dE'_p \left[\frac{dE'_p}{dx}\right]^{-1} \qquad (5)$$

where $dE'_p/dx \leq 0$ is the stopping power of the target material.

As the gamma rays are produced at increasing depth into the companion star, their probability of escaping out

of the companion material decreases exponentially. As a first approximation, we assume that all gammas produced within one attenuation length of the companion surface escape with 100% probability, and all those produced further in than one attenuation length are completely absorbed before escaping. Hence, for a given proton energy E'_p, we allow it to lose up to the energy loss at one attenuation length $\Delta(E'_p)$. Beyond that point, the proton cannot produce a gamma which will escape. Our gamma ray production probability is then

$$P(E'_p) = \int_{E'_p}^{E'_p+\Delta'(E'_p)} dE_p\, \sigma(E_p)\, n_a \left[\frac{dE_p}{dx}\right]^{-1} . \qquad (6)$$

The dependence on target density n_a is really artificial here. We assume the target density to be given by the nuclear number density times a typical ^{16}O stellar abundance. The stopping power dE_p/dx is also proportional to the nuclear number density, so that our result is independent of the density of the companion. This production probability is then folded with the proton spectrum $N_p(E'_p)$ from the pulsar which strikes the companion star to obtain the number of gamma rays per second produced,

$$N_\gamma = \int_{E_t}^{\infty} dE'_p\, N_p(E'_p) \int_{E'_p}^{E'_p+\Delta'(E'_p)} dE_p\, \sigma(E_p)\, n_a \left[\frac{dE'_p}{dx}\right]^{-1} , \qquad (7)$$

where E_t = 6.52 MeV is the threshold energy for production of the 6.13 MeV gamma ray. The proton spectrum is assumed to obey a power law and is normalized to N_p protons per second,

$$N_p(E'_p) = N_p \hat{N}_p(E'_p) = N_p K (E'_p)^{-\alpha} , \qquad (8)$$

so that normalization constant K is determined from

$$\int_{E_t}^{\infty} dE'_p\, \hat{N}_p(E'_p) = 1 . \qquad (9)$$

By inverting the order of integration and performing one integral analytically, we obtain

$$N_\gamma = \int_{E_t}^{\infty} dE_p \frac{n_a N_p}{(E_t)^{1-\alpha}} \sigma(E_p) \left[\frac{dE_p}{dx}\right]^{-1} \left\{ (E_p)^{\alpha+1} - (E_p+\Delta(E_p))^{\alpha+1} \right\} \qquad (10)$$

Data for the gamma production cross section are compiled from the literature (Dyer et al., 1981; Lang et al., 1987; Lesko et al., 1988). An analytic fit to stopping power data has been provided to us (Lang, 1993). The cross section peaks in the 10-15 MeV range and falls slowly with energy (See Fig. 1). The energy loss over one attenuation length is obtained from the stopping power

$$\Delta(E_p) = \int_0^{x_\gamma} dx \left[\frac{dE'_p}{dx}\right] , \qquad (11)$$

where the attenuation length x_γ is obtained by assuming a purely hydrogen composition for the companion (Zombeck, 1990).

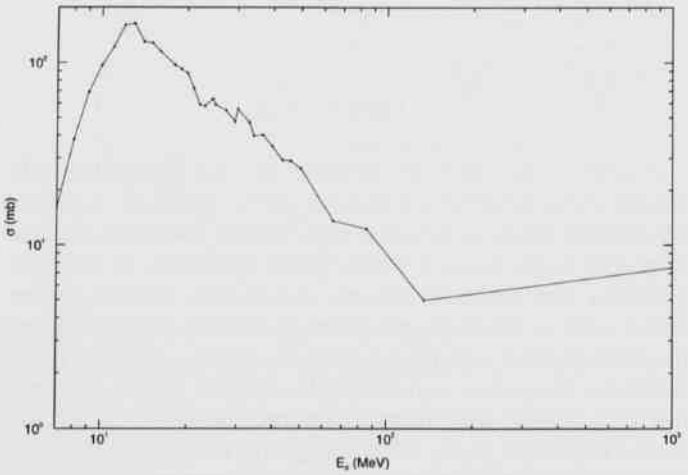

Fig. 1. Cross section for production of 6.13 MeV gamma rays by protons on ^{16}O.

Results and Discussion

The resulting integral is integrated numerically to obtain the number of gamma rays per second produced. We take the power factor for the proton spectrum to be a = 2. A proton influx of $N_p = 10^{41}/sec$ is taken as a baseline. This is an upper limit estimate for the Crab Pulsar based on the luminosity of the surrounding nebula (Zombeck, 1990).

The gamma ray production per unit energy of the incoming protons [the integrand of equation (10)],

$$\frac{dN_\gamma}{dE'_p} = Np(E'_p)\, P(E'_p) , \qquad (12)$$

shows a peak behavior similar to the gamma ray production cross section and 90% of the gamma rays are due to

protons with energies $E'_p \leq 50$ MeV (See Fig. 2).

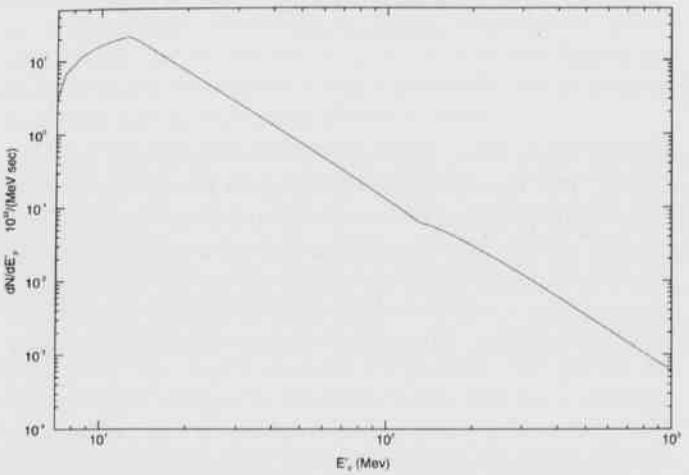

Fig. 2. Production rate of 6.13 MeV gamma rays as a function of energy of incoming protons from the pulsar.

The gamma ray flux at the Earth is obtained by dividing the gamma ray production rate by $4\pi d^2$ where d is the distance to the pulsar. Using 1000 light-years as the distance to the nearest pulsar we obtain

$$\phi_{6.13\gamma} = 2.4 \times 10^{-8}\ (cm^2\ sec)^{-1}\ . \qquad (13)$$

In order to determine if this flux is detectable from Earth, we need to consider the background signal which it must compete against. The observed energy flux from continuum gamma rays from the Crab Nebula is (Zombeck, 1990)

$$\frac{d\phi_E}{dE} = 10^2\ \frac{eV}{cm^2 sec MeV} \qquad (14)$$

At a gamma ray energy of 6.13 MeV, this provides a gamma ray flux of approximately

$$\frac{d\phi_\gamma}{dE} = \frac{d\phi_E/dE}{E\gamma} = 1.7 \times 10^{-5}\ (cm^2 sec\ MeV)^{-1}\ . \qquad (15)$$

We take this to represent a typical background signal. Since the 6.13 MeV gamma ray line from ^{16}O has a full width at half maximum of about 0.1 MeV, the flux from the line has a maximum of approximately

$$\frac{d\phi_{6.13\gamma}}{dE} = \frac{\phi_{6.13\gamma}}{0.1MeV} = 2.4 \times 10^{-7}\ (cm^2 sec\ MeV)^{-1}\ . \qquad (16)$$

Conclusions

We have found the flux of 6.13 MeV gamma rays to be about two orders of magnitude smaller than an estimated background signal. This is probably an order of magnitude below detection threshold. However, more effort needs to be devoted to investigating the proton flux and energy spectrum from pulsars and the calculation of the background signal before their detection is ruled out.

Acknowledgements

The authors are indebted to Dr. Carl Werntz and Dr. Fred Lang for introducting them to this problem and for much useful discussion regarding its solution. The hospitality of Dr. Carol Jo Crannell and the Solar Physics Branch of NASA-Goddard Space Flight Center during visits to NASA-Goddard is gratefully acknowledged. This work has been supported by NASA grant NAG8-277, Arkansas Space Grant Consortium grant NL-3013S, SILO Undergraduate Research Fellowship, and NASA-Goddard Space Flight Center NSF-REU Program.

Literature Cited

Chupp, E.L., D.J. Forrest, P.R. Higbie, A.N. Suri, C. Tsai and **P.P. Dunphy.** 1973. Solar gamma ray lines observed during the solar activity of August 2 to August 11, 1972, Nature 241:333-335.

Dyer, P., D. Bodansky, A.G. Seamster, E.B. Norman and **D.R. Maxson.** 1981. Cross sections relevant to gamma-ray astronomy: proton induced reactions, Phys. Rev. C 23:1865-1882.

Lang, F.L., C.W. Werntz, C.J. Crannell, J.I. Trombka and **C.C. Chang.** 1987. Cross sections for production of the 15.10-MeV and other astrophysically significant gamma-ray lines through excitation and spallation of ^{12}C and ^{16}O with protons, Phys. Rev. C 35:1214-1227.

Lang, F.L. 1993. Private communication.

Lesko, K.T., E.B. Norman, R.-M. Larimer, S. Kuhn, D.M. Meekof, S.G. Crane and **H.G. Bussel.** 1988. Measurements of cross sections relevant to gamma-ray line astronomy, Phys. Rev. C 37:1808-1817.

Werntz, C., F.L. Lang and **Y.E. Kim.** 1990. Solar flare gamma-ray line shapes, Ap. J. Suppl. 73:349-357.

Zombeck, M.V. 1990. Handbook of Space Astronomy and Astrophysics, Cambridge Press, New York, 440 pp.

Zeilek, M., S.A. Gregory and **E.V.P. Smith.** 1992. Introductory Astronomy and Astrophysics. Harcourt Brace Jovanovich, Orlando, 504 pp.

Laccase Production by *Chaetomium elatum*, a Soft-Rot Fungus

Wilson H. Howe
Department of Physics and Astronomy
University of Arkansas at Little Rock
Little Rock, AR 72204

Joyce M. Hardin
Department of Biology
Hendrix College
Conway, AR

Abstract

Though enzymes responsible for rotting wood have been studied for some time, the enzymes and enzymatic systems responsible for breaking down lignin have only begun to be discovered. The lignin-degrading enzymes produced by soft-rot fungi, in particular, have not been sufficiently studied. The present study presents evidence that the enzyme called laccase, known to be associated with lignin biodegradation, is produced by the species *Chaetomium elatum*, a soft-rot fungus. *Cerrena unicolor*, a positive control, and *Chaetomium elatum* were grown in culture. These species were tested for the presence of laccase using syringaldazine as a chromogenic substrate. As expected, *Cerrena unicolor* showed laccase production after two weeks of growth indicating the experimental procedures were working. After three weeks, *Chaetomium elatum* showed laccase production.

Introduction

Lignin is produced in large quantities as a byproduct of pulp production and currently has very little economic value. An understanding of lignin biodegradation may have a positive effect on several industries.

Several studies have illustrated the benefit of using fungal decay in the processing of wood for pulp manufacturing. Paszcynski et al. (1988) demonstrated how wood chips and pulps can be delignified by natural methods. Eriksson and Vallander (1980) showed that pretreating wood chips with wood-rotting fungi saves 30% in the energy demand for processing these wood chips into pulp.

A better understanding of the enzymatic mechanisms required for lignin biodegradation could lead to the ability to use waste lignin for the production of useful chemicals. For instance, S.L. Rosenberg and C.R. Wilke (1980) investigated the possibility of cheaply producing ethyl alcohol from cellulose by removing lignin via wood-rotting fungi. In particular, soft-rot fungi such as *Chaetomium* sp. may offer suitable strains for utilization in industry (Kirk et al., 1980).

Understanding lignin biodegradation is also important environmentally. For over a century, large amounts of lignin-related compounds have entered the environment from pulp production (Salkinoja-Salonen and Sundman, 1980). Understanding the biodegradability of these compounds is essential to understanding the impact of these compounds on the environment and how to cure any problems that occur.

One way of understanding lignin biodegradation is by studying the enzymes involved. Investigations of the enzymes of fungi are helpful in determining what fungi have and what they lack in wood-rotting capacity. Studying the enzymology of fungi proves in some ways to be more helpful in understanding lignin-degrading capacities of fungi than by observing fungi in their wild habitat.

Observation of fungi in their wild habitat gives limited evidence of their ability to degrade lignin. A given species may degrade a part of wood so slowly or incompletely that its degradation may not readily be observed in nature. A more-capable species, rotting wood at a faster rate, will take the place of a less-capable one before the slow-acting activity of the less-capable species takes place. In this way the slower-acting wood-rotting capacities of a given species are almost undoubtedly hidden from the observer (Garrett, 1963).

One of the first enzymes associated with lignin-biodegradation to be isolated was called laccase. Numerous researchers have suggested that laccase is necessary for complete lignin breakdown (Harkin et al., 1974; Szlarz et al., 1989), but the role of laccase in the long process of lignin metabolism is still not completely understood. It seems that laccase plays an indirect but necessary role, as a phenol-oxidizing enzyme, but that it does not structurally change lignin to a large degree (Kirk 1983; Kirk, 1984).

Recently, the enzymatic functions of laccase produced by *Coriolus versicolor* on polymeric lignin were determined by Iimura et al. (1991). Using ^{13}C and ^{14}C labeled synthetic high-molecular-mass lignin and ^{13}C-NMR spectroscopy, they found that laccase can degrade the framework of lignin and make lignin water soluable.

Since laccase is necessary for lignin biodegradation, it has been looked for primarily in fungi known to be lignin degraders. These fungi are called white-rot fungi because they degrade the cellulose, hemicelluloses, and lignin of wood evenly and equally, leaving the wood a light color during decay. Most other wood-rotting fungi are referred to as "brown-rot fungi" because they only metabolize cel-

lulose and hemicelluloses. Lignin is left behind in brown bands resulting in an erratic decay pattern in wood. These fungi attack some cells extensively while leaving others unharmed. They seem to have the necessary chemistry for the rudimentary processes of lignin degradation (Kirk, 1983). Since the brown-rot fungi are blocked by lignin, the decay of wood from these fungi is generally not as great as the decay due to white-rots (Deacon 1984).

The third and last type of wood-rot fungi is called soft-rot fungi. They are most commonly seen on wood that is in contact with water (Deacon, 1984). Soft-rots have not been studied as extensively as the other two types, and the enzymes necessary for lignin biodegradation by soft-rot fungi are not known (Raven et al., 1992).

Although the lignin-degrading enzymes used by soft-rot fungi have not been studied adequately, the extent to which soft-rot fungi can degrade lignin has been studied. A comparison of the weight losses resulting from attack by each wood-rotting type shows that soft-rot fungi do not degrade lignin nearly as quickly as white-rto fungi, but faster and to a larger degree than brown-rto fungi (Kirk, 1983). As one can see in the succession of fungi on trees or soil, soft-rot fungi prefer carbohydrates to lignin, degrading them much faster (Ander and Eriksson, 1978).

Eslyn et al. (1974) determined that the ability to degrade various parts of the wood varies greatly with each species of soft-rot fungi. An examination of the wood-rotting activities of just six soft-rot fungi indicated a range of 2 to 20% lignin depletion. The amounts of cellulose and hemicellulose depleted varied even more. With such varying degrees of wood-rotting capabilities, it could be assumed that the enzymology varies considerably as well.

The enzyme laccase is found in all white-rot fungi, but it has not been found in all soft-rot fungi. The goal of this research is to find laccase producing fungi among soft-rot species. Species belonging to the genus *Chaetomium* were tested for the ability to produce laccase. *Chaetomium* is a rather large genus containing more than eighty species (Ames, 1963), all of which are considered to be true soft-rot fungi. Three species found to grow on wood were chosen for study.

Materials and Methods

Chaetomium and *Cerrena* species were obtained from The American Type Culture Collection (Rockville, MD). Cultures were kept on 5% malt agar slants at about 20°C.

To test for laccase, cultures were transferred to a liquid medium using the methods described by Lindeberg and Fahraeus (1952). The medium contained in one l of H_2O: 1.8 g $NaNO_3$, 5 g glucose, 0.5 g $MgSO_4*7H_2O$, 0.47 g KH_2PO_4, 0.48 g Na_2HPO_4, 0.05 g $Ca(NO_3)_2*4H_2O$, 8.5 mg $Mn(CH_3COOO)_2$, 3.2 mg $FeC1_3*6H_2O$, 2 mg $Zn(NO_3)_2$, 2.5 mg $CuSO_4$, 0.05 mg thiamine, pH 5.6.

The fungi were grown in 250 ml Erlenmeyer flasks containing 50 ml of medium at 23° C for two weeks in a static culture. Eight cultures were grown for each species. Each of the cultures were tested for laccase activity at one week intervals for two months. *Cerrena unicolor* was used as a positive control to check testing procedures. A study by Harkin et al., (1974) confirmed that *Cerrena unicolor* shows signs of laccase activity.

Laccase activity was detected using syringaldazine as a chromogenic substrate. The reaction mixture contained in 1 ml: 0.4 Mellvaine buffer (0.2 M phosphate-0.1 M citrate), pH 6.5, 0.1 ml 1 mM syringaldazine (in an ethanol solution), and the medium sample. After the broth and mycelia have been mixed with syringaldazine, a pink color appears in the broth and mycelia when laccase activity is present (Szlarz et al., 1989). The reaction mixture was watched for two minutes.

Results

Species	Result	Growth	Reaction Time
Cerrena unicolor	positive	2 weeks	instant
Chaetomium elatum	positive	3 weeks	15 s
Chaetomium olivaceum	negative		
Chaetomium succineum	negative		

"Growth" refers to the length of time the species grew in the medium before a positive result was detected. "Reaction time" is the length of time the broth took to turn pink after it was added to the syringaldazine mixture.

Discussion

Harkin et al. (1974) tested over one hundred wood-rotting species and found that syringaldazine can be used for an indicator of the production of laccase. Before Harkin's discovery, tincture of guaiac was used as a test for laccase (Nobles, 1958). All species known to produce laccase tested positive to the Harkin test, and those known to lack the ability to produce laccase tested negative. Since their discovery, syringaldazine has repeatedly been used for detection of all types of laccases, even those produced by plants (Bao et al., 1993). Syringaldazine is thought, therefore, to be an accurate test for the presence of laccase.

It was determined that *C. elatum* is a laccase producing fungus. It is not certain that *C. elatum* degrades lignin simply because it produces laccase, an enzyme associated with

lignin biodegradation. Further research must be done to make the conclusion that it has lignin degrading abilities. The fact that the species is a laccase producer does make it a good candidate species for lignin biodegradation.

If it is a lignin-degrading fungus, it should be tested for evidence of activity of other enzymes associated with lignin degradation so that lignin degradation among soft-rot fungi can be better understood.

It has been noted that soft-rot fungi such as *Chaetomium* sp., which degrade wood differently than brown-rot or white-rot fungi, may offer suitable strains for utilization in industry, but too little is known of these species to say with certainty how useful they may be (Kirk et al., 1980). To determine the usefulness of *Chaetomium elatum* the extent to which it degrades other parts of wood and the ease with which its degrading ability can be manipulated should be tested.

Acknowledgements

The first author acknowledges financial support from the UALR Donaghey Scholars Program, The UALR Department of Physics and Astronomy and from the U.S. Department of Energy.

Literature Cited

Ander, P. and **K. Eriksson.** 1978. Lignin degradation and utilization by micro-organisms. Pro. Ind. Micro. 14:1-58.

Ames, L.W. 1963. A monograph of the chaetomiaceae. U.S. Army Research and Development Series No. 2.

Bao, W., D.M. O'Malley, R. Whetten, R.R. Severoff. 1993. A laccase associated with lignification in loblolly pine xylem. Science 260:672-674.

Deacon, J.W. 1984. Introduction to modern mycology 2nd ed. Blackwell Scientific Publications Boston.

Eriksson, K.E. and **L. Vallander.** 1980. Biomechanical pulping Pp. 213-224. *In* Lignin biodegradation: micro biology, chemistry, and potential applications. CRC Press, Baco Raton, Florida.

Eslyn, W.E., T.K. Kirk and **M.J. Effland.** 1974. Changes in the chemical composition of wood caused by six soft-rot fungi. Phytopatho. 65: 473-476.

Garrett, S.D. 1963. Soil fungi and soil fertility. Pp. 96-106. Pergamon, Oxford.

Harkin, J.M., J.L. Larsen and **J.R. Obst.** 1974. Use of syringaldazine for detection of laccase in sporophores of wood rotting fungi. Mycologia 66: 469-476.

Iimura, Y., K. Takenouch, Y. Katayama, M. Nakamura, S. Kawai, and **N. Morohoshi.** 1991. Elucidation of the biodegradation mechanism of ^{13}C-, and ^{14}C-labeled solid state lignin by *Coriolus versicolor.* Pp. 285-289. *In* Pro. 6th International Symp. on Wood and Pulp. Chem., Vol. 2.

Kirk, T.K., T. Higuchi and **H. Chang.** 1980. Lignin Biodegradation: Summary and Perspectives. Pp. 235-244. *In* Lignin Biodegradation: Microbiology, Chemistry and Potential Applications. CRC Press. Boca Raton, Florida.

Kirk, T.K. 1983. Degradation and converstion of lignocelluloses. *In* The filamentous fungi Vol. 4 Fungal Technology. Edward London Arnold Limited. Pp. 267-295.

Kirk, T.K. 1984. Microbial degradation of organic compounds. Edward London Arnold Limited. Pp. 399-430.

Lindeberg, G. and **G. Fahraeus.** 1952. Nature and formation of phenol oxidases in *Polyporus zonates* and *Polyporus versicolor.* Phy. Plant. 5:277-283.

Nobles, M.K. 1958. A rapid test for extracellular oxidase in cultures of wood-inhabiting hymenomycetes Can. J. Bot.

Paszczynski, A., R.L. Crawford, R.A. Blanchette. 1988. Delignification of wood chips and pulps by using natural and synthetic porphyrins: models of fungal decay App. Envir. Micro. 54: 62-68.

Raven, P.H., R.F. Evert, S.E. Eichhorn. 1992. Biology of Plants. 189, 199. New York Worth Publs.

Rosenberg, S. and **C.R. Wilke.** 1980. Lignin Biodegradation and the production of ethyl alcohol from Cellulose. Pp. 199-212. *In* Lignin Biodegradation: Microbiology, Chemistry and Potential Applications. CRC Press, Boca Raton, Florida.

Salkinoja-Salonen, M. and **V. Sundman.** 1980. Regulation and genetics of the biodegradation of lignin derivatives in pulp mill effluents, Pp. 179-198. *In* Lignin Biodegradation: microbiology, chemistry and potential applications. CRC Press, Boca Raton, Florida.

Szlarz, G., R. Antibus, R. Sinsabaugh and **A Linkins.** 1989. Production of phenol oxidases and peroxidases by wood-rotting fungi. Mycologia 81:234-240.

Yoshitake, A., Y. Katayama, M. Nakamura, Y. Iimura, S. Kawai and **N. Morohoshi.** 1993. N-linked carbohydrate chains protect laccase III from proteolysis in *Coriolus versicolor* J. of Gen. Microbiol. 139:179-185.

Barn Owl (*Tyto alba*) Food Habits in West-Central Arkansas

R.M. Huston and T.A. Nelson
118 Seebee Lane
Buckville, AR 71956

Department of Zoology
600 Lincoln Avenue
Eastern Illinois University
Charleston, IL 61920-3099

Abstract

This study was conducted on Holla Bend National Wildlife Refuge in west-central Arkansas to investigate the food habits of the common barn owl (*Tyto alba*). Three hundred thirty-eight pellets were collected from four barn owl nest boxes yielding the remains of 1003 individual prey items. Hispid cotton rats (*Sigmodon hispidus*) were eaten most frequently, comprising 46.8% of the diet by frequency. Results of this study are compared with those from other Arkansas ecoregions to assess regional variation in the diet of this endangered species.

Introduction

The barn owl (*Tyto alba*) is a species of special concern in Arkansas due to its low numbers. It is usually associated with open fields and agricultural land. While this species has been studied extensively throughout most of its range (Bent, 1938; Wallace, 1948; Boyd and Shriner, 1954; Banks, 1965; Bunn et al., 1982), few studies have been conducted in Arkansas. We are aware of only two food habits studies one conducted in northeast Arkansas (Paige et al., 1979) that examined the contents of 45 pellets, and another conducted in southwest Arkansas (Steward et al., 1988). Our study was conducted on Holla Bend National Wildlife Refuge (Pope County), located in the Arkansas River Valley in west-central Arkansas.

Materials and Methods

Over two years (1990 and 1991), 338 pellets from four nest boxes were collected and analyzed. The nest boxes were located in barns surrounded by farmland, primarily soybean and sorghum fields. Pellets were collected from nest boxes every two weeks, placed in bags, and labeled with the date and location. To analyze food contents, skeletal, hair, and feather remains were separated and identified. Remains were observed under a dissecting microscope and compared to standard keys (Glass, 1951; Sealander, 1979; Schwartz and Schwartz, 1981) and specimens in the Arkansas Tech University Vertebrate Collection. The importance of each species or group in the diet of barn owls was estimated from the percent frequency of occurrence in pellets.

Results and Discussion

The evaluation of food habits based on pellet analysis can be biased because foods differ in digestibility (Errington, 1932). The primary foods of barn owls are rodents whose skulls and teeth are difficult to digest (Errington, 1932). Because our sample size was large, we were confident that these data allow a general assessment of the raptor's diet in this region of the state.

Small mammals comprised the vast majority of the species consumed by barn owls on Holla Bend. Hispid cotton rats (*Sigmodon hispidus*) were the most important food item and were found in 46.8% of the sample (Table 1). The cotton rat was common on the study area, which is comprised of crop fields, fallow land, and old fields. The cotton rat prefers this type of habitat (Schwartz and Schwartz, 1981; Sealander and Heidt, 1990). The southern bog lemming (*Synaptomys cooperi*) has been documented as the dominant prey of barn owls in northeast Arkansas (Paige et al., 1979). Although there is suitable habitat, southern bog lemmings are not found in the study area (Sealander and Heidt, 1990). The woodland vole (*Mircotus pinetorum*) was the second most important food item in our study, comprising 14.2% of the prey consumed. Steward et al. (1988) reports the woodland vole and the cotton rat as the most numerous prey items in southwest Arkansas. The marsh rice rat (*Oryzmys palustris*) represented 13% of the food contents of the pellets. The combined percentage for all shrew species was 7.1%. The southeastern shrews (*Sorex longirostris*) are a county record and represent only the ninth Arkansas county from which the shrew has been taken (Sealander and Heidt, 1990). The remaining prey items were other rodent species and

birds.

Table 1. Food contents of barn owl pellets on Holla Bend National Wildlife Refug (Fall 1990 and 1991).

Food Item	No. of specimens	% Frequency
Hispid Cotton Rat (*Sigmodon hispidus*)	470	46.8
Woodland Vole (*Microtus pinetorum*)	142	14.2
Marsh Rice Rat (*Oryzomys palustris*)	130	13.0
Unidentified bird species (*passerines*)	88	8.8
House Mouse (*Mus musculus*)	46	4.6
Unidentified shrews (*Soricidae*)	39	3.9
Least Shrew (*Cryptotis parva*)	21	2.1
Fulvous Harvest Mouse (*Reithrodontomys fulvescens*)	20	2.0
Deer Mouse (*Peromyscus maniculatus*)	13	1.3
Unidentified species	9	0.9
Short-tailed Shrew (*Blarina carolinenis*)	8	0.8
Unidentified Cricetidae	7	0.7
Southeastern Shrew (*Sorex longirostris*)	4	0.4
Eastern Cottontail (*Sylvilagus floridanus*)	4	0.4
Unidentified rodents (*Rodentia*)	2	0.2
TOTAL	10003	100.1

Unidentified bird species (passerines) occured in 8.8% of our sample (Table 1). Red-winged blackbirds (*Agelaius phoeniceus*) were identified in two of the pellets. Red-winged blackbirds were also found in barn owl pellets from Ohio (Carpenter and Fall, 1967).

Our results show that rodent species are the primary prey consumed by barn owls. This is also supported by Paige et al. (1979) and Steward et al. (1988). As prey items, bird species were slightly more prevalent in our sample (8.8%) than those of Paige et al. (1979) (6.5%), and Steward et al. (1988), (2.2%). This could reflect differences in the availability of prey in differing habitats. Insectivore percentages in Steward et al. (1988), Paige et al. (1979), and our study were 3.4%, 5.4%, and 7.2%, respectively. Although prey availability probably varies among ecoregions in Arkansas, the relative importance of rodents, insectivores, and birds in the diets of barn owls appears to be consistent. These studies suggest that barn owls could be beneficial predators in agricultural communities by culling nuisance rodent species.

Acknowledgements

We appreciate the assistance and information provided by Martin Perry and his staff at Holla Bend National Wildlife Refuge. We also thank Karen Yaich of the Arkansas Game and Fish Commission for providing information concerning Barn Owl nest boxes and Charles B. Burrell for field assistance. Support for the study was provided by the U.S. Fish and Wildlife Service and Arkansas Tech University.

Literature Cited

Banks, R.C. 1965. Some information from barn owl pellets. Auk 82:506.

Bent, A.C. 1938. Life histories of north american birds of prey: part two. Dover Publications Inc., New York, 412 pp.

Boyd, E.M. and **J. Shriner.** 1954. Nesting and food of the Barn Owl (*Tyto alba*) in Hampshire Co. Mass. Auk 71:199-201.

Bunn, D.S., A.B. Warburton and **R.D.S. Wilson.** 1982. The Barn Owl. Buteo Books, Vermillion, South Dakota.

Carpeter, M.L. and **M.W. Fall.** 1967. The Barn Owl as a red-winged blackbird predator in northeastern Ohio. Ohio J. Sci. 67(5):317.

Errington, P.L. 1932. Techniques of raptor food habits study. Condor 34:75-86.

Glass, B.P. 1951. A key to the skulls of North American mammals. Burgess Publishing Co., Minneapolis, Minnesota, 71 pp.

Paige, K.N., C.T. McAllister and **C.R. Tumlison.** 1979. Unusual results from pellet analysis of the American Barn Owl *Tyto alba pratincola* (Bonaparte). Proc. Arkansas Acad. Sci. 33:88-89.

Schwartz, C.W. and **E.R. Schwartz.** 1981. The wild mammals of Missouri. University of Missouri Press and Missouri Dept. of Conservation, Columbia, 356 pp.

Sealander, J.A. 1979. A guide to Arkansas mammals. River Road Press, Conway, Arkansas, 313 pp.

Sealander, J.A. and **G.A. Heidt.** 1990. Arkansas mammals their natural history, classification, and distribution. The University of Arkansas Press, Fayetteville, Arkansas, 308 pp.

Steward, T.W., J.D. Whilhide, V.R. McDaniel, and D.R. England. 1988. Mammalian species recovered from a study of Barn Owl, *Tyto alba*, pellets from southwestern Arkansas. Proc. Arkansas Acad. Sci. 44:115-116.

Wallace, G.J. 1948. The Barn Owl in Michigan. Mich. State Coll. Agr. Exp. Sta. Tech. Bull. 208:1-61.

The Effect of Product Price, Interest Rates and Forestry Incentives on Financial Returns from Arkansas' Nonindustrial Private Forests

James R. Jolley and Richard A. Kluender
School of Forest Resources
University of Arkansas at Monticello
Monticello, AR 71656

Abstract

As the U.S. population increases, demand for Arkansas' forest production will continue to increase. Nonindustrial private forests (NIPF) will be increasingly relied upon to meet future demand. Restocking following harvest and good forest management techniques have not always been practiced on NIPF lands. Federal cost sharing programs exist which encourage investment in forestry; federal programs may pay up to half of establishment and management costs. Special federal capital gains treatment and other tax incentives also exist for nonindustrial landowners; however, nonindustrial use of incentives is not great.

Models were developed to determine whether actual stumpage prices and existing economic incentives were sufficient to cover the investment cost of establishment and owning and holding the stand. Using site indexes of 70 and 80 (base 50) for loblolly pine plantations, stand value and opportunity costs were compared annually over the life of a 40 year rotation. Long-term U.S. Treasury Bond rates and a flat 6% rate of return were used to estimate opportunity costs on an after tax basis. Investment costs were estimated with and without using existing economic incentives.

Results show that if front-end costs of establishment are low, stand value is virtually certain to be greater than opportunity costs. This was true even on low site index tracts with high opportunity costs. Without incentives, investment success is subject to stumpage price fluctuations especially when high opportunity costs are in place. Policy recommendations include increasing present efforts to inform NIPF landowners of incentive opportunities to encourage development of private forest resources. If private landowners have the proper information, they are more likely to improve their personal situation and enhance forest productivity.

Introduction

Non-industrial private landowners (NIPL) hold 57% (9.8 million acres) of the timber land in Arkansas. The forest industry controls 25% (4.4 million acres), and public agencies the remaining 18% (3.1 million acres) (USDA, 1992a). Approximately 52% of the Arkansas' softwood harvest and 29% of the hardwood harvest come from private forest industry lands. Public agencies supply 9% of the State's hardwood and softwood harvest. Nonindustrial private land provides the remaining 39% of the state's softwood harvest and 62% of the hardwood harvest (USDA, 1988).

In Arkansas during 1988 for all ownership and forest types (17.2 million acres), approximately 4.0 million acres (24%) were ready for final harvest. Some 8.0 million acres (46%) of the timberland supported young, well-stocked stands where no obvious treatment was required to enhance growth. However, about 2.9 million acres (17%) of the State's timberlands were so poorly stocked that establishment of new stands was needed. The remaining 2.4 million acres (13%) required commercial thinning or other stocking control. Of the 9.8 million nonindustrial acres in Arkansas, approximately 2.5 million acres (26%) were ready for final harvest. Some 4.1 million acres (41%) were in no obvious need of treatment to enhance prospective growth. About 1.3 million acres (13%) required commercial thinning or other stocking control. The remaining 1.9 million acres (20%) were poorly stocked and needed to be reestablished. Of the state's poorly stocked timberland requiring reestablishment, 67% was on nonindustrial private lands (USDA, 1992a).

After growth and removals from 1978 to 1988, the average annual net growth in Arkansas declined from 50 to 45 ft^3 per acre. The average annual net growth of pine was down 16%, while hardwood growth increased by 5%. Most of the reduction in pine growth occurred on nonindustrial private lands where net pine growth was down 22%. At the same time, most of the increase in net hardwood growth was on nonindustrial private lands (USDA, 1992a). It is not surprising that in a recent study Greene and Blatner (1987) found that over two thirds of the nonindustrial private landowners did not practice forest management, even though 38% of nonindustrial private landowners had named timber as a primary goal of holding forest land.

As the population in the U.S. increases, demand for Arkansas' forest production will increase. Public forests are increasingly coming under scrutiny. Limitations on

harvesting methods and annual harvest quotes are being enacted. Private industrial forests are producing at near maximum levels. Nonindustrial forests remain as the only domestic source to draw from (USDA, 1988).

Arkansas' nonindustrial forest landowners have cost sharing and tax incentives available to encourage investment in their forests; however, these incentives are often not used. Given the non-use of cost sharing and tax incentives, the question arises whether stumpage prices are sufficient for forestry investment to compete with alternative investment choices.

Cost Sharing Incentives.--Incentive programs have been instituted by Congress to encourage nonindustrial private landowners to establish and manage forests. The cost sharing programs include: the Stewardship Incentives Program (SIP), the Forestry Incentives Program (FIP), and the Conservation Reserve Program (CRP). In order to receive SIP funds, the landowner must have an approved management plan developed under the Stewardship Program (SP) which provides technical assistance instead of cost sharing (Arkansas Forestry Commission, 1990).

The SP began in 1990 and is administered by the USFS. The program is intended to promote and recognize good land stewardship by private nonindustrial landowners. To be eligible for the SP, a private landowner must own a minimum of 40 acres with at least 10 acres of it in forests, and must have the desire to manage the land for multiple resources (Arkansas Forestry Commission, 1990). SP is administered cooperatively at the state level by the Arkansas Forestry Commission (AFC) and several other agencies. Management objectives in addition to timber production include: wildlife, recreation, soil and water protection, and aesthetics. Once a landowner has an approved management plan. he can apply under SIP for cost share assistance to carry out recommended practices.

SIP cost sharing is set at 50% of the state wide average cost so the landowner must make a commitment to invest some his own capital as well. Areas of cost sharing include: 1) tree planting, 2) timber stand improvement, 3) soil/water protection and improvement, 4) riparian and wetlands protection and improvement, 5) fisheries habitat protection and improvement, 6) wildlife habitat protection and enhancement and 7) forest recreation enhancement.

FIP was authorized by Congress in 1973 to provide cost sharing with private landowners solely for tree planting and timber stand improvements. Funding for FIP ceases in 1995 and the program is being augmented/replaced by SIP (M. Phillips, pers. comm.). SIP has multiple management objectives, whereas FIP only has timber as the objective. The percentage of cost sharing is based on U.S. Forest surveys of total, eligible, private timber acreage and acreage potentially suitable for production of timber products. Cost sharing state wide for Arkansas is set at 50%. Cost share income is generally considered to be tax free (USDA, 1981). Monitoring for compliance with FIP regulations and technical assistance are provided by the Arkansas Forestry Commission (D. Grimmett, pers. comm.).

CRP was authorized by the Food Security Act in 1985. The intent of the program is to protect the nation's natural resource base by removing highly-erodible and eroding cropland out of production. In addition to protecting soil, benefits are expected to include: 1) improved water quality, 2) reduction in surplus commodities, 3) reduced sedimentation, 4) long-term timber supplies, 5) improved wildlife habitat (AGFC, 1986). CRP is administered by Agricultural Stabilization and Conservation Service (ASCS) at the federal level and carried out by the Soil Conservation Service (SCS) on the local level. Under CRP the landowner makes an agreement with the USDA to set aside an area of land for a period of at least ten years to establish trees. During the agreement period, the USDA pays the landowner up to $50 per acre annually for rent of the land and 50% of the establishment costs. When a landowner applies for CRP, the SCS informs the landowner how much will be paid in rent and cost-share benefits (M. Phillips, pers. comm.).

Nonindustrial Landowner Use of Cost Share Incentives in Arkansas.--Table 1 shows the number of acres planted in Arkansas under SIP, FIP, and CRP from 1986 to 1993. During the period from 1975 to 1989, the number of acres planted to trees under FIP and CRP was 247,931.2 acres. For the same period, 372,000 acres were planted on nonindustrial private lands (USDA, 1992a). Thus, approximately 67% of the acres planted on nonindustrial private lands was done with the benefit of FIP and CRP. Most nonindustrial private landowners do not exercise enough foresight to achieve adequate stocking using natural regeneration methods (D. Grimmett, pers. comm.).

Tax Incentives.--Federal tax legislation provides significant advantages to nonindustrial private forest landowners. The 1943 Revenue Act and Section 631 of the Internal Revenue Code allow income from both timber sales and timber use by owners to be taxed under capital gains rates which are lower than the marginal rates for ordinary income. This treatment continues to exist to present, although the capital gains rate is now significantly higher than it once was. In 1980 Public Law 96-451 was passed to encourage investment by nonindustrial landowners (USDA, 1988). This law stipulates a 10% investment tax credit plus an initial seven year amortization on the first $10,000 of capitalized reforestation expenditures during one year (USDA, 1988).

The Tax Reform Act of 1986 established two tax brackets of 15% and 28% (Church, 1986). The effect is that capitalized forestry expenses are taxed at the marginal tax rate. The seven year amortization schedule, 10% investment tax credit for reforestation, and the expensing of

annual management costs is retained (USDA, 1988). The Tax Reconciliation Act of 1993 added a 36% and 39.6% marginal tax rate to the existing 31% bracket for ordinary income. The 31% bracket was added under the 1990 Revenue Reconciliation Act. Timber income qualifying for capital gains treatment can take advantage of a substantially lower rate than required for ordinary income (Haney, 1993).

Table 1. Acres planted in Arkansas under various incentive programs, 1975 to 1993.[A]

Fiscal Year	CRP	FIP	SIP	Year Total	NIPF Area Planted [B]
1975-1982	-	67,328	-	67,328	118,000
1983	-	11,057	-	11,057	20,000
1984	-	11,925	-	11,925	16,000
1985	-	13,948	-	13,948	23,000
1986	10,487.2	13,823	-	24,310.2	24,000
1987	31,908.9	8,547	-	40,455.9	45,000
1988	27,523.3	11,146	-	38,669.3	64,000
1989	28,202.3	12,035.5	-	40,237.8	62,000
1990	13,464.4	12,618.8	-	26,083.4	C
1991	7,407.3	11,673.3	-	19,080.6	C
1992	7,962.9	12,652.4	-	20,615.3	C
1993	9,879.4	13,575.2	1,355.5	24,810.1	C
Totals	136,835.9	200,329.2	1,355.5	338,520.6	372,000

A Sources: U.S. Department of Agriculture, Agricultural Stabilization and Conservation Service. Internal Report, and U.S. Department of Agriculture. [Annual Issues.] Agricultural statistics 19xx. U.S. Government Printing Office, Washington: 19xx.
B Sources: U.S. Department of Agriculture, Forest Service, [Annual Issues.] U.S. forest planting report. Washington, DC.
C Data not available.

Nonindustrial Private Landowners as Forest Investors.--The main issue for nonindustrial land owners considering forest investment is whether or not forestry is as profitable as other investments. The forest investment must meet or exceed the rate of return on alternative investments or the investor faces an opportunity cost. The yearly opportunity cost of holding timber as a capital asset is the interest charge on the value of the timber. The appropriate rate of return is the highest rate that the investor could earn on capital invested elsewhere with similar risk and duration (Pearse, 1967). With an appropriate interest rate, the total holding cost of a stand can be compared annually to the value received if the standing timber were liquidated. If the stand value is greater than or equal to the total holding cost, then the nonindustrial owner knows that if he were to sell his timber, the price received would cover his owning and holding cost. Additionally, if this condition exists, then price is at least the long-run equilibrium price which is sufficient to prompt reinvestment.

Given the non-use of cost sharing and tax incentives, the question arises whether stumpage prices are sufficient for forestry investment to compete with alternative investment choices. The objectives of this research were: 1) to determine whether stumpage prices that a NIPF landowner would receive at any point in the rotation would cover the owning and holding costs of growing timber up to that time; 2) to examine historical trends in stumpage prices and existing economic incentives to determine if a suitable environment is present for the landowner to invest in forestry and; 3) to compare investment opportunities with and without forestry incentives.

Methods

The total cost of owning and holding and the value of a forest stand were examined annually for a nonindustrial private landowner. A routine treatment regime was used to simulate a cut-over loblolly pine plantation. PCWTHIN version 2.0, growth and yield forecasting and planning tool (Weih and Scrivani, 1990) was used to predict growth and yield for a 40 year sawtimber rotation in Arkansas. Assumptions for the simulation were that pine seedlings were hand planted with 8' by 10' spacing on two Coastal Plain soils having a site index of 70 and 80 (base 50). A site index of 70 is low for the Arkansas' Coastal Plain, while site index 80 is average. The two sites were used to determine the effect of timber volume changes in the model. Several treatments were applied during the simulated rotation. Site preparation consisted of a prescribed burn and single chop disking. A chemical release was performed to control undesirable vegetation. Prior to harvests, prescribed burns were performed to gain better access for subsequent inventory/marking and control of undesirable vegetation. Between harvests, a prescribed burn was executed for fuel reduction to decrease the risk of wildfire and to control undesirable vegetation. Tables 2 and 3 show the silvicultural activity, costs with and without SIP incentives, and timber volumes for the simulated stands. Estimated yields from the program for site 70 and site 80 were compared with actual yields in Arkansas to validate the model (R.A. Williams, pers. comm.).

Treatment costs (1992) were used for Coastal Plain sites were taken from Belli et al. (1993). Seedling costs (1993) were taken from Arkansas Forestry Commission nursery price schedules (D. Grimmett, pers. comm.). Stumpage prices for 1960 to 1992 in Arkansas were taken from Timber Mart-South (Data Resources Inc, 1986), and USFS data for Louisiana (USDA, 1990).

Table 2. Simulated treatments used in model development, Site index 70 (base 50).

Year	Activity	Cost*	Volumes**	
Date No.	Establishment, Harvest, or Treatment	Nominal / Real	Pulpwood Cords Bfr/After	Sawtimber BDFT Doyle BftAfter
1953 0	Prescribed burn, Single chop, Hand Plant 8x10, Chemical Release	216/154 / 110/78	0	0
1967 15	Prescribed Burn	8/6 / 3/2	7.8	0
1972 20	Prescribed Burn, Inventory, Marking, Row-Low Thin 1:4 Rows BA 60	21/15 / 16/12	14.4/ 10	262.6/ 241.1
1977 25	Prescribed Burn	8/6 / 3/2	9.8	1921.9
1982 30	Prescribed Burn, Inventory, Marking, Free Thin BA 60	21/15 / 16/12	9.6/ 4.7	4023.1/ 2802.4
1987 35	Prescribed Burn	8/6 / 3/2	3.8	4755.2
1992 40	Prescribed Burn, Inventory, Marking, Final Harvest	21/15 / 16/12	2.6/ 0	7196/ 0

*Cost $/acre without SIP/with SIP, constant dollar (real) dollars are from 1983 base. Amounts rounded to whole dollars.
**Volumes are on a per acre basis.

Table 3. Simulated treatments used in model development, Site index 80 (base 50)

Year	Activity	Cost*	Volumes**	
Date No.	Establishment, Harvest, or Treatment	Nominal / Real	Pulpwood Cords Bfr/After	Sawtimber BDFT Doyle BftAfter
1953 0	Prescribed burn, Single chop, Hand Plant 8x10, Chemical Release	216/154 / 110/78	0	0
1965 13	Prescribed Burn	8/6 / 3/2	9	0
1970 18	Prescribed Burn, Inventory, Marking, Row-Low Thin 1:4 Rows BA 70	21/15 / 16/12	14.5/ 11.6	482/ 445.4
1974 21	Prescribed Burn	8/6 / 3/2	11.4	2119.2
1977 25	Prescribed Burn, Inventory, Marking, Free Thin BA 70	21/15 / 16/12	11.2/ 6	3792.9/ 3079
1980 28	Prescribed Burn	8/6 / 3/2	5.3	4397
1984 31	Prescribed Burn, Inventory, Marking, Low Thin BA 60	21/15 / 16/12	4/ 1.6	7033/ 4978.3
1988 36	Prescribed Burn	8/6 / 3/2	1.5	6931.6
1992 40	Prescribed Burn, Inventory, Marking, Final Harvest	21/15 / 16/12	1.3/ 0	9335.9/ 0

*Cost $/acre without SIP/with SIP, constant dollar (real) dollars are from 1983 base. Amounts rounded to whole dollars.
**Volumes are on a per acre basis.

The cost of each management treatment was compounded from the year it was incurred during the rotation using annual yield (annual interest rate) during June for long-term U.S. Treasury Bonds. The U.S. Treasury Bond yields are commonly used in economic analysis as a comparison against forestry investments because the bonds are

of low risk and long duration. Treasury Bond yield data was obtained form the Federal Reserve Bank in Dallas, Texas (U.S. Federal Reserve, 1994a). The compounded costs were summed as they occurred. Since the nonindustrial private landowner owner makes the decision each year whether to liquidate the stand or allow it to grow, there is an annual opportunity cost in addition to the compounded costs. The annual opportunity cost was represented by multiplying the current value of the stand by the Treasury Bond annual yield. The annual opportunity cost was added to the compounded costs to simulate total holding cost for each year. The stand value for the year is the volume of the standing timber times the current price. Sawtimber and pulpwood were the only products considered in stand value. During harvest years, volume was removed form the stand. Stand value was accordingly reduced. The disposition of revenue garnered from harvests was not reinvested in the forest or used to diminish the total holding cost. Nonindustrial private forest owners commonly use the harvest revenue to purchase desired goods and services such as a new car, college education for children, etc. (R.L. Willett, pers. comm.). All dollar amounts were adjusted to constant dollars using average annual Consumer Price Index (CPI) data from the Federal Reserve Bank in Saint Louis, Missouri (U.S. Federal Reserve, 1994b). The previously cited CPI data was also used to adjust all annual interest rates to real interest rates (Buongiorno and Gilless, 1987). The equation used to calculate the annual stand value was:

$$S_t=(V_{Pt}xP_{Pt})+(V_{St}xP_{St})$$

S_t = Stand value at year t
V_p = Pulpwood volume, time t
P_p = Pulpwood price, time t
V_s = Sawtimber volume, time t
P_s = Sawtimber price, time t

The annual holding cost was calculated by:

$$TC_t=(S_t \cdot i_t)+\Sigma[c_n \cdot (1-m) \cdot (1+i_n)^{t-n}]$$

TC_t = Total holding cost in year t
S_t = Stumpage value of stand in year t
i_n = Annual yield or opportunity cost of alternative investment in year n
c_n = Treatment cost that occurred in year n
m = Marginal tax rate
t = Time (years) since rotation was initiated
n = Year treatment performed

The total holding cost was adjusted to an after-tax basis using both federal and state rates for Arkansas. The owner's income was assumed to be in the 28% bracket for federal and the 6% bracket for state taxes for an aggregate tax of 34%. (Arkansas Department of Revenue, 1993). Three pairs of total holding cost series were calculated. In the first pair, one series included the reduction of costs provided by SIP federal cost sharing funds along with seven year amortization of capitalized reforestation expenditures on federal income taxes. The other series did not include any incentives or tax considerations. The second pair was the same as the first except a 6% (after tax) rate for the entire period was used vice the Treasury Bond Yield rates. The 6% rate was used to show sensitivity to changes in rates and represents a realistic long-term rate for investment. The third pair used the 6% (after-tax) rate and average period constant-dollar prices (pulpwood \$12.58/cd, sawlogs \$132.40/mbf) to show sensitivity to stumpage price change.

Results

Figures 1 and 2 show constant dollar and nominal prices for pulpwood and sawtimber respectively. Constant dollar pulpwood prices increased from 1982-84 and decreased from 1985-91. Otherwise they remained relatively constant throughout the rotation. Constant dollar sawtimber prices increased from 1972-79 and in 1992. Otherwise prices remained relatively constant throughout the rotation.

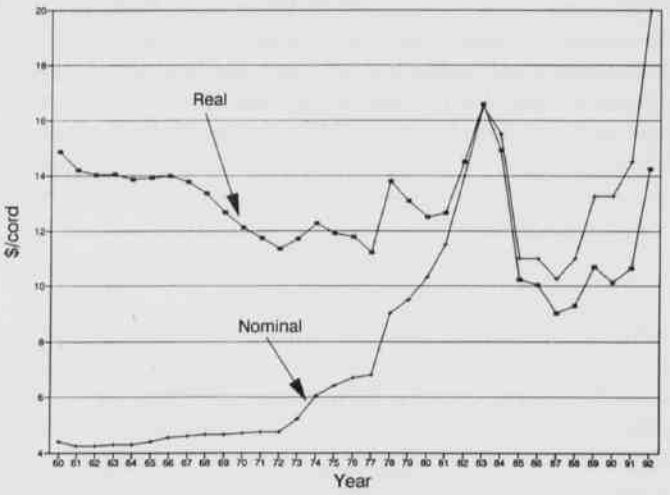

Fig. 1. Constant dollar and nominal pulpwood prices for Arkansas, 1960 - 1992.

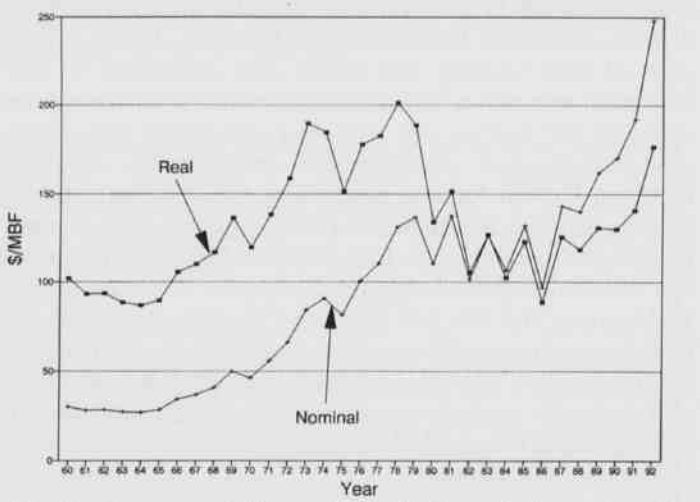

Fig. 2. Constant dollar and nominal sawtimber prices for Arkansas, 1960 - 1992.

Figure 3 shows the results for the model of the plantation on site index 70 with the yield of a then-current Treasury Bond (real) used as the investment opportunity cost to estimate total holding cost. When SIP and amortization incentives are used, the stand value clearly exceeds the total holding cost throughout the rotation after the trees reach merchantable size. When SIP and tax incentives are not included, the stand value exceeds the total holding cost from 1974 to the end of the rotation. Fig. 4 shows the model on site index 80 soil with Treasury Bonds (real) used to estimate total holding cost. With SIP and amortization, again the stand value overwhelmingly surpasses the total holding cost once the trees attain merchantable size. With no incentives, the stand value exceeds total holding cost from 1967-92, except in 1971 after the first thinning.

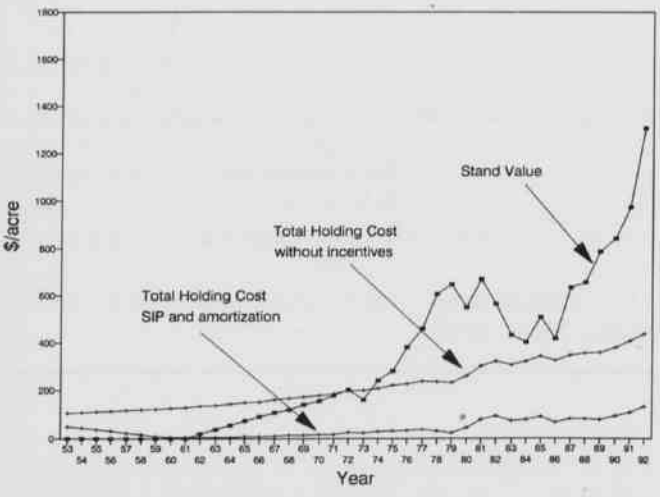

Fig. 3 Simulated stand value, and total owning and holding cost based on constant dollar stumpage prices with and without investment and tax incentives for SI 70, after tax basis using U.S. Treasury Bond interest rates (real) 1953-1992.

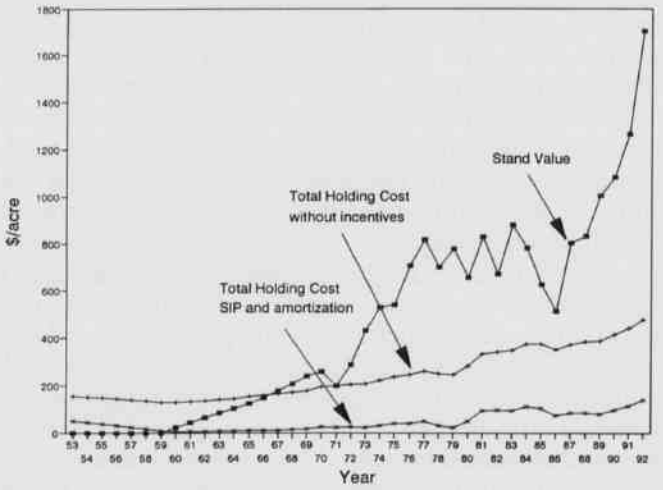

Fig. 4. Simulated stand value, and total owning and holding cost based on constant dollar stumpage prices with and without investment and tax incentives for SI 80, after tax basis using U.S. Treasury Bond interest rates (real), 1953-1992.

Figure 5 depicts the Treasury Bond annual yields (nominal and real) for each year during the rotation. Note when treatment costs were incurred, the real annual yields were between 2% and 4%. Exceptions were 9% in 1982 and 5% in 1970 for site indexes 70 and 80 respectively. Treatment costs during these years were low compared to the cost of establishment. Figures 6 and 7 portray the two simulated rotations with a flat 6% (real) rate during the entire rotation driving total holding costs. The 6% (real) rate causes the total holding costs to increase markedly and shift upward compared to the Treasury Bond (real) rates. Note that a 6% (real) rate more appropriately reflects a true opportunity cost for long-term investment than does the Treasury Bond (real) rate. For the site index 70 plantation, the stand value only surpasses the total holding cost from 1978-81 and in 1992 (Fig. 6). For site index 80, the stand value exceeds the total holding cost during 1973-84 and 1991-92 (Fig. 7). Recall that when the Treasury Bond (real) rates were used to estimate total holding costs, the periods which the stand value exceeded the total holding costs were much longer. Additionally, the margins between stand value and the total holding costs were greater. The 6% (real) rate used for estimating total holding costs shows that without SIP and tax incentives, nonindustrial private landowners are more susceptible to

loss when stumpage prices fall. At the 6% (real) rate, the problem is exacerbated when the site index is low (70) as shown in Fig. 6. The stand value only exceeds the total holding costs for brief periods. However, when the 6% rates were used along with SIP and tax incentives, for both site indexes, the stand value was greater than the total holding costs from the time the trees became merchantable until the end of the rotation.

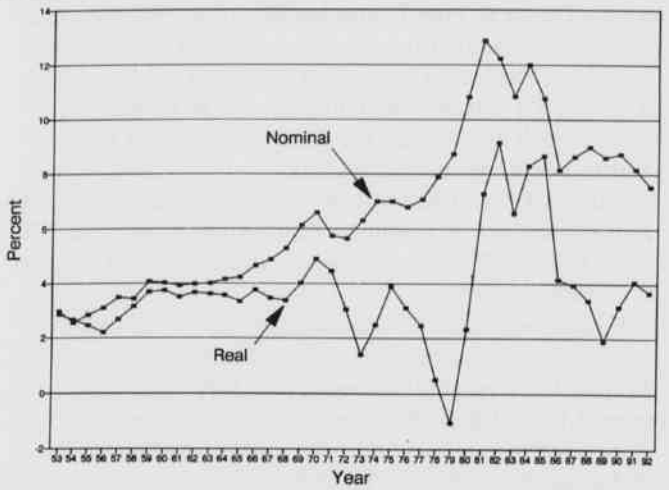

Fig. 5. U.S. Treasury Bond yield rate (nominal and real), 1953-1992.

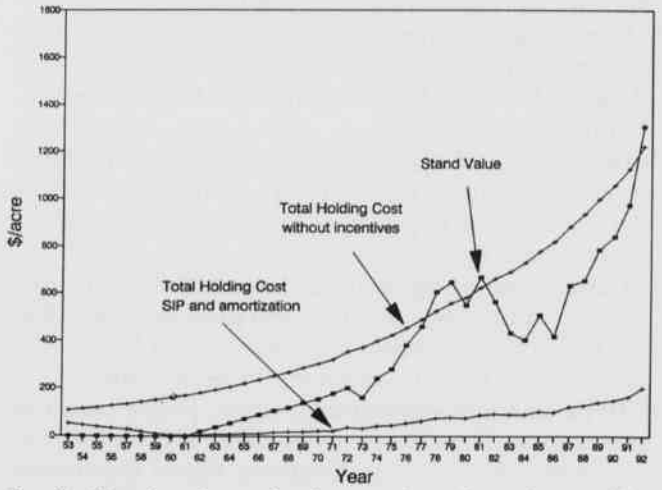

Fig. 6. Simulated stand value, and total owning and holding cost based on constant dollar stumpage prices with and without investment and tax incentives for SI 70, after tax basis using 6% real alternative interest rates, 1953-1992.

Figures 8 and 9 show the two site indexes with the 6% (real) rate and average period constant-dollar stumpage prices. Again for both site index 70 and 80 when SIP and

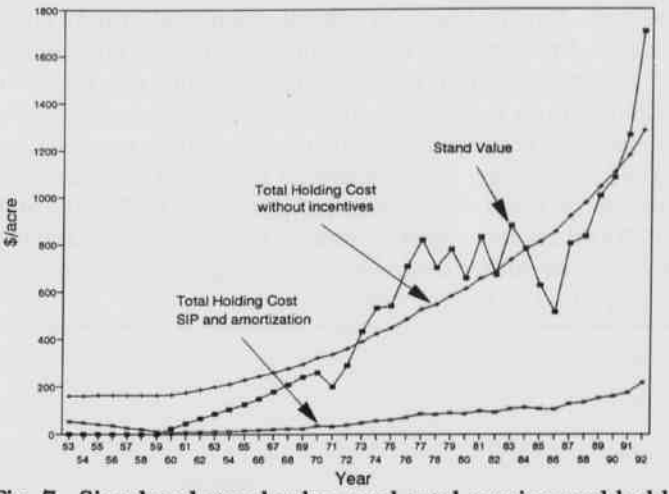

Fig. 7. Simulated stand value, and total owning and holding cost based on constant dollar stumpage prices with and without investment and tax incentives for SI 80, after tax basis using 6% real alternative interest rates, 1953-1992.

tax incentives are employed, stand value exceeds total holding cost for the entire period once timber is merchantable. However, for site index 80 without economic incentives, the number of years when stand value surpassed total holding cost decreased compared to when price were not averaged (Fig. 7). Similarly, without economic incentives on site index 70 (Fig. 8) stand value is never greater than total holding cost. Averaging prices over a long period such as a 40 year rotation removes the variability of business cycles from stumpage returns. It is this average price that an investor must use in making investment plans, although high markets concurrent with timber maturity are always yearned for.

Conclusions

Reducing or eliminating the high front-end costs (capitalized costs) of site preparation and planting is critical for NIPF landowners. Reduction of front-end costs becomes more important as opportunity costs rise and is especially critical on lower quality sites. Tax and cost sharing incentives available for regeneration and management activities can provide the single most effective means for overcoming front-end and opportunity costs for NIPF landowners once the decision concerning site preparation and regeneration method has been made. As the SI increases, the NIPF landowner is more assured of not suffering a loss when prices decrease. Better sites will always be better investments. NIPF landowner success in forest investment relies heavily on selling when product prices

are high. This is especially critical when opportunity costs are high. Product price information is critical to sale timing.

Policy recommendations following from this research include: (1) an increased educational effort by consultants, universities and extension agents should be targeted on NIPF landowners; (2) educational programs should stress the use of federal cost sharing programs (FIP, SIP, and CRP) and tax incentives to reduce front end costs; and (3) educational efforts should stress the importance of market timing in NIPF timber sales.

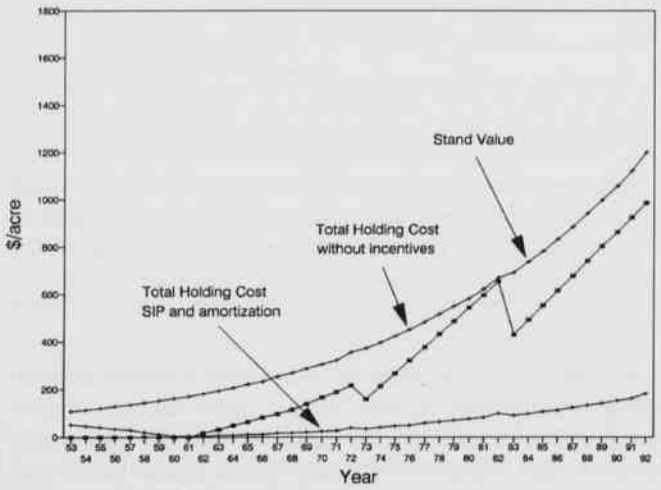

Fig. 8. Simulated stand value, and total owning and holding cost based on constant dollar average stumpage prices with and without investment and tax incentives for SI 70, after tax basis using 6% real alternative interest rates, 1953-1992.

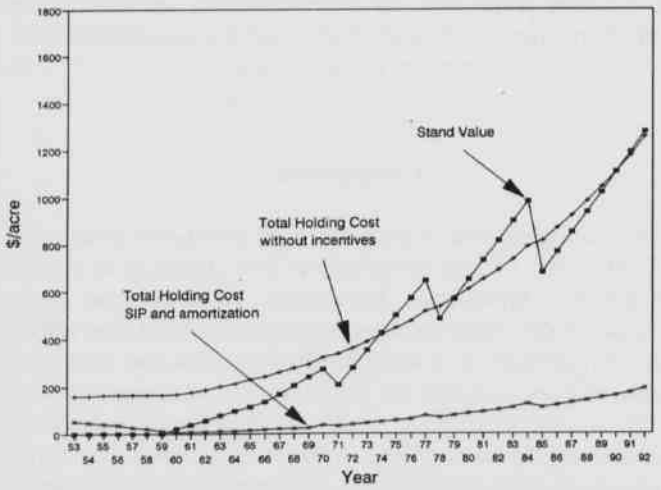

Fig. 9. Simulated stand value, and total owning and holding cost based on constant dollar average stumpage prices with and without investment and tax incentives for SI 80, after tax basis using 6% real alternative interest rates, 1953-1992.

Literature Cited

Arkansas Department of Revenue. 1993. Arkansas 1993 individual income tax booklet. State Income Tax. Little Rock, Arkansas.

Arkansas Forestry Commission. 1990. The Arkansas forest stewardship program. Pamphlet (no series number).

Arkansas Game & Fish Commission. 1986. Wildlife habitat improvements through the conservation reserve program. Pamphlet (no series number).

Belli, M.L., T.J. Straka, M. Dubois, and **W.F. Watson.** 1993. Costs and trends for forestry practices in the south. Forest Farmer. 52:25-31.

Buongiorno, J. and **J.K. Gilless.** 1987. Forest management and economics. MacMillian Publishing. New York, NY.

Church, G.J. 1986. The making of a miracle. Time. August 25, 1986, p 12-18.

Data Resources Inc. 1986. Stumpage prices for pine sawlogs and pine pulpwood in Arkansas. Timber Mart-South, 1984 yearbook. Lexington, MA.

Greene, J.L. and **K.A. Blatner.** 1987. Woodland owner characteristics associated with timber management. Arkansas Farm Research. 36:11.

Haney, H.L. 1993. Should you tailor forest management to current tax law?. Forest Farmer. 52:15-17.

Pearse, P.H. 1967. The optimum forest rotations. Forestry Chronicle. June, pp. 178-195.

U.S. Department of Agriculture. 1981. Forestry as an investment in the South. Forest Service. General Report SA-GR 20. Washington, D.C.: Government Printing Office.

U.S. Department of Agriculture. 1988. The south's fourth forest: Alternatives for the future. Forest Service. Forest Resource Report No. 24. Washington, D.C.: Government Printing Office.

U.S. Department of Agriculture. 1990. U.S. timber production, trade, consumption, and price statistics 1960-88. Forest Service. Misc. Publication No. 1486. Washington, D.C.: Government Printing Office.

U.S. Department of Agriculture. 1992a. Forest resources of Arkansas. Forest Service. Resource Bulletin SO-169. New Orleans, Louisiana. Southern Forest Experiment Station.

U.S. Department of Agriculture. 1992b. Stewardship incentives program - Arkansas. Soil Conservation Service. Amendment 3, Paragraph 21, p. 16-17. Washington, D.C.: Government Printing Office.

U.S. Federal Reserve Bank, Dallas, TX. 1994a. Long-term U.S. Treasury Bond rates time series. A dial-in computer bulletin board for statistical series.

U.S. Federal Reserve Bank, St. Louis, MO. 1994b. Long-term consumer price index time series. A dial-in com-

puter bulletin board for statistical series.

Weih, R.C., Jr. and **J.A. Scrivani.** 1990. PC THIN, a growth and yield simulator of loblolly pine. Virginia Polytechnic Institute and State University. School of Forest and Wildlife Resources.

Storm Dominated Channel Sequences on a Shallow Marine Shelf: Morrowan of Northwestern Arkansas

Kimberly R. Jones and Doy L. Zachry
Department of Geology
University of Arkansas
Fayetteville, AR 72701

Abstract

The Brentwood Member of the Bloyd Formation (Morrowan, Pennsylvanian) in northwestern Arkansas contains stratigraphic sequences deposted by tropical storms in middle shelf environments. The deposits are confined to shallow channels incised by strong unidirectional currents into an interval of shale deposited during fair weather conditions. Complete storm sequences reflect initial bottom currents of high competency that declined through time and were succeeded by wave generated oscillatory activity. The storm succession consists of an erosion surface followed by a basal pebble conglomerate, massive grainstone and packstone, whole-fossil wackestone, hummocky cross-strata and a swell lag of platy crinoid calyxes. As storm activity ceased, fairweather deposits of middle shelf clay blanketed the storm sequences.

Introduction

In recent years modern storm event shave caused storm deposits to be recognized as a normal part of the stratigraphic record. It is assumed that ancient storms would systematically effect coastal areas and adjacent continental shelves, and that these storm deposits would interrupt normal fairweather marine deposition. An understanding of storm processes has heightened the interest in ancient storm deposits and led to more frequenct recognition of such deposits in recent years.

Morrowan strata within the Bloyd Formation of northwest Arkansas contain depositional characteristics that can not be attributed to normal open marine, inner shelf depositional processes, but are compatible with storm depositional processes.

Geologic Setting.--Accumulation of early Morrowan sediment in northwest Arkansas occurred in a variety of marine and nonmarine environments on an inner shelf depositional surface inclined to the south at less than .01 degrees. A deeper outer shelf and slope marine environment lay to the south in central and southern Arkansas. Marine strata composed of shale, sandstone, and limestone were deposited in inner and middle shelf settings and dominate the Morrowan sequence.

The Hale and Bloyd Formations compose the Morrowan Series in northwest Arkansas (Fig. 1). The Hale Formation rests unconformably on rocks of Mississippian age. The Bloyd Formation conformably overlies the Hale. It is divided in ascending order into the Brentwood Member, the middle Bloyd sandstone, the Dye Shale Member and the Kessler Limestone Member (Fig. 1). All are marine deposits except for the middle Bloyd sandstone, a fluvial interval deposited by braided streams.

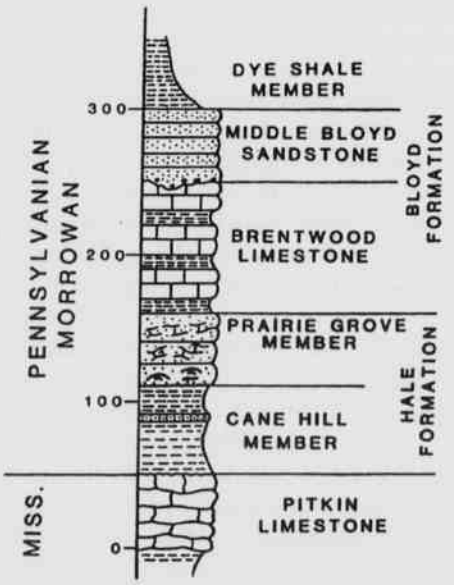

Fig. 1. Stratigraphic column of lower Pennsylvanian (Morrowan) strata of Madison County, Arkansas. Storm channel deposits occur in the upper Brentwood Member.

The Brentwood Member is composed of alternating beds of limestone and shale and ranges to 50 feet in thickness (Zachry, 1977). It conformably succeeds the Prairie Grove Member of the Hale Formation. The Prairie Grove accumulated in high-energy, inner shelf environments succeeded by transgression and the deposition of middle shelf shale and limestone beds of the Brentwood Member in slightly deeper water. Deposits

believed to be of storm origin have been identified in the upper part of the Brentwood Member (Fig. 1). They were deposited on an erosion surface formed on the middle shelf during maximum storm intensity and accumulated as storm current and wave intensity declined.

During the early Carboniferous, the southern part of North America was south of the equator. Arkansas was approximately 20 degrees south of the equator and bounded by an open sea and continential shelf (Smith et. al., 1981). Reconstructions suggest that the shelf was in a belt effected by tropical storm events.

Location.--The storm channel deposits are in the upper part of the Brentwood Member and are exposed along the east side of Highway 23 approximately 15 miles south of the city of Huntsville in central Madison County (T15N, R26W, Sec. 25; Fig. 2.). Exposures containing storm deposits range from 12 to 15 feet in thickness and extend for a distance of 432 feet.

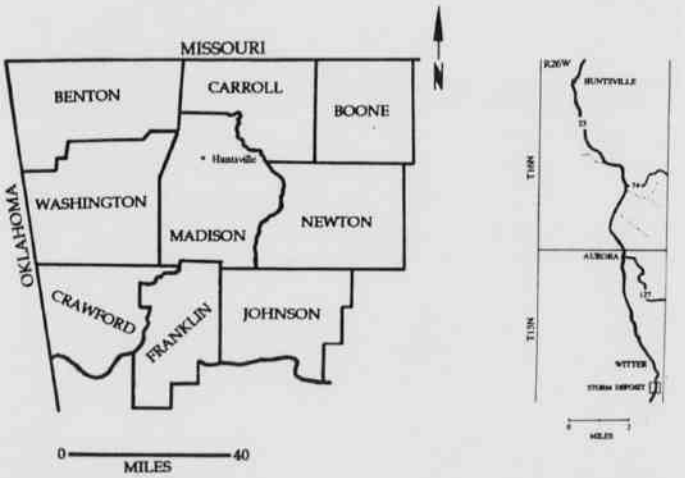

Fig. 2. Geographic locality map of the study area. Storm channel deposits occur along Highway 23, south of Huntsville in central Madison County.

Materials and Methods

Outcrop sections were measured with a Jocobs staff and measuring tape. Slabs and thin sections were prepared from outcrop samples collected from each unit, and detailed descriptions of sedimentary structures and lithic characteristics were made. X-ray diffraction analyses were conducted to compare the compositions of selected facies.

Discussion

Storm Facies.--Five storm facies are defined within the storm sequence that is confined above and below by fair-weather shale deposits. In ascending order they are the pebble conglomerate facies, the packstone facies, the wackestone facies, the hummocky corss-stratified facies, and the swell lag facies (Figs. 3 and 4).

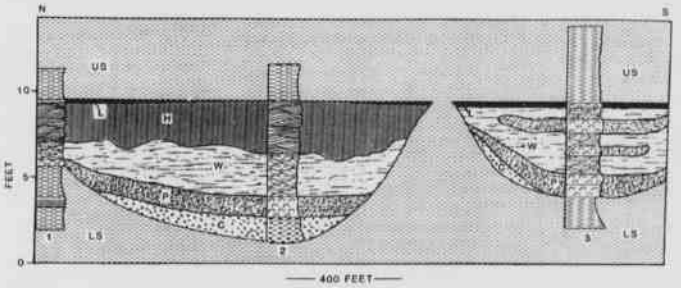

Fig. 3. Cross-section view of storm deposits and channel system. Measured sections include fair weather facies involving the lower shale (LS) and upper shale (US) and storm facies including the basal pebble conglomerate facies (C), athe packstone facies (P), the wackestone facies (W), the hummocky cross-stratification facies (H), and the swell lag facies (L).

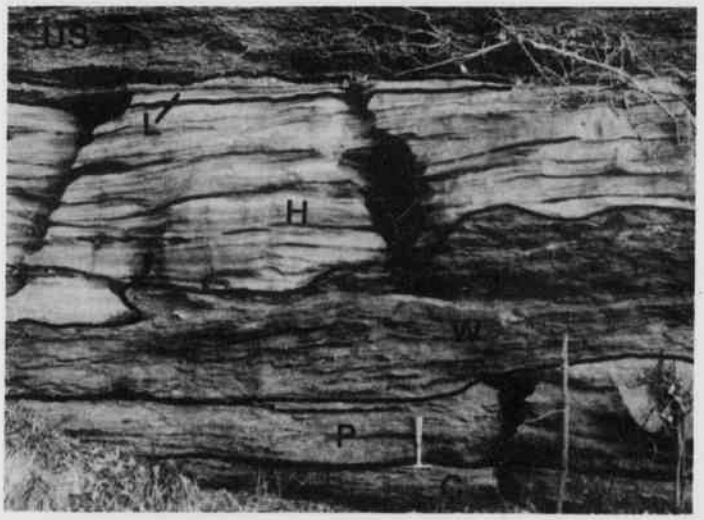

Fig. 4. Photograph of measured section 2 (Fig. 3) displaying the complete storm interval. Abbreviations same as in Fig. 3.

Storm deposits of the lower Brentwood are unconformably underlain throughout the outcrop area by an interval of black, fissile shale containing several thin beds of iron oxide cemented siltstone and ironstone concretions. The siltston beds are trucated by the erosion surface (Fig. 5). The shale is dominantly composed of illite and chlorite and is not calcareous.

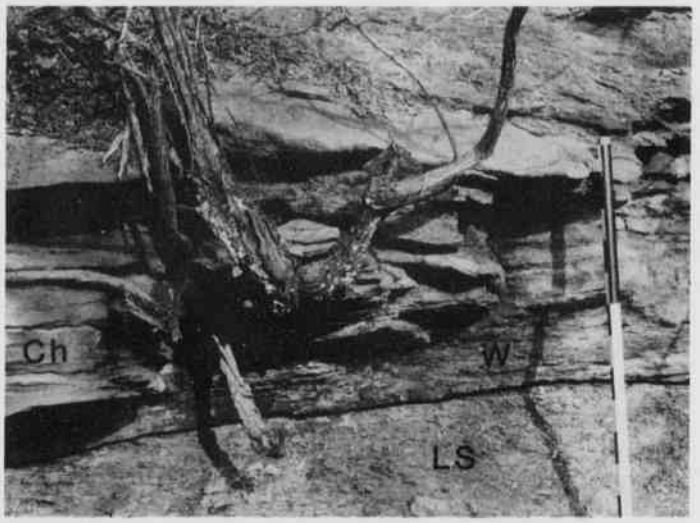

Fig. 5. Truncation of the lower shale unit by the storm channel erosion surface. The surface is indicated by the solid line with the lower shale (LS) below and the wackestone (W) and hummocky facies (Ch) above.

The pebble conglomerate facies rests on the erosion surface cut on the lower shale unit. It is composed of clay ironstone pebbles and cobbles from one to four inches in length. The particles are embedded in a matrix of course skeletal bioclasts (Fig. 6). The matrix is composed of subrounded crinozoan fragments (24%), ramose bryozoans (2%), and brachiopods (1%). Pebble and cobble clasts form 65% of the conglomerate. The remaining constituents are quartz sand (2%) and clay (6%). The facies ranges from 0.5 to three feet in thickness. The stratigraphic position of the pebble conglomerate suggests that the clasts were derived from the lower shale and formed during scouring of the channels.

Beds of the packstone facies directly overlie the pebble conglomerate. The facies consists of a lower bed of limestone composed of massive, ungraded grainstone. Fragments of coarse to very coarse, rounded crinozoan fragments (74%) are the dominate constituent (Fig. 7). Bryozoans (7%) and brachiopods (3%) are also present. Clay matrix (4%) and calcite cement (7%) occur in intergranular areas (Fig. 7).

The lower bed is overlain by a second limestone bed composed of massive, crinoid and bryozoan packstone. Crinozoans fragments compose 18% of the rock whereas various kinds of bryozoans form 65% of the rock. Skeletal fragments are horizontally to subhorizontally oriented. Clay matrix (24%) is pervasive in intergranular areas and calcite cement is absent.

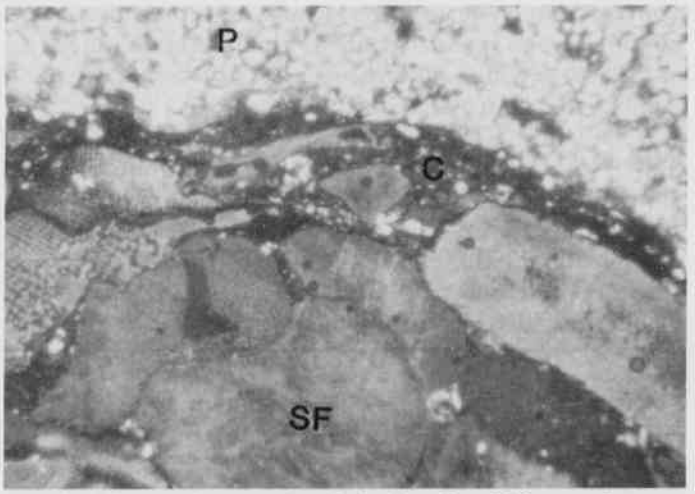

Fig. 6. Photomicrograph of the basal pebble conglomerate. The pebble (P) interpenetrates the crinoid skeletal fragments (SF). A thin layer of clay occurs between the pebble and crinoid fragment.

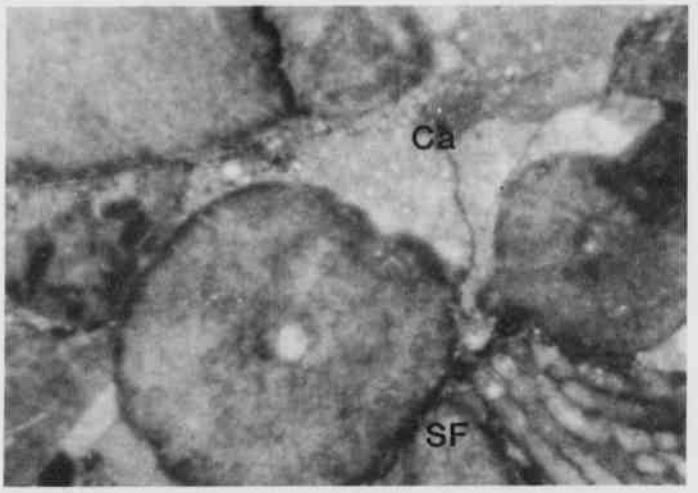

Fig. 7. Photomicrograph of the packstone facies with calcite cement (Ca) between skeletal fragments (SF).

Beds of the packstone facies are overlain by strata assigned to the wackstone facies (Figs. 3 and 4). Beds of the facies are gray and have a shaley appearance related to the presence of platy skeletal grains. Coarse to very

coarse, articulated crinoid stems ranging to eight inches in length are common. Platy fenestrate bryozoan fronds and occasional brachiopod valves are present. Calcite cement occurs, but most intergranular areas contain terrigenous clay.

The hummocky facies directly overlies beds of the wackestone facies and consists of sets of cross-strata from three to 8.5 feet in length and from four to 14 inches in thickness (Fig. 8). Foreset laminae dip less than 10 degrees and are clearly defined by oriented fenestrate bryozoan fronds along foreset boundaries (Fig. 8). A single hummocky set was collected from a wackestone interval. Polished slabs display foresets inclined from 5 - 15 degrees and composed of crinozoan and bryozoan fragments. Large tabulate coral fragments from 4 - 24 mm in diameter are scattered throughout the set. Intergranular terrigenous clay composes 27 - 30% of the rock. Micrite and calcite cement are essentially absent.

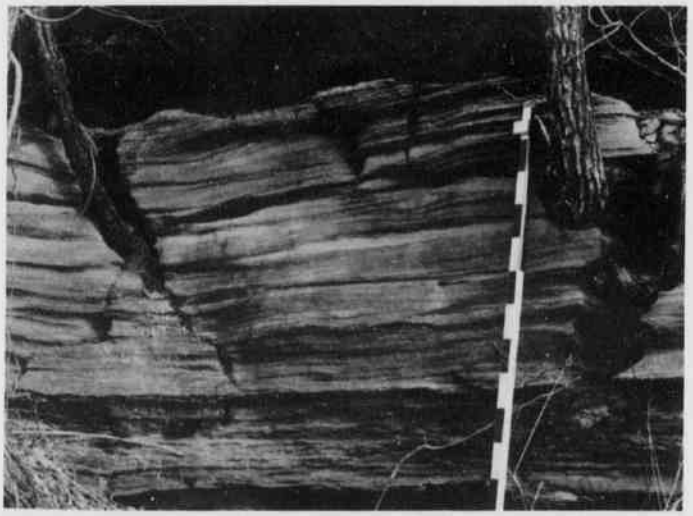

Fig. 8. Hummocky cross-stratification facies in the storm sequence. Note well defined foreset strata and inclination to the north (left).

Strata of the hummocky facies are overlain by a thin veneer of crinozoan calyx plates from two to three inches thick (Figs. 3 and 4). Individual plates are oriented with their convex side up. Other fossil fragments are absent. This veneer is assigned to the swell lag facies and is the uppermost facies in the storm sequence. The swell lag facies is overlain by black, fissile shale of the upper shale unit. This shale is not calcareous and fossil fragments are absent.

Outcrop Stratigraphy.--Storm deposits of the Brentwood Member fill two shallow channels in the outcrop area (Fig. 3). The channels are incised into the lower shale interval and have erosional relief of up to four feet. Complete storm sequences include the pebble conglomerate facies at the base of a channel succession followed by the packstone, wackestone, hummocky cross-stratification, and swell lag facies. This succession is bounded above by the upper shale unit (Figs. 3 and 4). A sharp contact exists between the top of the storm sequence and the upper shale.

Results and Conclusions

Depositional Synthesis.--Early Carboniferous paleographic interpretation by Smith et al., (1981) placed southern North America south of the equator with Arkansas at 15 degrees south latitude (Fig. 9) and bounded to the south and southeast by shelf, slope and oceanic basin environments. The area was a prime location for hurricanes and tropical storms that are capable of extensive shoreline erosion and sediment transport in shallow, marine depositional settings (Duke, 1985). Wind and pressure gradients generate wave and current forces operating far below fairweather wave base that erode and transport bottom sediment during storm events (Kreisa, 1981, Aigner, 1982; 1985 Snedden and Nummedal, 1991). Water driven onto inner shelf and coastal areas creates coastal buildups and generates high energy, seaward-directed return currents (Dot and Bourgeois, 1982; Hobday and Morton, 1984). As storm energy wanes unidirectional currents are gradually supplanted by wave processes that produce oscillatory flow (Leckie and Krystinik, 1989). Sediment is reworked under these conditions but sediment "migration" does not occur (Hunter and Clifton, 1881). Hummocky cross-stratified sets of reworked sediment are formed under these conditions (Snedden and Nummedel, 1991).

Onshore directional storm currents initially scoured channels into the lower shale unit on the middle shelf during the early phases of storm activity. These bottom currents transported sediment from a carbonate-dominated inner shelf to an outer shelf where terrigenous clay and silt had accumulated during fairweather conditions. Mass quantities of skeletal debris were moved from the inner shelf and combined with clay pebbles eroded from middle sheld clays during channel formation. This sediment was funnelled through and deposited in the shallow channel system. The basal claystone pebble conglomerate accumulated at the base of channels during the most competent phases of return current flow. The skeletal-rich packstone facies was depostied from waning but still competent return current systems. During the last phases of unidirectional flow from return currents, mass transport and deposition of poorly sorted sediment rich in

skeletal fragments and terrigenous mud formed the wackestone facies. During transport, boulder-sized bryozoan and cobble-sized tabulate coral fragments were suspended in a matrix of finer skeletal fragments and terrigenous clay.

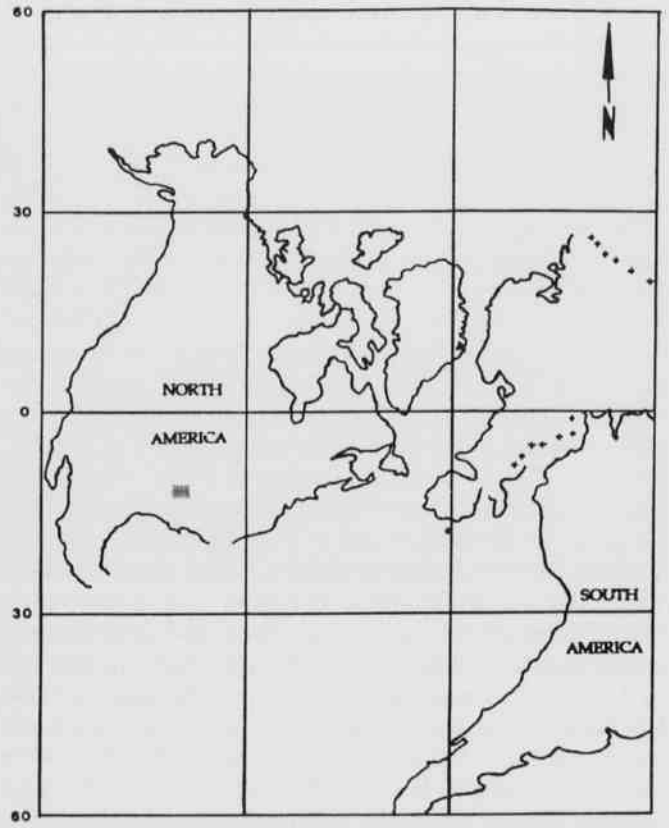

Fig. 9. Paleogeographic map of North America during early Carboniferous time (modified from Smith et al., 1981). Rectangle represents the position of the northwestern Arkansas and the study area during this time.

As storm intensity subsided wave activity replaced unidirectional currents as the dominant process in the water column. Oscillatory movement driven by waves impinged on the bottom and reworked the skeletal and terrigenous sediment of the wackestone facies forming hummocky corss-stratification. Platy calyx plates from crinoids remained suspended in the oscillatory regime after more spherical fragments were deposited and ultimately accumulated as a swell lag on the hummocky sets to complete storm deposition. Outer shelf clays blanketed the storm sequence with the return of fairweather conditions. Facies within the Brentwood storm sequence document phases of storm activity observed in modern coastal areas and indicate that mass transport of inner shelf carbonate sediment to middle-shelf environments during storms is a normal sedimentologic event.

Literature Cited

Aigner, T. 1985. Storm Depositional Systems. Springer-Verlag, Berlin, 157 pp.

Duke, W.L. 1985. Hummocky cross-stratification, tropical hurricanes and intense winter storms. Sedimentology 32: 167-194.

Dott Jr., R.H. and **J. Bourgeois.** 1982. Hummocky stratification: significance of its variable bedding sequences. Bull. Geol. Soc. Amer. 93: 6632-6680.

Hobday, D.K. and **R.A. Morton.** 1984. Lower Cretaceous shelf storm deposits, northwest Texas. Jour. Sed. Petrology 55: 205-213.

Hunter R.E. and **Clifton, H.E.** 1981. Cyclic deposits and hummocky cross-stratification of probable storm origin in upper Cretaceous rocks of the Cape Sebastian area, southwestern Oregon. J. Sed. Petrology 52: 127-143.

Kreisa, R.D. 1981. Storm generated sedimentary structures in subtidal marine facies with examples from the Middle and Upper Ordovician of southwest Virginia. J. Sed. Petrology 51: 823-848.

Leckie, D.A. and **Lee F. Krystinik.** 1989. Is there evidence for geostropic currents preserved in the sedimentary record of inner to middle shelf deposits. J. Sed. Petrology 59: 862-870.

Smith, A.G., A.M. Hurley and **J.C. Briden.** 1981. Phannerozoic Paleocontinental World Maps. Cambridge Univ. Press, London, 102 pp.

Snedden, J.W. and **D. Nummedal.** 1991. Origin and geometry of storm deposited sand beds in modern sediments of the Texas continental shelf. Int. Assoc. Sedimentologists. Special Pub. 14: 283-308.

Zachry, D.L. 1977. Stratigraphy of middle and upper Bloyd strata (Pennsylvanian, Morrowan) northwestern Arkansas. Oklahoma Geol. Surv. Guidebook 18: 61-66.

Genetic Variability in Developing Periodical Cicadas

Alvan A. Karlin, Eric C. Stout, Lance T. Adams, Lisa R. Duke and James J. English
Department of Biology
University of Arkansas at Little Rock
Little Rock, AR 72204

Abstract

There are few events in nature that are more predictable than the emergence of periodical cicadas. The insects emerge from the ground after 13 or 17 years (depending on brood and species) of development. Karlin et al., (1991) biochemically examined over 750 *Magicicada tredecassini* belonging to Brood XIX which emerged during the spring of 1985. In this study they found evidence for rapid deterioration of heterozygosity for two esterase loci, Gi-3-pdh and Gpi, and suggested that this deterioration may be related to differential mating classes. To test this hypothesis, we re-sampled from this same brood at the same location during fall (1993) and winter (1994), nine years into the 13 year development of this brood. The current biochemical data suggest no significant deviations from Hardy-Weinberg expectations for either Est-3, Gl-3-pdh or Pgm-1, but in several cases Est-1 or Est-2 displayed significant departures. Our failure to find excess heterozygosity in the nymphal sample is interpreted to support weakly the size-mediated mating system hypothesis.

Introduction

There are three morphologically identifiable species of periodical cicadas (genus *Magicicada*) each of which has 13- and 17-year life cycle forms. These are considered as six separate species (Alexander and Moore, 1962), although the recent findings for the Decim pair calls this treatment into question (Martin and Simon, 1988, 1990; Simon et al., 1993).

Periodical cicada year classes termed "broods", have been analogized with incipient species because adults of each year class are temporally reproductively isolated from all other year classes (Simon, 1988). Members of a year-class are synchronized. They emerge from the ground within a two week period with most of the individuals emerging during days two and three (Karban, 1982). The emergence occurs regularly, every 13 or 17 years depending on particular location (Marlatt, 1907; Alexander and Moore, 1962; Lloyd and Dybas, 1966; Lloyd and White, 1976). Thus, for the 17-year cicadas potentially 17 different year classes could exist (broods I-XVII), and for 13-year cicadas there could be 13 different reproductively isolated broods (XVIII-XXX) (Marlatt, 1898). Currently, only 12 17-year broods and three 13-year broods are known to exist (Simon, 1988). In this study we focused our attention on one species, *Magicicada tredecassini*, from Brood XIX in northwestern Arkansas.

In a previous study, Karlin et al. (1991) examined almost 500 individuals captured as they emerged from the ground and another 500 individuals captured three weeks later in chorus centers for several biochemical traits. They interpreted the data to suggest that heterozygosity for two esterase loci (Est-1 and Est-3), glyceraldehyde-3-phosphate dehydrogenase (Gi-3pdh), and glucose phosphate isomerase (Gpi) decreased markedly between sample periods. They proposed that the observed decline in heterozygosity could be a result of a phenotypic mating system linked to individual size as proposed by Karban (1982). If the larger (or smaller) males are more (or less) heterozygous, one class may mate earlier and hence be removed preferentially from the chorus population sample. Observations in support for this hypothesis include finding the larval population in Hardy-Weinberg equilibrium for the genes in question. Although finding Hardy-Weinberg equilibrium is a weak demonstration of support, if the genes are not in equilibrium frequencies, we can strongly reject the hypothesis.

One alternative hypothesis would implicate a constant decline in heterozygosity over the life cycle of the periodical cicadas. This hypothesis leads us to predict a heterozygote excess for these genes in the larval population allowing for the decline we observed in the adult population. Thus, we can use heterozygote excess as detected by deviations from Hardy-Weinberg expectations to support this hypothesis.

Materials and Methods

Nine-year-old nymphs of 13-year periodical cicadas (*Magicicada tredecassini*) were collected at a single locality, near Durham, Washington Co., Arkansas, in October, 1993 and February, 1994. The main study site used by Karlin et al. (1991) was revisited for this study.

Oak trees (*Quercus* sp.), hickory trees (*Carya* sp.) and black locust trees (*Robinia pseudoacacia*) showing obvious evidence of cicada galleries (scaring on the outer branches) were selected. We carefully dug 10 - 20 cm. into the ground approximately 1 - 2 m from the tree base and searched from nymphs. Once an individual was located, careful excavation followed to locate additional individuals. To insure genetic diversity, we sampled 5 - 15 individuals from each of 10 trees. Individuals collected from a tree were placed together into a plastic bag filled with dirt. The bag was refrigerated on ice until returned to the laboratory at University of Arkansas - Little Rock. Once in the lab, the bags were frozen at -70°C until used.

On the morning of electrophoresis, individual cicadas were partially thawed and their total length measured with vernier calipers. Measurements were recorded to the nearest 0.1 mm. To prepare proteins for electrophoresis, the thorax was macerated in an equal volume of double distilled water. The resultant slurry was absorbed onto two filter paper wicks (Whatman #3, 5 x 11 mm) for inoculation into starch slabs. Horizontal starch gel electrophoresis and histochemical staining followed the procedures outlined in Karlin et al. (1991) and Selander et al. (1971). The gel buffers and stains were as reported by Karlin et al. (1991).

Electrophoretic data were recorded as inferred individual enzyme genotypes for each polymorphic protein. To determine whether the genotype frequencies were in agreement with Hardy-Weinberg expectations based on gene frequencies, the data were analyzed using BIOSYS-1 (Swofford and Selander, 1981). Chi-square probabilities were modified (Harris, 1985) to account for the number of tests performed and for small sample sizes. To determine gene frequency differences between populations samples we used Nei's genetic distance and identity estimates (Nei, 1978).

Results and Discussion

Of the total of 113 individuals surveyed for esterases, Gi-3-pdh, Gpi, and Pgm-1, we found that glucosephosphate isomerase (Gpi) was not interpretable in any of the nymphs. Similarly, beta-naphtyl proprionate esterase-4 (Est-4) was not consistently interpretable on our gels. Although some individuals were not scorable for some enzymes, we were able to score 112 individuals for Est-1, 108 for Est-2, 112 for Est-3, 113 for Gi-3-pdh, and 77 for Pgm-1. We found significant ($P < 0.05$ adjusted) departures from Hardy-Weinberg expectations for Est-1 and Est-2 when the entire sample was considered (Table 1). In these two cases, the departure resulted from excess homozygosity (Fixation Index = +0.276 and +0.429 for Est-1 and Est-2 respectively) for Est-1^{aa}, Est-1^{bb}, Est-2^{bb} homozygotes (Table 1). When we pooled all rare homozygotes and all rare heterozygotes for Est-1, no significant deviations from equilibrium frequencies were observed. Hence, only Est-2 genotypes were not in equilibrium frequencies after pooling. Because we only found two of the four known genes for Est-2 (Karlin et al., 1991) in the nymphal sample, the absence of those genes could have resulted in the skewed genotype frequencies. We consider these results to indicate strongly no departures from Hardy-Weinberg expectations for the five proteins studied. In terms of the original hypotheses, the absence of excess heterozygosity suggests that heterozygosity does not decline steadily throughout the life cycle of periodical cicadas.

Table 1. Genotype frequencies for 5 polymorphic loci in *Magicicada tredecassini* from Durham, Arkansas, 1994.

Locus	Genotype	Observed Frequency	Expected Frequency[1]	Chi-Square
Est-1	AA	2	0.53	
	AB	12	9.18	
	AC	0	4.66	
	AD	0	1.08	
	BB	45	36.45	
	BC	26	37.45	
	BD	0	8.61	
	CC	15	9.33	
	CD	9	4.38	
	DD	3	0.47	34.38* df=6
Est-2	AA	76	68.4	
	AB	20	35.2	
	BB	12	4.4	18.33* df=1
Est-3	AA	64	58.48	
	AB	34	45.04	
	BB	14	8.48	5.87 ns df=1
Pgm-1	AA	22	20.13	
	AB	35	38.73	
	BB	20	18.14	0.463 ns df=1
Gl-3pdh	AA	82	79.80	
	AB	26	30.40	
	BB	5	2.8	1.569 ns df=1

1- Expectations are based on Hardy-Weinberg Equilibrium
*P <0.05

To evaluate gene frequency differences between the nymph population and the adult population sampled in 1985 (Karlin et al., 1991), we used genetic distance and identity estimates (Nei, 1978). Because we were not able to survey all of the enzymes as in Karlin et al., (1991), the adult data set was reduced to only those enzymes surveyed in the nymph population. Both the genetic distance (D = 0.03) and the genetic identity (I = 0.968) suggest that any differences in gene frequencies are due to chance. Although we found no differences in average

individual heterozygosity between the adult and nymph samples, Karlin et al., (1991) observed more alleles in the adult population. This was expected as a result of the smaller sample from the nymph population.

Karlin et al. (1991) suggested that the differences observed between emerging and chorus samples could have resulted from preferential mating patterns linked to individual size. Lloyd and Dybas (1966) found that cicada nymphs grow at different rates. Often at one site individuals of the same age class were in different instar stages. That suggests that one class grows rapidly and "waits" up to four years for the "slower" growing nymphs to catch-up. It is thus possible that nymphs of different sizes emerge differentially, and as predation pressure on adults is severe (see Karban, 1982), genotypic differences between emergent samples and chorus samples may result.

In this study we found two different size-class nymphs. One class, 48 individuals, was comprised of small individuals usually less than 16.5 mm in total length, while the other class was comprised of large nymphs (larger than 16.5 mm, 64 individuals). When we separated the population by size class and recomputed genotype frequencies (Table 2), we found no differences in gene frequencies between the two groups (D= 0.000, I=1.000), nor did we found evidence for genetic heterogeneity (Chi-square = 5.53, df=7, ns) across all proteins. Furthermore, no departures from Hardy-Weinberg expectations were observed for any enzyme in the small nymphs, while only Est-1 and Est-2 demonstrated departures in the large nymphs (Table 2). Once again, in the large nymphs, the departures were due to homozygote excesses for Est-1^{bb}, Est-1^{cc}, Est-2^{aa}, and Est-2^{bb}, and pooling eliminated the homozygote excess for Est-1. Again, these departures are in the opposite direction of what we would expect if there was a continual reduction of heterozygosity, and we interpret them to be consistent with the differential mating hypothesis.

Table 2. Genotype Frequencies for Large (> 16.5 mm) and Small (< 16.5 mm) *Magicicada tredecassini* from Durham, Arkansas, 1994.

		Large Cicadas			Small Cicades		
Locus	Class	Obs. Freq.	Exp. Freq.	Chi-Square	Obs. Freq.	Exp. Freq.	Chi-Square
Est-1	AA	1	0.22		1	0.29	
	AB	6	4.72		6	4.46	
	AC	0	2.33		0	2.35	
	AD	0	0.51		0	0.58	
	BB	28	21.85		17	14.50	
	BC	13	21.85		13	15.62	
	BD	3	4.72		0	3.90	
	CC	10	5.24		5	3.97	
	CD	4	2.33	21.81 (6)	5	2.06	8.69 (6)
	DD	2	0.22	$P<0.05$	1	0.22	ns
Est-2	AA	46	40.75		27	27.66	
	AB	7	17.47	18.94 (1)	13	17.67	2.37 (1)
	BB	7	1.76	$P<0.05$	5	2.66	ns
Est-3	AA	32	29.45		32	29.21	
	AB	23	28.08	1.53 (1)	11	16.58	4.11 (1)
	BB	9	6.45	ns	5	2.21	ns
Pgm-1	AA	10	9.88		12	10.49	
	AB	21	21.24	0.00 (1)	14	17.01	0.62 (1)
	BB	11	10.88	ns	8	6.49	ns
Gi-3 pdh	AA	44	42.57		38	37.16	
	AB	14	16.86	0.901 (1)	12	13.67	0.19 (1)
	BB	3	1.57	ns	2	1.16	ns

Combined Chi-Square of Homogeneity = 5.527 (df=7) ns

Finally, during the course of this investigation, we noticed that several individuals were infected with what appeared to be the fungal pathogen *Massospora cicadina*. We later identified the organism as a pathogenic bacterial agent, tentatively identified as *Bacillus sp.* Approximately half-way through the study, we noticed that the incidence was rather high, and at that point we began to keep records of infected vs. non-infected individuals. In the sub-sample (53 nymphs) in which we recorded pathogen incidence, we found 43% to be infected. We divided those genotypic data by presence of infection and reanalyzed the frequencies. Again we found no heterogeneity (Chi-square = 4.38, df=7, ns) and no differences in gene frequencies (D=0.00, I=1.00) between infected and non-infected individuals. Similarly, the groups did not differ from each other with respect to genotype frequencies (Table 3). We suggest that although this pathogen is not currently known to be a source of mortality, its high incidence suggests that it may have a role in regulating this population. As it produced no apparent genotypic bias in our study we suggest it represents a random factor.

Our observations that Est-2 demonstrated departure from Hardy-Weinberg equilibrium in the nymphs but not in the adults, and our failure to resolve Gpi in the nymphs may suggest specific gene expression in the nymphs. The results lead us to suggest that the genotype frequencies in the nymph population are in close agreement to expectations. Thus, we can not reject our initial hypothesis. We can, however, reject the notion that heterozygosity steadily decreases in this cicada population.

Table 3. Genotype Frequencies for *Magicicada tredecassini* infected with *Bacillus sp.* and those without infection from Durham, Arkansas, 1994.

		Infected Cicadas			non-Infected Cicades		
Locus	Class	Obs. Freq.	Exp. Freq.	Chi-Square	Obs. Freq.	Exp. Freq.	Chi-Square
Est-1	AA	1	0.22		0	0.10	
	AB	3	3.0		4	2.38	
	AC	0	1.55		0	1.19	
	AD	0	0		0	0.21	
	BB	9	7.80		12	9.84	
	BC	6	8.40		6	10.14	
	BD	0	0		0	1.79	
	CC	4	2.02		4	2.38	
	CD	0	0	2.63 (3)	3	0.89	6.83 (6)
	DD	0	0	ns	0	0.05	ns
Est-2	AA	19	16.46		24	21.61	
	AB	1	6.06	12.5 (1)	3	7.78	8.37 (1)
	BB	3	0.46	P<0.05	3	0.61	P<0.05
Est-3	AA	15	14.65		17	16.59	
	AB	6	6.67	0.006 (1)	10	10.81	0.01 (1)
	BB	1	0.65	ns	2	1.59	ns
Pgm-1	AA	3	2.69		1	1.78	
	AB	7	7.62	0.002 (1)	10	8.43	0.19 (1)
	BB	5	4.69	ns	8	8.76	ns
Gi-3 pdh	AA	18	16.46		20	20.63	
	AB	3	6.06	3.43 (1)	9	7.73	0.10 (1)
	BB	2	0.467	ns	0	0.63	ns

Combined Chi-Square of Homogeneity = 4.382 (df=7) ns

Acknowledgements

We thank Mr. Michael Cassidy for permission to sample cicada nymphs and for his generous cooperation in the field work. We also thank K. Smith, R. Dukes, J. Penor, and L. Lacer for their help in the field.

Literature Cited

Alexander, R. and **T. Moore.** 1962. The evolutionary relationships of 13- and 17-year periodical cicadas, and 3 new species. Mus. Zool. Misc. Publ. 121. Univ. Mich. Ann Arbor.

Harris, R.J. 1985. A primer of multivariate statistics. Harcort Brach Jovanovich, San Diego, California. 575 pp.

Karban, R. 1982. Increased reproductive success at high densities and predator satiation for periodical cicadas. Ecology 63:321-328.

Karlin, A.A., K.S. Williams, K.G. Smith and **D.W. Sugg.** 1991. Biochemical evidence for rapid changes in heterozygosity in a population of periodical cicadas (*Magicicada tredecassini*). Am. Midl. Nat. 125:213-221.

Lloyd, M. and **H. Dybas.** 1966. The periodical cicada problem. I. Population biology. Evolution 20:466-505.

Lloyd, M. and **J. White.** 1976. Sympatry of periodical cicada broods and the hypothetical 4-year acceleration. Evolution 30:786-801.

Marlatt, C. 1898. A new nomenclature for the broods of the periodical cicada. Bull. USDA. Div. Entomol. Bull. (new series) 18:52-58.

Marlatt, C. 1907. The periodical cicada. Bull. of the USDA, Bureau of Entomol. 71:1-181.

Martin, A.P. and **C.M. Simon.** 1988. Anomalous distribution of nuclear and mitochondrial DNA markers in periodical cicadas. Nature 336:237-239.

Martin, A.P and **C.M. Simon.** 1990. Differing levels of population divergence in the mitochondrial DNA of 13-verses 17-year periodical cicadas related to historical biogeography. Evolution 44:1066-1088.

Nei, M. 1978. Estimation of average heterozygosity and genetic distance from a small number of individuals. Genetics 89:583-590.

Selander, R.K., M.H. Smith, S.Y. Yang, W.E. Johnson and **J.B. Gentry.** 1971. Biochemical polymorphism and systematics in the genus *Peromyscus*. I. Variation in the old-field mouse (*Peromyscus polionotus*). Stud. Genet. VI. Univ. Texas. Publ. 7103:49-90.

Simon, C.M. 1988. Evolution of 13- and 17-year periodical cicadas (Homoptera: Cicadidae: *Magicicada*). Bull. Entomol. Soc. Am. 34:163-176.

Simon, C.M., C. McIntosh and **J. Deniega.** 1993. Standard restriction fragment length analysis of the mitochondrial genome is not sensitive enough for phylogenetic analysis or identification of 17-year periodical cicada broods (Hemiptera: Cicadidae): The potential for a new technique. Ann. Entomol. Soc. Am. 86:228-238.

Swofford, D.L. and **R.B. Selander.** 1981. BIOSYS-1: A FORTRAN program for the comprehensive analysis of electrophoretic data in population genetics and systematics. J. Hered. 72:281-283.

Distance of Interference of Red Rice (*Oryza sativa*) in Rice (*O. sativa*)[1]

Sam L. Kwon
Dept. of Agronomy
Univ. of Arkansas
Fayetteville, AR 72703

Roy J. Smith Jr.
Agric. Res. Serv.
U.S. Dept. Agric.
Stuttgart, AR 72160

Ronald E. Talbert
Dep. of Agronomy
Altheimer Lab
Univ. of Arkansas
Fayetteville, AR 72703

Abstract

Three rice cultivars were grown to determine the distance at which red rice affects growth and grain yield. Red rice reduced grain yield of Lemont when rice plants grew within 71 and 53 cm of red rice in 1986 and 1988, respectively. Grain yield of Newbonnet was reduced when grown within 53 cm of red rice in both years. Grain yield of Tebonnet was reduced when grown within 53 and 36 cm of red rice in 1986 and 1988, respectively. Grain yield reduction in influenced areas averaged 35, 26 and 21% for Lemont, Newbonnet, and Tebonnet, respectively. As the distance increased at 10-cm increments from the red rice row, Lemont, Newbonnet, and Teboment grain yields increased 49 to 85, 32 to 40, and 24 to 33 g/m^2, respectively. Rice straw dry weight was reduced when Lemont and Tebonnet were grown within 71 and 36 cm of red rice in 1986 and 1988, respectively. Straw dry weight of Newbonnet was reduced when grown within 36 cm of red rice in both years. As the distance increased at 10-cm increments from the red rice row, Lemont, Newbonnet and Tebonnet straw biomass increased 22 to 46, 10 to 18, and 12 to 20 g/m^2, respectively. Rice panicles/m^2 were reduced when Lemont, Newbonnet, and Tebonnet were grown within 36, 18, and 18 cm of red rice, respectively. Rice grains/panicle were reduced when rice was grown within 71, 71, and 36 cm of red rice for Lemont, Newbonnet, and Tebonnet, respectively.

[1]Published with the permission of the Director of the Arkansas Agric. Exp. Stn.

Introduction

Red rice is a competitive weed of rice in the southern U.S. A density of five plants/m^2 reduced rice grain yield by 22% (Diarra et al., 1985). Also, red rice is difficult to control in rice with herbicides because it is genetically and physiologically similar to commercial rice (Craigmiles, 1978; Hoagland, 1978) and is tolerant to most herbicides that are tolerated by rice cultivars.

Weed interference can be researched by different experimental methods (Connolly, 1988; Fernandez-Quintanilla, 1988; Oliver, 1988; Van Groenendael, 1988). The most common methods include studies in which weed density and duration of interference are varied. Usually in the area of interference studies, the effect of individual weeds on crops is determined, but in field situations the patchy distribution of weeds should be considered in assessing crop-weed interactions. From this standpoint the method used in this interference study would be comparable to high densities in patches of red rice infestations that frequently occur in rice field. Effects of area of influence or interference have been conducted with several weed in soybeans (*Glycine max* L. Merr.) (Monks and Oliver, 1988), cotton (*Gossypium hirsutum* L.) (Bridges and Chandler, 1986), and rice (Baker et al., 1987; Smith, 1987). However, research has not been reported on the area of influence of red rice on rice.

Development of integrated weed management systems must be supported by a thorough understanding of the dynamics of weed populations obtained from weed interference studies (Fernandez-Quintanillia, 1988). Understanding of interference thresholds, biology, and growth habits of weeds in essential to timely, effective, economical weed control technology for profitable rice production (Smith, 1988). An integrated weed management system for rice includes a directed agroecosystem approach for the management and control of weed populations at threshold levels to prevent economic damage in current and future crops (Shaw, 1982).

The objective of this study was to determine the distance at which red rice plants affected growth and yield of commercial rice cultivars.

Materials and Methods

Field experiments were conducted in 1986 and 1988 at the University of Arkansas Rice Research and Extension Center, Stuttgart, to determine the distance of interference of red rice on three rice cultivars. Plots were on a Crowley silt loam (Typic Albaqualfs) with a pH of 5.5 and 6.5 in 1986 and 1988, respectively, and 1% organic matter. Because growth and development of rice and red rice were injured by soil alkalinity in 1987, results for

that year are not reported.

Lemont, Newbonnet, and Tebonnet cultivars, with plant heights at maturity of 84, 102, and 112 cm (Ark. Coop Ext. Serv., 1990), respectively, were drill-seeded at 145, 123, and 134 kg/ha, respectively, in 18 rows with a row spacing of 18 cm in plots 3.2 m wide by 3 m long (Fig. 1). At the time of drill-seeding rice, red rice was hand seeded as a center (A) row of each plot at seeding rates equivalent to rice cultivars. In control plots the appropriate rice cultivar was substituted for the red rice in row A. The experiment was arranged as a split plot with three replications with rice cultivars in main plots and rice distance from red rice in subplots.

Rice and red rice were seeded on May 14, 1986 and May 16, 1988. Plants of both species emerged on May 22, 1986 and May 30, 1988 at an average density of 390 plants/m² which is a higher density than normal field populations of 220 to 320 plants/m² for rice (Ark. Coop. Ext. Serv., 1990).

For general weed control all plots were sprayed with a tank mixture of propanil [N-(3,4-dichlorophenyl) propanamide] plus bentazon [3-(1-methylethyl)-1H)-2,1,3-benzothiadiazin-4(3H)-one 2,2-dioxide] at 4 plus 0.6 kg/ha, respectively, in 190 L/ha with a backpack sprayer. These treatments did not injure rice or red rice.

All plots received a total of 202, 151, and 123 kg/ha nitrogen applied in three increments as urea for Lemont, Newbonnet, and Tebonnet, respectively, because each cultivar requires different rates of nitrogen for optimum grain yield (Ark. Coop. Ext. Serv., 1990). The first application was on dry soil when rice was in the 5-leaf stage just before flooding. The second increment was applied into the floodwater when rice internodes were 1.3 cm long, while the third increment was applied into the floodwater 7 to 14 days after the second application. In 1986 phosphorus (45 kg/ha) and potassium (90 kg/ha) were applied to the previous soybean crop, but they were applied preplant incorporated to rice in 1988. Chelated zinc at 2.2 kg/ha was applied preplant in 1988 to prevent rice injury from high alkalinity.

Measurements were recorded separately for each row in the plot. Before harvest five rice panicles from each row were randomly selected for determining the number of filled grains/panicle. Six rows of rice on each side of a red rice row were hand harvested. All measurements at the same distance on each side of the red rice row were averaged for each cultivar. Three outside border rows on each side of the plot were not harvested.

Panicles were separated from the straw, counted, and threshed. Rough rice yields were adjusted to 12% moisture. The straw was dried in a forced-air oven at 70°C for 48 hours and weighed. Data were subjected at analysis of variance and regression analysis.

Results

Data for weed-free plots were averaged for all 12 rows harvested because there were no significant differences among rows. The interaction of the year by distance by cultivar for rough rice yields and rice straw dry weights was significant at the 5% level; therefore, data are separated for each year and cultivar. Because the year by distance intereaction for panicles/m² and grains/panicle was not significant, these data were combined over years for each cultivar.

Growth and yield of Lemont.--In 1986 Lemont yield was reduced 11 to 68% for rice grown within 18 to 71 cm of red rice. Grain yield of Lemont in 1988 was reduced 16 to 56% for rice grown within 18 to 53 cm of red rice. Distance of influence of red rice on rice yield was less in 1988 than in 1986 because red rice lodged over rice plants in 1986. Linear regression models described grain yield response to increased distance from red rice in both years, but the slope was greater in 1986 than in 1988 (Fig. 2). The regression equations indicate that Lemont grain yields increased 85 and 49 g/m² in 1986 and 1988, respectively, for each 10-cm increase in distance from the red rice row; this is a 31 and 14% increase for the two years, respectively, for each 10-cm increment.

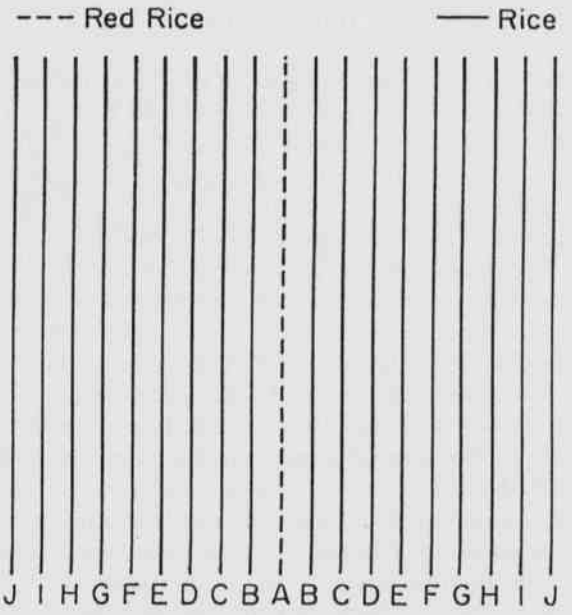

Fig. 1. Planting pattern for rice cultivars and red rice in plots. Data from rice rows B to G at the same distance on both sides of row A were combined and rows H, I, and J were borders. In the control plot the appropriate rice cultivars were substituted for red rice in row A.

Straw dry weight of Lemont was reduced within 71 and 36 cm from the red rice row in 1986 and 1988, respectively. Reductions were 16 to 46% and 14 to 35% in 1986 and 1988, respectively, compared to weed-free rice. Straw dry weight of Lemont increased linearly as the distance from red rice increased. (Fig. 3). Straw bionass increased 22 to 46 g/m² for each 10-cm increase that rice was grown form the red rice row.

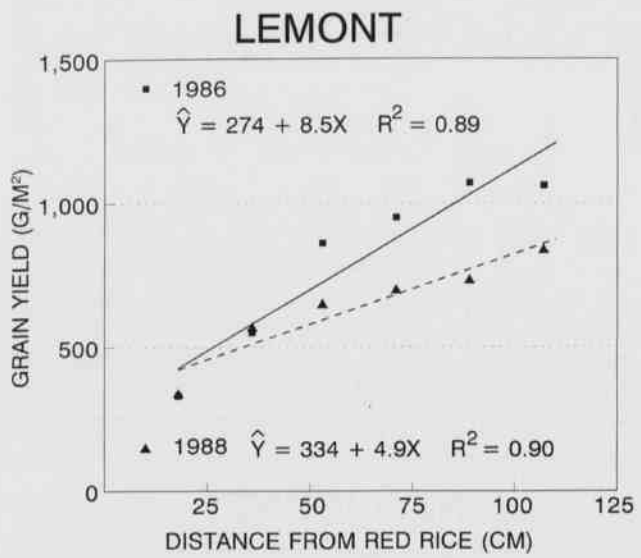

Fig. 2. Grain yield of Lemont rice when grown at different distances from red rice in 1986 and 1988. Grain yield of plots without red rice averaged 1080 and 765 g/m² in 1986 and 1988, respectively.

There was a quadratic response of rice panicles/m² with increased distance from red rice, but response of filled grains/panicle was linear (Fig. 4). Panicles/m² of Lemont were influenced within 36 cm of red rice with 19 to 37% reductions compared to weed-free rice. Filled grains/panicle were influenced within 71 cm from the red rice row with 13 to 55% reductions compared to weed-free rice. Shading of rice plants occurred by the red rice canopy over the rice because red rice was taller and had longer, droopier leaves than Lemont.

Growth and yield of Newbonnet.--Newbonnet grain yield was affected similarly in both years, although yields were greater in 1986 than in 1988 (Fig. 5). Red rice influenced grain yield of Newbonnet within 53 cm from red rice both years, with an average reduction of 26% and a range of 17 to 37% grain yield reduction when grown within 18 to 53 cm from the red rice row. Linear regression models described yield responses to increased distances from red rice (Fig. 5). Grain yields increased 32 to 40 g/m² for each 10-cm increase in distance that rice grew from the red rice row.

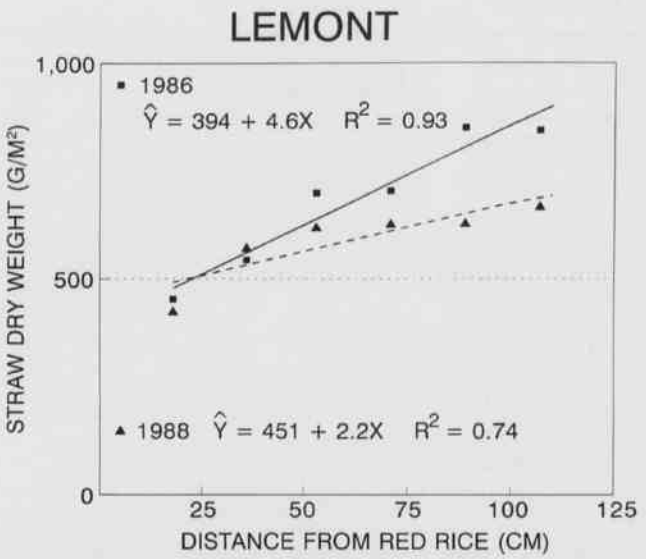

Fig. 3. Straw dry weight of Lemont rice when grown at different distances from red rice in 1986 and 1988. Straw dry weight of plots without red rice averaged 841 and 666 g/m² in 1986 and 1988, respectively.

Response of rice straw dry weight were similar to those of rice grain yield as distances increased form red rice (Fig. 6), but the affected distance was shorter for straw than for grain yield. Newbonnet straw biomass was reduced within 36 cm from red rice in both years, with an average reduction of 13% compared to weed-free rice. For each 10-cm increase in distance from the red rice row, grain yields improved 10 to 18 g/m².

Panicles/m² of Newbonnet were reduced within 18 cm from the red rice row with an 18% reduction at this distance, but filled grains/panicle were influenced with in71 cm from the red rice row, with 12 to 35% reductions compared to weed-free rice. The response of panicles/m² was quadratic, but that of filled grains/panicle was linear as the distance increased from the red rice row (Fig. 7).

Growth and yield of Tebonnet.--Grain yield of Tebonnet was reduced when rice was grown within 18 to 53 and 18 to 36 cm of the red rice row in 1986 and 1988, respectively. Red rice reduced grain yield of Tebonnet by 11 to 36% and 18 to 20% in 1986 and 1988, respectively, in affected distances compared with weed-free rice. Red rice reduced Tebonnet yield more in 1986 than in 1988 because red rice plants lodged on top of Tebonnet plants in 1986. A linear regression model described yield response to increased distances from the red rice row in both years, but the slope was greater in 1986 than in 1988

(Fig. 8). Tebonnet grain yields increased 24 to 33 g/m² for each 10-cm increment that the cultivar grew from the red rice row.

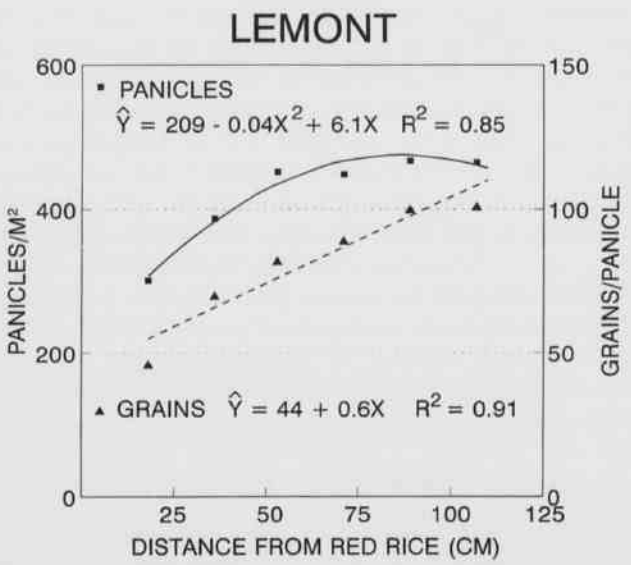

Fig. 4. Number of panicles and filled grains in panicles of Lemont rice when grown at different distances from red rice averaged for 1986 and 1988. Average values in control plots were 475 panicles/m² and 102 filled grains/panicle.

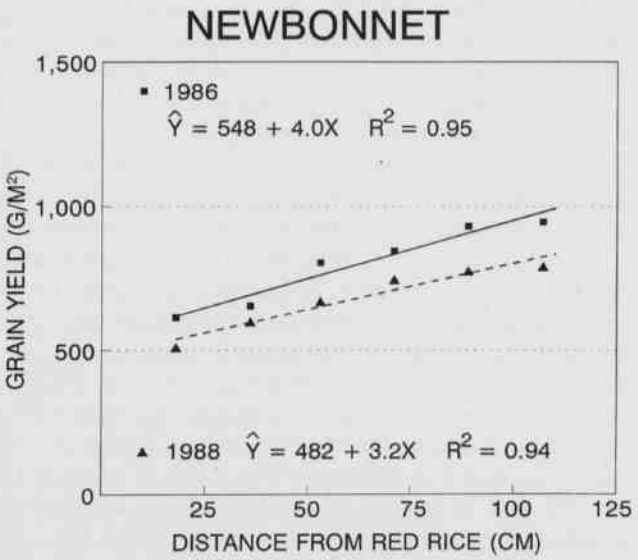

Fig. 5. Grain yield of Newbonnet rice when grown at different distances from red rice in 1986 and 1988. Grain yield of plots without red rice averaged 925 and 795 g/m² in 1986 and 1988, respectively.

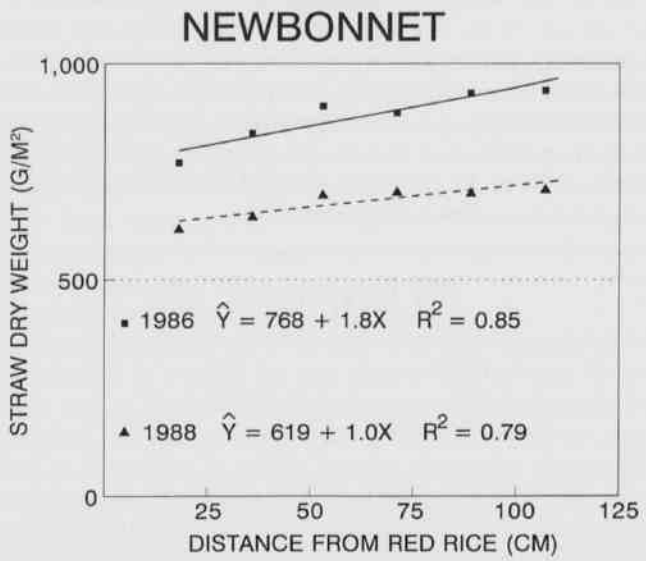

Fig. 6. Straw dry weight of Newbonnet rice when grown at different distances from red rice in 1986 and 1988. Straw dry weight of plots without red rice averaged 929 and 725 g/m² in 1986 and 1988, respectively.

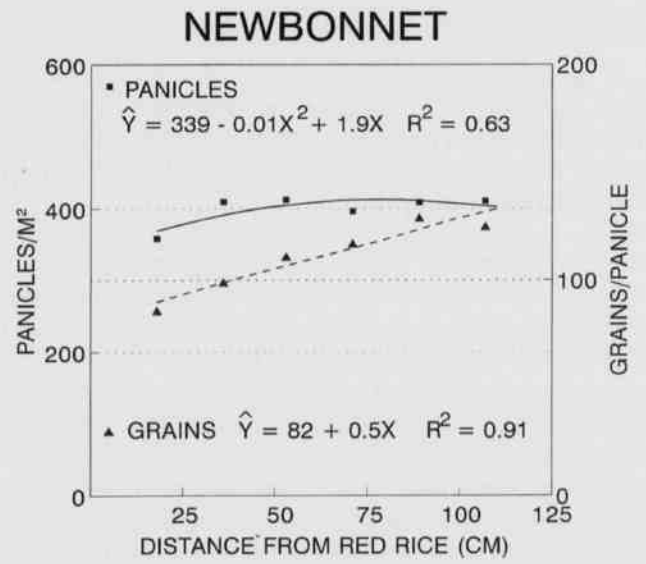

Fig. 7. Number of panicles and filled grains in panicles of Newbonnet rice when grown at different distances from red rice, averaged for 1986 and 1988. Average values in control plots were 438 panicles/m² and 133 filled grains/panicle.

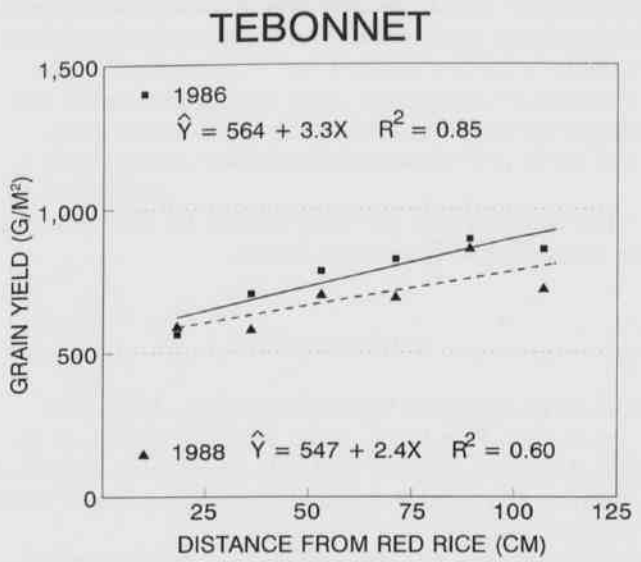

Fig. 8. Grain yield of Tebonnet rice when grown at different distances from red rice in 1986 and 1988. Grain yield of plots without red rice averaged 885 and 720 g/m² in 1986 and 1988, respectively.

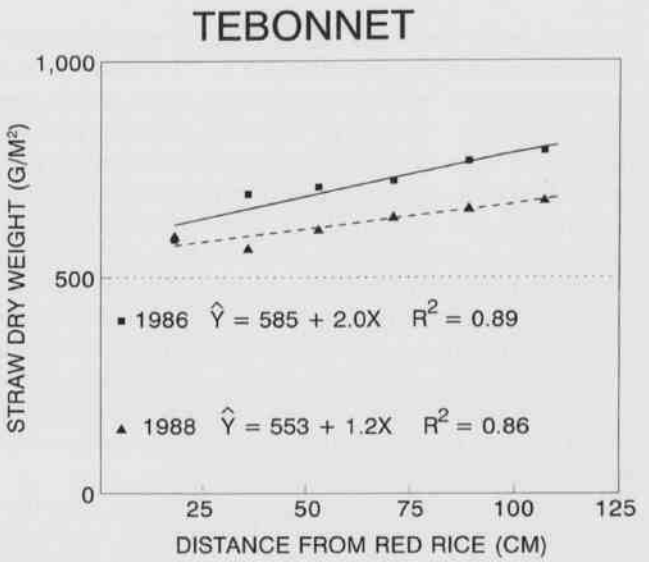

Fig. 9. Straw dry weight of Tebonnet rice when grown at different distances from red rice in 1986 and 1988. Straw dry weight of plots without red rice averaged 790 and 662 g/m² in 1986 and 1988, respectively.

Tebonnet straw dry weight was reduced within 71 and 36 cm from the red rice row in 1986 and 1988, respectively. Reductions of Tebonnet straw biomass were 8 to 26% and 10 to 14% for the two years, respectively compared with weed-free rice. Response of straw biomass was similar to that of grain yield of Tebonnet as the distance increased from the rice row. Tebonnet straw biomass increased 12 to 20 g/m² for each 10-cm increase in distance from the red rice row (Fig. 9). However, red rice reduced panicles/m² of Tebonnet in only the first rice row or 18 cm from the red rice row; a 10% reduction occurred when compared to weed-free rice. Red rice reduced filled grains/panicle in the first two rows or 36 cm of Tebonnet with a 17 to 28% reduction in affected distances. Filled grains/panicle was quadratic as distance from red rice increased (Fig. 10).

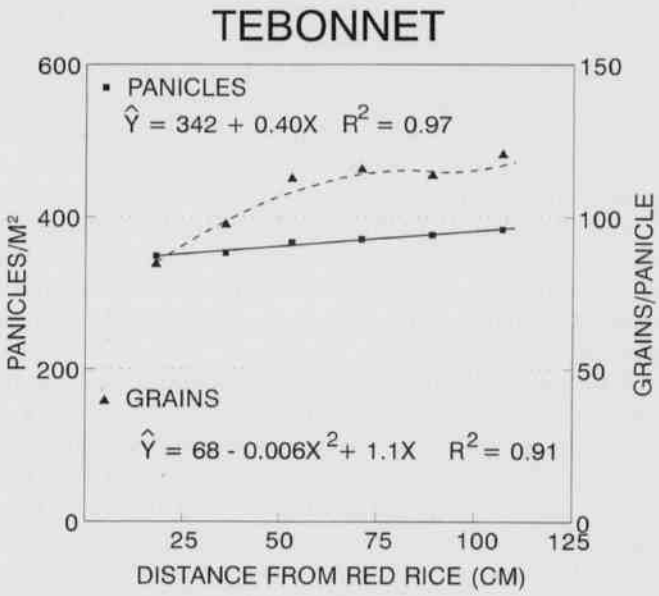

Fig. 10. Number of panicles and filled grains in panicles of Tebonnet rice when grown at different distances from red rice, averaged for 1986 and 1988. Average values in control plots were 389 panicles/m² and 118 filled grains/panicle.

Discussion

Lemont grain yield was reduced by an average of 35% when Lemont was grown within 53 to 71 cm of red rice. Reduction of grain yield averaged 26% when Newbonnet was grown within 53 cm of red rice. Grain yield was reduced 21% when Tebonnet was grown within 36 to 53 cm of red rice. Rice plants growing near red rice plants were affected more than those growing at greater distances from red rice. Lemont, Newbonnet, and Tebonnet at maturity have plant heights of 84, 102, and 112 cm, respectively (Ark. Coop. Ext. Serv., 1990). Short-statured crop plants compete less than tall plants with weeds (Jennings and Herrera, 1968; Smith, 1988). The use of plant growth regulators that would reduce plant height or biomass of red rice (Dunand et al., 1986) may reduce effects of red rice on rice.

Red rice interfered with grain yields of rice from greater distances than several weeds of soybeans. Common cocklebur (*Xanthium strumarium* L.), Palmer amaranth (*Amaranthus palmeri* S. Wats.), and tall morningglory (*Ipomoea purpuea* (L.) Roth) interfered with soybean yields when grown within 25, 25, and 12 cm, respectively of soybean plants (Oliver, 1988). However, devil's-claw (*Proboscidea louisianica* (Mill.) Thellung), velvetleaf (*Abutilon theophrasti* Medik.), and okra (*Abelmoschus esculentus* (L.) Moench) influenced cotton yields when grown within 2, 1, and 1 m, respectively, of cotton plants (Bridges and Chandler, 1986).

A basic assumption in weed-crop competition is that as a crop or weed plant grows from emergence to maturity, its interference zone form resources such as light, nutrients, and other growth requirements continues to expand until it meets another zone of neighboring plants (Fisher and Miles, 1973). The final dry matter yield of each plant is directly proportional to its area of interference. Generally plants first occupy space horizontally until all available horizontal space is occupied by either crop or weed plants.

The patchy distribution of weeds should be considered in assessing crop-weed interactions in the field. In interference studies it is commonly assumed that weeds are spatially homogeneously distributed and that they occur in monospecific stands in the field (Van Groenendael, 1988). Also, because the patchy distribution of weeds complicates crop-weed interactions, replacement method series are usually inadequate to assess competitive interactions in the field. Instead, additive experiments are more adequate to assess competition in field environments (Connolly, 1988). Therefore, use of regression response models relating crop growth and yield provides better methodology in assessing interactions involving patchy distribution of weeds. Although the method used in this study did not simulate the normal distribution of red rice in rice fields, red rice densities in the row would be comparable to high densities in patches of red rice infestations that frequently occur in rice fields.

Acknowledgements

This research was partially funded by The Arkansas Rice Research and Promotion Board.

Literature Cited

Arkansas Cooperative Extension Service. 1990. Rice Production Handbook. Misc. Publ. 192 (Rev.), 59 pp.

Baker, J.B., J.W. Shrefler and **K.P. Shao.** 1987. Sphere of influence of hemp sesbania in rice. Proc. South. Weed Sci. Soc. 40:304.

Bridges, D.C. and **J.M. Chandler.** 1986. Area of influence of selected weeds in Texas cotton. Proc. South. Weed Sci. Soc. 39:394.

Connolly, J. 1988. Experimental methods in plant population research in crop-weed systems. Weed Res. 28:431-436.

Craigmiles, J.P. 1978. Introduction. Pages 5-6 *In* E.F. Eastin, ed., Red rice research and control. Texas Agric. Exp. Stn. Bull. 1270.

Diarra, A., R.J. Smith, Jr. and **R.E. Talbert.** 1985. Interference of red rice (*Oryza sativa*) with rice (*O. sativa*). Weed Sci. 33:644-649.

Dunand, R.T., J.B. Baker, M.W. Brunson, R.R. Dilly, G.A. Meche and **J.W. Shrefler.** 1986. Plant growth regulator effect on rice. Pages 91-119 *In* Louisiana Agric. Exp. Stn., 78th Annu. Res. Rep., Crowley, LA.

Fernandez-Quintanilla, C. 1988. Studying the population dynamics of weeds. Weed Res. 28:443-447.

Fisher, P.R. and **R.E. Miles.** 1973. The role of spatial pattern in the competition between crop plants and weeds. A theoretical analysis. Math. Biosci. 18:335-350.

Hoagland, R.E. 1978. Isolation and some properties of an aryl acylamidase from red rice, *Oryza sativa* L., that metabolizes 3', 4'-dichloropropionanilide. Plant Cell Physiol. 19:1019-1029.

Jennings, P.R. and **R.M. Herrera.** 1968. Studies on competititon in rice. II. Competition in segregating populations. Evolution 22:332-336.

Monks, D.W. and **L.R. Oliver.** 1988. Interactions between soybean (*Glycine max*) cultivars and selected weeds. Weed Sci. 36:770-774.

Oliver, L.R. 1988. Principles of weed threshold research. Weed Technol. 2:398-403.

Shaw, W.C. 1982. Integrated weed management system technology for pest management. Weed Sci. 30:2-12.

Smith, R.J., Jr. 1987. Area of interference of hemp sesbania in rice. Proc. South. Weed Sci. Soc. 40:305.

Smith, R.J., Jr. 1988. Weed thresholds in southern U.S. rice, *Oryza sativa.* Weed Technol 2:232-241.

Van Groenendael, J.M. 1988. Patchy distribution of weeds and some implications for modelling population dynamics: A short literature review. Weed Res. 28:437-441.

Boron Phosphate and Aluminum Phosphate Aerogels

David A. Lindquist*, Steven M. Poindexter, Sterling S. Rooke, D. Ritchie Stockdale, Kirk B. Babb, Alison L. Smoot and William E. Young
The University of Arkansas at Little Rock
Department of Chemistry
Little Rock, AR 72204

*Author to whom correspondence should be addressed

Abstract

Anhydrous sol-gel condensation of triethyl phosphate [$(CH_3CH_2O)_3PO$] with boron trichloride (BCL_3) or triethyl aluminum [$(CH_3CH_2)_3Al$] in organic solvents, led to formation of metallophosphate gels. The pore fluid of the gels was removed under supercritical conditions in a pressurized vessel to form aerogels. The aerogels were then calcined at progressively higher temperatures to produce high surface area phosphates. Since the initial gel reagent mixtures contained several NMR active nuclei, the condensation chemistry prior to the gel point was monitored by solution ^{1}H,^{13}C,^{31}P,and ^{11}B NMR. The surface areas, distribution of pore sizes, and total pore volumes of the aerogel products were determined using nitrogen gas physisorption methods.

Introduction

The orthophosphate (MPO_4) compounds of boron, aluminum, and iron(III) may be described as covalent network solids of oxygen bridging alternating PO_4 and MO_4 tetrahedra (Van Wazer, 1958). These phosphates are consequently structurally isomorphous with one or more of the various forms of silica (SiO_2) and also share similar chemical and physical properties with silica. The formation of silica by sol-gel routes has been intensively studied for various applications such as coatings and formation of high surface area materials (Brinker and Scherer, 1990), but comparatively little has been written on the sol-gel preparation of covalent phosphates (Gerrard and Griffey, 1961; Kearby, 1967; Glenz et al., 1991; Rebenstorf et al., 1991).

Phosphate gels of aluminum and boron were prepared in this work; iron phosphate ($FePO_4$) will be described in future studies. Since phosphates of acidic metal cations have useful solid acid catalytic properties, it was desirable to prepare them with a high surface area. Aerogels have high surface areas since the liquid in the gels is removed under supercritical conditions, and collapse of the pore structure, which can be problematic for evaporatively dried gels, is greatly reduced. We chose to prepare gels under nonaqueous conditions because most organic solvents have a considerably lower critical temperature than water. A second rationale for anhydrous conditions is the difficulty in making stoichiometric phosphate compositions from aqueous solutions. In water solutions one may obtain some metal oxide phase in addition to the desired phosphate due to competing hydrolysis reactions.

Materials and Methods

Gel Syntheses and Aerogel Processing.--All solvents were dried under a dry nitrogen atmosphere by distillation from P_2O_5 in the case of chlorobenzene, potassium carbonate for acetone, and sodium benzophenone ketyl for pentane. The triethyl phosphate was also freshly distilled and all gel syntheses conducted under a dry nitrogen atmosphere using Schlenk techniques.

The boron phosphate gels in this work were synthesized using the method of Gerrard and Griffey (1959) by reaction of triethyl phosphate with boron trichloride to yield boron phosphate and ethyl chloride as a byproduct. To prepare the boron phosphate gels, 8 mL (46 mmol) of triethyl phosphate $(CH_3CH_2O)_3PO$ was dissolved in 18 mL of chlorobenzene. The solution was cooled in an ice bath and a flask containing 4 mL (46 mmol) of boron trichloride (BCL_3) was mated to the triethyl phosphate solution flask to allow condensation of the BCL_3 vapor into the stirring phosphate solution over a period of about three hours. During this time, the flasks were closed off from nitrogen purge so that no BCL_3 was lost from the system. The resulting solution of adduct was then aged at 60°C for 8 hours. During this time, the flask was periodically vented to allow for escape of the ethyl chloride byproduct. The gel point occurred, on average, 1 hour after beginning heating at 60°C. The gel was then allowed to age in a sealed flask at room temperature for two days.

The $AlPO_4$ gel was prepared by a novel method using triethyl aluminum instead of the chloride compound due to the low solubility of aluminum chloride in organic solvents. In a flask equipped with a water condenser, a neat

mixture of 10 mL (73 mmol) of $(CH_3CH_2)_3AL$ and 12.4 mL of $(CH_3CH_2O)_3PO$ (73 mmol) were heated to 175°C in an oil bath on a hot plate stirrer overnight. This formed an oligomeric oil. The oligomer (2 mL) was then dissolved in 24 mL of acetone and the solution cooled in a salt ice bath (-40°C). Anhydrous NH_3 was then bubbled vigorously through the solution with a syringe needle. After a few minutes the mixture gelled with a concomitant evolution of gas. The gel was then allowed to stand in a sealed flask at room temperature for two days.

The aged gels then were transferred to a soxhlet apparatus and the chlorobenzene or acetone exchanged for pentane by reflux overnight (15 hr). While in the soxhlet, the gels were kept in an open top glass container so that fresh refluxing pentane could condense and pour off the top of the gels without draining the pore liquid from the gels during each emptying cycle of the soxhlet. The solvent exchange through the gels could be monitored visually because the translucent gels became more opaque upon substitution of the pentane for chlorobenzene or acetone.

The pentane solvent exchanged gels were transferred to a one liter bomb (Parr® Instrument Co. Model 4500) along with an additional 100 mL of dry pentane. The vessel was then pressurized with nitrogen gas to 400 psi, heated over a period of one hour to 210°C, and held at this temperature under supercritical conditions for 0.5 hour. During heating, the vessel attained a maximum pressure of approximately 1000 psi; the critical point of pentane is 196°C and 480 psi. The supercritical pentane then was vented from the bomb while maintaining the temperature at 210°C. Portions of the prepared aerogels were subsequently heated in air in a muffle furnace at elevated temperatures of 200°C, 500°C and 800°C for one hour at each temperature. This heating was done in order to determine the effects of progressive calcining on the microstructure of the gels.

Characterization Methods.--The early stages of the condensation chemistry prior to the gel point could be monitored by multinuclear solution NMR. In the case of boron phosphate, the freshly prepared chlorobenzene adduct solution was examined by ^1H, ^{13}C, ^{31}P, and ^{11}B.

FT-NMR (Bruker Instruments 250 MHz FT-NMR). The NMR spectra were collected from samples in vacuum sealed NMR tubes containing $CDCl_3$ lock solvent. NMR spectra were also collected from heated and aged samples. Infrared spectra of aerogels were obtained as Nujol mulls. The instrument used was a Perkin Elmer Model 1600 FTIR. Surface characterization of solids by nitrogen physisorption, including isothermal desorption, multipoint Brunauer-Emmett-Teller (BET) surface area, total pore volume, and average pore radius were determined using a Quantachrome® Model NOVA 1000 instrument. Samples were outgassed at 200°C overnight under oil pump vacuum prior to physisorption measurements. Multipoint BET data were collected using a 4 point adsorption isotherm (P/P_0=0.05, 0.15, 0.25, and 0.35). The total pore volume was determined based on the quantity of N_2 adsorbed onto the sample at a relative pressure P/P_0=0.99. The average pore reaius in the gels was calculated by dividing twice the pore volume by the surface area. This method of calculating the value of the average pore radius assumes that the pores have a cylindrical geometry.

Results and Discussion

Polymerization of the boron phosphate gel proceeded by a condensation of B-O-P bonds with concomitant elimination of chloroethane (Gerrard and Griffey, 1959). Freshly prepared solutions of the metal chlorides and triethyl phosphate showed sharp NMR resonances attributable to a 1:1 adduct $[(CH_3CH_2O)_3P{=}O{:}BCl_3]$. The NMR characterization data for the $(CH_3CH_2O)_3P{=}O{:}BCl_3$ adduct in chlorobenzene solution with $CDCl_3$ lock solvent are as follows: ^1H δ 4.57 multiplet (CH_2 intensity 1.5), 1.58 multiplet (CH_3 intensity 1.0); $^{11}B(BF_3{\cdot}Et_2O)$ δ 5.4 (h/2~13 Hz): ^{13}C δ 63.6 (CH_2), δ 15.0 (CH_3); ^{31}P (85% H_3PO_4) δ -11.6. The ^{11}B resonance of the adduct was narrow due to the tetrahedral coordination of boron. NMR spectra collected after heating the sample at 50°C in water for 5 minutes, exhibited the emergence of peaks ascribed to ethyl chloride and a concomitant diminution of adduct peaks as condensation began. The ^{31}P spectrum of the heated sample also showed an additional resonance at -20 ppm pertaining to formation of $(CH_3CH_2O)_2P(O)OBCl_2$ by elimination of one equivalent of ethyl chloride from the adduct. After an additional two days of aging at room temperature only ethyl chloride could be seen in the NMR spectra since the boron and phosphorus had become incorporated into the crosslinked gel.

The structure of the oligomer formed by heating the neat mixture of $CH_3CH_2)_3A1$ and $(CH_3CH_2O)_3PO$ is not yet understood. The NMR data indicate that ethyl groups remain on both aluminum and phosphorus atoms. The proton NMR characterization data for the aluminum phosphate oligomer in $CDCl_3$ are as follows: 1H δ 4.05 multiplet [CH_2-(P) intensity 1.0), δ 1.35 triplet [CH_3-(A1) intensity 1.8]. δ 0.96 triplet [CH_3-(P) intensity 1.3], δ -0.23 quartet [CH_2-(A1) intensity 1.3]. Integration of the ^1H resonances indicated that there were more ethyl groups on aluminum that on phosphorus (4:3 ratio) instead of the expected 1:1 ratio. We are currently investigating the chemistry of this system to better understand it. Regardless of the chemistry which led to formation of the $A1PO_4$ gel, the aerogel product nonetheless had favor-

able properties as evidenced by its high surface area and the thermal stability of its microstructure.

Figures 1 and 2 illustrate the desorption isotherm data from the NOVA 1000 instrument for the three calcined BPO_4 aerogels and the three calcined $A1PO_4$ aerogels respectively. The 200°C BPO_4 aerogel and all three of the $A1PO_4$ samples exhibited Type IV isotherms (Brunauer et al., 1940). The adsorption of N_2 at both low and high relative pressures in these samples is indicative of materials with a distribution of pore radii, from micropores (r<15Å) to macropores (r≈1000Å). However, the 500°C and 800°C BPO_4 showed almost no desorption at low relative pressures illustrating a lack of microporosity. The 800°C BPO_4 sample was lacking in macroporosity as well. It is clearly evident in comparing Figs. 1 and 2 that the BPO_4 becomes increasingly dense and nonporous with increased heating, whereas the $AlPO_4$ largely maintains its original microstructure.

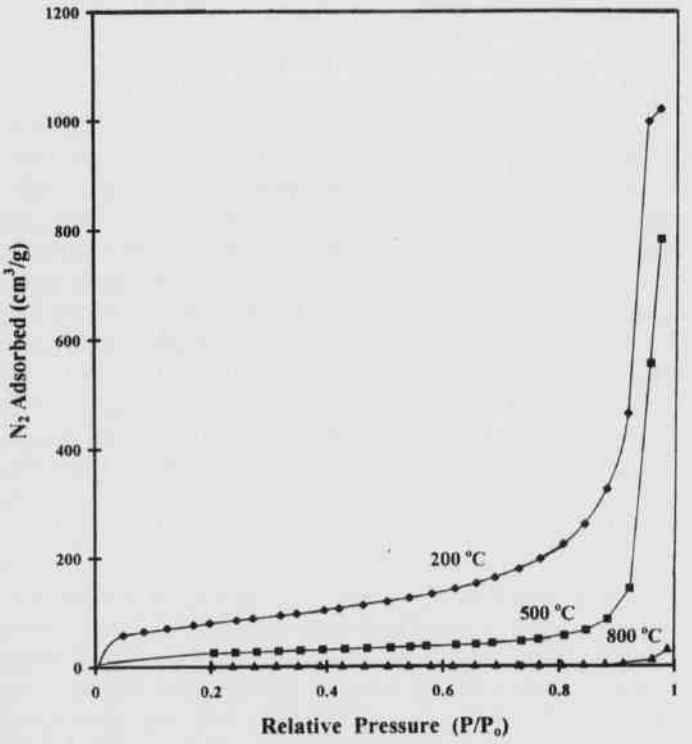

Fig. 1. N_2 desorption isotherm curves for BPO_4 aerogel heated to 200°C, 500°C, and 800°C.

There is an anomalous feature in Fig. 2; the 200°C isotherm is less than that of the 500°C sample. This might be explained as adsorbed water in the pore structure not removed during the 200°C outgassing procedure prior to the isotherm measurements. The presence of water

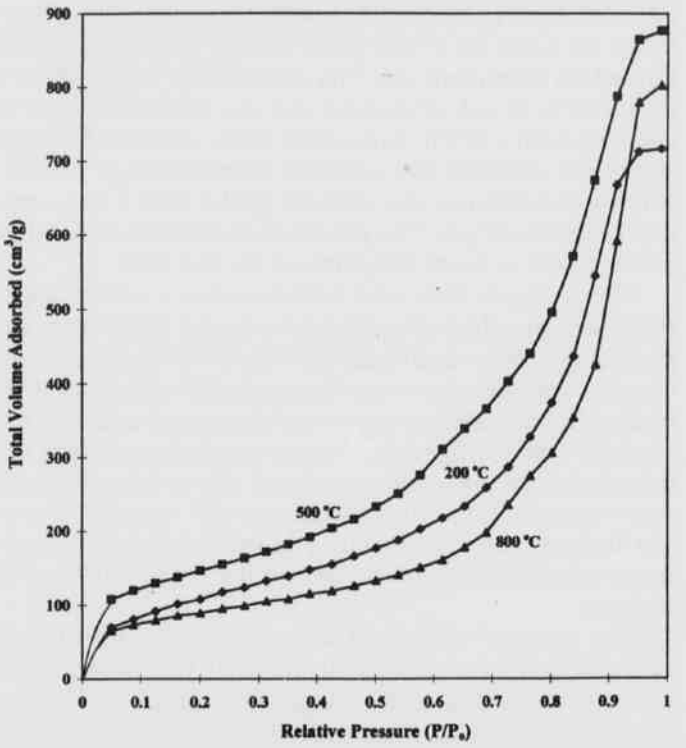

Fig. 2. N_2 desorption isotherm curves for $AlPO_4$ aerogel heated to 200°C, 500°C, and 800°C.

trapped in the micropores at temperatures below 500°C is reasonable since such high surface area materials make very good desiccants.

Table 1 is a complilation of the calculated specific surface area, total pore volume, and average pore radius for each of the heated aerogels. The microstructure becomes more course and the small pores are vanquished with increasing temperature. This is manifested as a decrease in total surface area and an increase in the average pore radius at higher temperatures and is a general phenomenon of sintering. There is not reported value for the average pore radius of the 800°C BPO_4 sample since the only "porosity" remaining would be the free space between the aerogel sample pieces which have already densified. The relatively constant total pore volume for the $AlPO_4$ aerogels reflects the stability of this material's microstructure.

Now that we have some basic understanding of these materials, we are currently working on developing applications for these phosphates. These applications include micro filtration membranes and catalytic membranes. In addition we hope to develop new types of crystalline catalysts by processing the solvent containing gels under similar conditions as those used to manufacture zeolites.

Table 1. Aerogel microstructural changes with increasing temperature.

$AlPO_4$	200°C	500°C	800°C
Surface Area (m^2/g)	410	530	320
Total Pore Volume (cm^3/g)	1.1	1.4	1.3
Average Pore Radius (Å)	54	51	77

BPO_4	200°C	500°C	800°C
Surface Area (m^2/g)	230	86	12
Total Pore Volume (cm^3/g)	1.7	1.0	0.05
Average Pore Radius (Å)	150	240	

Acknowledgements

This work was funded by the Arkansas Science and Technology Authority and faculty research grant from UALR. We would like to thank Mr. Alan Toland for his assistance in obtaining the NMR spectra.

Literature Cited

Van Wazer, J.R. 1958. Phosphorus and its compounds. Interscience Pub., N.Y.

Brinker, C.J. and **G.W. Scherer.** 1990. Sol-gel science. Academic Press, Inc., San Diego.

Gerrard, W. and **P.F. Griffey.** 1959. A novel preparation of boron phosphate, Chem. & Ind. 55.

Kearby, K.K. 1967. Compositions containing stable aluminum phosphate gel and methods of making and using same. U.S. Patent 3,342,750.

Glenza, R., Y.O. Parent and **W.A. Walsh.** 1991. Amorphous aluminum phosphate gels. ACS Symp. Ser. (Div. Petr. Chem.) 36: 369-477.

Rebenstorf, B., T. Lindblad and **S.L.T. Anderson.** 1991. Amorphous $AlPO_4$ as Catalyst Support. J. Catal. 128: 293-302.

Brunauer, S., L.S. Deming, W.S. Deming and **E. Teller.** 1940. On a theory of the van der Waals adsorption of Gases. J. Am. Chem. Soc. 62: 1723-1732.

Comparative Gas-Exchange in Leaves of Intact and Clipped, Natural and Planted Cherrybark Oak (*Quercus pagoda* Raf.) Seedlings[1]

Brian R. Lockhart[2]
School of Forest Resources
University of Arkansas at Monticello
P.O. Box 3468
Monticello, AR 71656-3468

John D. Hodges
Department of Forestry
Mississippi State University
P.O. Box 9681
Mississippi State, MS 39762-9681

[1]This paper is approved for publication by the Director of the Arkansas Agricultural Experiment Station.
[2]Author to whom correspondence should be sent.

Abstract

Gas-exchange measurements, including CO_2-exchange rate (net photosynthesis), stomatal conductance, and transpiration, were conducted on intact and clipped cherrybark oak (*Quercus pagoda* Raf.) seedlings growing in the field and in a nursery bed. Seedlings in the field, released from midstory and understory woody competition, showed significant increases in gas-exchange compared to non-released seedlings due to increases in light levels reaching seedlings. Concurrently, little difference occured in the CO_2-exchange rate between intact and clipped seedlings in the released treatment although clipped seedlings maintained a consistently greater rate of stomatal conductance. In order to reduce the high variability of light levels recorded in the field, gas-exchange measurements were conducted on intact and clipped cherrybark oak seedlings growing in a nursery bed under consistent light conditions. Again, no differences were found in the CO_2-exchange rate between intact and clipped seedlings. Furthermore, no differences were found in stomatal conductance and transpiration between intact and clipped seedlings. However, significant differences in gas-exchange were found between first-flush and second-flush leaves regardless of seedling treatment (intact or a sprout). Greater rates of gas-exchange in second-flush leaves can be attributed to developing third-flush steams and leaves.

Introduction

Cherrybark oak (*Quercus pagoda* Raf.) occurs throughout the southeastern United States on river and stream floodplains (USDA, 1990). Its rapid growth, high quality wood, and consistent mast production make this species a highly desired tree for timber and wildlife habitat management purposes. In fact cherrybark oak is considered to be the best red oak for management purposes in southern bottomland hardwood forests (Putnam et al., 1960). But a continuing problem in the management of oak stands, and cherrybark oak in particular, is securing adequate oak regeneration after a harvest cut. Reports indicate that many stands formerly dominated by oak are regenerating to species other than oak (Johnson, 1979; McGee, 1986; Cho and Boerner, 1991), even when silvicultural prescriptions designed to increase the oak component were used (Johnson and Krinard, 1976; Loftis, 1983). Reasons for these failures include an insufficient number and/or size of natural oak reproduction at the time of overstory removal and a slow early height growth rate of both natural and planted seedlings (Beck, 1970; Janzen and Hodges, 1987; Graney, 1989). Much of this past research was comprised of applied field studies attempting to regenerate oak stands. Recently, scientists have pointed to the need for more information on the basic biology of oak seedlings to better understand regeneration successes and failures (Hodges and Jazen, 1987; Crow, 1988; Lorimer, 1989; Johnson, 1993). Therefore, the objective of this study was to compare gas-exchange rates between intact and clipped, natural and planted cherrybark oak seedlings. Oak sprouts are believed to be more successful in regenerating hardwood stands than intact seedlings. We hyposthesized that the early rapid height growth of cherrybark oak sprouts can be attributed, in part, to greater rates of leaf gas-exchange compared to intact seedlings.

Materials and Methods

Natural cherrybark oak seedlings were located on three sites within the floodplains along Loakofoma Creek and the Noxubee River on the Noxubee National Wildlife Refuge, Oktibbeha and Noxubee Counties, Mississippi. Stand composition was either bottomland hardwood or old-field mixed pine and hardwood. All three stands were even-aged, with overstory ages ranging from 46 to 80 years depending on site. Soils were Stough fine sandy loam, Ochklockonee loam, and the Urbo series for Sites 1, 2, and 3, respectively. Site index, base age 50 years, for cherrybark oak ranged from 26-35 depending on site.

Seedlings selected for gas-exchange measurements were part of a larger study on the response of natural cherrybark oak seedlings to release from competing vegetation and seedling clipping (Lockhart, 1992). A 2 X 2 factorial arrangement in a split-plot block design with two replications per site was established in February, 1989, for Sites 1 and 2 and February, 1990, for Site 3. Treatments consisted of midstory and understory removal or no removal at the whole-plot level and seedling clipping or no clipping at the subplot level. All stems, excluding cherrybark oak seedlings, were removed by chainsaw felling. Immediately after each stem was cut, Tordon 101R® was applied to the stump using a mist-spray bottle. Seedling clipping consisted of severing one-half of the seedlings at 2.5 cm above groundline using a hand-held shear.

Leaf gas-exchange measurements were conducted using an ADC LCA-2 Infrared Gas Analyzer. Measurements were made of the CO_2-exchange rate (CER; net photosynthesis), photosynthetic photon flux density (PPFD; light), stomatal conductance, and leaf temperature. Since gas-exchange measurements in control plots showed very low levels of CER (data not shown), sampling involved randomly selecting five intact and five clipped seedlings within a single released plot, thereby focusing attention to those seedlings receiving increased levels of light. Individual seedlings were selected based on the following criteria: (1) lag, or resting, stage of development (Hanson et al., 1986), (2) equal number of terminal flushes, and (3) undamaged median leaves along the terminal flush. A single median leaf from each seedling was measured hourly from 9:00 a.m. to 5:00 p.m. CST at various times during the 1989 and 1990 growing seasons until gas-exchange equilibrium was reached.

Due to high variability in light levels experienced during field measurements, a second gas-exchange experiment was conducted to determine if differences in CER existed between intact and clipped planted cherrybark oak seedlings. Sixty, one-year-old cherrybark oak seedlings growing in a nursery bed at the Blackjack Research Facility, Mississippi State University, were flagged in February, 1991. Seedlings were watered two-three times per week through June, then daily for the remainder of the 1991 growing season. On six days during July and August, leaf gas-exchange measurements were conducted on five intact and five clipped seedlings as described above, except measurement times were 8:00 a.m., 11:00 a.m., 2:00 p.m., and 5:00 p.m.

Analysis of variance was used to determine if differences existed in gas-exchange between intact and clipped cherrybark oak seedlings. Dependent variables included CER, PPFD, stomatal conductance, leaf temperature, and time. Individual seedlings were treated as experimental units in all analyses (Kruger and Reich, 1993a). Differences in treatment means were considered to be significant at $P \leq 0.05$. All analyses were conducted using PC-SAS (SAS, 1985). Gas-exchange measurements for only one representative summer day for each of the two experiments are presented below.

Results

Natural Seedlings.--Gas-exchange measurements conducted on July 11, 1990 on Site 3 were selected as representative for measurements conducted in the field. Mean levels of CER for both intact and clipped cherrybark oak seedlings were 3.18 µmol CO_2 m^{-2} s^{-1}, ($F < 0.01$, $P=0.99$), although a significant difference did occur in the diurnal CER pattern ($F=6.36$, $P=0.01$; Fig. 1). Levels of CER were lowest at 9:00 a.m. with 1.5 and -0.9 µmol CO^2 m^{-2} s^{-1} for intact and clipped seedlings, respectively. CER levels then increased throughout the morning, more so for clipped seedlings than for intact seedlings. Maximum CERs were obtained at noon with 5.88 and 6.60 µmol CO^2 m^{-2} s^{-1} for intact and clipped seedlings, respectively. Thereafter, levels for CER steadily decreased throughout the afternoon, except for a small increase for intact seedlings at 3:00 p.m. Changes in diurnal CER patterns for both intact and clipped seedlings coincided with changes in the diurnal pattern of light interception (Fig. 2). Light levels were also initially low in the morning (< 200 PPFD), but showed a steady increase until noon for intact seedlings (1,250 PPFD) and 1:00 p.m. for clipped seedlings (1,400 PPFD). Light levels then decreased rapidly during the afternoon hours, due primarily to shading from both overstory and adjacent overstory/midstory canopies, except for a second peak for intact seedlings at 3:00 p.m. (950 PPFD).

As with earlier gas-exchange measurements, clipped seedlings showed considerably higher rates of stomatal conductance throughout the day than did intact seedlings ($F=28.70$, $P= 0.01$; Fig. 3). Rates of stomatal conductance for clipped seedlings were consistently 0.10-0.20 cm s^{-1} greater than intact seedlings throughout the day. The diurnal pattern of stomatal conductance was not significantly different, although rates slightly increased during the morning until noon when rates further increased by approximately 0.50 and 0.10 cm s^{-1} for intact and clipped seedlings, respectively. These increases coincided with maximum light levels for intact seedlings and relatively high light levels for clipped seedlings. Stomatal conductance rates then decreased throughout the afternoon indicating partial stomatal closure, which would partially explain the decreases in the diurnal patterns of CER experienced during the afternoon hours.

Differences in leaf temperature also existed between leaves of intact and clipped seedlings. Mean leaf temperatures were 21.3°C and 30.1°C for intact and clipped

Journal of the Arkansas Academy of Science, Vol. 48 [1994], Art. 1

seedlings, respectively (F=11.37; P<0.01). Diurnal patterns of leaf temperature followed similar patterns as the diunal light pattern (Fig. 4). Leaf temperatures steadily increased throughout the morning, reaching a maximum of 33°C for clipped seedlings at 2:00 p.m. This time coincided with higher light levels and was the only time leaf temperatures were greater for clipped seedlings. A maximum temperature for intact seedlings was 33.7°C at 3:00 p.m. Leaf temperatures for both intact and clipped seedlings decreased thereafter.

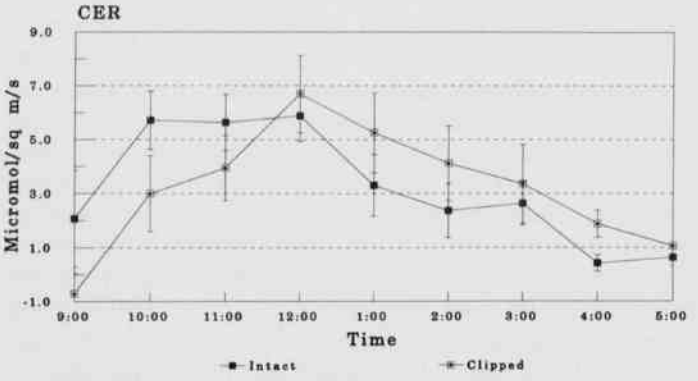

Fig. 1. Diurnal CO_2-exchange rates (CER) for intact and clipped natural cherrybark oak seedlings released from midstory and understory competition on the Noxubee National Wildlife Refuge, Noxubee County, MS. Gas-exchange measurements conducted on Site 3 on July 11, 1990. Vertical bars represent ± 1 SE.

Planted Seedlings.--No apparent differences in CER occurred between intact and clipped cherrybark oak seedlings in the field; thus, definite statements about gas-exchange similarities or differences could not be made. Reasons for this include differences in age of seedlings, high variability in light levels, and possible below ground competition from overstory trees. Therefore, additional gas-exchange measurements were conducted on clipped and intact cherrybark oak seedlings growing under more consistent environmental conditions in a nursery bed. Gas-exchange measurements conducted on August 24, 1991 were selected as a representative summer day for measurements conducted in the nursery bed.

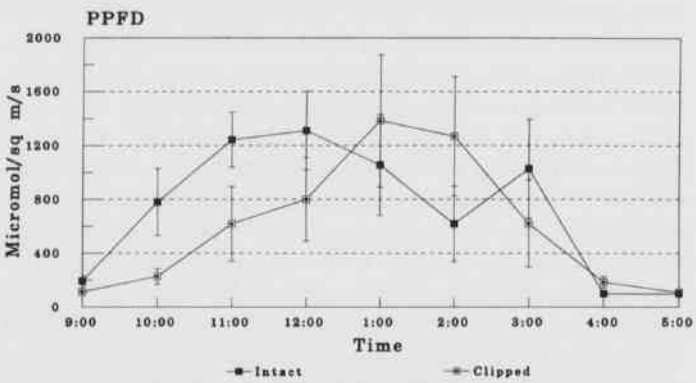

Fig. 2. Diurnal photosynthetic photon flux densities (PPFD) for intact and clipped natural cherrybark oak seedlings released from midstory and understory competition on the Noxubee National Wildlife Refuge, Noxubee County, MS. Gas-exchange measurements conducted on Site 3 on July 11, 1990. Vertical bars represent ± 1 SE.

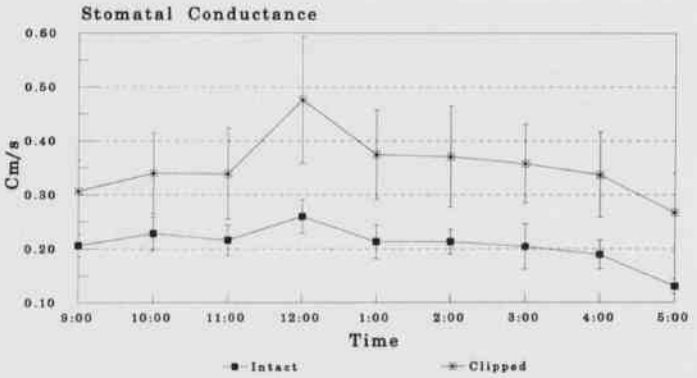

Fig. 3. Diurnal stomatal conductance rates for intact and clipped natural cherrybark oak seedlings released from midstory and understory competition on the Noxubee National Wildlife Refuge, Noxubee County, MS. Gas-exchange measurements conducted on Site 3 on July 11, 1990. Vertical bars represent ± 1 SE.

Clipped cherrybark oak seedlings had a slightly greater mean CER (5.86 µmol CO_2 m^{-2} s^{-1}) based on four measurements periods compared to intact seedlings (5.30 µmol CO_2 m^{-2} s^{-1}), although this diference was not significant (F=0/87, P<.36). However, differences were found between first-flush leaves and second-flush leaves. Mean CER during the day was 4.52 and 6.64 µmol CO_2 m^{-2} s^{-1} for first-flush and second-flush leaves, respectively

(F=12.34, P<0.01). Similar patterns of diurnal CER existed for intact and clipped seedlings regardless of flush number. CER increased for all seedlings from 8:00 to 11:00 before decreasing during the afternoon (Fig. 5).

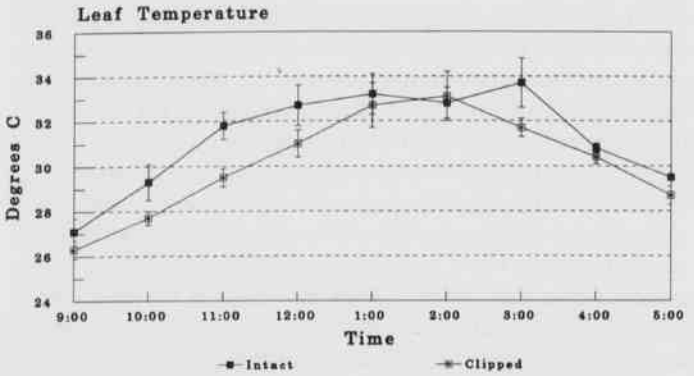

Fig. 4. Diurnal leaf temperatures for intact and clipped natural cherrybark oak seedlings released from midstory and understory competition on the Noxubee National Wildlife Refuge, Noxubee County, MS. Gas-exchange measurements conducted on Site 3 on July 11, 1990.

As expected, little difference was found in light levels between intact and clipped seedlings regardless of flush due to the open conditions that existed in the nursery bed. Second-flush leaves did receive slightly more light than first-flush leaves (Fig. 6). First-flush leaves, with their lower positions on the stem, were probably partially shaded by leaves from above even through attemps were made to avoid such situation. However, a diurnal pattern of light levels did exist, with greater levels occurring during the 11:00 a.m. and 2:00 p.m. measurement times compared to the 8:00 a.m. and 5:00 p.m. measurement times. Also, little difference was found for leaf temperatures between intact and clipped seedlings, regardless of flush (Fig. 7). As with light levels, a diurnal pattern of leaf temperature existed.

Differences is stomatal resistances (as measured with a LiCor Model LI-1600 steady-state porometer instead of stomatal conductance as measured with the ADC unit; stomatal resistance = 1/stomatal conductance) and transpiration rates between intact and clipped seedlings were small. Since porometer measurements were only conducted twice, at 11:00 a.m. and 2:00 p.m., diurnal patterns were not detected. But, as with previous nursey bed measurements and the CER measurements for this day, differences in stomatal resistance and transpiration existed between flushes. Second-flush leaves consistently had lower stomatal resistance rates, i.e., greater stomatal conductance rates, with 2.38 and 1.37 s cm^{-1} for intact and clipped seedlings respectively. These values were 3-4 times greater than for respective first-flush leaves (F=3.63, P<0.07). Furthermore, transpiration rates were 9.491 and 11.757 µgm m^{-2} s^{-1}, respectively, for intact and clipped seedlings. These values were 1-5 µgm m^{-2} s^{-1} greater than for first flush leaves (F=4.41, P=0.05).

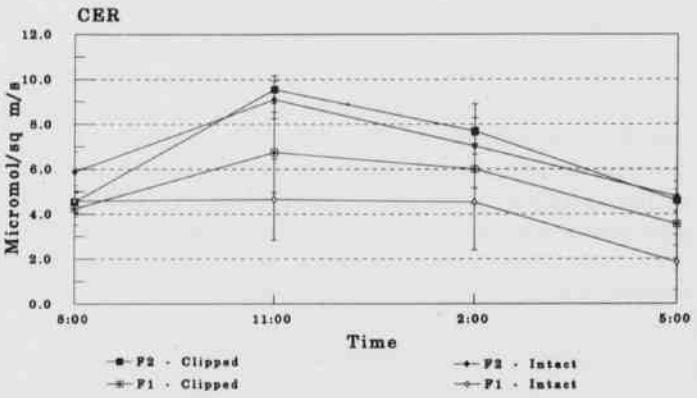

Fig. 5. Diurnal CO_2-exchange rates (CER) for intact and clipped planted cherrybark oak seedlings growing in a nursery bed at the Blackjack Research Facility, Oktibbeha County, MS. Gas-exchange measurements conducted on August 24, 1991.

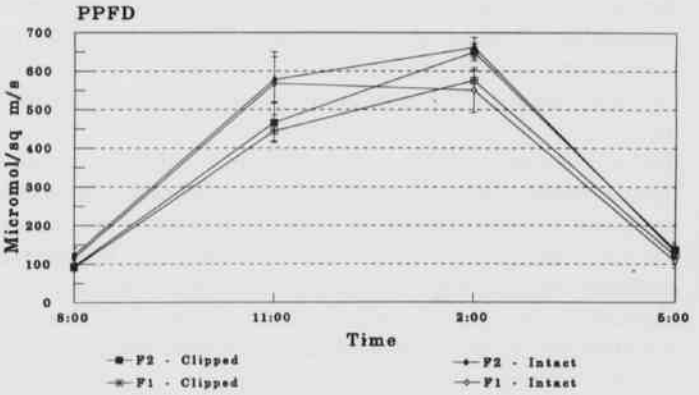

Fig. 6. Diurnal photosynthetic photon flux densities (PPFD) for intact and clipped planted cherrybark oak seedlings growing in a nursery bed at the Blackjack Research Facility, Oktibbeha County, MS. Gas-exchange measurements conducted on August 24, 1991.

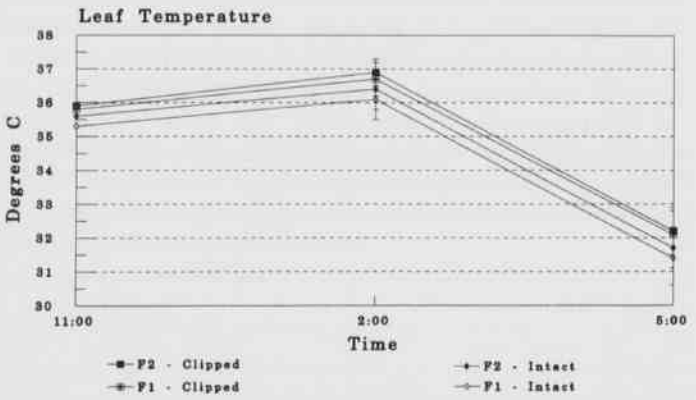

Fig. 7. Diurnal leaf temperatures for intact and clipped planted cherrybark oak seedlings growing in a nursey bed at the Blackjack Research Facility, Oktibbeha County, MS. Gas-exchange measurements conducted on August 24, 1991.

Discussion

Clipping of oak seedlings has been shown to increase the rate of height growth and could be beneficial in the natural regeneration of oak stands (Hodges and Janzen, 1987). In general, oak seedlings contain numerous buds at the base of their stem which sprout prolifically upon stem breakage (Matsubara and Hiroki, 1985). Reasons for the rapid growth of sprouts is not fully understood but may include favorable root/shoot ratios (Cobb et al., 1985), increased photosynthetic capacity of the leaves (Kruger and Reich, 1989), and increased water transport capabilities (Blake and Tschaplinski, 1986). Clipping oak seedlings also somewhat imitates the "shoot dieback/resprout" phenomenon prevalent among natural oak seedlings. Reasons for oak seedling dieback/resprouting events are presently unknown (Crow, 1988), but repeated sprouting events allow oak seedlings to build relatively large root systems compared to the shoot (Watt, 1979). Therefore, shoot dieback/resprouting may be a survival mechanism allowing oak seedlings to survive for longer periods of time in the understory while waiting for an opportunity to take rapid advantage of a canopy opening.

One reason commonly cited for greater growth of oak sprouts compared to intact seedlings has been greater gas-exchange, specifically greater rates of net photosynthesis of sprout leaves (Satoh et al., 1977; Heichel and Turner, 1983; Tschaplinski and Blake, 1989; McGraw et al., 1990; Kruger and Reich, 1993b). Kruger and Reich (1993b) showed that northern red oak sprouts (*Q. rubra* L.) had a distinctly different diurnal gas-exchange pattern compared to intact seedlings in the field. Both sprouts and intact seedlings reached maximum levels of CER in the mid-morning hours (approximately 10:00 a.m. CST). Thereafter, sprout leaves were able to maintain near maximum rates of both photsynthesis and stomatal conductance throughout the day while leaves of intact seedlings exhibited sharp declines throughout the day. Similar patterns in CER of natural cherrybark oak seedlings were not found in this study. This was due in part to the highly variable light conditions present in the field. During gas-exchange measurements, overstory trees occasionally shaded measurement seedlings. Greater CER of cherrybark oak sprouts in the field is possible given their consistently greater rates of stomatal conductance compared to intact seedlings. Similar patterns of stomatal conductance were found on three of the four other days gas-exchange measurements were conducted during the 1990 growing season (data not shown). Possible reasons for this consistent difference in stomatal conductance between intact and clipped seedlings include: (1) differences in stomatal pore opening, (2) differences in stomatal density per unit leaf area, and/or (3) differences in cuticular resistance to water vapor exchange.

No differences in CER were found between sprout and intact cherrybark oak seedlings growing under more consistent environmental conditions in the nursery bed. The influence of the developing third flush may have masked any possible differences. Hanson et al., (1986) showed, with northern red oak seedlings growing in a growth chamber, that development of a third flush of growth does affect the gas-exchange properties of the other two flushes, particularly the second flush. Flushing in oak seedlings has a profound effect on source-sink relationships. Increases in the gas-exchange of the second flush is in response to the increases in photosynthate demand by the developing third flush (Dickson, 1991).

While the question of "Why are sprouts able to grow more rapidly than intact seedlings?" was not answered by this study, results showed that cherrybark oak sprouts do have the potential for greater CER based on greater stomatal conductance. These results agree with the results of others working with oak sprouts (Heichel and Turner, 1983; McGraw et al., 1990; Kruger and Reich, 1993a, 1993b). Future work in the area of oak sprout ecophysiology should involve comparisons of anatomy and morphology of leaves and stems, photosynthate partitioning, nutrient dynamics, and water relations under both controlled and field conditions. These studies are needed in order to better understand the mechanisms that lead to greater initial growth in oak sprouts compared to intact seedlings.

Acknowledgements

We would like to acknowledge the assistance of Yanfei Guo, Tim Deen, Emile Gardiner, and Masato Miwa for their field assistance in conducting gas-exchange measurements. We would also like to acknowledge the U.S. Forest Service, Southern Hardwoods Laboratory, for partial funding of this project.

Literature Cited

Beck, D.E. 1970. Effect of competition on survival and height growth of red oak seedlings. USDA For. Serv. Res. Pap. SE-56, 7 pp.

Blake, T.J. and **T.J. Tschaplinski.** 1986. Role of water relations and photosynthesis in the release of buds from apical dominance and the early reinvigoration of decapitated poplars. Physiol. Plant. 35: 152-157.

Cho, D.S. and **R.E.J. Boener.** 1991. Canopy disturbance patterns and regeneration of *Quercus* species in two Ohio old-growth forests. Vegetatio 93: 9-18.

Cobb, S.W., A.E. Miller and **R. Zahner.** 1985. Recurrent shoot flushes in scarlet oak stump sprouts. For. Sci. 31: 725-730.

Crow, T.R. 1988. Reproductive mode and mechanisms for self-replacement of northern red oak (*Quercus rubra*) - a review. For. Sci. 34: 19-40.

Dickson, R.E. 1991. Episodic growth and carbon physiology in northern red oak. Pp. 117-124, in Proceedings of The Oak Resource in the Upper Midwest; Implications for Management (S. B. Laursen and J. F. DeBoe, eds.) Minnesota Extension Service Publication Number Nr-BU-5663-S, 309 pp.

Graney, D.L. 1989. Growth of oak, ash, and cherry reproduction following overstory thinning and understory control in upland hardwood stands of northern Arkansas. Pp. 245-252, *In* Proceedings of the Fifth Biennial Southern Silvicultural Research Conference (J. H. Miller, ed.) USDA Forest Service General Technical Report SO-74, 618 pp.

Hanson, P.J., R.E. Dickson, J.G. Isebrands, T.R. Crow and **R.K. Dixon.** 1986. A morphological index of *Quercus* seedling ontogeny for use in studies of physiology and growth. Tree Phys. 2: 273-281.

Heichel, G.H. and **N.C. Turner,** 1983. CO_2 assimilation of primary and regrowth foilage of red maple (*Acer rubrum* L.) and red oak (*Quercus rubra* L.): response to defoliation. Oecologia 57: 14-19.

Hodges, J.D. and **G.C. Janzen.** 1987. Studies on the biology of cherrybark oak: recommendations for regeneration. Pp. 133-139, *In* Proceedings of the Fourth Biennial Southern Silvicultural Research Conference (D.R. Phillips, ed.,), USDA Forest Service General Technical Report SE-42, 598 pp.

Janzen, G.C. and **J.D. Hodges.** 1987. Development of advanced oak regeneration as influenced by removal of midstory and understory vegetation. Pp. 455-461, *In* Proceedings of the Fourth Biennial Southern Silvicultural Research Conference (D. R. Phillips, ed.,), USDA Forest Service General Technical Report SE-42, 598 pp.

Johnson, P.S. 1993. Perspectives on the ecology and silviculture of oak-dominated forests in the central and eastern states. USDA For. Serv. Gen. Tech. Rpt. NC-153, 28 pp.

Johnson, R.L. 1979. Adequate oak regeneration - a problem without a solution. Pp. 59-65, *In* Management and Utilization of Oak, Proceedings of the Seventh Annual Hardwood Symposium of the Hardwood Research Council, Cashier, North Carolina, 125 pp.

Johnson, R. L. and **R.M. Krinard.** 1976. Hardwood regeneration after seed tree cutting. USDA For. Serv. Res. Pap. SO-123, 9 pp.

Kruger, E.L. and **P.B. Reich.** 1989. Comparative growth and physiology of stem-pruned and unpruned northern red oak. Pp. 302, *In* Proceedings of the Seventh Central Hardwood Conference (G. Rink and C. A. Budelsky, eds.), USDA Gen. Tech. Rpt. NC-132, 313 p.

Kruger, E.L. and **P.B. Reich.** 1993a. Coppicing affects growth, root:shoot relations and ecophysiology of potted *Quercus rubra* seedlings. Physiol. Plant. 89: 751-760.

Kruger, E.L. and **P.B. Reich.** 1993b. Coppicing alters ecophysiology of *Quercus rubra* saplings in Wisconsin forest openings. Physiol. Plant. 89: 741-750.

Lockhart, B.R. 1992. Morphology, gas-exchange, and ^{14}C-photosynthate allocations patterns in advanced cherrybark oak reporduction. Unpublished Ph.D. dissertation. Mississippi State University, Mississippi State, MS, 192 pp.

Loftis, D.L. 1983. Regenerating southern Appalachian mixed hardwood stands with the shelterwood method. South. J. Appl. For. 17: 75-79.

Lorimer, C.G. 1989. The oak regeneration problem: new evidence on causes and possible solutions. Pp. 23-40, *In* Proceedings of the Seventeenth Annual Symposium of the Hardwood Research Council, Merrimac, WS, 211 pp.

Matsubara, R. and **S. Hiroki.** 1985. Ecological studies on the plants of Fagaceae. IV. Reserve materials in roots and growth till five years old in *Quercus variabillis* Blume. Jap. J. Ecol. 35: 329-336.

McGee, C.E. 1986. Loss of *Quercus* spp. dominance in an undisturbed old-growth forest. J. Elisha Mitchell Sci. Soc. 102: 10-15.

McGraw, J.B., K.W. Gottschalk, M.C. Vavrek and **A.L.**

Chester. 1990. Interactive effects of resource availabilities and defoliation on photosynthesis, growth and mortality of red oak seedlings. Tree Phys. 7: 247-254.

Putnam, J.A., G.M. Furnival and **J.S. McKnight.** 1960. Management and inventory of southern hardwoods. USDA For. Serv. Agric. Hdbk. No. 181, 102 pp.

SAS. 1985. SAS/STAT guide for personal computers, version 6. SAS Institute, Inc., Cary, NC, 378 pp.

Satoh, M., P.E. Kriedemann and **B.R. Loveys.** 1977. Changes in photosynthetic activity and related processes following decapitation in mulberry trees. Physiol. Plant. 41: 203-210.

Tschaplinski, T.J. and **T.J. Blake.** Photosynthetic reinvigoration of leaves following shoot decapitation and accelerated growth of coppice shoots. Physiol. Plant. 75: 157-165.

USDA. 1990. Silvics of North America. Volume 2. Hardwoods. R.M. Burns and B.H. Honkala (tech. coord.). USDA For. Serv. Agriculture Handbook 654, 877 pp.

Watt, R.F. 1979. The need for adequate advance regeneration in oak stands. Pp. 11-17, *In* Proceedings on Regenerating Oaks in Upland Hardwood Forests (H. A. Holt and B. C. Fischer, eds.), Purdue University, 132 pp.

Concrete Beam Design Optimization with Genetic Algorithms

S. Malasri, D.A. Halijan and M.L. Keough
Department of Civil Engineering
Christian Brothers University
Memphis, TN 38104

Abstract

This paper demonstrates an application of the natural selection process to the design of structural members. Reinforced concrete beam design is used as the example to show how various chromosomes representing a design solution can be formulated. Fitter chromosomes (or better solutions) have a better chance of being selected for cross over; this in turn creates better generations. Random mutation is used to enhance the diversity of the population. The evolution progresses through several generations, and the best solution is then used in the design. The method gives reasonable results, but sometimes a local (as opposed to the global) optimized solution is obtained.

Introduction

Structural engineers traditionally design structural elements based on a trial-and-error process. An educated guess is made for a trial size of the member, then the performance is checked. Adjustments are then made for the next trial. An experienced designer normally starts with a reasonable trial size which a good design is obtained after a few iterations. For a typical new designer, this process can become tedious.

In recent years, genetic algorithms (GA) have been used in various optimization problems (Michalewicz, 1992). Structural design is another form of an optimization problem, in which the designer looks for the optimal solution (or a near-optimal solution) under a set of constraints. This paper demonstrates that GA can be applied to structural design problems by using the design of a reinforced concrete beam as an example.

Materials and Methods

The evolution process starts with a randomly created first generation. A generation consists of a constant population size, in which an individual in the population is represented by a chromosome. Each chromosome, consisting of genes, represents a design solution. A fitness value is then evaluated for each chromosome. Fitter chromosomes are assigned greater probabilities to be selected as parents for the next generation. Some of these selected chromosomes exchange genes with others during the crossover stage. Some genes are also randomly mutated. The process repeats through several generations. The fittest chromosome is then used as the design solution. The following sections will describe the details of this process in the context of reinforced concrete beam design.

Chromosome Formulation.--In designing a rectangular reinforced concrete beam for bending strength, the design solution consists of the section dimensions (width and effective depth) and the steel area, as shown in Fig. 1(a) where "b" is the section width, "d" is the section effective depth (the distance from the extreme compression fiber to the centroid of the tension steel), and "A_s" is the area of reinforcing steel.

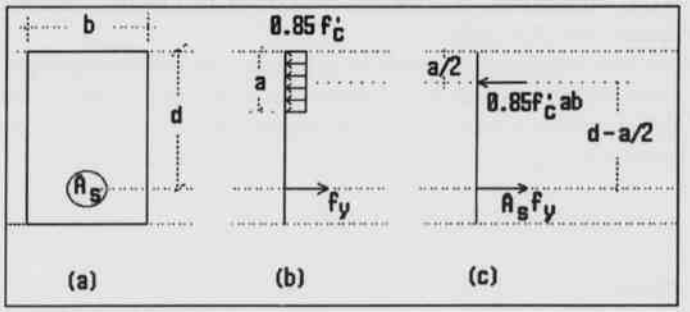

Fig. 1. Reinforced Concrete Beam: (a) Dimensions, (b) Stresses, and (c) Forces.

Thus, a chromosome must consist of three sets of genes representing these three quantities. In this particular implementation, each of these sets is represented by 12 binary digits, which gives the maximum decimal number of 4095. This maximum number is then divided by 100, so each parameter is in the range of 0 to 40.95. This range covers most of the practical problems. Fig. 2 shows a chromosome with its genes and the parameter range.

The First Generation.--Population in the first generation is created using random numbers. To avoid starting the sequence of random numbers at the same location

every time the program is executed, the current minute from the computer time clock is used as the seed value for the random number generator. If "r" is the random number generated for a gene, the value of the j-th gene of the i-th chromosome ($gene_{ij}$) is determined based on the following rule:

If $r < 0.5$ then $gene_{ij} = 0$, otherwise $gene_{ij} = 1$,
where $0 <= r <= 1$

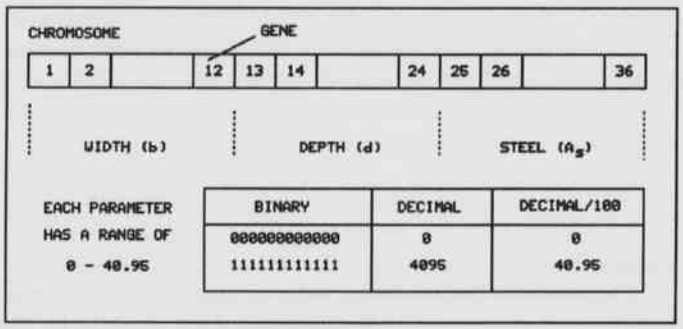

Fig. 2. Chromosome, genes and parameter range.

Fitness Evaluation.--Once the population in a generation is defined, the fitness of each chromosome can be evaluated. For the reinforced concrete beam problem, the fitness is determined based on its bending strenth (M_d), the section proportion (width/depth ratio), and the steel ratio ($A_s/(bd)$).

The bending strength is given by the following equation which was derived from engineering mechanics (Nawy, 1990) based on the stress and force diagrams shown in Fig. 1 (b) and (c).

$$M_d = (0.9)(A_s f_y)(d-a/2)$$

where

f_y = yield strength of reinforcing steel
a = $(A_s f_y) / (0.85 f'_c b)$
and f'_c = concrete strength at 28 days

This M_d is then compared with the required moment (M_u) which is specified as part of the input data. If M_d is greater than or equal to M_u, then the section is acceptable; otherwise, the section is rejected.

There are different section proportions that provide the desired strength. When "b" is too large compared with "d", the section is not economical. On the other hand, when "b" is too small compared with "d", the section is too slender and lateral buckling can occur. For a practical design, many designers keep the width/depth ratio around 0.5.

There are several combinations of section dimensions and steel reinforcement that provide sufficient bending strength. Larger sections require less steel, while smaller sections require more steel. There are minimum and maximum limits on the steel reinforcement set by the American Concrete Institute (American Concrete Institute, 1989) to avoid the sudden failure of concrete beams. Steel ratio is used in the comparison with these limits, as shown below:

$$200/f_y <= A_s/(bd) <= 0.75(0.85)\, B_1 f'_c(87000) / (f_y(87000+f_y))$$

where

$$B_1 = 0.85 - (f'_c - 4000)/1000$$

and $0.65 <= B_1 <= 0.85$

The fitness of a chromosome is then determined from the following rules:

1. The smaller the difference of M_d and M_u, the higher the fitness. When M_d is less than M_u, a penalty is applied.
2. The closer the b/d ratio is to 0.5, the higher the fitness.
3. When the steel ratio exceeds the maximum or minimum limits, a penalty is applied.

Based on these general rules, the fitness is determined by:

$$\text{Fitness} = 10^6 / (|M_d - M_u|)/(|0.5 - b/d|)/p_1/p_2$$

where

$|\ |$ = Absolute value
p_1 = Penalty factor for bending capacity
If $M_d >= M_u$, then $p_1=1$, otherwise $p_1=2$ (for $M_d < M_u$)
p_2 = Penalty factor for steel reinforcement If the steel ratio is within the minimum and maximum limits, $p_2=1$, otherwise $p_2=10$
10^6 = Scaling factor to make sure that the fitness value is not too small

Population Selection.--Once the fitness for each chromosome has been evaluated, they are selected according to a probability weighing scheme as an imaginary spinner. The fitter chromosomes occupy larger areas on the spinner. In this implementation, the relative probability is used to represent these areas on the spinner. Let p_i be the probability of the i-th chromosome. Thus, p_i can be computed from the following equation:

$$p_i = \text{Fitness}_i / \text{Fitness}_{gen},$$

where

Fitness_i = Fitness of the i-th chromosome,
and Fitness_{gen} = Summation of all fitnesses of the generation.

Let n be the number of chromosomes in a generation (population size). The spinner is spun "n" times, during which the new population is selected. The i-th chromosome is selected from a spin if the random number, r, satisfies the following condition:

$$(p_1+p_2+\ldots p_{i-1}) < r <= (p_1+p_2+\ldots p_i)$$

Cross Over.--After the spinner is spun and a new pool of chromosomes is selected, a number of chromosomes (based on the probability of crossover specified by the user) is selected for cross over. A cross over location is randomly determined. The two randomly selected chromosomes exchange their genes from this location to the rest of the chromosome. The two new chromosomes (offspring) are then used to replace the original two parents.

If the two parent chromosomes, each with 15 genes, are:

1 1 1 0 0 1 0 1 0 1 0 0 1 1 0,

and 1 0 0 1 0 1 1 0 0 1 0 1 0 0 0,

and the crossover location is right after the 6th gene, the two offsprings, which replace the two parents become:

1 1 1 0 0 1 1 0 0 1 0 1 0 0 0,

and 1 0 0 1 0 1 0 1 0 1 0 0 1 1 0.

Mutation.--Mutation is the process in which some genes change their genetic codes. In this implementation, mutation causes a gene to change its value from 0 to 1, or vice versa. After several generations, it is possible that a solution which is superior to the others but not really acceptable could take control of the entire population by spreading its genetic codes to others. A better solution would then become impossible. Mutation injects diversity to the population and often helps to move the evolution out from a local optimum situation.

Results and Discussion

As an example, a beam is to be designed for a bending moment (M_u) of 2,000,000 lb-in (226 kN-m) using the concrete strength (f'_c) of 4,000 psi (27.6 MPa) and the steel yield strength (f_y) of 60,000 psi (414 Mpa), as shown in Fig. 3.

```
Rectangular Beam Designer - (c) 1994 by S. Malasri
Concrete Strength - f'c (psi)     : ? 4000
Steel Yield Strength - fy (psi)   : ? 60000
Required Moment - Mu (in-lb)      : ? 2000000

Press any key to continue
```

Fig. 3. Input screen.

Other input parameters including the population size, the crossover probability, the mutation probability, and the number of generations are shown in Fig. 4. After 20 generations, a 11.96" by 30.29" section is obtained with the moment capacity (M_d) of 2,013,032 in-lb (which is very close to the required M_u). The steel ratio (Rho) of 0.0035 is also within the minimum steel ratio of 0.0033 and the maximum steel ratio of 0.0214. The width/depth ratio is 0.39 which is not too far from the desired 0.5. This, in fact, is a good design.

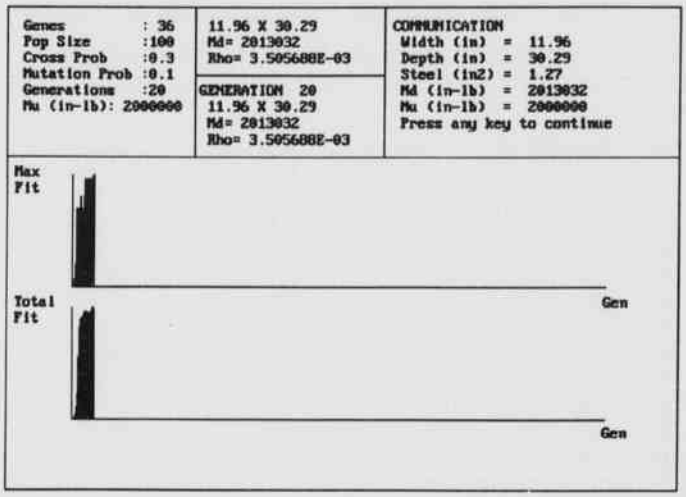

Fig. 4. Screen Showing the Evolution Process and Results.

Ten consecutive runs were made using different values of population size, crossover and mutation probabilities, and number of generations. They are summarized in Table 1. Most of the runs give good designs, except for the following:

1) Run number 3 has the steel ratio of 0.0012 which is lower than the minimum of 0.0033 allowed by the American Concrete Institute Code. The design engineer would reject this design.

2) Run number 6 has the steel ratio of 0.0248 which is greater than the maximum of 0.0214. This is not too bad, since theoretically, the maximum steel ratio in this case can go up to 0.0285. However, a conservative designer would reject this design.

3) Run numbers 7 and 9 are unnecessarily large, since they give the bending capacity of over 3,000,000 in-lb as compared to the required moment of 2,000,000 in-lb. This solution is safe but uneconomical.

Out of these 10 runs, six give acceptable solutions, two give safe but uneconomical solutions, one gives a working solution with less safety margin, and one gives an undesirable solution. Three of the four runs that have problems (run numbers 3, 7, and 9) use the same population size of 50. This population size probably does not provide

enough diversity. By increasing the mutation probability from 0.1 to 0.2 as in run number 10, an acceptable solution is obtained. Table 2 shows the evolution process that took place in run number 10. The solution starts from a very large section in the first generation that gives almost six times the desired bending capacity to an acceptable solution after 9 generations. After the only minor changes occur until the 51st generation. No better solution was found from the 51st generation to the 100th generation.

Table 1. Various Runs for the Same Design Problems.

Input*:

No.	Population Size	Crossover Probability	Mutation Probability	Number of Generations
1	150	0.3	0.1	20
2	100	0.3	0.1	20
3	50	0.3	0.1	20
4	100	0.3	0.3	20
5	100	0.3	0.1	20
6	100	0.3	0.1	20
7	50	0.3	0.1	20
8	150	0.3	0.1	20
9	50	0.3	0.1	40
10	50	0.3	0.2	100

* Other input data is shown in Fig. 3.

Output:

No.	Section b x d	b/d	M_d in-lb	Steel Ratio**	A_s in^2
1	8.63" x 18.02"	0.48	2,066,671	0.0159	2.47
2	10.83" x 19.90"	0.54	2,071,534	0.0098	2.11
3	18.98" x 40.94"	0.46	2,034,294	0.0012	0.93
4	11.28" x 13.93"	0.81	2,059,934	0.0214	3.38
5***	11.96" x 30.29"	0.39	2,013,032	0.0035	1.27
6	8.31" x 15.35"	0.54	2,051,439	0.0248	3.17
7	13.16" x 26.18"	0.50	3,479,880	0.0077	2.64
8	12.06" x 23.05"	0.52	2,046,162	0.0062	1.74
9	13.61" x 27.65"	0.49	3,789,192	0.0072	2.71
10	8.24" x 17.93"	0.46	2,099,687	0.0173	2.56

** Minimum Steel Ratio = 0.0033, Maximum Steel Ratio = 0.0214
*** Also shown in Fig. 4.

Table 2. Evolving from an Initial Random Solution to an Acceptable Solution.

Generation	Section	Md (in-lb)	Steel Ratio
1	21.75" x 38.75"	11,473,060	0.0069
2	11.99" x 16.35"	3,372,077	0.0250
3	8.22" x 14.29"	674,143	0.0080
4	21.75" x 38.77"	1,948,608	0.0011
6	14.35" x 18.09"	2,307,335	0.0100
8	8.22" x 14.29"	1,609,766	0.0220
9	7.95" x 18.09"	2,114,676	0.0179
11	8.23" x 18.09"	2,128,144	0.0173
12	8.27" x 18.09"	2,123,180	0.0171
24	7.95" x 17.93"	2,092,471	0.0180
25	7.99" x 17.93"	2,087,830	0.0179
51	8.24" x 17.93"	2,099,687	0.0173

Conclusion

This paper demonstrates that it is possible to automate the design process using the evolution process as seen in the reinforced concrete beam design example. The cumulative selection (as opposed to pure random selection) is a very powerful mechanism in evolution. As shown in the example, acceptable solutions are obtained quickly (within 20 generations). In this problem, the goal is to optimize the bending capacity with the three constraints: M_d is greater or equal to M_u, section proportion is around 0.5, and steel ratio should lie within the acceptable range. For a more complex problem with more constraints, more generations may be needed.

To a structural engineer, the design of a reinforced concrete beam is a simple problem and many design aids are available. But for other more complex problems where design aids are not available and a resonable trial section is hard to guess, this evolution approach becomes very useful. The current work includes the design of structural steel columns. This problem has more complex constraints. For example, steel sections come in standard sizes, a data base of the available standard section must be checked. This puts severe restrictions to the corss over and mutation mechanisms.

Literature Cited

American Concrete Institute. 1989. Building code requirements for reinforced concrete and

commentary. American concrete institute, Detroit, 353 pp.

Michalewicz, Z. 1992. Genetic algorithms + Data structures = evolution programs. Springer-Verlag, New York, 259 pp.

Nawy, E.G. 1990. Reinforced concrete a fundamental approach, 2nd edition. Prentice Hall, Englewood Cliffs, 734 pp.

Visualizing Electrostatic Phenomena Using Mathematica

Eric Mayes
Department of Computer Science, Mathematics and Physics
Arkansas State University
State University, AR 72467

Abstract

A set of packages for visualizing electrostatic phenomena was developed using *Mathematica* as a programming language. These packages allow users to plot potential fields, equipotential lines, 2-D and 3-D vector fields in order to gain a visual understanding of electrostatic charges. They would be useful in accompanying undergraduate physics labs pertaining to electrostatics, as they would enable students to connect experiment with mathematics through open-ended visual exploration.

Introduction

Mathematica (Wolfram, 1991) is a symbolic mathematics computer program that was first released in 1988. It can perform symbolic calculations, produce beautiful graphics, and give very accurate results limited only by the system that it is run on. Its most powerful feature, though, is that it is also a programming language. The purpose of this project was to visualize electrostatic phenomena and *Mathematica's* easily utilized, yet powerful, graphics abilities made it a perfect choice. The project is open-ended, in that others can easily create new change distributions and view them.

Theory

To produce the images of the electrostatic potentials and the electric fields, explicitly forms of the electric field and potential were used (Wangsness, 1986). The electric field is give by:

$$\mathbf{E}(\mathbf{r}) = \sum_{i=1}^{N} \frac{q_i \, \hat{\mathbf{R}}_i}{4\pi\epsilon_0 \, \mathbf{R}_i^2}$$

or more explicitly by:

$$\mathbf{E}(\mathbf{r}) = \sum_{i=1}^{N} \frac{q_i \left[(x-x_i)\hat{\mathbf{x}} + (y-y_i)\hat{\mathbf{y}} + (z-z_i)\hat{\mathbf{z}}\right]}{4\pi\epsilon_0 \left[(x-x_i)^2 + (y-y_i)^2 + (z-z_i)^2\right]^{\frac{3}{2}}}$$

Similarly the scalar potential is given explicitly by:

$$\phi(\mathbf{r}) = \sum_{i=1}^{N} \frac{q_i}{4\pi\epsilon_0 \left[(x-x_i)^2 + (y-y_i)^2 + (z-z_i)^2\right]^{\frac{1}{2}}}$$

These forms of the equations are easily manipulated using *Mathematica's* symbolic processing. A "Do Loop" adds up the contributions from each source point. For the electric field, a vector field is created; and for the electrostatic potential, a scalar field is created. These fields, through further manipulation, can be displayed on the screen or output in several forms, including printing to Post Script based laser printers.

Electrostatics Package

The first package (Listing 1), named "ElectroStatics," is loaded into *Mathematica Version 2.0* as:

```
In [1]:=<<ElectroStatics
```

There are four basic commands in this package. Two prompt the user for the charge distribution, and the other two accept list data types. The first command is "MakePField." This command is executed at the prompt in the form:

```
In[2]:=MakePField[N, {x, xmin, xmax}, {y, ymin, ymax},
(other opts)]
```

where "N" is the number of charger's in the distribution, "xmin, xmax, ymin, and ymax" are the bounds on the graph to be created and "other opts" specify other standard *Mathematica* graphics options. This command will return a 3-D surface. The Z-axis of the surface represents the magnitude of the electrostatic potential. Positive Z-axis values represent positive potentials, as negative values represent negative potentials. Note that *Mathematica* will chop off the tops and bottoms of charge's potentials as they diverge at the charge's locations. As an example:

```
In[2]:=MakePField[2, {x, -1, 2}, {y, -1, 2}, PlotPoints -> 40]
```

will prompt the user with:

```
Charge #1
-----------------
Charge: ?
```

The user can then enter the magnitude. The magnitude is entered in electrostatic units instead of Coulombs to keep the calculations simpler and faster. The user also enters the position of each charge up to "N" charges.

The second command is "MakeEField." This command takes the same form as the first, only it returns a plot of the electric field instead of the potential.

The third and fourth commands perform the same tasks as the first two, only they do not prompt the user for the magnitude and position. They expect to receive data of this form:

```
{charge, x coord, y coord, ...chargeN, xN coord, yN coord, N}
```

As an example:

```
In[3]:= PlotPField[{-1,1,1,1,-1,1,2}, {x,-2,2}, {y,-2,2}, PlotPoints -> 40]
```

These two commands were made so that the user could graph a function that would specify a specific charge distribution.

Figures 1a and 1b were created with the MakePField command, with N = 2. Figures 2a and 2b were created by displaying the result of 1a and 1b as contour plots using the standard *Mathematica* command:

```
Show [ContourGraphics["1a or 1b"], ContourShading -> False]
```

These plots are the equipotential lines for the charge distributions. Figures 3a and 3b were created for the same charge distribution with the MakeEField command. Figures 4a and 4b are combinations of 2a, 2b and 3a, 3b showing the electric field lines perpendicular to the equipotential lines. The third and fourth list input commands allow the user to display charge configurations generated by a function, rather then entering each charge individually.

As one way to utilize these commands, we can introduce a function like this:

```
RingOCharge[{x0_, y0_}, radius_, points_] :=
  Block[{i, theta, charges = {}},
    Do[AppendTo[charges,1];
    AppendTo[charges, (radius*Cos[theta] + x0)];
    AppendTo[charges, (radius*Sin[theta] +y0)];
    {theta, 0, 2*Pi, (2*Pi/points)}];
    AppendTo[charges, points]; charges]
```

It should be noted that the RingOCharge function sets the magnitude of each charge to 1. This function, when called with x0 and y0 being the center, will create a *Mathematica* list representing a ring of radius "radius" and approximated by "points" number of charges.

Figure 5 uses the third function, PlotPField with a list representing a ring of radius 3 centered at {0,0} approximated by 20 points. Figure 6 uses the fourth function, PlotEField with the same list.

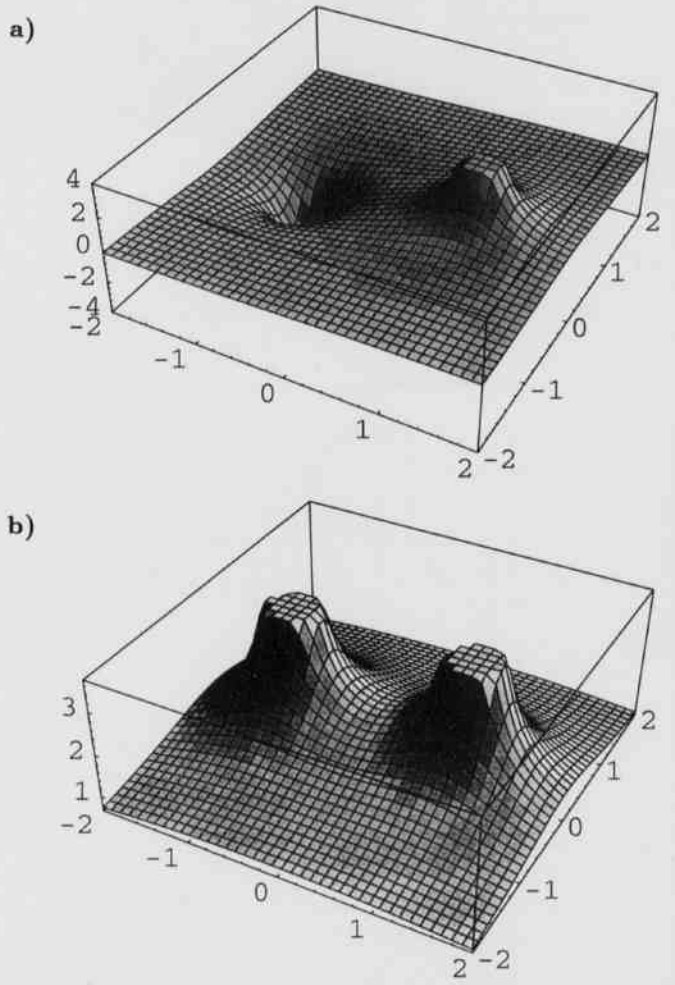

Fig. 1. a) Potential Energy Field for a Dipole [Inputs -1 at {-1,0} and 1 at {1,0}], b) Potential Energy Field for a Pair of Like Charges.

Electrostatics3D Package

The second package, "ElectroStatics3D," is loaded in the same manner:

```
In[1]:=<<ElectroStatics3D
```

There are only two commands in this package, one for

user input and the other for list input. Both commands create a 3-D plot of the electric field surrounding a set of charges. The first command, MakeEField3D, is called in almost the same manner as the MakeEField command, with the addition of a Z-coordinate:

In[2]:=MakeEFields3D[N, {x, xmin, xmax}, {y, ymin, ymax}, {z, zmin, zmax}, (other opts)]

Figure 7 is an example of this command with four co-planar charges.

Figure 8 demonstrates the second command in this package along with a slightly modified RingOCharge function in which the Z-coordinate was kept constant. This graph was produced from a list and the PlotEField3D command.

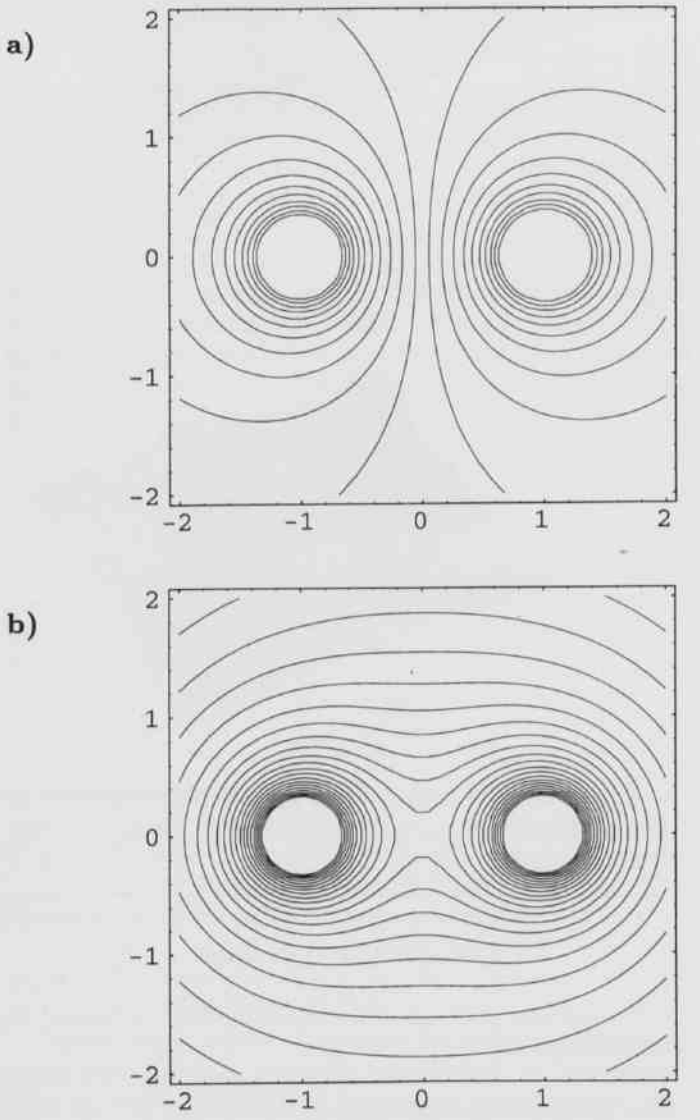

Fig. 2. a) Equipotential lines for a dipole, b) Equipotential lines for a pair of like charges.

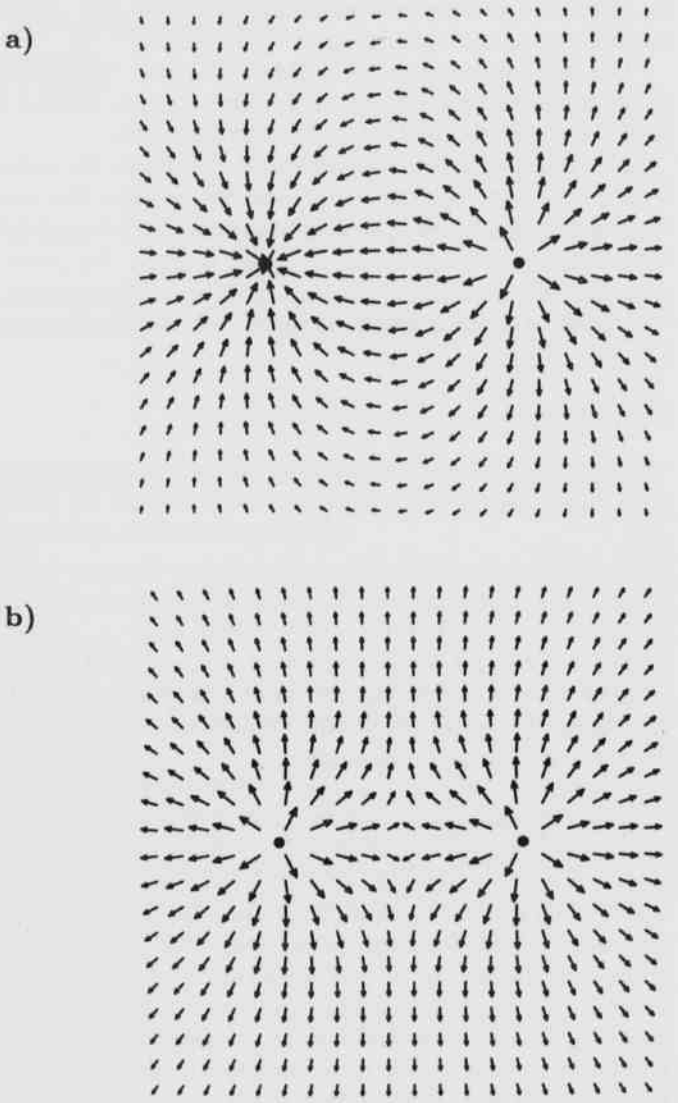

Fig. 3. a) Electric field vectors for a dipole, b) Electric field vectors for a pair of like charges.

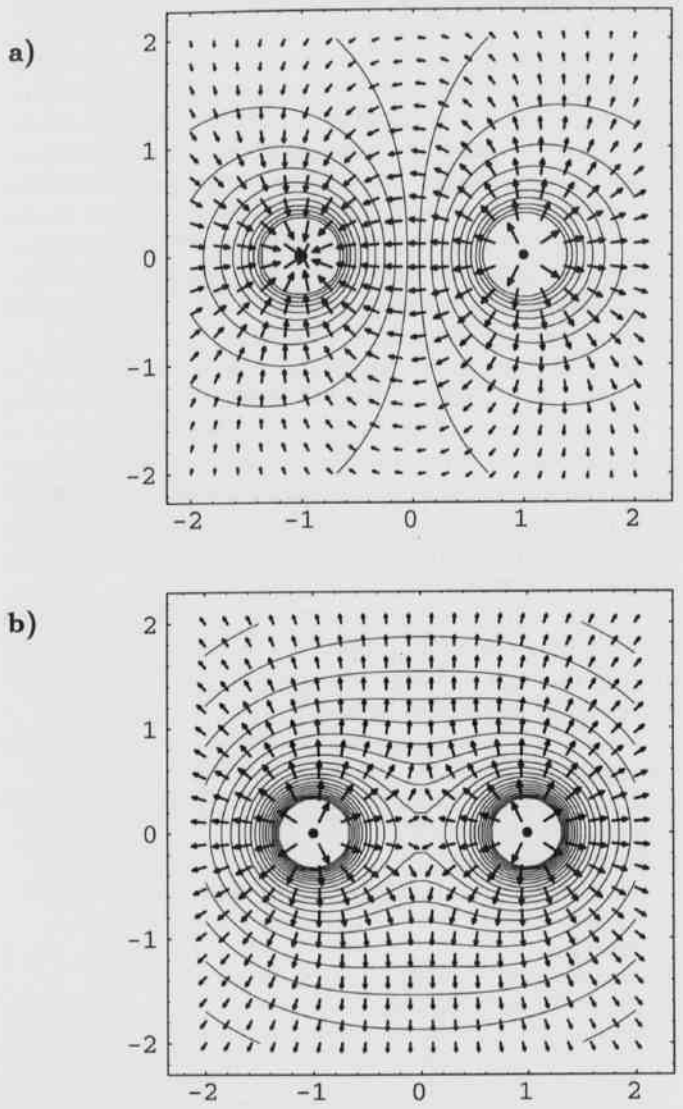

Fig. 4. Combination of equipotential lines and electric field vectors for two systems of charge. a) Dipole, b) Pair of like charges.

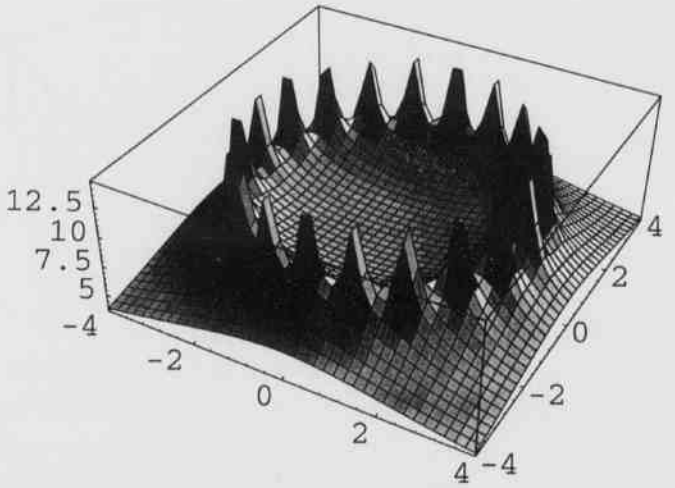

Fig. 5. Potential energy field for a ring of charge approximated by 20 point charges.

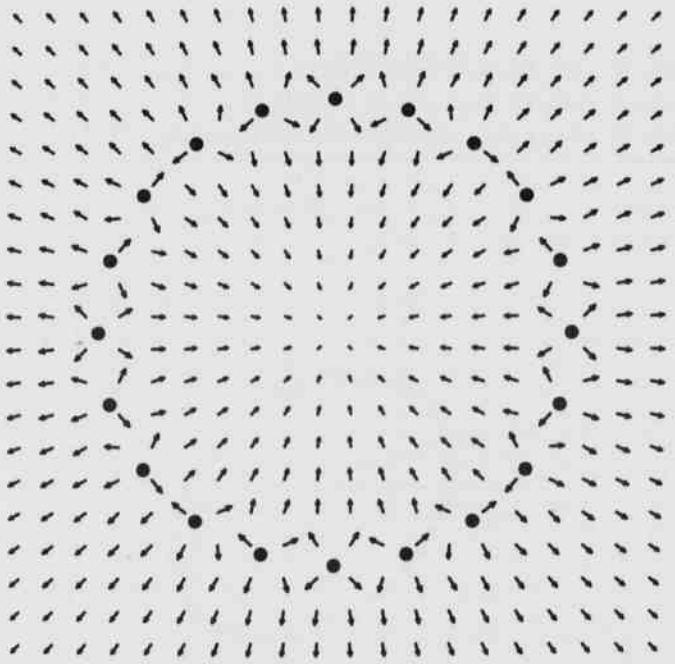

Fig. 6. Electric field vectors for a ring of charge approximated by 20 point charges.

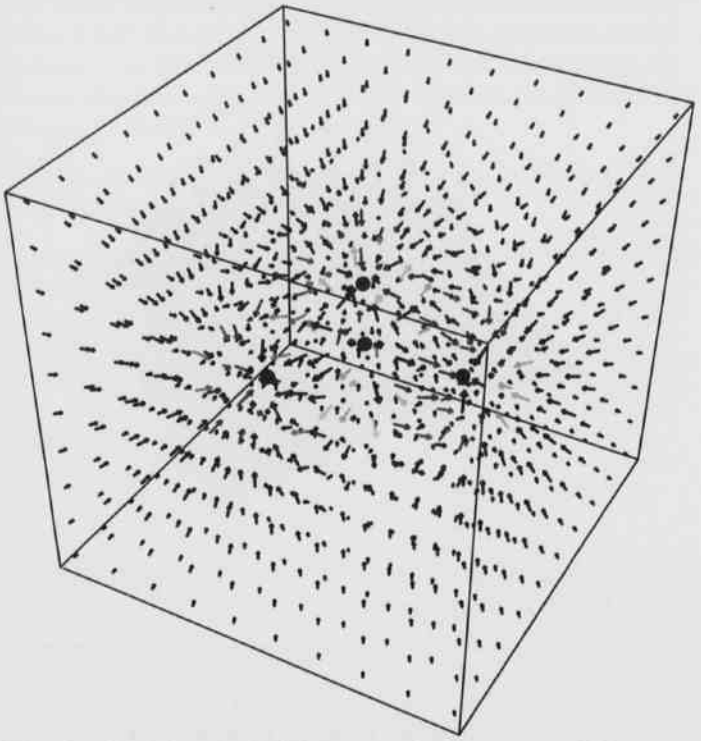

Fig. 7. 3-D Electric field vectors for a system of four coplanar charges [inputs 2 at {0,0,0}, -1 at {0,1,0}, {-0.866, -0.5, 0} where the -1 charges are separated by 120°].

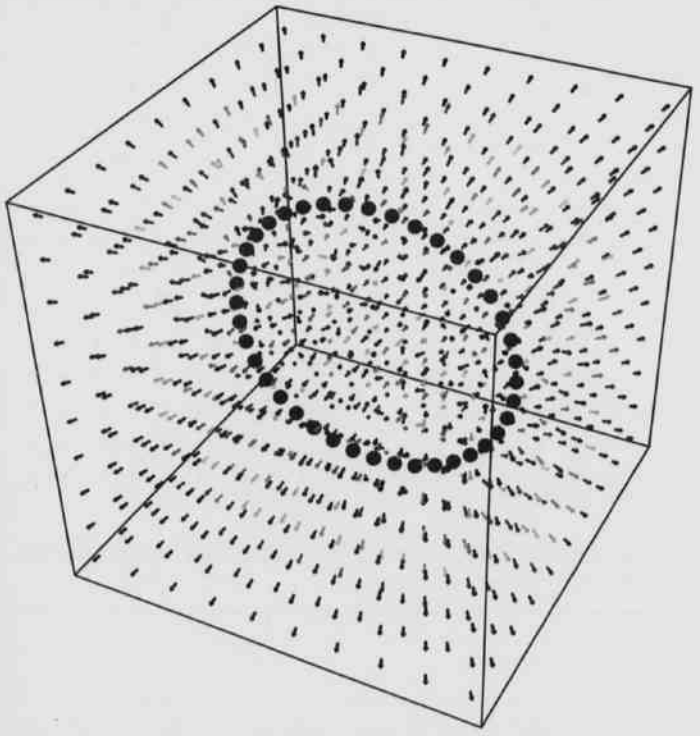

Fig. 8. 3-D electric field vectors for a ring of charge in the X-Z plane approximated by 40 point charges.

Discussion

These packages (See Listing 1 for ElectroStatics and Listing 2 for ElectroStatics3D) can be of educational value if combined with undergraduate physics labs pertaining to electrostatics. For labs that require the experimental mapping of equipotential lines, students could also model the lines on a computer using *Mathematica* and compare results. The packages may make learning electrostatics fun: making interesting charge distributions just to see what happens can be entertaining. *Programming in Mathematica* (Maeder, 1990) and *Mathematica, a System for Doing Mathematics by Computer* (Wolfram, 1991) are good references to help with such a lab.

Modeling complex distributions is time intensive. A Sun SPARC-IPC, with a SPARC RISC processor running at 15.8 MIPS and 1.7 MFLOPS, took about 35 minutes to complete Fig. 8. Unfortunately, *Mathematica* packages are not stand-alone. *Mathematica* has its own kernel which must be present in order to run the packages; so economic concerns could limit the packages' use, as *Mathematica* is rather expensive.

Future work on this project will utilize *Mathematica 2.0's* ability to animate graphics. Hopefully a test charge moving through a charge distribution can be modeled in a reasonable amount of time.

Listing 1. The Code for the "ElectroStatics" Package.

```
(*:Version: Mathematica 2.0*)
(*:Name: ElectroStatics' *)
(*:Title: Electric Potential and Field Plots for Static Charges *)
(*: Author:
    Eric Mayes
    Arkansas State University
    emayes@quapaw.astate.edu *)
(*:Summary: This package allows the user to input a set of static
    charges on the x-y plane. The results, depending on the selected
    function, will display either a graph of the magnitude of the electric
    potential over a region; or it will display a 2-D vector plot of the
    electric field. *)
BeginPackage["ElectroStatics'", "Graphics'PlotField'"]

MakePField::usage = "MakePField[N, {x,xmin,xmax}, {y,ymin,ymax},
    (other opts)] returns a 3-D graph of the potential field of a set of N
    charges specified by the user.";

MakeEField::usage = "MakeEField[N, {x,xmin,xmax}, {y,ymin,ymax},
    (other opts)] returns a graph of the electric field of a set of N
    charges specified by the user.";

PlotPField::usage = "PlotPField[list, {x,xmin,xmax}, {y,ymin,ymax},
    (other opts)] returns a 3-D graph of the potential field of a list of N
    charges that conform to the format {charge1,x1,y1...,chargeN,xN,yN
    ,N}.";

PlotEField::usage = "PlotEField[list, {x,xmin,xmax}, {y,ymin,ymax},
    (other opts)] returns a graph of the electric field of a list of N
    charges that conform to the format
```

```
    {charge1,x1,y1...,chargeN,xN,yN,N}.";

Begin["`Private`"]

MakePField[num_, {x0_, x1_, x2_}, {y0_, y1_, y2_}, opts___] :=
    Block[{i, chargelist = {}, potential = 0},
     Do[
        Print [" "];
        Print["Charge #",ToString[i]];
        Print["———"];
        answer = Input["Charge: "];
          AppendTo[chargelist,answer];
        answer = Input["X Coord: "];
          AppendTo[chargelist,answer];
        answer = Input["Y Coord: "];
          AppendTo[chargelist,answer],
    {i,num}];
    AppendTo[chargelist,num];
    Do[
        potential = potential + (Part[chargelist,i]/
        ((x0 - Part[chargelist, (i+1)])^2 +
          (y0 - Part[chargelist, (i+2)])^2)^.5),
    {i,1,(Last[chargelist]*3),3}];
    Plot3D[potential, {x0, x1, x2}, {y0, y1, y2}, opts]]

MakeEField[num_, {x0_, x1_, x2_}, {y0_, y1_, y2_}, opts___] :=
    Block[{i, vectorplot, dotsplot, chargelist = {}, dots = {}, field = 0},
     Do[
        Print[" "];
        Print["Charge #",ToString[i]];
        Print ["———"];
        answer = Input["Charge: "];
          AppendTo[chargelist, answer];
        answer = Input["X Coord: "];
          AppendTo[chargelist, answer];
        answer = Input["Y Coord: "];
          AppendTo[chargelist, answer],
    {i,num}];
    AppendTo[chargelist, num};
    Do[(field = field + ((Part[chargelist,i]*
        ({(x0 - Part[chargelist, (i+1)]),
          (y0 - Part[chargelist, (i+2)])}))/
        ((x0 - (Part[chargelist, (i+1)]+.0001))^2 +

    (* .0001 Added To Protect From Division By Zero *)

        (y0 - (Part[chargelist, (i+2)]+.0001))^2)^(3/2))),
    {i,1,(List[chargelist]*3),3}];
    vectorplot = PlotVectorField[field, {x0, x1, x2}, {y0, y1, y2}, opts,
    ScaleFunction->(Log[Log[Log[Log[Log[Log[#+1]+1]+1] +1]+1]+1]&),
    ScaleFactor -> .2, DisplayFunction -> Identity];

    Do[AppendTo[dots,Point[{Part[chargelist, (i+1)], Part [chargelist,
        (i+2)]}]], {i,1,(Last[chargelist]*3),3}];
    dotsplot = Graphics[{PointSize[0.02], dots}, Display Function->
        Identity];
    Show[vectorplot,dotsplot,DisplayFunction -> $Display Function]]

PlotPField[chargelist_, {x0_, x1_, x2_}, {y0_, y1_, y2_}, opts___] :=
    Block[{i, potential =0},
     Do[
        potential = potential + (Part[chargelist,i]/
        ((x0 - Part[chargelist,(i+1)]) ^2 +
         (y0 - Part[chargelist,(i+2)])^2)^.5),
    {i,1,(Last[chargelist]*3),3}];
    Plot3D[potential, {x0, x1, x2}, {y0, y1, y2}, opts]]

PlotEField[chargelist_, {x0_, x1_, x2_}, {y0_, y1_, y2_}, opts___] :=
    Block[{i, vectorplit, dotsplot, dots = {}, field = 0},
     Do[
        field = field + ((Part[chargelist,i]*
        ({(x0 - Part[chargelist, (i+1)]),
          (y0 - Part[chargelist, (i+2)])}))/
        ((x0 - (Part[chargelist,(i+1)]+.0001))^2 +
          (y0 - (Part[chargelist,(i+2)]+.0001))^2)^(3/2)),
    {i,1,(Last[chargelist]*3),3}];
    vectorplot = PlotVectorField[field, {x0, x1, x2}, {y0, y1, y2}, opts,
    ScaleFunction->(Log[Log[Log[Log[Log[Log[#+ 1]+1]+1]+1]+1]+1]&),
    ScaleFactor -> .2, DisplayFunction -> Identity];

    Do[AppendTo[dots,Point[{Part[chargelist, (i+1)], Part [chargelist,
        (i+2)]}]], {i,1,(Last[chargelist]*3),3}];
    dotsplot =Graphics[{PointSize[0.02], dots},DisplayFunction ->
        Identity];
    Show[vectorplot,dotsplot,DisplayFunction ->  $DisplayFunction]]

End [] (* ElectroStatics`Private` *)

Protect[MakePField, MakeEField, PlotPField, PlotEField]

EndPackage[] (* ElectroStatics` *)
```

Listing 2. The Code for the "ElectroStatics3D" Package.

```
(*:Version: Mathematica 2.0 *)

(*:Name: ElectroStatics3D` *)

(*:Title: 3-D Electric Field Plots for Static Charges *)

(*:Author:
    Eric Mayes
    Arkansas State University
    emayes@quapaw.astate.edu *)

(*:Summary: This packages allows the user to input a set of static
charges in 3-space. The result will be displayed in a 3-D vector field plot.
*)

BeginPackage["ElectroStatics3D`", "Graphics`PlotField3D`"]

MakeEField3D::usage="MakeEField3D[N, {x,xmin,xmax},{y,ymin,ymax},
    {z,zmin,zmax}, (other opts)] returns a 3-D graph of the electric
    field of a set of N charges specified by the user."

PlotEField3D::usage ="PlotEField3D[list, {x,xmin,xmax},{y,ymin,ymax},
    {z,zmin,zmax}, (other opts)] returns a 3-D graph of the electric
    field of a list of N charges that conform to the format
    {charge1,x1,y1,z1...,chargeN,xN,yN,zN,N}."

Begin["`Private`"]

MakeEField3D[num_, {x0_, x1_, x2_}, {y0_, y1_, y2_}, {z0_,  z1_, z2_},
        opts___] :=
    Block[{i, vectorplot, dotsplot, dots = {}, chargelist = {}, field = 0},
    Do[
        Print[" "];
        Print["Charge #",ToStrin[i]];
        Print["———"];
        answer = Input["Charge: "];
          AppendTo[chargelist,answer];
        answer = Input["X Coord: "];
          AppendTo[chargelist,answer];
        answer = Input["Y Coord: "];
          AppendTo[chargelist,answer];
        answer = Input["Z Coord: "];
          AppendTo[chargelist,answer],
```

```
    {i,num}];
    AppendTo[chargelist,num];
    Do[
        field = field + ((Part[chargelist,i]*
        ({(x0 - Part[chargelist, (i+1)]),
          (y0 - Part[chargelist, (i+2)]),
          (z0 - Part[chargelist, (i+3)])})/
        ((x0 - (Part[chargelist,(i+1)]+.0001))^2 +

        (*.0001 Added To Protect From Division By Zero *)

        (y0 - (Part[chargelist,(i+2)]+.0001))^2 +
        (z0 - (Part[chargelist,(i+3)]+.0001))^2)^(3/2)),
    {i,1,(Last[chargelist]*4),4}];
    vectorplot = PlotVectorField3D[field, {x0, x1, x2}, {y0, y1, y2},
    {z0, z1, z2}, opts, ScaleFunction -> (Log[Log[Log[Log[Log[Log[# +
     1]+1]+1]+1]+1]+1]&), ScaleFactor -> .2, DisplayFunction -> Identity];

    Do[AppendTo[dots,Point[{Part[chargelist,(i+1)],Part[chargelist, (i+2)],
        Part[chargelist, (i+3)]}]], {i,1,(Last[chargelist]*4),4}];
    dotsplot = Graphics3D[{PointSize[0.02], dots},DisplayFunction ->
        Identity];
    Show[vectorplot,dotsplot,DisplayFunction -> $DisplayFunction]]

PlotEField3D[chargelist_, {x0_, x1_, x2_}, {y0_, y1_, y2_}, {z0_, z1_, z2_},
        opts___] :=
    Block[{i, vectorplot, dotsplot, dots = {}, field = 0},
      Do[
        field = field + ((Part[chargelist,i]*
        ({(x0 - Part[chargelist, (i+1)]),
          (y0 - Part[chargelist, (i+2)]),
          (z0 - Part[chargelist, (i+3)])})/
        ((x0 - (Part[chargelist, (i+1)]+.0001))^2 +
         (y0 - (Part[chargelist,(i+2)]+.0001))^2 +
         (z0 - (Part[chargelist,(i+3)]+.0001))^2)^(3.2)),
    {i,1,(Last[chargelist]*4),4}];
    vectorplot = PlotVectorField3D[field, {x0, x1, x2}, {y0, y1, y2},
    {z0, z1, z2}, opts, ScaleFunction -> (Log[Log[Log[Log[Log[Log[# +
    1]+1]+1]+1]+1]+1]&), ScaleFactor -> .2, DisplayFunction -> Identify];

    Do[AppendTo[dots,Point[{Part[chargelist, (i+1)], Part[chargelist,
      (i+2)], Part[chargelist, (i+3)]}]], {i,1,(Last[chargelist]*4),4}];
    dotsplot = Graphics3D[{PointSize[0.02], dots},DisplayFunction ->
        Identity];
    Show[vectorplot,dotsplot,DisplayFunction -> $DisplayFunction]]

End [] (* ElectroStatics3D`Private` *)

Protect[MakeEField3D, PlotEField3D]

EndPackage[] (* ElectroStatics3D` *)
```

Acknowledgements

This work acknowledges Charles A. Hughes for his assistance and the Department of Computer Science, Mathematics, and Physics at Arkansas State University for the use of their facilities.

Literature Cited

Wangsness, R.K. 1986, Electromagnetic Fields, 2nd ed. John Wiley & Sons, Inc., New York, Pp. 51-82.

Maeder, R. 1990. Programming in Mathematica. Addison-Wesley, Redwood City, California.

Wolfram, S. 1991. Mathematica, a System for Doing Mathematics by Computer. Addison-Wesley, Redwood City, California.

Liver Lipids Profiles in Nude Mice Implanted Subcutaneously with Cells of Human Prostate Adenocarcinoma Grade IV

Lawrence M. Mwasi
Department of Biology
University of Arkansas at Pine Bluff
1200 N. University Drive
Pine Bluff, AR 71061

Abstract

Liver lipid changes in male BALB-c nude mice due to subcutaneously implanted human prostate metastatic grade IV adenocarcinoma was studied. The prostate cancer cells were cultured in F_{12} plus 7.5% horse serum and 25% fetal calf serum medium. When they reached confluence, some of these cells were fixed with glutaraldehyde and thoroughly washed with buffer then 4×10^7 cells were implanted into four mice. Four more mice were implanted with 4×10^6 viable, unfixed cells. Four uninjected mice served as controls. All the mice were sacrificed 18 days later. The total liver lipids (TLL) from each liver were extracted with chloroform:methanol and dried in separate vials under a stream of gaseous nitrogen. While being dried, the TLL of each liver sample were weighed intermittently until their weight remained constant. The weight of TLL in each vial was then divided by the wet weight of each corresponding extracted liver. This was done to normalize the liver lipids in terms of one gram of liver because livers of different wet weights were extracted. The TLL per gram of wet liver were similar in the control and livers of mice injected with viable cancerous cells and decreased in the livers of mice injected with glutaraldehyde-fixed cells. When the total lipids were fractionated into polar and non-polar lipids on silicic gels, entirely different changes were seen. The TLL of the mice injected with untreated viable cancer cells and those injected with glutaraldehyde-fixed cells were similar while the control liver lipids classes were significantly different. There was a decrease in the percentage of neutral lipids and an increase in the polar fractions in the two groups of mice injected with either cells. The growth of the viable injected prostate cells did not cause any unique lipid changes in these two lipid class profiles. However, the triglycerides and total cholesterol showed wide variations among the livers of mice injected with viable cancer cells. The ratio of the polar/neutral lipids did not differ between the mice injected with either cells. Thus, the present study does not support the accepted explanation that the rapidly growing cancer cells are mainly responsible for the lipid changes seen in animals implanted with other types of tumor cells.

Introduction

The idea that a growing tumor may influence metabolism in tissues remote from its site is a fascinating one since it implies the existence of a humoral agent that could possibly be intercepted to study and control tumor growth. Indeed, several investigators have obtained evidence that the turnover of liver lipids is profoundly changed in animals bearing a variety of tumors (Weber and Cantero, 1959; Stein et al., 1965; Stein et al., 1966; Wood, 1975; Ruggieri et al., 1976; Redgrave et al., 1984). These altered turnover rates are reflected in the composition of the liver lipids and may indeed reveal a major source of substrate and energy for tumor growth.

Stein and his co-workers (1965, 1966) considered that the adipose tissue may be the ultimate source of triglyceride fatty acids for this purpose, since it has been observed in many studies that this tissue is depleted during tumor growth (Wood et al., 1974). The consequent changes taking place in the liver may represent an intermediate transport mechanism by which the fatty acids are efficiently furnished to the neoplastic cells. These fatty acids could consist of the essential fatty acids necessary for membrane formation and cell growth as well as a general mixture of the usual 16-and 18- carbon acids for energy. Since fatty acids for these purposes may be derived from the diet, synthesized in other tissues, or released from stored trigylcerides, it has not been easy to predict in many cases, or to interpret the changes in the fatty acids themselves, particularly since some of the enzymes involved in fatty acids alteration are missing or have escaped control in the tumor (Chiappe et al., 1974). However, the changes in the lipids, which must be synthesized in the tissues themselves by known pathways, may be very revealing.

Nakazawa and Mead (1976) measured the alterations in liver lipids in female BALB-c nude mice bearing transplanted cells from a human ovarian adenocarcinoma and reported significant changes in the phospholipid:triglyceride (PL:TL) ratio brought about by increases in the

phospholipid fraction and decreases in the triglyceride fraction. This system was proposed as a model for studying similar changes seen in the liver lipids of human patients (Nakazawa and Yamagata, 1971). However, in these earlier experiments, the degree of tumor metastatic grade, as well as the cell numbers implanted in the mice were not characterized and quantified. Such lack of precise number of the implanted cells as well as varying degree of grades of the tumor metastasis level might have been the cause for the disparities seen in different studies done using freshly obtained human tissues as the source of cells to implant into mice.

In order to obviate some of the problems and gain further information on the mechanisms producing liver changes, the present study was done using an established clonal cell line derived from a human metastatic prostate grade IV adenocarcinoma. This permitted a more quantitative injection and, in addition, treatment of some of the cells by glutaraldehyde.

Materials and Methods

Chloroform, methanol, petroleum ether, and pentane were reagent grade and were distilled before use. Ethyl ether was used directly from a freshly opened can of reagent grade ether. Other reagents were also reagent grade. Standards for gas-liquid chromatography were obtained from NU-Chek Prep, Elysian, Minnesota and Applied Science Laboratory (State College, Pennsylvania).

Treatment of Animals.--Male BALB-c nude mice 19 weeks old were divided into three groups and treated as follows. Four control mice (group 1) were not injected. In group 2 four experimental mice were injected subcutaneously on the right side with 0.2 ml (4 by 10^6 cells) of cells from cell line PC_3, a human metastatic prostate grade IV carcinoma, cloned and cultured in F_{12} plus 7.5% horse serum and 25% fetal calf serum. Four mice, making group 3, were injected with the same type of cells but which had been fixed for one hour with 2.5% glutaraldehyde in 0.1 M sodium cacodylate pH 7.4 buffer and rinsed 20 hr. in 0.1 M sodium phosphate buffer, pH 7.4. The injected and the control mice were kept for 18 days before sacrifice by cervical dislocation. The livers were removed and frozen at -80°C until extraction.

Extraction and Analysis of Lipids.--Lipids were extracted from liver tissue with chloroform:methanol (2:1) and, after washing, the solvent was removed in a stream of nitrogen at less than 40°C. The total lipids in each sample were separated into non-polar and polar fractions by elusion from small silicic acid columns with chloroform and methanol, respectively.

Portions of neutral fractions were separated into components on thin-layer plates (silica gel GD. Merck, Darmstadt). The thin layer plates were developed using a mixture of solvents composed of ethyl ether (redistilled and collected between 60-70°C), petroleum ether, acetic acid (20:80:1), or chloroform. The developed plates were sprayed with cupric acetate-phosphoric acid reagent and charred in an oven at 140°C (Fewster et al., 1969). The relative proportions of the separated components were measured using a Kontes densitometer (K-495000 connected to K-495150 integrator), and quantified using comparison with standards spotted on the same plates.

Analysis of Component Fatty Acids.--Aliquots of lipid samples were converted into methyl esters by methanolysis, using 5% methanolic HCL. The methyl esters of the component fatty acids were separated and quantified on a Beckman gas chromatograph (6C-M) fitted with disc integrator and using a 6' x 3/8" column of siliac 10C. The chromatograph was operated at 185°C. Areas under the peaks were read from the integrator.

Table 1. Distribution of lipids in livers of control and injected mice.

	Treatment of Mice		
	Group 1 Uninjected Controls	Group 2 Viable Growing Cells Injected	Group 3 Glutaraldehyde Fixed Cells Injected
Total Liver Lipid[a]	23.2±0.16	23.2±0.04	19.7±0.05
Percent of Polar Lipids	70 ±4.4	78 ±2.3*	77 ±2.5*
Percent of Neutral Lipids	32 ±2.1	21 ±2.1*	22 ±1
Triglyceride[b]	69 ±2.9	71 ±12.5	65.4±4.4
Total Cholesterol	31 ±3.3	28 ±18.2	35 ±4.1
Ratio: Polar Lipid/Neutral Lipid	2.2±0.2	3.6±0.09*	3.5±0.26*
	(4) [c]	(4) [c]	(4) [c]

All statistical comparisons were done using student's test.

[a]Values are of mean ± S.D. of mg per g wet wt of livers.

[b]Triglyceride expressed as percent of neutral lipids.

[c]Number of mice in each group. The liver from each mouse was separately analyzed.

* Significantly different from controls at the 0.01 level.

Results

Distribution of Lipids.--The state of the injected cells did not change the total percentage of lipids profiles in the livers of mice (Table 1). However, there was a significantly higher proportion of polar lipid and a lower proportion of neutral lipid within the TLL in the mice injected with any of the cell preparations. This is reflected in a highly significant difference in the ratios of polar to neutral lipids between the controls and all treated groups.

Moreover, there were no significant differences in these values among the treated groups (Table 2).

Within the neutral lipid fractions, there was considerable variation in the proportions of triglycerides and total cholesterol as reflected in the standard deviations. This variability was also apparent in the distribution of free and esterified cholesterol. The meaning of these changes is not apparent. Among the fatty acids, there were no significant differences attributed to the treatment of the mice though the usual differences (Table 2) in neutral and polar lipids were seen.

Table 2. Distribution of major fatty acids in polar and neutral lipids of control and injected mice (mean of relative percentages ± SD)

A. *Polar Lipids*	16:0	16:1	18:0	18:1	18:2	20:4	22:6
Group 1 (4) Uninjected Control	22.8±4.6	1.03±0.7	18.6±1	11.6±0.95	20.6±5.01	17.2±0.24	4.8±0.81
Group 2 (4) Viable Cells Injected	27.9±4.5	0.25±1.0	12.0±7.8	14.9±4.04	18.4±6.02	18.8±1.82	4.0±1.75
Group 3 (4) Glutaraldehyde Fixed Cells Injected	25.3±3.7	0.2±0.02	21.1±0.07	12.3±1.3	16.0±1.05	20.4±1.35	3.3±2.25
B. *Neutral Lipids*							
Group 1 (4) Uninjected Control	30.9±2.88	2.03±1.25	3.08±0.43	39.4±4.57	16.88±2.13	1.2±0.78	0
Group 2 (4) Viable Growing Cell Injected	35.88±6.74	1.83±1.94	3.85±0.94	32.38±4.92	16.53±4.92	2.35±0.41	0
Group 3 (4) Glutaraldehyde Fixed Cell Injected	32.1±1.85	1.5±1.66	2.65±0.35	33.65±1.35	22.65±4.65	1.5±0.5	0

The number in parentheses is the number of mice receiving each treatment. Each liver was separately analyzed.

Discussion

The results of these experiments appear to confirm those of Nakazawa and Mead (1976) since there is an increase in the ratio of polar lipid to neutral lipid in mice injected with the neoplastic cells. They do not however, confirm the very large difference between control and experimental values shown in the prior study. Explanations for these differences are not difficult to suggest. First, whole tissue from an ovarian adenocarcinoma was injected in the earlier study, while known numbers of cells from an established line derived from a metastatic prostate adenocarcinoma were used in the present study with male mice. Second, two months elapsed between injection and sacrifice in the prior experiment, thus allowing for considerable cell proliferation. Third, male animals were used in the present study while females were used in the previous one. In the present study, only two weeks elapsed between injection and sacrifice with the hope that changes occurring before profound generalized metabolic changes occurred could be seen. Moreover, since numbers of cells were not known in the previous work, an attempt was made in the present study to compensate for the proliferation of the viable injected cells by injecting larger numbers of the non-growing cells. Whether for this or other reasons, no significant differences in total liver lipids were seen between the livers of mice injected with proliferating cells and uninjected controls. However, there was a significant decrease of total liver lipids in the livers of mice injected with non-proliferating cells. But, when the total liver lipids from each group were fractionated into polar and non-polar components and each component expressed as a percent of the total liver lipids for each experimental group, there was no significant difference between the percentages in the two groups injected with cells (Table 1). The observed changes, therefore, cannot be a result of rapid growth of the injected neoplastic cells, but must depend on some other unknown cause. Such a cause might be attributed to the reactions of the injected cells with the host animal immune response. The reaction may be to increase the availability to the foreign cells of fatty acids needed for growth and energy demands. In the present case however, only in one of the groups were the foreign cells able to utilize the fatty acids. With the possible exception of 18:1 and 16:1 (Table 2) the lack of significant change in the fatty acids of neutral and polar lipids may indicate that there was no selective use of theses as opposed to utilization of the entire complement of the lipid involved.

Kampschmidt and Upchurch (1966) have called attention to the fact that the site of tumor transplant in an animal may lead to variation in the results obtained. We do not know whether this is also true as far as lipids are concerned. Total cholesterol in the control mice was constant, whereas in the mice bearing cells, there were some fluctuations as reflected in the large standard deviations (Table 2) with most variations in the mice injected with viable cells. Failure to find a substantial decrease of triglycerides in the lipids of mice injected with viable cells does not seem to support the notion frequently cited that the decrease is due to the presence of a tumor (Stein et al., 1965; Stein et al., 1966). These animals did not show any gross pattern of lipid loss. It was not possible to tell the experimental from the control mice in this respect.

Literature Cited

Chiappe, L.E., M.E. DeTomas and **O. Mercuri.** 1974. In

vitro activity of -6 and -9 desaturases in hepatomas of different growth rates. Lipids 9: 489- 490.

Fewster, M.E., B.J. Burns and **J.F. Mead.** 1969. Quantitative densitometric thin-layer chromatography 43: 120-126.

Kampschmidt, R.F. and **H.F. Upchurch.** 1966. Some effects of tumor implantation site on tumor-host relations. Cancer Res. 26: 990-994.

Nakazawa, I. and **S. Yamagata.** 1971. Biochemical changes of lipid in biopsied livers of patients with neoplastic disease. Tohuku J. Exp. Med. 103: 129-139.

Nakazawa, I. and **J.F. Mead.** 1976. In vitro activity of fatty acyl desaturases of human cancerous and noncancerous tissue. Lipids 11: 79-82.

Redgrave. T.G., D.F. Devereux and **P.J. Decker.** 1984. Hyperlipidemia in tumor-bearing rats. Biochem. Biophys. Acta 795: 286-292.

Ruggieri, S., A. Fallani and **D. Tombaccini.** 1976. Effect of essential fatty acid deficiency on the lipid composition of the Yoshida ascites hepatoma (AH130) and the liver and blood plasma from host and normal rats. J. Lipid Res. 17: 456-466.

Stein, A.A., E. Opalka and **I. Rosenblum.** 1965. Hepatic lipids in tumor-bearing (glioma) mice. Cancer Res. 25: 957-961.

Stein, A.A., E. Opalka and **D. Serrone.** 1966. Sequantial hepatic triglycerides in tumor-bearing mice. Cancer Res. 26: 1707-1710.

Weber, G. and A. Cantero. 1959. Effect of neoplasia and fasting on phospholipid turn over rate in rat liver. Biochem. Biophys. Acta 35: 257-259.

Wood, R. 1975. Hepatoma, host liver, and normal rat liver phospholipid are affected by diet. Lipids 10: 736-745.

Wood, R., J. Falch and **R.D. Wiegand.** 1974. Hepatoma, host liver, and normal rat liver neutral lipids as affected by diet. Lipids 10: 202-207.

Burying Beetle (Coleoptera: Silphidae, *Nicrophorus*) Surveys on Poteau Ranger District, Ouachita National Forest

Joseph C. Neal, M. Earl Stewart and Warren G. Montague
Poteau Range District
USDA Forest Service
P.O. Box 2255
Waldron, AR 72958

Abstract

Surveys for American burying beetles (*Nicrophorus americanus* Oliver) were conducted in west-central Arkansas on Poteau Ranger District of the Ouachita National Forest in 1992 and 1993. A total of 2450 *Nicrophorus* specimens were captured in 1098 trap nights. The most frequently captured specimens were *N. orbicollis, N. tomentosus,* and *N. pustulatus*. One specimen of *N. americanus* was also captures. Other species of beetles were also trapped and identified in this survey. Habitats sampled were primarily well-drained uplands with proposed or recent harvests of shortleaf pine (*Pinus echinata*). It appears that these habitats may not harbor extensive populations of *N. americanus* on Poteau RD.

Introduction

The American burying beetle (*Nicrophorus americanus* Oliver) was added to the Federal list of endangered species in July 1989 (USF&WS, 1991). Beginning in September 1992, Ouachita National Forest (Ouachita NF) districts with historical records of *N. americanus* were directed to perform surveys prior to ground-disturbing activities (e.g., road construction, preparation of sites for tree planting) that might affect this species (J.M. Curran letter of Sept. 18, 1992). Surveys were initiated in fall 1992 on the Poteau Ranger District (Poteau RD) in west-central Arkansas.

Study Area

Poteau RD encompasses 69,659 ha of mixed forest consisting primarily of shortleaf pine (*Pinus echinata*) and various hardwood species in Scott, Polk, and Sebastian counties of west-central Arkansas. Most of these public lands are located on rugged uplands of east-west trending ridges typical of the Ouachitas. In general the cool north slopes favor hardwoods, while the warmer south slopes and ridge tops favor shortleaf pine. Privately-owned farmland occupies most extensive bottomlands within the boundaries of Poteau RD.

Trap lines were established on Poteau RD where projects were proposed that would involve various ground-disturbing activities including: 1) harvest of shortleaf pine timber, 2) construction of temporary roads to provide access to the harvest areas, 3) revegetation of eroded cut-over lands recently acquired by the Forest Service, and 4) various wildlife-related projects, including pond construction. Most of these activities occurred in well-drained areas with tree stands currently dominated by shortleaf pine or that were dominated by pine prior to recent harvest. No beetle trapping occurred on north-facing hardwood dominated stands, in bottomland pastures, or in open grasslands.

Methods

Surveys for American burying beetles were conducted on Poteau RD in Scott County from 7-13 October 1992, and from 22 June - 10 September 1993. In 1992 surveys totalled 351 trap nights; in 1993, 747 trap nights (one trap night = one baited pitfall trap in place for beetle trapping for one night).

Methods used were similar to nonlethal baited pitfall traps described in the recovery plan for *N. americanus* (USF&WS, 1991). A pit was formed by a single 16 ounce plastic cup set in the ground with the lip of the cup at ground level; a second cup was inserted into the first cup to facilitate removing trapped beetles. In 1992 and at the beginning of 1992, chicken gizzard bait was placed in the bottom of the second cup and the trap was covered with a rock or bark. This method was modified in 1993 with bait placed in a 1-2 ounce sauce cup suspended with flexible wire over the 16 ounce cup. The baited trap was covered by lids cut from plastic one gallon bleach jugs that were approximately 10 cm in height by approximately 15 cm in diameter. The lids were weighted with small stones or limbs. A severe thunderstorm blew the lid off one trap, causing the trap to fill with water; thereafter, small

drainage holes (diameter = 2 mm) were made in the bottom of all cups. Traps were checked for three consecutive mornings following the set-up day (for an equivalent of three trap nights).

In 1992 and at the beginning of 1993, frozen baits were thawed, then placed in an outdoor container and allowed to spoil for 2-4 days. Later in 1993 thawed baits (or unfrozen, fresh baits) were held in a cooler with ice to prevent rapid deterioration during intense summer heat.

Configuration of trap lines varied according to topography and proposed resource management project that prompted the survey. Pitfalls were often set 74 - 122 m apart on proposed road construction rights-of-way, allowing survey of the entire corridor. Shorter trap lines, with pitfalls 46 - 61 m apart, were set in other areas, such as those planned for control of soil erosion. Survey lines were within approximately 800 m of the project area.

Specimens of *Nicrophorus* and other beetles were identified in the field. Field identification was based upon preserved specimens that had been sent out for examination (see Acknowledgements). Many relatively small beetles were not identified in the field; these were entered on data sheets as "beetle species."

Results

In 1992 and 1993, 2450 specimens of *Nicrophorus* were captured in 1098 trap nights. *N. orbicollis* and *N. tomentosus* accounted for >90 percent of the total (Table 1). *N. pustulatus, N. marginatus,* and *N. americanus* were also captured in small numbers. A male *N. americanus* was trapped in compartment 1281, approximately 16 km southwest of Waldron, in Scott County, Arkansas, on 5 August 1993. Habitat at the capture site was a mixed stand of mature trees dominated by shortleaf pine adjacent a recently harvested stand in early regeneration (grasses, forbs, and seedling trees). In the same cup with *N. americanus* were four *N. orbicollis* and two *Canthon* sp.

Table 1. Captures per trap night of *Nicrophorus* sp. beetles on Poteau RD, Ouachita NF, 1992-1993.

Species	351 Trap Nights 1992	747 Trap Nights 1993
N. orbicollis	1.66	2.04
N. tomentosus	1.29	0.05
N. pustulatus	0.50	0.02
N. marginatus	<0.01	<0.01
N. americanus	<0.01	<0.01

Table 2. Sample of beetles attracted to ripened gizzard bait, Poteau RD, Ouachita NF, 1992-1993. Results are presented as captures per trap night.

Species	186 Trap Nights 1992	159 Trap Nights 1993
Deltochilum gibbosum	0.53	0.85
Canthon sp.	0.27	0.48
Necrodes surinamensis	0.02	0.38
Trox sp.	0.09	0.14
Necrophila americana	0.06	0.07
Geotrupes sp.	0.01	0.06

Other species of beetles were frequently trapped. A sample of these captures is present in Table 2. Specimens of the Scarabaeidae (especially *Deltochilum gibbosum* and *Canthon* sp.) were often identified in these samples. Other specimens regularly captured included *Trox* sp., *Geotrupes* sp. (Scarabaeidae) and other carrion beetles (e.g. *Necrophila americana, Necrodes surinamensis*). Rove beetles (Family Staphylinidae: e.g. *Creophilus maxillosus*) and hister beetles (Histeridae: e.g. *Ateuchus histeroides*) were occasionally common.

Discussion

Beetle surveys on Poteau RD varied seasonally and numerically between the two years (Table 1). While captures per trap night of *N. orbicollis* were similar between the two years, the capture rates for *N. tomentosus* and *N. pustulatus* were numerically dissimilar. *Nicrophorus tomentosus* is reproductively active in the fall (Wilson and Fudge, 1984), which likely explains why the trapping in October 1992 resulted in a higher rate of capture as compared to the summer trapping in 1993. *Nicrophorus pustulatus* is a woodland species active throughout the summer, but it seems very sensitive to a lack of moisture (K. Stephan, pers. comm.) Unlike October 1992 the 1993 trapping season was droughts from 27 June - 1 August, with 0.4 cm of rainfall and temperatures ranging from 33 to 39 degrees C (Poteau RD weather data). Five surveys during this period resulted in the capture of 161 *Nicrophorus* sp. in 258 trap nights, or 0.6 beetles per trap night, a rate lower than overall results for the two years (Table 1).

Pitfall traps baited with ripened carrion serve as a powerful attractant to carrion beetles, including *Nicrophorus* sp. (USF&WS, 1991), but ripening bait more than two days under very warm conditions during sum-

mer in western Arkansas may reduce the value of the bait as an attractant. On Poteau RD the fresh chicken gizzard bait changed from pink (relatively fresh, slight odor, few or no maggots), to gray (rotting, strong odor, small maggots), to black (putrid, overwhelming odor, numerous large maggots). These changes occurred slowly during the cool, fall weather of 1992, and quickly during the hot weather of 1993.

Bait in the pink to gray condition was effective in attracting *Nicrophorus* sp., but as the bait advanced toward the black, putrid condition, fewer *Nicrophorus* sp. were attracted, and there was an increase in *Necrodes surinamensis*, *Trox* sp. and other species. *Deltochilum gibbosum* was attracted at all stages of bait ripening, but numbers increased as the bait approached the gray and black stages. In 1993 *Geotrupes* sp. appeared most frequently with highest numbers of *Nicrophorus*. *Necrophila americana* did not seem to appear until the bait reached the gray stage. The apparent preference of *Nicrophorus* sp. for bait in the pink to gray condition may confer an adaptive advantage to the insects by allowing early colonization and thereby maximizing the nutritional resources available to larvae (May, 1993; C. Carlton, pers. comm.).

A relatively large population of these beetles has been documented at Ft. Chaffee, Arkansas, in habitats characterized as grasslands and open oak and oak-hickory woodlands or "oak savannas" (U. S. Army, 1993). Since September 1992, *N. americanus* has been captured on four ranger districts of the Ouachita NF in western Arkansas and eastern Oklahoma (Frazier, 1993; file data, Ouachita NF). Most captures occurred on the Tiak RD in McCurtain County, Oklahoma, and on the Cold Springs RD in Logan and Scott counties, Arkansas. Therefore, despite declining elsewhere in North America (USF&WS, 1991), a population persists along the eastern deciduous-western prairie econtone in western Arkansas and eastern Oklahoma.

The capture of *N. americanus* in compartment 1281 of Poteau RD in Scott County, Arkansas, was the only capture during surveys involving 25 of 127 district compartments. The closest other captures were more than 30 km northeast and west (file data, Ouachita NF). The capture on Poteau RD provided an additional link in the current range of this species in the western Arkansas-eastern Oklahoma prairie-forest ecotone.

Very little open, park-like oak-hickory forest and open grassland occurs within Forest Service boundaries on Poteau RD. It appears that typical well-drained upland sites most suitable for growth of shortleaf pine may have limited potential for populations of *N. americanus*.

Finally, no action taken by the US Forest Service may jeopardize critical habitat of federally listed species (Ouachita NF, 1990). These surveys satisfied that legal requirement. In addition, the surveys provided an opportunity to collect data on carrion beetles, an otherwise little-studied component of the Ouachita ecosystem.

Acknowledgements

Beetle identifications and careful readings of an earlier version of this manuscript were provided by Karl Stephen of Red Oak, Oklahoma, and Chris Carlton from the Department of Entomology, University of Arkansas-Fayetteville. J. McLemore, F. Rothwein, M. Lichtler, R. Bastarache, and J. Mawk (all from the USDA Forest Service) shared data about beetle trapping and distribution on other Ouachita NF districts. K. Piles, L. Shores, J. Ridenhour, and H. Johnson assisted on Poteau RD surveys. Chicken gizzards were donated by the Tyson Foods poultry processing plant in Waldron.

Literature Cited

Frazier, K. 1993. Current status of the American burying beetle within the midwest geographical recovery area. USF & WS, Div. Ecol. Serv., Tulsa, Oklahoma (letter Jan. 20, 1993).

May, M. 1993. Coleopteran child care. American Scientist 81: 20-22.

Ouachita National Forest. 1990. Amended Land and Resource Management Plan. USDA, Forest Service. Hot Springs, Arkansas.

U.S. Department of the Army. 1993. Biological assessment: for the American burying beetle at Fort Chaffee, Arkansas. 21 pp.

U.S. Fish and Wildlife Service. 1991. American burying beetle (*Nicrophorus americanus*) Recovery Plan. Newton corner, Massachusetts, 80 pp.

Wilson, D.S. and **J. Fudge.** 1984. Burying beetles: intraspecific interactions and reproductive success in the field. Ecol. Entomol. 9:195-203.

Hammett Correlations of Half-Wave Reduction Potentials in a Series of N-(Aryl substituted)-Dichloronicotinamides

Cecil C. Persons, Ali U. Shaikh, Julie Shiflett and Frank L. Setliff
Department of Chemistry
University of Arkansas at Little Rock
Little Rock, AR 72204

Abstract

Excellent correlations of Hammett substituent constants (σ_R) of a series of N-(R-substituted aryl) -2,6-, 2,5-, and 5,6-dichloronicotinamides with polarographic half-wave potentials were observed. Although the correlations demonstrate that all three series of amides experience comparable sensitivity to the R groups at the carbonyl reduction site, the relative ease of reduction varies according to the chlorine substitution pattern on the pyridine ring. These differences are suggested to be due to combinations of mesomeric, inductive, and field effects which operate differently in the three systems. Correlation analysis also revealed that Hammett heteroatomic replacement constants previously determined by NMR studies are valid in the present polarographic studies.

Introduction

In connection with our interest in the preparation of dihalonicotinic acids and their derivatives as potential agricultural agents (Setliff and Soman, 1992), we recently reported the excellent correlation of Hammett substituent constants (σ_R) with the amide proton chemical shift in several series of N- (R- substituted aryl) -dihalonicotinamides (Setliff et al., 1992). From the correlation equations obtained therefrom, we were subsequently able to determine Hammett pyridyl 3-aza and 4-aza replacement constants by measuring the amide proton chemical shifts of several N- (pyridyl substituted) -dihalonicotinamides (Setliff et al., 1993). This paper describes an extension of the study of structural and electronic effects in these systems by the use of polarography. The objectives of this research are as follows: 1) to investigate the electronic effects of R groups upon the half-wave reduction potentials in three series of N-(R-substituted-aryl)-dichloronicotinamides, and to determine if Hammett correlations exist, 2) if such correlations exist, to test the validity of the aza replacement constants previously determined by the NMR studies, and 3) To determine the relative reduction ease of the three systems as dictated by the substitution pattern of the chlorine atoms on the pyridine ring.

Materials and Methods

The preparation of the amides has been described previously (Setliff and Soman, 1992). Samples used had been recrystallized several times and had sharp melting points.

Polarographic reductions were conducted in anhydrous dimethylsulfoxide (DMSO) containing 0.01 M tetrabutylammmonium perchlorate (TBAP) as supporting electrolyte. A three-electrode polarographic analyzer, Model PAR 174 A (Princeton Applied Research Corporation, Princeton, NJ) with a dropping mercury electrode, and a drop-timer was used in conjunction with an X-Y recorder, Model 2200 (Houston Instruments, Austin, TX). The reference electrode was a specially prepared low-porosity calomel electrode (Fisher Scientific, Pittsburgh, PA) filled with a 0.40 M solution of tetraethylammonium chloride in order to adjust the potential to 0.00 volt vs. the saturated calomel electrode (SCE). The counter electrode was a platinum wire.

Exactly 10.00 mL of the TBAP/DMSO solution was poured into the electrochemical cell and was purged with dry nitrogen for about 30 min to remove dissolved oxygen. The nitrogen flow was then diverted above the solution, and the potential of the dropping mercury electrode was scanned between 0.00 volt and -2.5 volt vs. the SCE at a rate of 5 mV/sec to obtain the d. c. background polarogram. Approximately 1 - 2 mg of the test compound was then added, the solution purged again with nitrogen for 5 min to assure complete dissolution, and the potential was scanned as above. Polarograms of all samples were obtained using this procedure.

The half-wave potentials and the number of electrons involved in the reduction were determined from the direct current polarograms using the relationship:

$$E = E_{1/2} + (0.0591/n)\log[(i_d - i)/i] \text{ volts at } 25^\circ C$$

where $E_{1/2}$ is the half-wave potential, n the number of electrons, and i_d the diffusion current. E and i are the corresponding values of the potential and current at any

stage in the rising portion of the curve. $E_{1/2}$ and n were calculated by a least squares analysis of data using the above equation.

The plots of $E_{1/2}$ vs. σ_R were done using an Axum linear regression program available from Trimetrix, Inc., Seattle, WA.

Results and Discussion

The compounds studied are described in Fig. 1 and Table 1, and the half-wave reduction potentials together with the Hammett substituent constants (Exner, 1988) are shown in Table 2. Our calculations revealed a one electron reduction in each case. The excellent linear correlations of $E_{1/2}$ with σ_R in all three series are depicted in Fig. 2. Equations of the lines in slope intercept form are represented below with the correlation coefficients shown in parentheses.

Series I	$E_{1/2} = 0.176\ \sigma_R - 1.79$	($r^2 = 0.94$)
Series II	$E_{1/2} = 0.161\ \sigma_R - 1.71$	($r^2 = 0.96$)
Series III	$E_{1/2} = 0.164\ \sigma_R - 1.65$	($r^2 = 0.95$)

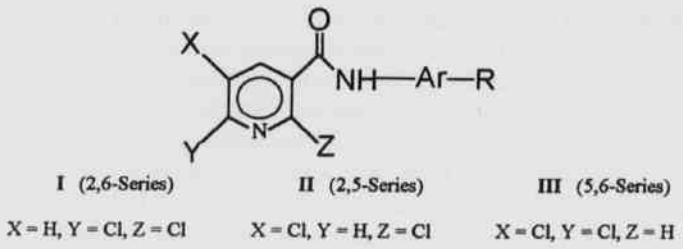

I (2,6-Series) X = H, Y = Cl, Z = Cl

II (2,5-Series) X = Cl, Y = H, Z = Cl

III (5,6-Series) X = Cl, Y = Cl, Z = H

Fig. 1. The N-(Aryl Substituted)-Dichloronicotinamide series.

Table 1. Aryl Substituents for the three Dichloronicotinamide series (Fig. 1).

Cpd.	Ar–R	R-group
a.	4-Methoxyphenyl	*p*-Methoxy
b.	4-Methylphenyl	*p*-Methyl
c.	Phenyl	----------
d.	4-Fluorophenyl	*p*-Fluoro
e.	3-Chloro-4-methoxyphenyl	*m*-Chloro *p*-Methoxy
f.	4-Chlorophenyl	*p*-Chloro
g.	3-Pyridyl	3-Aza
h.	4-Chloro-5-methyl-3-pyridyl	*m*-Methyl 3-Aza
i.	4-Trifluoromethylphenyl	*p*-Trifluoromethyl
j.	4-Pyridyl	4-Aza

Table 2. Hammett Substituent Constants (σ_R) and Half-wave Potential Values ($E_{1/2}$) for the three Dichloronicotinamide Series (Fig. 1).

Cpd.	R	σ_R	$E_{1/2}$ I	$E_{1/2}$ II	$E_{1/2}$ III
a.	O-CH_3	-0.28	-1.83 V	-1.76V	-1.69 V
b.	CH_3	-0.14	-1.82 V	-1.74 V	-1.67 V
c.	H	0.00	-1.79 V	-1.73 V	-1.66 V
d.	F	0.06	-1.80 V	-1.72 V	-1.65 V
e.	*p*-O-CH_3 *m*-Cl	$\Sigma_{\sigma R}$(*additive*) (0.09)	-1.77 V	-1.70 V	-1.65 V
f.	Cl	0.22	-176 V	-1.69 V	-1.62 V
g.	30aza	0.34	01.75 V	-1.67 V	-1.60 V
h.	3-aza *p*-Cl *m*-CH_3	$\Sigma_{\sigma R}$(*additive*) (0.50)	-1.70 V	-1.63 V	-1.57 V
i.	CF_3	0.53	-1.70 V	-1.65 V	-1.58 V
j.	4-aza	0.55	-1.68 V	-1.62 V	-1.54 V

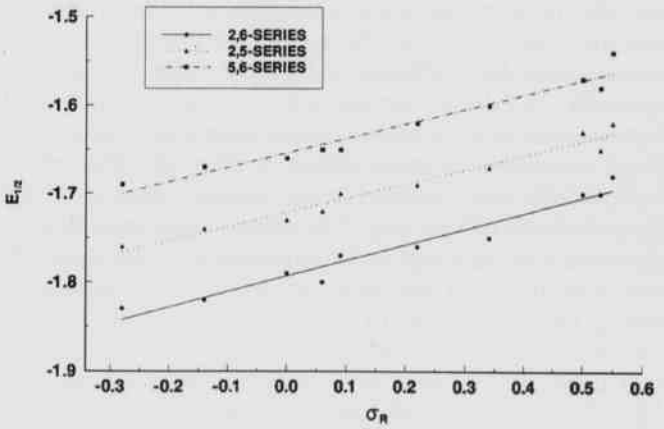

Fig. 2. Correlations of $E_{1/2}$ with Hammett σ_R values.

Substituents on the benzene ring affect the ease of reduction in the same way in the three series as evidenced by reducibility enhancement by the more electron withdrawing substituents. The similarity of the slopes (coefficients of σ_R corresponding to a Hammett ρ value) suggests that the reduction sensitivity to these groups is approximately the same. It is noteworthy that effects of substituent groups are additive in these systems. Disubstituted N-aryl compounds Ie, IIe, and IIIe gave $E_{1/2}$ values that correlate well with the their additive σ_R's. Furthermore, the heteroatomic replacement constants for 3-aza and 4-aza as determined previously by proton NMR studies (Setliff et al., 1993) correlate extremely well (compounds Ig, IIg, and IIIg, and Ij, IIj, and IIIj), and these replacement constants are additive with the Hammett σ_R

values as exhibited by compounds Ih, IIh, and IIIh.

The relative ease of reduction of the three series (as indicated by the magnitude of the $E_{1/2}$ values in Table 2 as well as the intercept values in the three correlation equations) is III > II > I. More specifically, the 5,6 series with the lowest potentials reduce the easiest, while the 2,6 series which requires the highest potentials is the most difficult to reduce. As mentioned previously the R groups affect all three systems to the same degree, so the difference in reducibility must be attributed to the positioning of the chlorine atoms on the pyridine ring.

Although detailed mechanistic studies are unavailable on polarographic reductions of amides, aldehydes and ketones have been studied extensively (Zuman, 1967). In these systems it has been established that reduction is initiated by a one electron attack at the carbonyl carbon, and our results suggest a similar process is likely in the amides. Amides are more difficult to reduce than aldehydes or ketones due to electron enrichment at their carbonyl carbon arising from resonance of the nitrogen lone pair. This process operates in all three of our amide systems, but most effectively in the 2,6-dichloro system (series I), and least effectively in the 5,6-dichloro system (series III). In the 2,6-series, we propose that the field effect of 2-chloro helps to stabilize the previously mentioned resonance form as shown in Fig. 3A. This effect coupled with the "through conjugation" (measomeric) effect of the 6- chloro (Fig. 3B) ensures appreciable electron density at carbonyl carbon, resulting in the most difficult reducibility of the three series. (The electron withdrawing inductive effect of 2-chloro is apparently neutralized by its mesomeric effect and does not have a net effect upon the electron density at the carbonyl carbon). In the 2,5- series the stabilizing field of the 2-chloro is still operative, but the 5-chloro, being incapable of any "through conjugation", can only exert an electron withdrawing inductive effect which partially offsets the electron enriching process. The net result is a slightly more positive carbonyl carbon. Finally, in the case of the 5,6-series the stabilizing field effect of 2-chloro is absent, and the weak mesomeric effect of 6-chloro is overshadowed by the significant electron withdrawing inductive effect of 5-chloro. The net result is the most positive carbonyl carbon of the three series. Similar combinations of field, inductive, and mesomeric effects have been used to rationalize reactivities of a series of substituted phenylpropiolic acids (Roberts and Carboni, 1955).

Future work will include electrochemical mechanistic studies with the goal of isolation and characterization of reduction products. Different solvent systems will also be investigated.

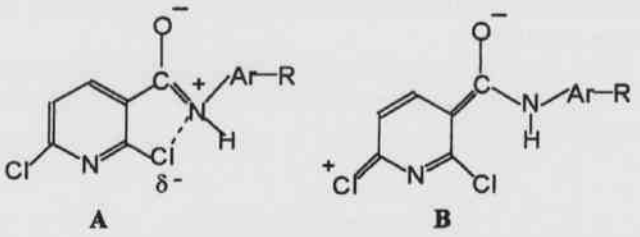

Fig. 3. Electron Enriching Processes at the Carbonyl Carbon.

Acknowledgements

The authors gratefully acknowledge Mr. Archie Stone for computer assistance on the Hammett plots and the UALR Faculty Research Fund for general financial support.

Literature Cited

Exner, O. 1988. Correlation analysis of chemical data, Plenum Press, New York, 275 pp.

Roberts, J.D. and **R.A. Carboni.** 1955. Electrical effects of substituent groups–reactivities of phenylpropiolic acids. J. Am. Chem. Soc. 77:5554-5558.

Setliff, F.L. and **N.G. Soman.** 1992. 4-Substituted anilides of 2,6-and 5,6-dichloronicotinic acids–potential agricultural agents. Proc. AR. Acad. Sci. 46:69-71.

Setliff, F.L., N.G. Soman, J.Z. Caldwell and **D.L. Rogers.** 1992. Hammett correlations in the ^{1}H nmr spectra of some N-aryldihalonicotinamides. Proc. AR. Acad. Sci. 46:72-74.

Setliff, F.L., N.G. Soman and **A.D. Toland.** 1993. Determination of Hammett pyridine 3-aza and 4-aza replacement constants by ^{1}H nmr studies of amide systems. Proc. AR. Acad. Sci. 47: 107-109.

Zuman, P. 1967. Substituent effects in organic polarography, Plenum Press, New York, 384 pp.

Tetraethylene Gycol - Based Electrolytes for High Temperature Electrodeposition of Compound Semiconductors

***Chris Poole, Robert Engelken, *Brandon Kemp, and *Jason Brannen**
Department of Engineering
Arkansas State University
P. O. Box 1740
State University, AR 72467

Abstract

We report an investigation of tetraethylene glycol (TEG) solutions of chloride salts ($CdCl_2$, $TeCl_4$, and $HgCl_2$) for electrodeposition of films of CdTe and $Hg_{1-x}Cd_xTe$, leading II-VI semiconductors. The high boiling point (314°C), below-room temperature (T) (-6°C) melting point, adequate metal chloride solubilities, and low toxicity of TEG make it a good candidate for electrodeposition at T > 200°C. Such temperatures tend to activate growth of larger crystallites than with aqueous electrolytes at T < 100°C, as are advantageous in optoelectronic applications.

Initial results do, indeed, indicate a dramatic increase in crystallinity with deposition temperature, especially for the CdTe films which are nearly amorphous when grown at room temperature. $Hg_{1-x}Cd_xTe$ films ($x < 0.5$) are marginally polycrystalline when grown at room temperature but also improve in crystallinity at higher growth temperatures. There appears to be a strong decrease in film adherence and uniformity as growth temperature increases for both materials probably because the greatly increased carrier concentrations at higher temperatures increase film conductivity which, in turn, supports easy electroplating of protruding loose dendritic and/or columnar crystallites, instead of the monolayer-by-monolayer growth of lower conductivity material as occurs at lower temperatures, especially in the higher bandgap/lower conductivity CdTe. The same increase in film conductivity with temperature is responsible for the decrease in the relative photosensitivity of both the CdTe and $Hg_{1-x}Cd_xTe$ with temperature. At all temperatures, the inferior adherence, uniformity, and photosensitivity as well as the superior crystallinity of $Hg_{1-x}Cd_xTe$ over that of the CdTe are also explained by its lower bandgap and higher conductivity. On balance, however, the initial results prove the utility of high temperature TEG electrolytes for electrodepositing CdTe and $Hg_{1-x}Cd_xTe$ films with much better crystallinity than for those grown at lower temperatures, notably in aqueous baths.

*Undergraduate Research Assistants

Introduction

Electrodeposition is a potentially advantageous method for producing materials used in solar cells and other optoelectronic devices. However, there are problems with electrodeposition that must be solved before it can be applied to optoelectronic device manufacturing. One is that electrodeposition tends to produce films that are amorphous or have relatively poor crystallinity. The research described herein is an effort to investigate one method to address this problem as a follow up to previous research on metal chalcogenide electrodeposition.

This work has focused on the growth of binary and ternary metal telluride semiconductor compounds at temperatures up to 200°C in organic solutions of tetraethylene glycol (TEG) (b.p. = 314°C). The compounds investigated thus far are CdTe and $Hg_{1-x}Cd_xTe$. It is hoped that growth of these at high temperatures (in principle up to the boiling point) will produce films with much larger grain (crystallite) sizes than in those grown at room temperature. More crystalline films should exhibit better performance in subsequent devices. Other attributes of high temperature growth include higher current densities which yield increased deposition rates and more complete diffusion of and reaction between the elements in the film (e.g., Cd, Hg, and Te) to produce a more homogeneous and stoichiometric compound phase. Since both diffusion and reactivity are temperature dependent (proportional to $\exp[-E_A/RT]$), moderate temperature increases could have dramatic effects.

Results thus far have indicated success in achieving the objective of enhanced crystallinity. CdTe films grown at elevated temperatures have exhibited much better crystallinity than those grown at room temperature, and the $Hg_{1-x}Cd_xTe$ films follow the same trend but not as dramatically.

Review of Literature

There has been much recent work on the electrodeposition of various semiconductor materials, including

CdTe (Takahasi et al., 1984; Darkowski and Cocivera, 1985; Engelken and Van Doren, 1985), $CuInSe_2$ (Pern, Goral, et al., 1988; Pern and Noufi, 1988), CdS (Baranski et al., 1981), SnS (Mishra et al., 1989), SnSe (Engelken et al., 1986), $Cu_{2-x}S$ (Engelken and McCloud, 1985), WSe_x (Engelken et al., 1985), and GaAs (Yang et al., 1992). Electrodeposition has even recently been applied to high temperature superconductors (Weston et al., 1992).

Various industrial groups have researched commercialization of solar cells that have involved one or more electrodeposition steps in their fabrication. Rockwell (Ogden and Tench, 1981), Monosolar (Rod et al., 1980), and AMETEK (Fulop et al., 1982) all investigated the electrodeposition of CdTe. The National Science Foundation has funded considerable work in this area, including that of one of the authors (Rajeshwar and Engelken, 1990). The U.S. Department of Energy and the Solar Energy Research Institute (SERI), now the National Renewable Energy Laboratory (NREL), conducted and/or sponsored investigation of electrodeposition of CdTe and $CuInSe_2$ (CIS) (Basol and Kapur, 1990; Kapur et al., 1987).

If fundamental problems with film (1) crystallinity (2) uniformity/adherence, and (3) stoichiometry/native doping can be effectively solved, electrodeposition can serve as an extremely convenient and low cost method for producing thin film-based optoelectronic devices.

Material and Methods

The apparatuses used in these experiments included an IBM EC 225 Voltammetric Analyzer, a Hewlett Packard 7046-B x-y-t recorder, a 300 ml Pyrex beaker, and a Teflon beaker cover with the appropriate holes. The anode was made of Poco pyrolyzed graphite and its submerged area was approximately 6 cm^2. The reference electrode was a Fisher Ag/AgCl reference electrode for measurements below 110°C or a piece of Poco pyrolyzed graphite for those above 110°C. The cathode clamp was constructed of Poco graphite and Teflon bolts and nuts, and the cathode substrates were Balzers 50 ohms/square ITO glass with approximately three cm^2 submerged. Other items included a Fisher Hg-filled thermometer and a Teflon coated stir bar.

Supplies and reagents used included Fluka tetraethylene glycol, and Johnson-Matthey $CdCl_2$, $TeCl_4$, $HgCl_2$, and ultra-pure NaCl.

A Rigaku D-MAX x-ray diffractometer was used to characterize crystallinity. A Perkin-Elmer Lambda 19 UV/VIS/NIR spectrophotometer was used for optical absorbance spectroscopy.

The ITO glass substrates were prepared by washing with Comet cleanser and tap water, followed by thorough rinsing in distilled water and drying with a hot air blower. The solutions contained 100 ml of tetraethylene glycol, with 10^{-3} M $TeCl_4$ and 0.05 M $CdCl_2$ for CdTe deposition, or 10^{-3} M $HgCl_2$, 2.10^{-3} M $TeCl_4$, and 0.05 M $CdCl_2$ for $Hg_{1-x}Cd_xTe$ deposition. The salts generally took overnight to dissolve completely in the viscous organic solutions.

The films were grown at cathode voltages ranging from -0.6 to -0.8 V referenced to the Ag/AgCl electrode. The deposition voltage was determined by analyzing photovoltammograms to find the region exhibiting the largest photocurrents which indicate semiconducting behavior. Deposition temperatures ranged from room temperature (21°C) to 170°C. The deposition times required to obtain reasonably thick films ranged from approximately 24 hours at room temperature (current densities less than 100 $\mu A/cm^2$) to 2-3 hours at the highest temperatures (current densities close to $1mA/cm^2$). This was due to the standard increase in current density versus temperature at a given voltage. The solutions were slowly stirred to help improve the uniformity of the films. During film growth, the substrate was occasionally illuminated with white light to monitor the photosensitivity of the film versus time and thickness. Films were rinsed in a tetraethylene glycol bath at the same temperature as the deposition bath and were allowed to cool slowly to room temperature in that bath to prevent cracking and flaking. The films were then rinsed in pure distilled water and were allowed to dry in the hood air stream. The films were stored in either ziplock bags or plastic Petri dishes.

Results and Discussion

Photovoltammograms were run for both the CdTe and the $Hg_{1-x}Cd_xTe$ deposition baths in order to determine the voltammetric structure and, thus, the voltage region in which semiconducting CdTe or $Hg_{1-x}Cd_xTe$ (versus nonstoichiometric and/or mixed phase) plating was occurring. Figure 1 shows the voltammetric structure of the CdTe bath at 60°C. The pure, metallic Cd cathodic deposition wave is not seen on this voltammogram because it occurs at a considerably more negative (over 0.3 V) potential in tetraethylene glycol than in water (-0.40 V (SHE)). The elemental tellurium and "Cd_xTe" waves are apparent as well as anodic strippint peaks associated with electrochemical dissolution of Cd out of the surface of the CdTe and the subsequent dissolution of the remaining Te and CdTe. This voltammogram exhibits conspicuous cathodic photocurrents, indicative of semiconducting material.

Figure 2 shows the voltammetric structure of the CdTe solution at 135°C. The cathodic deposition and anodic stripping waves are much larger in this case, due to the increased current and, hence, amount of material

plated at the higher temperatures. The photocurrents appear to be smaller, but this is primarily due to the higher current scale used versus that of Fig. 1.

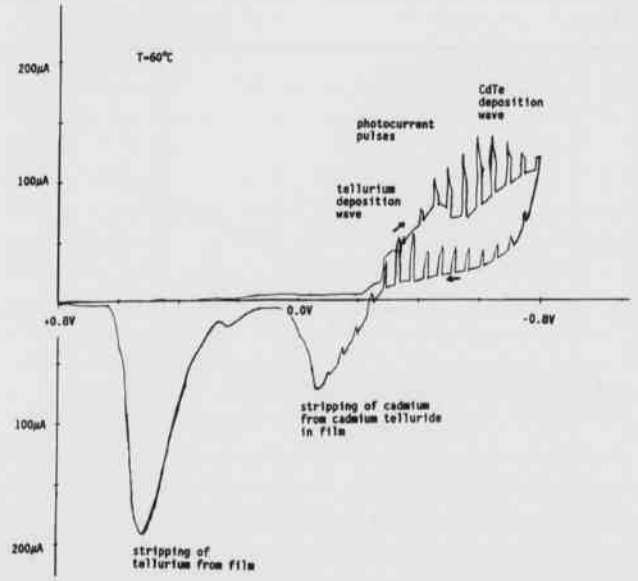

Fig. 1. Cyclic voltammogram (current-voltage curve) for an indium-tin oxide coated glass cathode in a tetraethylene glycol solution of 0.05 M $CdCl_2$, 10^{-3} M $TeCl_4$, and 0.10 M NaCl at 60°C. The sweep rate was 5 mV/s and the reference electrode was Ag/AgCl. Note the cathodic photocurrent pulses at the more negative voltages, indicative of semiconducting material.

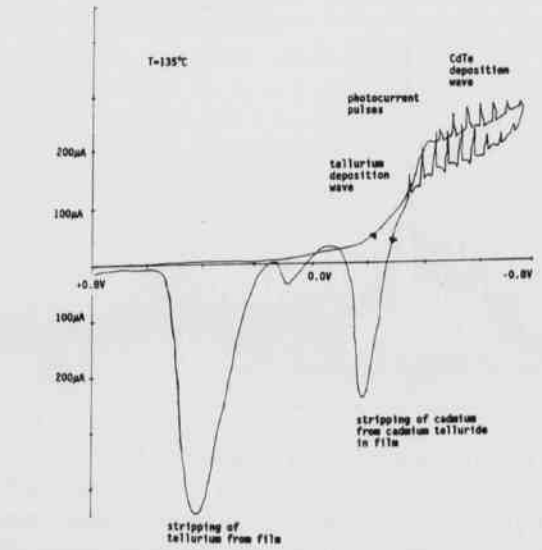

Fig. 2. Cyclic voltammogram as with Fig. 1 except that T = 135°C and a graphite strip was used as a reference electrode. Note the increase in the current levels.

Figure 3 shows the voltammetric structure for the CdTe solution at 165°C. Once again, the currents in the deposition and stripping waves have increased with temperature. In this case, there seems to be a true reduction in photocurrent from that at lower temperatures, perhaps due to drastically increased carrier densities and conductivity at this temperature.

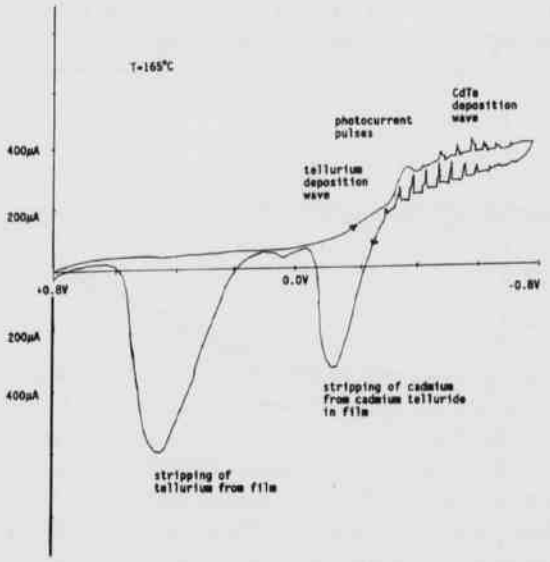

Fig. 3. Cyclic voltammogram as with Fig. 2 except that T = 165°C. Note the increase in the current with temperature and an apparent decrease in the relative photocurrent.

The voltammetric structure for the $Hg_{1-x}Cd_xTe$ bath at room temperature is shown in Fig. 4. The currents and the photocurrent pulses in this case are small. Also, the separate deposition and stripping waves are not as distinct as in the CdTe solution probably due to the mutual underpotential deposition of both Hg and Te into HgTe in one broad wave/reaction. The small but distinct photocurrent is indicative of semiconducting $Hg_{1-x}Cd_xTe$ rather than "metallic" HgTe (no bandgap). Fig. 5 shows the voltammetric structure of the $Hg_{1-x}Cd_xTe$ solution at 100°C. In this case, the currents are much larger, but no photocurrents can be seen, probably because at this temperature, the low bandgap material has itself been driven nearly "metallic" (huge carrier concentrations).

Figure 6 shows the x-ray diffractometer (XRD) (Cu-kα) plot of intensity versus goniometer angle (2θ) for a CdTe film grown at room temperature. The peaks seen in this plot correspond directly with the indium tin oxide (ITO) substrate coating. The vertical lines on the plot indicate where the peaks for CdTe should lie (i.e., the "standard"

Journal of the Arkansas Academy of Science, Vol. 48 [1994], Art. 1

powder diffraction file date). The absence of peaks other than those from ITO indicates that the material on the substrate was amorphous. Figure 7 shows the XRD plot from a CdTe film grown at 90°C. This plot shows very large CdTe peaks, indicating much better crystallinity for this film. Figure 8 shows the XRD plot for a CdTe film grown at 170°C. This plot also shows large peaks, although not as large as before. The reason for the smaller peaks in this latter case is probably not decreased crystallinity, but a much smaller film thickness which reduced the strength of the diffracted X-ray signal.

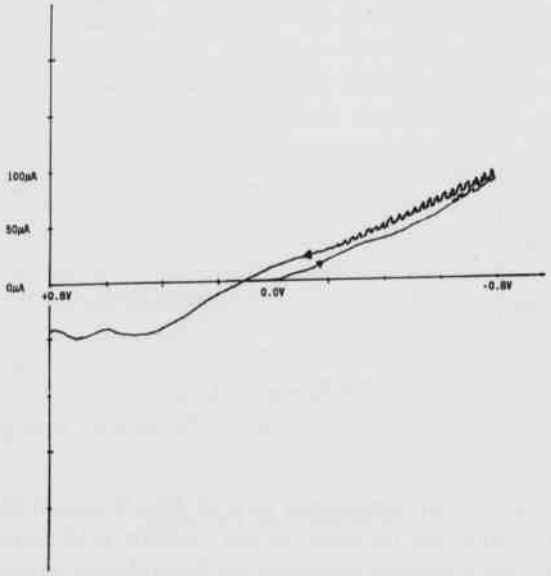

Fig. 4. Cyclic voltammogram (5 mV/s) for a ITO-coated glass cathode in a TEG bath 10^{-3} M in $HgCl_2$, $2 \cdot 10^{-3}$ M in TeC14, and 0.05 M in $CdCl_2$. Note the single, broad cathodic wave starting near O V (Ag/AgC1), probably indicative of mutual underpotential deposition of Hg and Te into HgTe. The subsequent appearance of cathodic photocurrent is indicative of incorporation of Cd into the film and deposition of semiconducting $Hg_{1-x}Cd_xTe$ at the more negative voltages.

Figure 9 shows the XRD plot for an $Hg_{1-x}Cd_xTe$ film grown at room temperature. The vertical lines on the plot show the locations of the peaks for a commercial sample of $Hg_{1-x}Cd_xTe$ ($x \approx 0.2$) donated by Johnson-Matthey. The relatively large intensity of the peaks on this plot indicates very good crystallinity for a film grown at room temperatures. Figure 10 shows the XRD plot for an $Hg_{1-x}Cd_xTe$ sample grown at 100°C. This plot shows slightly larger peaks, indicating better crystallinity for the higher deposition temperature (although relatively not as large an increase as for CdTe). The high conductivity of $Hg_{1-x}Cd_xTe$ leads to much easier growth of dendritic crystallites at low temperature than with much lower conductivity CdTe which tends to grow "layer-by-layer" in an amorphous to small grained manner due to the relatively high resistance of the growing film due to its much higher bandgap.

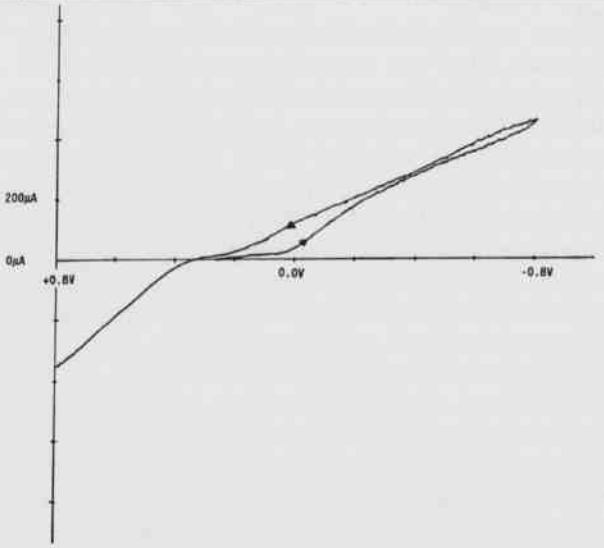

Fig. 5. Cyclic voltammogram as in Fig. 4 except that T = 100°C. Note the disappearance of photocurrent pulses, probably became the low bandgap/high conductivity material has been driven nearly "metallic" by the high temperatures.

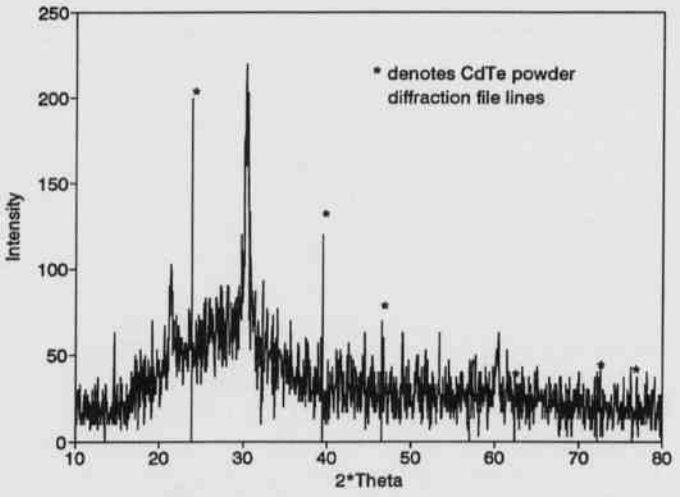

Fig. 6.. X-ray diffraction data for a CdTe film electrodeposited onto ITO-coated glass from a bath as described in Fig. 1 and at room temperature. The visible peaks match the indium-tin oxide and there are no large peaks definitely above the noise that match the standard CdTe Powder diffraction file peaks indicated by the vertical lines and stars.

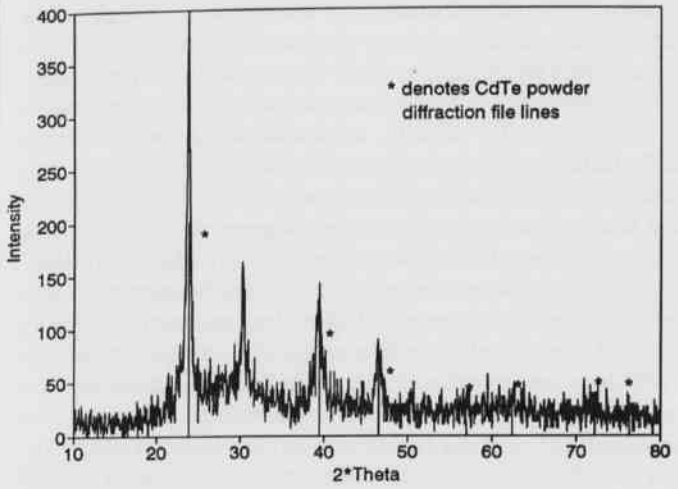

Fig. 7. XRD data as in Fig. 6 but for a film grown at 90°C. Note the appearance of significantly larger peaks matching the CdTe file data and indicating relatively large grain CdTe.

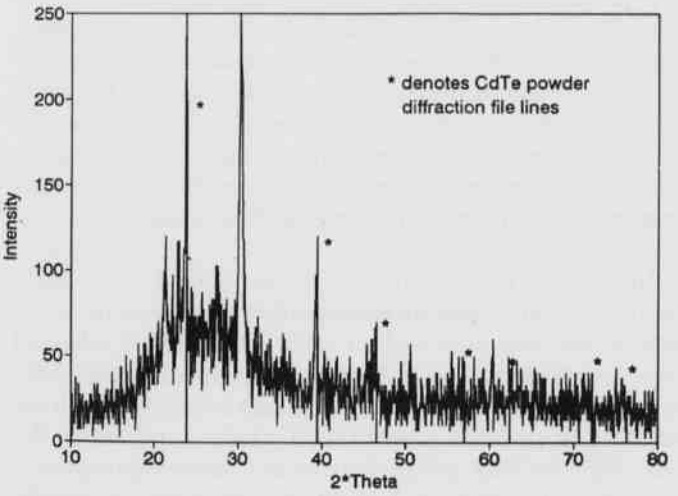

Fig. 8. XRD data as in Figs. 6 and 7 but for a CdTe film grown at 170°C. Again, note the large CdTe peaks. However, they are less intense than in Fig. 7 primarily because of the thinness of this last sample.

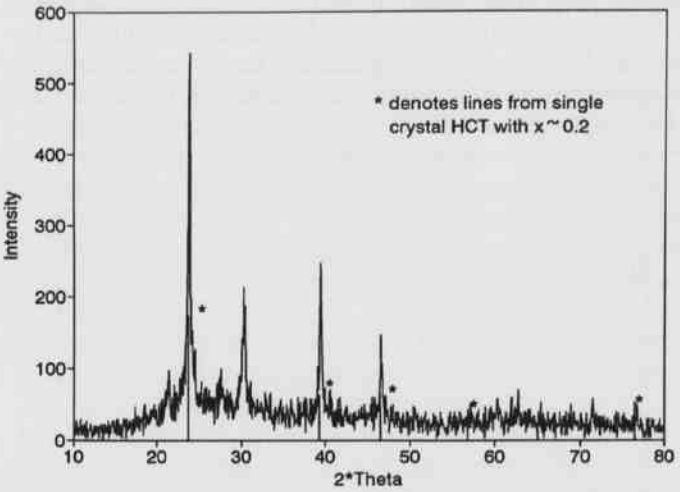

Fig. 9. XRD data for a $Hg_{1-x}Cd_xTe$ film electrodeposited on ITO at room temperature. Note the good alignment with the lines representing peak centroid for a single crystal $Hg_{1-x}Cd_xTe$ (x=0.2) sample. However, the slight mismatch probably represents a somewhat smaller value of x than 0.2 (i.e., the film peaks are shifted slightly toward those of HgTe). It is significant that the film exhibits good polycrystallinity even when grown at room temperature; this is probably a result of the much greater conductivity of the low bandgap $Hg_{1-x}Cd_xTe$ over that of CdTe.

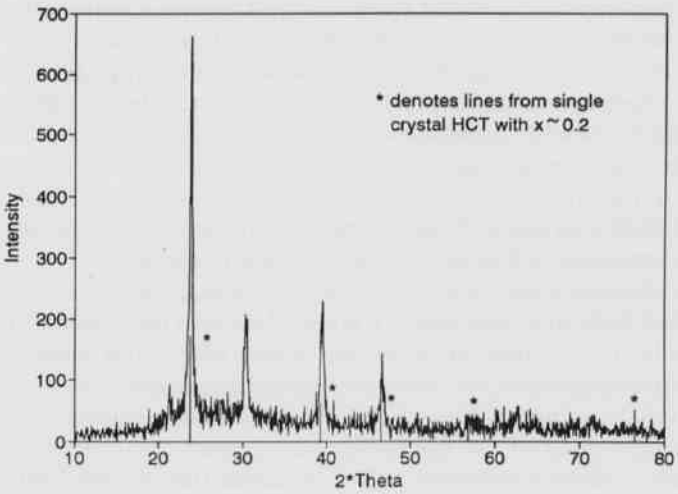

Fig. 10. XRD data as in Fig. 9 except that the deposition temperature was 100°C. Note the slight increase in crystallinity in this case (i.e., peak intensities) over that of the room temperature-grown and comparably thick film in Fig. 9.

A plot of optical absorbance vs. wavelength for a CdTe film is shown in Fig. 11. This plot shows an absorption edge at approximately 800 - 850 nm, consistent with CdTe's 1.5 eV direct bandgap. Problems with film uniformity and adherence (i.e., pinholes) have thus far prohibited good absorption data from being obtained for the $Hg_{1-x}Cd_xTe$ films.

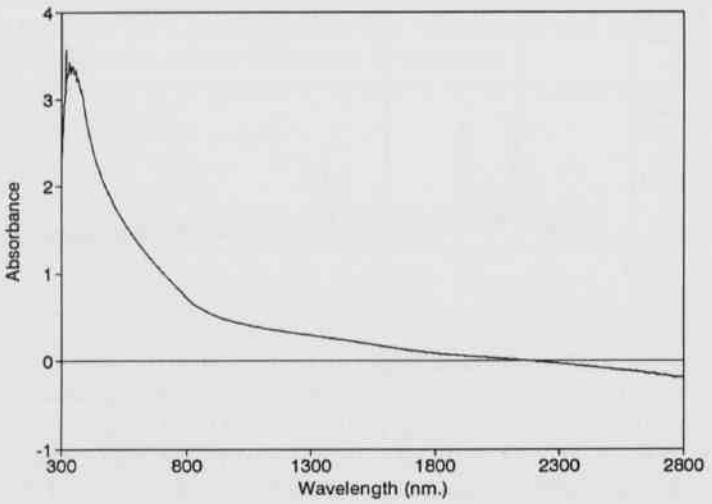

Fig. 11. Optical absorbance vs. wavelength spectrum for a CdTe film electrodeposited from the TEG solution. Note the absorption edge in the 800-850 nm range, consistent with CdTe's 1.5 eV bandgap.

In general, the $Hg_{1-x}Cd_xTe$ films, although definitely polycrystalline, are not as morphologically uniform or adherent as the CdTe films. Again, the relatively large crystallinity may be due to dendritic type growth that leads to less structurally sound and uniform deposits.

Problems encountered in this work included producing films with good uniformity and adherence. CdTe films grown at high temperatures tended to be more nonuniform that those grown at low temperatures. Also, films grown at high temperatures were much more prone to cracking and flaking upon cooling and rinsing.

An unusual effect was observed in the CdTe deposition bath at temperatures above 135°C. First, the bath took on a cloudy appearance. Then, when film growth was attempted at or above this temperature, copious, dendritic, spongy material was observed growing on the sharp edges of the parallelepiped-shaped cathode. This material was assumed to be cadmium metal but XRD analysis identified elemental tellurium as the only crystalline phase. The actual composition of the material is still under study.

There are some distinct bath color changes at temperatures approaching 200°C. First, the baths rather quickly turn a yellow-brown (but still transparent) color whereas the TEG is clear to just the slightest yellow color at room temperature. Since the yellow color remains after the bath cools, it is likely that it is due to simple oxidation ("charring") in the presence of atmospheric oxygen. We plan on conducting future depositions under an inert atmosphere (N_2, argon, etc.) to circumvent this problem.

We also observe an additional gray color appearing in the solution at T > 200°C, accompanied by effervescent gas bubbles in the solution and misty vapor above the solution. This bubbling is not wholesale boiling of the TEG but appear to be due to homogeneous creation of a gaseous product throughout the solution which condenses into a vapor above the solution. This phenomenon also correlates with decreased deposition currents. A likely (but still unproven) mechanism is the reduction of the Te(IV) ions into a gray elemental tellurium suspension by the TEG, itself oxidized into a lower b.p. organic after this occurs, consistent with removal of tellurium ions.

The minute ($\approx 10^{-3}$ M) concentrations of Hg(II) and Te(IV) required to avoid gross Hg and/or Te richness in the deposits (due to their relatively positive reversible potentials and, thus, the need for their currents to be diffusion-limited) are depleted after several depositions and lead to a continuous decrease in their concentrations that makes exact control of stoichiometry more challenging.

Conclusions

In this project we have shown the CdTe and $Hg_{1-x}Cd_xTe$ films electrodeposited at higher temperatures from tetraethylene glycol solutions exhibit better crystallinity than films grown at room temperatures. However, problems exist with high temperature deposition; these include noumiformity and flaking of the films and chemical changes in the electrolyte. On balance, the preliminary results are encouraging and indicative of the utility of TEG-based electrolytes for electrodeposition of large-grained polycrystalline metal chalcogenide films for optoelectronic applications.

In the future, we plan to investigate other solvents for the deposition baths, including other high boiling point organic solvents and molten salts. The molten salts will allow experimentation at even higher temperatures. Also, we will soon begin electrodeposition of other semiconductor compounds, including $CuInSe_2$ and from the same high boiling point electrolytes. Inert atmospheres will also be investigated to avoid oxidation of organic phases at high temperature and the deposited films will be characterized in more detail.

Acknowledgements

The described work is being jointly funded by the NASA JOint VEnture (JOVE), NASA ESPCoR, and NSF/Arkansas Science Information Liaison Office (SILO) Undergraduate Research Fellowship (SURF) Programs as a follow up to an earlier grant from the Arkansas Science and Technology Authority.

Dr. Robert D. Engelken is working with Dr. Frank Szofran of the Electronic and Photonic Materials Branch of the Space Science Laboratory at NASA Marshall Space Flight Center in Huntsville, Alabama under the JOVE Program; the Program is designed to bring together university professors and NASA personnel to work together on mutually interesting projects. R.D.E.'s work involves electrochemical preparation and characterization of compound semiconductors such as $Hg_{1-x}Cd_xTe$ and $Hg_{1-x}Zn_xTe$, both of interest to NASA for both fundamental materials studies (e.g., crystal growth) and device applications. The deposition of high quality films by electrodeposition has emerged as important for producing samples of varying stoichiometry ("x") for subsequent "calibration" of other electrochemical methods being investigated for mapping stoichiometry.

The SILO SURF Program provided additional funding for Chris Poole to continue electrodeposition research through an undergraduate research fellowship. The Program seeks to dramatically increase the involvement of undergraduates in cutting-edge research within Arkansas to improve the technical base and economic competitiveness of the state.

The recently commenced (May, 1994) Arkansas NASA EPSCoR Project includes the Advanced Photovoltaic Materials Research Cluster of which R.D.E. is a participant along with faculty from the University of Arkansas - Fayetteville and University of Arkansas - Little Rock. The Cluster is investigating photovoltaic materials, configurations, and processes, including additional work on electrodeposition of CdTe and $CuInSe_2$ from nonaqueous electrolytes.

Literature Cited

Baranski, A., W. Fawcett, W. McDonald, R. deNobriga and **J. MacDonald.** 1981. The structural characterization of cadmium sulfide films grown by cathodic electrodeposition. J. Electrochem. Soc. 128:963-968.

Basol, B. and **V. Kapur.** 1990. Deposition of $CuInSe_2$ films by a two-stage process utilizing e-beam evaporation. IEEE Trans. on El. Dev. 37:418-421.

Darkowski, A. and **M. Cocivera.** 1985. Electrodeposition of cadmium telluride using phosphine telluride. J. Electrochem. Soc. 132:2768-2771.

Engelken, R. and **H. McCloud.** 1985. "Electrodeposition and material characterization of Cu_xS films. J. Electrochem. Soc. 132:567-573.

Engelken, R. and **T. Van Doren.** 1985. Ionic electrodeposition of II-IV and III-V compounds - Parts I and II. J. Electrochem. Soc. 132:2904-2919.

Engelken, R., T. Van Doren, J. Boone, A. Berry and **A. Shahnazary.** 1986. Electrodeposition and analysis of tin selenide films. J. Electrochem. Soc. 133:581-585.

Engelken, R., T. Van Doren, J. Boone, A. Berry and **A. Shahnazary.** 1985. "Growth of tungsten selenide films through pyrolytic conversion and electrooxidation of ammonium selenotungstate ($(NH_4)_2WSe_4$). Mat. Res. Bull. 20:1173-1179.

Fulop, G., M. Doty, P. Meyers, J. Betz and **C. Liu.** 1982. High efficiency electrodeposited cadmium telluride solar cells. Appl. Phys. Lett. 40:327-328.

K. Mishra, K. Rajeshwar, A. Weiss, M. Murley, R. Engelken, M. Slayton and **H. McCloud.** 1989. Electrodeposition and characterization of SnS thin films. J. Electrochem. Soc. 136:1915-1923.

Kapur, V., B. Basol and **E. Tseng.** 1987. High efficiency, copper ternary thin film solar cells - final report. Prepared under SERI/DOE Contract CE-AC02-83CH10093.

Ogden, C. and **D Tench.** 1981. Electrodeposition of device quality semiconductor materials - final report. Rockwell, International. Prepared under U.S. DOE Contract AC02-77CH00178.

Pern, F. and **R. Noufi.** 1988. One-step electrodeposition of polycrystalline $CuInSe_2$ thin films and their properties. Electrochemical Society Extended Abstracts Vol. 88-2. pp. 539-540.

Pern, F., J. Goral, R. Matson, T. Gessert and **R. Noufi.** 1988. Device quality thin films of $CuInSe^2$ by a one-step electrodeposition process. Solar Cells. 24:81-90.

Rajeshwar, K. and **R. Engelken.** 1990. Novel approaches to the electrodeposition of compound semiconductors - final report. Prepared under National Science Foundation Grant MSM-8617850.

Rod, R., R. Bunshah, O. Stafsudd, B. Basal and **P. Nath.** 1980. Emerging materials for solar cell applications: electrodeposited CdTe - final report. Monosolar, Inc. Prepared under U.S. DOE Contract DE-AC04ET23008.

Takahasi, M., K. Uosaki and **H. Kita.** 1984. Electrochemical deposition, optical properties, and photoelectrochemical behavior of CdTe films. J. Electrochem. Soc. 131:2304-2307.

Weston, A., S. Lalvani, F. Willis and **N. Ali.** 1992. Electrodeposition of YBaCuO and ErBaCuO super conductor precursor films. J. Alloys and Compounds. 181:233-239.

Yang, M., U. Landau and **J. Angus.** 1992. Electrodeposition of GaAs from aqueous electrolytes. J. Electrochem. Soc. 139:3480-3488.

Analysis of Ammunition by X-Ray Fluorescence

Michael W. Rapp and Teddy L. Townsend
Department of Chemistry
University of Central Arkansas
Conway, AR 72035

Abstract

Nondestructive analysis of lead shotgun pellets by X-ray fluorescence (XRF) shows considerable promise in assignment of the identity of the ammunition source. X-ray fluorescence spectra of various shotgun pellets and of standard alloys were obtained using an energy-dispersive instrument and an Am-241 source. The correlation obtained between the precent antimony in the standard alloys and the intensity of the K_a fluorescence peak from antimony was excellent. Peak areas from antimony in shotgun pellets were measured and compared to calibration plots from the standard alloys. The method was capable of distinguishing among lead-based alloys, such as ammunition, with antimony content as high as 10%.

Introduction

X-ray fluorescence (XRF) has become a standard method of analysis over the past 25 years (Leyden, 1987) and has been used for many years in analysis of ammunition (Brunelle et al., 1970). A principal advantage of XRF analysis is that there is often no need to dissolve the sample, to remove interferences, or other-wise to prepare the sample. Measurements can even be made directly on solid samples. While XRF measurements will not reveal the particular chemical forms of the elements present, simultaneous determination of the amounts of several elements is possible as long as the peaks do not overlap in the XRF spectrum. The intensity (peak area) of the fluorescent radiation from a given element varies somewhat according to texture, particle size, and the matrix in which the element is found. However, adjustments in the way a sample is prepared or in the way the data are interpreted can ameliorate those effects (Jenkins et al., 1981).

The principal elements present in leaded ammunition are lead, tin, and antimony. Lead shotgun pellets contain between 0.5% and 8% antimony, but very little tin (Grayson, 1984). Lead shot manufactured by Federal Cartridge Co. (Anoka, Minnesota) contains between 1.5% and 6% antimony, with higher precentages for more expensive loads (Gronfor, 1994). X-ray fluorescence analysis could be the method of choice for ammunition, since significant peaks for antimony, tin, and lead fall in the range of 10-30 keV and there is little interference due to overlap of peaks. This study was undertaken to determine whether direct measurement of the XRF peaks from lead or antimony could provide a rapid, reliable method of determining the composition and identity of lead shotgun pellets.

Materials and Methods

A 100-millicurie americium-241 source (Amersham Corporation, Arlington Heights, Illinois), placed in a lead cylinder to shield the operator from radiation, was used as the exciting source. An energy-dispersive X-ray fluorescence instrument (EG&G ORTEC, Oak Ridge, Tenn., Model # 7016-6165) with a Si-Li detector was used to measure the XRF signals. The system included a preamplifier, a 30 L liquid nitrogen Dewar, a 0.0127 mm thick beryllium detector window, and the Si-Li crystal diode (6 mm thick by 30 mm^2 area) centered about five cm below the surface of the sample position.

Shotgun pellets of different size and from different suppliers were obtained. Alloys of known composition (purchased from Brammer Standard Company, Houston, and National Institute of Standards and Technology, U.S. Dept. of Commerce, Gaithersburg, Maryland) were used for calibration of the method. Alloys were chosen so their composition encompassed the percentages of antimony expected in the shotgun pellets. The composition of these standards is given in Table 1.

Spectra of the standard alloys and the shotgun pellets were taken by exposing the samples to the radiation from the Am-241 source. Small plastic cuvettes with bottoms made of thin mylar film were used to hold granular samples. Acquisition and manipulation of data were facilitated by software provided by EG&G ORTEC. Command files were written and executed to collect XRF spectra for each sample. Assignment of peaks was made according to reference tables (Johnson and White, 1985). Computer programs were written to extract data from the "channel files" that the software created. A commercial program, QuattroPro (version 5.0), was then used to perform a regression analysis (correlating peak intensity and com-

postion) and to generate the graphs shown below.

Table 1. Composition of standard alloys.

Standard Alloy and Description	Elemental Composition (%)		
	Lead	Tin	Antimony
"Lead Setting Up Sample" Cylinder Brammer Cat. # RPb15/5	64	30	1.6
"Lead Base Alloy" Granules Brammer Cat. # GBW2401	65.72	15.97	16.09
"Lead Base Alloy" Granules Powder Brammer Cat. # GBW2402	76.22	5.69	15.02
"Lead Base Bearing Metal" Cylinder NIST Cat. # 1132	83.7	5.84	10.26
"Lead Base White Metal" Small Granules Brammer Cat. # 177/2	84.5	5.07	10.10
"Hard Lead" Cylinder Brammer Cat. # IMN-PE1	99.36	0.59	0.053
"Hard Lead" Cylinder Brammer Cat. # IMN-PE2	99.27	0.50	0.27
"Hard Lead" Cylinder Brammer Cat. # IMN-PE3	99.13	0.38	0.49
"Hard Lead" Cylinder Brammer Cat. # IMN-PE4	98.99	0.31	0.70
"Hard Lead" Cylinder Brammer Cat. # IMN-PE5	98.90	0.21	0.89
"Hard Lead" Cylinder Brammer Cat. # IMN-PE6	99.07	0.40	0.53

Results and Discussion

A portion of the XRF spectrum of one of the "hard lead" standards (Catalog No. IMN-PE6 from Brammer Standards Co.) is given in Fig. 1. The spectrum was obtained by irradiation of the alloy for one hour. The vertical scale for the plot was chosen in order to expand the important fluorescence peaks from tin and antimony. Table 2 gives the assignment of the peaks of interest for lead, tin, and antimony.

Figure 2 gives the XRF spectrum of a particular sample of shotgun pellts (#6 shot from a 12 gauge Remington shell). As expected, comparison of the XRF spectrum of the shotgun pellets to that of the standard in Fig. 1 shows that the relative size of the peak for antimony has increased, while no peak occurs for tin in the spectrum of the shotgun pellets.

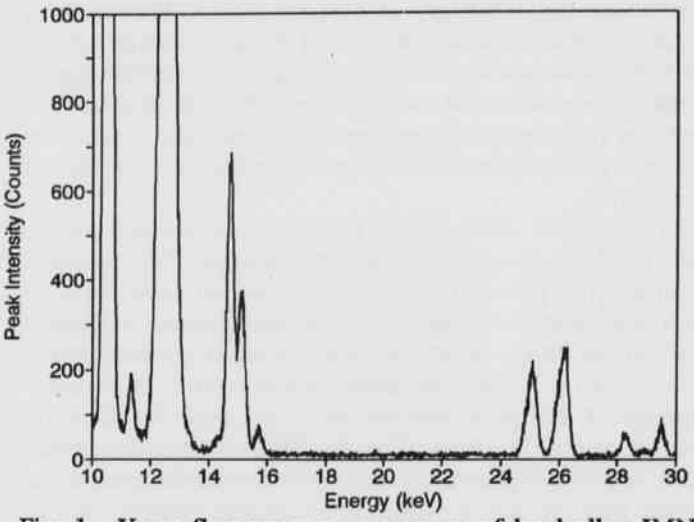

Fig. 1. X-ray fluorescence spectrum of lead alloy IMN-PE6.

Table 2. Peak assignment for XRF spectra of Pb, Sn, Sb alloys.

Energy (keV)	Assignment
10.6	lead - $L_{\alpha 1}$
12.6	lead - $L_{\beta 1}$
25.2	tin - $K_{\alpha 1,2}$
26.3	antimony - $K_{\alpha 1,2}$

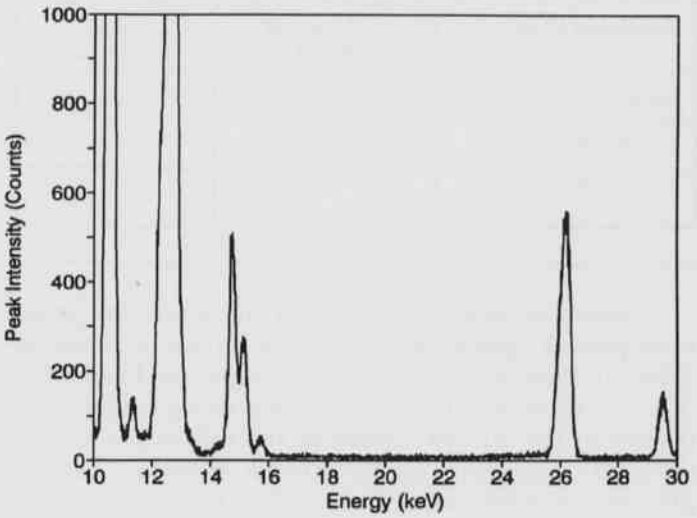

Fig. 2. X-ray fluorescence spectrum of remington #6 shot.

Ten spectra were taken for each sample in order to determine the reliability of measurements. The areas of peaks of interest were calculated for each sample from the ten spectra taken, along with averages of the areas. Typical standard errors were about 1% of the average values and repeated measurements after an interval of many months gave values in close agreement (less than 2% difference).

Peak areas were found to vary considerably as the nature of the sample's surface was changed. For example, compressing pellets into a disk caused all peak areas to increase. Such a behavior is entirely expected, since a greater surface area of the disk will be irradiated by the source and a larger fluorescence will result. As a consequence of this phenomenon an error arises in comparison of peak intensities between samples of different texture (e.g. - using a calibration plot prepared from standards that are metal cylinders to predict composition of shotgun pellets). In order to compensate somewhat for differences in sample texture, peak areas were scaled so that the elastic scattering (Rayleigh peak at 59.5 keV) from each spectrum had a value of 10,000 "counts." Table 3 compares "scaled" and "unscaled" areas for the antimony peak (26.3 keV) in one sample. Although the scaled value still differs from the value obtained for the compressed disk by about 10%, such an agreement is sufficiently close to distinguish many different shotgun pellets. Table 4 gives average areas and scaled areas for each of the standards. Ten spectra were obtained for each sample.

Table 3. Comparison of "scaled" and "unscaled" areas with changes in texture.

Remington #9 Shot	"Unscaled" Peak Area	"Scaled" Peak Area
Pellets	32,828	29,350
Compressed Disk	43,604	32,450
Percent Difference	25%	10%

Scaled and unscaled areas for the antimony peaks were plotted against percentages of antimony (listed in Table 1). Each gave an excellent straight-line fit (correlation coefficients > 0.9997). The plot using scaled areas (shown in Fig. 3) was chosen as the calibration plot in order to compensate for differences in texture of samples, as described above. The standard error (uncertainty in the value for area) according to the regression analysis was 1540 counts, a vertical distance on the plot which is less than half the height of the filled triangle marker.

Table 4. Intensities of peaks in standard alloys.

Sample Description	Average Area (59.5keV)	Scaled Area (59.5keV)	Average Area (26.3keV)	Scaled Area (26.3keV)
Brammer RPb 15/5	12,309	10,000	33,255	27,017
Nist 1132	13,101	10,000	220,315	168,167
Brammer 177/2	13,025	10,000	211,095	162,069
Brammer IMN-PE1	13,858	10,000	1,405	1,014
Brammer IMN-PE2	13,913	10,000	5,260	3,781
Brammer IMN-PE3	13,738	10,000	9,306	6,774
Brammer IMN-PE4	13,797	10,000	12,526	9,079
Brammer IMN-PE5	13,740	10,000	15,968	11,622
Brammer IMN-PE6	13,687	10,000	10,237	7,479

Inspection of Fig. 3 reveals the clear correlation of percent antimony with peak areas and, even though the available standards did not have percentages of antimony distributed evenly across the range of 0-10%, one expects the correlation to hold well throughout that range. In contrast, peak intensity at 12.6 keV could not be correlated well with percent of lead present. A plot of peak areas for lead (12.6 keV) versus percent lead for a number of standards is given in Fig. 4. Poor correlation may be due to a "saturation" that has occurred at higher concentrations. That is, a large concentration of lead present is quite efficient at absorbing the radiation, such that the amount of radiation absorbed does not increase linearly with increasing concentrations of lead.

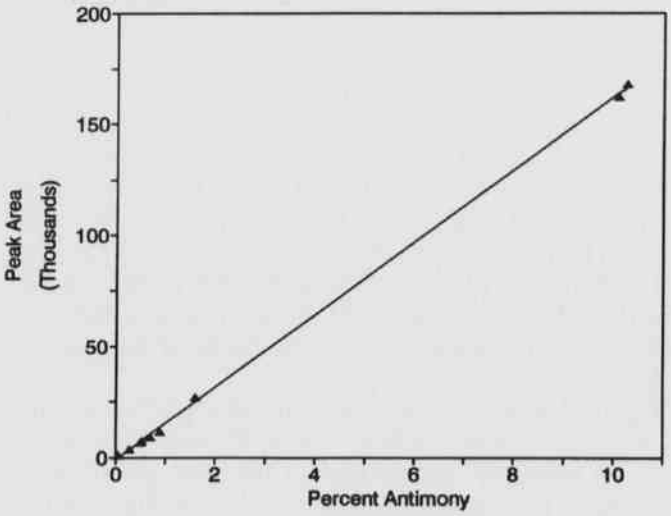

Fig. 3. Calibration plot of percent antimony vs. peak areas.

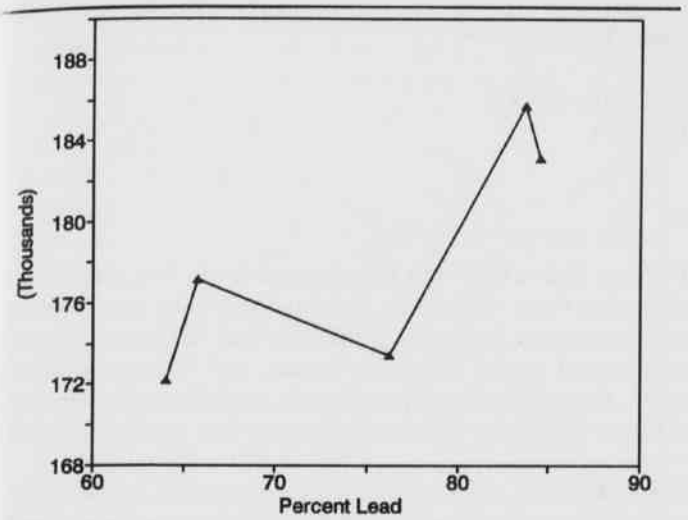

Fig. 4. Peak area from lead (12.6 keV) vs. percent lead.

Several different shotgun pellets were examined. The shot were donated by individuals or retail stores and were not identified other than by brand and shot size. The scaled areas of peaks from these shot are shown in Table 5, along with the percentages of antimony as predicted by the calibration plot.

Table 5. Comparison of spectra - shotgun pellets.

Sample Description	Pb Peak (12.6keV)	Sn Peak (25.2keV)	Sb Peak (26.3keV)	Percent Antimony
Federal No. 2	164463	0	8405	0.58
Peters Buckshot	160710	0	1523	0.16
Winchester No. 7.5	159620	0	17244	1.12
Remington No. 6	162167	0	22441	1.44

For these pellets, XRF measurements can clearly distinguish samples on the basis of peak intensity for antimony. According to information from Federal Cartridge Company (Gronfor, 1994), the less expensive shot ("promotional loads") have a lower percent antimony than the more expensive shot ("target loads"). Based on this information, the shot used in this study were likely the less expensive "promotional loads."

Acknowledgements

The authors would like to thank the University of Central Arkansas for its financial assistance, through the University Research Council, and the Arkansas Space Grant Consortium, for support throught a Faculty Enhancement Grant and Student Fellowship.

Literature Cited

Brunelle, R.L., C.M. Hoffman and **K.B. Snow.** 1970. Comparison of elemental composition of pistol bullets by atomic absorption. J. AOAC 53 (3) :470-474.

Grayson, M., editor. 1984. Kirk-Othmer concise encyclopedia of chemical technology, 3rd edition. Wiley, New York.

Gronfor, G. 1994. Personal Communication. Federal Cartridge Company, Anoka, Minnesota (Product Service Representative).

Jenkins, R., R.W. Gould and **D. Gedcke.** 1981. Quantitative X-ray spectrometry. Marcel Dekker, Inc., New York, 586 pp.

Johnson, G. Jr. and **E.W. White.** 1985. X-ray emission wavelengths and keV tables for nondiffractive analysis (ASTM Data Series DS 46). American Society for Testing and Materials.

Leyden, D.E. 1987. Energy-dispersive X-ray spectrometry. Spectroscopy. 2 (6) :28-36.

A Long-Term Study of Benthos in Dardanelle Reservoir

John D. Rickett and Robert L. Watson
Biology Department
University of Arkansas at Little Rock
Little Rock, AR 72204

Abstract

Winter, spring, summer, and autumn samples were collected with a 15.24x15.24-cm Ekman grab from five stations on Dardanelle Reservoir, Pope County, Arkansas during the 24-year period from 1970-1993. Twenty-three taxa representing the eight phyla, Cnidaria, Nematoda, Nematomorpha, Entoprocta, Ectoprocta, Mollusca, Annelida, and Arthropoda, were collected. Numerically, oligochaetes comprised 36%, whereas chironomid larvae, *Chaoborus* larvae, and *Hexagenia* naiads mad up 29.7, 17, and 12%, respectively, of the samples. Asiatic clams, fingernail clams, amphipods, and *Urnatella* were collected frequently during the last 10 years but were not abundant. Other taxa were taken infrequently but consistently during the study period.

Densities of all taxa fluctuated widely but generally not in close association with season, station, or year. A few significant differences (t-tests; α=0.05) occurred between stations 5 (discharge) vs. 16 (intake) and 5 vs. 21 (upstream control), but most of them were due to natural differences in substrate composition. Margalef's Richness and Shannon's Heterogeneity Indices did not identify any time-based trends and, with one exception, did not indicate any significant differences between stations.

Introduction

Dardanelle Reservoir was created about 1965 by Dardanelle Lock and Dam, a part of the Kerr-McClellan Navigation System build on the Arkansas River. The reservoir has a surface area of 13,720 ha, mean depth of 4.3 m, and volume of 656x10^6 m^3. The watershed of the reservoir proper (not including the river upstream) is approximately 40,000 ha, and the mean river discharge at the dam-sited gauging station is 1103 m^3/s. Dardanelle is a somewhat typical flow through reservoir with low velocity, having a mean residence time of 6.9 days (Rickett and Watson, 1985). The Illinois Bayou enters the north side of the reservoir approximately 5.6 km above the dam where a large, shallow (except for the Illinois Bayou channel) embayment is created, having physicochemical characteristics quite different from those of the Arkansas River mainstream.

Unit I of Arkansas Power and Light/Energy Corporation's nuclear generating station on Dardanelle Reservoir (Russellville, Arkansas) uses reservoir water for condenser cooling once-through at the approximate rate of 48 m^3/s when operating at optimal commercial capacity. In 1968 a project was begun to evaluate the impact of construction and operation of the plant on the ecological integrity of the reservoir. This project has generated previous reports addressing physicochemical characteristics (Rickett and Watson, 1985), the phytoplankton (Rickett and Watson, 1983a, 1992a), and the zooplankton (Rickett and Watson, 1983b, 1992b). In general, previous reports have documented considerable natural fluctuations in most physicochemical variables and plankton populations and have determined these natural variations exceeded impacts of the power plant construction and operation. This report describes the benthic community for the period 1970-1993.

Methods

Five sampling stations were established on Dardanelle Reservoir (Fig. 1). Stations 16 and 5 were at the mouths of the intake and discharge bays, respectively, Station 21 was an upstream control, Station 11 was a mid-reservoir control to monitor the extent of the discharge plume, and Station 15 was a downstream control established to detect any overall change of the reservoir water, if present.

Two samples were taken quarterly at each station from 1970 through 1993 with a tall 15.24 by 15.24-cm Ekman equipped with heavy duty closure springs. Samples were washed free of most sediment in a sieving bucket having a 0.5-mm mesh screen. Some sediment residue with organisms was transported to the lab in Whirlpak bags on ice. The organisms were sorted, identified, and counted as soon as possible. Specimens were preserved in 70% ethanol. Organisms were identified using Edmondson (1959) and Pennak (1989). Counts for each taxon were multiplied by 43.055 and recorded as organisms per square meter.

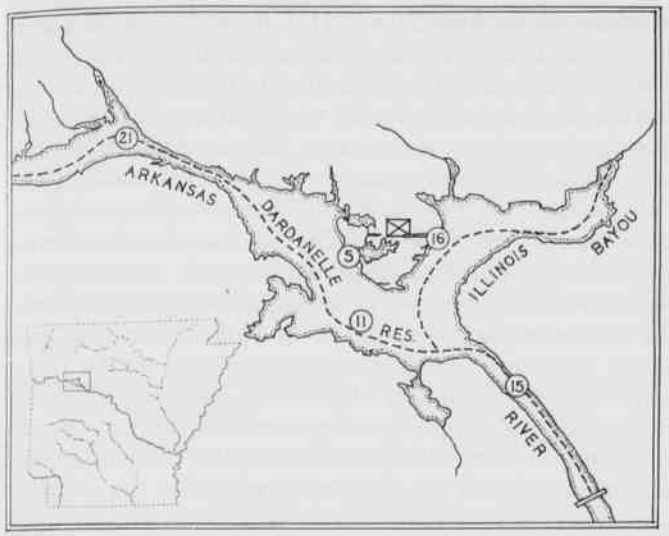

Fig. 1. Sampling stations on Dardanelle Reservoir, Arkansas, 1970-1993.

A description of the sediment and a battery of physicochemical variables in the water just above the sediment were recorded for possible correlation with variations in benthos abundance. Hutchinson's (1993) benthos categorization was also used to try to correlate abundance with preferred habitat, where known. Margalef's richness and Shannon's heterogeneity indices were calculated for each sample. Tests of significant difference were conducted to compare data between Stations 16 (intake) and 5 (discharge) and between 5 and 21 (upstream control). The F-statistic was used to check for similarity of internal variation of each data set pair. Then the Mann-Whitney U test or student's t-test was used to test for significant difference between data sets if the F test was or was not significant, respectively.

Results and Discussion

Sediment characterization.--Sediment at Stations 5 (mouth of discharge bay), 15 (downriver control), and 21 (upriver control) was dominated by finely divided, organic-rich silt, ideal for optimal reproduction and growth of most benthic organisms. At station 11 (mid-reservoir) sand was a significant component. In the vicinity of Station 11 some areas had sand overlying the silt, whereas in other areas the two strata were inverted. For any of these specific areas around Station 11, the sediment apparently shifted occasionally in response to velocity and discharge variations. At Station 16 (mouth of intake channel) the bottom contour was irregular, and hard clay with a few rocks (20-50 mm) overlain with woody detritus dominated the sediment. Prior to 1976 samples at Station 16 were taken a short distance within the intake mouth, but the removal of the softer silty components by the flow created by the Unit I intake pumps required that we move about 120 m further out into the reservoir.

Taxa, Abundance and Trends.--Twenty-five taxa representing eight phyla were recorded (Table 1). Aside from some seasonal variation, oligochaetes, chironomid larvae, *Chaoborus* larvae, and *Hexagenia* naiads were regularly abundant, together comprising 77.1 to 99.9% by number of all samples. Oligochaetes averaged 36%, whereas chironomids, *Chaoborus*, and *Hexagenia* averaged 29.7, 17, and 12%, respectively. The introduced Asiatic clam (*Corbicula fluminea*), fingernail clams (Sphaeriidae), amphipods (*Corophium*), and the entoproct, *Urnatella*, were collected frequently over the last 10 years but were not particularly abundant. Other taxa were taken infrequently but consistently during the 24-year period. All of the following abundance and diversity figures showed a sharp decline during 1975-77, apparently as a result of a chemical spill upstream from Dardanelle Reservoir (S. Hardin, pers. comm.), but the community recovered by 1979, exhibiting essentially the same abundance and diversity as before.

Table 1. Taxonomy of benthic organisms collected in Dardanelle Reservoir, 1970-1993.

Phylum	Class	Order	Family	Genus
Cnidaria	Hydrozoa			*Hydra*
Nematoda				
Nematomorpha				
Entoprocta				*Urnatella*
Ectoprocta				*Pectinatella*
Mollusca	Bivalvia		Corbiculidae	*Corbicula*
			Sphaeriidae	*Sphaerium*
			Unionidae	
	Gastropoda		Planorbidae	
			Pleurocercidae	*Pleurocerca*
Annelida	Oligochaeta			
	Hirudinea			
Arthropoda	Crustacea	Amphipoda	Corophiidae	*Corophium*
	Arachnida	Hydracarina		
	Insecta	Ephemeroptera	Ephemeridae	*Hexagenia*
			Caenidae	
		Odonata		
		Coleoptera	Elmidae	
		Diptera	Chaoboridae	*Chaoborus*
			Chironomidae	
			Heleidae	
		Megaloptera	Sialidae	*Sialis*
		Trichoptera		

The six categories of benthos recognized by Hutchinson (1993) are:

(1) haptobenthos – attached, sessile organisms
(2) lasion (=psudoperiphyton) -- organisms which move around among the haptobenthos
(3) eubenthos – crawlers on surface of sediment and objects
(4) nektobenthos – swimmers which may spend significant time in the water just above the substrate but feed on other benthos
(5) herpobenthos – those which burrow into the mud, usually in deeper areas
(6) psammon – those which burrow into sandy substrates, usually in shallower areas

Table 2 gives an adaptation of Dardanelle taxa to these categories based on known characteristics and stations of greatest or least abundance and on an evaluation of their adherence to predicted microhabitats.

Table 2. Benthos categorization after Hutchinson (1993), applied to Dardanelle Reservoir taxa, Arkansas, 1970-1993.

Haptobenthos	Lasion	Eubenthos
Hydra	Nematoda	Planorbidae
Urnatella	Nematomorpha	*Pleurocerca*
Pectinatella	Heleidae	snail
	some chironomids	Hirudinea
	Chaoborus	*Corophium*
	(occasionally)	Elmidae
		Chaoborus
		Trichoptera
Nektobenthos	**Herpobenthos**	**Psammon**
Hydracarina	*Corbicula*	*Hyallela*
Odonata	Sphaeriidae	
Sialis	Unionidae	
	Oligochaeta	
	Hexagenia	
	Caenidae	
	some chironomids	

The total range of the number of oligochaetes was zero to 11,322 per m², although most samples ranged from 80 to 2000. A standard error of 160 indicated wide variation among the samples. Annual means of abundance are given in Fig. 2. By averaging all seasons per year, Station 21 had the largest number 16 of 24 years, whereas Station 5 exhibited the fewest oligochaetes 13 of 24 years. Between 1978 and 1993, overall abundance of oligochaetes at all sampling stations rose and fell cylicly, but the overall rise was slightly more than the fall, exhibiting a long-term gradual increase (Fig. 3). The years 1988, 1989, 1991, and 1992 exhibited the greatest densities. Winter was generally the period of greatest abundance, while summer was the least (Fig. 4). According to Hutchinson's (1993) categorization scheme, oligochaetes are herpobenthos and should be found in greater densities at stations with abundant soft, silty sediment. This was true for Stations 15 and 21, but not 5. For the winter, spring, and autumn samples, the Mann-Whitney U test revealed significant differences ($\alpha = 0.05$) between Stations 5 and 21 (Table 2), with Station 21 consistently having the greater abundance. Substrate characteristics and physio-chemical variables were not essentially different between the two stations. Heated water should not have affected oligochaetes at Station 5 as the heated water from the power plant dispersed laterally and on top of the cooler reservoir water. The water temperature immediately above the substrate was not significantly different at the two stations. Perhaps more curious was the lack of significant difference of oligochaete abundance between the intake and discharge, regardless of the fact that the substrate was very different between the two stations and was less than ideal for oligochaete growth at the intake.

Table 3. Results of the F, t-, and Mann Whitney U tests on selected benthic taxa, Dardanelle Reservoir, Arkansas 1970-1993. (** = significant at α=0.05)

	station 5 vs. 16			station 5 vs. 21		
	F	t-test	MW-U	F	t-test	MW-U
Oligochaeta						
winter	**			**		**
spring	**			**		**
summer	**			**		
autumn				**		**
Chironomidae						
winter						
spring						
summer				**		**
autumn						
Chaoborus						
winter	**		**	**		**
spring						
summer	**			**		
autumn						
Hexagenia						
winter	**					
spring						
summer	**			**		
autumn				**		

The total range of chironomid abundance was zero to 1,938 per m², although most samples ranged between 300 and 800 (S.E. = 58) (Fig. 2). When seasons were combined, Station 15 exhibited the largest numbers 11 of the 24 years (Fig. 5), whereas the lowest abundance varied randomly among the other stations. When stations were combined, the winter samples contained the most chironomids 12 of the 24 years, and the samples with fewest varied randomly among the other seasons (Fig. 6). Only one of the eight Station 5 vs. 16 and 5 vs. 21 tests was significantly different (summer samples), with Station 5 having the greater number compared to Station 21. Of the eight tested pairs (see Table 2), more chironomids were collected at Station 5 than either Stations 16 or 21 seven

times, though not at significantly different numbers each time. There seemed to be an interaction occurring between chironomids and oligochaetes at Station 5. For most samples, particularly the high abundance years of 1988, 89, 91, and 92, when the oligochaete numbers were higher than the mean, the chironomid numbers were lower than the mean, and vice versa. This relationship was not apparent at the other stations, but additional data examination needs to be done. Chironomids are diverse enough to be categorized as herpobenthos, lasion, and probably psammon. Numbers collected at the various stations also reflected this diversity of microhabitat choice.

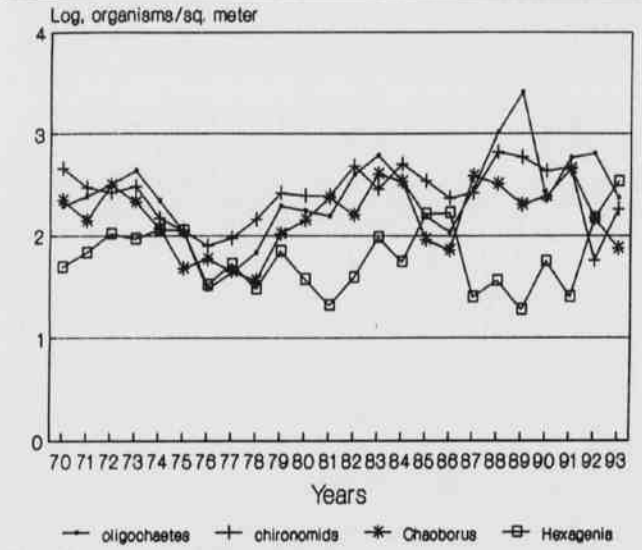

Fig. 2. Annual means of major taxa, I, Dardanelle Reservoir, Arkansas, 1970-1993.

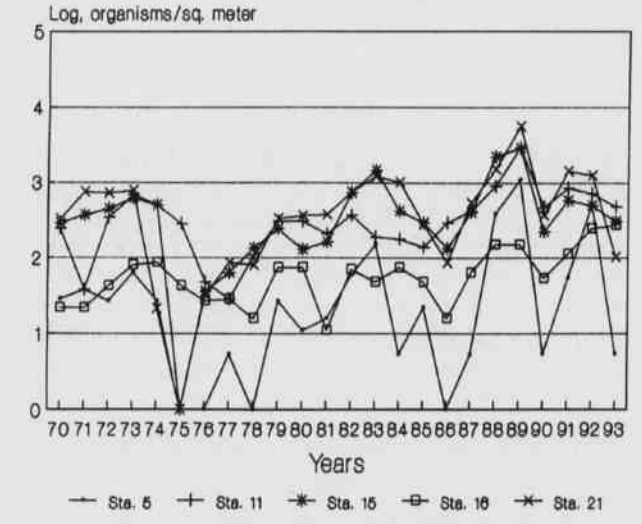

Fig. 3. Oligochaetes, means of all seasons per station, Dardanelle Reservoir, Arkansas, 1970-1993.

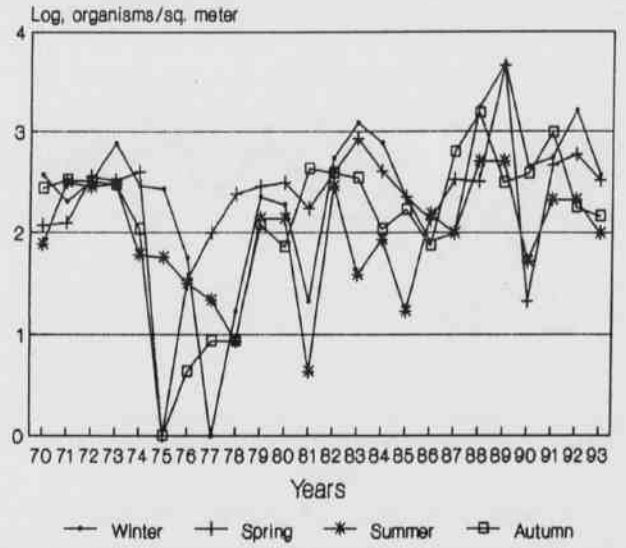

Fig. 4. Oligochaetes, means of all stations per season, Dardanelle Reservoir, Arkansas, 1970-1993.

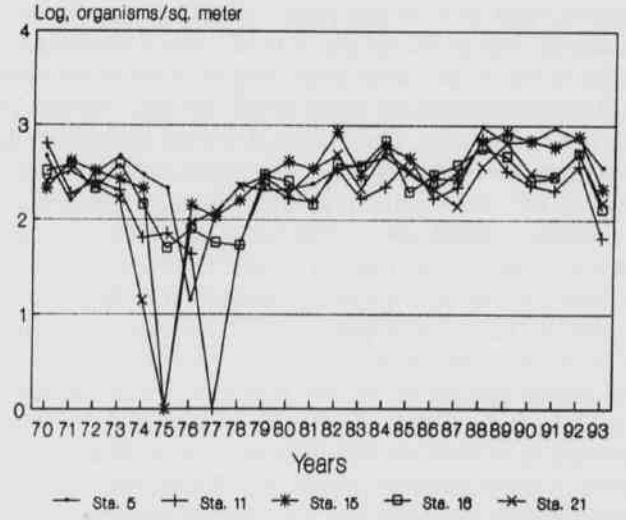

Fig. 5. Chironomids, means of all seasons per station, Dardanelle Reservoir, Arkansas, 1970-1993.

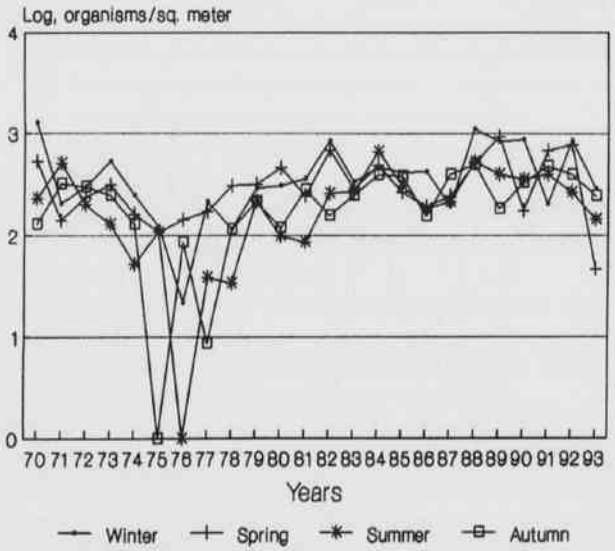

Fig. 6. Chironomids, means of all stations per season, Dardanelle Reservoir, Arkansas, 1970-1993.

The total range of *Chaoborus* larvae numbers was zero to 2,670 per m², but most samples contained approximately 40-400 (S.E. = 48) (Fig. 2). When seasons were combined, the greatest abundance were recorded at Station 15 for 17 of the 24 years (Fig. 7). Station 11 exhibited the lowest numbers eight of the 24 years. When stations were combined, *Chaoborus* were most abundant during autumn 13 of the 24 years and least abundant during spring 11 of the 24 years. (Fig. 8). Only during the winter were there significant differences (α=0.05) between Stations 16 vs. 5 and 5 vs. 21 (Table 2). Station 5 of the first pair and station 21 of the second pair had greater abundance. The relative paucity of *Chaoborus* at station 16 was apparently due to the scoured clay substrate covered with coarse pieces of woody detritus. In the study of other lakes (Lake Maumelle, for example), we have observed that fine woody debris may encourage the growth of the *Chaoborus* population. *Chaoborus* is primarily a eubenthic predator but may occasionally search for prey around sessile organisms and, therefore be classed as lasion. Their use of these microhabitats was supported by our data. Most peaks of abundance were at stations with soft, silty sediment (Stations 5, 15, and 21), but occasionally we collected large numbers at station 16 where they may have been cruising the attached *Urnatella* colonies for prey.

The total abundance range of *Hexagenia* naiads was zero to 2,412 per m², whereas, most samples contained 10 to 200 individuals (S.E. = 57) (Fig. 2). Years of greatest abundance were 1985, 86, 92, and 93. When stations were combined and seasons were combined, both exhibited about equal frequencies of greatest and least abundance (Fig. 9 and 10, respectively). Stations 16 vs. 5 and 5 vs. 21 did not exhibit significant differences, although mayfly collections at Stations 16 and 21 were less consistent than at Station 5 (Table 2). Winter and spring samples more consistently contained naiads than summer and autumn samples. Hutchinson's (1993) classification scheme would determine *Hexagenia* as herpobenthos (burrowers in mud), and our data revealed greatest densities were observed most frequently at Station 15 where soft, silty sediment was abundant.

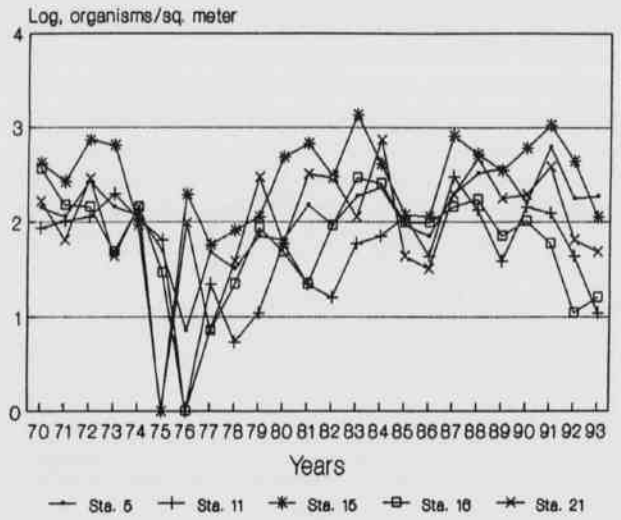

Fig. 7. *Chaoborus*, means of all seasons per station, Dardanelle Reservoir, Arkansas, 1970-1993.

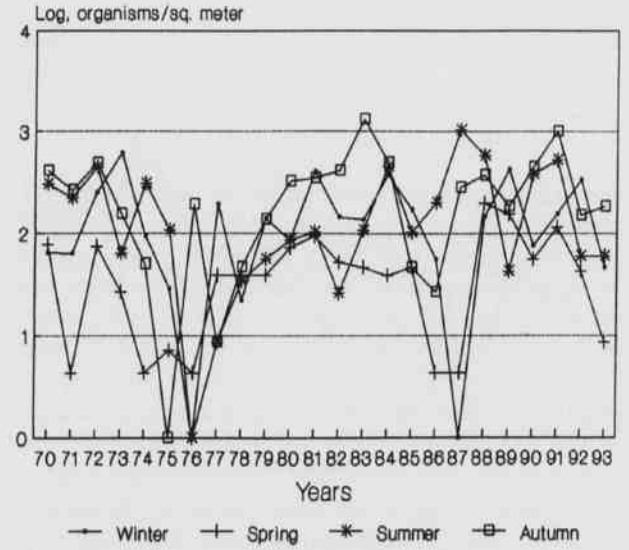

Fig. 8. *Chaoborus*, means of all stations per season, Dardanelle Reservoir, Arkansas, 1970-1993.

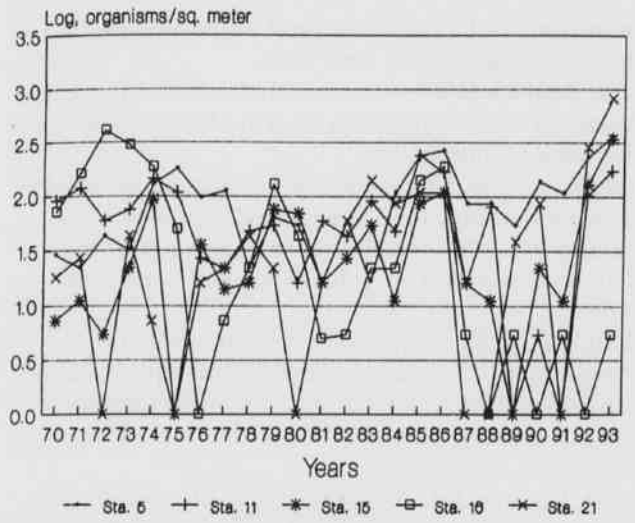

Fig. 9. *Hexagenia*, means of all seasons per station, Dardanelle Reservoir, Arkansas, 1970-1993.

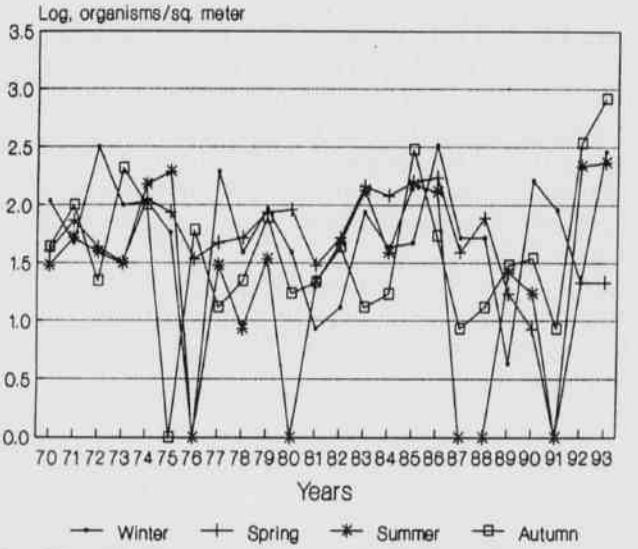

Fig. 10. *Hexagenia*, means of all seasons per station, Dardanelle Reservoir, Arkansas, 1970-1993.

The Asiatic clam, *C. fluminea*, was first collected in 1983, reached greatest abundance during that year and 1984, then declined and was represented by a sporadic appearance in the samples during alternate years until 1993 (Fig. 11). At present their abundance seems to be low but holding steady. Fingernail clams, *Sphaerium*, were present throughout the study period, and their numbers increased rather steadily from 1983 to 1993 (Fig. 11). The presence of Asiatic clams in Dardanelle has not reduced the population of fingernail clams as they did in the Saline River (Rickett, 1989).

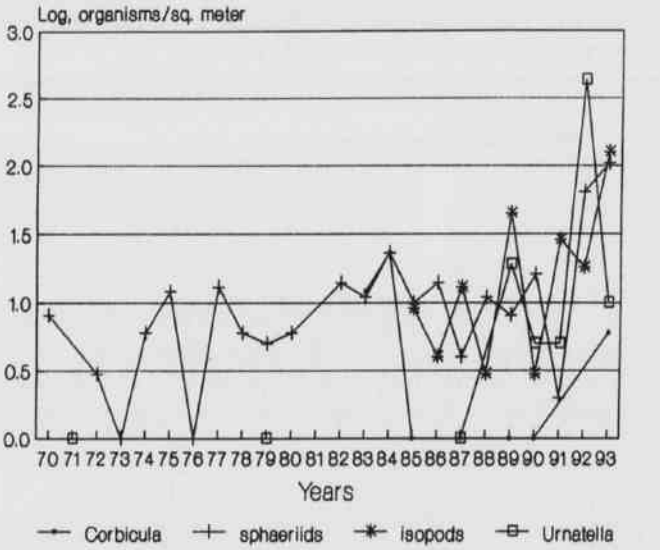

Fig. 11. Annual means of major taxa, II, Dardanelle Reservoir, Arkansas, 1970-1993.

The estuarine amphipod, *Corophium lacustrae*, was first collected in 1985, reached a peak of abundance in 1986-87, declined through 1988-91, and increased strongly again 1992-93 (Fig. 11). Amphipods were consistently most numerous at Station 16 (mouth of the intake channel), except during 1993 when we apparently took an aggregation of juveniles which had not yet dispersed at Station 11. This euryhaline species has been historically characteristic of tidal mud flats and open bay bottoms along the Louisiana and Texas coasts (Heard, 1982), and its presence here represents a significant range extension.

The colonial entoproct, *Urnatella*, was first collected in low numbers in 1971, but no additional specimens were taken from 1972-78. They were present again in 1979, absent from 1980-86, present again in 1987, and have been generally increasing in number since 1987 (Fig. 11). Prior to 1993 they were, with few exceptions, taken only at Station 16. *Urnatella* colonies were usually found attached to pieces of woody detritus, and to the extent such material occurs in other areas of the reservoir, they are probably spreading.

Diversity Indices.--Margalef's Richness and Shannon's Heterogeneity Indices were calculated to try to identify trends or significant differences between stations regarding benthic community diversity. Margalef's index considers the number of taxa and the number of individuals comprising those taxa, whereas Shannon's index also considers how the individuals are distributed among the taxa. Both indices exhibited many fluctuations but no discernable trends over time. With one exception no significant differences between the station pairs 5 vs. 16 and 5 vs. 21 were observed for either index. The exception was

Shannon's Heterogeneity comparison between Stations 5 vs. 21 for winter samples; at Station 5 bethos was more heterogenous than at Station 21 (Fig. 12).

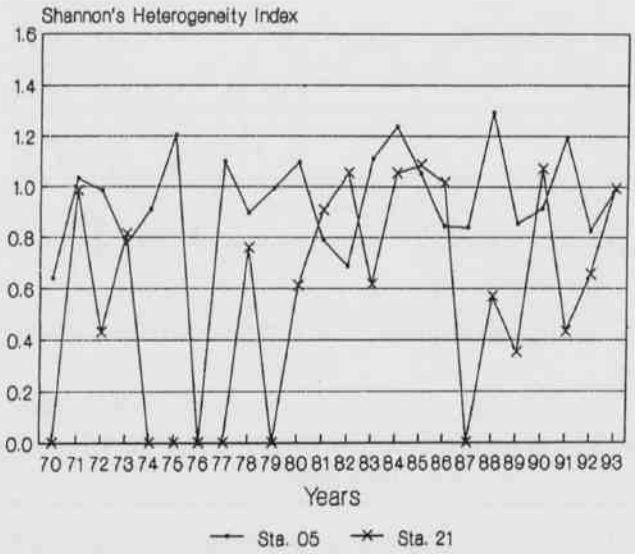

Fig. 12. Shannon-Weiner Heterogeneity Index, winter bethos, Dardanelle Reservoir, Arkansas, 1970-1993.

Summary

Twenty-three taxa representing eight phyla were collected at five stations over a 24-year period in Dardanelle Reservoir. Sample densities varied widely, but overall, oligochaetes comprised 36%, chironomid larvae 29.7%, *Chaoborus* larvae 17%, and *Hexagenia* naiads 12%. Asiatic clams, fingernail clams, isopods, and *Urnatella* mad up most of the remaining 5.3% particularly during the most recent 10 years, whereas the remaining 16 taxa occurred consistently but in low numbers. Within the four most numerous taxa, six significant differences occurred between station pairs (5 vs. 16 and 5 vs. 21), but these were due primarily to innate differences in substrate quality. Community diversity, as indicated by Margalef's Richness and Shannon's Heterogeneity, fluctuated widely but did not exhibit any time-based trends. With one exception (winter samples, Station 5 vs. 21) no significant differences of diversity between stations were observed.

Acknowledgements

The authors wish to thank Energy Corporation, formerly Arkansas Power & Light Company, for funding this project. We also thank the personnel at Arkansas Nuclear One for their cooperation.

Literature Cited

Edmondson, W.T., ed. 1959. Freshwater biology, 2nd ed. John Wiley and Sons, New York.

Heard, R. 1982. Guide to common tidal marsh invertebrates of the northeastern Gulf at Mexico. Miss-Ala Sea Grant Consortium.

Hutchinson, G.E. 1993. Treatise on Limnology, vol. IV: The zoobenthos. John Wiley and Sons, New York.

Pennak, R.W. 1989. Freshwater invertebrates of the United States, 3rd ed. John Wiley and Sons, New York.

Rickett, J.D. 1989. Dispersal and abundance of the Asiatic clam, *Corbicula fluminea*, in the upper Saline River, southcentral Arkansas. Poster presented at annual meeting of Amer. Soc. Limn. and Oceanogr., Fairbanks, Alaska.

Rickett, J.D. and **R.L. Watson.** 1983a. Phytoplankton community structure in Dardanelle Reservoir, Arkansas. 1975-82. Proc. Arkansas Acad. Sci. 37:70-73.

Rickett, J.D. and **R.L. Watson.** 1983b. Zooplankton community structure in Dardanelle Reservoir, Arkansas, 1975-82. Proc. Arkansas Acad. Sci. 37:65-69.

Rickett, J.D. and **R.L. Watson.** 1985. Fluctuations and relationships of selected physicochemical parameters in Dardanelle Reservoir, Arkansas, 1975-82. Proc. Arkansas Acad. Sci. 39:98-102.

Rickett, J.D. and **R.L. Watson.** 1992a Phytoplankton community abundance and diversity in Dardanelle Reservoir, Arkansas, 1981-90. Proc. Arkansas Acad. Sci. 46:53-56.

Rickett, J.D. and **R.L. Watson.** 1992b. Zooplankton community abundance and diversity in Dardanelle Reservoir, Arkansas, 1981-90. Proc. Arkansas Acad. Sci. 46:57-60.

Thermal Decomposition Studies of Selected Transition Metal Polysulfide Complexes. II. Effect of Atmosphere on Decomposition

Benjamin Rougeau and M. Draganjac
Department of Chemistry and Biochemistry
Arkansas State University
State University, AR 72467

Abstract

Initial studies involved the thermal decomposition profile of five polysulfide complexes in air up to 550°C. Since our first report to the Academy in 1990, we have obtained the capability to run samples up to 1500°C under various gases. Thermal Gravimetric Analysis (TGA) and Differential Thermal Analysis (DTA) of a series of transition metal polysulfide complexes are presented. Compounds analyzed included Cp_2TiS_5, MoS_9^{2-}, $MoOS_8^{2-}$, $Zn(S_x)^{2-}$, $Cd(S_x)^{2-}$, $Fe_2S_{12}^{2-}$ and NiS_8^{2-}.

Introduction

Binary and tertiary metal sulfides have many important uses including catalysis, batteries and electrical devices (Greenwood and Earnshaw, 1984). More efficient methods for preparing these materials may employ the use of a large class of compounds known as transition metal polysulfides as precursors. Though polysulfide complexes are known for most transition metals (Draganjac and Rauchfuss, 1985), few studies have focussed on the reactivity and applicability of these compounds. Our interests involve possible use of metal polysulfides as sulfur transfer reagents, particularly in the vulcanization of rubber. To understand their usefulness in this capacity, we have begun a systematic study of the thermal stability of a series of transition metal polysulfides. Herein, we report on the thermal decomposition profiles for several of the transition metal polysulfide complexes.

Methods and Materials

Reactions were carried out on a dual manifold vacuum line using Schlenk techniques, Kewaunee Inert Atmosphere Box or in a Vacuum Atmosphere Dual Station Dry-Box under N_2. Reagents were used as purchased without further purification. Polysulfide complexes were prepared as described in the literature: Cp_2TiS_5 (Kopf et al., 1968), $(Et_4N)_2MoS_9$, $(Ph_4P)_2MoOS_8$ (Draganjac, 1983), $(Ph_4P)_2Fe_2S_{12}$ (Coucouvanis et al., 1979), $(Et_4N)_2ZnS_8$, $(Ph_4P)_2CdS_{10}$ and $(Ph_4P)_2NiS_8$ (Coucouvanis et al., 1985). The polysulfide complexes were characterized and compared with literature values to assure the identity of the products before thermal analysis. Thermal gravimetric analyses (TGA) were obtained on a Seiko TG/DTA 320 instrument. All samples were run at heating rates of 20°C/min up to 1000°C. Gas flow rates (either air or N_2) were set at 300 mL/min. Scanning Electron Microscopy (SEM) X-ray Fluorescence measurements were obtained on a JEOL-100CX II with Tracor Northern 2000 X-ray detection system.

Results and Discussion

Depending on the atmosphere employed (air vs. nitrogen), differences occurred in the thermal decomposition of the transition metal polysulfides. All of the samples run in air flow showed exothermic behavior in the Differential Thermal Analysis (DTA). This could be explained by the burning of the C- and S-containing moieties. The differences in the mass loss can also be explained by the reaction of O_2 with the polysulfide complexes.

Figure 1 shows the Thermal Gravimetric Analysis (TGA) curves for Cp_2TiS_5. Under N_2, a total of 33.7% mass loss has occurred by 1000°C. The compound is still losing mass at this temperature. Loss of two $CpS_{1.5}$ units and subsequent coupling of the remaining Ti fragments to give to Cp_2TiS_7 species would account for 33.5% mass loss. Giolando and Rauchfuss (1984) have demonstrated Cp migration from the Ti in Cp_2TiS_5 to the pentasulfide ring at elevated temperature (boiling xylenes, b.p. 137-144°C for 24 hr under N_2). Mass change in Cp_2TiS_5 begins at 132°C. Further decomposition to TiS_x would be expected at higher temperatures. In air, the total mass loss of 77.8% approximates the formation of TiO_2 (76.4%). The decomposition left a white powder in the sample pan. SEM X-ray fluorescence measurements showed presence of Ti and a trace of S. A large exotherm at 563.9°C is seen in the DTA plot for Cp_2TiS_5 in air.

Figure 2 shows the TGA curves for $(Et_4N)_2MoS_9$. In N_2, beginning at 153.0°C, a total mass loss of 67.0% is observed. SEM measurements show only Mo. Due to

overlap of the Mo and S peaks, it is not possible to conclude the presence of S. The gray appearance of the decomposition product suggests MoS_x. Calculations based on MoS_3 would indicate a 70.2% mass loss. An extremely bad odor was given off during this reaction. In air, MoS_9^{2-} shows a step-wise decomposition. The first step at 183.5°C could be a possible loss of two Et_3N and five eq. of S atoms leaving $(EtS)_2MoS_2$ (56.2% loss). Further heating associated with the exotherm at 579.5°C is explained by the formation of MoO_3. A small endotherm corresponds with the melting of MoO_3 at 795°C. Under the flow of air, possibly the MoO_3 is vaporized, explaining the total mass loss of 98.5%.

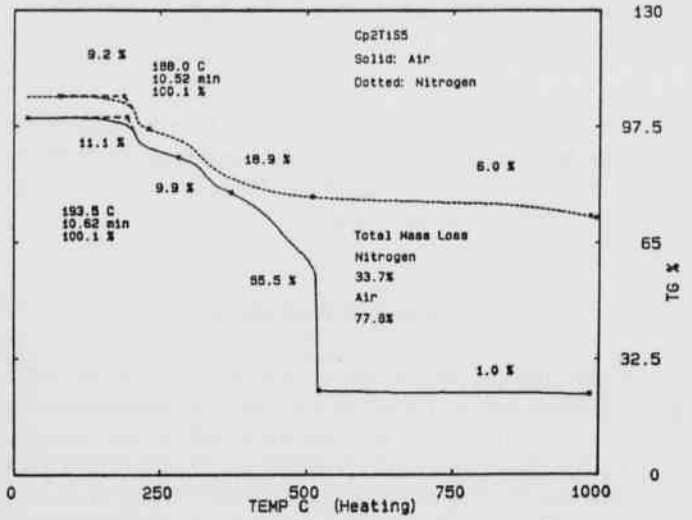

Fig. 1. TGA curves for Cp_2TiS_5. The air curve has been offset by -6%.

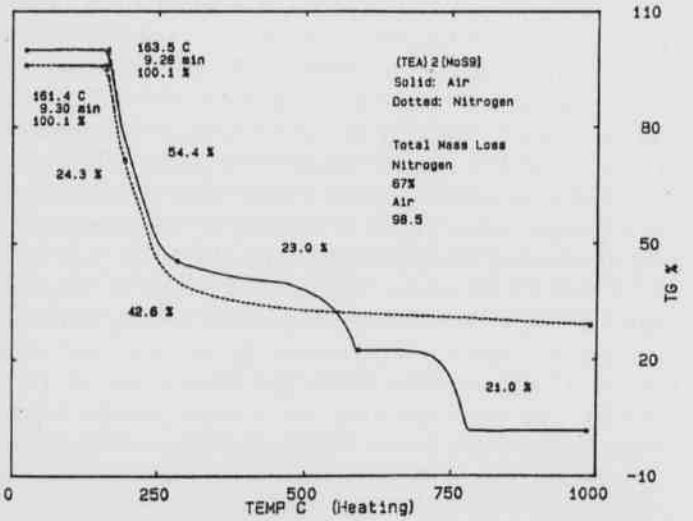

Fig. 2. TGA curves for $(Et_4N)_2MoS_9$. The N_2 curve has been offset by -4%.

The TGA curves for $(Ph_4P)_2Fe_2S_{12}$ (Fig. 3) show greater mass loss for the run under N_2 than in air. Under N_2, the final product appears to be FeS_2. The total mass loss of 80.6% agrees with the calculated value of 80% for the iron disulfide. In air, the decomposition product had a reddish color and the SEM showed only the presence of Fe and P. A mixture of iron oxides and phosphates is proposed at this time. Further study of the decomposition products is underway.

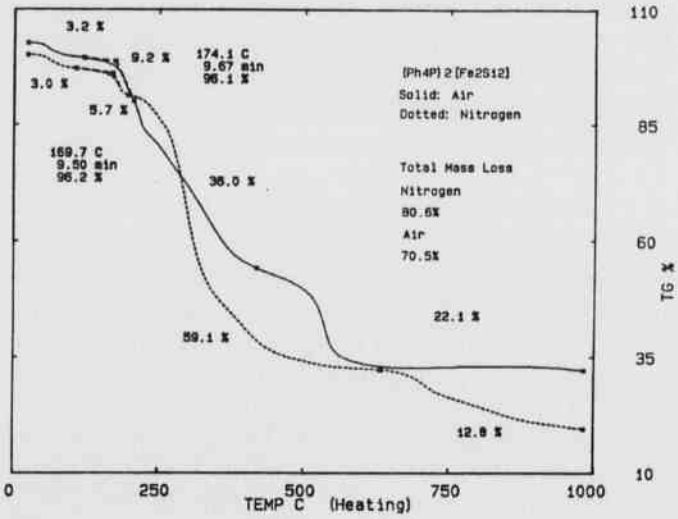

Fig. 3. TGA curves for $(Ph_4P)_2Fe_2S_{12}$. The N_2 curve has been offset by -2.5%.

The decomposition curves for $(Ph_4P)_2MoOS_8$ (Fig. 4), $(Et_4N)_2ZnS_8$ (Fig. 5), $(Ph_4P)_2CdS_{10}$ (Fig. 6) and $(Ph_4P)_2NiS_8$ (Fig. 7) are shown for comparison. Calculations based on expected products do not conform to total mass loss for these four compounds.

The authors caution the readers that the proposed intermediate and product structures in the discussion above are speculative at best. Attempts to isolate and characterize the intermediates and final decomposition products for all seven of the polysulfide complexes will be undertaken. The main intent of this report is to show the effect of differing atmospheres on the decomposition profiles. Due to their ease of preparation, Cp_2TiS_5 and $(Et_4N)_2MoS_9$ are currently being tested for their ability to vulcanize rubber.

Acknowledgements

Funding for the TG/DTA provided by the National Science Foundation (Grant No. DUE-9351560).

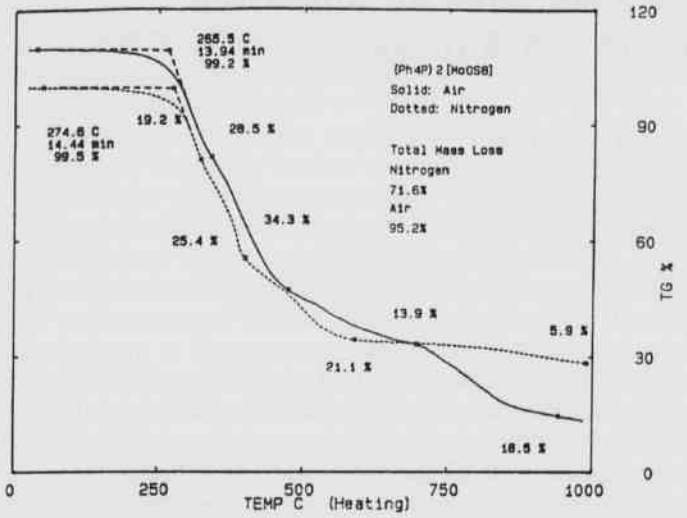

Fig. 4. TGA curves for $(Ph_4P)_2MoOS_8$. The air curve has been offset by +5%.

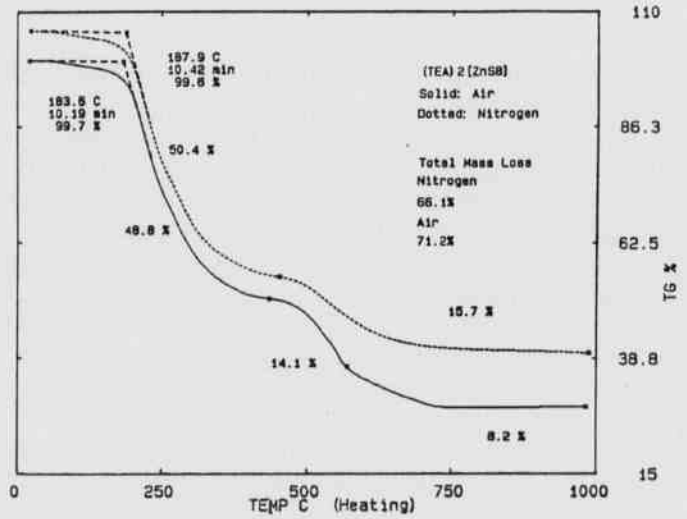

Fig. 5. TGA curves for $(Et_4N)_2ZnS_8$. The N2 curve has been offset by +6%.

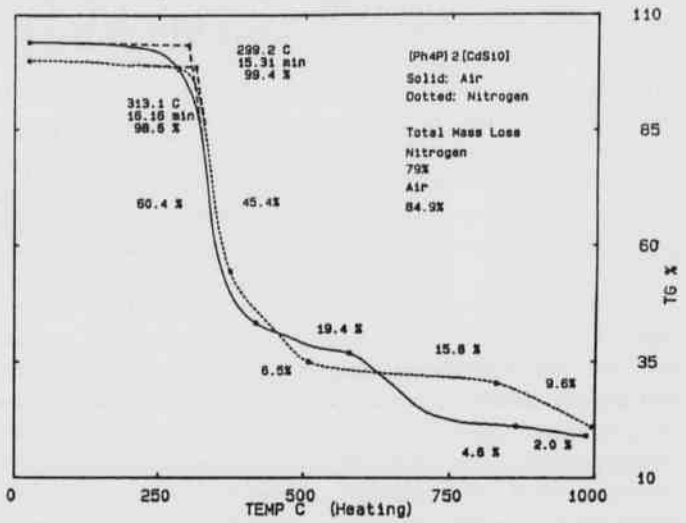

Fig. 6. TGA curves for $(Ph_4P)_2CdS_{10}$. The air curve has been offset by +5%.

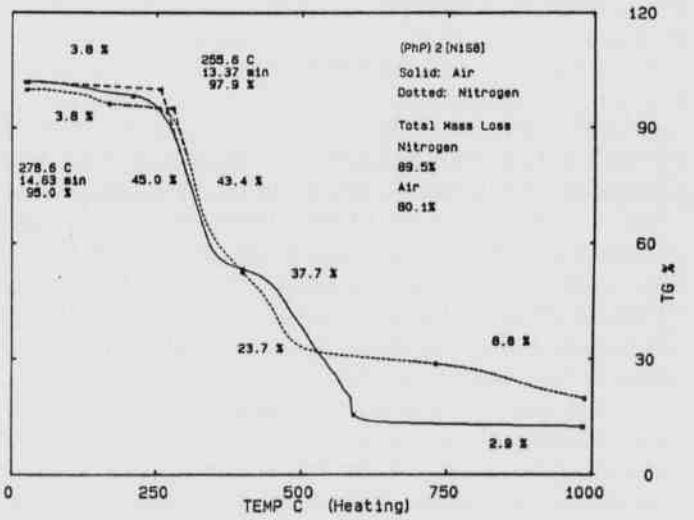

Fig. 7. TGA curves for $(Ph_4P)_2NiS_8$. The air curve has been offset by +2%.

Literature Cited

Coucouvanis, D., D. Swenson, P. Stremple and **N.C. Baenziger.** 1979. Reaction of $[Fe(SC_6H_5)_4]^{2-}$ with organic trisulfides and implications concerning the biosynthesis of ferredoxin. Synthesis and structure of $[(C_6H_5)_4P]_2Fe_2S_{12}$ complex. J. Am. Chem. Soc. 101:2293-3393.

Coucouvanis, D., P.R. Patil, M.G. Kanatzidis, B. Detering and **N.C. Baenziger.** 1985. Synthesis and reactions of binary metal sulfides. Structural characterization of the $[(S_4)_2Zn]^{2-}$, $[(S_4)_2Ni]^{2-}$, $[(S_5)Mn(S_6)]^{2-}$, and $[(CS_4)_2Ni]^{2-}$ anions. Inorg. Chem. 24:24-31.

Draganjac, M. 1983. Synthesis, structure and reactivity of binary molybdenum sulfur compounds. Ph.D. Thesis, University of Iowa.

Draganjac, M. and **T.B. Rauchfuss.** 1985. Transition metal polysulfides: coordination compounds with purely inorganic ligands. Angew. Chem. Int. Ed. Engl. 24: 742-757.

Giolando, D. and **T.B. Rauchfuss.** 1984. Rearrangement of $(C_5H_5)_2TiS_5$ involving migration of the organic fragment from metal to sulfur. J. Am. Chem. Soc. 106:6455-6456.

Greenwood, N.N. and **A. Earnshaw.** 1984. Chemistry of the elements. Pergamon Press, Tarrytown, New York, 1542 pp.

Kopf, H., B. Block and **M. Schmidt.** 1968. Di-π-cyclopen tienyl-titan(IV)-pentaselenid und -pentasulfd, zwei hetero-cyclo-hexachalkogene in fixierter konformation. Chem. Ber. 101:272-276.

The Vegetation of Maple-leaved Oak Sites on Sugarloaf and Magazine Mountains, Arkansas

David W. Rouw and George P. Johnson
Department of Biological Sciences
Arkansas Tech University
Russellville, AR 72801

Abstract

We conducted an analysis of the vegetation of the maple-leaved oak sites on Sugarloaf and Magazine Mountains, Arkansas, during September and October of 1993. The woody vegetation was sampled using the point-quarter method; on Sugarloaf Mountain five transects were sampled (950 m) and on Magazine Mountain four transects were sampled (710 m). Soil samples from each site were collected and analyzed for 15 factors. In total 27 species were recorded and measured for both sites, 18 for Sugarloaf and 19 for Magazine. The Sugarloaf site can be described as a *Quercus-Juniperus* community and the Magazine site can be described as a *Juniperus-Carya-Fraxinus* community. Qualitative observations for the maple-leaved oak sites on Porter and Pryor Mountains, Arkansas, are also included.

Introduction

Until 1991 the maple-leaved oak (*Quercus shumardii* Buckl. var. *acerifolia* Palmer) was only known from Magazine Mountain, Logan County, Arkansas (Palmer, 1927). Discoveries on Pryor Mountain, Montgomery County and Sugarloaf Mountain, Sebastian County (Johnson, 1992) extended the known sites to three. In 1993 an additional population was discovered on Porter Mountain, Polk County, bringing the total known populations to four (Johnson, 1994).

Only one of these sites, Magazine Mountain in the Ozark National Forest, has been studied; these studies include Pyle's study of the herbaceous flora (1939) and Tucker's classification of the plant communities and habitat types of the slopes and plateau surface (1989). Tucker included the maple-leaved oak in the Mesic Bluffline Community and noted the probable occurrence of impure limestone in the rock underlying this community type. Tucker suggested that there may be a correlation between the presence of limestone and the high species diversity in that area. The soils associated with this community are of the Linker and Nella-Mountainburg Associations (U.S.D.A., 1975a).

The Sugarloaf site was briefly described by Johnson (1992). Unlike the Magazine site, this site is a xeric, east-facing bluffline and an adjacent, highly-eroded glade-like area. The soils are thin, have a significant shale component, and are of the Enders-Mountainburg Association (U.S.D.A., 1975b).

The Pryor and Porter Mountain sites in the Ouachita National Forest are physically similar, i.e. steep novaculite glades, and each supports few maple-leaved oak plants. The Pryor site supports a population of *Polymnia cossatotensis* (Johnson, 1992), which occurs on basic soils (Bates and Pittman, 1991).

We conducted this study to: 1) qualitatively and quantitatively document the woody vegetation of the two largest population sites of the maple-leaved oak; 2) determine the similarities and differences in the vegetation of these two sites; 3) determine if soil factors, especially pH play a role in the oak's distribution; 4) develop a list of species associated with the Maple-leaved oak so that the occurrence of new sites may be predicted more accurately; and, 5) provide a baseline for detecting changes in these communities over time. The oak site on Sugarloaf is privately owned and the Magazine site has been proposed as the site of a state park (Gandy et al., 1993).

Materials and Methods

Sampling took place during September and October of 1993 and utilized the point-quarter method (Mueller-Dombois and Ellenberg, 1974). For each species encountered, number of points of occurrence, number of individuals, and total basal area were measured. These data were used to calculate relative frequency, relative density, relative dominance, and importance value. On Sugarloaf, the five transects that were sampled were chosen to represent the extent of the vegetation and topography of the oak population. Three transects paralleled the bluffline (topographically below, at, and above the bluffline) (200 m each) and two ran perpendicular to the bluffline (210 and 140 m). At the Magazine site, four transects were sampled representing the Brown's Spring and Dripping Springs Oak populations. Three transects paralleled the bluffline (two topographically at the bluffline and one

above) (270, 80, and 180 m, respectively) and one ran perpendicular to the bluffline (180 m). All transects were sampled at 10 m intervals.

Soil samples from the upper 20 cm of the soil profile were taken along the transects at points representative of variations in elevation, topography, soil type and appearance, and vegetational composition. The samples included: Sugarloaf (10 samples), Magazine (6 samples), Pryor (1 sample), and Porter (1 sample). They were analyzed by the Arkansas Agricultural Extension Service Soil Testing Laboratory at Fayetteville, Arkansas. Analysis included the following factors: pH, percent organic matter (P.O.M.), P, K, Ca, Na, Mg, SO_4-S, Fe, Mn, Cu, Zn, NO_3-N, cation exchange capacity (C.E.C.), and percent base saturation (% B.S.). References used for identification and nomenclature were Radford et al. (1968), Tucker (1976), Smith (1988), Preston and Wright (1988), and Harlow et al. (1991).

Results and Discussion

Soils.--Soil sample data are presented in Table 1. The soils for all sites were moderately acidic, and pH decreased as altitude decreased at the Sugarloaf and Magazine sites. The lowest pH, 4.1, was recorded on Magazine in moist, rich soil on the upper slope below the bluffline. Our initial thoughts that the distribution of maple-leaved oak might be correlated with near-neutral or basic soils were not supported by the data, although the oaks may be influenced by high pH material not evident in the surface soil layer.

Vegetation.--In total 27 species were recorded and measured for both sites, 18 for Sugarloaf and 19 for Magazine (Tables 2 and 3, respectively). On Sugarloaf *Q. stellata* represented one-third, *Q. shumardii* var. *acerifolia* and *Juniperus virginiana* represented another one-third, and the other 15 species represented the final one-third of the total importance value. As a result, the woody vegetation of Sugarloaf's maple-leaved oak habitat can be characterized as a *Quercus-Juniperus* community, consisting of many smaller plants with a number of larger specimens of *Q. stellata* and *J. virginiana* interspersed among them. The latter point is evident when comparing the number of trees and total basal area for *Q. stellata* (123 trees, 27.38 sq. m) with *Q. shumardii* var. *acerifolia* (100 trees, 14.24 sq. m) and *Q. marilandica* var. *ashei* (36 trees, 1.67 sq. m). The largest maple-leaved oak plants were found on the summit and also on the upper slopes below the bluffline along with larger specimens of *Q. rubra, Q. muehlenbergii,* and *Carya tomentosa*.

On Magazine, *J. virginiana* represented one-third, *C. texana, Fraxinus americana, C. glabra,* and *Q. shumardii* var. *acerifolia* represented another one-third, and the other 14 species represented the remaining one-third of the total importance value. As a result, the woody vegetation of Magazine's maple-leaved oak habitat can be characterized as a *Juniperus-Carya-Fraxinus* community. Four zones of woody vegetation were encountered proceeding from the bluffline on the perpendicular transect: 1) *Q. shumardii* var. *acerifolia, Q. stellata, C. texana,* and low *Vaccinium;* 2) *Q. shumardii* var. *acerifolia, J. virginiana, Fraxinus americana, Chionanthus virginicus,* and *Amelanchier arboreum*; 3) *J. virginiana*; and, 4) *Q. alba, Q. velutina,* and clumps of *C. glabra* with understory species *Ostrya virginiana* and *Robinia pseudoacacia. Juniperus virginiana* was ubiquitous, and the larger maple-leaved oaks were found in zone 2 a short distance from the bluffline within the encroaching trees.

In comparison there are some notable differences between these two maple-leaved oak sites and their vegetation. First, three species very common on Sugarloaf, *Q. stellata, Q. shumardii* var. *acerifolia,* and *Q. marilandica* var. *ashei,* are much less common on Magazine. Second, Sugarloaf is more open with smaller trees; this is consistent with Sugarloaf's smaller values for trees/ha and basal area/ha (Tables 2 and 3). Third, Sugarloaf supports an Oak population of over 350 plants while Magazine supports a population of approximately 200 individuals. Fourth, the average oak on Magazine (.214 sq. m/tree) is larger than on Sugarloaf (.142 sq. m/tree). Magazine has a smaller population of larger individuals with the larger individuals located mainly 10-15 m above the bluffline. Conversely, Sugarloaf has a larger population of smaller

Table 1. Soil sample data for maple-leaved oak sites.

Site	Number of soil samples	pH range	% Organic Matter (P.O.M.)	P (ppm)	K (ppm)	Ca (ppm)	Mg (ppm)	Na (ppm)	SO_4-S (ppm)	Fe (ppm)	Mn (ppm)	Cu (ppm)	Zn (ppm)	NO_3-N (ppm)	Cation Exchange Capacity (C.E.C.)	% Base Saturation (%B.S.)
Sugarloaf	10	4.6-5.8	2.25	8	135.4	587.75	474.6	54.3	13.9	88.95	52.4	1.41	3.15	0.95	14.3	48.53
Magazine	6	4.1-5.3	3.95	15.1	92.9	522.75	67.65	54.15	32.85	81.5	48.75	0.74	5.55	17.85	14.2	23.9
Porter	1	5.1	4.3	26.5	189	1325	160.5	47	18	39.5	151	1.7	3.55	57	21	40.7
Pryor	1	4.7	4.3	79	148.5	870.5	53	55	41	118	78	0.95	4	6.5	17	31.8
Mean			3.04	15.35	124.95	622.75	298.1	53.9	21.95	85.4	58.1	1.2	4.02	10	14.8	39

individuals with the larger individuals located on the upper slopes below the bluffline and on the summit. Additionally, Sugarloaf has three highly disturbed areas: an abandoned road bed, an existing road leading to the former site of a fire tower, and a power line right-of-way extending to the tower site. These areas are highly eroded, yet the maple-leaved oak is flourishing on them.

Table. 2. Vegetational data for Sugarloaf Mountain.

Species	Number points of occurrence	Number of Trees	Total Basal Area (sq. m)	Relative Frequency (F) %	Relative Density (D) %	Relative Dominance (Do) %	Importance Value (F+D+Do)
Quercus stellata	68	123	27.378	26.772	30.750	40.088	97.610
Quercus shumardii var. *aceri*	55	100	14.239	21.654	25.000	20.849	67.503
Juniperus virginiana	27	43	6.030	10.630	10.750	8.829	30.209
Quercus marilandica var. *ash*	23	36	1.662	9.055	9.000	2.434	20.489
Quercus rubra	13	15	6.779	5.118	3.750	9.926	18.794
Carya texana	18	25	1.622	7.087	6.250	2.375	15.712
Quercus muehlenbergii	16	17	2.607	6.299	4.250	3.817	14.366
Ulmus alata	10	13	2.271	3.937	3.250	3.325	10.512
Pinus echinata	6	6	1.770	2.362	1.500	2.592	6.454
Carya tomentosa	4	6	2.032	1.575	1.500	2.975	6.050
Prunus serotina	3	3	1.353	1.181	0.750	1.981	3.912
Viburnum rufidulum	3	5	0.074	1.181	1.250	0.108	2.539
Prunus mexicana	2	2	0.093	0.787	0.500	0.136	1.424
Rhus copallina	2	2	0.028	0.787	0.500	0.041	1.328
Quercus velutina	1	1	0.332	0.394	0.250	0.486	1.130
Ptelea trifoliata	1	1	0.013	0.394	0.250	0.019	0.663
Diospyros virginiana	1	1	0.008	0.394	0.250	0.012	0.655
Crataegus intricata	1	1	0.004	0.394	0.250	0.006	0.650
(Total)	254	400	68.295	100.000	100.000	100.000	300.000
Total distance (m) =	1115.840						
Avg. distance (m) =	2.790						
Trees/100 sq. m =	12.850	(1285.04/ha)					
Total basal area (sq. m) =	68.295						
Avg. basal area/tree (sq. m) =	0.171						
Basal area/100 sq. m =	2.194	(219.4/ha)					

Table 3. Vegetational data for Mountain Magazine.

Species	Number points of occurrence	Number of Trees	Total Basal Area (sq. m)	Relative Frequency (F) %	Relative Density (D) %	Relative Dominance (Do) %	Importance Value (F+D+Do)
Juniperus virginiana	47	101	20.285	23.5	33.667	32.072	89.239
Carya texana	26	40	7.473	13.0	13.333	11.815	38.149
Fraxinus americana	23	33	5.859	11.5	11.000	9.264	31.764
Carya glabra	11	17	5.251	5.5	5.667	8.302	19.469
Quercus shumardii var. *aceri*	14	17	3.637	7.0	5.667	5.750	18.417
Chionanthus virginicus	17	19	1.418	8.5	6.333	2.242	17.075
Quercus stellata	10	10	2.803	5.0	3.333	4.432	12.765
Amelanchier arboreum	9	13	2.159	4.5	4.333	3.414	12.247
Quercus velutina	4	5	5.379	2.0	1.667	8.505	12.171
Ostrya virginiana	11	16	0.696	5.5	5.333	1.100	11.934
Pinus echinata	8	8	2.271	4.0	2.667	3.591	10.257
Quercus alba	3	3	4.204	1.5	1.000	6.647	9.147
Ulmus alata	4	4	0.524	2.0	1.333	0.828	4.162
Robinia pseudoacacia	3	4	0.518	1.5	1.333	0.819	3.652
Acer saccharum	3	3	0.686	1.5	1.000	1.085	3.585
Ptelea trifoliata	4	4	0.068	2.0	1.333	0.108	3.441
Sassafras albidum	1	1	0.011	0.5	0.333	0.017	0.851
Quercus marilandica var. *ash*	1	1	0.003	0.5	0.333	0.005	0.838
Rhus copallina	1	1	0.003	0.5	0.333	0.005	0.838
(Total)	200	300	63.248	100.0	100.000	100.000	300.000
Total distance (m) =	778.000						
Avg. distance (m) =	2.593						
Trees/100 sq. m =	14.873	(1487.3/ha)					
Total basal area (sq. m) =	63.248						
Avg. basal area/tree (sq. m) =	0.211						
Basal area/100 sq. m =	3.136	(313.6/ha)					

These data suggest that the maple-leaved oak may be an early successional taxon that thrives in open-canopy, disturbed situations. If so, this might also explain the smaller importance value for maple-leaved oak on Magazine compared to Sugarloaf. At the turn of the century the plateau surface of Magazine had been settled and cleared, and in the first description of the oak, Palmer (1927) said it was found "in open woods bordering the cliffs and along their margins." Then Magazine might have offered opportunities similar to those now present on Sugarloaf. In the absence of recent major disturbances, the oak habitat on Magazine is undergoing change, and many of the oak trees are now surrounded by larger trees of other species. Furthermore, the small populations of maple-leaved oak on Porter and Pryor Mountains are found, along with *Q. marilandica* var. *ashei*, *Q. stellata*, *J. virginiana*, and *Ilex vomitoria*, on open, thin soils of steep, novaculite glades and appear to be doing passably in what might be termed an early successional area.

Conclusions

Sugarloaf Mountain, having a wide range of size classes, is presently optimal habitat for the maple-leaved oak. Sugarloaf has highly-eroded, heavily-disturbed areas, and it appears that the oak has spread from the summit and bluffline to fill these disturbed areas. Although Mount Magazine might have been optimal habitat in the past, it now represents marginal habitat. Magazine's oak population has more individuals in the larger size classes, and as surrounding trees continue to grow, the canopy is beginning to enclose the larger oak specimens located up from the bluffline. Based on the data collected, it appears that the maple-leaved oak is a member of the *Quercus-Juniperus* community and flavors early successional habitat.

Acknowledgements

We would like to thank the U.S.D.A. Forest Service for providing access to the Mt. Magazine study site, David M. Hunt for providing positive identification of *Q. marilandica* var. *ashei*, Gary Tucker for assistance in identification of *Carya glabra* on Mt. Magazine, and the Arkansas Agricultural Extension Service Soil Testing Laboratory at Fayetteville, Arkansas for providing soil analysis. We also thank Arkansas Tech University for its support.

Literature Cited

Bates, V. and **A.B. Pittman.** 1991. A review of the status of *Polymnia cossatotensis* Pittman and Bates (COMPOSITAE) or the "Cossatot leafcup". Report submitted to Arkansas Natural Heritage Commission, 41 pp.

Gandy, L.C., C.R. Britton, R.S. Caldwell, R.K. Ford, C.R. Laurin, R.E. McDaniel, S. Noland, C.S. Spears, J.L. Spellman and **G.E. Tucker.** 1993. Mount Magazine State Park, Final Environmental Impact Statement. F.T.N., Inc., Little Rock, 468 pp.

Harlow, W.M., E.S. Harrar, J.W. Hardin and **F.M. White.** 1991. Textbook of dendrology. McGraw-Hill, Inc., New York, 501 pp.

Johnson, G.P. 1992. Noteworthy collections-Arkansas: *Quercus shumardii* Buckl. var. *acerifolia* Palmer (FAGACEAE). Castanea 57:150-151.

Mueller-Dombois, D. and **H. Ellenberg.** 1974. Aims and methods of vegetational ecology. John Wiley and Sons, New York, 547 pp.

Palmer, E.J. 1927. On Nuttall's trail through Arkansas. J. Arnold Arboretum 8:24-55.

Preston, R.J. and **V.G. Wright.** 1988. Identification of southeastern trees in winter. North Carolina Agricultural Extension Service, Publ. AG-42, Raleigh, 113 pp.

Pyle, H.R. 1939. The herbaceous flora of Magazine Mountain. M.S. thesis. Univ. Arkansas, Fayetteville, 38 pp.

Radford, A.E., H.E. Ahles and **C.R. Bell.** 1968. Manual of the vascular flora of the Carolinas. The University of North Carolina Press, Chapel Hill, 1183 pp.

Smith, E.B. 1988. An atlas and annotated list of the vascular plants of Arkansas, 2nd ed. Kinko's Copies, Fayetteville, 489 pp.

Tucker, G.E. 1976. A guide to the woody flora of Arkansas. Ph. D. diss. Univ. Arkansas, Fayetteville, 147 pp.

Tucker, G.E. 1989. A survey of the botanical features of Magazine Mountain on the slopes and plateau surface. 26 pp.

U.S. Dept. Agri., Soil Conservation Service. 1975a. Soil Survey of Logan County. Arkansas Agricultural Experiment Station, U.S. Forest Service, and U.S. Department Agriculture, Washington, DC.

U.S. Dept. Agri., Soil Conservation Service. 1975b. Soil Survey of Sebastian County. Arkansas Agricultural Experimental Station, U.S. Forest Service, and U.S. Department Agriculture, Washington, DC.

The Complexity of Fetal Movement Detection Using A Single Doppler Ultrasound Transducer

William A. Russell, Jr.[1], Curtis L. Lowery[2], Patrick J. Baggot[2], James D. Wilson[1], Robert Walls[3], Roger M. Hawk[1], and Pam Murphy[2]

University of Arkansas at Little Rock[1]
Department of Electronics and Instrumentation
2801 S. University
Little Rock, AR 72204

University of Arkansas for Medical Sciences (UAMS)[2]
Department of Obstetrics and Gynecology
4301 West Markham
Little Rock, AR 72205

University of Arkansas for Medical Sciences (UAMS)[3]
Division of Biometry
4301 West Markham
Little Rock, AR 72205

Abstract

The objective of this paper is to discuss the complexity of fetal movement detection encountered during development and implementation of an automated single Doppler ultrasonic transducer based instrument. The single transducer instrument was intended to better quantify the duration, velocity, and magnitude of fetal movements. A Corometrics Model 116 fetal heart rate monitor was modified, and a fetal movement detection algorithm (Russell Algorithm) was developed to detect fetal movements on one and two (data fusion) transducers. A Hewlett-Packard (HP) M-1350-A fetal monitor and the Russell Algorithm were used to detect and record fetal movements concurrently on sixty patients between the gestation ages of 31 to 41 weeks. Using a computer-controlled SVHS PC-VCR, the instrumental detection of fetal movements was time-linked with real-time video ultrasound. This allowed the fetal movements to be scored by expert examiners on a second-per-second basis. A total of 52,478 seconds of fetal movements was scored using this system. Neither system could accurately define the entire duration, velocity, or magnitude of the fetal movements as detected by real-time ultrasound. The complexity of detecting fetal movements using only one transducer has many shortcomings, such as: the amplitude of the returning Doppler signal, the small area of the fetus monitored by a single transducer, the position of the fetus, the type and variety of fetal movements, and material size and shape.

Introduction

Clinicians today are becoming increasingly impressed with the importance of fetal movements as an assessment of fetal well-being (Neldam, 1980). Fetal movements may be classified as: general body, breathing, hiccups, and isolated extremity movements such as arms, legs, and head (Rayburn, 1982, 1987).

Maternal perception of fetal movements is an inexpensive method of assessing fetal well-being, but maternal perception of fetal movements may vary statistically due to subjective thresholds (Johnson et al., 1990; Schmidt et al., 1984). Differentiation between types of movement such as, extremity kicks, movement of the head, or gross body movements, are difficult, if not impossible, to determine by the mother (Rayburn, 1982). Maternal perception of short duration or weak movements tend not to be recorded by the mother.

Researchers are currently investigating Doppler instrumentation to detect fetal movements to alleviate the dependence on maternal perception (Wheeler et al., 1987; Besinger et al., 1989; Johnson et al., 1990; Melendez et al., 1989). They have shown that a single transducer Doppler instrument has the same problems as maternal perception. Current manufactures of fetal-movement detection instrumentation include Hewlett Packard and Toitu. The Hewlett Packard includes in their fetal heart rate monitor a circuit for one transducer movement detection that can detect simple gross body movement. Toitu of Japan produces an actocardiograph that provides the physician with unprocessed Doppler signals which are plotted on a strip chart recorder.

Over the last two years, we have been developing an automated Doppler ultrasound-based fetal-movement-detection instrument which will better define the duration, velocity, and amplitude of fetal movements. We have found that the detection and subsequent classification of fetal movements using only one Doppler ultrasonic transducer is very complex. The difficulties were linked to four major areas: 1) The Doppler frequency shift is dependent on the direction of fetal movement. 2) The amplitude of the returning signal is dependent on the angly of incidence and the attenuation of the signal due to the tissue. 3) The diameter of the Doppler signal is

only five m 4) The fetus is a very complex reflecting surface moving in complex patterns.

Doppler Effect.--The Doppler effect is defined as a frequency change in the carrier source due to the motion of the emitter or reflecting target (Sabbagha, 1980). The Doppler frequency shift is given by

$$fd = \left[\frac{2f_o v}{c}\right]\cos(\theta)$$

where f_d = Doppler frequency shift, f_o = carrier or transmitter frequency, v = velocity of the reflector, c = speed of sound in the medium, and θ = angle of incidence (Sabbagha, 1980). The accepted speed of sound in the medium is 1540m/s (Sabbagha, 1980). The Doppler frequency shift equation is very dependent on the angle at which the target is moving. A target moving directly toward or away from the source will produce the greatest frequency shift since $\cos(\theta) = 1$.

Propagation of Sound in Soft Tissue.--The amplitude of the sound wave is directly proportional to the generating source, and as the sound wave propagates through soft tissues, it is attenuated or absorbed by the tissue. For simplicity, fat, muscle, spleen, bladder, liver, kidney, and brain will be categorized as soft tissues; therefore, the equation

$$\alpha = af^b$$

can be used to approximate the attenuation of signal in soft tissue, where α = attenuation of signal in *dB / cm - MHz*, f = transmitter frequency (MHz), a and b are tissue coefficients (Ziskin et al., 1993). Using average values for a and b, then

$$\alpha = 0.70f^{1.1}.\text{(Ziskin et al., 1993)}$$

Many authors generally accept 1dB/cm-MHz for soft tissue attenuation (Wells, 1977). If the propagating sound wave encounters a medium change or a boundary, then reflection, refraction, and transmission will affect the amplitude and/or direction of the sound wave as illustrated in Fig. 1.

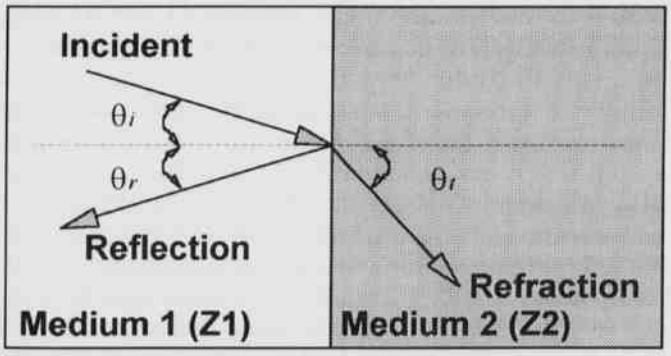

Fig. 1. Porpagating Sound Wave Encounters a Medium Change.

Snell's Law applies in soft tissue if the wavelength is short in comparison with the size of the tissue at the boundary (Ziskin et al., 1993). Snell's Law is given by

$$\frac{\sin(\theta_i)}{\sin(\theta_t)} = \frac{c_1}{c_2}$$

where c_1 = speed of sound in medium one and c_2 = speed of sound in medium two and

$$\theta_i = \theta_r.$$

Using conservation of energy, it can be shown that

$$E_i + E_r = E_t,$$

where the impedance of a medium is

$$Z = \rho c,$$

and ρ = density of the medium, and c = speed of sound in the medium (Sabbagha, 1980, Ziskin et al., 1993). Using Snell's Law, the conservation of energy, and the impedance of the medium, the amplitude ratio of the reflected sound to the incident wave is given by:

$$R = \frac{Z2*\cos(\theta_i) - Z1*\cos(\theta_t)}{Z2*\cos(\theta_i) - Z1*\cos(\theta_t)}$$

where $Z = \rho c$ (Sabbagha, 1980, Ziskin et al., 1993). The impedance of different materials is provided in Table 1.

The interface between fat and bone will produce a very high amplitude reflection ratio compared to fat and muscle as shown in the calculations below:

$$R = \frac{Z2 - Z1}{Z2 + Z1} = \frac{1.38\text{-}0.92}{1.38\text{+}0.92} = 0.2 \text{ Bone to Fat Interface}$$

$$R = \frac{Z2 - Z1}{Z2 + Z1} = \frac{1.07\text{-}0.92}{1.07\text{+}0.92} = 0.075 \text{ Muscle to Fat Interface}$$

where the calculations assumed $\theta i = 0$. This difference in amplitude reflections is the physical property used in medical imaging instrumentation.

Table 1. Impedance of different mediums (Wells, 1977; Sabbagha, 1980).

Material	Density (g/ml)	Velocity (m/s)	Impedance $10^6 kg/(m^2\text{-}s)$
Bone (skull adult)	1.38-1.81	4080	3.75-7.38
Fat	0.92	1460	1.35
Muscle	1.07	1600	1.65-1.74
Water	1.00	1480	1.52
Air	0.00112	330	0.0004

Materials and Methods

A Corometrics Model 116 dual fetal heart rate monitor (Coro 116) was modified to allow fetal movement detection on one or both transducers. The One or Two (data fusion) Transducer Russell algorithm and analog electronics were developed to detect fetal movements using the Coro 116. The Coro 116 fetal heart rate monitor uses a nine element transducer which produces a transmitted beam diameter of approximately five centimeters. The diameter which remains approximately five cm in diameter within the desired viewing volume (O'Connell, 1994).

Russell Algorithm.--The Russell one and two (data fusion) transducer fetal-movement detection algorithm was developed for Corometrics Medical Systems, Inc. in Wallingford CT. The primary specification for the Russell algorithm was it had to be as-good-as the Hewlett Packard M-1350-A fetal monitor. Due to the proprietary nature of the Russell algorithm, it will not be published or discussed further. However, the one transducer Russell algorithm has been tested extensively and is undergoing FDA 510K clinical trials in a Corometrics Medical Systems Model 150 fetal monitor.

A Hewlett-Packard (HP) M-1350-A fetal monitor was used with the Russell algorithm to detect and record fetal movements concurrently on sixty patients between the gestation ages of 31 and 41 weeks.

A computer-controlled NEC SVHS PC-VCR was used to time-link the instrumental detection of fetal movements with two 3.5 NHz real-time ultrasounds. The real-time ultrasounds were a Corometrics Aloka Model 620 and a General Electric Model 3000. The two video images of the fetus were compressed onto the video section of the NEC SVHS PC-VCR.

The time synchronization of the real-time video images of the fetus and the instrumental detection of fetal movements allowed the expert examiners to score the VCR tapes on a second per second basis and store the scored results in a time-linked file. A total of 52,478 seconds (14.6 hours) of fetal movements was scored using this system.

The measurement of fetal motion on a second per second basis provides a simple way to objectively measure the performance of any fetal motion detector. During each second of measurement, the machine either agrees with the expert file or it does not. Scoring movements on a second per second basis has provided information that allows calculated values not previously reported by other authors. Common indices of agreement (or disagreement) are now weighted in proportion to time while the measurements of previous investigators were not.

Indices of Agreement or Disagreement.--The indices of agreement or disagreement used in the statistical study are sensitivity, specificity, positive and negative predictive values, and odds ratio (Rosner, 1990). A frequency summary will aid in the calculations of the indices of agreement of disagreement and is presented in Table 2.

Table 2. Frequency summary table.

Frequency Table	Expert Movement	Expert Non-Movement	Total
Machine Movement	A	B	A+B
Machine Non-Movement	C	D	C+D
Total	A+C	B+D	N

The counts or frequencies (A,B,C,D) are based on the second-per-second resolution of the PC-VCR tapes. On the second-per-second basis the expert or machine will either score a movement or a non-movement. The counts A and D are the number of seconds that the expert and machine agree and counts B and C are the number of seconds that the expert and machine do not agree. The indices of agreement or disagreement are further defined by: (Rosner, 1990)

Sensitivity: The conditional probability that the expert and machine both indicate a movement. SEN = A/(A+C)

Specificity: The conditional probability that the expert and machine both indicate a non-movement. SPEC = D/(B+D)

Positive Predictive Value: The posterior probability of a movement given a score by the machine. PPV = A/(A+B)

Negative Predictive Value: The posterior probability of a non-movement given a non-movement score by the machine. NPV = D/(C+D)

Results

During this study, we conducted a total of 60 examinations with fetal gestation ages between 31 and 41 weeks. Upon investigation of several maternal demographic factors, we concluded that their affect on the common indices of agreement were insignificant. AT any time, there was transducer movement on the real-time ultrasounds which was excluded from the analysis, due to lack of visualization of the fetus. AFter removal of transducer movements, we had a total of 52,478 seconds (14.6 hours) of fetal movements for analysis. The movement detection results from the One Transducer Russell algorithm and the HP M-1350-A and the movement detection results from the Two Transducer (data fusion) Russell algorithm are presented in Table. 3.

Journal of the Arkansas Academy of Science, Vol. 48 [1994], Art. 25

Table 3. One and two transducer russell algorithm and the Hewlett Packard M-1350-A Statistics.

Number of Patients = 60	Sensitivity	Specificity	Positive Predictive Value	Negative Predictive Value
One Transducer	43.66	90.65	50.28	89.80
Two Transducer (Data Fusion)	63.47	90.51	52.91	92.95
HP	31.12	90.05	33.61	88.28

Discussion

The fetus is a very complex reflecting surface for Doppler instrumentation. The fetus also is capable of moving in complex patterns (Rayburn, 1982, Rayburn, 1987). A representation of the fetus and the Doppler transmitter beam is illustrated in Fig. 2.

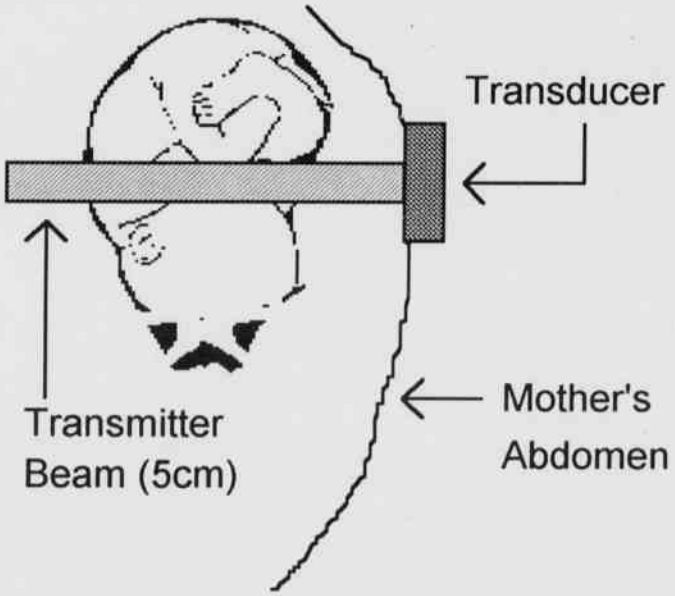

Fig. 2. Fetal representation.

Even though the fetus is enclosed in a small space (the uterus), it still has many degrees of freedom of movement. The directional vectors of the movements are directly linked to the cos(θ) in the doppler frequency shift equation, resulting in a spectrum of Doppler shift frequencies received. The signal is further complicated by the complex biophysical profile of the fetus and its reflecting surfaces. As the fetus moves, highly reflective and poorly reflective surfaces are presented to the transmitter at different angles of incidence. During this type of movement, Snell's Law and the amplitude ratio of the reflected sound become the dominate factors influencing the complexity of the returning signal. The combination of these three factors working together on the returning signal, results in the detection-skip-detection pattern of movement scoring. The fetal head and extremities can also become active reflectors for the transmitting signal during a fetal movement.

A solution to correct the one transducer Doppler and Snell's Law dependence on the cos(θ) could be to increase the number of transducers as with the Two Transducer (data fusion) Russell algorithm. The Two Transducer (data fusion) Russell algorithm statistics did indicate that a substantial increase in sensitivity could be achieved. The data fusion increase was almost 20% better than the one transducer method. The switch from Doppler detection to pulse-echo (A-mode) detection of fetal movements could also be a viable detection technique.

Figure 2 clearly illustrates that the entire fetus is not covered by the five-cm transmitter beam. Increasing the beam diameter is not an option to increase fetal movement coverage. If the beam diameter is increased, the transmitter power (W/cm^2) also must be increased to counteract the soft tissue signal attenuation. Increasing the transmitted power would increase the risk of over exposure of ultrasound for the mother, since, the transducer is making contact with the maternal abdomen in one small area. However, the entire fetal area could be covered by placing more transducers on the maternal abdomen without increasing the single transducer transmitter power.

Conclusions

Our research goal was to develop a one transducer Doppler ultrasonic fetal-movement detection algorithm that was as-good-as the HP M-1350-A fetal monitor. Table 3 clearly indicates that the one transducer Russell algorithm made a statistical improvement over the HP M-1350-A. During development of the one transducer algorithm, we encounter several limiting factors for detecting fetal movements with only one transducer as discussed earlier. To prove that two transducers are better than one, we added another transducer. Using an adapted Russell algorithm and data fusion, the sensitivity increased to 63.4% (see Table 3). The two transducer Russell algorithm was 32.4% better in sensitivity than the HP M-1350-A. The two transducer Russell algorithm reassured us that increasing the number of transducers will increase the fetal movement detection sensitivity and

eliminate some of the one transducer limiting factors.

Literature Cited

Neldam S. 1980. Fetal movements as an indicator of fetal well being, Lancet, Vol. 2, 1222 pp.

Rayburn W. 1982. Clinical implications from monitoring fetal activity. American Journal of Obstetrics and Gynecology, Vol. 144, 967 pp.

Rayburn W. 1987. Monitoring fetal body movements, Clinical Obstetrics & Gynecology, Vol. 3, No. 4, 899 pp.

Johnson T., E. Jordan, and **L. Paine.** 1990. Doppler recordings of fetal movement: II. Comparison with maternal perception, Obstetrics & Gynecology, Vol. 76, 42 pp.

Schmidt W., I. Cseh, K. Hara and **F. Kubli.** 1984. Maternal perception of fetal movements and real-time ultrasound findings, Perinatal Medicine. Vol. 12, 313 pp.

Wheeler T., K. Roberts, J. Peters and **A. Murrills.** 1987. Detection of fetal movement using doppler ultrasound. Obstetrics and Gynecology, Vol. 70, No. 2, 251 pp.

Besinger R., and **T. Johnson.** 1989. Doppler recordings of fetal movement: clinical correlation with real-time ultrasound. Obstetrics & Gynecology, Vol. 74, No. 2, 227 pp.

Melendez T., W. Rayburn and **C. Smith.** 1992. Characterization of fetal body movement recorded by the Hewlett-Packard M-1350-A fetal monitor, American Journal of Obstetrics & Gynecology, Vol. 167, No. 3, 700 pp.

Sabbagha R. 1980. Diagnostic Ultrasound Applied to Obstetrics and Gynecology, J.B. Lippincott Company, Philadelphia.

Ziskin M. and **P. Lewin.** 1993. Ultrasonic Exposimetry, CRC Press Inc., Boca Raton, Florida.

Wells P.N.T. 1977. Biomedical Ultrasonics, Academic Press, New York.

O'Connell B. 1994. Personal Communications, Corometrics Medical System Inc. Wallingford, Connecticut.

Rosner B. 1990. Fundamentals of Biostatistics, Third Edition, PWS-Kent Publishing Company, Boston, Massachusetts.

Pleistocene and Holocene Remains From The Red River, Southwest Arkansas

Terry A. Sanders
Taylor High School
506 East Pine
Taylor, AR 71861

Abstract

Vertebrate remains have been found on gravel bars of the Red River in southwest Arkansas, northeast Louisiana, and east Texas. The majority of these specimens were recovered by amateur archaeologists and Dr. Frank Schambach of the Arkansas Archaeology Survey. Extinct species of bison (*Bison* sp.), mastodon (*Mammut americanum*), pampathere (*Holmesina septentrionalis*), llama (*Palaeolama mirifica*), tortoises (*Geochelone* sp.), and (*Terrapene* sp.) indicate a Pleistocene component in the region's alluvium. The giant tortoise, pampathere, and llama represent first known occurrences of these species for the state of Arkansas. Search times between finds were recorded for seven localities. The richest gravel bar averaged one man-minute per find. The least productive bar averaged 82.5 man-minutes per find. The average collection rate for all bars was one find per 19.5 man-minutes.

Introduction

In the past 70 years, 200 specimens of vertebrate remains have been recovered from the Red River drainage of Arkansas, Louisiana, and Texas. Hay (1924) Reported an *Equus complicatus* molar from a gravel bar near Shreveport, Louisiana. Slaughter and Hoover (1963) mentioned that channelizing of the Sulphur River in northeast Texas in 1929 had exposed Pleistocene alluvium. In processing "several tons of matrix," they recovered nine coyote-sized or larger and thirteen small mammals. Hemmings (1982) identified 15 taxa: Chelonia, *Megalonys jeffersoni, Canis familaris, Canis* sp., *Ursus americanus, Felis* sp., *Equus caballus, Equus* sp., *Mylohyus nasutus, Odocoilius virginianus, Bos tarurus, Bison bison, Bison* sp., *Mammut americanum,* and *Homo sapiens* from point and channel bars of the Red River in southwest Arkansas. Over several years, F. Schambach of the Arkansas Archaeology Survey and several amateur archaeologists have collected other vertebrate remains form gravel bars along the Red River.

Other vertebrate remains have been recovered from Arkansas beyond the Red River drainage. Brown (1908) reported the excavation of Conard Fissure in Newton County and the recovery of eleven large mammals and forty-five microvertebrates. Hay (1924) noted the finds of mastodon near Helena, Trumann, and Lake Chicot. Davis (1969) and Quinn (1972) reported on their excavation of Peccary Cave, also in Newton County. Semken's (1984) interpretation of the Peccary Cave chronology is the most extensive evaluation to date of Pleistocene and Holocene climates in Arkansas.

Gravel bar sites were first located from the river channel, and their positions were estimated by using aerial photos and topographic maps. The localities were later confirmed by going to each site from fixed positions on land after gaining permission from the land owners. Table 1 provides the locations of fossil producing sites.

Table 1. Locations of fossil producing sites along the Red River, southwest Arkansas.

Locality Designation	Description	Section	Township	Range
G.C.-1	head of chute	25	T14S	R26W
G.C.-2	head of chute	13	T15S	R26W
G.C.-3	channel bar	NW,22	T14S	R26W
F.-4	head of chute	NE,24	T16S	R26W
F.-5	Kitchens Island	17	T18S	R25W
F.-8	channel bar	27	T16S	R25W
Ful.-9	mouth of Little River	19	T13S	R26W
Ful.-10	channel bar	31	T13S	R26W
Ful.-11	channel bar	5	T14S	R26W

Two collecting methods were employed to determine the abundance of vertebrate remains on gravel bars of the Red River in southwest Arkansas. In the timed method, a group of collectors searched until a specimen was found. All collectors stopped while the recorder noted the time elapsed and labeled the specimen. All would resume collecting simultaneously when the clock was reset. Other collections were made without measuring the time elapsed. The number of fossils collected per bar during 1992 and the number of man-minutes per find on the seven bars in which timed collections were made are presented in Table 2.

Table 2. Number of specimens collected during 1992 from seven gravel bars of the Red River, southwest Arkansas.

Locality Designation	Man-minute per find	Total Specimens Collected
G.C.-1	13.2	58
G.C.-3	11.0	6
F-4	14.9	12
F-5	82.5	8
F-8	1.0	89
Ful-9	4.1	13
Ful-11	9.5	6
Mean	19.5	192

Due to uncertain boundaries along the Red River, many of the county lines are listed as "indefinite" or "approximate," reflecting the ever-changing position of the channel. Further, the exact position of many of the gravel bars has not been located to any greater precision than one square mile section. All the "channel bars" localities are on the right bank of the river.

Unless otherwise noted, all bone measurements are of total lengths, taken by using a bone-board. Other critical measurements were taken with calipers. The degree of fossilization in each specimen was determined by using the criteria mentioned by Hemmings (1982). The three levels were "modern" indicating bone with ivory-like color with some elasticity, "subfossil" determined by pale brown to brown color with observable weight increase or loss of elasticity; and "fossil" noted by very dark color with increased weight and hardness.

Faunal List (*denotes extinct species)

Class: Reptilia
Terrapene sp. *
Geochelone sp. (giant tortoise) *
Macroclemys temminckii (alligator snapping turtle)
Apalone spinifera (spiny soft-shell turtle)
Alligator mississippiensis (American alligator)
Class: Aves
Antatidae (duck)
Chen hyperborea (snow goose)
Meleagris gallopavo (turkey)
Class: Mammalia
Order: Marsupialia
Dedelphis virginiana (opossum)
Order: Edentata
Holmesina septentrionalis (pampathere) *
Order: Lagomorpha
Lepus californicus (black-tailed jack rabbit)
Order: Rodentia
Castor canadensis (beaver)
Order: Carnivora
Canis latrans (coyote)
Canis familaris (dog)
Urus americanus (black bear)
Procyon lotor (raccoon)
Felis rufus (bobcat)
Order: Artiodactyla
Palaeolama mirifica (Ilama) *
Sus scropha (pig)
Odcoileus virginianus (white-tail deer)
Bison sp. (bison) *
Bos sp. (cow)
Capra hircus (goat)
Order: Proboscidea
Mammut americanum (mastodon) *

Notes On Pleistocene Species

Terrapene sp.

Specimens examined: (6) *Terrapene ornata*

Specimen referred: (1) plastron fragment G.C.-1-2

Remarks: The specimen G.C.-1-2 is judged to be a fragment of a plastron of *Terrapene* due to its growth lines on the abdominal surface anterior to the hinge line, but it has more nearly square edges than the recent turtle specimens examined. The fossil specimen is 8 mm thick as compared to 3 mm in the known *Terrapene* specimen. The fossil specimen is dark brown, well mineralized, and may represent the extinct Pleistocene form, *T. carolina putnami*.

Geochelone sp.

Specimens examined: (2) *Terrapene ornata*

Specimen referred: (1) plastron fragment G.C.-1-3

Remarks: After comparison with modern *Terrapene* specimens, the fragment is interpreted as a portion of the left half of a plastron. The fossil specimen displays a portion of the suture or hinge line and is 23 mm thick.

Holmesina septentrionalis

Specimen examined: (1) *Holmesina septentrionalis*

Specimen referred: (1) buckler osteoderm G.C.-1-5

Remarks: The specimen G.C.-1-5 (Fig. 1) displays the depressed marginal band completely around the osteoderm mentioned to be characteristic of pampatheres (Edmund, 1987). Inside the marginal band is a pitted ridge 1.0 mm to 3.0 mm wide, and there is a slight ridge extending from the marginal band to the center. The fossil specimen is more nearly square than an SAU specimen of *Holmesina septentrionalis* collected from the Sulphur River in east Texas by Davis and Ball (1991). The localities in east Texas are less than 200 miles west of the collection site of the specimen G.C.-1-5.

Palaeolama mirifica

Specimens examined: (1) *Bison bison*, (1) *Ovibos sp.*, (4) *Palaeolama*, (1) *Alces alces*, (1) *Oreamnos americanus*

Specimen referred: (1) distal scapula 85-389

Fig. 1. The external view of a buckler osteoderm from *Holmesina septentrionalis.* Scale 3 cm.

Remarks: The fossil specimen was compared to several recent ruminants because it displays an abrupt rise from the glenoid cavity and neck to the spine, a feature not seen in horses (Fig. 2). The dorsoventral dimension of the articulation surface in specimen 85-389 is 48 mm as compared to an average of 50 mm is four fossil specimens of *Palaeolama* from south Texas (observed range 49 mm to 51 mm). The lateromedial width of the articulation surface in specimen 85-389 is 63 mm as compared to an average of 61 mm in the known *Palaeolama* specimen (observed range 59 mm to 64 mm). A third measure was taken on all specimens between the glenoid and the lateral process. The Red River fossil specimen measured 31 mm, and all of the known *Palaeolama* specimens measured 30 mm for this width. Webb (1974) reviewed North American Ilama specimens and revised their taxonomy. *Palaeolama mirifica,* originally known from Seminole Field, Pinellas County, Florida, is now regard as extending around the Gulf Coast to Texas, based on the work of Lundeilus (1972) at the Ingleside local fauna. Although a partial skeleton of *Palaeolama* was recovered from the "boot heel" of Missouri (R.W. Graham, per. comm., April, 1993), it is thought the specimen at hand represents the first known occurrence for the state of Arkansas.

Bison sp.

Specimens examined: (3) *Bos* sp., (3) *Bison antiques,* (1) *Bison bison*

Specimen referred: (1) ischium F-5-1

Remarks: The fossil specimen was nearly two times longer and wider than the ischium of an adult male *Bison bison.* The fossil specimen was also compared to a *Bison antiquus* pelvis. From the tuber ischia to the medial process of the ischium, the *Bison antiquus* measured 100 mm as compared to 135 mm in the fossil specimen. The width anterior to the tuber ischia in the *Bison antiquus* was 95 mm as compared to 115 mm in the fossil specimen. The fossil specimen appears to be the same size as a *Bison* antiquus specimen mounted and displayed at the University of Kansas Museum.

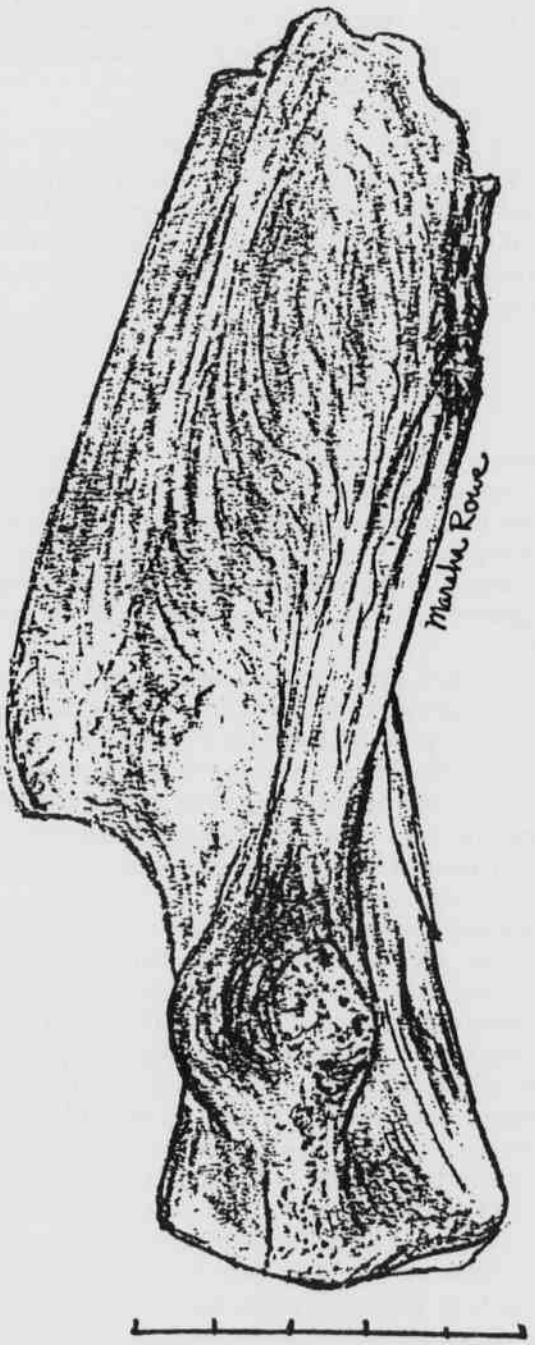

Fig. 2. Anterior view, distal portion of the right scapula of *Palaeolama mirifica.* Scale 5 cm.

Mammut americanum

Specimen referred: (1) M3 and several bone fragments

Remarks: The fossil specimen commonly referred to as the Mud Creek mastodon is highly fragmented. Identification was based on the upper third molar which displayed the characteristic high crest or cusps of mastodon teeth, in contrast to mammoths (Olsen, 1960). One proximal femur among the post-cranial fragments has a diameter of 159 mm.

cf. *Mammut americanum*

Specimen referred: (1) tusk fragment 3MI-45

Remarks: The specimen is tentatively assigned to *Mammut americanum* due to the fact it was found several miles down stream from the Mud Creek locality and due to the abundance of the species during the late Pleistocene.

Discussion

Abundance Of Specimens.--Of the seven gravel bars (Table 1) on which collections were timed, specimens were found in the greatest abundance on G.C.-1 and F-8 which are separated by about 12 miles. Man-minutes per find was chosen as the index for concentration of specimens on gravel bars due to the varying size of the groups collecting.

G.C.-1 yielded four Pleistocene species (four specimens), F-8 two Pleistocene species (three specimens), and four other sites produced only one specimen each. The ratio between the Pleistocene specimens and the total number of specimens varies between 0.33 and 0.55 for seven sites, and shows little correlation to total number of specimens collected. There is no apparent point source for the Pleistocene specimens.

Climatic Implications.--Of the remains collected along the Red River, the black-tailed jack rabbit, alligator snapping turtle and the American alligator have the most significant modern ranges. The jack rabbit is a prairie dweller while the alligator snapping turtle and the American alligator are limited by their need for warm temperatures and bodies of water. An area of sympatry (region where a portion of the ranges of all the species recovered overlap, Fig. 3) is located at the junction of southeast Oklahoma, northeast Texas, and southwest Arkansas. Another small area of sympatry in coastal southeast Texas near the Louisiana border does exist, but the region is at least 270 miles from the Red River in southwest Arkansas, and it is not thought to be relevant. The Arkansas, Texas, and Oklahoma area is near the boundary between the western plains and the eastern forests. The area of sympatry for the surviving animals is so near where their remains were found that apparently, even in this boundary area, there is no evidence of significant climatic shift in the span of time represented by the fossil remains.

Of the 23 species of vertebrates, *Terrapene* sp., *Geochelone* sp., *Holmesina septentrionalis,* and *Palaeolama mirifica* represent the first known occurrences in Arkansas. Also collected were an extinct *Bison* and *Mammut americanum* which are also part of the Pleistocene megafauna that became extinct 10 to 11 thousand years ago. All other species encountered are either present or have been recently extirpated in this area.

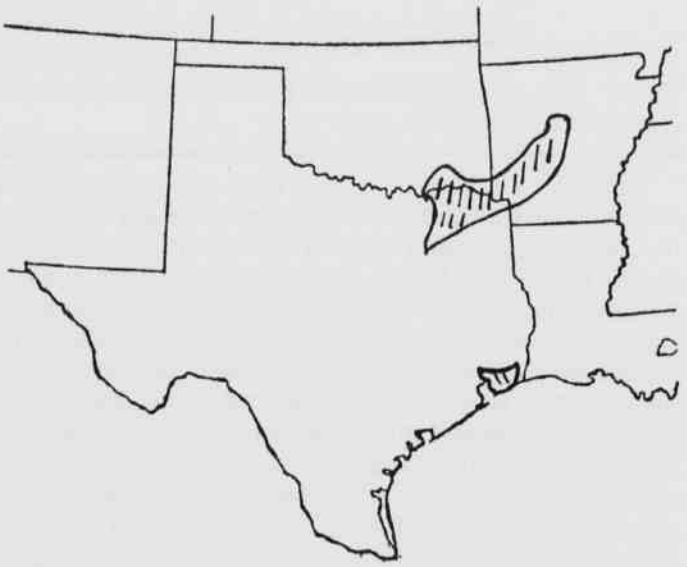

Fig. 3. Area of sympatry for modern vertebrates recovered from the Red River alluvium. Animals ranges after Burt and Grossenheider (1964) and Conant and Collins (1991).

Acknowledgements

I would like to thank K. Ball, D. Nelson, and E. Millican for field assistance. F. Schambach granted access to most of the specimens in this study. L.D. Martin, R. Timm, M. Hilmann, and E. Lundelius, Jr., provided specimens for comparisons. M. Rowe provided the illustrations and L.C. Davis provided valued consultations. D. Jean helped determine site locations. R. Eichenbuger and D. Nelson read the manuscript.

Literature Cited

Brown, B. 1908. The Conard Fissure, a Pleistocene bone deposit in northern Arkansas: with descriptions of two new genera and twenty new species of mammals. Mem. Amer. Mus. of Nat. Hist. 9 (4) 157-208.

Burt, W.H. and **R.P. Grossenheider.** 1994. A field guide to the mammals. Houghton Mifflin Co. Boston: 249 pp.

Conant, R. and **J.T. Collins.** 1991. Reptiles and amphibians. Houghton Mifflin Co. Boston: 450 pp.

Davis, L.C. 1969. The Biostratigraphy of Peccary Cave, Newton County, Arkansas. Proc. Arkansas Acad. Sci. 23: 192-195.

Davis, L.C. and **K.M. Ball.** 1991. Pleistocene mammals From The South Sulphur, Hunt County, Texas. Proc. Arkansas Acad. Sci. 45: 22-24.

Edmund, A.G. 1987. Evolution Of The Genus *Holmesina* (PAMPATHERIIDAE, MAMMALIA). Pearce-Sellards Series No. 45. Texas Memorial Mus., University of Texas, Austin. 1-20.

Hay, O.P. 1924. The Pleistocene of the Middle Region of North America. Washington: Carnegie Institution of Washington. 322A.

Hemmings, E.T. 1982. Vertebrate fossils from Recent Red River point bars and channel bar deposits in the Great Bend Region. Contributions to the Archeology of the Great Bend Region. 22: 30-38.

Lundelius, E.L. 1972. Fossil Vertebrates from the Late Pleistocene Ingleside fauna, San Patricio County, Texas. bur. Econ. Geol., Rep. Inveest. 77: 1-74.

Olsen, S.J. 1960. Post-cranial skeleton characters of *Bison* and *Bos*. Papers of Peabody Museum of Archeology and Ethnology, Harvard University. Vol. XXXV (no. 4): 15.

Quinn, J.H. 1972. Extinct mammals in Arkansas and related C-14 data circa 3000 years ago. 24th International Geological Congress. Sec. 12: 89-96.

Semken, H.A. 1984. Paleoecology of a Late Wisconsinan/Holocene Micromammal Sequence in Peccary Cave, Newton County, Northwest Arkansas. *In* H.H. Genoways and M.R. Dawson (Ed.), Contributions In Quaternary Vertebrate Paleontology: A Volume In Memorial To John E. Guilday. Pittsburgh: Carnegie Museum Of Natural History. 405-431.

Slaughter, B.H. and **B.R. Hoover.** 1963. Sulphur River Formation and the Pleistocene Mammals of the Ben Franklin Local Fauna. J. Grad. Res. Center. 31: 133-148.

Webb, S.D. 1974. Pleistocene Llamas of Florida, with a Brief Review of the Lamini, *In* Pleistocene Mammals of Florida. University Presses of Florida, Gainesville. 265.

Pre-spawning Migration of Channel Catfish into Three Warmwater Tributaries–Effects of a Cold Trailwater

Gary L. Siegwarth[1] and James E. Johnson
National Biological Survey
Arkansas Cooperative Fish & Wildlife Research Unit
Department of Biological Sciences
University of Arkansas
Fayetteville, AR 72701

Abstract

Spring migrations of channel catfish (*Ictalurus punctatus*) into the Kings, Mulberry and Buffalo rivers, Arkansas, were compared to determine adult catfish migration into a warmwater river that flows into a cold tailwater. The Buffalo River flows into a cold tailwater reach of the White River and supports a sparse channel catfish population compared to similar rivers in the region that do not flow into cold tailwaters. This is an important factor because many recent studies have demonstrated that channel catfish make pre-spawning migrations into tributary streams and may contribute significantly to tributary populations. To assess channel catfish migration, hoop nets were deployed at the confluence of the three rivers and fished continuously from 29 March to 22 April 1992, with total catches used as an index of the relative number of fish migrating into each river. Movements of channel catfish into the three rivers were observed throughout April; however, the relative number migrating into the Buffalo River (n=33) was significantly less than the Kings (n=169) or Mulberry (n=263) Rivers. Water temperature differed significantly between the White and Buffalo Rivers during the sampling period, but did not differ between the Kings or Mulberry, and their respective confluence. Although cold, White River tailwaters do not totally inhibit overwintering and migration of adult channel catfish into the Buffalo River, reduced numbers of migratory catfish may partially account for the river's low reproductive output and sparse adult population.

[1]Present address: Iowa Department of Natural Resoures, Northeast District Headquarters, Route 2 Box 269, Manchester, Iowa 52057

Introduction

An increasing numer of tagging studies have shown that channel catfish (*Ictalurus punctatus*) exhibit extensive spring migrations from larger rivers or lakes into tributary streams. These spring migrations have been documented for river systems in a wide range of geographical locations. Humphries (1965) reported that channel catfish in the Savannah River, Georgia, made an upstream migration into a tributary stream during May and June, followed by downstream movement back into the river during July. In South Dakota, June (1977) reported that channel catfish in Lake Oahe moved into tributary rivers prior to spawning. Channel catfish movements into or out of tributaries have also been observed for river systems in Florida (Hale et al., 1986), Iowa (Welker 1967), Louisiana (Perry et al., 1985), Missouri (Newcomb, 1989; Dames et al., 1989), Wisconsin (Ranthum, 1971), and Wyoming-Montana (Smith and Hubert, 1989). These movements as well as channel catfish migrations reported from other investigations, are believed to be associated with spawning.

Annual migrations of channel catfish appear to be in response to either a lack of overwintering habitat in the tributary (Newcomb, 1989) or a lack of suitable spawning habitat in the confluence system (Gerhardt and Hubert, 1990). Channel catfish appear to require substantially different habitat areas for overwintering and spawning. Newcomb (1989) found that deep scour-holes in the Missouri River provide valuable overwintering habitats; during winter, channel catfish were only collected in depths greater than 3.7 m and water velocities less than 0.3 m/s. He reported a general pattern of channel catfish movement from these overwintering habitats into tributaries in spring, summer and fall. Use of deep-water (4.9 to 7.6 m) habitats by winter aggregations of channel catfish have also been reported for the Mississippi River (Hawkinson and Grunwald, 1979). Gerhardt and Hubert (1990) concluded that more abundant spawning habitat in a Wyoming tributary explained the substantial use by channel catfish during the spawning period.

Many small rivers may not provide both suitable spawning habitat and deep overwintering areas for channel catfish (Newcomb, 1989; Gerhardt and Hubert, 1990). Although tributary channel catfish populations may depend upon annual inputs from spring migrations of catfish which overwintered in other waters, information is not available on the importance of these annual migra-

tions for maintaining tributary populations. In the Wisconsin River, it is estimated that greater than 75% of the channel catfish population migrates into overwintering habitats in the upper Mississippi River, and that an absence of migrating adults would result in a significantly reduced catfish population in the Wisconsin River (T.D. Pellett and D. Fago, Wisconsin Department of Natural Resources, unpublished data).

In Arkansas, a significantly lower abundance of young-of-year (YOY) channel catfish has been observed in the Buffalo River relative to similar, nearby warmwater, Ozark rivers (Siegwarth, 1992). The Buffalo River also supports a sparse natural adult catfish population; previously stocked, hatchery-reared catfish make up a significant (>93%) portion of the population (Siegwarth, 1994). One possible reason for the low reproductive output and recruitment observed in the Buffalo River is that, unlike other rivers examined, the Buffalo River flows into a cold tailwater. The sparse catfish population in the Buffalo River may result from these cold tailwaters if historic annual inputs of migrating adults have been reduced or eliminated.

The objective of this study was to determine if the cold tailwater reach of the White River has eliminated pre-spawning migration of channel catfish into the Buffalo River. This was tested by comparing relative numbers of catfish migrating into similar, nearby rivers which do not flow into cold tailwaters. Knowledge of cold tailwater effects on channel catfish migration will aid in assessing reasons for the lack of natural reproduction and sparse channel catfish populations observed in the Buffalo River.

Materials and Methods

Study Sites.--Pre-spawning migration of channel catfish was assessed for the Kings, Mulberry and Buffalo

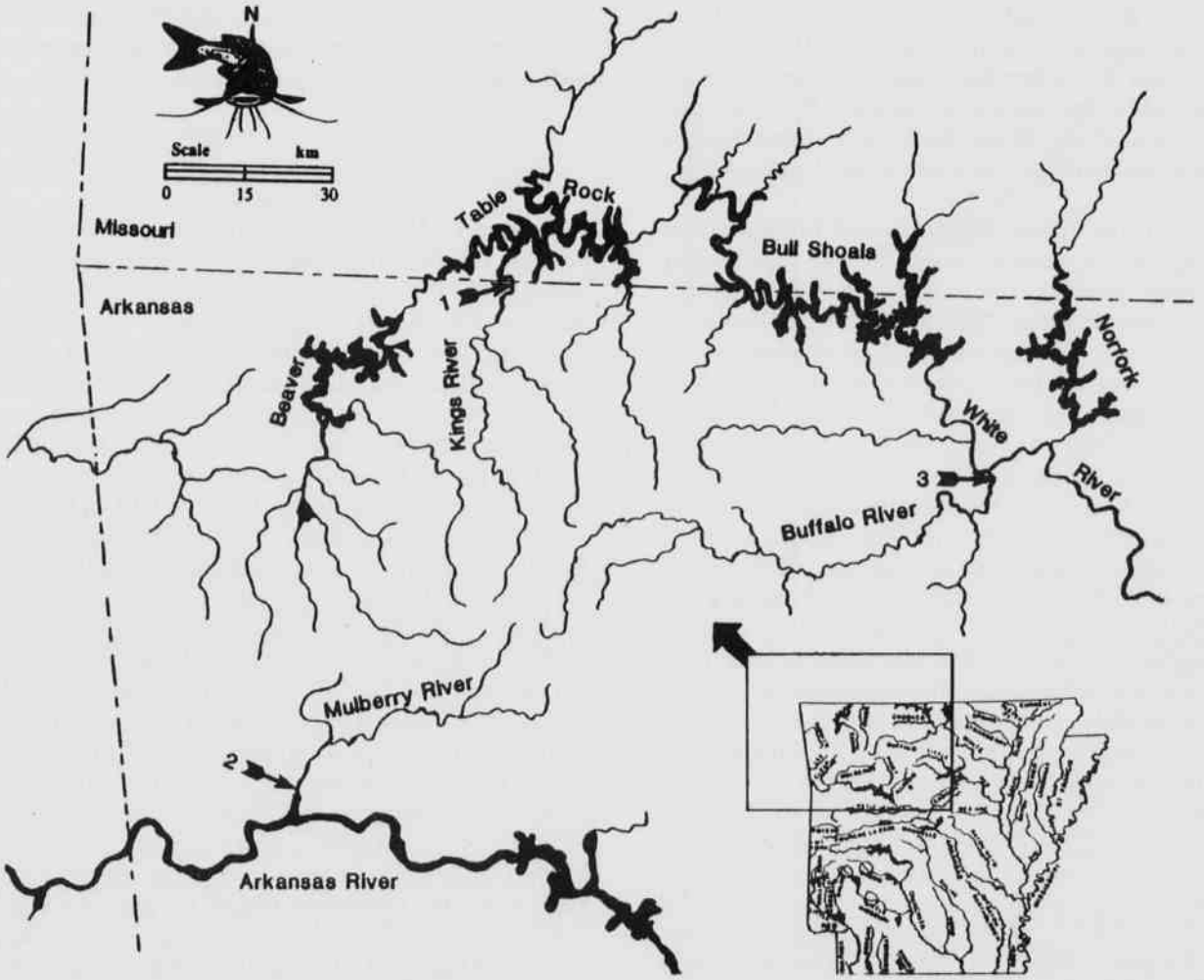

Fig. 1. Study sites at the mouth of the Kings (1), Mulberry (2) and Buffalo (3) rivers of northeastern Arkansas.

Rivers of northwestern Arkansas (Fig. 1). These three rivers originate in the Boston Mountains and are typical clear-water, Ozark streams characterized by long pools separated by short riffles. Substrate is primarily gravel and rubble in the headwater sections; rubble, boulder and bedrock in the middle reaches; with some deposits of sand and silt in the lower reaches. Land use in the Kings and Mulberry river watersheds is a combination of agriculture and forestry. The Buffalo river flows through U.S. Forest Service and National Park Service (NPS) lands and has been managed by NPS since 1972. The Kings, Mulberry and Buffalo rivers are free-flowing upstream from their confluence with Table Rock Reservoir, the Arkansas River, and the White River tailwater below Bull Shoals Dam, respectively (Fig. 1).

Cold tailwaters of the White River extend 160 km downstream from Bull Shoals Reservoir, including a second input of cold tailwater from the North Fork of the White River below Norfork Reservoir which joins the White River approximately 17 km below the confluence of the Buffalo River. Tailwaters created from these impoundments support an important put-and-take fishery for rainbow trout (*Oncorhynchus mykiss*) and brown trout (*Salmo trutta*). Although warmwater streams flow into this coldwater stretch of the White River, the mainstream is not warmed sufficiently to eliminate trout (Aggus et al., 1977).

Discharges of the Kings, Mulberry and Buffalo rivers vary seasonally, with a general pattern of high flow during spring and early summer followed by relatively low flow in late summer and autumn. Local storm events, however, can produce flooding in any season. Low discharge during late summer and autumn results in intermittent flow in headwater reaches. Average annual discharge for Kings River is 12 m^3/s and ranges from 0.01 to 35.3 m^3/s (USGS 1988). The Mulberry River has a slightly higher gradient (4.3 m/km) than the other two rivers; average annual discharge is 15.3 m^3/s (USGS 1988). Average annual discharge reported for the middle reach of the Buffalo River is 25.8 m^3/s and ranges from 0.04 to 555.0 m^3/s (USGS 1988).

Assessment of Channel Catfish Migration.--One sampling site each was selected at the mouth of the Kings, Mulberry and Buffalo rivers (Sites 1, 2 and 3; Fig. 1). Four hoop nets were deployed within the main channel at each site. Hoop nets were of two designs; one large net (3.2 cm web, double finger throated, with seven 1.1 m diameter hoops) and one small net (1.9 cm web (bar measure, double finger throated, with six 0.6 m diameter hoops) were fished in tandem (one hoop net-set) continuously from 29 March through 22 April, after which sampling was terminated due to heavy rainfall and flooding. One net fished for a 24 h period represented one net-day of effort (CPUE). Nets were emptied and cleaned every three or four days (5 sampling dates x 4 nets = 20 net samples/river) and all channel catfish collected were enumerated, measured for total length (TL), marked (adipose fin clip), and a pectoral spine was removed before being returned alive to the river. Spine cross-sections of all catfish were examined to identify any hatchery-reared fish stocked in previous years (Siegwarth, 1994). Water temperature (°C) was measured for each river and its respective confluence on the dates nets were sampled.

Differences in catch rates of channel catfish and water temperature among rivers (and their confluences) were compared by analysis of variance (ANOVA) using the Statistical Analysis System (SAS Institute 1988). If a significant difference was found ($P < 0.05$), the ANOVA was followed by Bonferroni's Multiple Range Test to identify rivers that differed from one another. To satisfy the assumptions of the statistical analysis (i.e., constant variance of catches among rivers and normal distribution of residuals), total catch/net sample was transformed using a standard $\ln(x+1)$ transformation (Box and Cox 1964). Regression analysis was used to identify potential relationships between catch rates and water temperature within each river.

Results

A total of 465 channel catfish was collected from 276 net-days of effort from the three rivers during March and April 1992. The largest numbers were collected from the mouths of the Kings (n=169) and Mulberry rivers (n=263), while the fewest were collected from the Buffalo River (n=33). Of the 33 channel catfish collected from the Buffalo River, 25 were determined to hatchery origin. Mean catch per net sample among rivers was significantly ($P<0.5$) lower for Buffalo River than the Kings and Mulberry rivers (Table 1). Overall CPUE for the large nets was 4.3, 3.5 and 0.7 for the Mulberry, Kings and Buffalo rivers, respectively; CPUE for small nets was 1.4, 0.1 and <0.1 for the three rivers, respectively. No previously marked channel catfish were recaptured.

Water temperatures observed during the sampling period did not differ ($P>0.05$) among the Kings, Mulberry and Buffalo rivers. However, water temperatures differed significantly ($P<0.05$) between the White and Buffalo rivers, but not between the Kings River and Table Rock Reservoir or between the Mulberry and Arkansas rivers (Table 2). Water temperature among the Mulberry/Arkansas rivers, and Kings River/Table Rock Lake exhibited consistent trends throughout April, while the Buffalo and White rivers had increasingly larger differences (Fig. 2). Catch rates of channel catfish during March and April were not significantly correlated with water temperature within any of the three rivers ($r^2<0.80$

for each river).

Table 1. Comparison of mean (±SE) catch/hoop net-set of channel catfish migrating into the Kings, Mulberry and Buffalo rivers. Values in each row without a letter in common are significantly different (P<0.05)[a].

Variable	River		
	Buffalo[b]	Kings	Mulberry
Mean catch/net-set	3.3	16.9	26.3
	±1.5	±4.4	±8.2
Transformed ln(x+1) mean catch/net-set	0.8[Y]	2.2[Z]	2.2[Z]
	±0.3	±0.3	±0.4

[a]Comparisons were not made between mean catch/net-set due to violations of statistical assumptions (unequal variance among rivers).

[b]Includes 2.5 fish/net-set which were determined to have a hatchery origin.

Table 2. Comparison of mean (±SE) water temperatures (°C) among the Kings, Mulberry, and Buffalo rivers and their confluence.

River	Confluence	P-Value
Kings	Table Rock Lake	
13.9 (±1.8)	14.3 (±1.9)	P>0.05
Mulberry	Arkansas River	
13.6 (±1.9)	15.5 (±1.8)	P>0.05
Buffalo	White River	
14.8 (±1.6)	9.9 (±0.7)	P<0.05

Discussion

Although several factors can influence CPUE results (Ricker, 1975) and hoop net catches (Muncy, 1957; Mayhew, 1973; Hubert and Schmitt, 1982), comparative catches of channel catfish in the present study are believed to be reliable because of similar limnological and climatic conditions among the Kings, Mulberry and Buffalo rivers during the sampling period, and because of the restricted channel widths of these tributaries. Muncy (1958) and others have shown that adult channel catfish are highly susceptible to capture in hoop nets during the spawning season. Smith and Hubert (1989) concluded that seasonal trends in hoop net catches within a Great Plains river system were associated with spawning migrations into tributary creeks. In this study, CPUE of hoop net samples represents the proportional abundance of channel catfish migrating into each tributary prior to spawning. Thus, despite the shortened sampling interval, spring hoop net sampling measured the relative numbers of channel catfish migrating into the Kings, Mulberry and Buffalo Rivers, with the assumption that catfish collected at the mouth of each tributary were migrating into that tributary. This assumption was supported by an absence of recaptures, and the fact that a number of marked catfish were recaptured 50 to 60 km upstream within the tributaries later in the summer.

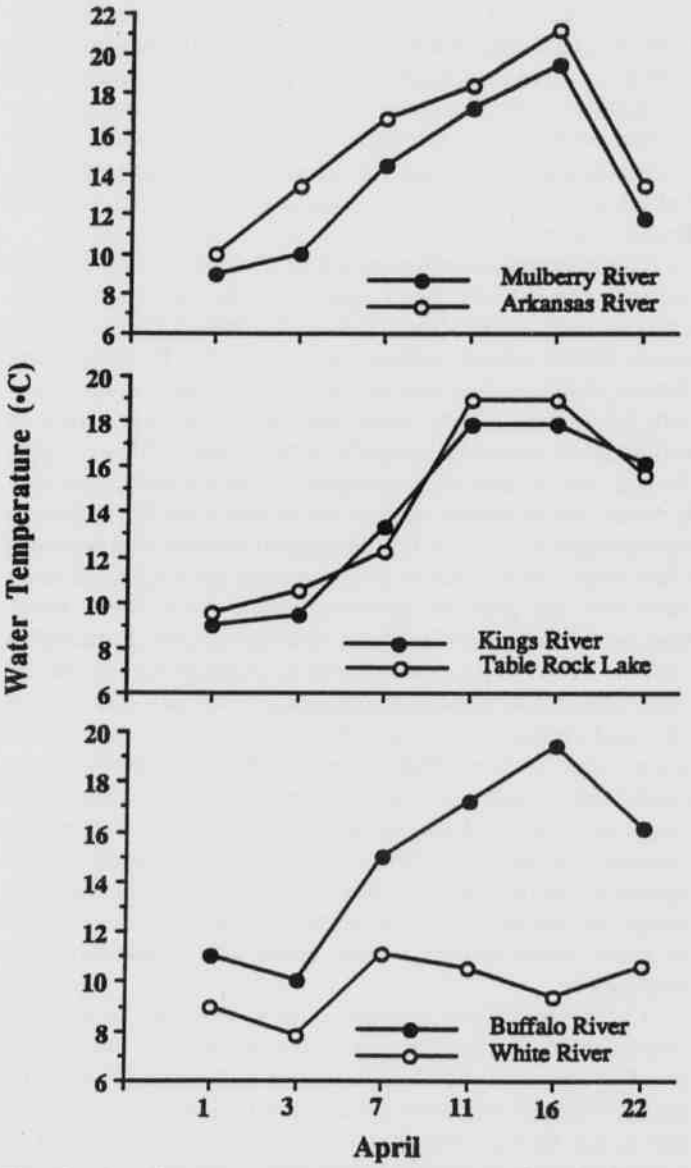

Fig. 2. April water temperature patterns for the Kings, Mulberry and Buffalo rivers, and their respective confluence.

The appearance of channel catfish moving into the Kings, Mulberry and Buffalo rivers conforms with similar patterns of spring movements reported for other waters (e.g., Humphries, 1965; June, 1977; Smith and Hubert,

1989). However, the number of channel catfish migrating into the Buffalo River was significantly less than was observed in the Kings or Mulberry rivers, although the measured physical characteristics (water temperature, turbidity, total discharge) did not significantly vary among these tributaries. Similarly, Brown (1967) reported a lack of spring channel catfish movements into the Buffalo River. This suggests that reduced inputs from migratory stocks of channel catfish since completion of Bull Shoals Dam in 1952 may partially account for the lower reproductive output and sparse adult population observed in the Buffalo River. In Wisconsin, it has also been suggested that without annual migrations of channel catfish, the population in the Wisconsin River would be sparse (T.D. Pellett and D. Fago, Wisconsin Department of Natural Resources, unpublished data).

The relatively small number of channel catfish migrating into the Buffalo River appears to be due to the presence of cold White River tailwaters, which had a significantly lower mean temperature than the Buffalo River during the sampling period. Studies on other cold tailwaters have shown that spawning of warmwater fishes is inhibited by release of hypolimnetic waters (Pfitzer, 1962; Brown, 1967), and that changes in water quality, especially water temperature, appear to be the most likely factors associated with disruption of natural stream communities (Edwards, 1978). Prior to construction of Bull Shoals Reservoir, the present coldwater reach of the White River had an historically abundant channel catfish population (Keith, 1964). The subsequent hypolimnetic release of cold water below Bull Shoals Reservoir has eliminated channel catfish (Brown, 1967) as well as other native warmwater species (Hoffman and Kilambi, 1971) from coldwater reaches of the White River. The coldwater reach may also eliminate temperature cues needed by channel catfish for spring migration. In contrast, no apparent barriers to migration exist downstream from the Kings or Mulberry Rivers; thus, channel catfish are able to move freely between these rivers and their respective confluence.

Cold White River tailwaters act as a barrier to channel catfish migration similar to that reported from other studies. For example, McCammon and LaFaunce (1961) suggested that the relatively closed population of channel catfish in the Sacramento River, California, was the result of a cold tailwater which inhibited movement up-river, increased salinity inhibited down-river movement, and the presence of a diversion dam prevented migration into a major tributary. Similarly, Welker (1967) reported that a lowhead dam appeared to inhibit up-stream movement of channel catfish in the Little Sioux River, Iowa, and McCammon (1956) found that the Palo Verde Weir on the lower Colorado River acted as a barrier to upstream channel catfish movement because tagged fish were caught at the base of the weir and few, if any, catfish moved upstream across the barrier.

Newcomb (1989) recognized the importance of excluding structures that hinder channel catfish passage to important seasonal habitat areas in the Missouri River and its tributaries. Sparse populations of channel catfish observed in some waters may be due to restrictions on catfish migration if suitable habitats for both spawning and overwintering are not available. The need for these specific habitat areas is illustrated by the extensive upstream or downstream movements documented from channel catfish tagging studies. Although clear-water Ozark streams such as the Kings, Mulberry and Buffalo rivers have abundant spawning habitat such as large boulders and rock crevasses, suitable overwintering areas appear to be limited because there are relatively few deep pools (>5 m), especially in downstream reaches.

Results from this study suggest that the sparse channel catfish population in the Buffalo River may be partially attributed to reduced inputs from historic migratory stocks due to cold White River tailwaters. Additional research is needed to quantify the importance of annual pre-spawning migrations for long-term maintenance of tributary channel catfish populations.

Acknowledgements

Funding for this project was provided by the National Park Service (NPS). Thanks are extended to J. Pitlo for review of the manuscript, and T.D. Pellett and W. Hubert for advice. Special thanks to University of Arkansas students J. Walters, D. Bowman, A. Thompson, L. Aberson, and M. Means for field assistance. Arkansas Game and Fish Commission and NPS provided permits for this study.

Literature Cited

Aggus, L.R., D.I. Morais and **R.F. Baker.** 1977. Evaluation of the trout fishery in the tailwater of Bull Shoals Reservoir, Arkansas, 1971-73. Proc. Annu. Conf. Southeast. Assoc. Fish and Wildl. Agencies 31:565-573.

Box, G.E.P. and **D.R. Cox.** 1964. An analysis of transformations. J. Royal Stat. Soc. B 26:211-243.

Brown, J.D. 1967. Study of the fishes of the tailwaters of three impoundments in northern Arkansas. M.S. Thesis. Univ. of Arkansas, Fayetteville.

Dames, H.R., T.G. Coon and **J.W. Robinson.** 1989. Movements of channel and flathead catfish between the Missouri River and a tributary, Perch Creek. Trans. Am. Fish. Soc. 118:670-679.

Edwards, R.J. 1978. The effect of hypolimnion reservoir releases on fish distribution and species diversity. Trans. Am. Fish. Soc. 107:71-77.

Gerhardt, D.R. and **W.A. Hubert.** 1990. Spawning habitat of channel catfish in the Powder River system, Wyoming-Montana. Prairie Nat. 22:155-164.

Hale, M.M., J.E. Crumpton and **D.J. Renfro.** 1986. Catfish movement and distribution in the St. John's River, Florida. Proc. Annu. Conf. Southeast. Assoc. Fish and Wildl. Agencies 40:297-306.

Hawkinson, B. and **G. Grunwald.** 1979. Observation of a wintertime concentration of catfish in the Mississippi River. Minn. Dept. of Nat. Res., Div. of Fish and Wildl., Fisheries Section Invest. Report 365, St. Paul.

Hoffman, C.E. and **R.V. Kilambi.** 1971. Environmental changes produced by coldwater outlets from three Arkansas reservoirs. Water Resour. Res. Center Pub. No. 5, Univ. of Arkansas, Fayetteville.

Hubert, W.A. and **D.N. Schmitt.** 1982. Factors influencing hoop net catches of channel catfish in Pool 9, upper Mississippi River. Proc. Iowa Acad. Sci. 89:84-88.

Humphries, R.L. 1965. A study of movements of the channel catfish (*Ictalurus lacustris punctatus*), in the Savannah River and one of its tributaries within the AEC Savannah River operations area. U.S. Atomic Energy Comm. Rep. TID-21791, Institute of Radiation Ecology, Univ. of Georgia, Athens.

June, F.C. 1977. Reproductive patterns in seventeen species of warmwater fishes in a Missouri River reservoir. Env. Biol. Fishes 2:285-296.

Keith, W.E. 1964. A pre-impoundment study of fishes, their distribution and abundance in the Beaver Lake drainage of Arkansas. M.S. Thesis, Univ. of Arkansas, Fayetteville.

Mayhew, J. 1973. Variations in the catch of channel catfish and carp in baited hoop nets. Proc. Iowa Acad. Sci. 80:136-139.

McCammon, G.W. 1956. A tagging experiment with channel catfish (*Ictalurus punctatus*) in the lower Colorado River. California Fish and Game 42:323-335.

McCammon, G.W. and **D.A. LaFaunce.** 1961. Mortality and movement in the channel catfish population of the Sacramento Valley. California Fish and Game 47:5-23.

Muncy, R.J. 1957. Factors affecting hoop-net and trap catches of channel catfish. pp. 23-28 *In* K.D. Carlander, ed. Symposium on evaluation of fish population in warm-water streams. Iowa State College, Ames.

Muncy, R.J. 1958. Movements of channel catfish in Des Moines River, Boone County, Iowa. Iowa State College J. of Sci. 32:563-571.

Newcomb, B.A. 1989. Winter abundance of channel catfish in the channelized Missouri River, Nebraska. N. Am. J. Fish. Manage. 9:195-202.

Perry, G.W., H. Rogillio, T. Morrison and **I. Dares.** 1985. Preliminary findings of channel catfish tagging study on the Salvador Wildlife Management Area. Proc. Louisiana Acad. Sci. 48:59-64.

Pfitzer, D.W. 1962. Investigations of waters below large storage reservoirs in Tennessee, 1951-1954. Tenn. Game and Fish Comm., Dingell-Johnson Rep., Project F-1-R.

Ranthum, R.G. 1971. A study of the movement and harvest of catfish tagged in the lower Trempealeau River and Trempealeau Bay. Wis. Dept. Nat. Res. Manage. Rep. No. 50.

Ricker, W.E. 1975. Computation and interpretation of biological statistics of fish populations. J. Fish. Res. Board of Canade, Bul. 191.

SAS Institute. 1988. SAS/STAT user's guide, release 6.03 edition. SAS Institute, Cary, N. Carolina.

Siegwarth, G.L. 1992. Channel catfish of the Buffalo National River, Arkansas: population abundance, reproductive output, and assessment of stocking catchable size fish. M.S. Thesis, Univ. Arkansas, Fayetteville.

Siegwarth, G.L. 1994. Identification of hatchery-reared channel catfish by means of pectoral spine cross-sections. Trans. Am. Fish. Soc. 123:830-834.

Smith, J.B. and **W.A. Hubert.** 1989. Use of a tributary by fishes in a great plains river system. Prairie Nat. 21:27-38.

USGS (U.S. Geological Survey). 1988. Statistical summary of selected water-quality data (water years 1975 through 1985) for Arkansas rivers and streams. U.S. Geological Survey Water-Resources Investigations Report 88-4112, Washington, D.C.

Welker, B. 1967. Movement of marked channel catfish in the Little Sioux River, Iowa. Trans. Am. Fish. Soc. 96:351-353.

Evaluation of Photodiode Arrays for Use in Rocket Plume Monitoring and Diagnostics

Dallas Snider, M. Keith Hudson, Robert Shanks and Reagan Cole
Department of Electronics and Instrumentation
University of Arkansas at Little Rock
2801 S. University ETAS 575
Little Rock, AR 72204

Abstract

The spectroscopic analysis of plume emissions is a non-intrusive method which has been used to check for fatigue and possible damage throughout the pumps and other mechanisms in a rocket motor or engine. These components are made of various alloys. Knowing the composition of the alloys and for which parts they are used, one can potentially determine from the emissions in the plume which component is failing. Currently, Optical Multichannel Analyzer systems are being used which utilize charge coupled devices, cost tens of thousands of dollars, are somewhat delicate, and usually require cooling. We have developed two rugged instruments using less expensive linear photodiode arrays as detectors. A high resolution system was used to detect atomic emission lines while a low resolution system was used to detect molecular emission bands. We have also written data acquisition software and built electronic circuits to control the arrays and collect data. While NASA has used similar systems for characterization of the Space Shuttle Main Engine, the emissions from other rocket systems have not been surveyed as well. The two instruments described will be utilized to study hybrid rocket emissions at the UALR hybrid rocket facility.

Introduction

Over the past decade, the National Aeronautics and Space Administration (NASA) has been plagued with several manned and unmanned mission mishaps costing taxpayers millions of dollars. The most infamous of these mishaps was the *Challenger* disaster in 1986. Because these events cause negative public option toward NASA, coupled with the need to cut federal spending and the effect of increasing foreign competition, more pressure has been put on NASA needs to be assured that its boosters will perform satisfactorily at each launch.

One way to assure the proper performance of launch vehicles is to employ extensive engine ground testing on test stands designed for this purpose at research facilities. Using spectroscopic analysis of plume emissions, the "health" of the engine (that it is performing well, not failing), particularly combustion efficiency and the existence of component fatigue, can be determined. The high temperatures and pressures found in a rocket plume make excellent sources for atomic line and molecular band emissions from the near ultraviolet to middle infrared. Currently, monitoring systems are being used which employ charge coupled devices and/or Fabry-Perot interferometers, cost tens of thousands of dollars, are somewhat delicate, and usually require cooling.

A spectrometer using a rugged photodiode array mounted in the focal plane of an imaging spectrograph can be used for the analysis of UV-V is emissions from rocket plumes. Gases such as CN, CO, N_2, and NH_3, and molecular species such as OH, C_2, and CH_2, emit in the visible region and can potentially be monitored. Also, most metals emit in the visible region, which is beneficial for detecting component fatigue or failure. Prior research conducted on the liquid-fueled Space Shuttle Main Engine (SSME) has shown the ability to detect wear from several alloys along the hot gas path.

Plume emission technology can also be applied to jet engines, especially military jets with afterburners. Other military applications include increasing the stealth capabilities of aircraft by reducing air-to-air and air-to-ground missile emission, which is possible through analysis of this type of data. Furthermore, high speed monitoring of the emissions produced by the combustion of propellant in all types of guns and explosives can be used to enhance their performance. Additionally, emission spectroscopy can be used to monitor the efficiency of oil-or coal-fired power plant furnaces.

Materials and Methods

Low Resolution Spectrometer.--A low resolution spectrometer for molecular band emission studies was constructed as shown in Fig. 1. The components for the spectrometer were positioned in a similar manner as a standard flame emission spectrometer (Ingle and Crouch, 1988). The components include the photodiode array

with associated timing and output electronics, the collection optics, an imaging spectrograph, an oscilloscope, and a computer.

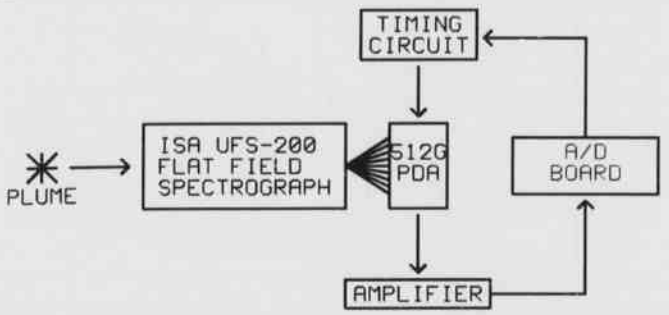

Fig. 1. Block diagram for the low-resolution spectrometer.

The photodiode array used in the low-resolution spectrometer was an EG&G Reticon 512G monolithic, self-scanning, linear array. This array has 512 photodiodes on 25 μm centers, thus giving a sensitive length of 12.8 mm. Each photodiode is 26 μm in height, which is relatively small when compared to the height of the slit on the spectrograph. Because of the array's monolithic, dual-inline-package (DIP) design, it was mounted into an 18-pin DIP socket that in turn was mounted to a circuit board. According to the manufacturer, this array was designed for use in low-cost facsimile and optical character recognition applications. While not optimized for spectroscopy, it offered a low cost alternative and was readily available.

Timing signals needed to drive the array were generated externally. The three required signals, clock, start, and reset, are shown in Fig. 2 and were produced by the circuit in Fig. 3. The circuit that produced the timing signals was mounted on a circuit board separate from the board to which the photodiode array was mounted. Pins 8 and 9 on the 512G array produce a video and dummy output respectively. These outputs were sent to a differential amplifier to extract the video signal and then through a low-pass filter before being sent simultaneously to the oscilloscope and to the Channel 0 High input on the analog-to-digital converter board installed in the computer. Fig. 4 shows the circuit board with the array and video output circuit (G Series, 1992).

The detector circuit board was positioned so the photodiodes in the array are in the focal plane of an Instruments SA UFS-200 Flat Field Spectrograph (UFS-200). The UFS-200 employs an aberration corrected concave holographic grating. This grating is 70 mm in diameter and is blazed with 200 grooves/mm. Its spectral range is from 200 to 800 nm with a dispersion of 24 nm/mm. The entrance slit is 3.8 mm high and 100 μm wide.

The collection optics were simply a convex lens and aperture stop. The lens was made of glass and housed in an aluminum bracket. It was 10.1 cm in diameter and had a focal length of 23 cm. This lens was able to focus a small part of the flame on the entrance slit. Using a glass collection lens was justified since the window on the photodiode array was also made of glass. The aperture was mounted to the lens housing and used to control the amount of light reaching the entrance slit. It had a maximum diameter of 9.78 cm and a minimum diameter of 0.56 cm.

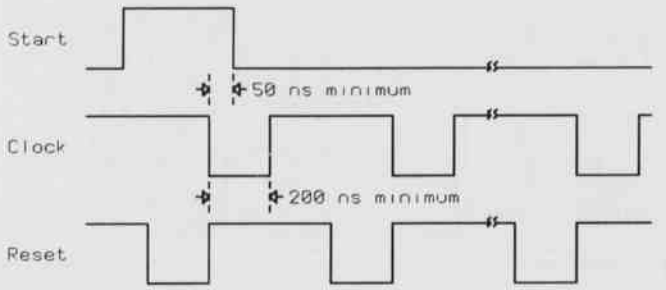

Fig. 2. Timing signals required for operation of the 512G.

A Zenith 80286AT personal computer equipped with an 80287 math coprocessor, and Computer Boards C10-AD16JR-AT analog-to-digital conversion board (A/D board) was used to collect and store data. Data acquisition was controlled by a Borland Turbo C program. The program first prompts the user for the name of the file to which the data were to be written, the number of scans to be taken, and the amount of time delay between scans. Next, a TTL pulse was sent out from the Digital Output 0 (Dig Out 0) to the circuit on the array board shown in Fig. 4. The signal produced by this circuit was sent to the Digital Input 0/Trigger (Dig. In/TRIGGER) on the A/D board. The signal to the Dig. In 0/TRIGGER was in sync with the clock pulses, however, they only occur after the start pulse and only for 512 pulses. Therefore, there was one sample collected per pixel. The program stopped data collection after 512 pulses and resets the LS7474 flip-flop to await the next scan. A timing diagram for these pulses is shown in Fig. 5 (Schildt, 1990; CIO-AD16JR, 1991). The collected data for each scan was stored via Direct Memory Access (DMA) to a specified memory segment. After all scans had been taken, the data were saved, along with all corresponding pixel numbers, to a file on the computer's internal hard disk drive. The data were written to an ASCII file in a format that allows them to be read and plotted by the graphing program. SPLOT.

High Resolution Spectrometer.--The high-resolution spectrometer for atomic line emission and detailed molecular band studies was constructed as shown in Fig. 6.

Again, the components for the spectrometer were positioned in a similar manner as a standard flame emission spectrometer (Ingle and Crouch, 1988). The components include a photodiode array with associated timing and output electronics, the collection optics, an imaging spectrograph, an oscilloscope, and a computer.

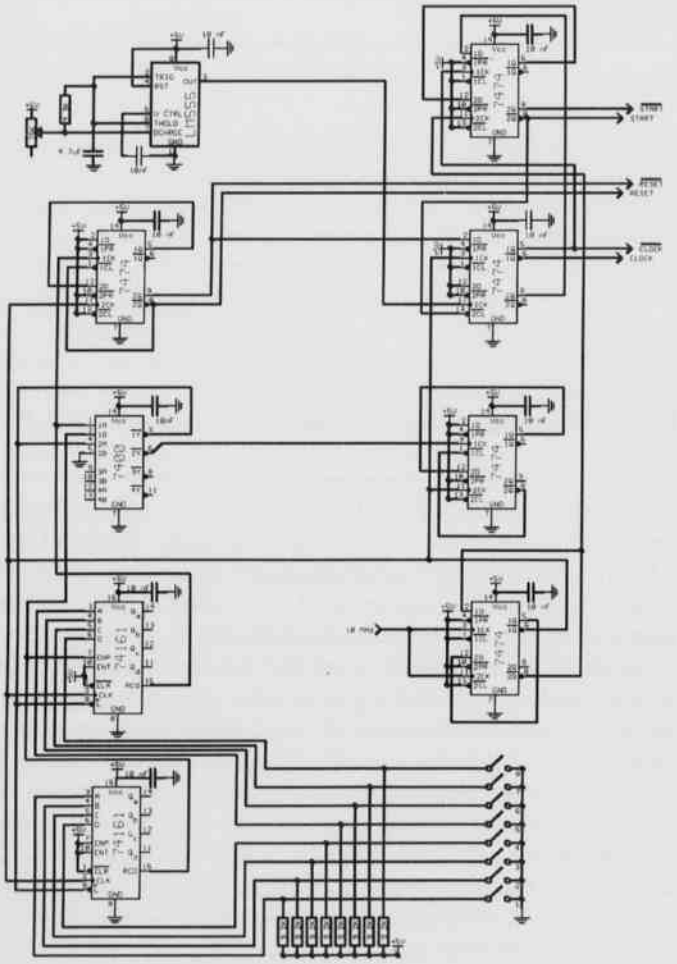

Fig. 3. Circuit to produce the timing signals in Fig. 2.

The photodiode array used in the high-resolution spectrometer was an EG&G Reticon 1024S monolithic, self-scanning, linear array. This array had 1024 photodiodes on 25 µm centers, thus giving a sensitive length of 25.6 mm. Each photodiode array was 13 µm wide and 2.5 mm high. According to the manufacturer, the 1024S was designed for spectroscopic studies. The slit-like geometry of each photodiode allows for the maximum amount of light possible to strike the photodiodes (S Series, 1991). The photodiode array was set in an EG&G Reticon RC1001 Satellite Board.

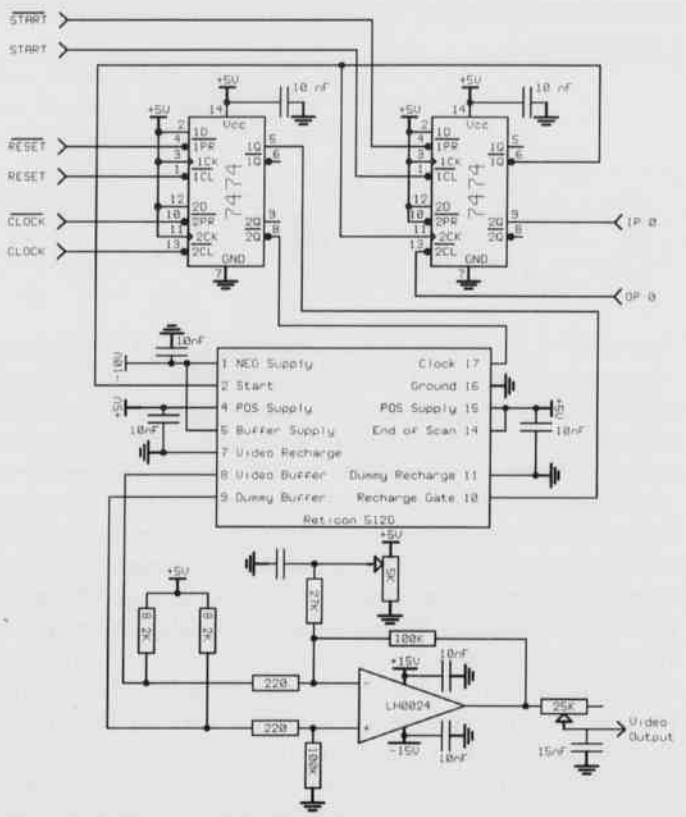

Fig. 4. Sensor board schematic.

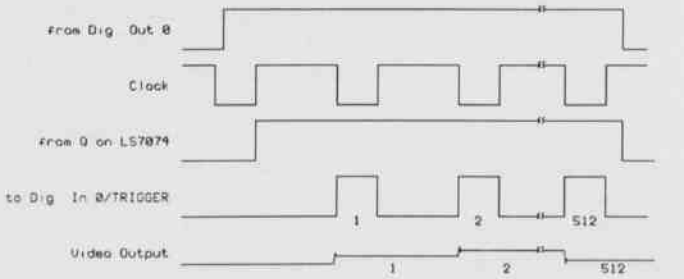

Fig. 5. Timing diagram for interfacing the 512G and A/D board.

The satellite board was connected to an EG&G Reticon RC1000 Mother Board via a 16-pin ribbon cable for digital signals and a six lead cable for analog signals. The RC1000 produces the required timing signals for the array, and it also has the necessary video processing circuitry. A single BNC connector allows the video signal to be output to an oscilloscope. In this setup, the video signal was sent to an oscilloscope and the computer as used previously (RC1000/RC1001, 1991).

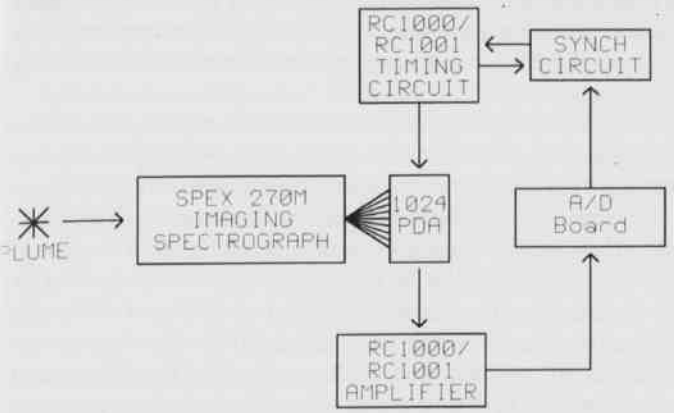

Fig. 6. Block diagram for the high-resolution spectrometer.

The combination of the EG&G Reticon RC1000 and RC1001 was designed for evaluation of photodiode arrays. It comes from the manufacturer ready to be hooked up to an oscilloscope, but not to a data acquisition system. A circuit was designed to interface between the RC1000 and a Computer Board CIO-AD16Jr-AT analog-to-digital converter board. This interface circuit is shown in Fig. 7. It produces a start pulse which was sent to the external start input on the RC1000. The circuit also produces active high TTL signals to the Dig. In O/TRIGGER input on the A/D board. These signals were synchronized so that one sample was taken for each pixel of the 1024S photodiode array. Fig. 8 shows the timing diagram for the interface circuit. In order for the interface circuit to perform properly, the start pulse input jumper on the RC1000 had to be set from internal to external. The timing and signal processing circuitry that was designed and built for the low resolution system (Figs. 3 and 4) was not necessary for the high resolution unit because of the outstanding performance of the RC1000/RC1001.

The 1024S photodiode array was positioned in focal plane of a SPEX 270M Imaging Spectrograph. The 270M employs two holographic gratings mounted on a motorized turret, so the optimum grating could be chosen depending on the wavelength to be analyzed. Both gratings have 1200 grooves/mm, one blazed for 250 nm and the other for 630 nm. Its spectral range was from 0 to 1100 nm with a dispersion of 3.1 nm/mm. The flat field area in the focal plane was 25 mm wide by 12 mm high, which gives 77 nm of coverage over the 25-mm width. The motorized turret allows a specific range of wavelengths to be observed. The entrance slit was 1.52 cm high and its width variable in 12.5 μm steps. The settings on the 270M were selected using the SPEX Hand Scan hand-held controller. This controller allows the user to select the desired grating, wavelength range, and entrance slit width (270M, 1993; Hand Scan, 1993).

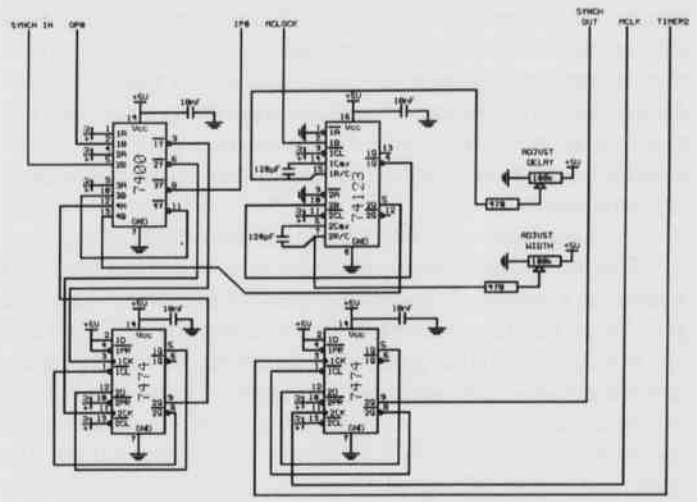

Fig. 7. Schematic for the interface circuit.

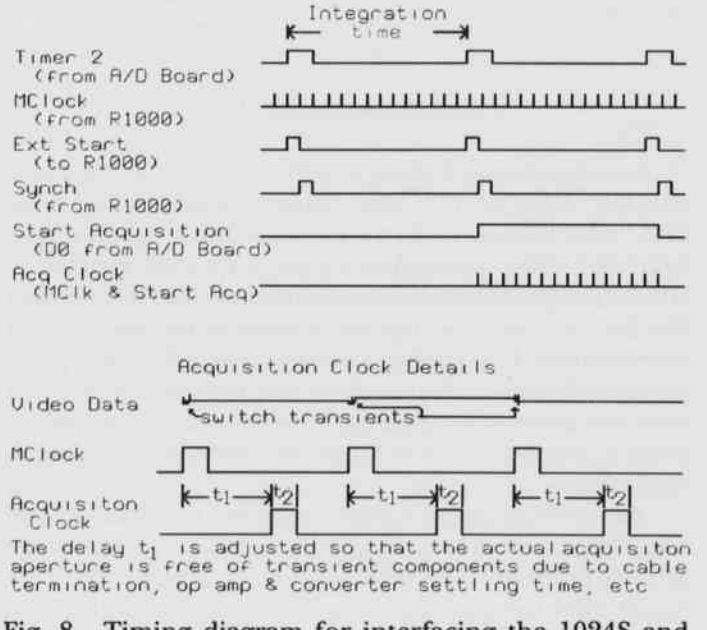

Fig. 8. Timing diagram for interfacing the 1024S and A/D board.

A BK Precision 20 MHz Model 2120A was used for alignment and calibration of the instrument. It was also used to set the proper integration time to attain a maximum signal without saturation. Channel 1 was used to monitor the video output. The sync output from Pin M on the RC1000 was sent to Channel 2 to provide a trigger pulse.

A Gateway 2000 486 personal computer with Computer Boards CIO-AD16JR-AT A/D board was used to collect and store data. Data acquisition was controlled by a Borland Turbo C program. The program first

prompts the user for the name of the file to which data was to be written, the number of scans to be taken, and the amount of time delay between scans. The program then prompts the user for the integration time or exposure. The value entered for the integration time was not the actual exposure time, but was the value written to Counter 2. To determine the integration time the following equation was used:

Integration time = (256 * Counter 2 value)/1,000,000.

The integration time pulse was sent out from the A/D board on Counter 2 out to the interface board. The pulse sent from the interface board to the Dig. In 0/TRIGGER on the A/D board triggers the sampling of the video signal which was coming in on Channel 0 High. The collected data for each scan was stored via DMA to a specified memory segment. After all scans have been taken, the data was saved, along with its corresponding pixel number, to an ASCII file on the computer's internal hard disk drive. The data was written to the file in a format to be read and plotted by the graphing program SPLOT (Schildt, 1990).

Results and Discussion

Low Resolution Software.--The Reticon 512G has a sensitive width of 12.8 mm. When mated with the UFS-200, which has a dispersion of 24 nm/mm, the 512G/UFS-200 combination gives a spectral window of 307.2 mm. Because this window does not cover the entire 200-800 nm range of the spectrograph, the array board was positioned in varying locations along the focal plane to see different portions within the UV-Vis region. Each time the array was repositioned, a scan of the emissions from a Pen-Ray mercury lamp was taken for wavelength calibration.

To obtain a useful spectra from the raw data, several steps have to be taken, all of which are carried out in the SPLOT program. The first step was to subtract the dark signal from the data. This step takes out most of the fixed pattern noise, which is common in photodiode arrays operating at room temperature. Being able to do this allowed us to decrease costs because the array does not have to be cooled. The next step was to convert the x values of the data from pixel number to wavelength. This was accomplished by scaling the x value by an amount determined by the following equation:

Scaling factor = -(Dispersion * Sensitive Length)/Number of Pixels

which has a value of -0.6 for the 512G/UFS-200 combination. The scaling factor was negative because the data was collected in decreasing values of wavelength with increasing values of pixel number. After multiplying by this negative value, the data has increasing wavelength values along the increasing x-axis of the plot. The next step was to offset the x-axis by 307.2 so the first point of the spectra was at zero nanometers. Finally, the appropriate amount of offset on the x-axis was determined by the Hg lamp spectra.

Initial studies were conducted by analyzing the flame produced by a Perkin-Elmer Atomic Absorption (AA) burner. The acetylene/air mix was adjusted to produce a lean flame with a bright blue interconal region. The spectra of this interconal region is shown in Fig. 9. The molecular bands centered at 463, 509, and 559 were created by the C_2 species. The bands centered at 382 and 427 were created by the CH series (Gaydon, 1974). The hump centered at 587 is not due to an emission band but was caused by fixed pattern noise.

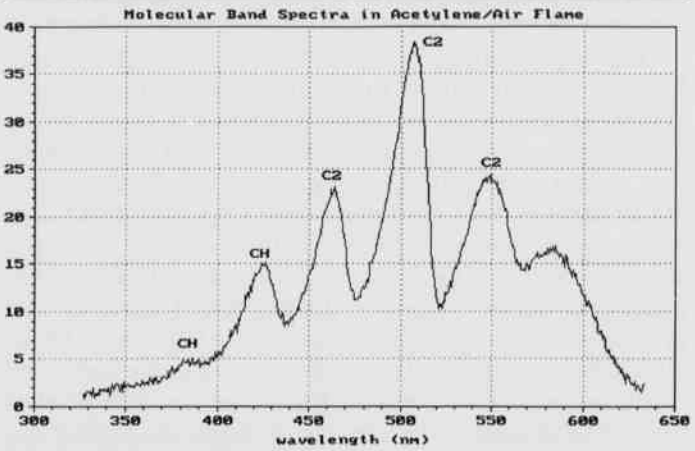

Fig. 9. Spectra of the interconal region of a C_2H_2/air flame recorded with the low-resolution spectrometer system.

Studies have also been done by aspiring NaC1 solutions of varying concentration into the AA burner to determine how well the low resolution unit could detect atomic emission lines. Fig. 10 shows the Na emission line at 598 nm for concentrations of 5, 10, 15, and 20 ppm. As expected, the peak intensity at 598 nm increased linearly with increasing Na concentration (Fig. 11).

High Resolution Spectrometer.--The Reticon 1024S has a sensitive width of 25.6 mm. When mated with the SPEX 270M, which has a dispersion of 3.1 nm/mm, the 1024S/SPEX 270M combination gives a spectral window of 79.36 nm. Because of this narrow window, the wavelength selector on the 270M was always set to center the atomic line emission wavelength of the species to be observed.

For the high-resolution spectrometer, only two steps have to be taken to obtain a useful spectra from the raw data. Again these steps were carried out in the SPLOT program. Unlike the low-resolution unit, the dark signal does not have to be subtracted because of the reduced fixed pattern noise and high quality video signal output of the RC1000/1001. The first step was to convert the x

values of the data from pixel number to wavelength. This was accomplished by scaling the x values by an amount determined by the following equation:

Scaling Factor = (Dispersion * Sensitive Length)/Number of Pixels

which has a value of 0.0775 for the 1024S/SPEX 270M combination. The scaling factor was positive for the high-resolution unit because the data was collected in increasing values of wavelength with increasing values of pixel number. The next step was to offset the x-axis by the value for the wavelength selector minus 39.68. This was done because the wavelength selector determined the wavelength falling on the center pixel, so half of the spectral window, 39.68 nm, must be subtracted, to allow the proper wavelength values to be assigned to the spectra.

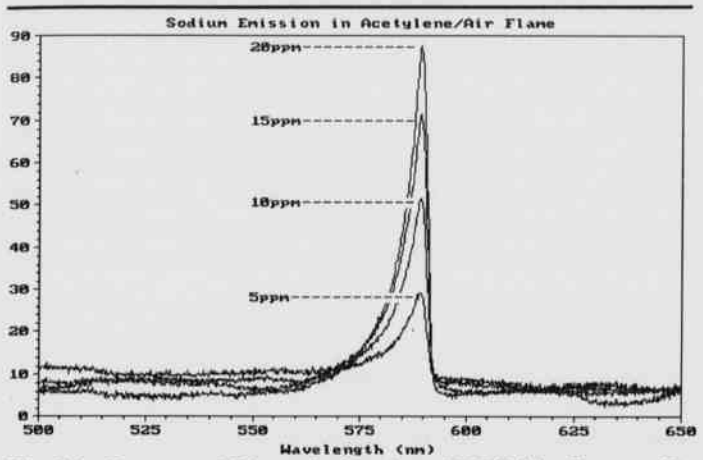

Fig. 10. Spectra of Na emission in a C2H2/air flame with varying concentrations of Na recorded with the low-resolution system.

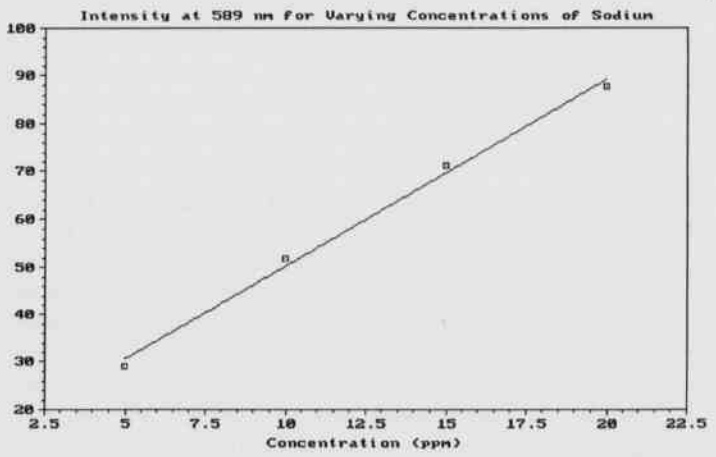

Fig. 11. Plot of peak intensity vs. concentration at 579 nm showing a linear increase in intensity with increasing Na concentration.

Several studies were being conducted on the emissions radiating from the plume of the hybrid rocket motor at the University of Arkansas-Little Rock's Combustion Diagnostics Facility, During initial tests of the high resolution unit, data was collected on the Na emission line at 589 nm and K emission lines at 763 and 766 nm. Na and K are evidentally present in the hydroxyl-terminated polybutadiene fuel grain as contaminant's from the manufacturing process. Data for Na and K were taken for three-second burns.

Figure 12 shows that the Na emission gradually rises throughout the burn. After the oxidizer was shut off at three seconds, the blackbody curve rises which is indicative of fuel rich combustion. After four seconds, the N_2 purge gas extinguishes all combustion.

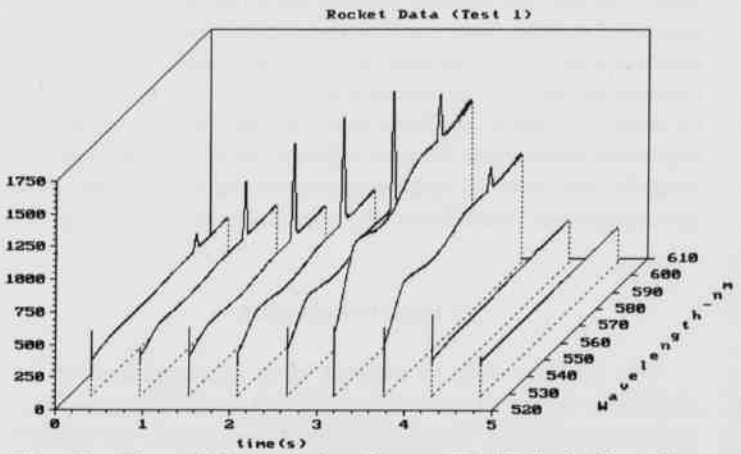

Fig. 12. Plot of Na emission from a HTPB hybrid rocket grain during a three second firing.

Figure 13 shows that the K emission starts off strong, but was overwhelmed by the blackbody radiation. Part of this was due to the fact that the region in which the K lines are present is approaching the near IR where blackbody radiation curves are more predominant.

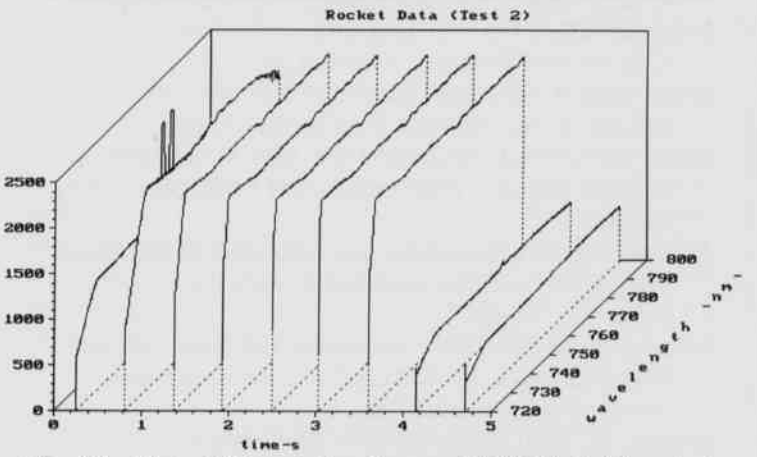

Fig. 13. Plot of K emission from a HTPB hybrid rocket grain during a three second firing.

Journal of the Arkansas Academy of Science, Vol. 48 [1994], Art. 1

Conclusions

Future studies will involve casting hybrid rocket fuel grains with known concentrations of metal salts to simulate wear within a launch scale hybrid rocket motor. We have seen that the 512G detector in the low resolution spectrometer is effective for characterizing band spectra, however, the signal-processing electronics need to be modified to decrease the fixed pattern noise which could be interpreted as a nonexistent emission band. Additionally, an improved low-resolution unit could be build by replacing the 512G photodiode array with a 1024S.

The 1024S detector has provided excellent results. By speeding up the timing and decreasing the integration time, we should have an instrument that can perform, in many applications, as well as or better than commercial Optical Multichannel Analyzers, without the higher cost or need for cooling. The planned improvement of the high-resolution unit by controlling the 270M through its RS-232 port should also enhance the spectrometers performance and capabilities.

Acknowledgements

The authors wish to express their appreciation to the National Aeronautics and Space Administration, the Arkansas Space Grant Consortium, and Hercules Aerospace for support of this work.

Literature Cited

CIO-AD16JR-AT User's Manual. 1991. Computer Boards, Inc., Mansfield, Massachusetts, 103 pp.

G Series: 128, 256, 512 and **1024 Elements.** 1992. EG&G Reticon Data Sheet, Sunnyvale, California, 8 pp.

Gaydon, A.G. 1974. The spectroscopy of flames. Capman and Hall, London, 412 pp.

Hand Scan Hand-Held Controller Manual. 1993. SPEX Industries, Inc., Edison, New Jersey, 32 pp.

Ingle, J.D. and **S.R. Crouch.** 1988. Spectrochemical analysis. Prentice Hall, Englewood Cliffs, New Jersey, 590 pp.

RC1000/RC1001 Operation and Alignment Instructions. 1991. EG&G reticon data sheet, Sunnyvale, California. 10 pp.

S Series Solid State Line Scanners: 128, 256, 512, and **1024 Elements.** 1991. EG&G reticon data sheet, Sunnyvale, California, 6 pp.

Schildt, H. 1990. Turbo C/C++: The complete reference. Osborne McGraw-Hill, Berkeley, California, 1016 pp.

UFS-200 Flat Field Spectrograph. Instruments S.A. data sheet, Metuchen, New Jersey, 5 pp.

270M Rapid Scanning Imaging Spectrograph/Monochromator User Manual. 1993. SPEX Industries, Inc., Edison, New Jersey, 79 pp.

Multisite Microprobes for Electrochemical Recordings in Biological Dynamics

G. Sreenivas, S.S. Ang, R.M. Ranade, A.S. Salian and W.D. Brown
Department of Electrical Engineering
University of Arkansas
Fayetteville, AR 72701

Abstract

For over 30 years, techniques have been developed that allow for the microscale (10-30 μm) measurement of chemical signals with high temporal resolution (1-200 Hz). Such measurements, called *in vivo* electrochemical recordings, allow for the direct determination of neurotransmitter molecules and related compounds in biological systems. Multiple recordings, simultaneously performed at different, closely spaced, well defined locations throughout a three-dimensional tissue volume in the brain, are of interest in neuroscience. Developments in microelectronic techniques enable the fabrication of multi-electrode microprobes for recording extracellular action potentials generated by individual neurons simultaneously. A high-yield microfabrication process has been successfully developed for the fabrication of a novel semiconductor-based, four-site silicon microprobe that involves a three-mask process and standard UV photolithography. A plasma process has been developed for dry etching of the gold electrodes and conducting lines. The electrochemical behavior of the microprobe is investigated by a high-speed computer-based *in vitro* electrochemical recording system. The electrochemical signals are measured at 5 Hz and varying gain. It is found that a selectivity of over 500:1 is achieved, and the signal to noise ratio of the recorded signal is particularly suitable for *in vivo* recordings.

Introduction

One of the central challenges in neuroscience is associated with the development of improved instrumentation for studying the central nervous system (CNS). Such instrumentation is needed both to better understand the information processing techniques used in neural structures and to aid in the development of a variety of closed-loop neural prostheses (Hoogerwerf and Wise, 1991). Multiple recordings, simultaneously performed at different, closely spaced, well defined locations throughout a three-dimensional tissue volume in the brain are of interest in neuroscience to derive useful prosthetic control signals (Prohaska et al., 1986). For over 30 years, the principle technique for studying the neural activity has been insertion of fine-tipped microelectrodes into the brain to record the extracellular action potentials generated by individual neurons (Rose and Mountcastle, 1954).

Developments in microelectronic techniques enable the fabrication of extremely small and precise structures that can be laid out in any desired way to match the recording site pattern for simultaneous neural recordings. Some of the valuable advantages offered by the thin film microprobes include a high degree of reproducibility, a precise knowledge of spatial distribution of electrode area, a high packaging density for a given implanted volume, and distribution of electrodes in a specific geometry pattern. Also, such multi-site semiconducting microprobes reduce the number of experiments necessary to collect the required data.

The John Hopkins' microprobes (Blum et al., 1991), consisting of a molybdenum-polyimide structure, exhibits poor mechanical strength, and the fabrication process yield is about 10% (all four good sites). Another major shortcoming of these probes is the polyimide dielectric material which is not suitable for chronic implants. The Michigan probe (BeMent et al., 1986), with a typical process yield of over 80%, has been fabricated on a silicon substrate with the thickness of the probes determined by the depth of a deep level boron diffusion.

In this paper, a new microfabrication technique for the fabrication of four-site semiconducting microprobes is presented. Figure 1 shows a three-dimensional view of one such four-site microprobe. The sensing electrodes of area 5580 μm^2 (155 μm by 36 μm) are placed on the tip of the microprobe and are spaced 200 μm from the center of the adjacent site. Bond pads are situated on the rear end of the microprobe and allow for external electronic connections. The microprobes are characterized *in vitro* using a high-speed computer-based electrochemical recording system. Also, the impedance and the integrity (lifetime) of the microprobe are investigated.

Materials and Methods

Microfabrication of the microprobes (electrodes) begins with a 3 milli-inches (mil) p-type <100> oriented sil-

icon wafer that acts as the host substrate. Silicon nitride (Si_3N_4) depositions are performed in a parallel-plate, capacitively-coupled, 13.56 Mhz Reinberg-type reactor (Texas Instruments Model A24C) by plasma decomposition of monosilane (SiH_4), ammonia (NH_3), and nitrogen (N_2). A modified Perkin Elmer Model 2400 sputtering machine is used to sputter successive layers of titanium-tungsten and gold on the patterned substrates. Patterns are transferred onto the substrates using a Quintel mask aligner/exposure system by a standard UV photolithography process. A Plasma Therm Model 520, parallel-plate reactive ion etcher (RIE) is used for selective dry etching of Si_3N_4, gold, and Hunt HPR-204 positive photoresist. Flow rates during both deposition and etching processes are electronically controlled by mass flow controllers. The microprobes are then separated from the host substrate by orientation dependent etching. The microprobes are then mounted on a custom made printed circuit board (PCB) carrier and either ultrasonically wire bonded using 3 mm aluminum wire with an Orthodyne Model 20 wire bonder or epoxy bonded, using ABLEBOND*967-1, to the printed circuit board carrier which allows for external electronic connections and acute recordings. A high-speed computer-based *in vivo* electrochemistry recording system is used for characterizing and qualifying the microprobes for *in vivo* recordings. Furthermore, the frequency response and impedance characteristics of the microprobes are also measured.

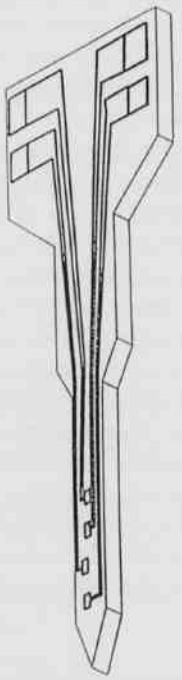

Fig. 1. Three-dimensional view of the four-site silicon microprobe.

Fabrication Process.--A typical process sequence is shown in Fig. 2. As shown, the fabrication process begins with a three-mm silicon wafer as the host substrate material and involves three masking steps. Silicon is strong, yet flexible when thinned, and is inert in the body. Therefore, it qualifies as a suitable substrate for chronic implants over other substrate materials.

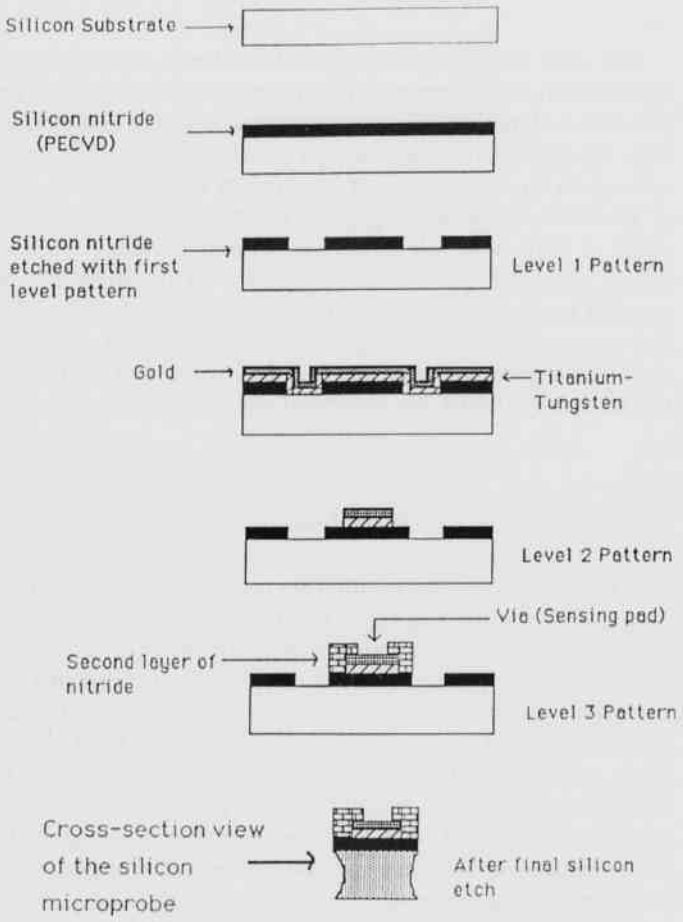

Fig. 2. A typical process sequence for the fabrication of the four-site silicon microprobe.

A sufficiently thick layer of silicon nitride, grown by plasma-enhanced chemical vapor deposition (PECVD), serves as a dielectric layer between the electrodes and the host substrate. Silicon nitride is a preferred choice since it is impervious to extracellular fluid. It is deposited by gas phase dissociation of monosilane (SiH_4), ammonia (NH_3), and nitrogen (N_2). This mixture of gases is excited by an RF plasma in which high-energy electrons dissociate reactant gases to allow deposition of solid material on the substrate at moderate temperatures (300°C). The silicon nitride deposition conditions are summarized in Table 1.

The outline of the microprobe is defined with a first-level photomask using a standard UV photolithographic process by which a pattern of photo-sensitive masking material is applied to the surface of a silicon substrate. The silicon nitride is subsequently etched from exposed areas by reactive ion etching. Table 2 provides source gases, etch rates, and other etch parameters for different materials used to fabricate the microprobes.

Table 1. The processing parameters used to deposit silicon nitride (Si_3N_4) films.

Experimental conditions:	
Deposition power (RF)	100 W (28 mW/cm^2)
Deposition frequency (RF)	13.56 MHz
Deposition temperature	300°C
Deposition rate	120 Å/min
Total gas pressure	1 Torr
Gas flow rates:	
Silane	100 sccm
Ammonia	80 sccm
Nitrogen	200 sccm

Table 2. Source gases, etch rates, and other etch parameters used to etch different materials.

Material	Gases/flow rate	Power	Pressure	Etch rate
Silicon nitride	CF_4 (25 sccm)	200 W	500 mT	200 Å/min
Gold/Ti-W	CF_4 (17 sccm) CCl_4 (25 sccm)	450 W	150 mT	914 Å/min
Photo resist	Oxygen (89 sccm)	450 W	700 mT	650 Å/min

The next step in the process is the sequential sputtering of ≈250Å of titanium-tungsten (Ti-W) and 2500 to 3000Å of gold (Au) onto the patterned microprobe. Gold, being highly electropositive and non-corrosive, is an excellent metal for chronic implants. Unfortunately, the adhesion of gold to silicon nitride is a major metallization problem. However, the thin layer of Ti-W acts as a barrier layer and promotes adhesion. In the sputtering process, the required coating material is dislodged and ejected from a target by momentum transfer due to energetic particles (argon ions and radicals in this case). A second-level mask is used to photolithographically define the Au and Ti-W to form the sensing electrodes, conducting lines, and bonding pads. As shown in Table 2, the etch rate for Au/Ti-W is ≈914 Å/min with an etch selectivity of 1.5 over positive photoresist (Ranade et al., 1993).

Figure 3 shows a scanning electron micrograph (SEM) of several 3 μm gold conductors etched using reactive ion etching. Good edge definition is achieved without significant undercutting implying that gold etching is primarily anisotropic.

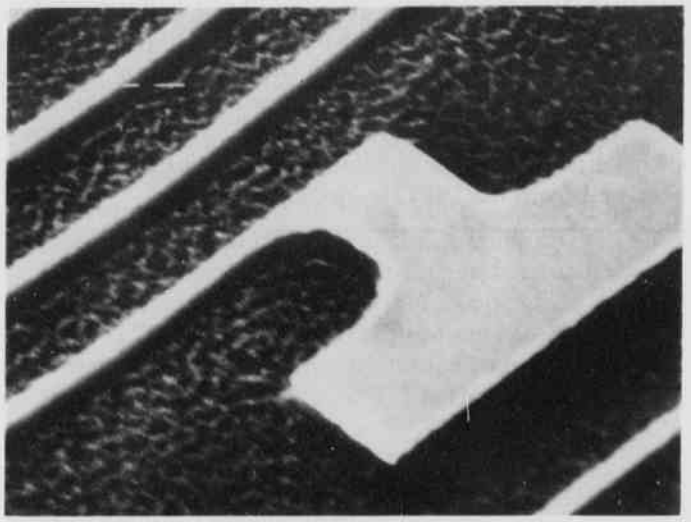

Fig. 3. Scanning electron micrograph (5000X) of several 3 μm lines etched using RIE.

A second layer of silicon nitride is then deposited, photolithographically defined, and etched to provide openings for sensing electrodes and bonding pads. Finally, the silicon microprobes are separated by an orientation-dependent etchant, ethylene-diamine pyrocatechol (EDP) in water. The thickness of the probes can be tailored to meet any requirement. The final thickness of these four-site silicon microprobes is about 50 μm. The fabrication processes are controlled to obtain a typical yield in the 70 to 80% range.

After separation, the good microprobes are mounted onto a custom made printed circuit board (PCB) carrier and wires are either ultrasonically or epoxy bonded from the microprobe to the PCB as shown in Fig. 4.

Characterization.--In vitro tests are performed to obtain most of the information required to qualify an electrode for electrochemical and electrophysiological studies. Quantitative measurements of microamines are performed with the microelectrodes using a high-speed chronoamperometric recording technique. Fig. 5 shows typical chronoamperometric measurement data. The microelectrodes were dip-coated with a thin layer of nafion, a perfluorosulfonated derivative of Teflon, to increase the selectivity of cationic neurotransmitters such as dopamine, norepinephrine, and serotonin *in vitro*. Their selectivities versus anionic interferents such as ascorbic acid in extracellular recording were also characterized (Van Horne et al., 1990). Dopamine calibration in 2 μM increments, challenged with 250 μM ascorbate, was

Journal of the Arkansas Academy of Science, Vol. 48 [1994], Art. 1

performed to the study sensitivities and recording characteristics of sensing electrodes. Square-wave pulses of 0.0 to +0.55 V, with respect to a Ag/AgCl reference electrode, were applied to the working electrode. The measurements are performed at 5 Hz and varying gain settings. The resulting oxidizing and reducing currents were digitally integrated for a fixed recording period. Figure 6 shows linear regression data for the sensing electrode obtained from the IVEC recording system.

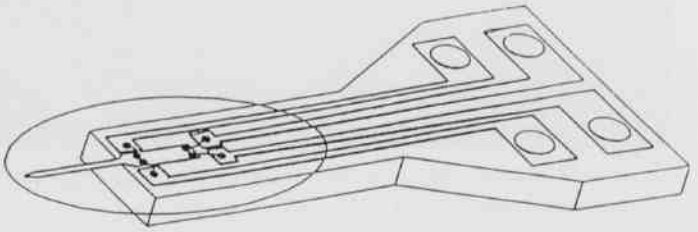

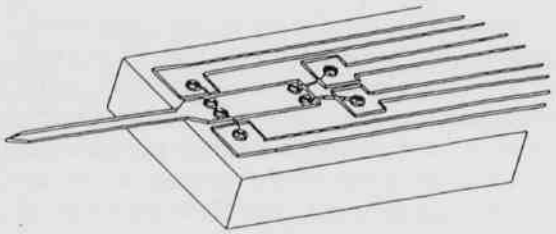

Fig. 4. A complete probe assembly consisting of microprobes bonded onto a printed circuit board carrier.

Results and Discussion

As can be seen in Fig. 6, the electrode responded linearly to increasing concentrations of dopamine with the linear regression correlation coefficient of the calibration curves being greater than 0.998. Typical selectivities for dopamine detection versus ascorbic acid achieved lie in the range of 300-900:1. Furthermore, the detection limit of the microelectrodes range from 25-150 nano-molar at a signal-to-noise ratio of 3. Current state-of-the-art carbon fibre probes have less than a 50 nano-molar detection limit at a signal-to-noise ratio of 3 (Gerhardt et al., 1984). The oxidation curve is found to have a slope of better than 100,000. A typical red-ox current ratio of about 0.6 to 0.8 was recorded.

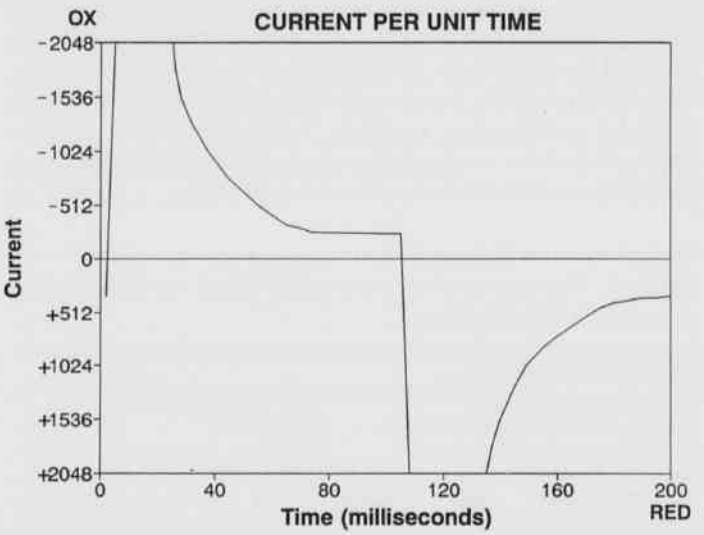

Fig. 5. Typical calibration data for the sensing electrode recorded using chronoamperometry.

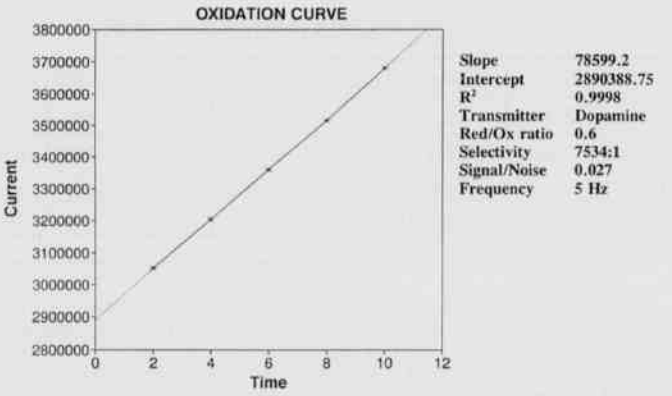

Fig. 6. Linear regression data for oxidation of the sensing electrode of Fig. 5.

An impedance tester was used to measure the impedance of each of the recording sites. The recording site impedance depends on the site material, site area, surface roughness, electrolyte, signal frequency, and current density (Prohaska et al., 1986). The measured impedance of the electrode is based on the potential developed at the electrode-electrolyte interface. A typical site impedance of 2 to 5 MΩ is measured at 2 KHz, which is in the appropriate range for a good neuronal recording (Ang et al., unpublished). Furthermore, tests of probe lifetime for continuous immersion in physiological saline solution

conducted on the microelectrodes over an extended period of time (180 hours), suggest that the site impedance remains relatively stable over the soak duration (Ang et al., unpublished). Such measurements are accomplished by calibrating the system using resistors for the microelectrode and correlating the measured potentials with a resistor value.

Summary and Conclusions

A high-yield microfabrication process has been successfully developed for the fabrication of a novel semiconductor-based, four-site silicon microprobe for electrochemical and electrophysiological recordings. The electrochemistry of these silicon microprobes was characterized quantitatively by *in vitro* measurements.

The microprobes were characterized for the sensitivity and recording characteristics of dopamine calibrated against ascorbic acid. A typical selectivity of over 500:1 for dopamine versus ascorbic acid was achieved. Also, the microelectrodes responded linearly to increasing stock solution (concentrations) of dopamine. Furthermore, the detection limit of the microelectrodes was found to lie in the range of 25-150 nano-molar at a signal-to-noise ratio of 3.

A typical electrode site impedance, in the range of 2 to 5 MΩ, was measured at a frequency of 2 KHz. The integrity of the microprobe dielectrics was examined by observing the stability of the site impedance during a 180 hour soak test in a saline solution. Finally, the results of this work suggest that semiconductor microprobes will play an important role as real time biological sensors to analyze presynaptic neurotransmitter dynamics and activity of multiple neurons.

Acknowledgements

The authors would like to express their appreciation to Biographics, Inc., Winston-Salem, North Carolina and Rocky Mountain Center for Sensor Technology, Denver, Colorado for their financial support.

Literature Cited

Ang, S.S., G.A. Gerhardt, G. Sreenivas, A.S. Salian, R.M. Ranade, B.J. Hoffer and **D.J. Woodward.** Unpublished data.

BeMent, S.L., K.D. Wise, D.J. Anderson, K. Najafi and **K.L. Drake.** 1986. Solid state electrodes for multi channel multiplexed intracortical neuronal recording, IEEE Trans. Biomed. Eng. BME-33: 230-241.

Blum, N.A., B.G. Carhuff, H.K. Charles, Jr., R.L. Edwards, and **R.A. Meyer.** 1991. Multisite microprobes for neural recordings: IEEE Trans. Biomed. Eng. BME-38: 68-74.

Gerhardt, G.A. A.F. Oke, G. Nagy, B. Moghadda and **R.N. Adam.** 1984. Nafion-coated electrodes with high selectivity for CNS electrochemistry, Brian Research, 290: 390-395.

Hoogerwerf, A.C. and **K.D. Wise.** 1991. A three-dimensional neural recording array. International Conference on Solid-State Sensors and Actuators, IEEE Electron Devices Soc. 120-123 pp.

Prohaska, O.J., F. Olcaytug, P.Pfundner and **H. Dragaun.** 1986. Thin-film multiple electrode probes: possibilities and limitations, IEEE Trans. Biomed. Eng. BME-33 (2): 223-229.

Ranade, R.M., S.S. Ang and **W.D. Brown.** 1993. Reactive ion etching of thin gold films, J. Electrochem. Soc. Vol. 140 (12): 3676-3678.

Rose, J.E and **V.B. Mountcastle.** 1954. Activation of single neurons in the tactile thalamic region of the cat in response to a transient peripheral stimulus, Bull. The Johns Hopkins Hospital, 94: 238-282.

Van Horne, C.G., S. Bement, B.J. Hoffer and **G.A. Gerhardt.** 1990. Multichannel semiconductor-based electrodes for in vivo electrochemical and electrophysiological studies in rat CNS,: Neurosci. Let. 120: 249-252.

Aquatic Macrophytes of Two Small Northwest Arkansas Reservoirs

John J. Sullivan and Arthur V. Brown
Department of Biological Sciences
University of Arkansas
Fayetteville, AR 72701

Abstract

Lake Fayetteville and Lake Wedington are small reservoirs of about the same size and age that are located in northwestern Arkansas. We collected macrophytes from eleven transects around each reservoir in the autumn of 1993. *Justicia* (waterwillow), *Typha* (cat-tail), *Scirpus* (bulrush), *Potamogeton* (pondweed), and *Zannichellia* (horned pondweed) occur in both reservoirs. *Justicia* occurs most commonly in both reservoirs. The macrophytes of Lake Wedington are organized in a characteristic zonation pattern with bands from shore toward open water of emergent, floating-leaved, then submersed macrophytes. Macrophyte zonation was not as evident in Lake Fayetteville because of the low occurrence of floating-leaved and submersed macrophytes in 1993. Early studies of Lake Wedington found that the dominant macrophytes were *Cyperus, Echinochloa, Lotus,* and *Sagittaria,* all of which were absent during this study. *Potamogeton, Scirpus,* and *Typha* were also found to be dominant during 1952 studies, but occurred in lesser amounts in the current study. Previous studies (1956, 1967, 1977) on Lake Fayetteville stated that *Sagittaria* and *Nelumbo* were dominant macrophytes, but we found none in 1993. *Juncus, Potamogeton, Scirpus,* and *Typha* were common in the early studies but occurred infrequently in our collections. Macrophyte composition in Lake Fayetteville in 1993 was attributable to an herbicide application that occurred in spring, 1992. As for the changes in Lake Wedington, we assume that the *Justicia* has out-competed those macrophytes that were in the reservoir in 1952, or that normal lake ontogeny during the intervening 40 years has altered habitat conditions to now favor *Justicia.*

Introduction

Aquatic macrophytes are an important component of many ecosystems. They are indicators of the existing physical environment, and they are also the agent of many changes to the environment in the water and sediments beneath them. Macrophytes also have important roles as intermediates in many biotic interactions.

Physical factors of the environment affect macrophyte distribution. In a survey of 139 lakes, Duarte et al. (1986) reported that the biomass of emergent macrophytes was proportional to lake size, but biomass of submersed macrophytes was inversely proportional to lake size. Lake basin slope has a negative influence on macrophyte biomass, especially emergent macrophytes (Duarte et al., 1986; Duarte and Kalff, 1990; Rorslett, 1991). Light is most often the limiting factor on submersed macrophyte biomass (Duarte et al., 1986). Rorslett (1991) determined that small fluctuations in water level greatly increased macrophyte diversity perhaps as a result of a supression of a dominant species that might competitively exclude others (Ward and Stanford, 1983). Duarte and Kalff (1990) reported a decrease in macrophyte biomass as wave action increased.

Water chemistry has a strong influence on macrophyte species distribution. Alkalinity, pH, dissolved organic matter, nitrogen, phosphorous, chloride, and sulfate all affect macrophyte species distribution (Pip, 1979). Duarte and Kalff (1990) reported that an incrase in macrophyte biomass corresponded to an incrase in alkalinity. Friday (1987) found that pH was the most important factor limiting macrophyte species diversity in small ponds in Great Britain.

Macrophytes can also effect changes in their abiotic environment. They decrease currents and, as a result, increase sedimentation (Spence, 1982; Carpenter and Lodge, 1986; James and Barko, 1990). The composition of the sediments beneath macrophyte beds differs considerably from other sediments. Nitrogen, phosphorus, calcium and organic compounds are present in higher quantities beneath macrophytes (James and Barko, 1990). The sediments beneath macrophytes are enriched by decaying material from the plant bed (Carpenter and Lodge, 1986). Macrophytes alter the quantity and quality of light beneath them. The reduction in the amount of light causes the water under the macrophytes to be cooler than the surrounding water (Carpenter and Lodge, 1986). Water chemistry is also influenced by macrophytes. Oxygen and carbon dioxide levels fluctuate more in the littoral than the limnetic zone as the macrophytes respire and photosynthesize. Organic and inorganic carbon levels in the water are increased by macrophytes while inorganic nutrient levels are generally reduced (Carpenter and Lodge, 1986).

Aquatic macrophytes play a pivotal role in the biotic interactions of the littoral zone. They provide an area of refuge and forage for fish (Rozas and Odum, 1988). Macrophytes serve as a substrate for periphyton and invertebrates (Carpenter and Lodge, 1986; Cyr and Downing, 1988). Many invertebrates inhabit the rich substrate created beneath the macrophytes (Becket et al., 1992).

Many studies have investigated the trophic links between periphyton, periphyton grazers, macrophytes, and predators (Price et al., 1980; Bronmark, 1985; Cyr and Downing, 1988; Chambers et al., 1990; Hanson et al., 1990; Steinman 1991). Bronmark (1985) found that when grazing snails were present, macrophyte growth increased due to the lesser amounts of epiphyton, but when fish ate the snails, macrophyte growth decreased. Studies by Chambers et al. (1990) and Hanson et al. (1990) were not as conclusive. They found differences in effect between male and female crayfish and species of plant because the crayfish ate snails and macrophytes. Macrophytes serve as a direct food source to many herbivorous invertebrates such as crayfish (Lorman and Magnuson, 1978; Price et al., 1980; Chambers et al., 1990; Hanson et al., 1990), and some fish (Carpenter and Lodge, 1986).

All of the above interactions may affect macrophyte frequency and biomass, but features of the plants themselves will also affect distribution. Some species of macrophytes can exclude other species (Pip, 1979; Grace, 1985). The shape of some macrophytes determines the environment that they may inhabit (Duarte and Roff, 1991). The aquatic macrophytes in the littoral zone of lakes are arranged in specific zones (Spence, 1982; Wetzel, 1983). Emergent macrophytes occur nearest the shore, the floating macrophytes occupy the intermediate zone, and the submersed macrophytes are farthest from shore.

In man-made lakes the succession of invading aquatic macrophytes follows a predictable course (Correll and Correll, 1975). The first aquatic macrophytes to become established are cat-tails (*Typha*) followed closely by bulrush (*Scirpus*). both of these have small wind-blown seeds which make them good colonizers. These macrophytes spread within the reservoir by means of rhizomes that stabilize the substrate and allow colonization by other macrophytes. Therefore, there should be an evident change in macrophyte composition between the early studies on Lakes Wedington (Allman, 1952; Owen, 1952) and Fayetteville (Hulsey, 1956; Browne, 1967; Jackson, 1977) and the present.

In reservoirs each of these zones is inhabited by certain plants (Correll and Correll, 1975). The emergent macrophytes are primarily of the following genera: spike rush (*Eleocharis*), sedge (*Carex*), bulrush, bur-reed (*Sparganium*), cat-tail, water plantain (*Alisma*), and arrowhead (*Sagittaria*). Common floating macrophytes in reservoirs are water shield (*Brasenia*), yellow cow lily (*Nuphar*), water lily (*Nymphaea*), pondweed (*Potamogeton*), water fern (*Azolla*), floating fern (*Ceratopteris*), water hyacinth (*Eichhornia*), and water meat (*Wolffia*). Submersed macrophytes found in reservoirs include water milfoil (*Myriophyllum*), coontail (*Ceratophyllum*), water nymph (*Najas*), *Egeria*, waterweed (*Elodea*), fanwort (*Cabomba*), and the macroalgae *Chara* and *Nitella*.

Previous research on other characteristics of Lakes Wedington and Fayetteville often included a description of the dominant genera or species of plants in the lakes. Hulsey (1956) reported that the only macrophyte found in Lake Fayetteville was watercress (*Rorippa*). Browne (1967) found that in Lake Fayetteville the dominant plant genera were bulrush, cat-tail, rush (*Juncus*) and a few patches of arrowhead. Jackson (1977) reported that his study sites were dominated by yellow lotus (*Nelumbo*) at the shallow sites and pondweed at the deeper sites.

Owen (1952) reported that the macrophyte population in Lake Wedington was dominated by the following genera: *Potamogeton, Lotus, Scirpus, Sagittaria*, and *Typha*. Owen also found that the aquatic macrophytes were most abundant on the western banks, with a lesser number of macrophytes also occurring on the northern shores. Allman (1952) found that the aquatic macrophytes in Lake Wedington grew primarily in the western ends of the coves. He found the following species: *Sagittaria cantata, s. latifolia, s. platyphylla, Echinochloa crusgalli, Cyperus escalenta, Scirpus americanus, Scirpus* spp., and *Eleocharis* spp.

Macrophytes of the littoral zone are important parts of many reservoir environments yet few studies of macrophytes exist for this latitude of North America, and no studies have been done solely on the macrophytes of Lakes Wedington and Fayetteville. The objectives of this study were to compare aquatic macrophytes between Lakes Fayetteville and Wedington regarding:

1) dominant genera, past and present;
2) above-substrate biomass;
3) zonation patterns.

Study Sites

We collected macrophytes from the littoral zones of Lake Fayetteville and Lake Wedington. Both reservoirs are located in Washington County, Arkansas. Lake Fayetteville is located north of Fayetteville and is an impoundment of about 69 ha on Clear Creek that was constructed in 1949-1950 (Hulsey, 1956; Browne, 1967; Jackson, 1977). Lake Wedington is located about 32 km west of Fayetteville. It was impounded in 1937 and covers an area of 33 ha (Allman, 1952; Owen, 1952).

Methods

Macrophytes were collected using methods similar to those used by Lillie (1990). We collected along transects spaced about 500 m apart for a total of eleven transects per lake. One 0.1 m² quadrat was sampled every two meters starting at the shoreline and proceeding through the littoral zone. All macrophytes in each quadrat were cut at the level of the substrate and counted, with each plant shoot that grew from one point out of the substrate counted as one plant. Macrophytes were identified to generic level using Correll and Correll (1975). Flowers and fruits were not available for identification to the specific level. The macrophytes were oven-dried for seven days at 55°C to determine biomass/m² for each genus. We used occurrence, shoot frequency, and biomass in determining genera dominance. Total biomass for both reservoirs was estimated using shoreline measurements from theses by Hulsey (1956) and Owen (1952), mean distance the macrophytes grew from the shore, and the mean biomass of macrophytes collected.

Results

A total of 11 genera of aquatic macrophytes was collected from both reservoirs. Water willow (*Justicia*), cattails, bulrush, pondweed, and horned pondweed (*Zannichellia*) occurred in both reservoirs. Rushes, coontail, and buttonbush (*Cephalanthus*) were collected only in the littoral zone of Lake Fayetteville. We observed duckweed in the littoral zone of Lake Fayetteville, but none was present in our sampled quadrats. Water lily, spike rush, and smartweed (*Polygonum*) were collected only in Lake Wedington. We observed sedge and coon-tail in the littoral zone of Lake Wedington, although none were present in our samples. The macrophyte composition was very smililar between lakes, with a similarity index of 73%.

The most dominant plant in both reservoirs based on occurrence in quadrats was water willow, occurring in 50% of the quadrats in Lake Wedington and 58% of the quadrats in Lake Fayetteville. Other macrophytes only occurred in 0 to 10.5% of the quadrats (Fig. 1).

Based on shoot frequency, water lily was the dominant macrophyte in Lake Wedington, comprising 72% of the plant shoots, while in Lake Fayetteville the rush was the most frequently occurring plant, making up 66% of the macrophyte shoots. Water willow was the second most frequent macrophyte in both reservoirs, comprising 20% of the plants in Lake Wedington and 27% of the plants in Lake Fayetteville. The other macrophytes represented less than 6% of the shoot frequency (Fig. 2).

Water willow dominated the biomass of Lake Fayetteville, making up 57% of the total. In Lake Wedington cat-tails and water willow accounted for about equal portions of the biomass, 37% and 34% respectively. Cat-tails comprised only a minor portion (6%) of the biomass in Lake Fayetteville. Rushes constituted 18% of the total biomass in Lake Fayetteville, while water lilies made up just under 18% of the biomass in Lake Wedington. The other macrophytes only contributed minor portions of the total biomass (Fig. 3).

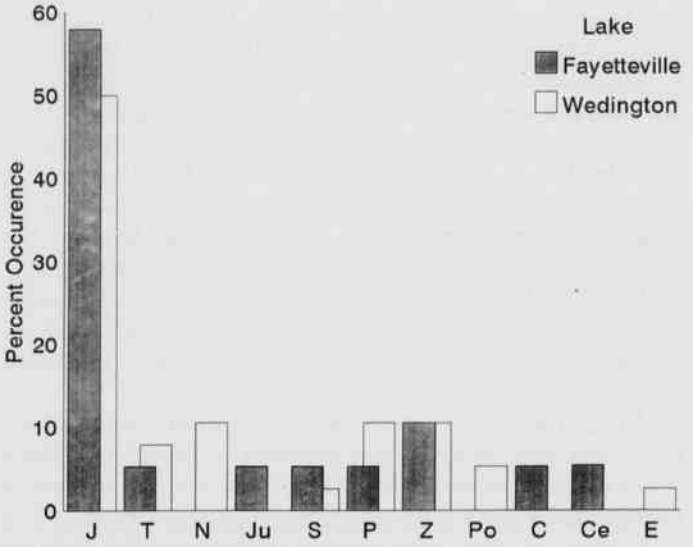

Fig. 1. Percent occurrence of macrophytes in quadrats from Lake Fayetteville and Lake Wedington in October, 1993. J=*Justicia*, T=*Typha*, N=*Nymphaea*, Ju=*Juncus*, S=*Scirpus*, P=*Potamogeton*, Z=*Zannichellia*, Po=*Polygonum*, C=*Ceratophyllum*, Ce=*Cephalanthus*, E=*Eleocharis*.

The shoreline of Lake Fayetteville, as reported by Hulsey (1956), is 8,420 m. The macrophytes in our transects extended to a mean distance of 2.45 m from the shoreline. This yields an estimated littoral zone of 20,667.3 m². In our collections we calculated a mean biomass of 110.6 g/m², for an estimated total biomass for standing crop of macrophytes of 2,285.8 kg (Table 1).

The shoreline of Lake Wedington is 6,122 m (Owen, 1952) and the macrophytes extended to a mean distance of 3.9 m from shore, yielding a littoral zone of 23,892.8 m², roughly equal to that of Lake Fayetteville. We calculated a mean biomass of 143.6 g/m² from our quadrats. This gave an estimate for the total standing crop biomass of 3,430.9 kg for Lake Wedington (Table 1).

A pattern of zonation in both reservoirs was obvious (evident to direct observers) but rather weak. Floating-leaved macrophytes occurred in only one quadrat along one transect in Lake Fayetteville. In Lake Wedington floating-leaved macrophytes occurred in only 3 of 11 tran-

sects. Submersed macrophytes were also relatively rare occurring in three transects each in Lake Fayetteville and Lake Wedington.

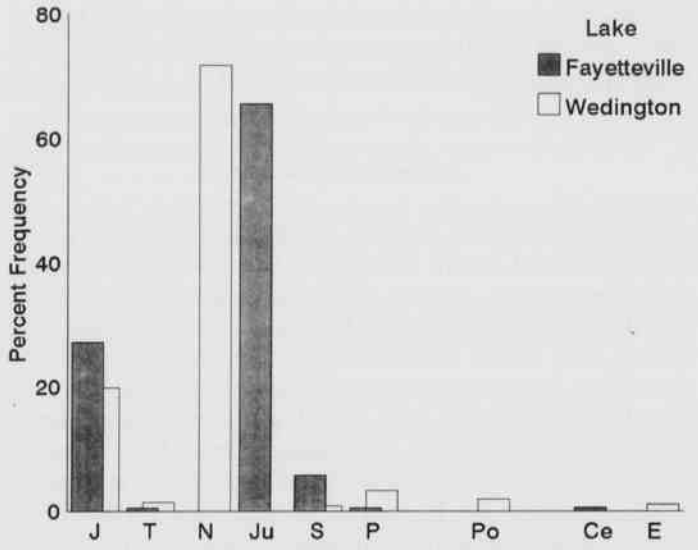

Fig. 2. Percent shoot frequency of macrophytes form Lake Fayetteville and Lake Wedington in October, 1993. J=*Justicia*, T=*Typha*, N=*Nymphaea*, Ju=*Juncus*, S=*Scirpus*, P=*Potamogeton*, Po=*Polygonum*, Ce=*Cephalanthus*, E=*Eleocharis*.

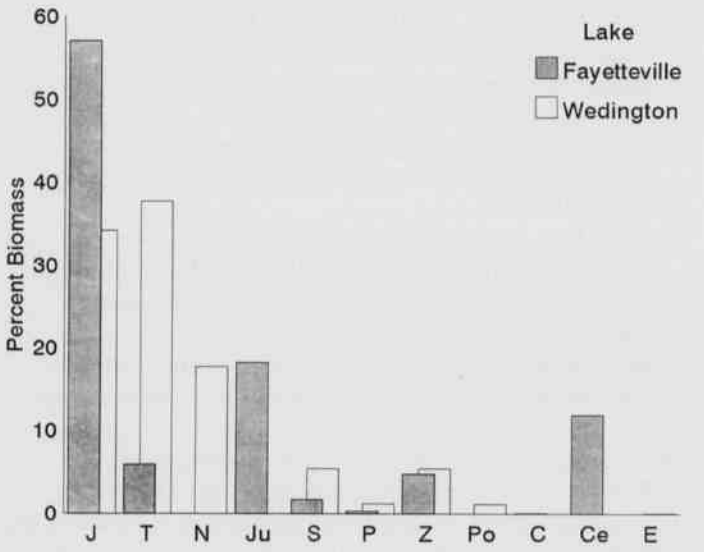

Fig. 3 Percent total biomass of macrophytes in Lake Fayetteville and Lake Wedington in October, 1993. J=*Justicia*, T=*Typha*, N=*Nymphaea*, Ju=*Juncus*, S=*Scirpus*, P=*Potamogeton*, Z=*Zannichellia*, Po=*Polygonum*, C=*Ceratophyllum*, Ce=*Cephalanthus*, E=*Eleocharis*.

Table 1. Littoral characteristics and total macrophyte standing crop biomass for Lakes Fayetteville and Lake Wedington in northwestern Arkansas during October, 1993.

	Wedington	Fayetteville
Surface Area (ha)	33	69
Mean Littoral Extension (m)	3.9	2.45
Shoreline (m)	6,122	8,420
Littoral Area (m2)	23,893	20,667
Mean Macrophyte Biomass (g/m^2)	143.6	110.6
Standing Crop Biomass (kg)	3,431	2,286

Discussion

Water willow was the most dominant macrophyte in both reservoirs. The high frequencies of water lily and rush were the result of a large shoot number occurring in very few quadrats, and is, therefore, over-emphasized in Fig. 2. Even though cat-tails had a low frequency and occurrence, in Lake Wedington they contributed a large amount of biomass. All other macrophytes were of minor importance in comparison to these.

The standing crop biomass of Lake Wedington was much larger than in Lake Fayetteville even though Lake Fayetteville has a larger shoreline and a shallower, potential littoral zone than Lake Wedington. Observations in other recent years indicate that the anomalous results of 1993 could have been caused by the application of an herbicide in 1992 (Hal Brown, pers. comm.).

The pattern of zonation in both reservoirs was weakly developed. In Lake Wedington only three transects contained all three zones, and the reservoir had two areas of extensive water lily growth. In Lake Fayetteville the data from transects did not support the weak zonation pattern observed. Only one floating-leaved macrophyte was collected and submersed macrophytes occurred in only three quadrats.

In Lake Fayetteville we collected four macrophytes (cat-tails, bulrushes, rushes, and pondweed) that were also present in early studies (Hulsey, 1956; Browne, 1967; Jackson, 1977). Macrophytes found in past studies that did not occur in our samples included arrowhead, yellow lotus, and watercress. The most notable macrophyte we collected that was not present in the past studies was water willow. The buttonbush that was growing four meters from the shore in the littoral zone was rooted on a raised tree bole and therefore might not be considered to be a truly littoral plant. However, buttonbush was relatively abundant in the wet soil near the water. The submersed macrophytes, horned pondweed and coontail, may possibly have been present but not detected in the past studies (Table 2).

In Lake Wedington, macrophytes collected that were also present in the studies of 1952 (Allman, 1952; Owen, 1952) include cat-tails, bulrushes, pondweed and spike rush. Macrophytes noted by Owen and Allman that we did not collect were arrowhead, yellow lotus, watercress, and water hyacinth. Macrophytes collected in 1993 that did not appear in the studies of 1952 were water willow, water lily, and smartweed. As with Lake Fayetteville, it is possible that the submersed macrophye, horned pondweed, was present in 1952 but not detected (Table 3).

Table. 2. Comparison between macrophytes found in early studies (Hulsey, 1956; Brown, 1967; and Jackson, 1977) and those found in Lake Fayetteville during October, 1993.

Early	1993
Typha	*Typha*
Scirpus	*Scirpus*
Juncus	*Juncus*
Potamogeton	*Potamogeton*
Sagittaria	*Justicia*
Nelumbo	*Cephalanthus*
Rorippa	*Ceratophyllum*
	Lemna

Table 3. Comparison between macrophytes found in early studies (Allman, 1952; Owen, 1952) and those found in Lake Wedington during October, 1993.

1952	1993
Typha	*Typha*
Scirpus	*Scirpus*
Eleocharis	*Eleocharis*
Potamogeton	*Potamogeton*
Sagittaria	*Justicia*
Lotus	*Nymphaea*
Echinochloa	*Zannichellia*
Cyperus	*Polygonum*
	Carex
	Ceratophyllum

Conclusions

The changes in both reservoirs are at least partially due to recent disturbance events. In the spring of 1992 most of the macrophytes in Lake Fayetteville were eliminated by herbicide poisoning. In the spring of 1991 the water level of Lake Wedington was lowered by 2 meters for a construction project. Both events probably altered the littoral zones, but since Lake Wedington may have been less-severely affected and had longer to recover, it has a greater biomass and was farther along in re-establishing a zonation pattern. Water willow had probably become the dominant macrophyte due to its ability to resist disturbance, supported by its widespread occurrence in Ozark streams which experience frequent harsh floods and droughts. The presence of watercress in these two reservoirs during the early studies (1950s) suggests a lingering stream influence at that time. The abundance of *Justicia* during our study and the disappearance of several other species which were reported earlier suggests that it has displaced some of the earlier species.

Acknowledgements

We thank Hal Brown at the Lake Fayetteville Environmental Study Center for the use of canoes and other equipment. Special thanks are due Carrie Sullivan for sitting in those canoes in rather chilly weather and taking field notes. Numerous students assisted with the extensive survey phase of this study including Yolanda Aguila, Zack Brown, Tim Burnley, Kenda Flores, Keith Harris, Dianne Melahn, Brian Shreve, and Imes Vaughn. We appreciate assistance with preparation of the manuscript by Kristine Brown. Constructive criticism by Stanley Trauth and an anonymous reviewer substantially strengthened the paper.

Literature Cited

Allman, J.F. 1952. Phytoplankton studies of Lake Wedington. Unpublished MS. Thesis, University of Arkansas, Fayetteville. 31 pp.

Beckett, D.C., T.P. Aartila and **A.C. Miller.** 1992. Contrasts in density of benthic invertebrates between macrophyte beds and open littoral patches in Eau Galle Lake, Wisconsin. Am. Midl. Nat. 127:77-90.

Bronmark, C. 1985. Interactions between macrophytes, epiphytes and herbivores: an experimental approach. Oikos 45:26-30.

Browne, L.E. 1967. Some aspects of the limnology of Lake Fayetteville in its fifteenth year of impoundment. Unpublished M.S. Thesis, University of Arkansas, Fayetteville. 48 pp.

Carpenter, S.R. and **D.M. Lodge.** 1986. Effects of submersed macrophytes on ecosystem processes. Aquat. Bot. 26:241-370.

Chambers, P.A., J.M. Hanson, J.M. Burke and **E.E. Prepas.** 1990. The impact of the crayfish *Orconectes virilis* on aquatic macrophytes. Freshwater Biol. 24:81-91.

Correll, D.S. and **H.B. Correll.** 1975. Aquatic and wetland plants of the Southwestern United States. Stanford University Press, Stanford, 2 Vol., 1777 pp.

Cyr, H. and **J.A. Downing.** 1988. The abundance of phytophilous invertebrates on different species of submerged macrophytes. Freshwater Biol. 20:365-374.

Duarte, C.M. and **J. Kalff.** 1990. Patterns in the submersed macrophyte biomass of lakes and the importance of scale of analysis in the interpretation. Can. J. Fish. Aquat. Sci. 47:357-363.

Duarte, C.M., J. Kalff and **R.H. Peters.** 1986. Patterns in biomass and cover of aquatic macrophytes in lakes. Can. J. Fish. Aquat. Sci. 43:1900-1908.

Duarte, C.M. and **D.A. Roff.** 1991. Architectural and life history constraints to submersed macrophyte community structure: a simulation study. Aquat. Bot. 42:15-19.

Friday, L.E. 1987. The diversity of macroinvertebrate and macrophyte communities in ponds. Freshwater Biol. 18:87-104.

Grace, J.B. 1985. Juvenile vs. adult competitive abilities in plants: size-dependence in cattails (*Typha*). Ecology 66:1630-1638.

Hanson, J.M., P.A. Chambers and **E.E. Prepas.** 1990. Selective foraging by the crayfish *Orconectes virilis* and its impact on macroinvertebrates. Freshwater Biol. 24:69-80.

Hulsey, A.H. 1956.Limnological studies in Arkansas VI physical, chemical, and biological features of Lake Fayetteville in its first year of impoundment. Unpublished M.S. Thesis, University of Arkansas, Fayetteville.

Jackson, D.C. 1977. Littoral and limnetic zooplankton dynamics in Lake Fayetteville, Arkansas. Unpublished M.S. thesis, University of Arkansas, Fayetteville. 172 pp.

James, W.F. and **J.W. Barko.** 1990. Macrophyte influences on the zonation of sediment accretion and composition in a north temperate reservoir. Arch. Hydrobiol. 120:129-142.

Lillie, R.A. 1990. A quantitative survey of the submersed macrophytes in Devil's Lake, Sauk County, with a historical review of the invasion of Eurasian water milfoil, *Myriophyllum spicatum* L. Trans. Wisconsin Acad. Sci. Arts Lett. 78:1-20.

Lorman, J.G. and **J.J. Magnuson.** 1978. The role of crayfishes in aquatic ecosystems. Fisheries 3:8-10.

Owen, B.G. 1952. Limnological studies in Arkansas IV: chemical, physical, and biological features of Lake Wedington in its thirteenth and fourteenth years of impoundment. Unpublished M.A. Thesis, University of Arkansas, Fayetteville. 31 pp.

Pip, E. 1979. Survey of the ecology of submerged aquatic macrophytes in central Canada. Aquat. Bot. 7:339-357.

Price, P.W., C.E. Bouton, P. Gross, B.A. McPheron, J.N. Thompson and **A.E. Weis.** 1980. Interactions among three trophic levels: influence of plants on interactions between insect herbivores and natural enemies. Annu. Rev. Ecol. Syst. 11:41-65.

Rorslett, B. 1991. Principal determinants of aquatic macrophyte richness in northern European lakes. Aquat. Bot. 39: 173-193.

Rozas, L.A. and **W.E. Odum.** 1988. Occupation of submerged aquatic vegetation by fishes: testing the roles of food and refuge. Oecologia 77:101-106.

Spence, D.H.N. 1982. The zonation of plants in freshwater lakes. Adv. Ecol. Res. 12:37-125.

Steinman, A.D. 1991. Effects of herbivore size and hunger level on periphyton communities. J. Phycol. 27:54-59.

Ward, J.V. and **J.A. Stanford.** 1983. The intermediate-disturbance hypothesis: An explanation for biotic diversity pattens in lotic ecosystems. Pages 347-357, *In* Dynamics of lotic ecosystems (T.D. Fontaine and S.M. Bartell, eds.) Ann Arbor Science Publishers, Ann Arbor, 494 pp.

Wetzel, R.G. 1983. Limnology. Saunders College, Fort Worth, 767 pp.

A Method for Determining Atmospheric Aerosol Optical Depth Using Solar Transmission Measurements

Felix Tendeku
Department of Industrial Technology
University of Arkansas at Pine Bluff
Pine Bluff, AR 71601

Abstract

A multiple wavelength radiometer instrumentation has been developed and used to measure solar irradiance in a water vapor absorption band in the near-infrared region. From these measurements the total atmospheric optical depth at each wavelength of observation is deduced using a linear least-squares fitting method. An iteration technique, based on a power law wavelength dependence of aerosol optical depth, is employed to retrieve aerosol optical depth from the total optical depth data. The technique permits simultaneous determination of precipitable water vapor amount.

Introduction

Information concerning the properties of atmospheric aerosols has been obtained from solar transmission measurements in the ultra-violet, visible, and near-infrared regions. King and Byrne (1976) used solar irradiance data, measured at varying solar zenith angles, to obtain both aerosol optical depth and total ozone content. More recently, Flittner et al. (1993) proposed a technique for inferring total ozone and aerosol optical depths using similar radiometric data. Several researchers (Yamamoto and Tanaka, 1969; Quenzel, 1970; Grassl, 1971; and King et al., 1978) have also demonstrated that parameters describing aerosol size distribution can be deduced from wavelength dependent aerosol optical depth data. This data is usually obtained from total atmospheric optical depth measurements by making corrections for molecular scattering and absorption due to atmospheric constituents such as water vapor, carbon dioxide and ozone. Whereas the contribution due to scattering can be easily calculated, molecular absorption can only be avoided if spectral measurements are made at wavelengths where there is no molecular absorption. However, from the ultra-violet to the near-infrared region there are spectrally broad absorption bands. Two such broadband absorption regions are the Chappuis band due to ozone, ranging from 440 to 800 nm, and the water vapor absorption band ranging from about 880 to 980 nm. Taking measurements outside these regions may lead to the loss of significant spectral information. In this work, measurements were made in five spectral channels between 700 and 975 nm. Three of the channels were located in the water vapor absorption region. A method is described for extracting both aerosol optical depth and precipitable water vapor amount.

Materials and Method

Determination of Aerosol Optical Depth.--The directly transmitted solar irradiance may be given by Beer-Lambert law as

$$F(\lambda) = F_0(\lambda) \exp[-\tau_t(\lambda) m(\theta_0)] \quad (1)$$

where $F(\lambda)$ is the solar irradiance at wavelength λ reaching a ground-based detector; $F_0(\lambda)$ the irradiance incident on top of the atmosphere; $m(\theta_0)$ the atmospheric air mass, a function of the solar zenith angle θ_0; and $\tau_t(\lambda)$ the total optical depth. Air mass is defined as the ratio of the slant path length for the solar rays through the atmosphere to the path length if the sun were in the zenith. This ratio is usually equal to the secant of the solar zenith angel, except for large angles when atmospheric refraction and earth curvature need to be taken into account. Taking the natural logarithm of (1) yields

$$\ln F(\lambda) = \ln F_0(\lambda) - \tau_t(\lambda) m(\theta_0) \quad (2)$$

A plot of $\ln F(\lambda)$ versus $m(\theta_0)$, known as Langley plot, yields a straight line with negative slope $\tau_t(\lambda)$, and y-intercept of $\ln F_0(\lambda)$, assuming the optical depth remains constant during the course of measurement. Thus, using irradiance measurements made at varying air mass, the Langley plot may be used to obtain the total optical depth, $\tau_t(\lambda_i)$, at each wavelength of observation. From the values of total optical depth, τ_t, corresponding values of aerosol optical depth, τ_a, are determined by subtracting contributions due to molecular (Raleigh) scattering, τ_R, and water vapor absorption, τ_W. Thus

$$\tau_a = \tau_t - \tau_R - \tau_W \quad (3)$$

An expression for τ_R, given by Hansen and Travis (1974) for standard surface pressure, P_0 = 1013.25 mbar, is

$$\tau_R(\lambda,P_0) = 0.008569\lambda^{-4}(1 + 0.0113\lambda^{-2} + 0.0013\lambda^{-4}) \quad (4)$$

where λ is the wavelength in μm. At pressure P, τ_R may be expressed as

$$\tau_R(\lambda,P) = \frac{P}{P_0}\tau_R(\lambda,P_0) \quad (5)$$

The water vapor optical depth may be given by

$$\tau_W = \zeta \cdot \alpha(\lambda) \quad (6)$$

where $\alpha(\lambda)$ is the water vapor absorption coefficient (per cm) at wavelength λ, and ζ the water vapor amount (cm). Substituting (5) and (6) in (3) gives

$$\tau_a(\lambda,P,\zeta) = \tau_t(\lambda) - \tau_R(\lambda,P) - \zeta.\alpha(\lambda) \quad (7)$$

Since ζ is unknown, τ_a cannot be calculated directly from (7). Instead, an iteration technique, similar to the method of King and Byrne (1976) is used to retrieve the mean water vapor density, ζ_0. The method described here is based on the Ångström power law which expresses the wavelength dependence of aerosol optical depth as

$$\tau_a = \beta\lambda^{-\upsilon} \quad (8)$$

where β and υ are constants. As the unknown parameter, ζ, takes on values from zero to a maximum value, ζ_{max}, aerosol optical depths calculated from (7) are fitted to the model (8) in order to obtain β and υ, as well as the statistic given by

$$\chi^2 = \sum_i \frac{1}{\sigma_i^2}[\tau_a(\lambda_i,P,\zeta) - \beta\lambda_i^{-\upsilon}]^2 \quad (9)$$

where the summation is made over the wavelengths of observation, λ_i, and σ_i represent the standard deviations of $\tau_a(\lambda_i, P, \zeta)$ values. Also, the partial derivative of χ^2 with respect to ζ is determined as

$$\frac{\partial\chi^2}{\partial\zeta} = -2\sum_i \frac{1}{\sigma_i^2}[\tau_a(\lambda_i,P,\zeta) - \beta\lambda_i^{-\upsilon}] \cdot \alpha(\lambda_i) \quad (10)$$

When χ^2 attains a minimum, its partial derivative with respect to ζ is zero, and the corresponding water vapor amount, ζ_0, represents the mean value for the period of measurement. Having obtained the constants β and υ, aerosol optical depths may be computed from (8).

Instrumentation.--The radiometer instrumentation comprises a telescope, a motorized filter wheel and controller, an enclosed variable frequency optical chopper and controller, an infrared detector, and a digital lock-in amplifier. The schematic diagram is shown in Fig. 1.

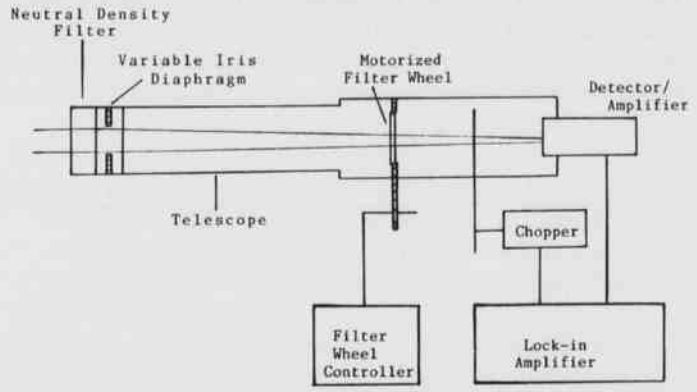

Fig. 1. Schematic diagram of the radiometer instrumentation.

The filter wheel holds five 25-mm diameter interference filters and permits automated wavelength selection. The telescope comprises a 20-cm tube, a neutral density filter, and an aperture stop. The aperture stop is a variable iris diaphragm used to set the field of view to about 3.5°. A neutral density filter is placed at the entrance of the telescope to reduce the intensity of solar flux to a measurable level for the detector. The detector is a radiometrically calibrated silicon photodiode with the National Institute of Standards and Technology (NIST) traceable calibrated responsivity factors for the 400 to 1100 nm range. The digital lock-in amplifier is model 70100 from Oriel Corporation.

Results and Discussion

Solar irradiance measurements at varying solar zenith angles were made on February 16, 1994 at University of Arkansas campus at Pine Bluff (latitude 34.13°N, longitude 92.0°W). Measurements were made with interference filters centered at 700, 875, 903, 941, and 975 nm, respectively. The full bandwidth at half-peak transmittance of each filter is less than 11.5 nm. Readings were taken at approximately 20-minute intervals from 8:00 to 17:00 local time (CST). Solar zenith angels were computed using well-known astronomical formulas and tabulated values taken from the *Astronomical Almanac for the year 1994* (U.S. Naval Observatory, 1993). Fig. 2 illustrates the variation of air mass with local time for the day. Fig. 3 indicates the plot of the natural logarithm of the measured solar irradiance, $\ln F(\lambda)$, versus air mass, $m(\theta_0)$, for the five spectral channels. The lines are the best least-square fit to the data while the resulting slopes give the total atmospheric optical depths for the respective wavelengths. The iteration procedure described above is performed with ζ given values from zero to ζ_{max} in order to determine the constants β and υ, as well as χ^2 and $\partial\chi^2/\partial\zeta$.

The value of ζ_{max} may be deduced from (7) as the maximum value of ζ which produces zero aerosol optical depth. In the region of measurement, the strongest water vapor absorption occurs at about 941 nm, thus

$$\zeta_{max} = \frac{\tau_t(941) - \tau_R(941)}{\alpha(941)} \qquad (11)$$

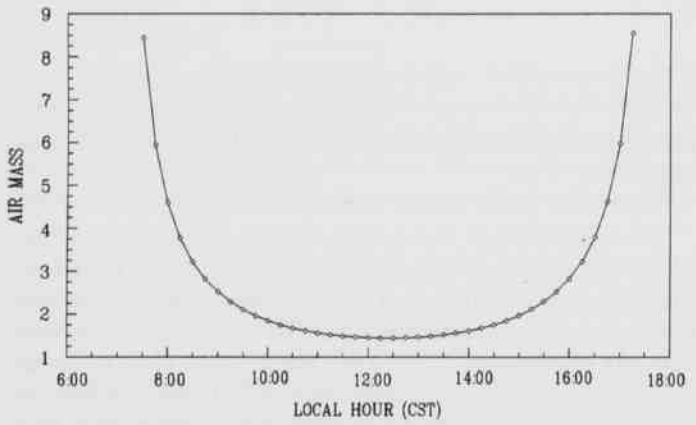

Fig. 2. Variation of atmospheric air mass with local time at Pine Bluff on February 16, 1994.

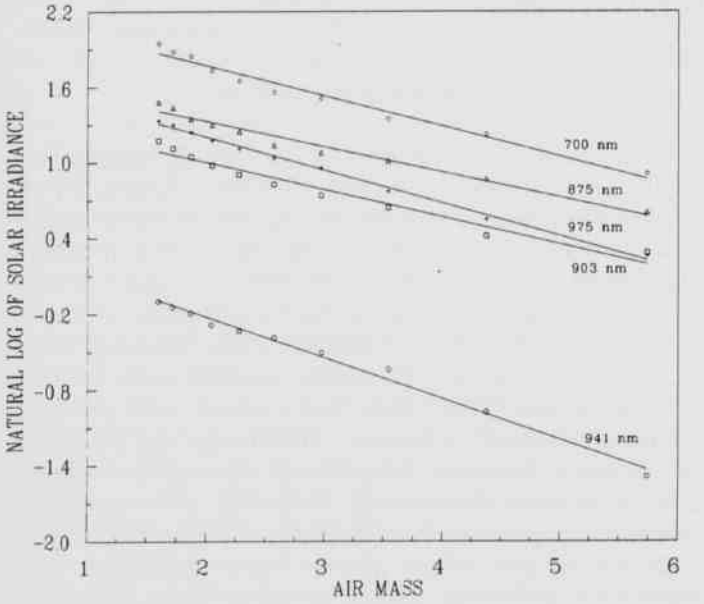

Fig. 3. The natural logarithm of solar irradiance versus atmospheric air mass.

Water vapor absorption coefficients used in this algorithm were taken from the revised Neckel and Labs spectrum in Bird (1984). Figure 4 shows the variation of χ^2 and $\partial\chi^2/\partial\zeta$ with water vapor amount, ζ. The mean water vapor amount, ζ_0, was determined to be 2.2 mm while β = 0.186 and υ = 0.225. The resulting values of aerosol optical depth are shown in Fig. 5.

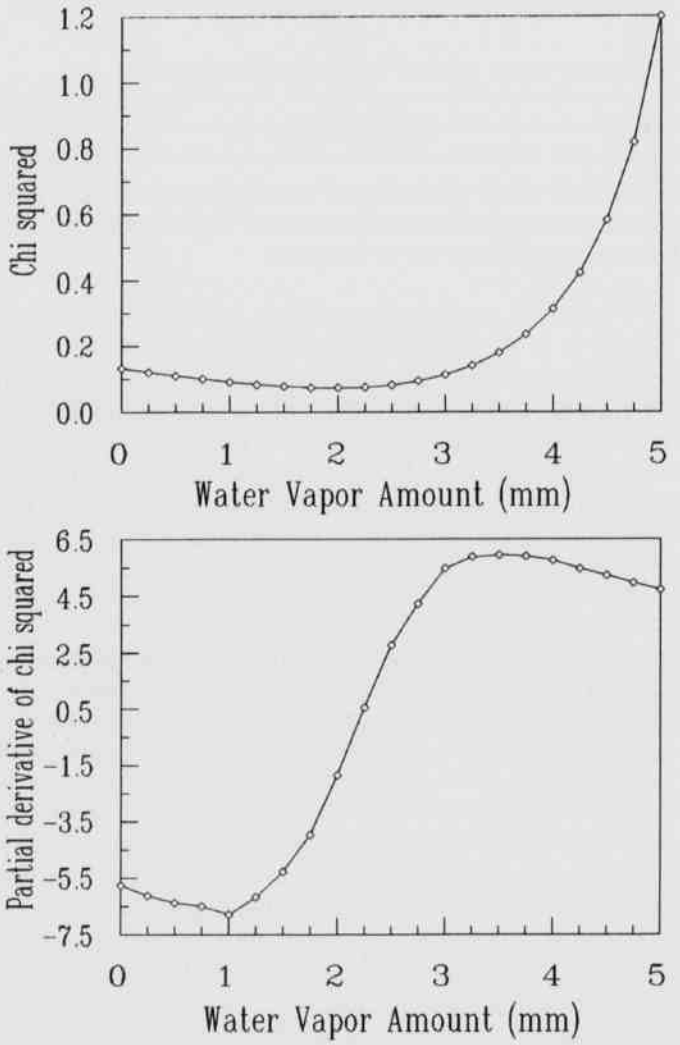

Fig. 4. The relationship of chi-squared statistic and its partial derivative with water vapor amount.

The mean columnar water vapor amount obtained from this algorithm was verified using the well-known differential absorption technique as described in Reagan et al. (1992) and Thome et al. (1992). Here, the two radiometric channels utilized were the 941 nm channel inside the water vapor absorption region and the 875 nm channel outside the absorption region. The ratios of the two radiometric channel measurements were used in a modi-

fied Langley plot. The water vapor amount was retrieved using the transmittance model developed by Thomason (1985). The retrieved value agrees, within an error of 10%, with the amount obtained by the algorithm described above.

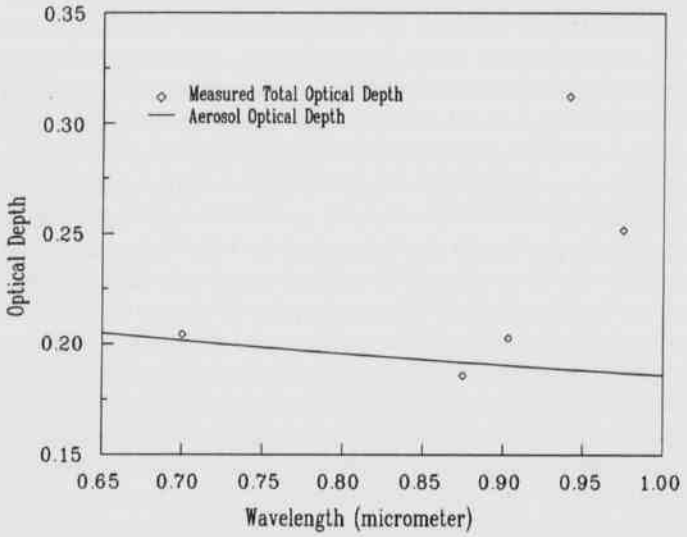

Fig. 5. Atmospheric optical depths measured at Pine Bluff.

Conclusions

The application of the algorithm described in this paper permits the retrieval of aerosol optical depths at wavelengths within water vapor absorption band in the near infrared region. The mean precipitable water vapor amount is obtained through nonlinear least squares fitting by minimizing the χ^2 statistic. The principal assumption upon which the technique is based is that aerosol optical depths can be adequately described by the Ångstöm power law within a relatively narrow wavelength region.

Acknowledgements

This project was undertaken with support from the University of Arkansas at Pine Bluff and partly with a grant received from the Arkansas Space Grant Consortium. I thank Bruce Gary at the Jet Propulsion Laboratory, Pasedena, for his encouragement and support; and K.J. Thome at the Remote Sensing Group, University of Arizona, Tucson, for his assistance in providing the software on the Thomason model. The support received from David L. Lickteig is very much appreciated.

Literature Cited

Bird, R.E. 1984. A simple, solar spectral model for direct-normal and diffuse horizontal irradiance. Solar Energy 32:461-471.

Flittner, D.E., B.M. Herman, K.J. Thome, J.M. Simpson and **J.A. Reagan.** 1993. Total ozone and aerosol optical depths inferred from radiometric measurements in the Chappuis absorption band. J. Atmos. Sci. 50:1113-1121.

Grassl, H. 1971. Determination of aerosol size distributions from spectral attenuation measurements. Appl. Opt. 10:2534-2538.

Hansen, J.E. and **L.D. Travis.** 1974. Light scattering in planetary atmosphere. Space Sci. Rev. 16:527-610.

King, M.D. and **D.M. Byrne.** 1976. A method for inferring total ozone content from spectral variation of total optical depth obtained with a solar radiometer. J. Atmos. Sci. 33:2242-2251.

King, M.D., D.M. Byrne, B.M. Herman and **J.A. Reagan.** 1978. Aerosol size distributions obtained by inversion of spectral optical depth measurements. J. Atmos. Sci. 35:2153-2167.

Quenzel, H. 1970. Determination of size distribution of atmospheric aerosol particles from spectral solar radiation measurements. J. Geophys. Res. 75:2915-2921.

Reagan, J.A., K.J. Thome and **B.M. Herman.** 1992. A simple instrument and technique for measuring columnar water vapor via near-IR differential solar transmission measurements. IEEE Trans. Geos. Remote Sensing. 30:825-831.

Thomason, L.W. 1985. Extinction of near infrared solar radiation as a means for remote determination of atmospheric water vapor. Ph.D. dissertation, University of Arizona, 125 pp.

Thome, K.J., B.M. Herman and **J.A. Reagan.** 1992. Determination of precipitable water vapor from solar transmission. J. Appl. Meteor. 31:157-167.

Yamamoto, G. and **M. Tanaka.** 1969. Determination of aerosol size distribution from spectral attenuation measurements. Appl. Opt. 8:447-453.

U.S. Naval Observatory. 1993. The Astronomical Almanac for the year 1994. U.S. Govt. Printing Office, Washington, D.C., 539 pp.

Female Reproductive Traits in Selected Arkansas Snakes

Stanley E. Trauth, Robert L. Cox, Jr., Walter E. Meshaka, Jr., Brian P. Butterfield and Anthony Holt
Department of Biological Sciences, Arkansas State University, State University, AR 72467-0599 (SET, AH),
RLC (Deceased), Archbold Biological Station, P.O. Box 2057, Lake Placid, FL 33852 (WEM),
Department of Zoology and Wildlife Science, Auburn University, Auburn, AL 36849 (BPB)

Abstract

Female reproductive characteristics of 17 genera of Arkansas snakes (27 species and subspecies) were examined. Most of the snakes (n = 495) were collected over a 10-year span (1984-1993). Methods used to estimate clutch and/or litter size were as follows: 1) counts of previtellogenic ovarian follicles, 2) counts of vitellogenic ovarian follicles, 3) counts of oviductal eggs or embryos, 4) counts of corpora luteal scars, and 5) counts of neonates from egg clutches or litters. In several species, Method 1 tended to overestimate clutch size as determined by Method 2 by as much as 100% (e.g., in *Diadophis punctatus, Elaphe obsoleta,* and *Lampropeltis getula*), whereas these methods produced similar counts in *Virginia striatula* and *Thamnophis proximus*. The largest clutch size as estimated by Method 1 was 79 ova in a 744 mm in snout-vent length (SVL) individual of *Thamnophis sirtalis*; the smallest clutch size as recorded by this method was in *Carphophis vermis* (2 ova; 182 mm in SVL). Method 2 reduces the total egg count by one third over Method 1 in most species, and this count was very similar to the estimates obtained by Method 3, the most reliable way to estimate clutch or litter size (without actually having counts from egg clutches or litters). The presence of atretic ovarian follicles accounts for discrepancies found between clutch size estimates using Methods 1 and 2 as compared to Method 3. Comparisons of clutch sizes in Arkansas specimens to those recorded for snake species in neighboring states revealed similar sizes in 13 species; counts were larger in 8 species from Arkansas and smaller in only one species.

Introduction

Baseline reproductive data have been compiled for many wide-ranging North American snake species (Wright and Wright, 1957; Fitch, 1970, 1985; Seigel and Ford, 1987; Ernst and Barbour, 1989; Ford et al., 1990). There remain, however, large geographic regions in the United States that lack such life history data. Geographic variation in snake reproductive traits does exist (Fitch, 1985), but seasonal and annual variation in reproductive traits within and between populations of a species are less well documented. Some species, such as *Storeria occipitomaculata*, show little latitudinal population variation in female reproductive traits between Michigan and South Carolina (Semlitsch and Moran, 1984), whereas Fitch (1985) found that 60% of 25 snake species in the United States showed a northward increase in clutch/litter size.

Few detailed studies on snake reproductive biology have been conducted on snake populations within the state of Arkansas (Plummer, 1983, 1984, 1992; Trauth, 1991; Robinette and Trauth, 1992) when compared with surrounding states [see snake accounts for Kansas (Collins, 1993), Oklahoma (Carpenter and Krupa, 1989), Louisiana (Dundee and Rossman, 1989), Missouri (Anderson, 1965; Johnson, 1987), and Texas (Dixon, 1987). In 1984 a statewide field survey of Arkansas snakes was initiated by one of us (SET) to attain large samples in an effort to establish baseline life history data on snake populations dwelling within the state. Herein, we report on reproduction in 27 species and subspecies representing 17 genera (and two families) of Arkansas snakes by an analysis of museum specimens. We hope our effort will stimulate more intensive studies of geographic and temporal variation on snake reproductive parameters within the state.

Materials and Methods

Reproductive data were derived via gross dissection of 495 preserved females comprised within two snake families (Colubridae and Viperidae) and 27 species and subspecies; this equates to approximately 66% of the known species and subspecies of snakes currently found in Arkansas. Nomenclature followed Conant and Collins (1991). Most snakes were collected from habitats throughout Arkansas between 1984 and 1993; voucher specimens are deposited in the Arkansas State University herpetology museum. Additional Arkansas specimens were borrowed from the Milwaukee Public Museum. Among the variables recorded from each specimen were the following: 1) snout-vent length (SVL), 2) number and size (greatest length = diameter, in some cases) of previtellogenic ovarian follicles (**POF**), 3) number and size (greatest length) of vitellogenic ovarian follicles (**VOF**), 4) number of oviductal eggs and/or oviductal embryos

(OE/OEM), and 5) number of corpora lutea (CL). In most specimens, at least 10 (if present) of the largest ovarian follicles per specimen were counted and measured. Immature ova less than 2 and 3 mm in small and large snakes, respectively, were not counted. In several instances, egg clutches deposited in captivity or collected in nature as well as litters born to females held in confinement provided additional data on clutches. Estimation of clutch or litter size can be based upon a combination of the above methods; however, follicular atresia is common to all size classes during vitellogenesis in snakes (Aldridge, 1979; Fitch, 1985). Thus, the most reliable technique is to use only greatly enlarged VOF (in most cases, > 5 mm in length in small snakes, > 10 mm in intermediate-sized snakes, and > 20 mm in large snakes) when incorporating counts of developing ova. For the purpose of contrasting variation in reproductive potential based on breeding condition within and among species, all methods were employed to some extent. Along with female clutch characteristics mentioned above, we report on other pertinent life history information; the data are from mostly spring and summer samples. Figures 1-9 detail the relationships among date of collection, female SVL, female fecundity (= clutch/litter size; see Ballinger 1978), and stage of reproduction on 21 species, in some instances, reporductive data from injured or abnormal females were omitted from Figs. 1-9, but were included elsewhere. In each species summary (discussed below), we have compiled the data into groups based upon the species; size, mode of reproduction (oviparous = egg layers vs viviparous = livebearers), and family (Colubridae or Viperidae). Colubrids are either oviparous or viviparous, whereas all viperids in Arkansas are viviparous: In all species we state which method (or combination of methods) was used to determine fecundity; mean values for clutch size data as well as for other parameters are, in most instances, accompanied by ± 2 SE (standard error), range, and sample size. Unless stated otherwise, all lengths are in mm.

Results and Discussion

Small Oviparous Colubrid Species.--Four relatively small secretive species were examined in this category. Each deposits one clutch of eggs from late May to mid-June. Hatching occurs around 50 to 60 days following oviposition. In the western worm snake (*Carphophis vermis*), clutch size averaged 3.4 ± 0.5 (2-5; n = 17) using only VOF (> 3 mm in length). This mean was similar to the value reported by Fitch (1985–data from Clark, 1970) for Kansas (3.3; n = 47; value derived by combining VOF and early OE). No females contained OE, and we discovered no egg clutches. Mean adult SVL of reproductive females in Arkansas was 222.6 ± 22.3 mm (186-263; n = 17), whereas 216 mm in SVL was the smallest adult female in Kansas (Clark, 1970). This species produces from 1 - 6 eggs in Missouri (Johnson, 1987). By mid-April in Arkansas, most adult females possessed VOF averaging 9.4 mm ± 1.45 (6.6-13.0; n = 11), although one female with two VOF ($\bar{x}$ = 12.5 mm) was collected on 18 March 1980. Aldridge and Metter (1973) indicated that vitellogenesis begins in ova prior to hibernation in October in Missouri.

In Arkansas clutch size of the northern scarlet snake (*Cemophora coccinea copei*) averaged 4.3 (4-11; n = 3) and was derived using VOF and OE. Developing ovarian follicles averaged 7.9 and 19.7 in two females (336 and 355 mm in SVL, respectively) collected on 20 May 1987 and 26 June 1989, and the one female (289 mm in SVL) possessing OE was collected on 14 June 1989. The largest specimen, a postreproductive female (382 mm in SVL), was taken from Dallas County on 27 July 1991. No egg clutches were discovered during the present study; however, eggs (as well as adults) have been found in sandy and/or red clay soils (Sutton and McDaniel, 1979; Trauth, 1982). Ford et al. (1990) reported a single clutch of six eggs laid by a captive female on 27 June 1988.

Clutch size in the prairie ringneck snake (*Diadophis punctatus arnyi*) was determined as follows: 1) by using POF, clutch size averaged 5.3 (4-8; n = 7), 2) by using VOF, the mean was 3.8 (2-5; n = 8), and 3) with OE, the mean was 4.0 (3 and 5; n = 2). By combining the latter two methods, clutch size averaged 3.8 ± 0.6 (2-5; n = 10). Fitch (1985) reported an average of 3.9 (1-10; n = 300) in northeastern Kansas using the first two methods, whereas Johnson (1987) stated that in Missouri this species may produce from one to ten eggs. Vitellogenesis in Arkansas specimens occurred rapidly after ova reach a length of around 7.0 mm. By mid-April most adult females possessed VOF averaging at least 9.0 mm in length; OE first appeared in mid-May. One female (282 mm in SVL) contained enlarged ova averaging 13.9 mm in length on 5 June 1980. Fitch (1975) provided the most detailed study on female reproduction for this subspecies.

The smallest snake species found in Arkansas is the flathead snake (*Tantilla gracilis*); adult females averaged 161.1 ± 14.0 mm in SVL (133-180; n = 16). This species emerges from hibernation as early as late March in Arkansas and, at that time, has previtellogenic ova averaging less than 3.0 mm (Fig. 1). Mean clutch size, using all methods, was 4.9 ± 1.3 (2-12; n = 16) and using VOF and OE, was 3.1 ± 0.7 (2-4; n = 7). Clutch size as reported by Force (1935) and Carpenter (1958) in Oklahoma populations is generally 2-3 eggs; in Kansas, 1-3 eggs (Fitch, 1985); in Missouri, 1-4 eggs (Johnson, 1987), and in Texas, 2-3 eggs (Cobb, 1990).

Medium-sized Oviparous Colubrid Species.--Two snake species examined during this study fall into this category;

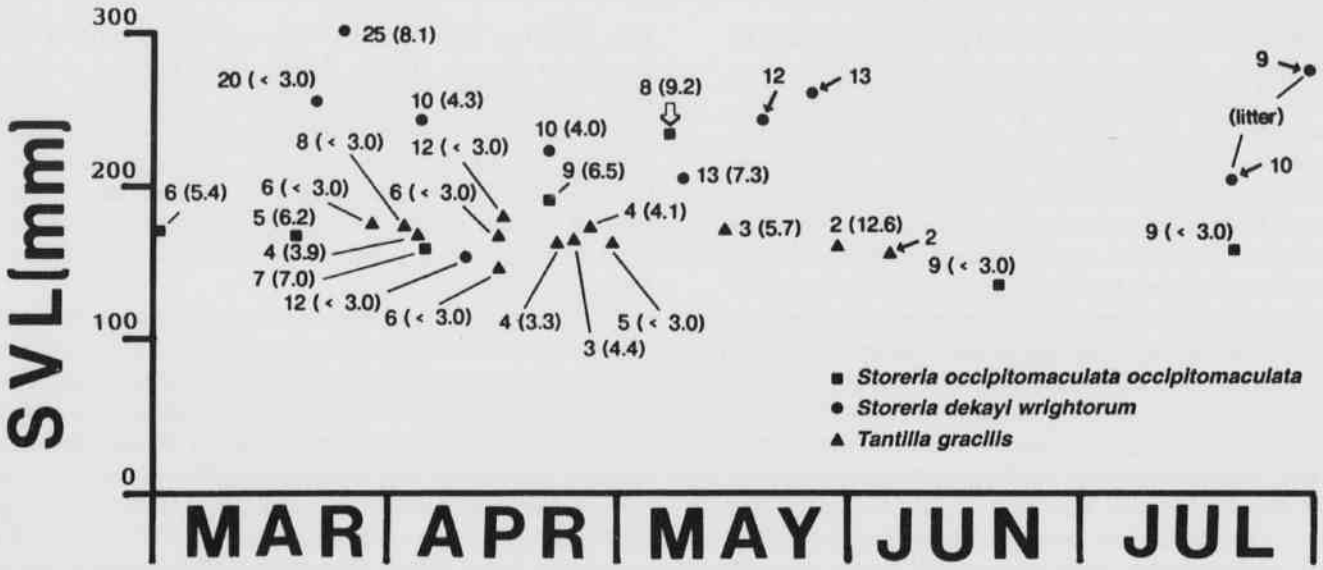

Fig. 1. Relationship between female body size (SVL) and reproductive condition in samples of three Arkansas snakes (*Storeria occipitomaculata occipitomaculata*. *S. dekayi wrightorum*. and *Tantilla gracilis*) according to month. Numerals (outside parentheses) = total number of ovarian follicles, oviductal eggs/embryos (designated with arrows), or neonates (of litters) for each snake. Other numerals (inside parentheses) = average length of ovarian follicles or designate size of previtellogenic follicles (open arrow = average length of oviductal eggs).

both are found throughout most of Arkansas. Clutch characteristics for the eastern hognose snake (*Heterodon platirhinos*) are shown in Fig. 2. Clutch size averaged 22.2 (20-44; n = 4), 25.2 ± 6.1 (15-44; n = 11), and 20.5 (15 and 26; n = 2) using **POF**, **VOF**, and **OE**, respectively. Using only **VOF** and **OE**, the average was 24.5 ± 5.4 (15-44; n = 13). Regression analysis revealed a significant positive correlation (r = 0.75; n = 13; $P < 0.01$) between clutch size (CS) using **VOF** and **OE** and SVL. The regression equation (CS = 30.7895 + 0.0850SVL) predicts that for an increase of 12 mm in SVL, a concomitant increase of one in clutch size would be observed. Enlarged ova were present in adult females in early March; the smallest female (531 mm in SVL) with advanced **VOF** was captured on 16 May 1993. Oviductal eggs were found in one female in early May. Females with a SVL of less than 500 mm were considered immature; this was also true for populations studied by Platt (1969). In addition, Platt (1969) summarized the literature on clutch size and reported a mean of 22.3 eggs (4-61; n = 59). Ford et al. (1990) reported on a clutch of 30 eggs laid by a captive female (660 mm in SVL) on 18 June 1988.

Figure 3 summarizes clutch characteristics on nine individuals of the Louisiana milk snake (*Lampropeltis triangulum syspila*). Vitellogenesis begins in early April in females greater than 325 mm in SVL. Clutch size was derived from counts of **POF**, **VOF**, and **OE**; the average was 8.0 ± 3.2 (4-13; n = 7). The largest vitellogenic ova observed in this subspecies averaged 23.2 mm in length in an early June specimen measuring 730 mm SVL. One female collected on 26 June 1976 contained **OE**; no egg clutches were discovered in this subspecies. Williams (1988) stated that nine clutches from Missouri averaged 5.2 eggs (4-7) and were deposited between 18 June and 22 July; however, Anderson (1965) reported from 6 to 12 eggs per clutch in Missouri. Fitch (1970) reported an average clutch size of 10.2 for 20 clutches (for all subspecies), but in his summary on reproduction on this subspecies (Fitch, 1985), he gives an average clutch size of 6.3 for northeastern Kansas.

Large Oviparous Colubrid Species.--This group of seven large-bodied snakes includes several of the longest and fastest snakes that occur in Arkansas; each species lays a single clutch of eggs per reproductive season. There are few documented records of the Great Plains rat snake (*Elaphe guttata emoryi*) from Arkansas; only a single adult female (of 10 animals) contained 12 **POV** on 4 April 1992. [Recently, the subspecific name (*emoryi*) of Arkansas populations was changed to *meahllmorum* (Smith et al., 1994).] On the other hand, the black rat snake (*Elaphe obsoleta obsoleta*) is a very common species in Arkansas and becomes active in early April. Previtellogenic ova (< 10 mm in diameter) dominated ovaries throughout April (Fig. 2). Clutch size using **POF** averaged 24.0 ± 3.1 (16-33; n = 10) and was approximately twice the size of the mean (12.1; 7-17; n = 7) derived using **VOF**. A grand mean of 11.6 ± 2.7 (7-17; n = 9) was found using **VOF**, **OE**, and one egg clutch. This two-fold decrease in clutch size is possibly the result of an especially high rate of follicular atresia in *E. o. obsoleta*. Rat snakes produce relatively large

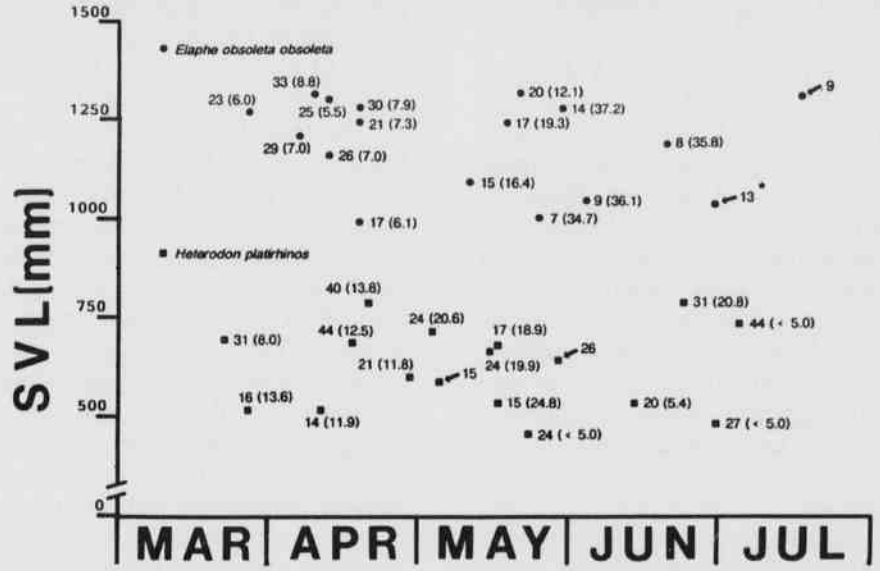

Fig. 2. Relationship between female body size (SVL) and reproduction condition in samples of two Arkansas snakes (*Elaphe obsoleta obsoleta* and *Heterodon platirhinos*). See Fig. 1 for explanation of numerals.

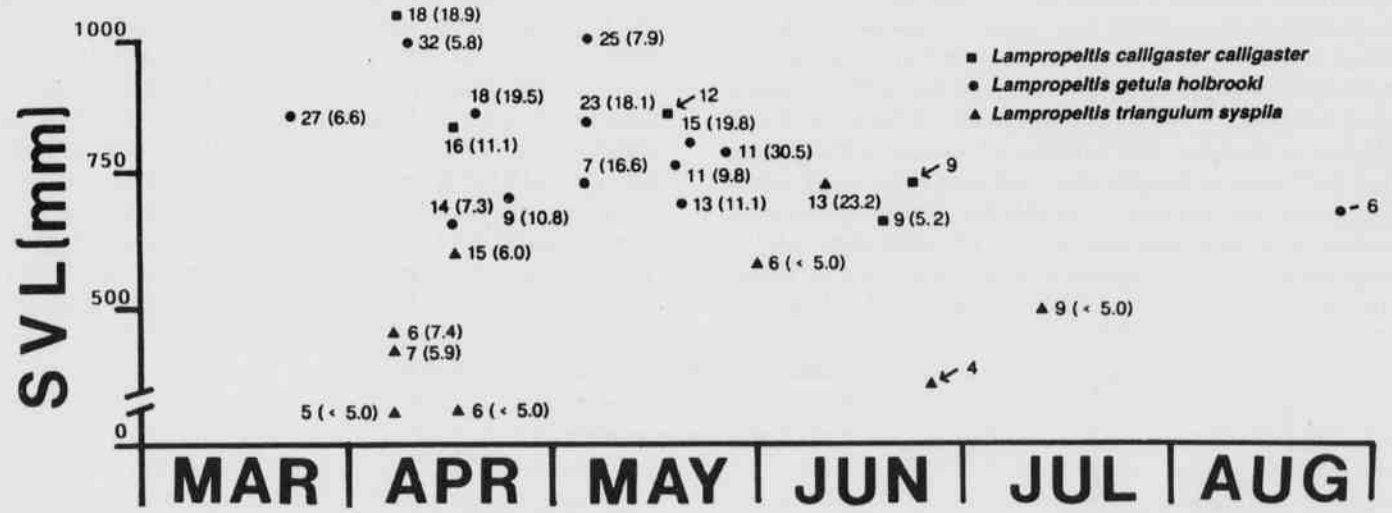

Fig. 3. Relationship between female body size (SVL) and reproduction condition in samples of three species of *Lampropeltis* from Arkansas. See Fig. 1 for explanation of numerals.

eggs (see below), and their coelomic cavity may be unable to expand in order to accomodate the potentially large numbers of eggs as evidenced by counts of **POF**. Fitch (1985) summarized the many records for clutch size in this species throughout its range in the United States; he reported mean clutch sizes (states grouped on a regional basis) to be the following: 13.9 (northeast), 11.2 (north-central), and 14.1 (southern). The mean for Arkansas specimens is closest to the northcentral states (Kansas and Missouri). In our study, only one female (a large specimen, 1308 mm SVL collected 16 July 1989), contained **OE** which numbered 9. (Early embryogenesis had begun within these eggs; the average crown-rump length of these embryos was around 5 mm.) Egg length and width of these eggs averaged 53.4 mm by 24.2 mm, whereas the average dimensions of two egg clutches of 8 and 9 eggs (collected in fallen trees on 30 July 1991 and 7 August 1986) were 47.0 mm by 26.6 mm and 41.4 mm by 25.4 mm, respectively. Corpora lutea (n = 13) were counted in one postreproductive female collected 30 June 1986.

Three subspecies of racers (*Coluber constrictor*) occur in Arkansas; two of these (*anthicus* and *priapus*) were examined during this study. A single specimen of the buttermilk racer (*C. c. anthicus*) yielded a clutch size of 16 (Fig.

4); otherwise, the rest of the reproductive data was derived from specimens of the southern black racer (*C. c. priapus*). Using counts obtained from **POF**, **VOF**, and **OE**, mean clutch sizes were 25.0 ± 4.2 (17-29; n = 7), 15.6 ± 2.2 (8-23; n = 13), and 16.3 ± 6.9 (14-26; n = 6), respectively. By combining the latter two methods, a grand mean was calculated to be 16.9 ± 2.0 eggs per clutch (8-26; n = 19). Racers begin vitellogenesis when follicles are approximately 6.0 mm in diameter; vitellogenic follicles reach a maximum of around 25.0 mm. Ovulation occurs in larger females by mid-May and in smaller females by late May. Oviposition occurs from mid-June until mid-July (Fitch, 1963). Fitch (1985) stated the *C. c. priapus* produced an average of 12.0 eggs per clutch in southern states (South Carolina, Florida, and Georgia) and that the maximum clutch size tended to occur in more northern populations of the species.

Two kingsnakes, the prairie kingsnake (*Lampropeltis calligaster calligaster*) and the speckled kingsnake (*L. getula holbrooki*), are common throughout Arkansas; clutch characteristics for both species are found in Fig. 3. Reproductive information on *L. c. calligaster* was limited; the largest female (1040 mm in SVL) contained large **VOF** ($\bar{x}$ = 18.9 mm in diameter) in early April. Clutch size based upon combined counts of **VOF** and **OE** averaged 14.0 ± 3.9 (9-20; n = 6). One specimen (908 mm in SVL) collected in October 1973 contained enlarged **POF** averaging 9.23 mm in length; this indicates that, as in some other snake species (e.g., *Carphophis vermis* and *Nerodia sipedon*--Aldridge and Metter, 1973; Aldridge, 1979, respectively), previtellogenic ova showed some enlargement prior to hibernation. Fitch (1985) noted that southern populations of prairie kingsnakes (specifically, southern parts of Illinois and Missouri) have clutch sizes averaging 11.0 (5-17; n = 9). Oviposition was observed in late June in Missouri (Johnson, 1987).

The transition from previtellogenic to vitellogenic follicles in female *L. g. holbrooki* occurred at approximately 8.0 mm in length. By early May, most large females have greatly enlarged **VOF**; yet, several specimens (both large and small) still possessed early-developing **VOF** in mid-May. Clutch size ranged from 14 to 32 ($\bar{x}$ = 23.5; n = 4) using **POF**, whereas the average was 13.1 ± 3.3 (7-23; n = 9) using **VOF**. Here again, the discrepancy between clutch size estimates using numbers of follicles may be similar to that observed in *Elaphe obsoleta* (i.e., a reduction in the reproductive potential due to follicular atresia). No females contained **OE**; however, one specimen (675 mm in SVL) in August exhibited six **CL**. Anderson (1965) reported egg laying in captive females in early July in Missouri. Average clutch size for southeastern states as reported by Fitch (1985) was 9.8 (5-17; n = 15).

The reproductive biology of the eastern coachwhip (*Masticophis flagellum flagellum*) is poorly known throughout its range in the United States; nothing has been published on its reproduction in Arkansas. Only two specimens of the eastern subspecies (*M. f. flagellum*) yielded data on clutch size (Fig. 4); one of these, an individual (1272 mm in SVL) collected 18 May 1986, had the largest average **VOF** (37.2 mm; n = 18) of all the large, oviparous colubrids examined during this study. The other specimen contained 14 **OE**; together, a mean clutch size of 16.0 was recorded. Postovipositional females (1265 mm in SVL, 19 June 1987; 1272 mm in SVL, 29 June 1986; 1148

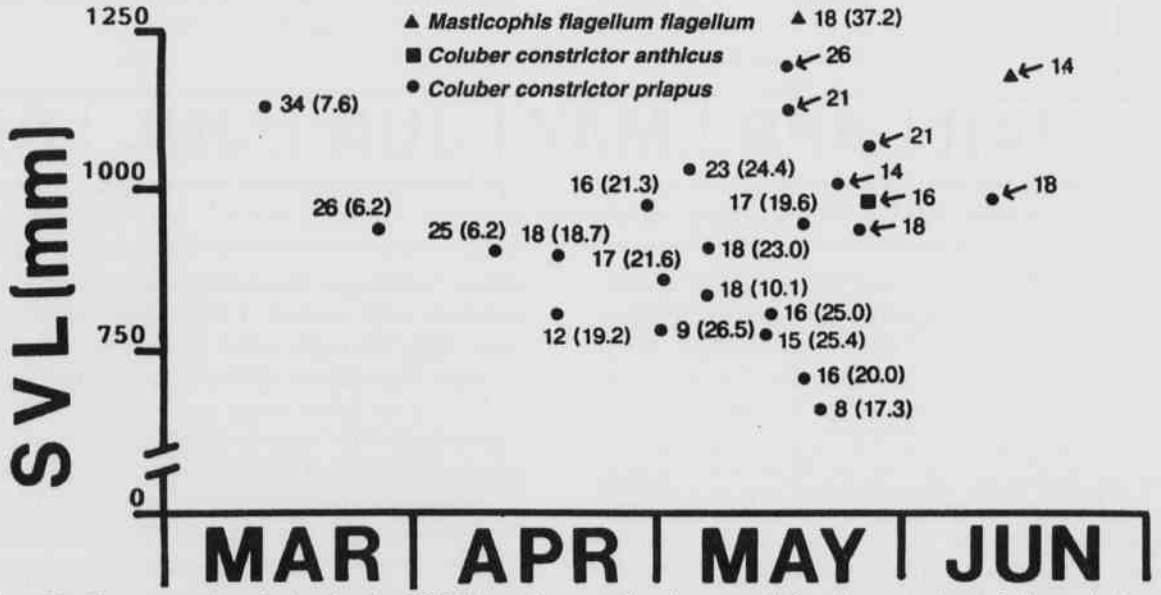

Fig. 4. Relationship between female body size (SVL) and reproduction condition in samples of three Arkansas snakes (*Masticophis flagellum flagellum, Coluber constrictor anthicus,* and *C. c. priapus*). See Fig. 1 for explanation of numerals.

mm in SVL, 6 July 1975) were also observed. From 8 to 24 eggs have been reported for this species in Missouri (Johnson, 1987), and Ford et al. (1990) recorded a clutch of 11 eggs in a female (1160 mm in SVL) in northeastern Texas. Ernst and Barbour (1989) determined that for 16 clutches ranging from 4 to 24 eggs, clutch size averaged 12.3 eggs.

Small Viviparous Colubrid Species.--Two genera comprising four species fall within this category of small woodland snakes; there exists a considerable amount of reproductive data on these species from the literature. Clutch and/or litter characteristics for the midland brown snake (*Storeria dekayi wrightorum*) and the northern redbelly snake (*S. occipitomaculata occipitomaculata*) are shown in Fig. 1. In *S. d. wrightorum*, vitellogeneis begins in ova around 3.0 mm in length sometime in late March or early April. Clutch size averages using **POV** and **VOF** were 16.5 (12-20; n = 4) and 13.8 (10-25; n = 6), respectively. Two litters averaged 9.5 neonates; a grand mean of 14.0 ± 2.8 (10-25; n = 12) was found when utilizing all methods. One female (205 mm in SVL) gave birth on 18 July 1989; the total lengths (in mm) of all young were as follows: 72, 74, 79, 83, 84, 85, 85, 87, 87, and 89. In addition, this female exhibited four large atretic follicles. Another female gave birth to a litter of 9 young on 4 August 1987 (no measurements available for these young). Fitch (1970) reported a mean of 14.0 (3-27) in 62 litters (a value identical to what we found as a grand mean). In Louisiana, Kofron (1979a) also reported a similar mean litter size of 14.9 (using several methods), whereas Ford et al. (1990) found a lower average litter size of 9.3 (4-15; n = 15) in northeastern Texas. Carpenter (1958) observed three litters (8, 12, and 9) in Oklahoma; dates of parturition were 26 July, 7 August, and 12 August, respectively.

There have been few studies that have adequately documented the reproductive biology of *S. o. occipitomaculata* in the southwestern portions of its range as compared to studies in other regions (Blanchard, 1937; Semlitsch and Moran, 1984; Brodie and Ducey, 1989). In Arkansas, redbelly snakes emerge from hibernation in March and have ovaries with developing follicles soon thereafter. Using counts of **POF**, **VOF**, and **OE**, a mean clutch size of 7.6 ± 1.2 (5-9; n = 7) was found. The largest female (235 mm in SVL) available for examination contained **OE** on 7 May 1994 (Fig. 1). Average litter size varies according to geographic region–8.2 (3-15) in the northeastern region, 7.2 (1-15) in the northcentral region, and 9.7 (3-18) in the northwestern region (Fitch, 1985). In Texas, Ford et al. (1990) reported on two litters (10 and 15) in *S. o. obscura* with females giving birth in July.

The rough earth snake (*Virginia striatula*) is one of the most common species of small snake encountered during the spring in Arkansas. Mean clutch size was calculated using **POF** (7.3 ± 0.8; 3-10; n = 18), **VOF** (7.0 ± 1.1; 5-9; n = 8), and **OE** (6.5; 4-9; n = 4). A grand mean using all methods was 7.1 ± 0.3 (3-10; n = 30). In our study, clutch size (using only greatly enlarged **VOF**) was positively correlated with SVL (r = 0.76; $P < 0.01$; n = 22). The regression equation (CS = - 5.5560 + 0.0620SVL) predicts that for every increase of 16 mm in SVL, and accompanying increase in one in clutch size will be observed. Atretic follicles were prevalent in most adult females examined; for example, the following data compares a series of clutches (using **VOF** and **OE**) and the number of atretic follicles encountered (clutch size/number of atretic follicles): 5/4, 6/4, 9/0, 7/4, 3/6, 10/3, 6/4, 7/1, 8/4, 10/5, 6/1, and 9/1. Clutch characteristics are shown in Fig. 5; no litters were examined during this study. The smallest reproductively-active female measured 147 mm in SVL; the mean SVL of adult females was 194.2 mm ± 3.8 (153-236; n = 32). Reproductive data are available from numerous published reports; litter size apparently varies little throughout this species' range (Fitch, 1985). For example, Fitch (1970) reported an average litter size of 4.9 (3-8; n = 16) from all regions, whereas in Texas, Clark and Fleet (1976) found 4.8 young per litter, and Ford et al. (1990) reported an average of 4.5 in two litters. In Oklahoma, Carpenter (1958) found litter size averaging 5.0 (3-6; n = 3); however, in a large sample, Stewart (1989) reported an average of 6.7 ± 0.4 (4-10; n = 33) from eastern Oklahoma. The similarity in fecundity between our sample and that of Stewart was not surprising considering his sample of snakes (from eastern Oklahoma) as well as most of ours was taken from the Interior Highlands Region.

Clutch characteristics (Fig. 5) of the smooth earth snake (*Virginia valeriae elegans*) in Arkansas are similar to those of the *V. striatula*. Mean clutch size using **POF** was 9.7 (7-14; n = 7), with **VOF**, 6.2 (6-7; n = 4), and with **OE**, 5.0 (5 and 5; n = 2). A grand mean using only **VOF** and **OE** was 5.8 (5-7; n = 7). As in *V. striatula* atretic follicles were numerous. Data on atretic follicles as above were as follows: 6/3, 6/3, 8/2, 9/2, 11/6, 6/3, and 8/2. Mean adult body size was 202.6 ± 9.4 mm in SVL (175-237; n = 13). For the southern states, Fitch (1985) compiled a mean litter size of 6.1 (4-14; n = 22), whereas Ford et al. (1990) indicated that two captive females in northeastern Texas had litters of 3 and 6.

Medium-sized Viviparous Colubrid Species.--Three natricine snakes were represented in this group. One was Graham's crayfish snake (*Regina grahamii*); a majority of these specimens was taken in a series collected in 1988 from Mallard Lake in Mississippi County (northeastern Arkansas). Females possessing **POF** were mostly collected in March and early April. The transitional size from **POF** to **VOF** was approximately 9.0 mm in length; this condition was evident in several females on 14 April 1988. By

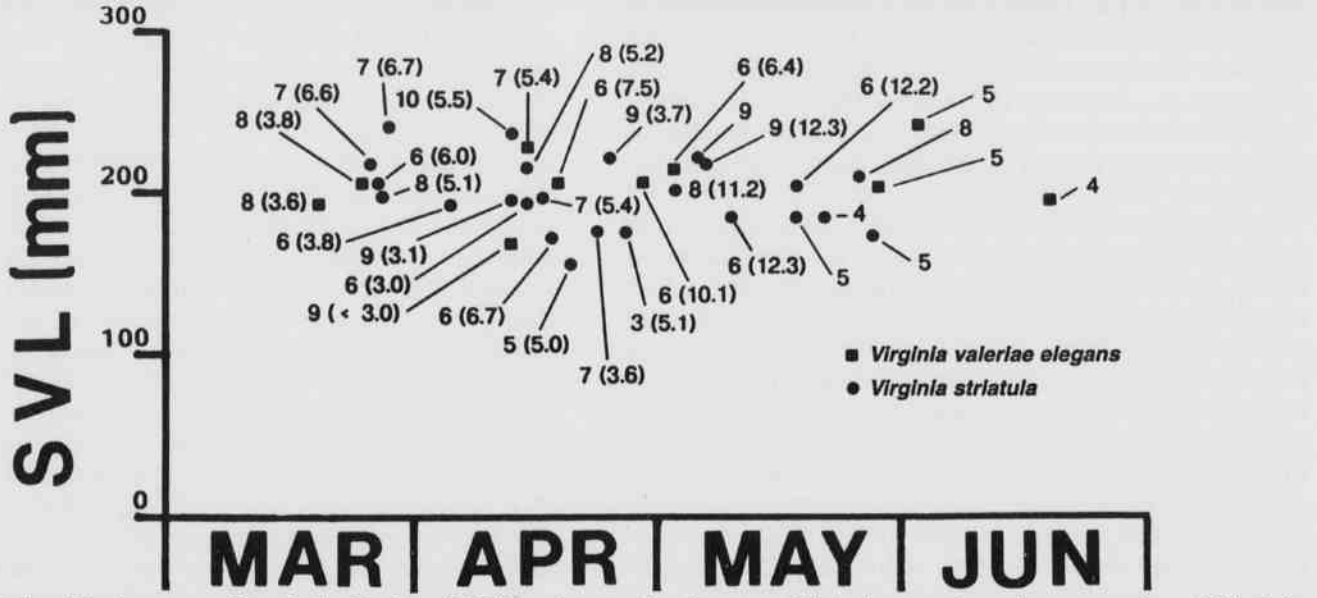

Fig. 5. Relationship between female body size (SVL) and reproduction condition in samples of two species of *Virginia* from Arkansas. See Fig. 1 for explanation of numerals.

early May most females contain **VOF** greater than 15 mm in diameter. A female containing the largest **VOF** ($\bar{x}$ = 23.5; n = 16) was collected on 8 June 1989; the only specimen with **OE** was collected on 29 May 1988. Using counts of **POF** and combined **VOF** and **OE**, mean clutch sizes were 32.9 ± 4.8 (18-44; n = 12) and 22.8 ± 3.7 (16-33; n = 10), respectively. Adult females (those with enlarged **VOF** or **OE**) averaged 703 ± 33.6 mm in SVL (625-775; n = 10). Data illustrated by Kofron (1979b) on reproduction in *R. grahamii* in Louisiana allowed for direct comparisons of the largest **VOF** between the Arkansas and Louisian females. Kofron found vitellogenesis beginning in ova 16 mm in length, whereas we found this to occur at around 9 mm. Kofron failed to mention an average clutch or litter size for *R. grahamii*; however, for northern states of Kansas, Missouri, Illinois, and Iowa, Fitch (1985) provided a combined average litter size of 16.4 (4-39; n = 24).

The other two species within this category are in the genus *Thamnophis*: for the most part, both have been well studied in most geographic areas in North America, except for the southcentral portions of their ranges (including Arkansas). In Arkansas the western ribbon snake (*T. proximus proximus*) becomes active on the first warm days in mid-March. Vitellogenesis generally begins in ova greater than 8.0 mm in length (Fig. 6). Mean clutch/litter size was generated using counts of **POV** (19.5 ± 4.3; 13-26; n = 6), **VOF** (20.3 ± 4.4; 8-34; n = 13), and **OE/OEM** (17.0; 12-26; n = 4). Using the latter two methods, a mean of 19.5 ± 3.7 (8-34; n = 17) was calculated; all methods are fairly consistent predictors of clutch/litter size. One female (642 mm in SVL collected 12 May 1988) contained large unovulated ova (n = 5) and one atretic follicle along with 26 **OE**. Another female (564 mm SVL collected 15 April 1968) contained a well-developed embryo (145 mm in SVL) in her right oviduct; this unusual occurrence would indicate a failure of this female to give birth to all offspring during the preceding late summer/early fall birthing period. The earliest data observed for **OE** was 19 May and the latest was 30 June. Clutch/litter size was generally much greater in Arkansas populations than what was found in other geographic areas. For example, Fitch (1985) gave a mean value of 11.6 (4-24; n = 41) for the central states (Oklahoma, Texas, and Louisiana) and only 12.4 (6-28; n = 14) for the northwestern states (Kansas, Nebraska, and Missouri). In another study, Clark (1974) reported an average of 8.4 (6-13; n = 8) in a Texas population.

The geographic variation in litter size of the eastern greater snake (*T. sirtalis sirtalis*) has been extensively documented (Fitch, 1970, 1985); however, nothing has been published on this subspecies in Arkansas. Clutch characteristics for 10 females are shown in Fig. 6; using counts of **VOF** and **OE/OEM**, mean clutch/litter sizes of 29.3 (26-33; n = 6) and 18.5 (16 and 21), respectively, were calculated. Combining these methods yielded a grand mean of 26.6 ± 4.0 (16-33; n = 8). Oviductal eggs were first noted in early May; only one female (517 mm in SVL collected 14 June 1993) contained **OEM** during the present study. Fitch (1985) summarized the literature on litter size in this species. The subspecies *sirtalis* in Canada exhibited average litter sizes of 25.0 (n = 14) and 29.0 (12-49; n = 7) in two separate studies. These estimates are similar to mean values of Arkansas specimens (using mostly ovarian counts), whereas Fitch (1970) found a mean of 14.5 in

132 gravid females (oviductal counts) of the subspecies *parietalis* in Kansas. Year-to-year intrapopulation variation in clutch size was documented in Kansas populations of *parietalis* (Seigel and Fitch, 1985). Several exceedingly large litters have been reported for this species (Fitch, 1985) and, especially, for the subspecies *sirtalis*; Dyrkacz (1975) reported a litter of 103 young of a captive female (1005 mm in SVL). Consequently, it was not surprising to find that the largest female (744 mm in SVL) observed during the present study contained a total of 79 **POF**.

Large Viviparous Colubrid Species.--Four of the five species of large aquatic natricine snakes of the genus *Nerodia* were examined during this study. The fifth species, the diamondback water snake (*N. r. rhombifer*), has been intensively studied in Arkansas (Plummer, 1992) as well as in the surrounding states of Louisiana (Kofron, 1979b), Missouri (Betz, 1963), and Texas (Ford et al., 1990). Plummer found an average litter size of 23.1 (12-48) in 21 litters, whereas Betz determined this to be 40.6 (28-56; n = 10). Ford et al. (1990) reported litters of 26, 37, and 30 in this species. Trends in geographic variation in litter size for this species are not fully understood (Fitch, 1985).

Reproduction in the Mississippi green water snake (*N. cyclopion*) is the least known of the water snakes in this group. In Arkansas, an average clutch size using combined counts of **POF**, **VOF**, and **OE/OEM** was 24.1 ± 7.3 (8-40; n = 11). If only **OE/OEM** are used, this count would be 18.3 (8-34; n = 3). Kofron (1979b) found a similar average count of 18.4 in 16 litters; he also stated that litter size generally increased in larger females. The smallest mature female (collected in April) measured 658 mm SVL; based upon size/age classes for this species as reported by Trauth (1990), she was in her third year of life. A similar size for the smallest mature female (measuring 637 mm SVL on 30 April 1976) was reported in Louisiana by Kofron (1979b). The largest female in the present study measured 961 mm in SVL and contained 34 well-developed embryos on 24 July 1988 (Fig. 7); this individual was estimated to be in her fifth year of life.

A large series of the yellowbelly water snake (*N. erythrogaster flavigaster*) yielded the following average clutch/litter sizes: **POF** = 34.6 ± 5.1 (22-57; n = 21), **VOF** = 21.6 ± 4.2 (9-33; n = 16), and **OE/OEM** = 21.8 (17-32; n = 4). By combining counts of **VOF** and **OE/OEM**, the average was 21.1 ± 9.4 (9-33; n = 20). Although female *N. e. flavigaster* become active in Arkansas starting in mid-March, vitellogenesis does not intensify until late April or early May (Fig. 8). This delay in ovarian development was also observed in Louisiana for this species (Kofron, 1979b) and was observed in other *Nerodia* species examined during the present study (Figs. 7 and 8). (Compare ovarian enlargement in *Nerodia* to *Agkistrodon* species–Fig. 9, or *Lampropeltis* species–Fig. 3). The smallest mature

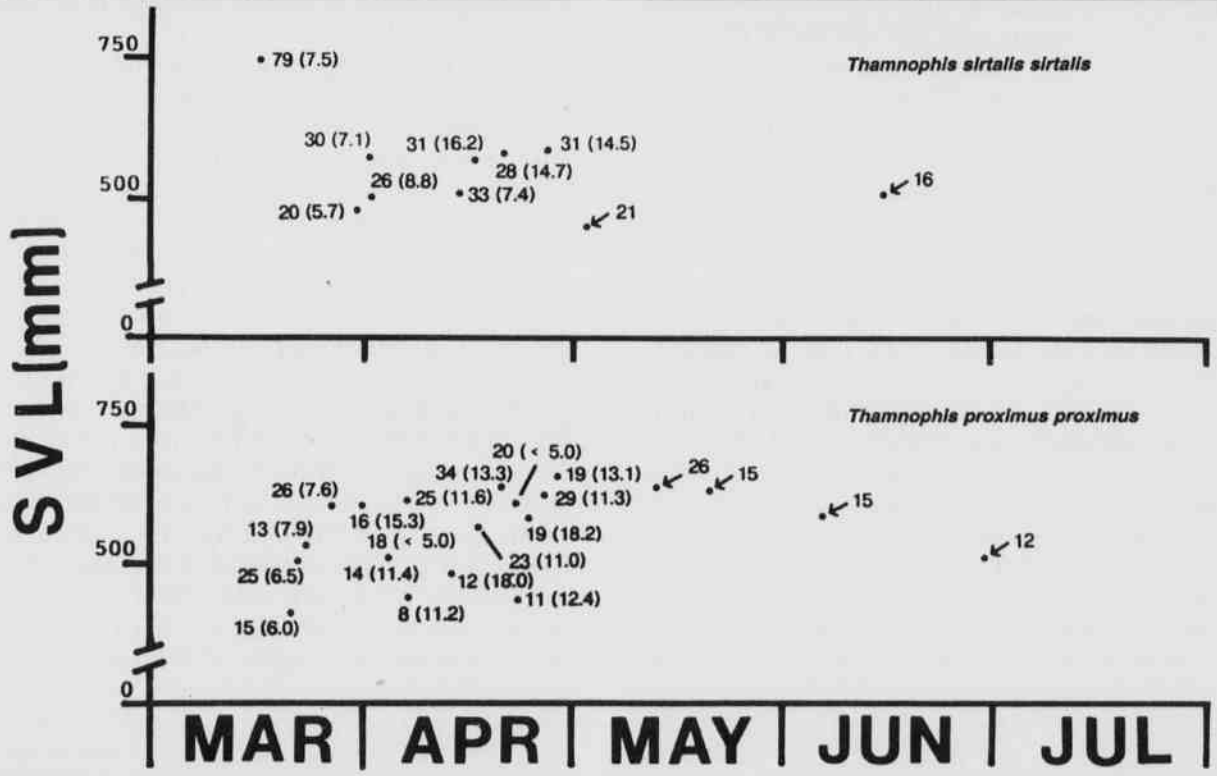

Fig. 6. Relationship between female body size (SVL) and reproduction condition in samples of two species of *Thamnophis* from Arkansas. See Fig. 1 for explanation of numerals.

female in the present study, measuring 638 mm in SVL on 15 May 1987, contained 13 **VOF** averaging 18.9 mm in length; on the other hand, the largest individual (a senescent female measuring 1167 mm in SVL on 29 May 1987), exhibited 57 **POF** averaging 6.4 mm in length. Kofron (1979) reported a female 734 mm SVL that showed the earliest onset of vitellogenesis. The transition between **POF** and **VOF** occurred in ova approximately 7.5 mm in length; the largest average of **VOF** was 27.7 mm. Failure of **POF** to develop accounted for about a 38% decrease in available ova for maturation. A significant positive correlation ($r = 0.67$; $n = 20$; $P < 0.01$) between CS and SVL was found. The regression equation (CS = -10.3546 + 0.0374SVL) indicates that as SVL increases by 27 mm, clutch size will be expected to increase by one. Fitch (1985) reported a much smaller average litter size (12.0; 4-22; n = 10) for southern population in this species and only a slightly larger average (15.7; 8-30; n = 20) for northern populations.

Anderson (1965) briefly mentioned litter sizes of 7, 13, and 19 (born in July and August) for Arkansas specimens of the broad-banded water snake (*N. fasciata confluens*). In our study average clutch size was determined (using **POF**, **VOF**, and **OE/OEM**, respectively) to be 33.6 ± 8.1 (19-56; n = 10), 20.2 ± 4.8 (12-31; n = 11), and 19.4 (17-25; n = 5). A combination of the latter two methods yielded an average of 20.6 ± 3.3 (12-31; n = 16). This estimate of litter size was similar to litter size in eastern states ($\bar{x} = 20.5$; n = 97), but larger than the average of 16.5 (n = 22; from Fitch, 1985) from Louisiana specimens. Regression analysis between CS and SVL in Arkansas specimens yielded the equation, CS = - 17.7703 + 0.0534SVL; as a result, for every increase of 19 mm in SVL, clutch size should increase by one. A significant positive correlation ($r = 0.71$; $P < 0.01$) was also observed between CS and SVL. The smallest mature females ranged between 523 and 558 mm in SVL; regardless of female body size, active vitellogenesis did not begin for most specimens until the month of May (Fig. 7). This general timing of vitellogenesis in Arkansas specimens contrasts sharply with the timing in Louisiana (Kofron, 1979b) populations which experience ova development as early as 27 March. Likewise, oviductal eggs were first observed during early June in Arkansas, whereas May was the rule in Louisiana populations. Interspecific comparisons revealed late June for the presence of **OE** in *N. e. flavigaster* and early July for *N. sipedon pleuralis* (Fig. 7).

Clutch characteristics in the midland water snake, *N. s. pleuralis*, were from samples taken mostly from the northeastern part of its range in Arkansas. We found average clutch sizes of 29.7 ± 7.2 (18-48; n = 10), 26.1 ± 5.7 (15-46; n = 9), and 19.0 (6-40; n = 3) using **POF**, **VOF**, and **OE/OEM**, respectively; a combined value of 24.3 ± 6.5 (6-46; n = 12) was calculated using the latter two methods. A significant positive correlation ($r = 0.76$; $P < 0.01$) existed between CS and SVL. The regression equation (CS = -32.4074 + 0.0793SVL) indicates that for every increase of 13 mm in SVL, clutch size will increase by one. Vitellogenesis occurred rapidly during the latter half of May; this feature was also observed in the northern water snake, *N. s. sipedon*, in Missouri (Bauman and Metter, 1977). The smallest mature female with **VOF** measured 593 mm in SVL was collected in mid-May (Fig. 7); this size was also similar to the value found by Aldridge (1982) in Missouri. The largest female (a specimen 940 mm in SVL collected in Crawford County on 8 August 1990) contained 40 well-developed embryos. We found two nonreproductive females of mature size in July and August; as pointed out by Collins (1993) for females in Kansas, all females may not breed annually. Fitch (1985) summarized the geographic variation in litter size in this species and found no clear trends; moreover, our estimate of litter size was slightly smaller than the average value (25.7) indicated for the subspecies *sipedon* for Missouri.

In general the reproductive traits in four of the five *Nerodia* species in Arkansas can be summarized as follows: 1) average litter size ranged from approximately 18 to 25, 2) minimal size at maturity ranged from 550 to 650 mm in SVL, 3) rapid development in ovarian follicles began in May, 4) the range in numbers of **POF** was from 15 to 60, and 5) the degree of follicular atresia appeared greatest in *N. erythrogaster* and *N. fasciata* and least in *N. cyclopion* and *N. sipedon*.

Small Viperid Species.--One species, the western pigmy rattlesnake (*Sistrurus miliarius streckeri*), falls into this category. An average clutch/litter size of 10.0 ± 2.2 (6-14; n = 8) was generated using combined counts of **POF**, **VOF**, and **OE/OEM**. Six **OE** averaging 17.1 mm in length were recorded from a female (338 mm in SVL) collected on 22 May 1994, and six well-developed embryos were observed in a female 420 mm in SVL collected on 29 June 1972. A litter of 13 neonates was born to a female of undetermined size on 9 September 1988 collected near Batesville (Independence County). Fitch (1985) and Ford et al. (1990) reported an average litter sizes of 8.6 (3-32; n = 9) and 7.4 (6-9; n = 5), respectively, for this subspecies from Texas; Anderson (1965) found litter size to range from 3 to 7 young in Missouri.

Medium-sized Viperid Species.--Two species of *Agkistrodon* are represented in this group. The southern copperhead, *A. contortrix contortrix*, is distributed throughout most of the eastern and southern parts of Arkansas; in the northwestern region of the state, this subspecies intergrades with *A. c. phaeogaster*. Most of the copperheads in our study were collected in northeastern Arkansas. The average clutch/ litter size using counts of **POF**, **VOF**, and **OE/OEM** (and neonates from litters) were 15.2 (12-18; n = 4), 12.4 ± 2.8 (7-25; n = 10), and 9.9

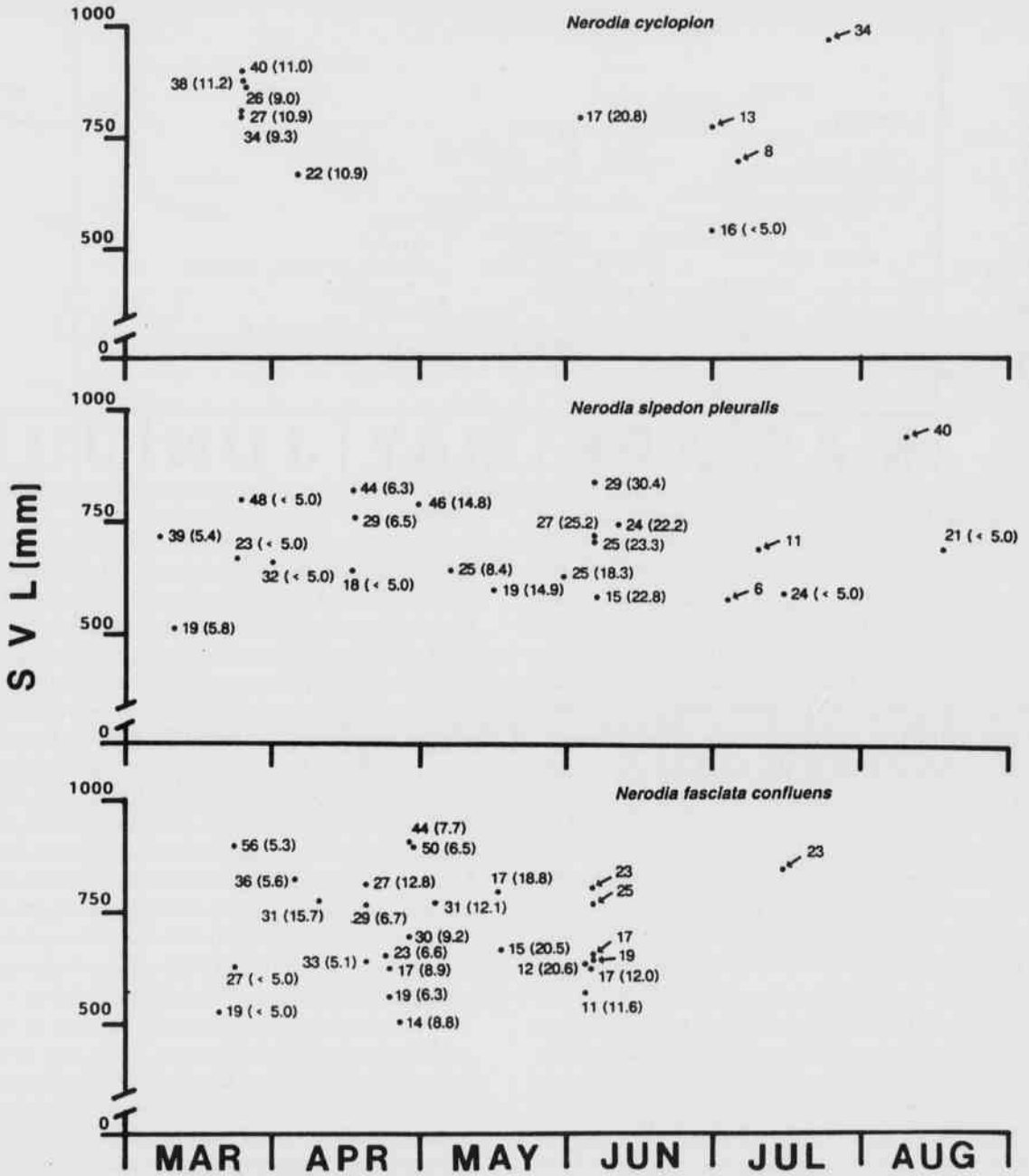

Fig. 7. Relationship between female body size (SVL) and reproduction condition in samples of three species of watersnakes (genus *Nerodia*) from Arkansas. See Fig. 1 for explanation of numerals.

± 3.7 (4-16; n = 7), respectively. [Litter sizes from Meshaka et al. (1989) were included in the latter estimate.] By combining the latter two counts, a mean of 11.4 ± 2.3 (4-25; n = 17) was determined. Clutch size was significantly correlated with SVL (r = 0.63; $P < 0.01$). The regression equation (CS = -11.8802 + 0.0353SVL) indicates that for every increase of 28 mm in SVL, an accompanying increase of one would occur in clutch size. Fitch (1985) reported litter size for the subspecies *contortrix* in the southeastern United States to average 6.6 (5-11; n = 17), whereas Ford et al. (1990) found an average of 6.9 (4-10; n = 8) in populations in northeastern Texas. The relatively high estimate of litter size as well as the actual high litter sizes observed in northeastern Arkansas (Fig. 9) may be a reflection of a locally-abundant food source (i.e., a possible increased availability of small mammals in this region related to intensive grain agriculture) or may be directly ralated to larger female body size attained in this region of the state.

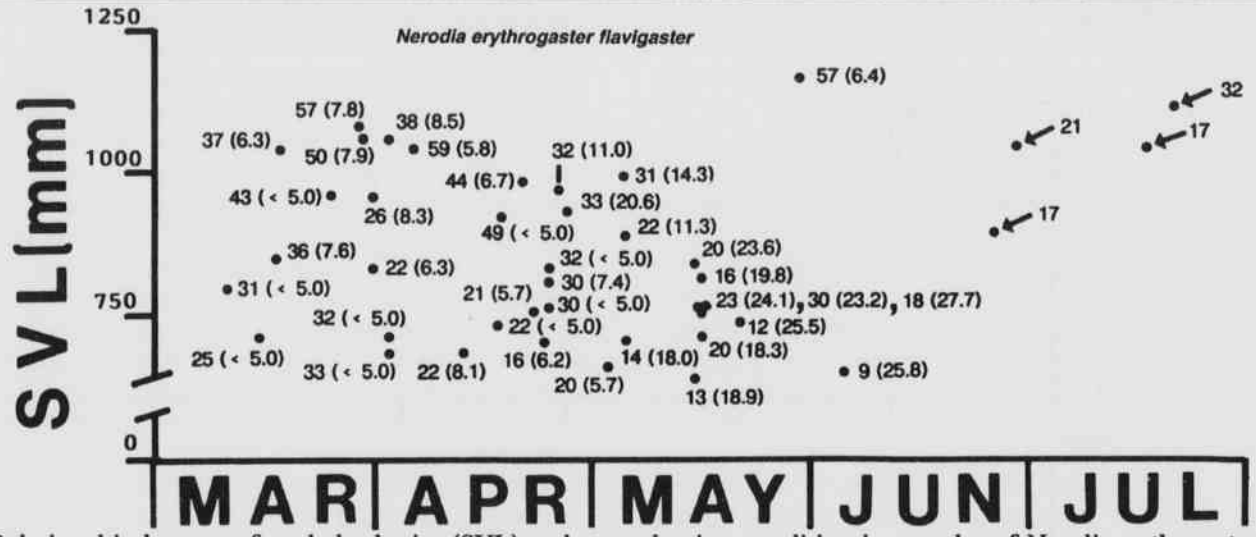

Fig. 8. Relationship between female body size (SVL) and reproduction condition in samples of *Nerodia erythrogaster flavigaster* from Arkansas. See Fig. 1 for explanation of numerals.

Mature females ranged in size from a little over 500 to around 750 mm in SVL. The largest female in a Texas sample as reported by Ford et al. (1990) was 600 mm in SVL, and Fitch (1960) reported no females greater than 690 mm in SVL. A biennial breeding pattern is common in this species (Fitch, 1960, 1970, 1985); Seigel and Ford (1987) reported that 60% of the mature females were gravid, whereas we found 86% of the adult females to be reproductively active.

Clutch characteristics of the western cottonmouth (*A. piscivorus leucostoma*) were compiled from samples taken from all parts of Arkansas. Using counts of **POF**, **VOF**, and **OE/OEM**, average clutch/litter sizes were 11.9 ± 2.5 (4-17; n = 10), 7.2 ± 1.3 (5-12; n = 12), and 4.8 (3-6; n = 4), respectively; a mean generated by combining the latter two methods yielded a value of 6.6 ± 1.2 (3-12; n = 16). Clutch size was not significantly correlated with SVL ($r = 0.49$; $P > 0.05$). In Louisiana Kofron (1979b) found 87% of female *A. p. leucostoma* gravid, whereas in eastern Texas, Burkett (1966) found only 42% (29 of 69). We determined that 67% of females we collected were reproductively active; this suggests a biennial reproductive cycle in this species in Arkansas. Our estimation of litter size was similar to a value of 6.8 (2-15; n = 21) reported by Fitch (1985) for specimens from the western and northwestern portions of its range. Vitellogenesis was underway in late March; the first **OE** were observed in late May. The smallest mature female was around 540 mm in SVL.

Large Viperid Species.--The timber rattlesnake (*Crotalus horridus*) is the lone representative in this category. [There are no records on reproduction in the western diamondback rattlesnake (*C. atrox*) from Arkansas, but see Fitch and Pisani (1993) for Oklahoma populations.] In Arkansas timber rattlesnakes usually emerge from hibernation dens sometime in April. Of the five female specimens collected in April, three exhibited **POF** averaging 12.3 in number and 6.1 mm in length (female SVL's = 1234, 977, and 948 mm); the other two females (1055 and 1008 mm in SVL) contained 16 greatly enlarged **VOF** averaging 37.6 mm in length and nine **OE** averaging 42.0 mm in length, respectively. (The latter female was collected on 19 April but was not killed until 4 June). Another female (908 mm in SVL collected 6 July 1985) exhibited **POF** < 5.0 mm in length. Vitellogenesis requires more than a single activity season (usually around 13-14 months–Martin, 1993). The reproductive pattern in this species is low-frequency birthing and delayed maturity (Brown, 1993). Geographic variation in litter size was summarized by Fitch (1985) with southern populations averaging 9.7 (7-11; n = 7) young per litter.

Conclusions

Our study focused on presenting female reproductive information, including such traits as clutch or litter size and the timing of ovarian development, on a large number of Arkansas snake species; this kind of data was inadequately known or unavailable for most snakes within the state. The results of our work provide pertinent life history data that will hopefully enable future researchers to include Arkansas populations when making geographic comparisons on intraspecific variation in snake ecology. Because our study included reproductive data from females collected from different populations over several years, data for each species included possible annual, seasonal, and geographic variation in parameters. Nearly one half (n = 13) of the 27 species and subspecies examined

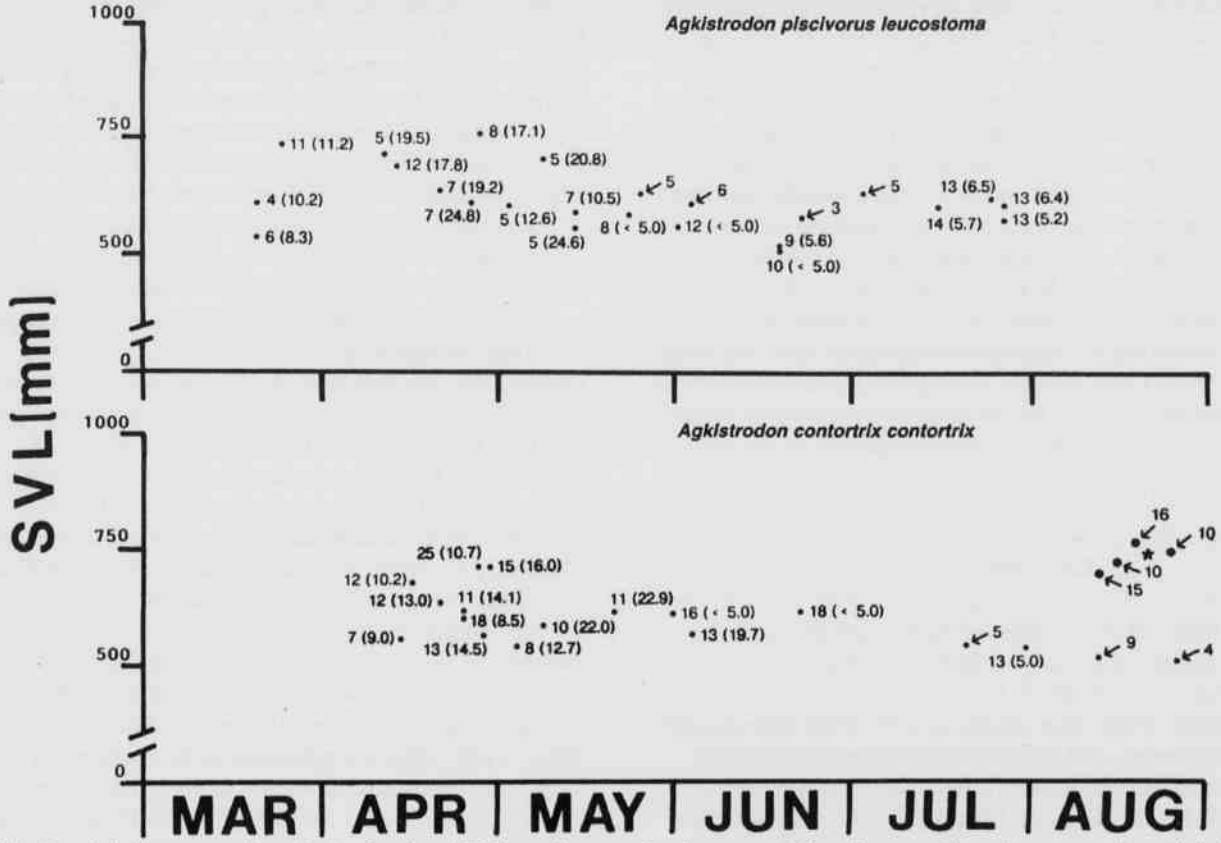

Fig. 9. Relationship between female body size (SVL) and reproduction condition in samples of two species of *Agkistrodon* from Arkansas. Asterisk denotes data (four litters) extracted from Meshaka et al. (1989). See Fig. 1 for explanation of numerals.

exhibited very similar clutch characteristics to populations in states bordering Arkansas. On the other hand, eight species had greater values with only one species exhibiting a smaller value.

Researchers in the field of snake reproductive ecology have focused their attention in recent years on identifying factors affecting the total reproductive investment by female snakes, and, especially, on those factors independent of phylogeny or less attributable to a female's genetic makeup (see reviews in Seigel and Fitch, 1985; Seigel et al., 1986; Seigel and Ford, 1987; Dunham et al., 1988). Any number of proximate environmental conditions (e.g., female nutritional state and food availability) can greatly influence critical reproductive parameters (clutch frequency and size). This is true in temperate zone snakes (and probably for tropical forms as well), a group whose overall reproductive biology is the best known of the ophidians. For many snakes species, increases in female body length are generally associated with greater clutch or litter size (e.g., Aldridge, 1982; Plummer, 1984; Seigel and Ford, 1987; Ford and Seigel, 1989); however, from year to year, female snakes sometimes increase offspring number and at the same time reduce offspring size, or vice versa. Some temperate zone viviparous species, especially viperids, exhibit a biennial reproductive cycle (Fitch, 1970; Aldridge, 1979). Blem (1982) noted, however, that female *Agkistrodon piscivorus* lacking sufficient amounts of stored lipids did not reproduce annually and that large cottonmouths were gravid more frequently than small ones. Short-term reproductive studies may fail to detect these types of variation in clutch data, whereas significant annual variation has been demonstrated in some species studied over periods of time up to 30 years (Seigel and Fitch, 1985). Consequently, long-term field investigations on snake reproductive biology are essential to our understanding of the multitude and complexity of factors related to reproductive success and must be undertaken to provide important data to support generalizations concerning reproductive characteristics of a given species.

Acknowledgements

Many students, friends, associates, colleagues, and family members kindly assisted in the collection of snakes, and we express our appreciation to all of them.

Among those who generously devoted much time and effort in the field are Blake Bevill, Betty G. Cochran, Patrick Daniel, Doug Fletcher, George L. Harp, Lewis Hunt, David H. Jamieson, Chris T. McAllister, Rusty McAllister, John W. Robinette, David A. Saugey, J.D. Wilhide, and Mr. Charles West of Marianna. William W. Bryd, Earl L. Hanebrink, and V. Rick McDaniel contributed greatly to the collection of specimens prior to 1984. Partial funding for field work was provided by the Arkansas Game and Fish Commission through research grants to SET during 1988 and 1989. Collections from 1984-1993 were under the authorization of the Arkansas Game and Fish Commission through scientific collection permits issued to SET. The critical remarks of two anonymous reviewers greatly improved the quality of the manuscript.

Literature Cited

Aldridge, R.D. 1979. Female reproductive cycles of the snakes *Arizona elegans* and *Crotalus viridis*. Herpetologica 35:256-261.

Aldridge, R.D. 1982. The ovarian cycle of the watersnake *Nerodia sipedon*, and effects of hypophysectomy and gonadotropin administration. Herpetologica 38:71-79.

Aldridge, R.D. and **D.E. Metter.** 1973. The reproductive cycle of the worm snake, *Carphophis vermis*, in Missouri. Copeia 1973:472-477.

Anderson, P. 1965. The reptiles of Missouri. Univ. Missouri Press, Columbia, xxiii + 330 pp.

Ballinger, R.E. 1978. Variation in and evolution of clutch and litter size. Pp. 789-825, *In* The vertebrate ovary (R.E. Jones, ed.) Plenum Press, New York, xxiii + 853.

Bauman, M.A. and **D.E. Metter.** 1977. Reproductive cycle of the northern watersnake, *Natrix s. sipedon* (Reptilia, Serpentes, Colubridae). J. Herpetol. 11:51-59.

Betz, T.W. 1963. The gross ovarian morphology of the diamond-backed water snake, *Natrix rhombifera*, during the reproductive cycle. Copeia 1963:692-697.

Blanchard, F.N. 1937. Data on the natural history of the red-bellied snake, *Storeria occipito-maculata* (Storer), in northern Michigan. Copeia 1937:151-162.

Blem, C.R. 1982. Biennial reproduction in snakes: an alternative hypothesis. Copeia 1982:961-963.

Brodie, E.D., III and **P.K. Ducey.** 1989. Allocation of reproductive investment in the redbelly snake *Storeria occipitomaculata*. Amer. Midl. Nat. 122:51-58.

Brown, W.S. 1993. Biology, status, and management of the timber rattlesnake (*Crotalus horridus*): a guide for conservation. Soc. Stud. Amph. Rept. Herpetol. Circ. No. 22, vi + 78 pp.

Burkett, R.D. 1966. Natural history of the cottonmouth moccasin, *Agkistrodon piscivorus* (Reptilia). Univ. Kansas Publ. Mus. Nat. Hist. 17:435-491.

Carpenter, C.C. 1958. Reproduction, young, eggs, and food of Oklahoma snakes. Herpetologica 14:113-115.

Carpenter, C.C. and **J.J. Krupa.** 1989. Oklahoma herpetology: an annotated bibliography. Univeristy of Oklahoma Press, Norman, vii + 258.

Clark, D.R., Jr. 1970. Ecological study of the worm snake *Carphophis vermis* (Kennicott). Univ. Kansas Publ. Mus. Nat. Hist. 19:89-194.

Clark, D.R., Jr. 1974. The western ribbon snake (*Thamnophis proximus*): ecology of a Texas population. Herpetologica 30:372-379.

Clark, D.R., Jr. and **R.R. Fleet.** 1976. The rough earth snake (*Virginia striatula*): ecology of a Texas population. Southw. Nat. 20:467-478.

Cobb, V.A. 1990. Reproductive notes on the eggs and offspring of *Tantilla gracilis* (Serpentes: Colubridae), with evidence of communal nesting. Southw. Nat. 35:22-24.

Collins, J.T. 1993. Amphibians and reptiles in Kansas. 3rd ed. Univ. Kansas Mus. Nat. Hist. Publ. Edu. Ser. No. 13:1-397.

Conant, R. and **J.T. Collins.** 1991. A field guide to reptiles and amphibians of eastern and central North America. Houghton Mifflin Co., Boston, 450 pp.

Dixon, J.R. 1987. Amphibians and reptiles of Texas with keys, taxonomic synopses, bibliography, and distribution maps. Texas A&M University Press, College Station, 434 pp.

Dunham, A.E., D.B. Miles, and **D.N. Reznick.** 1988. Life history patterns in squamate reptiles. Pp. 441-522, *In* Biology of the reptilia, Vol. 16 and ecology B, defense and life history, (C. Gans and R.B. Huey, eds.). Alan R. Liss, Inc., New York, xi + 659 pp.

Dundee, H.A. and **D.A. Rossman.** 1989. The amphibians and reptiles of Louisiana. Louisiana State Univ. Press, Baton Rouge, xi + 300 pp.

Dyrkacz, S. 1975. Life history (litter size): *Thammophis s. sirtalis*. Herpetol. Rev. 6:20.

Ernst, C.H. and **R.W. Barbour.** 1989. Snakes of eastern North America. George Mason Univ. Press, Fairfax, VA, vii + 282 pp.

Fitch, H.S. 1960. Autecology of the copperhead. Univ. Kansas Mus. Nat. Hist. 13:85-288.

Fitch, H.S. 1963. Natural history of the racer *Coluber constrictor*. Univ. Kansas Publ. Mus. Nat. Hist. 15:351-468.

Fitch, H.S. 1970. Reproductive cycles in lizards and snakes. Univ. Kansas Mus. Nat. Hist. 52:1-247.

Fitch, H.S. 1975. A demographic study of the ringneck snake (*Diadophis punctatus*) in Kansas. Univ. Kansas Mus. Nat. Hist. Misc. Publ. 62:1-53.

Fitch, H.S. 1985. Variation in clutch and litter size in New World reptiles. Univ. Kansas Mus. Nat. Hist. 76:1-76.

Fitch, H.S. and **G.R. Pisani.** 1993. Life history traits of the western diamondback rattlesnake (*Crotalus atrox*)

studied from roundup samples in Oklahmoma. Univ. Kansas Mus. Nat. Hist. Occ. Pap. No. 156:1-24.

Force, E.R. 1935. A local study of the opisthoglyph snake *Tantilla gracilis* Baird and Girard. Papers Michigan Acad. Sci., Arts Letters 20:645-659.

Ford, N.B., V.A. Cobb and **W.W. Lamar.** 1990. Reproductive data on snakes from northeastern Texas. Texas J. Sci. 42:355-368.

Ford, N.B. and **R.A. Seigel.** 1989. Relationships among body size, clutch size, and egg size in three species of oviparous snakes. Herpetologica 45:75-83.

Johnson, T.R. 1987. The amphibians and reptiles of Missouri. Missouri Dept. Cons., Jefferson City, xi + 368 pp.

Kofron, C.P. 1979a. Female reproductive biology of the brown snake, *Storeria dekayi*, in Louisiana. Copeia 1979:463-466.

Kofron, C.P. 1979b. Reproduction of aquatic snakes in south-central Louisiana. Herpetologica 35:44-50.

Martin, W.H. 1993. Reproduction of the timber rattlesnake (*Crotalus horridus*) in the Appalachian Mountains. J. Herpetol. 27:133-143.

Meshaka, W.E., S.E. Trauth, B.P. Butterfield and **A.B. Bevill.** 1989. Litter size and aberrant pattern in the southern copperhead, *Agkistrodon contortrix contortrix*, from northeastern Arkansas. Bull. Chicago Herpetol. Soc. 24:91-92.

Platt, D.R. 1969. Natural history of the hognose snakes *Heterodon platyrhinos* and *Heterodon nasicus*. Univ. Kansas Publ. Mus. Nat. Hist. 18:253-420.

Plummer, M.V. 1983. Annual variation in stored lipids and reproduction in green snakes (*Opheodrys aestivus*). Copeia 1983:741-745.

Plummer, M.V. 1984. Fèmale reproduction in an Arkansas population of rough green snakes (*Opheodrys aestivus*). Pp. 105-113, *In* Vertebrate ecology and systematics: a tribute to Henry S. Fitch. (R.A. Seigel, L.E. Hunt, J.L. Knight, L. Malaret and N.L. Zuschleg, eds.). Univ. Kansas Mus. Nat. History, Lawrence, viii + 278 pp.

Plummer, M.V. 1992. Relationships among mothers, litters, and neonates in diamondback water snakes (*Nerodia rhombifer*). Copeia 1992:1096-1098.

Robinette, J.W. and **S.E. Trauth.** 1992. Reproduction in the western mud snake, *Farancia abacura reinwardtii* (Serpentes: Colubridae), in Arkansas. Proc. Arkansas Acad. Sci. 46:61-64.

Seigel, R.A. and **H.S. Fitch.** 1985. Annual variation in reproduction in snakes in a fluctuating environment. J. Anim. Ecol. 54:497-505.

Seigel, R.A. and **N.B. Ford.** 1987. Reproductive ecology. Pp. 210-252, *In* Snakes: Ecology and evolutionary biology (R.A. Seigel, J.T. Collins, and S.S. Novak, eds.). Macmillan Publ. Co., New York, xiv + 529 pp.

Seigel, R.A., H.S. Fitch and **N.B. Ford.** 1986. Variation in relative clutch mass in snakes among and within species. Herpetologica 42:179-185.

Semlitsch, R.D. and **G.B. Moran.** 1984. Ecology of the redbelly snake (*Storeria occipitomaculata*) using mesic habitats in South Carolina. Amer. Midl. Nat. 111:33-40.

Stewart, J.R. 1989. Facultative placentotrophy and evolution of squamate placentation: quality of eggs and neonates in *Virginia striatula*. Amer. Nat. 133:111-137.

Smith, H.M., D. Chiszar, J.R. Staley, II and **K. Tepedelen.** 1994. Populational relationships in the corn snake *Elaphe guttata* (Reptilia: Serpentes). Texas J. Sci. 46:259-292.

Sutton, K.B. and **V.R. McDaniel.** 1979. Unusual concentration of scarlet snakes (*Cemophora coccinea*) in Village Creek State Park, Arkansas. Proc. Arkansas Acad. Sci. 33:92.

Trauth, S.E. 1982. *Cemophora coccinea* (Scarlet Snake). Reproduction. Herpetol. Rev. 13:126.

Trauth, S.E. 1990. Flooding as a factor in the decimation of a population of green water snakes (*Nerodia cyclopion cyclopion*) from Arkansas. Bull. Chicago Herpetol. Soc. 25:1-3.

Trauth, S.E. 1991. Distribution, scutellation, and reproduction in the queen snake, *Regina septemvittata* (Serpentes: Colubridae), from Arkansas. Proc. Arkansas Acad. Sci. 45:103-106.

Williams, K.L. 1988. Systematics and natural history of the American milk snake, *Lampropeltis triangulum*. Milwaukee Publ. Mus., Milwaukee, WI x + 176 pp.

Wright, A.H. and **A.A. Wright.** 1957. Handbook of snakes of the United States and Canada. Comstock Publ. Associates, Cornell Univ. Press, Vol. 1, xviii + 564 pp; Vol. 2, ix + 565-1105 pp.

Reproductive Cycles in Two Arkansas Skinks in the Genus *Eumeces* (Sauria: Scincidae)

Stanley E. Trauth
Department of Biological Sciences
Arkansas State University
State University, AR 72467-0599

Abstract

Reproductive cycles of the southern coal skink (*Eumeces anthracinus pluvialis*) and the five-lined skink (*E. fasciatus*) were studied by examining museum specimens collected in Arkansas. Histological preparations of testes from each species revealed eight spermatogenic stages. Male coal skinks produced sperm by late February, at least one month before male five-lined skinks. Height of the testicular cycle (maximum sperm production–stage 6 = spermiogenesis) in *E. a. pluvialis* occurred in March and early April, whereas in *E. fasciatus*, spermiogenesis reached a peak in May. Testicular recrudescence began in late May in *E. a. pluvialis* and mid-July in *E. fasciatus*. The reproductive condition of female skinks was determined by counting and measuring enlarged ovarian follicles and oviductal eggs. Female coal skinks contained vitellogenic ovarian follicles starting in mid-March; vitellogenic ova reached their maximum size by mid-April. Oviductal eggs were recorded from early April to mid-May. Clutch size in *E. a. pluvialis* averaged 10.5 (5 - 17; n = 27) based on vitellogenic ova and 9.6 (8 - 13; n = 21) based on oviductal eggs. No egg clutches of *E. a. pluvialis* were discovered. In female *E. fasciatus*, a rapid increase in the rate of vitellogenesis began in late April; yolking ova were last observed in an individual in mid-June. Oviductal eggs were recorded from mid-May to late June; average clutch size based on vitellogenic ova was 10.0 (7 - 15; n = 34), whereas oviductal eggs yielded an average clutch size of 8.4 (6 - 12; n = 13). Atresia of ovarian follicles may explain the difference between counts. Clutch size as determined from five nests discovered in June and July was 8.2 (7 - 10). Intraspecific synchrony of annual sexual cycles occurs between the sexes of each skink, while only a marginal overlap exists between the two species.

Introduction

Northern Hemisphere *Eumeces* (Scincidae) are represented in the southcentral United States (Zug, 1993) by four oviparous species (*E. anthracinus, E. fasciatus, E. inexpectatus,* and *E. laticeps*). Compared to the other three species, surprisingly little is known about the reproductive ecology of the coal skink, *E. anthracinus*, a member of the *anthracinus* group of eastern four-lined skinks (Smith, 1946). Moreover, reproduction in this species has received no detailed study; published information on clutch size in brooding females has appeared anecdotally (Sexton, 1984) or as brief accounts in state herpetology books (e.g., Mount, 1975; Johnson, 1987; Dundee and Rossman, 1989; Collins, 1993). Fitch (1970, 1985) had no data on coal skinks in his general summaries on lizard reproduction. In contrast, the life history and reproductive biology of the five-lined skink (*Eumeces fasciatus*), a member of the *fasciatus* group of five-lined skinks (Smith, 1946) and a species common throughout much of the eastern and central United States (Conant and Collins, 1991), have been well documented (Fitch, 1954, 1970, 1985; Vitt and Cooper, 1986; Shadrix et al., 1994).

The coal skink has a relatively broad but patchy range east of the Mississippi River, whereas it has a nearly continuous distribution throughout the Interior Highlands of Arkansas, Missouri, Kansas, and Oklahoma; its range also extends into portions of northern Louisiana and eastern Texas (Conant and Collins, 1991). The southern coal skink, *E. a. pluvialis*, is known to occur in at least 34 of the 75 counties in Arkansas (Trauth, unpubl.). Collection of this species in Arkansas is mostly sporadic at best. Individuals are often observed in forest habitats near streams although they can also be taken in moist areas along cedar glades (see Sexton, 1984). Sampling is mostly confined to late winter and spring months. On the other hand, *Eumeces fasciatus* is encountered in a variety of habitats in Arkansas, especially in pine and oak-hickory forests from March through October. These two species have similar morphologies and are sympatric in Arkansas; yet they prefer slightly different habitats. In the present study the reproductive ecology of *E. anthracinus* was compared to that of sympatric *E. fasciatus* to determine whether any observed differences might represent higher taxonomic level (species group) differences.

Materials and Methods

Reproductive data were amassed from 64 adult *E. a. pluvialis* (21 males; 43 females) and 219 adult *E. fasciatus* (112 males; 107 females) during this study. Most coal skinks (n = 30) and five-lined skinks (n = 167) were collected over a 10-year span (1984-1993). Sampling occurred primarily within the Ozark Mountains of northeastern Arkansas; museum voucher specimens from Arkansas were also examined. Skinks were obtained by hand and were processed in the lab at Arkansas State University within 48 hr after capture. Lizards were killed with an intraperitoneal injection of a dilute solution of sodium pentobarbitol and fixed in 10% formalin. Following fixation, the snout-vent length (SVL) was measured to the nearest mm. Specimens were later transferred to 70% ethanol for permanent storage.

Routine histological techniques were used to prepare testes and attached epididymides for light microscopy. Tissues were dehydrated in a graded series of ethanol, cleared in xylene, embedded in paraffin, sectioned into 10 μm serial strips (affixed to glass slides using Haupt's adhesive), and stained using Harris hematoxylin followed by counterstaining with eosin (H & E). The testicular cycle was staged according to spermatogenic condition (Mayhew and Wright, 1970). Testicular stage refers to spermatocytogenic development starting with spermatogonia and ending with the release of sperm into lumina of the seminiferous tubules; these eight stages, briefly summarized, are as follows: 1) division of germinal cells, 2) primary spermatocytes predominate within tubules, 3) secondary spermatocytes reside at luminal borders, 4) undifferentiated spermatids at luminal borders, 5) metamorphosing spermatids at luminal borders, 6) mature sperm at luminal borders and within expanded lumina, 7) early epithelial regression with some sperm at luminal borders and within lumina, and 8) complete epithelial regression with no sperm within lumina. A morphometric analysis of both the seminiferous and epididymal tubules was performed to evaluate variation in size of these structures. The procedure involved tracing of tubule perimeters onto a digitizing tablet (The Morphometer^R, Woods Hole Educational Associates, Woods Hole, MA) using a cursor and a compound light microscope (at 150X mounted with a camera lucida). The system was interfaced with a Zenith Data System ZVM-1380-C computer; summary statistics for perimeter data were compiled as a feature of the software. In most cases, 25 true to nearly true cross sections of tubules were selected for quantification. Because epididymal tubules vary regionally, tubules were chosen primarily within the most columnar region of the epididymis. In addition, tubule epithelial height was measured with a compound light microscope (at 400X) with the aid of an ocular micrometer.

In females the diameter (to the nearest 0.1 mm) and number of vitellogenic ova were recorded along with the number of oviductal eggs. Measurements were taken with vernier calipers or with an ocular micrometer and dissecting microscope.

Voucher specimens and prepared histological slides are deposited in the Arkansas State Univeristy Herpetology Museum. Additional museum specimens examined during the study were from the Milwaukee Public Museum, University of Kansas Museum of Natural History, and the Carnegie Museum. Specimens examined from these museums that were catalogued without a day of collection were not included on any figure warranting an exact date. All descriptive statistics are given as means $\pm$ two standard error (2SE). Parametric (least square regression) and nonparametric tests (Mann-Whitney rank sum test) were employed; an alpha level of 0.05 was set.

Results

***Testicular Cycle in* Eumeces anthracinus pluvialis *and Comparisons with* Eumeces fasciatus.**--Evaluation of the testicular histology of *E. a. pluvialis* revealed seven of the eight spermatogenic stages (stage 4 not observed). At the onset of seasonal activity in early February, seminiferous tubules were in stage 3 (Fig. 1B); the secondary spermatocytes appeared scattered along the luminal margins and were only one or two cell layers in thickness. Average seminiferous tubule perimeters were nearly twice the size as seen in stage 2 tubles (found in only one specimen in October); this dramatic increase in volume was a consequence of a gain in luminal size rather than an increase in tubule epithelial height which had remained relatively unchanged (Table 1). Spermiogenesis (stages 5 and 6) occurred from late February to late April at the same time seminiferous tubles had reached their maximum perimeter size. During stage 5, large numbers of nutritive Sertoli cells were evident throughout the germinal epithelium (Fig. 1C). Stage 6 commenced as aggregates of transforming spermatids formed pyramid-like clusters about the Sertoli cells (Fig. 1D), whereas loosely-packed sperm formed masses inside lumina. At these two stages, the epididymal tubule epithelial height had doubled in thickness over stage 3 (Fig. 2C, D; Table 1) in preparation for receiving sperm. Spermatocytogenesis did not appear to continue beyond stage 6; this resulted in a decrease by over 50% in the height of the germinal epithelium from stage 6 to stage 7. Accordingly, there was a marked decrease (37%) in the average size of seminiferous tubules (Fig. 2A). Epididymal tubules had also reached their maximum size during stage 6. Most testes were in either stage 7 or 8 by mid-April, although some sperm were still being released from the germinal epithelium

during stage 7. The spent testis (stage 8) was characteristically devoid of all sperm within the seminiferous as well as the epididymal tubules (Fig. 2B, F). Cellular debris could be found within lumina in either case. The germinal epithelium exhibited one or two layers of cells, commonly known as the germinal-Sertoli cell syncytium, and had a height equal to less than 20% of its maximal thickness at stage 5. Interstitial cells with highly eosinophilic cytoplasms resided conspicuously between adjacent seminiferous tubules. The epididymal tubules, as stated above, undergo a cyclicity in volume and epithelial height similar to that experienced by the seminiferous tubules (Table 1; Fig. 2C-F). When sperm were present, the epithelium changed from irregular low columnar cells in stage 3 (Fig. 2C) to tall cells with basal nuclei (Fig. 2D). As these secretory columnar cells lost their integrity by providing nourishment (exocytosis?) or support (possibly in conjunction with extracellular tubules; see Newton and Trauth, 1992) prior to ejaculation, the epithelium became hetermorphic, less uniform, and was depleted of cytoplasmic materials (Fig. 2E). Consequently, sperm masses within the tubules often appeared eosinophilic as a result of these added cellular constituents following staining with H & E. At stage 8, the columnar epithelial cells appeared pseudostratified with greatly reduced cytoplasms.

Testicular histology of *E. fasciatus* (Fig. 3) conformed closely to that previously described for *E. a. pluvialis*. All eight spermatogenic stages were observed (Table 1; Fig. 3). Table 1 shows a morphometric comparison of the seminiferous and epididymal tubules of the two species.

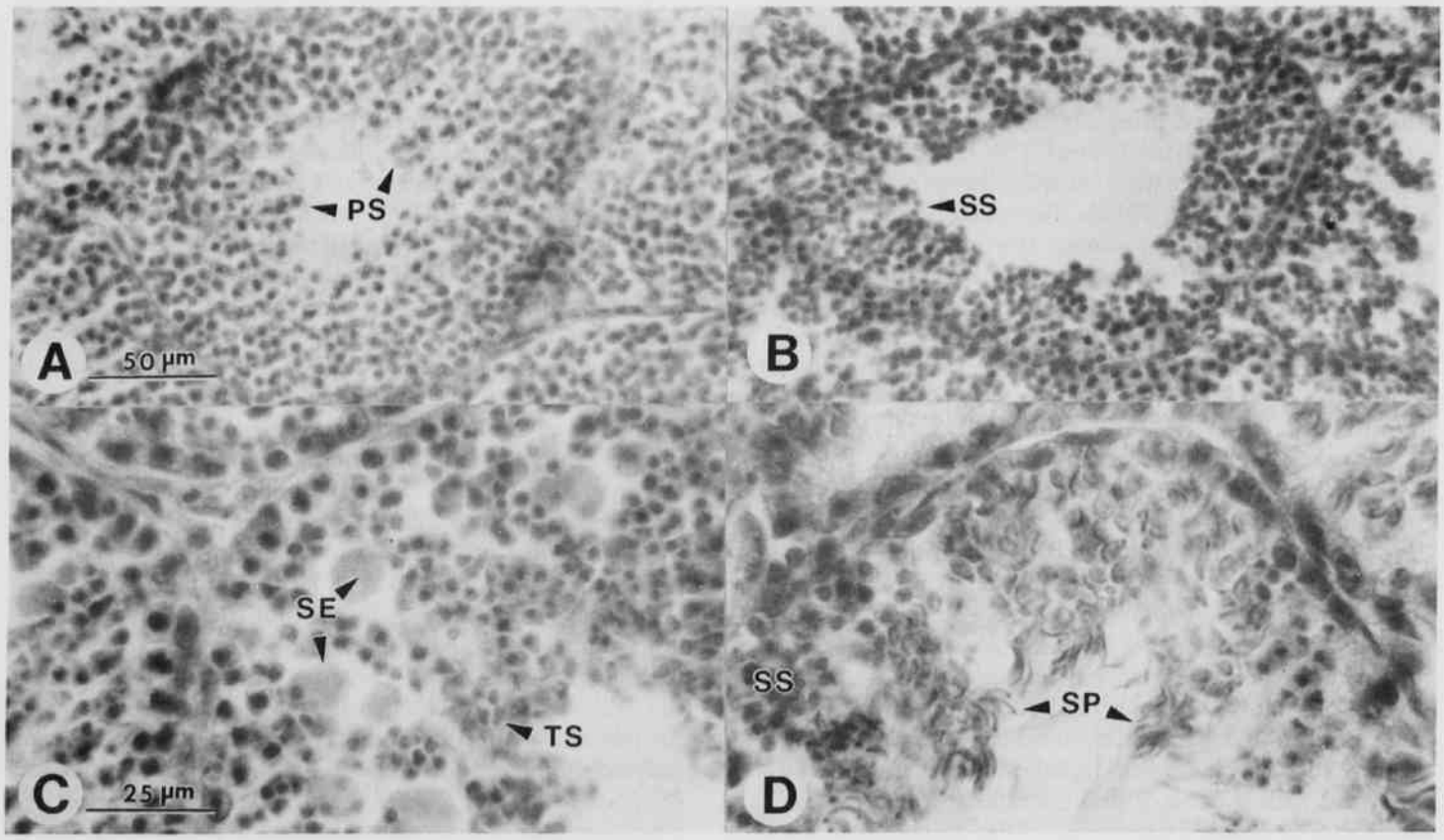

Fig. 1. Photomicrographs of seminiferous tubules of *Eumeces anthracinus pluvialis* collected in Arkansas. A. Section through a tubule illustrating stage 2 from specimen collected in October; PS = primary spermatocyte. B. Seminiferous tubule in stage 3 in early February; SS = secondary spermatocytes. C. Magnification of a tubule (stage 5) showing several nutritive (Sertoli) cells (SE) and transforming spermatids (TS) at the luminal margin. D. Portion of a tubule (stage 6) from a specimen collected in late March; SP = sperm. Scale lines in A and C also refer to B and D, respectively.

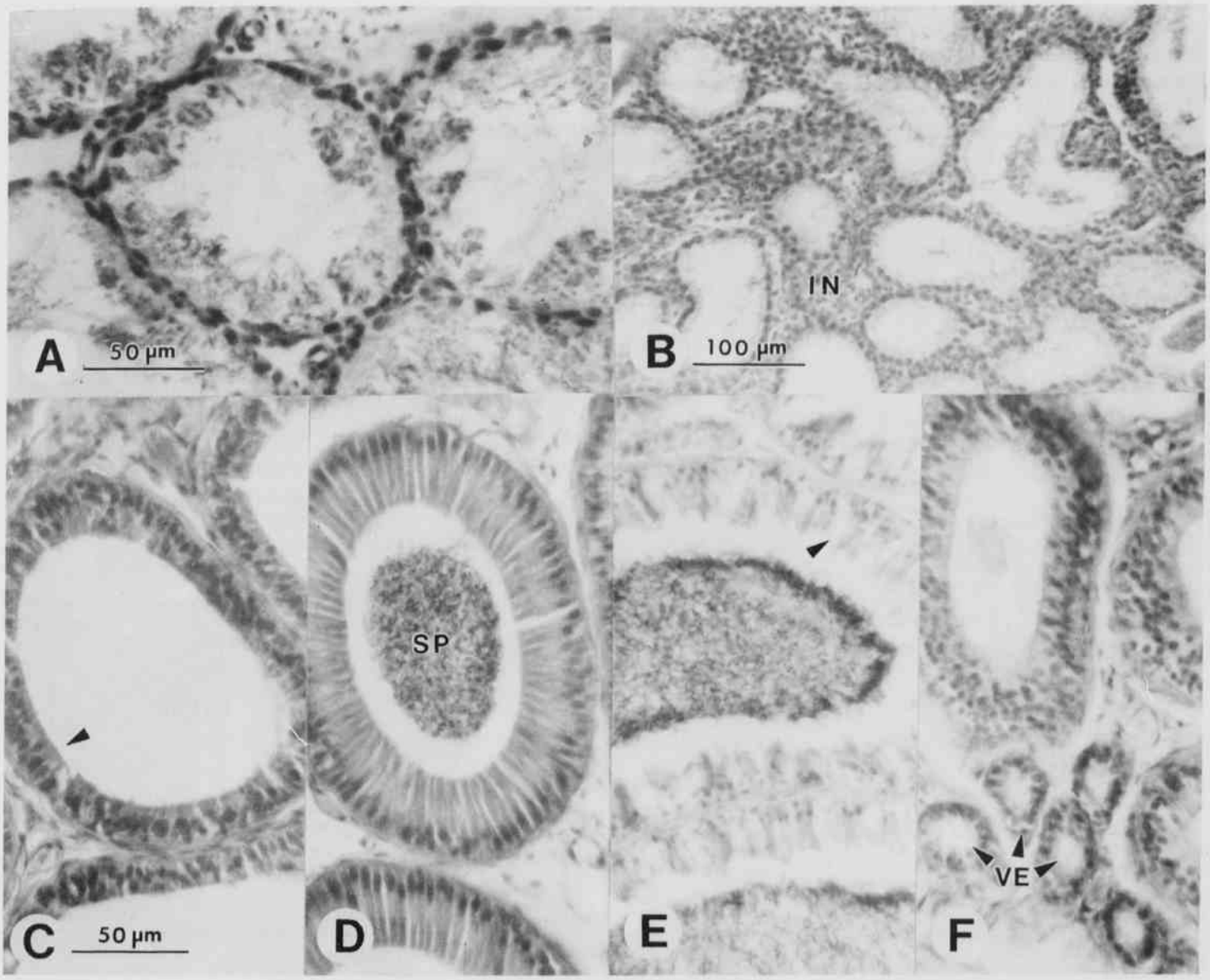

Fig. 2. Photomicrographs of seminiferous (A and B) and epididymal tubules (C-F) of *Eumeces anthracinus pluvialis* collected from Arkansas. A. Seminiferous tubules in stage 7 in late March specimen. B. Section showing completely-regressed testis in stage 8 (early April). Empty tubules are surrounded by interstitial cells (IN). C-F. Epididymal tubules showing cyclic nature of the columnar epithelial cells (arrows) from low (C) to tall (D) and then heteromorphic (E) to pseudostratified (F). See text for further explanations. VE = vas efferens. Scale line in C refers also to D-F.

There were some minor size differences between the two skinks when mean values (according to spermatogenic stages) were matched. In both species the maximum diameter of epididymal tubules was reached during stage 6. Major differences were apparent in the timing and duration of the testicular cycles between the two skinks. For example, Fig. 4 illustrates the degree of synchrony in spermatogenic stages between the two species. The time of sperm release from the testis (Stage 6) can be inferred as an approximation of the mating season for the species. Most male coal skinks exhibited stage 6 testes during March and April, whereas the same stage in five-lined

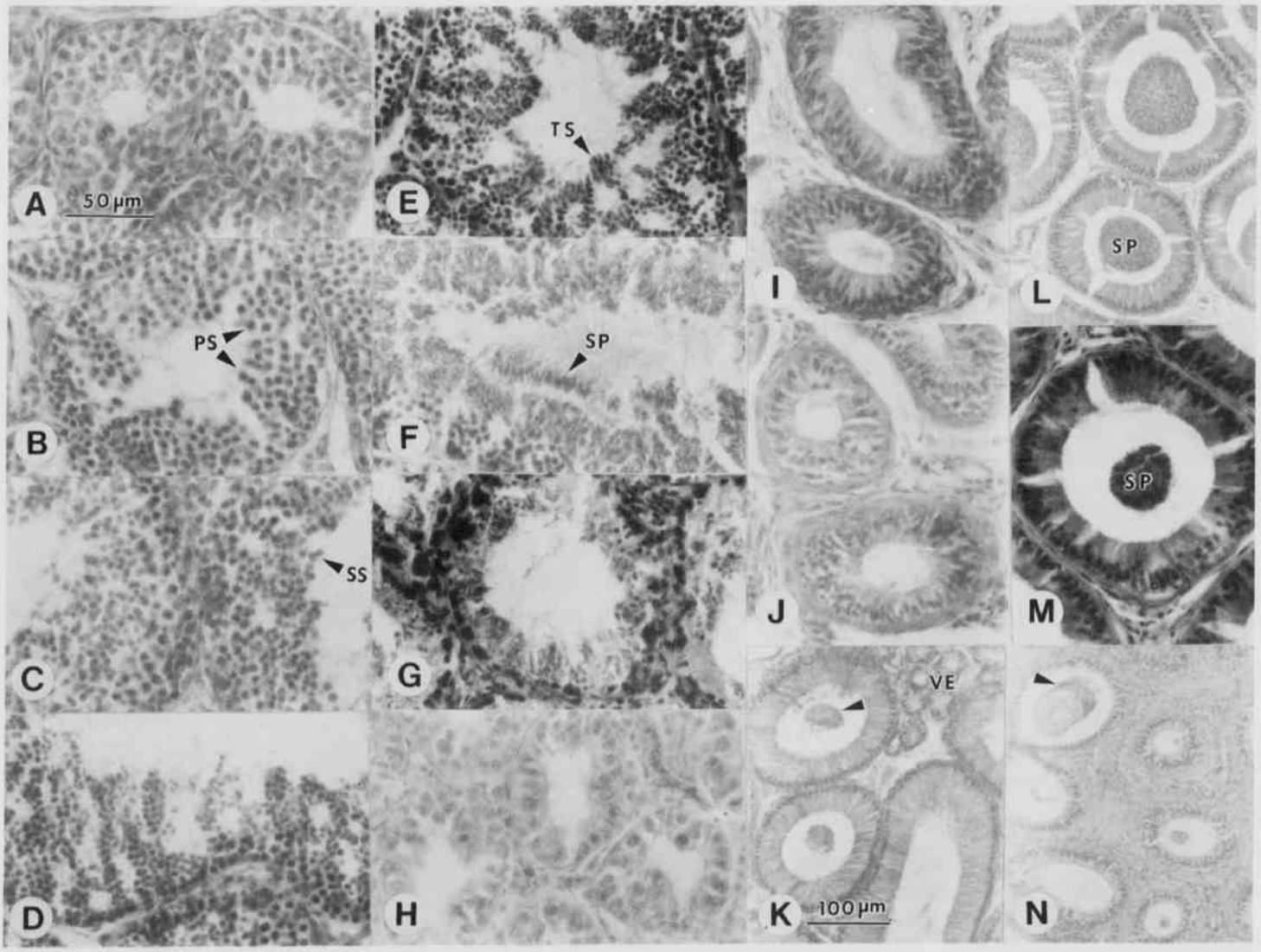

Fig. 3. Photomicrographs of seminiferous (A -H) and epididymal tubules (I - N) of *Eumeces fasciatus* collected in Arkansas. A- H. Spermatogenic stages 1-8, respectively; scale line in A the same for A-J, M; line in K the same for L and N. Abbreviations are the same as in Figs. 1 and 2. I-N. Spermatogenic stages corresponding to the epididymal tubules are: 2-I, 1-J, 5-K, 6-L, 6-M, and 7-N. See text for histological explanations.

skinks occurred in April and May. Animals entering overwintering retreats had testes in stage 2.

Fig. 4. Spermatogenic stages in *Eumeces anthracinus pluvialis* (small numerals) and *Eumeces fasciatus* (large numerals) as a function of body size (SVL) and date of collection. Asterisk denotes skink with and SVL of 50 mm exhibiting spermatogenic stage 5.

***Ovarian Cycle in* Eumeces anthracinus pluvialis *and Comparisons with* Eumeces fasciatus.**--Female *E. a. pluvialis* emerge from hibernation in northern Arkansas in early March with ovaries containing many white-to-opaque, non-vitellogenic ova. Vitellogenesis begins immediately thereafter; Fig. 5 shows the average diameter of vitellogenic ova for females ≥ 54 mm SVL (the approximate minimum adult size in females). The largest ova averaged 6.5 mm in diameter; vitellogenic ova require around one month to reach maximum size. No females had vitellogenic ova later than 29 April, whereas females had oviductal eggs as early as 9 April (Fig. 6). There was little size difference between females containing vitellogenic ova (60.0 ± 1.1 mm) and those containing oviductal eggs (56.0 ± 1.3 mm). The largest female with oviductal eggs measured 66 mm in SVL, and no ovigerous females were collected after mid-May. The ovarian cycle in this species lasted a little over two months. A common regression equation comparing all clutch size (CS) data and SVL was as follows: CS = 19.809 + 0.497SVL; a statistically significant positive relationship ($r = 0.53$; $P < 0.05$) was found between CS and SVL; this indicated that as SVL increased by 1.8 mm, there is a concurrent increase

Table 1. Dimensions (in μm) of seminiferous and epididymal tubules according to spermatogenic stage in *Eumeces anthracinus pluvialis* (above) followed by comparisons with *Eumeces fasciatus* (below).

Spermatogenic Stage	No. of Specimens	Seasonal Occurrence	Mean Perimeter ± 2SE		Mean Epithelial Height ± 2SE	
			Seminiferous Tubules	Epididymal Tubules	Seminiferous Tubules	Epididymal Tubules
1	-	-	-	-	-	-
2	1	October	194.2 ± 7.5 (159.1 - 231.4)	-	63.1 ± 7.3 (46.2 - 119.4)	-
3	2	February	393.1 ± 11.0 (337.2 - 452.8)	281.1 ± 11.9 (220.5 - 338.3)	51.8 ± 3.2 (38.5 - 65.4)	17.7 ± 12.6 (15.4 - 19.2)
4	-	-	-	-	-	-
5	2	February	441.4 ± 20.6 (312.7 - 529.6)	287.5 ± 8.6 (254.9 - 325.6)	65.4 ± 2.7 (57.8 - 73.2)	36.2 ± 2.1 (30.8 - 42.4)
6	8	Late February - Late April	423.8 ± 18.1 (334.9 - 536.8)	388.8 ± 18.1 (322.2 - 531.9)	61.3 ± 1.8 (50.0 - 65.4)	38.1 ± 1.8 (30.8 - 42.4)
7	3	Late March - Mid-April	271.2 ± 10.4 (223.2 - 338.8)	329.9 ± 8.3 (281.5 - 368.2)	28.3 ± 2.9 (19.2 - 42.4)	31.6 ± 3.2 (23.1 - 34.6)
8	2	Early April - Late April	180.2 ± 8.6 (148.6 - 242.3)	295.1 ± 13.8 240.6 - 338.7)	14.1 ± 1.0 (9.5 - 19.0)	20.7 ± 12.4 (15.2 - 26.6)
Eumeces fascitatus						
1	3	Mid-July - Late September	221.9 ± 9.7 (174.8 - 309.3)	169.6 ± 18.7 (136.6 - 197.6)	-	20.9 ± 2.3 (17.1 - 26.6)
2	4	Late August - Mid-March	360.3 ± 7.4 (292.6 - 404.6)	190.6 ± 6.6 (155.7 - 218.4)	-	21.9 ± 0.7 (19.0 - 24.7)
3	4	Mid-March - Mid-April	471.2 ± 17.3 (376.9 - 545.1)	241.1 ± 11.3 (196.7 - 288.7)	-	22.4 ± 0.9 (20.9 - 24.7)
4	1	-	-	-	-	33.2 ± 1.7 (30.4 - 34.2)
5	4	Late April - Early May	438.8 ± 10.3 (367/4 - 508.8)	323.4 ± 9.4 (272.7 - 374.8)	-	46.9 ± 2.1 (41.8 - 53.9)
6	5	Mid-April - Early June	484.1 ± 16.8 (389.9 - 600.3)	477.5 ± 18.0 (397.1 - 589.9)	-	50.5 ± 2.1 (38.5 - 57.8)
7	5	Late May - ?	263.6 ± 6.3 (230.6 - 304.3)	337.9 ± 12.9 (299.5 - 384.4)	-	37.2 ± 1.4 (34.6 - 42.4)
8	3	Early August - Late August	234.8 ± 13.0 (165.6 - 280.5)	295.1 ± 13.8 (240.6 - 338.7)	-	14.7 ± 1.8 (7.7 - 19.2)

of one in CS. By subjecting the regression residuals from the correlation to a Mann-Whitney rank sum test (to provide a size-free comparison), no statistically significant difference (T = 325; $P = 0.313$) was found between CS as estimated using females with vitellogenic follicles ($\bar{x}$ = 10.5 ± 1.2; 5-17; n = 27) and CS as determined with oviductal eggs ($\bar{x}$ = 9.6 ± 0.7; 8-13; n = 21). The average CS using both methods was 10.1 ± 1.6 (5-17; n = 43). Nevertheless, the coefficient of determination ($r^2 = 0.28$) predicts that only 28% of the variability in CS is explained by its linear relationship to SVL.

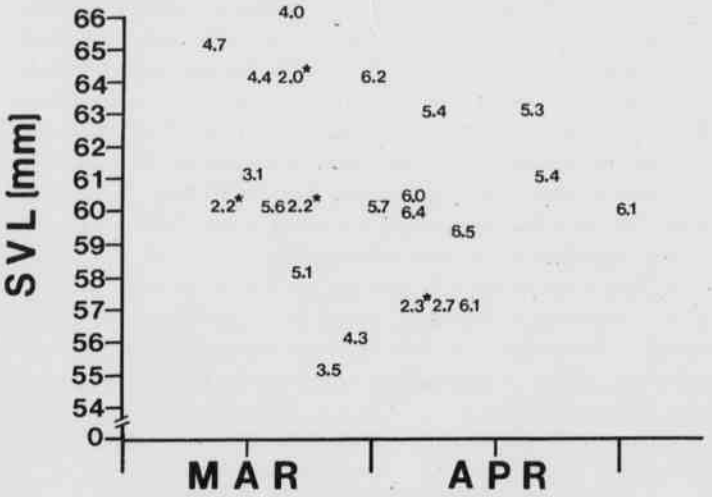

Fig. 5. Average diameter of vitellogenic ova per female as shown as a function of body size (SVL) and date of collection in *Eumeces anthracinus pluvialis* from Arkansas. Asterisk denotes females with a majority of non-vitellogenic ova.

The ovarian cycle of *E. fasciatus* is illustrated in Fig. 7. Female *E. fasciatus* emerge from overwintering dens sometime in March in northern Arkansas; however, ovarian enlargement does not accelerate for nearly a month. A dramatic increase in vitellogenic activity occurred in late April, especially in older females. No females contained vitellogenic ova later than mid-June. Minimal adult body size was estimated to be 60 mm in SVL; no female was larger than 69 mm in SVL. Ovulation commenced by mid-May in females of all sizes. One ovigerous female (60 mm in SVL) was captured on 19 June. Clutch size based on counts of vitellogenic ova averaged 10.0 ± 0.7 (7 -15; n = 34), whereas CS based upon counts of oviductal eggs averaged 8.4 ± 1.0 (6-12; n = 13). A significant positive correlation (r = 0.51; $P < 0.01$) was found between CS (using vitellogenic ova) and SVL, and a regression equation, CS = 13.8660 + 0.3763SVL, was calculated. This relationship predicts that for every increase of 3.1 mm in SVL, there is a concordant gain of one in CS. Atretic ovarian follicles (AOF) were observed in several females with enlarged vitellogenic ova. For example, a female (65 mm in SVL collected 14 April) whose 12 ova averaged 2.4 mm in diameter exhibited 5 AOF. The difference between the two estimates of CS may be the result of AOF. Egg clutches (n = 5; 7-10; $\bar{x}$ = 8.2) accompanied by brooding females were discovered under rocks and inside of rotting logs from early June to early July. The grand mean CS found by combining counts based upon oviductal eggs and laid eggs averaged 8.3 ± 0.8. In this case the correlation between CS and SVL (r = 0.49; $P > 0.05$) was not significant.

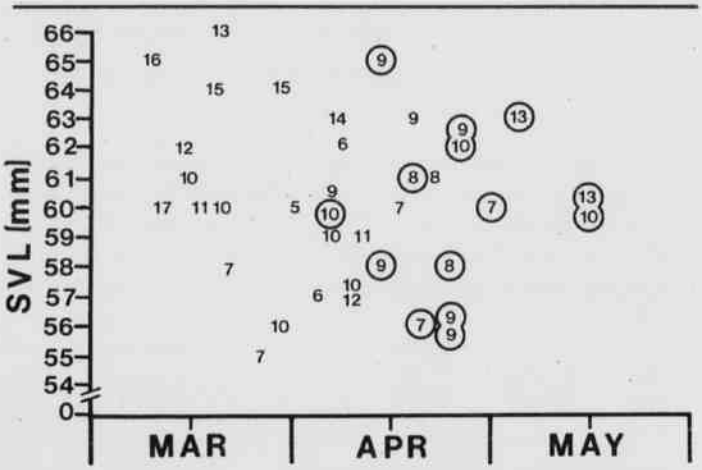

Fig. 6. Clutch size as a function of body size (SVL) and date of collection in *Eumeces anthracinus pluvialis* from Arkansas. Circled numerals represent counts of oviductal eggs and those without circles are counts of vitellogenic ova.

The major difference between the ovarian cycles of the two skink species was the timing of vitellogenesis. In *E. a. pluvialis* yolk deposition began by mid-March and extended until late April, whereas this process began in late April and extended until mid-June in *E. fasciatus*. Although both species differed in maximum adult body size (*E. fasciatus* being larger), the average CS of the two species was very similar.

Timing of the Reproductive Cycles.--Timing of critical reproductive events (i.e., vitellogenesis and spermiation) between sexes in these species was concordant. In *E. a. pluvialis*, the synchrony between vitellogenesis in females and sperm production in males lasted from early March to late April. In *E. fasciatus*, these events occurred from mid-April to mid-June. Consequently, the mating period between the two species overlapped marginally (see discussion).

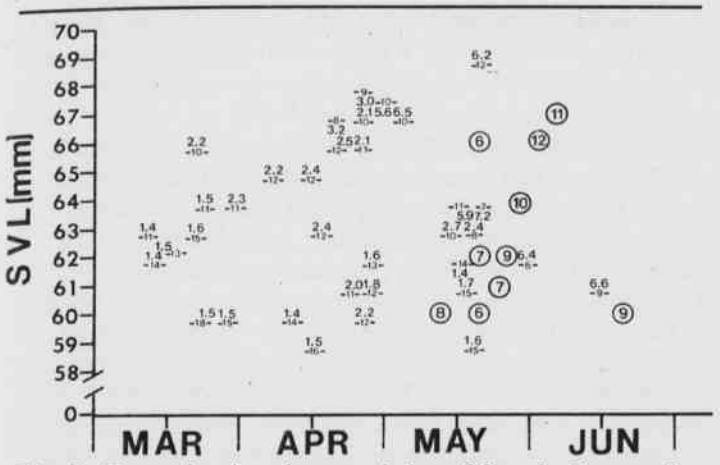

Fig. 7. Reproductive characteristics of female *Eumeces fasciatus* from Arkansas (samples selected from collections made from 1984 - 1993) as a function of body size and date of collection. Large numerals with decimals represent the average diameter of ovarian follicles per female and are matched with small numerals within dashes which represent the total number of ovarian follicles > 1.0 mm in diameter of each female. Circled numerals denote the number of oviductal eggs of individual females.

Discussion

Clutch size, time of mating, and oviposition are the best documented reproductive characteristics in *E. a. pluvialis*. In Missouri, Anderson (1965) mentioned a single clutch of 8 eggs laid on 27 May, and Sexton (1984) collected a clutch in the process of hatching on 7 July. Collins (1993) noted that clutches of from 8-11 eggs were laid between 21 and 23 June in Kansas. A clutch of five eggs was reported for northern Louisiana (Dundee and Rossman, 1989). Although no egg clutches of *E. a. pluvialis* were discovered during the present study, my data suggest that the month of May is the most likely time for oviposition to take place in Arkansas. Mount (1975) observed a pair of captive coal skinks copulating in March in Alabama; this observation would occur within the period of spermiation in Arkansas. Because of the paucity of reproductive data on this species, other authors (e.g., Johnson, 1987) have presumed that reproduction in this species was comparable to *E. fasciatus*, or they reported its reproduction using published data outside of a localized geographic region. In fact only the stages of the ovarian and testicular cycles in *E. a. pluvialis* closely resemble those of *E. fasciatus*.

The reproductive characteristics in *E. fasciatus* have been reported from many parts of its range (Reynolds, 1943; Fitch, 1970, 1985; Sexton, 1984; Vitt and Cooper, 1986; Shadrix et al., 1994). Reynolds (1943) presented histological stages of the testicular cycle for *Eumeces fasciatus* from several states; however, he divided the cycle according to monthly intervals rather than spermatogenic stages and probably included other *Eumeces* species in his analysis. Both the present study and that of Reynolds indicated that May was the primary month for spermiation and that seminiferous and epididymal tubules reached their maximum diameter during May. An average CS of 8.4 (6-10; n = 6) was given for females from Oklahoma and Arkansas by Fitch (1985); a recent report for Oklahoma (Shadrix et al., 1994) included a CS averaging 10.8 (7-14; n = 10) in females 55 - 70 mm in SVL. In South Carolina, Vitt and Cooper (1986) reported a CS of 8.6 (6-11; n = 7) in females 60 - 70 mm in SVL. In 24 females (65 - 70 mm in SVL) from Kansas, the average CS was 8.2 (Fitch, 1970). These estimates are similar to the 8.3 eggs per clutch for Arkansas females of comparable size. In general, older and larger females produce more eggs than younger and smaller females (Fitch, 1954; Vitt and Cooper, 1986), although the correlation between CS (using oviductal and laid eggs) was not significant in neither the Arkansas sample (n = 18) nor the South Carolina sample (n = 28).

As a rule, synchronization of male and female reproductive cycles occurs in most oviparous lizard species (e.g., see Shrank and Ballinger, 1973; Trauth, 1979); yet, there are some exceptions within viviparous species in montane regions in which females will store sperm for several months (Mendex de la Cruz et al., 1988) prior to fertilization. This phenomenon may even occur in some *Eumeces* (Guillette, 1983) which have an asynchronous cycle, where timing of fertilization occurs soon after ovulation (or, in effect, after copulation), and sperm storage is not utilized or is of little importance. Male *E. a. pluvialis* are reaching maximal production of sperm in March, whereas male *E. fasciatus* are reaching this peak in May. There are numerous advantages to synchronization of courtship and mating with to ovulation. The ovigerous period (Figs. 6 and 7) in the present study tends to match the peak in spermiation (Fig. 4) for both species and, thus, illustrates a maximizing of reproductive efficiency.

In conclusion, it is apparent that the timing and duration of the reproductive season in *E. a. pluvialis* differ markedly from that of *E. fasciatus*. Moreover, the peak in breeding condition and sexual activity in each species appears to be highly synchronized for both sexes. This peak showed little interspecific overlap at the level of species groups. Males of species within *Eumeces* of the *fasciatus* group can discriminate cloacal ordors (via tongue-flicking behavior) between conspecifics (and heterospecifics) and can identify sexual receptivity (Cooper and Vitt, 1986). Under normal circumstances, interspecific aggression in *Eumeces* occurs infrequently (Vitt and Cooper, 1986). Evolutionary differences in behavior, microhabitat preferences, and activity may restrict social

contact between these skinks in Arkansas; however, at present, any social or competitive interactions between the two species remain to be determined in Arkansas.

Acknowledgements

I wish to express my appreciation to the numerous students and colleagues who participated in collecting trips or provided field assistance in obtaining specimens. In particular, I thank Brian P. Butterfield, Phyllis Chaffin, Robert L. Cox, Jr., Betty G. Cochran, Anthony Holt, David H. Jamieson, Chris T. McAllister, Walter E. Meshaka, David A. Saugey, and J.D. Wilhide. I am also grateful to the curatorial staffs at the Milwaukee Public Museum, University of Kansas Museum of Natural History, and the Carnegie Museum for the loan of specimens. Partial funding for this work was provided by research grants from the Arkansas Game and Fish Commission during 1988 and 1989. Permits for scientific collection were provided by the Arkansas Game and Fish Commission. The critical comments by three anonymous reviewers greatly improved the manuscript.

Literature Cited

Anderson, P. 1965. The reptiles of Missouri. Univ. Missouri Press, Columbia, xxxiii + 330 pp.

Collins, J.T. 1993. Amphibians and reptiles in Kansas. 3rd. ed. Univ. Kansas Mus. Nat. Hist. Publ. Edu. Ser. No. 13:1-397.

Conant, R. and **J.T. Collins.** 1991. A field guide to reptiles and amphibians of eastern and central North America. Houghton Mifflin Co., Boston, 450 pp.

Cooper, W.E., Jr. and **L.J. Vitt.** 1986. Interspecific odour discriminations among syntopic congeners in scincid lizards (genus *Eumeces*). Behaviour 97:1-9.

Dundee, H.A. and **D.A. Rossman.** 1989. The amphibians and reptiles of Louisiana. Louisiana State Univ. Press, Baton Rouge, xi + 300 pp.

Fitch, H.S. 1954. Life history and ecology of the five-lined skink, *Eumeces fasciatus*. Univ. Kansas Publ. Mus. Nat. Hist. 8:1-156.

Fitch, H.S. 1970. Reproductive cycles in lizards and snakes. Univ. Kansas Mus. Nat. Hist. Misc. Publ. No. 52, 247 pp.

Fitch, H.S. 1985. Variation in clutch and litter size in New World reptiles. Univ. Kansas Mus. Nat. Hist. Misc. Publ. No. 76, 76 pp.

Guillette, L. J., Jr. 1983. Notes concerning the reproduction of the montane skink, *Eumeces copei*. J. Herpetol. 17:144-148.

Johnson, T.R. 1987. The amphibians and reptiles of Missouri. Missouri Dept. Cons., Jefferson City, 368 pp.

Mayhew, W.W. and **S.J. Wright.** 1970. Seasonal changes in testicular histology of three species of the lizard genus *Uma*. J. Morphol. 130:163-186.

Mendez de la Cruz, F.R., L.J. Guillette, Jr., M.V. Santa Cruz and **G. Casas-Andreu.** 1988. Reproductive and fat body cycles of the viviparous lizards, *Sceloporus mucronatus* (Sauria: Igunaidae). J. Herpetol. 22:1-12.

Mount, R.H. 1975. The reptiles and amphibians of Alabama. Auburn Univ. Agri. Exp. Sta., Auburn, 347 pp.

Newton, W.D. and **S.E. Trauth.** 1992. Ultrastucture of the spermatozoon of the lizard *Cnemidophorus sexlineatus* (Sauria: Teiidae). Herpetologica 48:330-343.

Reynolds, A.E. 1943. The normal seasonal reproductive cycle in the male *Eumeces fasciatus* together with some observations on the effect of castration and hormone administration. J. Morph. 72:331-377.

Schrank, G.D. and **R.E. Ballinger.** 1973. Male reproductive cycles in two species of lizards (*Cophosaurus texanus* and *Cnemidophorus gularis*). Herpetologica 29:289-293.

Sexton, O.J. 1984. Life history notes on the terrestrial vertebrates inhabiting some glades of eastern Missouri with emphasis on amphibians and reptiles. Missouri Acad. Sci. Occas. Pap. 7:21-65.

Shadrix, C.A., D.R. Crotzer, S.L. McKinney and **J.R. Stewart.** 1994. Embryonic growth and calcium mobilization in oviposited eggs of the scincid lizard, *Eumeces fasciatus.* Copeia 1994:493-498.

Smith, H.M. 1946. Handbook of lizards. Comstock Publ. Co., Ithaca, New York, xiv + 557 pp.

Trauth, S.E. 1979. Testicular cycle and timing of reproduction in the collard lizard (*Crotaphytus collaris*) in Arkansas. Herpetologica 35:184-192.

Vitt, L.J. and **W.E. Cooper, Jr.** 1986. Skink reproduction and sexual dimorphism: *Eumeces fasciatus* in the south eastern United States, with notes on *Eumeces inexpectatus*. J. Herpetol. 20:65-76.

Zug, G.R. 1993. Herpetology: an introductory biology of amphibians and reptiles. Academic Press Inc., San Diego, California, xv + 527 pp.

Use of Visual and Tactile Behaviors by Rats (*Rattus norvegicus*) in an Object Discrimination Swimming Task

Todd Wiebers
Department of Psychology
Henderson State University
Arkadelphia, AR 71999

Abstract

When challenged with a cognitive task, rats demonstrate a behavioral fexibility in use and preference of sensory modalities. The present study describes visual and tactile behaviors used by rats in a two choice object discrimination swimming task. The task was designed to preclude use of other sensory modalities and could not be solved via spatial strategies. Fourteen rats learned to criterion a series of 10 discrimination problems. Rats exhibited three stereotypic visual and two stereotypic tactile behaviors over the course of the study. Data analyses indicated that rats demonstrated these behaviors more frequently as they became more familiar with the task. However, once they became proficient, a significant increase in tactile behaviors paralleled a significant decrease in visual behaviors. Reports on the use of visual and tactile behaviors by wild rats are discussed to help interpret the laboratory data from an evolutionary perspective.

Introduction

When exploring the cognitive abilities of animals in a laboratory setting, it is imperative that psychologists be sensitive to specific behaviors and sensory processes of the species under investigation (Lorenz, 1952; Breland and Breland, 1961; Bolles, 1970). From this perspective, the present report describes the development of a swimming task designed to assess the ability of Norway rats to form a learning set concept via use of visual and tactile behaviors. Behavioral procedures from a previous study are presented to familiarize the reader with our task, and then a recent experiment is presented that quantifies the use of visual and tactile behaviors by rats over the course of the learning process. Results are discussed relative to the use of these sensory behaviors by wild rats.

In the psychological literature, learning set is considered a cognitive, conceptual type of learning in which animals demonstrate an increase in performance across a series of novel discrimination problems (Harlow, 1949; Warren, 1965; Schrier, 1984). Mammals such as apes, monkeys, cats, and dogs have demonstrated such learning, as have certain species of birds. Similar studies with rats show them quite capable when challenged with olfactory, gustatory, auditory, or spatial discriminations. However, numerous attempt to demonstrate visual discrimination learning sets have not been conclusive, and few data are available for tactile discriminations (for review, see Wiebers, 1992). Thus, our original objective was to design an object discrimination task for rats that might be more conducive to their use of visual and tactile sensory modalities.

In designing our task, we opted to use a large circular watering trough for our testing arena because rats are known to be natural swimmers (Barnett, 1975; Morris, 1981). Moreover, while rats are motivated to find a way out of water, this procedure is far less invasive than traditional motivational methods such as shock or food deprivation. During learning, our rats would be started at one end of the pool, on the other side of which were two visible objects (plastic or metal junk objects of varying size, form, and luminance). These objects were affixed to underwater escape platforms. If a correct choice was made, the animal could displace the object and escape from the water. Conversely, the platforms and objects could be lowerd below the surface of the water if an incorrect choice was made, thus forcing the animal to continue swimming. The task could not be solved via spatial strategies, and precautions were taken to preclude use of any sensory modalities except visual and tactile processes. Wiebers (1992) provides methodology for controlling use of auditory and olfactory cues in our swimming task.

Our original study used a learning to criterion procedure in which rats learned a total of 51 novel discrimination problems. Rats learned at their own pace, and while there were admittedly individual differences in performance, group performance was significantly above chance, thus suggesting evidence of a learning set concept using visual and tactile behaviors. However, two other findings of the original study are particularly relevant to the current report. First, certain problems proved to be of inherently low, moderate, or high difficulty regardless of when they were encountered during the

learning process. We identified three respective difficulty clusters of five problems each, via data analyses and four decision rules. Second, rats consistently demonstrated three stereotypic tactile behaviors over the course of the study. These sensory behaviors are the focus of the following experiment and will be discussed as they relate to the learning process and also to the behaviors of wild rats.

Materials and Methods

Fourteen adult male Long Evans hooded rats were used. From the time of weaning, they were group housed and received frequent social interaction sessions with humans and each other as part of an inter- and intra-species socialization process. Rats always had food and water available and received a variety of foods in addition to the standard Purina chow diet.

A general overview of the swimming task has already been given in introducing this paper. For a detailed description of the apparatus and specific procedures, see Wiebers and Hothersall (1994). For purposes of this report, only a few design issues are of particular importance. First, this study was conducted in two phases. In the first phase, rats were randomly assigned to one of two groups, Low Difficulty (LD rats) and High Difficulty (HD rats). During this learning phase, LD and HD rats received five low or high difficulty problems, respectively. For the second learning phase, all rats received five identical moderate difficulty problems. Animals proceeded at their own pace and were required to make 10 correct choices out of 12 trials during a single day's session before moving on to their next problem.

The second design issue is critical to this paper and involves the observation and recording of stereotypic visual and tactile behaviors. Five specific behaviors, with the first three being visual and the last two being tactile, were defined as follows:

1) VTEs (Vicarious Trial & Errors) – en route to the platforms, the rat exhibits a multiple series of head turns directed at each of the two objects (Tolman, 1948).
2) VEERs – the rat begins his approach directly toward one platform and then makes a sharp body turn in the direction of the opposite platform.
3) SPINs – en route to the platforms, the rat stops in the water, does a compact, full, body spin and then resumes his approach.
4) PUSH AWAYs – upon arrival at a platform, the rat pushes off the underwater platform and/or object with his front paws.
5) LEAPs – upon arrival at a platform, the rat pushes off the underwater platform (possibly making body contact with the object) with his rear paws and proceeds to the other platform – often, becoming completely airborne.

These behaviors were observed consistently in our original study and were demonstrated by all of the rats. However, individual rats tended to have preferred behaviors. It should be noted that these behaviors were regularly observed on both correct and incorrect trials. These behaviors were operationally defined prior to data collection in the current experiment and were recorded systematically as they occurred.

Results

All rats successfully solved their respective 10 problems. Figure 1 depicts sessions to criterion for LS and HD rats (i.e., number of sessions needed to attain at least 10 correct choices within a single session). While there are several interesting results that could be discussed from a psychological learning perspective, it is sufficient for the reader to note the learning curve demonstrated by the HD rats. Since their significant decrease in sessions to criterion across the first five problems was not attributable to decreasing problem difficulty, these rats clearly demonstrated a learning set concept using visual and tactile behaviors. However, the primary focus of this paper is the use of these behaviors by rats in our task.

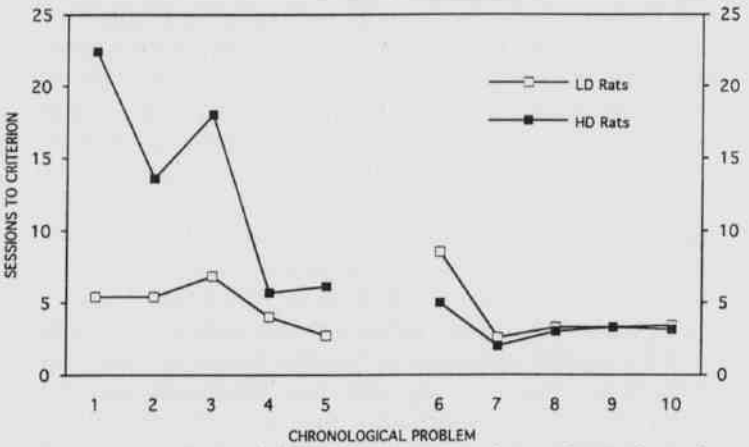

Fig. 1. Sessions to criterion across chronological problem.

All rats exhibited the five stereotypic behaviors over the course of the study, and no new or novel behaviors were observed. Percent of trials in which the behaviors were observed was used as a dependent measure for analysis. Visual and tactile data were initially analyzed separately. For each modality, a between/within (group by chronological problem) ANOVA was conducted for each of the two learning phases. In each modality analysis, no

differences were detected between LD and HD rats in either learning phase, nor were there any significant interaction effects. However, significant effects were detected for prevalence of both visual and tactile behaviors across chronological problems in both learning phases. Use of both visual and tactile behaviors significantly increased during the first learning phase, F (4, 48) = 3.52, P <.02 and F (4, 48) = 5.65, P <.001, respectively. Curiously during the second learning phase, a significant decrease in visual behaviors, F (4, 48) = 3.83, P <.01, contrasted with a continued significant increase in tactile behaviors, F (4, 48) = 3.19, P <.02.

Given the lack of any differences between LD and HD rats with regard to use of visual and tactile behaviors in our task, we thought it interesting to directly compare the utilization of these sensory behaviors by rats over the course of learning. In so doing, we used the data from all 14 rats and conducted two-factor repeated measures ANOVAs for the two learning phases, specifically sensory modality by chronological problem. Figure 2 depicts percent of trials in which visual and tactile behaviors were observed across the two learning phases. During the first learning phase, a significant effect of sensory modality indicated that rats were relying on visual behaviors to a greater extent than tactile behaviros, F (1, 13) = 4.76, P<.05. In addition, a significant effect of chronological problem reflected a steady increase in use of both sensory behaviors, F (4, 52) = 10.89, P <.001. For the second learning phase, the only significant effect was an interaction between sensory modality and chronological problem, F (4, 52) = 4.75, P <.01. As can be seen in Fig. 2, this finding is particularly interesting because it indicates that once rats became proficient in our learning task, a continued preference for tactile behaviors coincided with a significant decrease in visual behaviors.

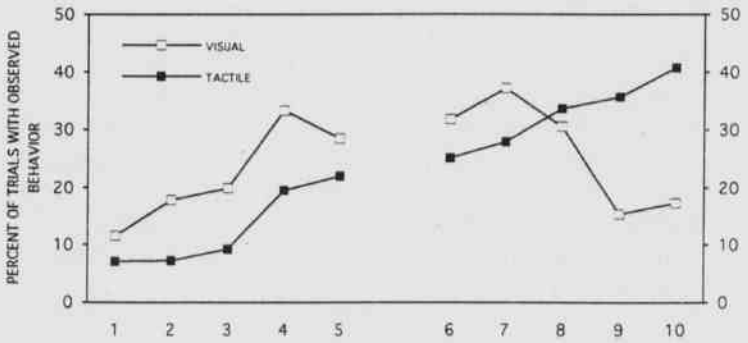

Fig. 2. Percent of visual and tactile behaviors observed across chronological problem.

Discussion

We have described a laboratory situation which requires Norway rats to utilize visual and tactile sensory modalities in solving a cognitive discrimination task. These data provide evidence that rats exhibit a certain behavioral flexibility when conditions require them to do so. In psychological learning theory, rats are often described as olfactory or spatially oriented animals, and are often profiled as having notoriously poor visual systems. Moreover, they are often lauded as having well developed auditory systems and extremely sensitive vibrissae for spatial detection; yet little attention is given to their ability for object manipulation. While there are valid reasons for such contentions, our study has provided evidence that visual and tactile modalities in rats are probably better developed than is generally acknowledged. We can further develop our case by addressing behaviors of both new and old world rats under natural conditions. Whereas wild rats have occasion to rely on visual and tactile behaviors for survival, we might expect laboratory rats to share a similar behavioral repertoire.

As exemplars of new and old world rats, let us use the wood rat (*Neotoma floridana*) and Norway rat (*Rattus norvegicus*), respectively. First, consider predator situations when visual behaviors might be necessary for survival. As a wild rat, visually detecting the silhouette of an appoaching raptor in the absence of olfactory, auditory, or spatial warning signals could be a matter of utmost significance (McFarland, 1985). Moreover, many predators will approach their prey from down wind, suggesting a rat being hunted must rely primarily on auditory and visual simuli. Additional examples might include the need to visually seek out shelter when confronted with an unexpected emergency encounter in a strange locale. These are certainly realistic situations for rats in rural communities. It is easy to imagine numerous other situations encountered by the often more urbanized Norway rat whose primary predators are humans.

Tactile behaviors and object manipulations are also of survival value for wild rats. Consider rats living along the banks of the Po River in Italy. Part of their food acquisition involves diving to the bottom of the river and retrieving molluscs (Galef, 1980). These animals are certainly using tactile and perhaps visual behaviors in their efforts. Also, Twigg (1975) describes a "search grasp" behavior used by rats, wherein they sift dirty or muddy water through their hands in hopes of finding morsels of food.

Another aspect of object manipulation involves the nest building behavior of wood rats, perhaps better known as pack or trade rats. These rats are continually bringing objects back to their nest sites, supposedly to reinforce their homes. However, if they happen to wander through your campsite, they will readily leave a hand-

some stick or stone in trade for your shiny new Swiss army knife or pocket watch (Caras, 1967). Wild Norway rats are also known for their knack of collecting seemingly useless objects, though they do not construct the elaborate nests of their new world counterparts (Barnett, 1975). Three possible explanations may be given for these types of behaviors in wild rats. Perhaps object manipulation is reminiscent of what has been called their "hoarding instinct", though Barnett (1975) argues against such a simple explanation. Another thought is that while wood rats might have a legitimate use for objects in nest building, this analogous behavior in Norway rats may have become a vestigial behavior after their liaison with *Homo sapiens*. Finally, Renner (1988) argues that exploratory behavior is of critical survival value in rats, and furthermore, this behavior not only consists of movements through space, but also tactile manipulations of novel inanimate objects. Approaches to objects vary between laboratory and wild rats, but nevertheless, object manipulation appears a necessary behavioral component (Dewsbury and Rethlingshafer, 1973).

Having discussed the significance of visual and tactile behaviors by wild rats, we can draw the following conclusions from the laboratory data presented in this paper. First, we suggest that if animal behaviorists observe depressed performance by their rats in learning tasks requiring visual and tactile modalities, they should be cautious in attributing such data to poorly developed sensory processes. Rather, they might consider that the task was not properly designed with regard to the rat's behavioral and biological repertoire. Second, our data suggest that rats probably have a preferential hierarchy with regard to use of their sensory modalities. For example, rats in our study demonstrated a significant preference for use of tactile behaviors once they became proficient at the task. Thus, they will exhibit a behavioral flexibility in adapting to various environmental demands. Finally, it would be interesting to explore whether wild rats in natural aquatic situations exhibit the stereotypic behaviors observed in our study. Perhaps some or all of these behaviors might not only be task specific, but species specific as well.

Acknowledgements

I would like to thank David Hothersall of The Ohio State University, and Marian Breland Bailey and Michael D. Murphy of Henderson State University for helping with various stages of the manuscript preparation.

Literature Cited

Barnett, S.A. 1975. The rat: A study in behavior. University of Chicago Press, Chicago, 318 pp.

Bolles, R.C. 1970. Species-specific defense reactions and avoidance learning. Psych. Rev. 77:32-48.

Breland, K. and **M. Breland.** 1961. The misbehavior of organisms. Amer. Psych. 16:681-684.

Caras, R.A. 1967. North American mammals. Galahad Books, New York, 578 pp.

Dewsbury, D.A. and **D.A. Rethlingshafer.** 1973. Comparative psychology: A modern survey. McGraw-Hill, New York, 625 pp.

Galef, B.G., Jr. 1980. Diving for food: Analysis of a possible case of social learning in wild rats (Rattus norvegicus). J. Comp. Physio. Psych. 94:416-425.

Harlow, H.F. 1949. The formation of learning sets. Psych. Rev. 56:51-65.

Lorenz, K.Z. 1952. King Solomon's ring. Harper and Row, New York, 225 pp.

McFarland, D. 1985. Animal behavior: Psychobiology, ethology, and evolution. Benjamin/Cummings, Menlo Park, 576 pp.

Morris, R.G.M. 1981. Spatial localization does not require the presence of local cues. Learn. Motiv. 12:239-260.

Renner, M.J. 1988. Learning during exploration: The role of behavioral topography during exploration in determining subsequent adaptive behavior. Intern. J. Comp. Psych. 2:43-56.

Schrier, A.M. 1984. Learning how to learn: The significance and current status of learning set formation. Primates, 25:95-102.

Tolman, E.C. 1948. Cognitive maps in rats and men. Psych. Rev. 55:189-209.

Twigg, G. 1975. The brown rat. Latimer Trend, Great Britain, 150 pp.

Warren, J.M. 1965. Primate learning in comparative perspective. Pp. 249-281 in Behavior of nonhuman primates (Vol. 1) (A.M. Schrier, H.F. Harlow, and F. Stollnitz, eds.) Academic Press, New York, 285 pp.

Wiebers, T. 1992. Object quality learning set: Further evidence for the cognitive capacities of *Rattus norvegicus*. University Microfilms Inc., Ann Arbor, 83 pp.

Wiebers, T. and **D. Hothersall.** 1994. Object quality learning set in rats (*Rattus norvegicus*). HSU Academic Forum, 11:90-109.

Monte Carlo Simulation of The Scintillating Optical Fiber Calorimeter (SOFCAL)

Zibin Yang, Russell Gillum and Donald C. Wold
Department of Physics and Astronomy
University of Arkansas at Little Rock
Little Rock, AR 72204

Abstract

A scintillating optical fiber calorimeter (SOFCAL) is being developed by NASA/Marshall Space Flight Center for use in balloon-borne emulsion chambers to study the spectrum of high-energy cosmic rays and gamma rays. SOFCAL will not saturate for long exposures, and the detector will be helpful for the study of primary cosmic-ray nuclei energies from 100 GeV to 1,000 TeV. For a given incident particle and energy, computer simulations of electromagnetic cascades allow computation of energy deposited in different regions of the calorimeter. For these initial simulations, a 5-cm x 5-cm x 7-cm calorimeter was used. Each subsection contained a 0.4-cm thick lead plate or two 0.2-cm lead plates and two layers of optical fibers, 90° to each other. There were 100 square fibers in a layer, and the length of an edge was 0.5 mm. For incident gamma ray energies of 0.5 to 1.5 TeV, the energy deposited in each layer of fibers was computed. Due to the limited dynamic range of the imaging electronics, a window for the energy deposition (ΣE_γ) in the fibers was explored to determine the best measure of energy deposition in the calorimeter.

Introduction

The Monte Carlo method in GEANT (CERN, 1992a) was used to simulate the photon and electron events in the Scintillating Optical Fiber Calorimeter (SOFCAL), which is under development at NASA/Marshall Space Flight Center for future applications in cosmic ray and gamma ray measurements.

Emulsion chambers employing calorimeters have been used for direct measurements of cosmic-ray composition (protons through Fe) between 10^{12} and 10^{15} eV using balloon-borne emulsion chambers (Kaplon et al., 1952; Minakawa et al., 1958; Niu et al., 1971; Burnett et al., 1986; Burnett et al., 1987; Parnell et al., 1989; Burnett et al., 1990; Asakamori et al., 1991). The emulsion chamber shown in Fig. 1 is composed of four parts: (1) a charge-determination module, (2) a target module with ~0.2 vertical interaction mean free paths for protons, (3) a spacer module, and (4) an emulsion calorimeter module with about fourteen vertical radiation lengths. In one emulsion chamber (Burnett, et al., 1986), the thickness of each part was as follows: primary charge detector, 1.78 cm; target module, 15.92 cm; drift space, 12.08 cm; and calorimeter section, 6.30 cm. The thickness was measured along an axis perpendicular to the plates. The simulations described here are for a scintillation optical fiber counterpart to the calorimeter section in the emulsion chamber.

The part of the primary energy going into gamma-rays, ΣE_γ, is the parameter most easily related to the primary cosmic ray spectrum in emulsion chamber experiments. The ability to measure energies of electron-photon cascades is one of the most important functions of the calorimeter. Following an interaction above or in the top of the calorimeter, a fraction of the total primary energy (5 - 25% of the energy released depending on impact parameters and atomic mass numbers of the colliding nuclei), will be deposited in the calorimeter in the form of photon energy, ΣE_γ. The photons originating from an interaction will develop individual electromagnetic cascades in the calorimeter. For these simulations, a calorimeter module with ten vertical radiation length of Pb was used. In the geometrical configuration shown in Fig. 2, each subsection of the calorimeter consisted of a 4-mm lead block, 100 square fibers (each 0.5-mm thick) in the x-direction and 100 square fibers (each 0.5-mm thick) in the y-direction. In these initial simulations, this lead and optical fiber combination was repeated fourteen times.

Materials and Methods

The Monte Carlo Method in GEANT.--GEANT and PAW (CERN, 1992b) are a system of detector description and simulation tools developed by CERN. The Monte Carlo simulations, which used GEANT Version 3.21, were done on DEC 5000 workstations. The principal application of GEANT in High Energy Physics are (1) the track-

Charge Detector: Measure Z by δ ray counting in emulsions and etch pit size in CR39.
Target: Interaction probability ~ 0.2 for protons and ~ 0.9 for iron nuclei.
Spacer: Primary fragments
- Produce $\pi^{\pm}$, and
- Gamma rays from π^0 decay spread out so they may be measured individually.
- θ (typical) = 2×10^{-3} radians at 10^{12} eV/amu.

Calorimeter: Gamma rays produce
- Copious $e^{\pm}$, γ's in lead.
- Number of $e^{\pm}$ counted in emulsions or X ray film.
- Optical density measured = ΣE_{γ} .

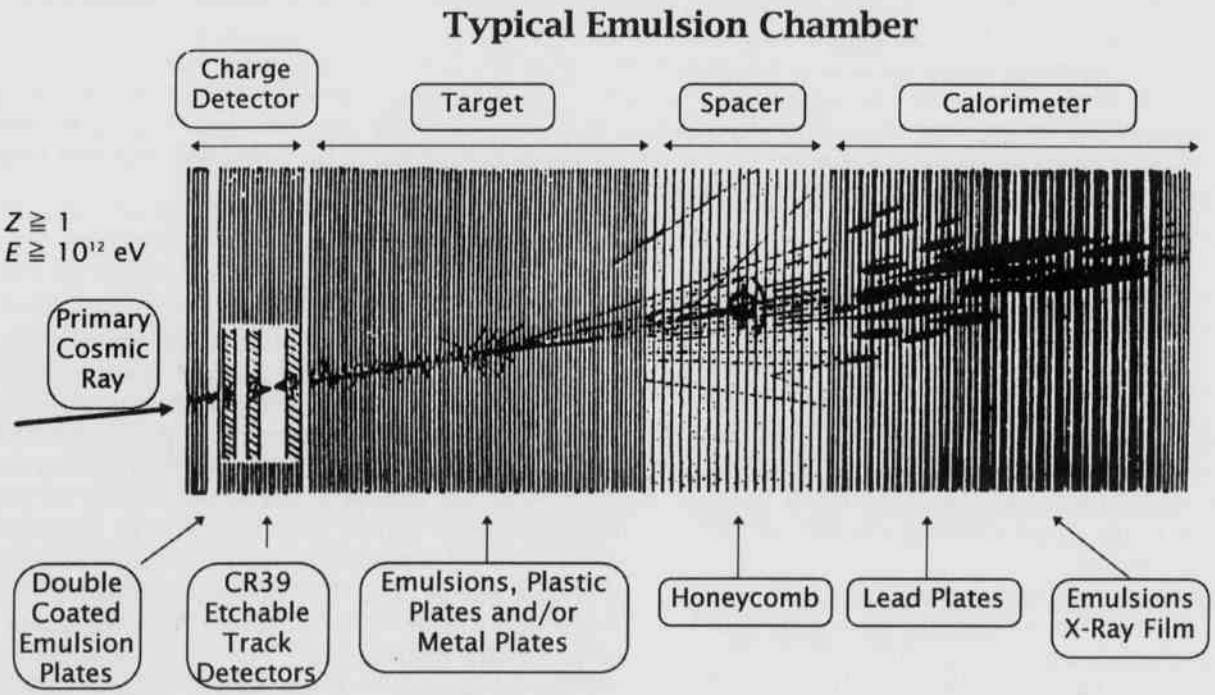

Fig. 1. Schematic diagram of an emulsion chamber.

ing of particles through an experimental setup for simulation of detector response, and (2) the graphical representation of the setup and of the particle trajectories. These two are often combined interactively in simulations.

The methods in these simulations include the following steps:

(1) ***Describe an experimental setup using geometry setup routines.*** The setup is represented by a structure of geometrical volumes. Each volume is given a medium number by the user. Different volumes may have the same medium number. A medium is defined by the so-called tracking medium parameters, which include reference to the material filling the volume.

(2) ***Accept events simulated by standard Monte Carlo generators.*** The Monte Carlo method is based on a statistical theorem which says that the distribution of a Cumulative Distribution Function is uniform. So random seeds generated by a random number generator (uniform) can be used to calculate events in a certain distribution. GEANT is interfaced with the event generator, FRITIOF. This Monte Carol program (Lönnblad, 1992) simulates events of hadron-hadron, hadron-nucleus, or nucleus-nucleus collisions at high energies.

(3) ***Simulate the transport of particles through the various***

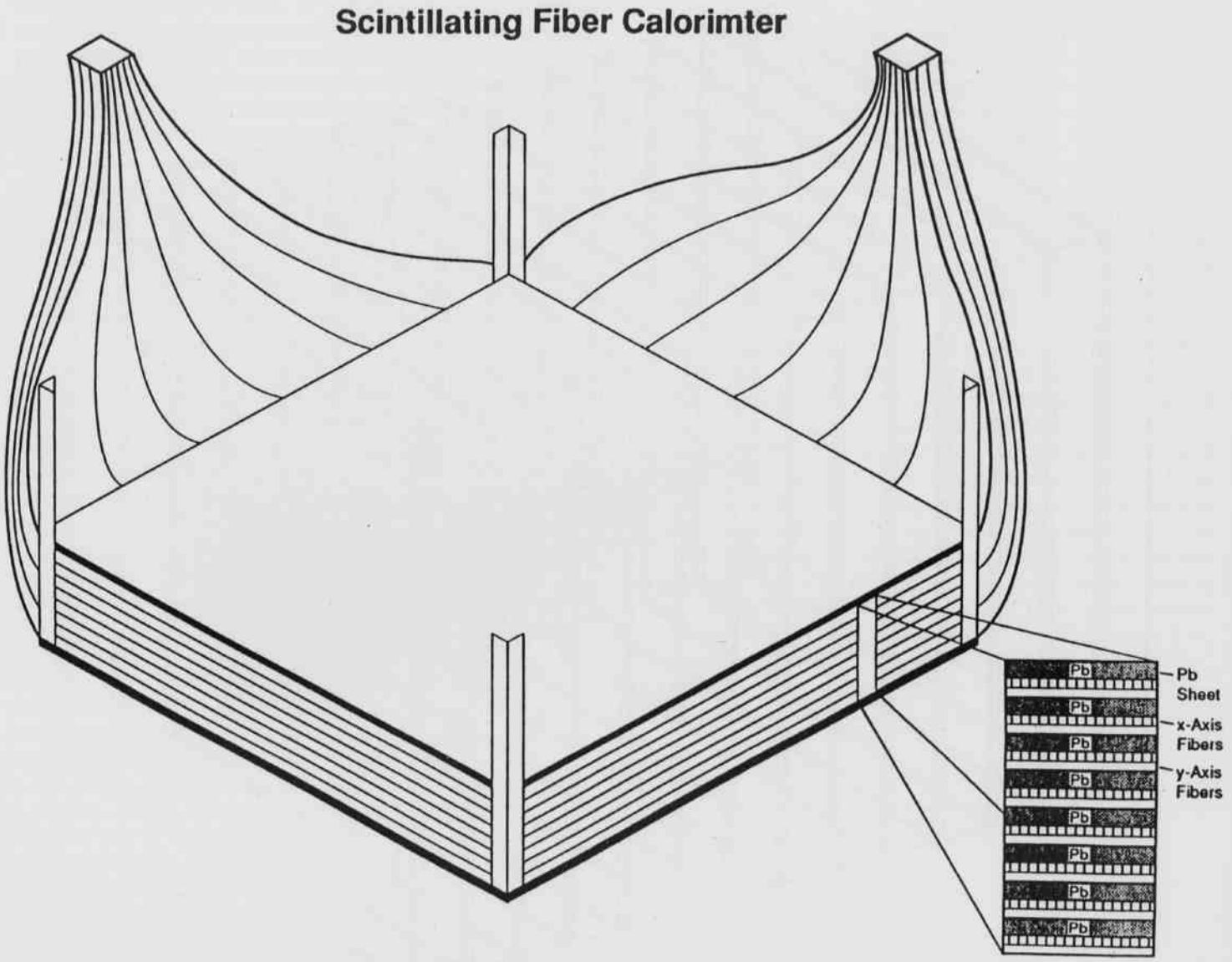

Fig. 2. Geometry of Scintillating Fiber Calorimeter (SOFCAL).

regions of the setup. GEANT can take into account the interactions of these particles with the matter and the boundary of the setup. GEANT is able to simulate the dominant processes which can occur in the energy range from 10 kV up to 10 TeV.

(4) ***Record elements of the particle trajectories and the response from the sensitive detectors.***

(5) ***Visualize the detectors and the particle trajectories.***

The Monte Carlo Program for SOFCAL Simulations (SOFCALS).--The process of optimization requires frequent design changes, so users should be able to change the geometry easily. The time required to modify GEANT programs containing geometry information about the detector can be enormous. Therefore a subroutine was developed to read in the geometrical configuration from a separate file in an ASCII format. This subroutine reads not only detector setup, but also other parameters needed for the simulation such as tracking medium parameters. The data are stored and later used for computing energy deposited by each particle in the cascade (Fig. 3) which was initially produced by a gamma ray.

Energy deposition is calculated from the lowest level geometry. Total energy deposition is integrated using step functions. When a threshold is imposed due to limi-

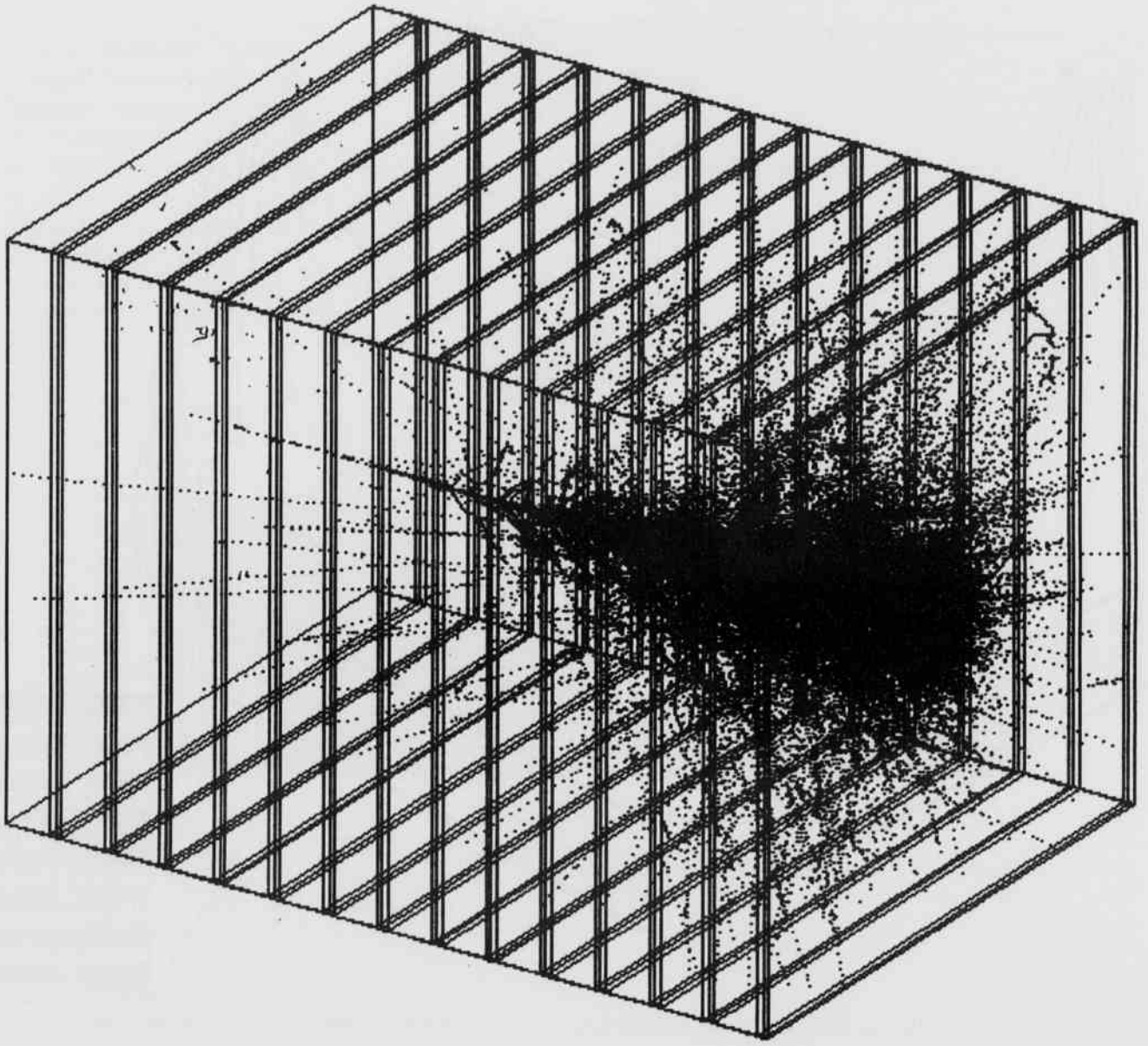

Fig. 3. The trajectories of a photon event with energy of 0.1 TeV.

tations in the electronic read out devices, then the measured energy is less than the energy actually deposited in each fiber. The program SOFCALS has interactive routines which are called to draw the trajectories of an individual gamma ray event.

Results

Energy Deposition Transition Curve and the Shower Event.--The typical detector (emulsion chamber) shown in Fig. 1 has a "target section" and "calorimeter section" designed for measuring produced charged particles and gamma rays, respectively. The target section includes many layers of nuclear emulsion plates to measure the charge of the incident particle and the emission angles of

the produced charged particles with high accuracy (0.01 mrad). The spacer section is a drift space that permits closely collimated gamma rays from an upstream vertex to diverge from each other before cascade development in the downstream calorimeter. The calorimeter includes layers of nuclear emulsion and X-ray film among lead plates to measure the electron distributions from the electromagnetic cascades initiated by gamma rays from π^0 decay. The calorimeter is used to measure the spectrum of energy deposition ΣE_γ from which the primary energy spectrum is derived.

It is difficult to measure the momenta of produced charged particles in emulsion chambers. However gamma rays from the π^0 decay are observed in the calorimeter and the emitted angles and energies can be measured individually if they are well separated. For high multiplicity events, they overlap in the forward region.

The incident energy of the cosmic ray projectile is not measured directly, but it can be estimated from the total gamma ray energy. The angular distribution and energy distribution of gamma rays from each π^0 decay are needed. Isospin symmetry is assumed so the number of π^0s which decay into pairs of gamma rays is about half that of the charged π mesons.

Figure 3 illustrates the cascade of electrons and photons produced by an incoming gamma ray with incident energy of 0.1 TeV. Figure 4 shows the energy deposited in each x-layer of fibers as a function of distance through the calorimeter. The incident particle is a gamma-ray with energies of 0.5, 1.0, and 1.5 TeV. The three curves are based on ten events each.

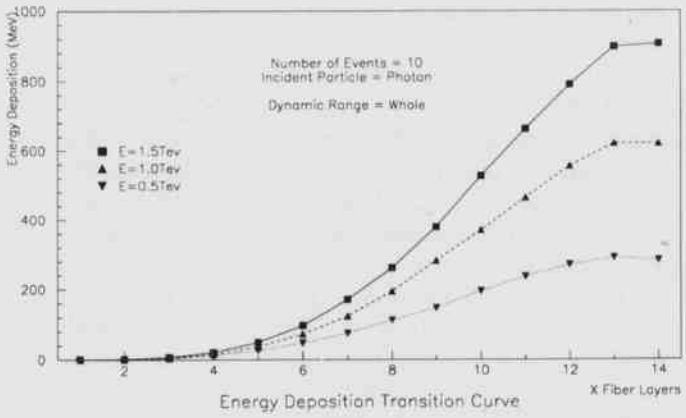

Fig. 4. The energy transition curve of a photon with energies of 0.5 TeV, 1 TeV, and 1.5 TeV.

Discussion

In these simulations of gamma rays incident on the SOFCAL detector, the direction of the incoming photon lies along the z-axis which is normal to the plane of each lead plate and layer of fibers. The energy transition curves show the energy deposited in each layer of optical fibers. They are used to determine parameter settings of the data acquisition devices.

The dynamic range is one limitation of the output image intensifier CCD electronics. Typical devices are limited to a dynamic range of approximately 256. For example, if the threshold energy is set to 1 MeV, then the highest energy which can be measured is only 256 MeV. Due to this limitation, a specific threshold and window may be needed to optimize the measurements. For these initial simulations of SOFCAL, a dynamic range of 100 was used. In Fig. 5, a threshold of 2 MeV appears to be optimal. Figures 5 to 8 show that the 2-MeV to 200-MeV range differentiates between gamma ray energies from 0.5 to 1.5 TeV better than other ranges. These figures should be compared with the energy deposition curve in Fig. 4, for which no threshold or range limitation has been imposed. For simulations of the primary cosmic rays, calculations must be performed with event generators, such as FRITIOF, to predict the distributions in ΣE_γ and then use GEANT for associated optimum "window" settings.

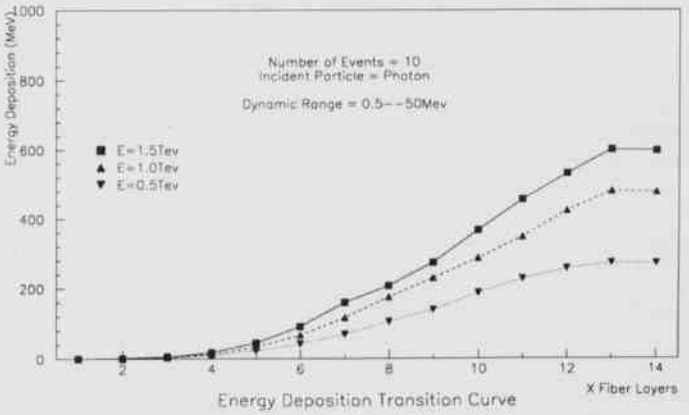

Fig. 5. The energy transition curves of photons with different energies. The dynamic range is 0.5 MeV to 50 MeV.

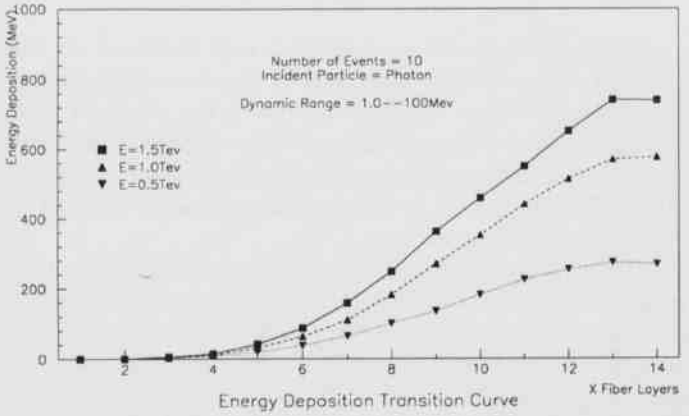

Fig. 6. The energy transition curves of photons with different energies. The dynamic range is 1 MeV to 100 MeV.

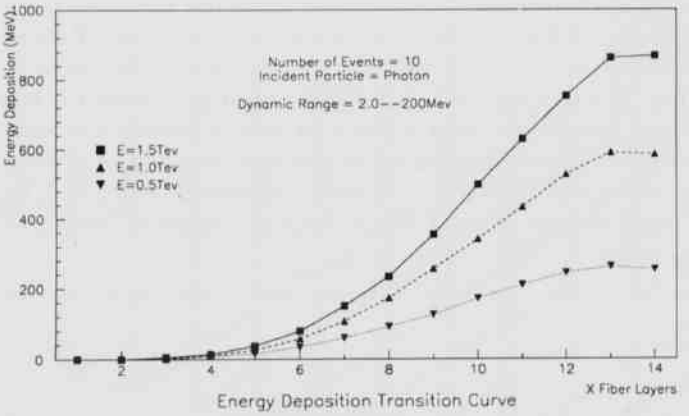

Fig. 7. The energy transition curves of photons with different energies. The dynamic range is 2 MeV to 200 MeV.

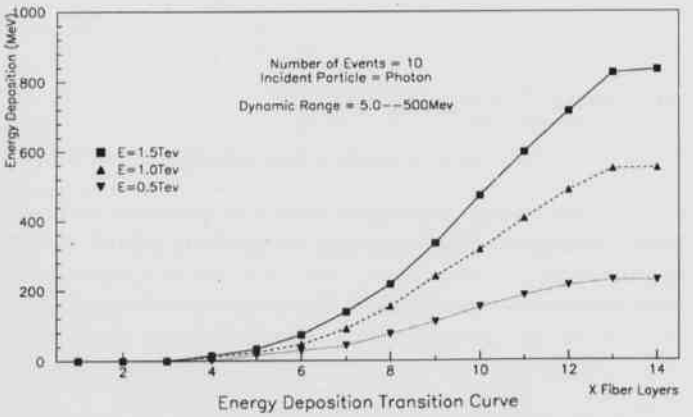

Fig. 8. The energy transition curves of photons with different energies. The dynamic range is 5 MeV to 500 MeV.

Acknowledgements

The authors acknowledge the help of colleagues at the NASA George C. Marshall Space Flight Center, Huntsville, Alabama and the University of Arkansas at Little Rock. Dr. Thomas A. Parnell, Dr. Geoffrey N. Pendleton, and Ms. F. Ellen Roberts generously gave the authors valuable support. Mr. Charles Byrd and Ms. Christine Byrd installed GEANT on the DEC-5000 workstations, while Dr. Marcus D. Gabriel and Mr. Lon Jones III maintained the workstations. This work was supported in part by NASA and funding for the project was provided by the NASA/University Joint Venture (JOVE) Program.

Literature Cited

Asakamori, K., T.H. Burnett, M.L. Cherry, M.J. Christl, S. Dake, J.H Derrickson, W.F. Fountain, M. Fuki, J.C. Gregory, T. Hayashi, R. Holynski, J. Iwai, A. Iyono, W.V. Jones, A. Jurak, J.J. Lord, O. Miyamura, H. Oda, T. Ogata, T.A. Parnell, F.E. Roberts, S. Strausz, Y. Takahashi, T. Tominaga, J.W. Watts, J.P. Wefel, B. Wilczynska, H. Wilczynski, R.J. Wilkes, W. Wolter and **B. Wosiek.** 1991. Energy spectra and composition of cosmic rays above 1 TeV per nucleon. Proc. 22nd Internat. Cosmic Ray Conf. (Dublin). 2:57-60.

Burnett, T.H., S. Dake, M. Fuki, J.C. Gregory, T. Hayashi, R. Holynski, J. Iwai, W.V. Jones, A. Jurak, J.J. Lord, O. Miyamura, H. Oda, T. Ogata, T.A. Parnell, T. Saito, T. Tabuki, Y. Takahashi, T. Tominga, J.W. Watts, B. Wilczynska, R.J. Wilkes, W. Wolter and **B. Wosiek.** 1986. JACEE emulsion chambers for studying the energy spectra of high energy cosmic ray protons and helium. Nucl. Instr. Meth. A251:583-595.

Burnett, T.H. S. Dake, J.H. Derrickson, W.F. Fountain, M. Fuki, J.C. Gregory, T. Hayashi, T. Hayashi, R. Holynski, J. Iwai, W.V. Jones, A. Jurak, J.J. Lord, C.A. Meegan, O. Miyamura, H. Oda, T. Ogata, T.A. Parnell, F.E. Roberts, T. Saito, S. Strausz, T. Tabuki, Y. Takahashi, T. Tominaga, J.W. Watts, B. Wilczynska, R.J. Wilkes, W. Wolter and **B. Wosiek.** 1987. Nucleus-nucleus interactions between 20 and 65 GeV per nucleon. Phys. Rev. D. 35:824-832.

Burnett, T.H. S. Dake, J.H. Derrickson, W.F. Fountain, M. Fuki, J.C. Gregory, T. Hayashi, R. Holynski, J. Iwai, W.V. Jones, A. Jurak, J.J. Lord, O. Miyamura, H. Oda, T. Ogata, T.A. Parnell, F.E. Roberts, S. Strausz, T. Tabuki, Y. Takahashi, T. Tominaga, J.W. Watts, J.P. Wefel, B. Wilczynska, H. Wilczynski, R.J. Wilkes, W. Wolter and **B. Wosiek.** 1990. Energy spectra of cosmic rays above 1 TeV per nucleon. Ap.J.

349:L25-L28.

CERN. 1992a. GEANT3 User's Guide. Internal Report CERN Data Division. CERN Program Library Office, CERN-CN, CH-1211 Geneva 23, Switzerland.

CERN. 1992b. PAW Physics Analysis Workstation. CERN Program Library Long Write-up Q121. CERN Geneva, Switzerland.

Kaplon, M.F., B. Peters, H.L. Reynolds and **D.M. Ritson.** 1952. The energy spectrum of primary cosmic radiation. Phys. Rev. 85:295-309.

Lönnblad, L. 1992. Status of the MC++ event generator toolkit. Proceedings of the International Conference on Computing in High Energy Physics '92. Proceedings (CERN 92-07), Annecy, France, 21-25 Sept. 1992 (Geneve, Switzerland: CERN 1992), p. 531-4.

Minakawa, O., S. Hasegawa, M. Tsuzki, Y. Nishimura, H. Yamanouchi, H. Aizu, H. Hasegawa, Y. Ishii, S. Tokunaga, K. Nishikawa, K. Imaeda, M. Kazuno, H. Mori, Y. Fujimoto, J. Nishimura and K. Niu. 1958. Studies on transverse momenta of high-energy jets with emulsion cloud chambers. Nuovo Cimento Suppl. 8:761-9.

Niu, K., E. Mikumo and **Y. Maeda.** 1971. A possible decay in flight of a new type of particle. Prog. Theor. Phys. 46:1644-6.

Parnell, T.A., T.H. Burnett, S. Dake, J.H. Derrickson, W.F. Fountain, M. Fuki, J.C. Gregory, T. Hayashi, R. Holynski, J. Iwai, W.V. Jones, A. Jurak, J.J. Lord, O. Miyamura, H. Oda, T. Ogata, T.A. Parnell, F.E. Roberts, S. Strausz, T. Tabuki, Y. Takahashi, T. Tominaga, J.W. Watts, J.P. Wefel, B. Wilczynska, H. Wilczynski, R.J. Wilkes, W. Wolter and **B. Wosiek.** 1989. in Proc, COSPAR 1988, Direct measurement of the composition and spectra of cosmic rays above 1 TeV/amu from JACEE. Adv. Space Res. 9:45-54 (JACEE Collaboration).

Takahashi, Y., S. Miyaji, T.A. Parnell, M.C. Weisskopf, T. Hayashi and **K. Nomoto.** 1986. Enhancement of high-energy cosmic ray spectrum by type-II super novae. Nature. 321: 839-841.

Sex Ratio and Success, an Assessment of *Lindera melissifolia* in Arkansas

Robert D. Wright
68 Crestview Road
Conway, AR 72032

Abstract

Lindera melissifolia pondberry, is a federally endangered dioecious shrub found in Arkansas and four other southeastern states. Although by far the greatest area exists in Arkansas, it is broken into numerous small single-sex clones concentrated in two locations. Several stands have been lost during the 1980's according to records of the Arkansas Natural Heritage Commission. Even casual observation reveals that there are more males than females. This suggests dependence on vegetative reproduction, with possible bias against females. This paper reports on work investigating this suggestion. It was found that a 7:1 bias in area covered favors males. Poor survival of seedlings and transplants indicates that only apomictic reproduction is successful. Females allocate 45 times more resources to reproduction than males. Stem dieback occurs in both sexes but regrowth is vigorous. Shoot moisture stress and response of net photosynthesis and conductance favor growth of males.

Introduction

Dioecious plant species, in order to maintain sex ratios balanced near 1:1, must be able to compensate for the reproductive resource allocation devoted to production of fruits by females (Lloyd, 1974). In the shrubby New Zealand species *Hebe subalpina* females produce greater numbers of leaves early in the season (Delph, 1990). Leaves of female *Simmondsia chinensis* in the deserts of California and Baja California store more water, female plants allocate a greater proportion of growth resources to leaves, and females have a more open growth form. This results in females having enhanced potential for photosynthesis (Wallace and Rundel, 1979). In five wind-pollinated species of various growth forms in northern Utah, males predominate on xeric microsites and females on moister sites, thus minimizing competition between the sexes (Freeman et al., 1976). In *Lindera benzoin*, a close taxonomic and ecological relative of *Lindera melissifolia*, female growth and reproduction are favored in canopy gaps (Niesenbaum, 1992). In all the above dioecious species with the exception of *Lindera melissifolia*, sex ratios are 1:1.

Bias in sex ratios seems to be the exception among dioecious plants (Meagher, 1984). In one reported case, *Silene alba* populations in Massachusetts were female biased, especially in moister sites and at higher desities (Lovett Doust et al., 1987). *Acer negundo* populations showed a non-significant male bias, but there was no clear implication of reproductive resource allocation (Ramp and Stevenson, 1988).

Materials and Methods

Stand Characteristics.—In 1991 all the known stands of pondberry in Arkansas were surveyed. Each stand was found to be comprised of one or more single-sex groups of stems, referred to hereafter as clones. Limited excavation revealed stems to be connected by vigorous subsurface rhizones. This plus the single-sex grouping indicates that each clone is indeed a single biological individual. Occasionally isolated stems of one sex were found in a clone of the other sex, but usually clone boundaries were distinct. A number of clones were isolated from each other by distances of 10 to 100 m. Taken together, total area of all the known pondberry clones in Arkansas was 2.7 ha in 1991. Virtually all of this area was in two locations, one in the vicinity of Swifton in Lawrence County and the other northwest of Corning in Clay County. Although this survey revealed a number of previously unmapped clones, in 1992 additional clones were discovered in the vicinity of Swifton (Tom Foti, personal communication), but these additional clones are not covered in this paper. The clones known prior to 1992 are in 9 distinct stands: 3 in Clay County, 5 in Lawrence County, and a single clone in Woodruff County.

Based on census data taken during anthesis, area covered was biased toward males by a ratio of 7:1, with 86.7% male and 13.3% female. In several of the 9 stands there were only male plants. The stand with the greatest coverage of female plants had 42% females by area. Not only were female clones absent from some stands, they tended to be smaller than male clones in stands where both sexes were represented. There was a total of 42 female clones and 63 male clones, plus another 13 clones discovered after anthesis. Although no fruit was present

on these 13, they could conceivably have been females too far from males for pollination to occur, so they were assigned to neither sex. Thus of the number of clones sexed, the ratio was 1.5: 1.0 in favor of males. Clones that had been sexed in previous years (Wright 1989a, b) had not changed in sex or location.

Stem density varied widely from clone to clone, ranging between 44 and 0.8 stems per m^2, but no sex difference in density was apparent. Typical densities in robust clones were 10-15 stems per m^2. Highest densities were in clones recovering from ground fire the year before. Densities below 5 stems per m^2 were associated with some form of disturbance, which could include water levels too high or too low, or heavy interference from shrubs and vines where canopy removal had occurred. Canopy closure ranged from 0-100%, with closure of 75% or more where no recent disturbance had occurred. Shrub-vine interference ranged from 0-85% of clone area, and was typically under 25% where no recent disturbance to the canopy had occurred. Of the 9 stands, 3 showed no disturbance to the forest, one had evidence of logging but not recently, one was undisturbed except for damage by ground fire, one showed some logging and windthrow, one had just been logged, one had been recently logged and drained, and one had excessively deep water during the growing season. In cases of recent logging, drainage, or deep flooding, stand condition was judged to be poor; thus four of the nine clusters were in poor condition.

Seedlings and transplants.--Regeneration of pondberry occurs naturally from vigorous rhizome sprouts (Wright, 1989b). Successful seed reproduction is rare, as indicated by the observation that plants seldom occur in mixed populations of both sexes, but seeds are viable and can be induced to germinate in nature by trampling them into a pond bottom when the pond is flooded (Wright, 1989b). Follow-up observations on the above experimental sowing revealed that the seed bank survived into the second season, when there was slight additional germination of trampled seed plus about 10% delayed germination of the untrampled control. Although seedling survival was excellent, seedlings grew very slowly, reaching an average height of 7.9 cm after two growing seasons. First year growth tended to die back, causing second year growth to originate near ground level and reach no higher than that of the first season. There was no indication when flowering would begin.

Transplantation of vigorous greenhouse-grown seedlings met with some success the first year (Wright, 1989b). By the end of the third growing season, however, only 3 of 61 transplants survived.

Predominance of vegetative reproduction was borne out by isozyme studies using starch gel electrophoresis. Comparisons among individuals of both sexes from the same stand and different stands revealed no isozyme differences for the 10 loci assayed. There were also several fixed heterozygotes, a condition not predicted when reproduction is sexual. These findings parallel those of Hooyschuur (1990).

Morphometric Comparisons.--Morphometric comparisons between sexes in adjacent pairs of clones revealed no discernable differences in leaf shape or stem height, but a tendency for males to have more leaves and branches per stem. In an earlier study, Richardson et al. (1990) found no significant morphometric differences between sexes except the production of fewer flowers and leaves by females. Richardson and Wright (unpubl. data) found morphometric differences between clones from different counties, but intersex difference was not studied.

Reproductive Resource Allocation.--Male bias in sex ratio can be taken as indicating effects of unequal reproductive resource allocation. Effects of unequal allocation would be amplified when reproduction was apomictic, since sexual regeneration would not be able to restore a 1:1 ratio.

Male stems produced more flowers than female stems, with mean dry biomass per stem 0.147 g for males and 0.067 g for females (n = 20). Mature fruit biomass, however, exceeded male flower biomass by over an order of magnitude, averaging 6.57 g per stem (n = 20). This means that total reproductive resource allocation was 6.64 g for females and 0.147 g for males, a ratio of 45:1. Although stems that had fruited often died back partially or completely the next growing season, dieback of male stems was also common. Measurements of dieback revealed nearly identical values for the sexes in proportion of stems dying back, length of dieback, and proportion of stems dead to the ground line.

Net Photosynthesis and Stomatal Conductance.--Gas exchange of carbon dioxide and water vapor was determined for 50 leaves of each sex in adjacent clones on five dates during the 1991 growing season, using a LICOR 6200 Portable Photosynthesis System. Data were analyzed with the SAS statistical package. The general linear models procedure revealed no significant differences between sexes in photosynthesis, light, temperature, or CO2, but a highly significant difference between sexes in stomatal conductance (Pr>F0.0007). Males had the higher conductance by about 20%. Multivariate ANOVA revealed a highly significant overall sex effect (Pr>F0.0001). Stepwise discriminate analysis gave rankings as follows:

	Partial R2	Prob. > F
1 Conductance	.0231	.0007
2 Temperature	.0189	.0021
3 Photosynthesis	.0082	.0431

Higher stomatal conductance for males indicates that transpiration occurs at a greater rate, and implies that net

photosynthesis could also be greater since both processes depend upon adequate numbers of stomates and stomatal aperture. Under field conditions, however, net photosynthesis did not differ between sexes.

Shoot Water Potential.--Under typical field conditions, soil moisture remains adequate for most of the growing season in the seasonal ponds where pondberries are found. This suggests that shoot water potential (WP) remains high, and such was the case in 1991. At the site and dates of gas exchange determination, mean shoot water potential was measured on samples of 5 to 10 detached shoots of each sex using a PMS pressure bomb. Mean WP never fell lower than - 1.27 MPa. Although sample sizes were too small to yield significant differences, male WP was lower than female WP on each date, with differences ranging from 5 to 30%.

Discussion

Unequal reproductive resource allocation in a female: male ratio of 45:1 suggests that to maintain a 1:1 sex ratio, *Lindera melissifolia* would need to possess compensating properties in its species biology favoring females. This study has revealed little evidence of such compensating properties. The smaller number and size of female clones indicates that reproductive load on females is not compensated. Absence of females from some stands implies their elimination from these stands. Where both sexes were present, this study found no differences in stem density; however, Richardson et al. (1990) did find a distinction, with female stem density only 60% that of male stem density. Taken as a whole, the above evidence indicates that females have suffered a decline disproportionate to that of males in this endangered species.

There is only limited evidence for genetic distinctions between the sexes. Morphometrically, females have lower numbers of leaves and flowers. Limited electrophoretic data revealed no differences between sexes, and indeed no differences at all among the populations of several stands. This plus the presence of fixed heterozygotes is consistent with the thesis that apomictic reproduction predominates. There is also no evidence that females can photosynthetically compensate for unequal reproductive resource allocation. Net photosynthesis was the same between the sexes, while stomatal conductance was higher in males. If anything, this bias in conductance should favor male photosynthesis, although a compensating bias may occur during infrequent late-season drought stress as recorded by Wright (1989a). Males would be expected to suffer drought stress sooner due to their higher stomatal conductance.

If sexual reproduction were competent, this would be expected to reduce the bias in sex ratio, but the species does not produce significant numbers of seedlings under natural conditions. Growth of the few seedlings is slow, unable to compete effectively with apodictic regeneration from rhizome sprouts. Shoots die back readily, and although new rhizome sprouts appear abundant, females clearly have not maintained themselves by this means. In contrast, the ubiquitous *Lindera benzoin*, with a 1:1 sex ratio (Niesenbaum, 1992), does not appear to spread by rhizome sprouts into large single sex clones. Although *Lindera benzoin* females can produce numerous fruits, they do it on much larger and longer-lived stems that apparently are able to survive the burden of unequal reproductive resource allocation.

Failure of females to maintain themselves in natural populations is likely accelerating the demise of this endangered species, *Lindera melissifolia*. As Wright (1989a) has previously suggested, only managed sexual reproduction has the potential of maintaining females and thus the biological integrity of the species.

Acknowledgements

The author is indebted to Margaret Post for assistance with both field and laboratory portions of this study. The work was supported by a contract from the Arkansas Natural Heritage Commission.

Literature Cited

Delph, L.F. 1990. Sex-differential resource allocation patterns in the subdioecious shrub *Hebe subalpina*. Ecology 71: 1342-1351.

Freeman, C.D., L.G. Klikoff and **K.T. Harper.** 1976. Differential resource utilization by the sexes of dioecious plants. Science 193:597-599.

Hooyschuur, E. 1990. Electrophoretic analysis of genetic variation among clones and populations of pondberry, *Lindera melissifolia*. Unpublished thesis, University of Central Arkansas.

Lloyd, D.G. 1974. Theoretical sex ratios of dioecious and gynodioecious angiosperms. Heredity 32: 11-34.

Lovett Doust, J., G. O'Brien and **L. Lovett Doust.** 1987. Effect of density on secondary sex characteristics and sex ratio in *Silene alba* (Caryophyllaceae). Amer. J. Bot. 74: 40-46.

Meagher, T.R. 1984. Sexual dimorphism and ecological differentiation of male and female plants. Ann. Missouri Bot. Gard. 71: 254-264.

Niesenbaum, R.A. 1992. Sex ratio, components of reproduction, and pollen deposition in *Lindera benzoin* (Lauraceae). Amer. J. Bot. 79: 495-500.

Ramp, P.F. and **S.N. Stephenson.** 1988. Gender dimor-

phism in growth and mass partitioning by Box-elder (*Acer negundo* L.). Amer. Midl. Natur. 119: 420-430.

Wallace, C.S. and **P.W. Rundel.** 1979. Sexual dimorphism and resource allocation in male and female shrubs of *Simmondsia chinensis*. Oecologia 44: 34-39.

Wright, R.D. 1989a. Species biology of (*Lindera melissifolia* Walt.) Blume. in northeast Arkansas. Pp. 176-179 *in* Ecosystem management: rare species and significant habitats (R.S. Mitchell, C.J. Sheviak, and D.J. Leopold, eds.) Proc. 15th Annual Natural Areas Asso. Conf., New York State Museum, Albany Bull 471, 314 pp.

Wright, R.D. 1989b. Reproduction of *Lindera melissifolia* in Arkansas. Proc. Arkansas Acad. of Sci. 43: 69-70.

Correlation Between Chromatid Deletion Production and Progression of the DNA Replication Fork in UV-Irradiated S Phase *Xenopus* Cells

Daniel M. Yoder
John Brown University Box 2244
Siloam Springs, AR 72761

Jason M. Hiles
John Brown University Box 2042
Siloam Springs, AR 72761

Gaston Griggs
John Brown University Box 3024
Siloam Springs, AR 72761

Abstract

Experimentation was performed primarily to determine whether progression of the DNA replication fork along segments of S phase *Xenopus* chromosomes, which contain UV-induced pre-aberrational lesions, plays a significant role in conversion of these lesions into chromatid deletions. Specifically, a *Xenopus* chromosome that was both easy to identify and that possessed a single DNA replication fork in one arm was found and used to conduct the experimentation. This chromosome was exposed to UV in early S phase and a Bromodeoxyuridine/Giemsa differential staining technique was applied in conjunction with conventional aberrational techniques to correlate progression of the DNA replication fork through segments of this arm with chromatid deletion production in these segments. The results point to "direct" evidence for the role of the DNA replication fork in converting some UV-induced pre-aberrational DNA damage into chromosomal deletions.

Introduction

Earlier studies of UV-induced chromosomal aberration production and related repair in interphase *Xenopus* tissue culture cells (Griggs and Bender, 1972; Bender et al., 1973; Griggs and Orr, 1979; Griggs and Payne, 1981;) have yielded essentially two key results. First, low UV (254 nm) fluences administered to interphase cells induced lesions that, if not repaired, led to a significant frequency of chromosomal aberrations observable at the first mitosis following the exposures. Second, when cells were exposed to relatively low fluences of UV in early G1 phase and then exposed to photoreactiveable light as a function of time, most of the UV-induced aberrational damage was photoreactivable through G1 phase, but as the cells entered S phase, their photoreactive capacity ceased. The intracellular process responsible for this alteration in photoeactiveability as the *Xenopus* cells enter S phase has not yet been properly elucidated. Currently, we are in the process of performing experimentation designed primarily for this purpose. Since DNA replication is a predominant cellular activity during S phase, an attempt to obtain "direct" evidence for the role of DNA replication in the process would appear to be the indicated initial effort.

The rationale for our initial experimentation was based on the following. Since it has been shown that the only photoreactivable aberrational damage in DNA is pyrimidine dimmers (Smith and Hanawalt, 1969), it is reasonable to expect that dimmers might distort the normal DNA configuration in such a manner as to interfere with the natural functioning of the DNA replication fork and associated mechanisms. Thia altered functioning might then be responsible for producing DNA breaks. A significant fraction of these breaks would lead to chromatid deletions observable at the first succeeding mitosis. Consequently, it should be possible to observe a definite correlation between the chromatid deletion positions on the chromosomes and the DNA replication fork position on the chromosomes if a technique were available for determining the positions of the DNA replication forks in chromosomes as a function of time during the replication of extended segments of the S phase chromosomes. Such a correlation would constitute "direct" evidence for an integral role of the DNA replication fork in (at least some) categories of chromosomal aberration production. Therefore, we report here an attempt to develop appropriate techniques to accomplish this and to describe the proposed correlation.

Materials and Methods

Cell line used, routine maintenance.--All experiments were conducted using the A87 *Xenopus* cell line that was cloned from the A8W243 line described by Griggs and Bender (1972). This line is maintained in the dark at approximately 23 degrees Celsius. Monolayers were present in large plastic bottles (Falcon) in F10 medium. This medium was supplemented with a 10% fetal calf serum solution (Hazleton) and buffered with $NaHCO_3$ (0.065 M) and HEPES (0.01 M) (Calbiochem.).

At this temperature in exponential growth, these cells usually exhibit a plating efficiency of at least 85%. The

average cell cycle time was 52 hours, including 12 hours for G1, 30 hours for S, and 10 hours for G2 and mitosis. The cell line, which contains cells that possess 36 easily identifiable chromosomes, provided adequate cytological material for chromosomal analysis, including deletion detection.

A more detailed description of this cell line and these procedures can be found in previous publications (Griggs and Bender, 1972; Griggs and Orr, 1979; Griggs and Payne, 1981; Kulp and Griggs, 1989; Laswell et al., 1991). Techniques employed for mitotic index determinations, colony assays, cell plating, cell synchronizations, mitotic arrest, survival curve analysis, and chromosome spreads did not differ significantly from the procedures outlined in the publications mentioned above.

Bromodeoxyuridine (BrdU) labeling.--A 5-bromodeoxyuridine (BrdU) solution (5 by 10^{-4} M) /Giemsa differential staining method was used in this experiment to determine the presence and location of any DNA replication forks. Synchronized momolayers of cells were allowed to progress through S phase in the BrdU medium. Then, after the cells had entered the first mitosis (M1), they were stained with Giemsa as described by Perry and Wolff (1974). Mitotic selection at M1 produced cultures of unifiliarly labeled cells.

Flash labeling experiments were also conducted in connection with the procedure described above. Synchronized cultures were placed in BrdU medium at two hour intervals that spanned the entire S phase. Beginning at 10 hours after shake off, different synchronized cultures were placed in the BrdU medium for 25 minutes every two hours ending at 42 hours after shake off. The labeled portion of the chromatid in the flash labeling procedure appears as only a small section of the entire chromatid (as opposed to continuous labeling where the entire chromatid is labeled) and allows for a more accurate determination of the presence of different replication forks and their location throughout S phase.

A similar labeling procedure was developed by Perry and Wolf (1974) who described the essentials of this technique in more detail. Also, similar work was conducted by Laswell et al. (1991) who give a complete discussion of the metaphase spread techniques employed in this experiment.

UV irradiation.--The source of the UV-irradiation was composed of four 15-W germicidal lamps (Sylvania G15T8) mounted at the top of a small cabinet. Irradiation of the monolayers occurred at 254 nm using thin sheets of plastic between the lamps and the sample radiation surface for does rate control. Techniques did not differ significantly from those described in greater detail by Griggs and Orr (1979).

Results and Discussion

The determination of which chromosome or chromosomes would be appropriately suited for our experimentation rested on the following two conditions: (1) the chromosome must have been easily identifiable and distinguishable in a chromosome spread, and (2) to facilitate ease of data interpretation, the chromosome would preferably contain a chromatid with a single replication fork that replicated an extended section of DNA. A chromosome that met the criteria was found in the cells of the A87 *Xenopus* cell line.

First, the chromosome we used was easy to identify. It is easily distinguishable because one arm projecting from the centromere is normal and the other two arms are not - they are both shorter and appear to have undergone abnormal supercoiling. Second, within the limits of resolution of the labeling we used, the chromosome appeared to possess a single DNA replication fork that replicated all the DNA of the normal chromatid, beginning at the centromere and ending near the telomere (Fig. 1).

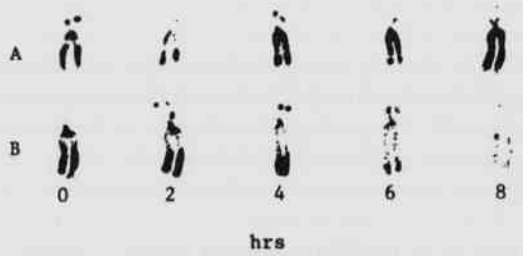

Fig. 1. BrdU labeled *Xenopus* chromosome at two hour intervals during S phase (numbers correspond to hours after S phase has begun). Set A contains the chromosome when flash labeled. Set B contains the chromosome when continuous labeling was employed. The chromosome exhibited a labeling pattern that indicated the presence of only one DNA replication fork that began at the centromere and ended near the telomere.

In the process of examining whether the chromosome met the second criterium, an accurate measure of the *Xenopus* cell cycle was determined - especially in regard to S phase when the DNA replication fork is present. Figure 2 contains data relating the BrdU labeling time with the number of chromosomes labeled at the following mitosis. Because BrdU is only incorporated into DNA during S phase when the DNA replication fork is present and synthesizing new DNA, only chromosomes that were in S phase during the flash labeling will appear labeled at M1. Therefore, from Fig. 2, it is readily apparent that S phase begins approximately 12 hours after shake off and appears to last until approximately 44 hours after shake

off, as is evidenced by the drop in labeled cells at M1 at this time (i.e., G2 is beginning here).

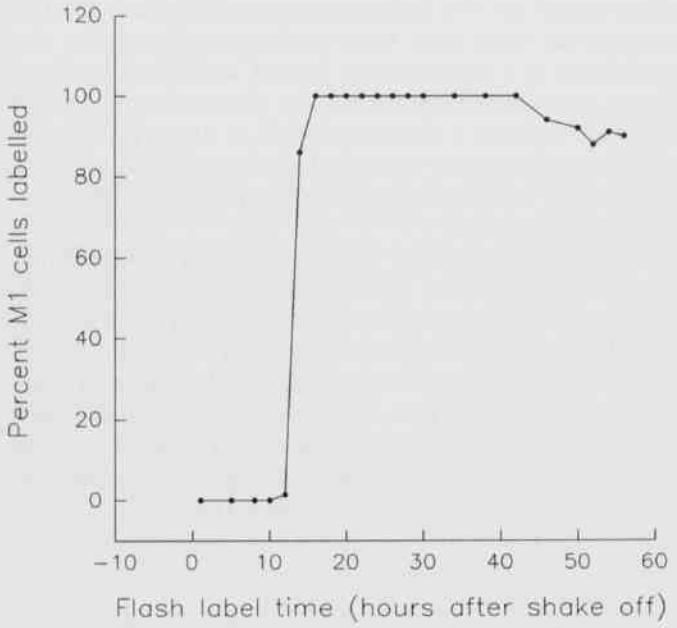

Fig. 2. Flash labeling curve to determine the duration of the cell cycle phases for synchronized G1 *Xenopus* cells. As indicated by the sharp rise in labeled cells, S phase begins at approximately 12 hours after shake off.

In addition to elucidating the S phase duration, it was necessary to our experiment to choose a proper UV fluency that produced sufficient damage to the chromosomes. However, it was also important that this UV fluency did not cause excessive damage which would possibly interfere with or prevent the DNA replication fork from interacting with the lesions. Figure 3 shows the effect of various UV fluences on both cell cycle time and mitotic index. The graph indicates that the cell cycle time is lengthened with increased UV fluency and that the mitotic index decreases with increased UV fluency, possibly because the repair mechanisms need additional time to carry out their functions (increased cell cycle time), and with more damage there is a greater chance that the cells will never be fully repaired and capable of entering mitosis (decreased mitotic index).

Based on Fig. 3, we felt the fluency that would best be suited for our experiment would be 9 J/m² - it would produce an adequate amount of damage, yet it would not cause so much damage that the interaction of the DNA replication fork with the lesions produced would be significantly altered or impaired. Figure 4 supports this assertion. Figure 4 is intimately related to Fig. 2. However, Fig. 4 plots the BrdU flash label time versus the percentage of labeled cells at M1 when 9 J/m2 was

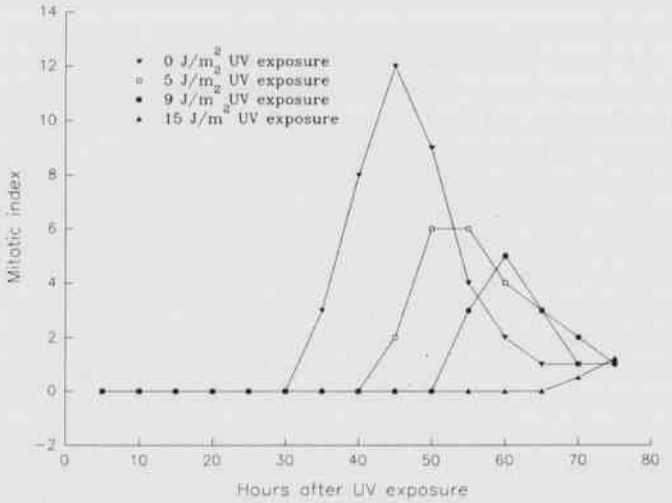

Fig. 3. Time course curve to determine the effect of various UV fluences on *Xenopus* cell cycle duration and mitotic index. UV radiation was administered at the onset of S phase (12 hours after shake off) at the indicated fluences.

administered at 12 hours after shake off, or the beginning of S phase. In contrast to Fig. 2, the cells represented in Fig. 4 were still in S phase even up to 70 hours after shake off. The best conclusion for the increased time spent in S phase is that intracellular repair mechanisms were functioning and required additional time to act. Thus, this data indicate there was indeed significant damage to the chromosomes caused by the 9 J/m² fluency used.

Figure 5 provides the data that ultimately led to our conclusion about the involvement of the DNA replication fork progression in converting the UV-induced lesions into chromosomal deletions. Figure 5 is a plot of the time at which the UV fluency of 9 J/m² was administered versus the percentage of chromosomes that possessed deletion at M1. The trend is obvious - the percentage of cells expressing deletions is indirectly proportional to the time at which the UV fluency was given. To best analyze Fig. 5, it is necessary to choose several points on the graph and describe in detail what we postulate is occurring.

Point A corresponds to the UV fluency given at approximately 12 hours after shake off where S phase is just beginning and the DNA replication fork is at its nearest to the centromere. When the UV fluency is administered, random lesions are produced all along the chromatid. Now, as the DNA replication fork moves down the chromatid toward the telomere, it has the highest probability of encountering the most number of lesions (i.e., it

interacts with the maximum amount of irradiated DNA that is possible for it to encounter). If the DNA replica

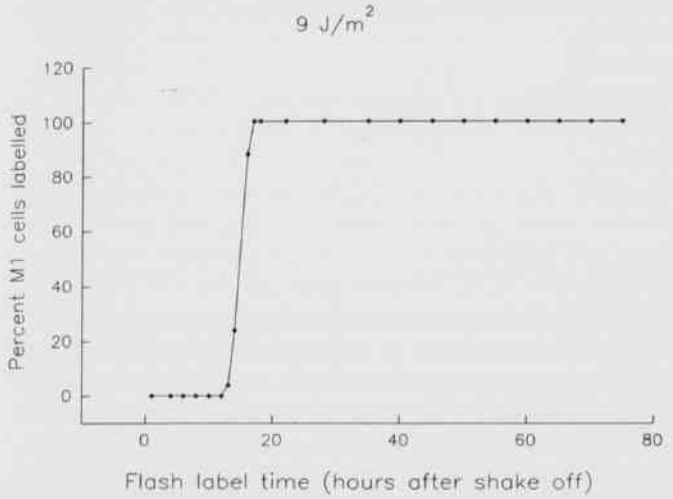

Fig. 4. Flash labeling curve to determine the duration of the cell cycle phases of synchronized G1 phase *Xenopus* cells following exposure to a 9 J/m² UV fluency administered at the onset of S phase (12 hours after shake off).

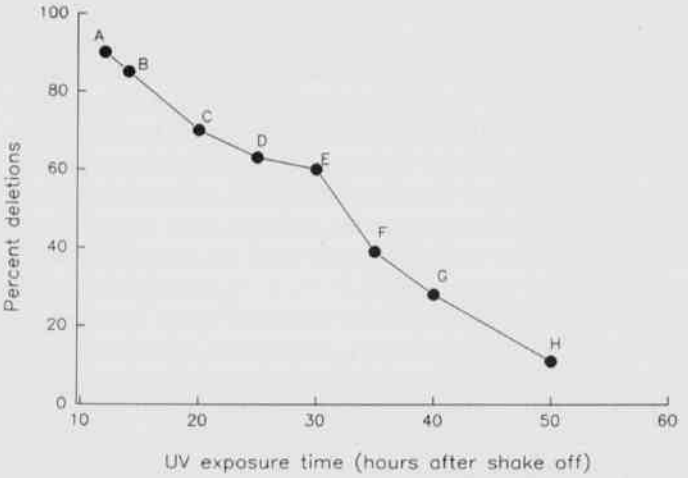

Fig. 5. Percentage of synchronized G1 phase *Xenopus* cells exhibiting chromatid deletions at M1 versus time of UV fluency (9 J/m²) administrations.

tion fork is involved in converting these UV-induced lesions into deletions, then point A should have the highest percentage of deletions - as it does.

Point E corresponds to the group of cells that were irradiated at approximately 30 hours after shake off. This is roughly half-way through the S phase. For illustrative purposes it is assumed that the DNA replication fork is essentially half-way through its trek along the chromatid when the UV fluency is given. Again, random lesions are produced all along the chromatid. However, in this case the DNA replication fork will encounter a lesser amount of irradiated DNA than points A, B, C, and D did. Thus, at point E the DNA replication fork has a lower probability of encountering as many lesions as it does at points A through D. Therefore, as stated above, if the DNA replication fork does play a role in converting these lesions into deletions, then point E should have a lower percentage of deletions than points A through D (and, using the same logic, point E should have a higher percentage of deletions than points F, G, and H) - as it does.

Finally, point H represents the group of cells that were irradiated when the DNA replication fork was at its closest point to the telomere. Here the DNA replication fork would interact with the least amount of DNA after UV exposure. Again, if the DNA replication fork is involved in the lesion to deletion process, point H should have the lowest percentage of deletions - as it does.

The data from a number of previous studies of UV-induced aberration production in interphase eukaryotic cells (Griggs and Bender, 1972; Wolff, 1972; Bender et al., 1973; Griggs and Payne, 1981) have been interpreted as indicating that dark radiation repair mechanisms, similar to excision or post-replication repair in *E. coli* (Rupp and Howard-Flanders, 1968; Walker et al., 1985) are intricately involved in aberrational processes. The essence of this interpretation is the idea that as damaged cells progress through the cell cycle, the repair mechanisms attempt to remove or circumvent the damage in various ways. The mechanisms are not 100% efficient and a number of aberrant structures result, including chromatid deletions, that appear with significant frequencies. The correlation between the DNA replication fork locations and the deletion frequencies at these locations suggests that some form of post-replication repair is more likely to play a significant role in deletion production than some type of excision repair. Post-replication repair is closely correlated with the replication fork and functions exclusively in S phase on portions of chromosomes that have already been replicated. On the other hand, excision repair is more of a random process that appears to function independently of the replication fork and in all phases of the cell cycle, not just in S phase (Walker et al., 1985).

In summary, the data described herein constitute "direct" evidence that the DNA replication fork is intricately involved in the conversion of some UV-induced lesions into chromatid deletions. Furthermore, these data, coupled with the results of earlier studies mentioned above, support the assertion that as the DNA replication fork attempts to replicate a section of DNA containing one of these lesions, an aberrant structure results,

which, if not corrected by post-replication repair, ultimately leads to a chromatid deletion.

Literature Cited

Bender, M., G. Griggs and **P. Walker.** 1973. Mechanisms of chromosomal aberration production. Mutation Res. 20:387-402.

Griggs, G. and **M. Bender.** 1972. Ultraviolet and gamma-ray induced reproductive death and photoreactivation in a *Xenopus* tissue culture cell line. Photochem. and Photobiol. 15:517-526.

Griggs, G. and **T. Orr.** 1979. Chromosomal aberrations resulting from ultraviolet exposures to G1 *Xenopus* cell. Photochem. and Photobiol. 30:363-368.

Griggs, G. and **J.D. Payne.** 1981. Time course of photore activation of UV induced chromosomal aberrations and lethal damage in interphase *Xenopus* cells. Photochem. and Photobiol. 35:57-62.

Kulp, S. and **G. Griggs.** 1989. Photoreactivation of lethal damage and damage leading to chromatid deletions induced in G1 phase hamster x *Xenopus* hybrid cells by UV. Photochem. and Photobiol. 50:185-191.

Laswell, D., J. Barber and **G. Griggs.** 1991. Photoreactivation of UV-induced damage in G1 phase *Xenopus* cells that leads to sister chromatid exchanges and cell death. Proceedings Arkansas Academy of Science 45:52-56.

Perry P. and **S. Wolff.** 1974. New Giemsa method for differential staining of sister chromatids. Nature 251:156-158.

Rupp, W.D. and **P. Howard-Flanders.** 1968. Discontinuities in the DNA synthesized in an excision defective strain of *E. coli* following ultraviolet irradiation. S. Mol. Biol. 31:291-304.

Smith, K.C. and **P.C. Hanawalt.** Molecular Photobiology, Academic Press, New York, 1969.

Walker, G., L. Marsh and **L. Dodson.** 1985. Genetic analysis of DNA repair: Inference and Extrapolation. An. Rev. Genetics. 19:103-126.

Wolff, S. 1972. Chromosome aberrations induced by ultraviolet radiation, *In* A.C. Giese (ed.), Photophysiology, 7: Academic Press, New York.

GENERAL NOTES

Bryophyte and Pteridophyte Distribution Records of Southern Arkansas

James R. Bray, Greg A. Whitehead, Daniel L. Marsh and Dennis W. McMasters
Department of Biology
Henderson State University
Arkadelphia, AR 71999-0001
Winfred D. Crank
328 Houston Drive
Hot Springs, AR 71913

This note catalogs distributional records for 22 species of hepatics and pteridophytes in southern Arkansas. We hope inclusion of four hepatics may stimulate more interest in the bryophytes of Arkansas. We wish either to initiate or contribute to the eventual preparation of an atlas and annotated list of the bryophytes of Arkansas in a format similar to that which Smith (1988) published for the vascular plants, an also to compile a photographic collection of the bryophytes to supplement the pteridophyte photographic collection compiled earlier by Crank.

Trichocolea tomentella (Ehrh.) Dumort. is a strikingly beautiful leafy liverwort (Order Jungermanniales) often mistaken for a delicate fern moss. Because of this appearance we use "mossy hepatic" as our English designation. It is widely distributed in the Northern Hemisphere, but is restricted to wet, low-acid sites often along mountain streams. The only location in Arkansas given by Schuster (1966) is at Camp Albert Pike in Montgomery Co. After studying that site, we located additional stands in Montgomery Co. Bray later found a new location in Garland Co. and another extensive stand in Hot Spring Co. We expect to find sites in other counties of the Interior Highland.

Another leafy liverwort which can form conspicuous mats is *Scapania nemorosa* (L.) Dumort., southern scapania or "carpet hepatic." It is widely distributed in the eastern half of North America and in Europe from 30-55° N. latitude. Schuster (1974) includes Arkansas and the adjacent states in the range, but gives no specific sites in Arkansas. This highly polymorphic species tolerates broad ranges of light, moisture, and soils, and it is likely to be found throughout the state. It forms extensive carpets in a city park in Arkadelphia and in a nearby cemetery (Clark Co.). Marsh has collected it from DeGray Lake State Park (Hot Spring Co.) and from the Ouachita National Forest south of Aplin in Perry Co. In addition we have student collections from Camp Albert Pike in Montgomery Co. and Neddle's Eye Mountain in Hot Spring Co.

One of our most common ribbon-mosses (Order Metzgeriales) is *Pallavicinia lyellii* (Hook.) Carruthers, which we usually call "winged liverwort" because the thalli are clearly differentiated into a midrib and lateral wings which are only one cell layer thick. It is common in bogs and on wet creek banks in our area. Schuster (1992) lists sites in 19 counties of Arkansas: Baxter, Conway, Cross, Franklin, Garland, Greene, Hempstead, Lafayette, Little River, Miller, Montgomery, Nevada, Newton, Polk, Pulaski, Saline, Stone, Union, and Van Buren. We have documented additional sites in Clark, Ouachita, and Pike counties.

The only member of the bottle hepatics (Order Sphaerocarpales) which we have found in Arkansas is *Sphaerocarpos texanus* Aust., which we call "Texas bottlewort." It is notable for the bottle-shaped involucres covering the sex organs and for being the first plant in which sex chromosomes were discovered. Schuster (1992) lists it for nine counties of Arkansas: Benton, Calhoun, Conway, Faulkner, Hempstead, Lafayette, Polk, Pulaski, and Washington. The new locations are in Clark, Dallas, Hot Spring, and Ouachita counties (the last was found by Michael Shepherd). Although it can be found on a wide variety of bare soils, it is undoubtedly much overlooked because of its small size and short growing season in cool weather.

In the fall of 1992 McMasters found a single shoot of the whisk-fern, *Psilotum nudum* (L.) Beauv., at the base of a retaining wall while cleaning out a dense growth of English ivy in the yard of his home in Arkadelphia. The aerial portion died during the late winter of 1993, possibly because it was no longer protected by the vine. This occurrence is documented by photographs but not by an herbarium collection. Presumably there was at least one gametophyte present in the soil, but the sporophyte could have developed apogamously. The nearest cultivated *Psilotum* is less than a mile from this site at the greenhouse on the Henderson State University campus. Several potted *Psilotum* plants there produce abundant spores, and young plants are found from time to time as weeds in pots containing other species. At present we regard this occurrence as a waif, but we suggest that botanists should be alert to the possibility that this species may occur as an escape. A stand of *Psilotum* was reported near Ruston, Louisiana (Rhodes, 1970) only 35 miles south of Arkansas within a forested area. Thieret (1980) indicates the species in both Lincoln and Ouachita parishes in northern Louisiana. In the case of occurrences under heavy

cover, as at Arkadelphia, the species could be easily overlooked.

Lycopodiella prostrata (Harper) Cranfill, creeping foxtail club-moss, was first reported in Arkansas by Peck et al. (1987) who discovered it in Calhoun Co. Later it was reported in Saline Co. by Bray and Marsh (1993). We have now located it in Clark Co. associated with *L. appressa*.

Selaginella eclipes Buck, Buck's meadow spikemoss, is shown only for northern counties in Taylor (1984) and Smith (1988). An extension to Montgomery Co. in southern Arkansas was reported by Bates (1993). We have found the species in Garland and Hot Spring counties. It probably occurs in other counties in the Ouachita division, where it has perhaps been taken for *S. apoda*. For many years we have regularly visited one of the Hot Spring Co. sites north of Bismarck on Highway 7 but we had incorrectly identified the plant as *S. apoda*. The two taxa are morphologically similar, and it has been suggested that *S. eclipes* might prove to be a subspecies of *S. apoda* (Valdespino, 1993). The two taxa have remained distinctive under cultivation in the Henderson State University greenhouse.

We have found single county extensions for the following pteridophytes: *Isoëtes melanopoda* Gay & Durieu, black-footed quillwort, in Cleveland Co.; *Equisetum hyemale* L., scouring rush, in Hot Spring Co.; *Asplenium bradleyi* D.C. Eat., Bradley's spleenwort, in Hot Spring Co.; *Asplenium resiliens* Kunze, black-stemmed spleenwort, in Montgomery Co.; *Cystopteris tennesseensis* Shaver, Tennessee bladder fern, in Montgomery Co.; *Pellaea atropurpurea* (L.) Link, purple-stemmed cliff brake, in Hot Spring Co.; *Thelypteris kunthii* (Desv.) Morton, southern shield fern, in Garland Co.; and *Thelypteris noveboracensis* (L.) Nieuwl., New York fern, in Hot Spring Co.

We report the mosquito fern *Azolla* in Clark and Ouachita counties, found without the sori needed to determine whether *A. caroliniana* Willd. or *A. mexicana* Presl. was represented. Thieret (1980) listed *A. caroliniana* as the only mosquito fern in adjacent Louisiana. Taylor (1984), with reservations, and Smith (1988) listed our mosquito fern as *A. mexicana*. Lumpkin (1993) included Arkansas in the mapped distributions of both species, but stated that the maps are tentative pending resolution of taxonomic difficulties. He pointed out that about 80% of the specimens studied lack sori.

During the last two years we have given some attention to the distribution of the Ophioglossales and have a number of additions to the county records provided by Taylor (1984) and Smith (1988). *Botrychium lunarioides* (Michx.) Sw., winter grape fern, was known in four counties; we have found a number of sites in four more counties: Clark, Dallas, Hot Spring, and Nevada. (The last was found by Tim Golden.) All of these locations are in rural cemeteries.

Ophioglossum crotalophoroides Walt., bulbous adder's tongue, was also found in four more counties: Garland, Montgomery, Pike, and Saline. The location of *O. engelmannii* Prantl, limestone adder's tongue, in a cemetery at Okolona is a new record for Clark Co. This is in the calcareous blackland prairie region. *O. nudicaule* L. f., least adder's tongue, was found in four new counties: Calhoun, Clark, Dallas, and Pike, doubling the number of counties recorded. *O. petiolatum* Hook., stalked adder's tongue, was previously known in four counties. We have found a site in Clark Co. where it is locally rather common in a rural church yard, mixed with a population of *O. crotalophoroides*. *O. vulgatum* L., southern adder's tongue, was found in three additional counties: Clark, Garland, and Montgomery.

Based on published reports and our work, Clark Co. is the only county presently known to contain all five of the Arkansas adder's tongues. This is obviously because we have concentrated much field work there. Distributions of these five species in the southeastern United States (Wagner and Wagner, 1993) and particularly in northern Louisiana (Thieret, 1980) strongly suggest that they all could be found in most counties in the southern one-third of Arkansas.

Voucher specimens of all the species cataloged above, except *Psilotum nudum*, have been placed in the Henderson State University Herbarium.

Literature Cited

Bates, V. 1993. Ouachita National Forest. Vol. 1. Overview of plant communities and an inventory of natural area. A cooperative project supported by Arkansas Nature Conservancy; Arkansas Natural Heritage Commission; U.S. Forest Service, Southern Region, iii + 144 pp.

Bray, J.R. and **D.L. Marsh.** 1993. Additional occurrences of the bog clubmosses in southern Arkansas. Proc. Ark. Acad. Sci. 47:131-132.

Lumpkin, T.A. 1993. Azollaceae. Pp. 338-342, *In* Flora of North America north of Mexico. Vol. 2. Pteridophytes and gymnosperms. Oxford University Press, New York xvi + 475 pp. 338-342.

Peck, J.H., C.J. Peck, S.L. Orzell, E. Bridges and **C. Amason.** 1987. Discovery of *Lycopodium* communities in the Gulf Coastal Plain region of Arkansas. Proc. Ark. Acad. Sci. 41: 112-113.

Rhodes, D.G. 1970. *Psilotum nudum* (Psilotaceae) in north Louisiana. Sida 3:525.

Schuster, R.M. 1966. The Hepaticae and Anthocerotae of North America east of the hundredth meridian, Vol. 1. Columbia University Press, New York, xvii + 802 pp.

Schuster, R.M. 1974. The Hepaticae and Anthocerotae of North America east of the hundredth meridian, Vol. 3. Columbia University Press, New York, ix + 880 pp.

Smith, E.B. 1988. An atlas and annotated list of the vascular Plants of Arkansas, 2nd ed. Kinko's Copies, Fayetteville, Arkansas, iv + 448 pp.

Taylor, W.C. 1984. Arkansas ferns and fern allies. Milwaukee Public Museum, Milwaukee, Wisconsin, 262 pp.

Thieret, J.W. 1980. Louisiana ferns and fern allies. Lafayette Natural History Museum, Lafayette, Louisiana, vi + 124.

Valdespino, I.A. 1993. Selaginellaceae. Pp. 38-63, *In* Flora of North America north of Mexico. Vol. 2. Pteridophytes and gymnosperms. Oxford University Press, New York, xvi + 475 pp.

Wagner, W.H. and **F.S. Wagner.** 1993. Ophioglossaceae. Pp. 85-106, *In* Flora of North America north of Mexico. Vol. 2 Pteridophytes and gymnosperms. Oxford University Press, New York, xvi + 475 pp.

A Recent Record of the Plains Minnow, *Hybognathus placitus* Girard, from Arkansas

Thomas M. Buchanan
Department of Biology
Westark Community College
Fort Smith, AR 72901

Henry W. Robison
Department of Biological Sciences
Southern Arkansas University
Magnolia, AR 71753

Robison and Buchanan (Fishes of Arkansas), Univ. Arkansas Press, 1988) reported the plains minnow, *Hybognathus placitus* Girard, had not been collected in Arkansas in over two decades, and was probably extirpated from the state. The last previously known collection of this species in Arkansas was a single specimen (TU 54530) taken from the Mississippi River in Mississippi County, 2.2 mi. NE of Butler, AR. on 8 October 1968. The only other Arkansas records of *H. placitus* were listed by Black (The Distribution of the Fishes of Arkansas, Ph.D. disseration, Univ. Michigan, 1940). A collection of three specimens was taken from the Red River in Hempstead County on 8 July 1939, and an unspecified number of individuals was taken from four Arkansas River localities between Fort Smith in Sebastian County and the mouth of Piney Creek in Logan County during the 1890s and 1930s. Black also collected this species from the Mississippi River in Mississippi County in the 1930s.

This note reports the first vouchered record of *H. placitus* from Arkansas in over 25 years. A single individual was collected by T. M. Buchanan and Westark Community College students on 28 July 1993, from the Arkansas River, 400 m downstream from Trimble Lock and Dam in Crawford County. The specimen was 46 mm in total length and was deposited in the Westark Zoology Collection. It had 16 scale rows below the lateral line, a narrow, rodlike basiocciptal process, and the eye width divided into the head length went 4.4 times. It was taken during unusually high water levels behind a submerged sandbar at a depth of approximately 1 m over a predominately sand substrate having patches of gravel in a slight current using a 9 m nylon seine of 3.2-mm mesh. Other species collected were: *Dorosoma cepedianum, D. petenense, Cyprinella lutrensis, Notropis atherinoides, N. blennius, Gambusia affinis, Menidia beryllina,* and *Micropterus salmoides.*

Hybognathus placitus is almost exclusively a Great Plains species where it is still abundant in the main channels of turbid, silt and sand-bottomed streams and rivers (Robison and Buchanan, loc. cit.). It is a common species in the Arkansas River drainage of northern and western Oklahoma, and Arkansas is near the southeastern margin of its range. It is not known whether a reproducing population of the plains minnow has ever existed in Arkansas, although one may have been present in the Arkansas River near Fort Smith prior to the 1940s. A resident population is not known to exist in the state.

The specimen in this report probably represents a waif from an existing upstream population which was displaced downstream by the high water levels in the Arkansas River that occurred from December 1992, through early August 1993. On 28 July 1993, the discharge reported for the Arkansas River in the vicinity of this collection locality was 60,000 cfs. This compares with the normal July discharge rate of approximately 12,000-15,000 cfs. The submerged sandbar near the collecting site is normally above water. During the last 22 years, two to four annual collections have been made by seine at this locality. In addition over 100 samples have been taken since 1971, by seine, electroshocker, and rotenone in a 20-km section of the Arkansas River near Fort Smith without finding *H. placitus*.

Renewal and Recovery: Shortleaf Pine/Bluestem Grass Ecosystem and Red-cockaded Woodpeckers

George A. Bukenhofer, Joseph C. Neal and Warren G. Montague
Ouachita National Forest
P.O. Box 2255
Waldron, AR 72958

The Ouachita National Forest (Ouachita NF) is comprised of 666,046 ha of pine and mixed hardwood forests in west-central Arkansas and southeastern Oklahoma. The Ouachita NF has proposed landscape-scale habitat restoration that would lead to renewal of once widespread habitat (Mattoon, 1915) dominated by shortleaf pine (*Pinus echinata*) and bluestem grasses (*Andropogon spp.*) on approximately 40,000 ha of the forest area (Fig. 1). This project is unique because of its size, scope of activities, and ecosystem management approach. As renewal of this ecosystem proceeds, it is reasonable to predict improved habitat conditions for numerous species of plants and animals, including Red-cockaded Woodpeckers (*Picoides borealis*).

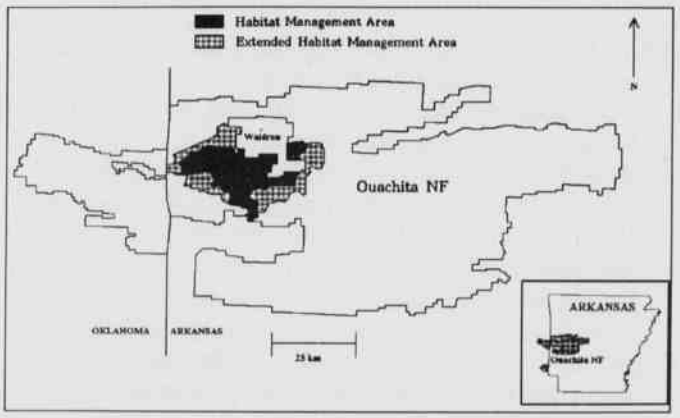

Fig. 1. Area of proposed shortleaf pine/bluestem grass ecosystem renewal on the Ouachita National Forest, Arkansas. The habitat management area is the minimum area required to maintain the existing population of Red-cockaded Woodpeckers. The extended area will be necessary to recover the population and to achieve landscape-scale goals of shortleaf pine/bluestem grass ecosystem renewal.

Historical accounts support the concept that open woodlands dominated by shortleaf pines and a lush herbaceous understory comprised of bluestem grasses and various forbs occurred widely in the Ouachita Mountains (Little and Olmstead, 1931; Smith, 1986a, 1986b; Jansma and Jansma, 1991). This association also occurred elsewhere in the southeastern U.S. (Jackson, 1988; Dickson, 1991; Waldrop et al., 1992). Frequent anthropogenic and lightning caused fire maintained the open condition of these stands in the Ouachitas (Foti and Glenn, 1991; Masters et al., 1993) and elsewhere in the southeast (Waldrop et al., 1992). Fire control efforts have reduced the incidence of wildfire, leading to widespread habitat changes, especially encroachment of dense mid-stories of pine and hardwood trees.

Recent work in the Ouachitas has shown that re-introduction of fire and re-establishment of open conditions in pine-dominated habitats results in increases of understory species diversity as compared to controls (Wilson et al., 1995). Habitat restoration produces changes in the composition of small mammal and breeding bird communities (Lochmiller et al., 1993; Wilson and Masters, 1993). Therefore, based upon historical accounts of habitat and results of this recent research, we hypothesize that other elements of the Ouachita biota have been negatively affected by widespread habitat change. Habitat renewal through forest management can improve conditions for communities of plants and animals affected by past land-use patterns.

The core area for proposed habitat renewal involves 40,000 ha of National Forest lands in Scott and Polk counties, Arkansas (Fig. 1). This area contains a population of Red-cockaded Woodpeckers (Neal and Montague, 1991), a federally-listed species considered a key indicator of pine-grass habitat maintained in an open condition by periodical fire (USF&WS, 1985; Jackson, 1988). The area proposed for habitat renewal was delineated by the known range of the species during the last 20 years (Neal and Montague, 1991). Current planning goals (Ouachita NF, 1990) include 50 breeding groups of Red-cockaded Woodpeckers. The current population estimate for the Ouachita NF is approximately 15 breeding groups (Ouachita NF unpubl. data). Habitat renewal would increase diversity of plants and animals that were likely present during presettlement times, including a recovered population of approximately 250 breeding groups of Red-cockaded Woodpeckers.

The goal of increasing the Red-cockaded Woodpecker population on the Ouachita NF to 250 groups has been made more realistic due to recent advances in management techniques. Translocation of individual birds between populations (Allen et al., 1993), installation of artificial cavities and modification of natural cavities (Carter et al., 1989; Allen, 1991; Copeyon et al., 1991), and the reduction of predation and interspecific cavity competition (Neal et al., 1992; Withgott et al., 1993; Montague et al., 1993; Montague, unpubl.) are now management options.

Continuing traditional use of the forest's resources is integral to the project's success. Scenarios have been proposed which would provide for integrated management in forest ecosystem including both wildlife and economic objectives (Seagle et al., 1987; Franklin, 1989; Hyde, 1989). In this project area, timber harvest levels would remain close to present levels, but their purpose would be redirected toward ecosystems management objectives (Fig. 2). With or without this restoration project, long term harvest levels will experience a modest decline.

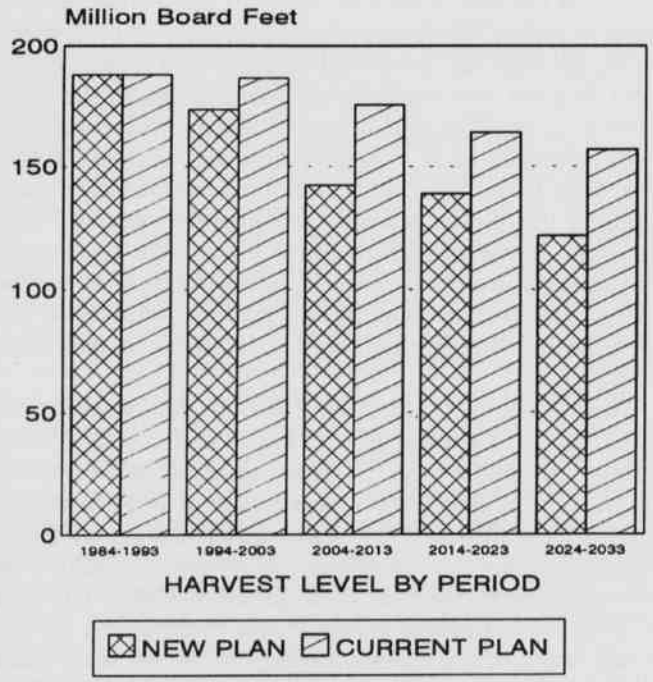

Fig. 2. Projected timber volume for next 50 years from shortleaf pine/bluestem grass ecosystem renewal area, Ouachita National Forest, Arkansas.

Shortleaf pine/bluestem grass ecosystem renewal would be achieved by the use of natural events such as fires, storms, and insect outbreaks and by emulating these events through the use of prescribed fire and timber harvest. The following are key elements of this approach: 1) using fire and tree cutting to simulate natural disturbance patterns, 2) using natural events such as insect outbreaks and wind storms to provide open conditions and opportunities for natural forest regeneration, 3) increasing the minimum time between regeneration cutting from 70 years to 120 years, which would allow for development of older trees required by Red-cockaded Woodpeckers and other cavity-using species, 4) maintaining mixtures of native pines and hardwoods, 5) developing and maintaining forested linkages between mature forest habitats, 6) minimizing ecotonal differences between contiguous stands and reducing habitat fragmentation, and 7) recognizing that people are an important part of this system by permitting a variety of economic, recreation, and scientific activities within the restoration area.

Human intervention in resource management is essential, given the inability of natural processes to function at pre-settlement landscape scales in a modern world. Renewal and restoration in the shortleaf pine/bluestem grass ecosystem should permit recovery of a diverse biota that has declined throughout this century.

Literature Cited

Allen, D.H. 1991. An insert technique for constructing artificial Red-cockaded Woodpecker cavities. Gen. Tech. Rep. SE-73. Asheville, NC: USDA, For. Serv, Southeast. For. Exp. Sta. 19 pp.

Allen, D.H., K.E. Franzreb and **R.E.F. Escano.** 1993. Efficacy of translocation strategies for Red-cockaded Woodpeckers. Wildl. Soc. Bull. 21:155-159.

Carter, J.H., III, J.R. Walters, S.H. Everhart and P.D. Doerr. 1989. Restrictors for Red-cockaded Woodpecker cavities. Wildl. Soc. Bull. 17:68-72.

Copeyon, C.K., J.R. Walters and **J.H. Carter III.** 1991. Induction of Red-cockaded Woodpecker group formation by artificial cavity construction. J. Wildl. Manage. 55:549-556.

Dickson, J.G. 1991. Birds and mammals of pre-colonial southern old-growth forests. Natural Areas J. 11:26-33.

Foti, T.L. and **S.M. Glenn.** 1991. The Ouachita Mountain landscape at time of settlement. Pp. 49-65, *In* Proceedings of a conference on restoring old growth forests in the Interior Highlands of Arkansas and Oklahoma (L. Hedrick and D. Henderson, eds.) USDA For. Serv., Hot Springs, Arkansas.

Franklin, J. 1989. Toward a new forestry. Am. Forests. Nov/Dec: 37-44.

Hyde, W.F. 1989. Marginal costs of managing endangered species: the case of the Red-cockaded Woodpecker. J.

Ag. Econ. Research 41:12-19.

Jansma, J. and **H.J. Jansma.** 1991. George Engelmann in the Arkansas Territory. Arkansas Historical Quarterly. Vol. L:225-248.

Jackson, J.A. 1988. The southeastern pine forest ecosystem and its birds: past, present, and future. Pp 119-159, *In* Bird Conservation 3 (J.A. Jackson, ed) Int. Council for Bird Pres., Univ. of Wisc. Press, Madison.

Little, E.L., Jr. and **C.E. Olmstead.** 1931. An ecological study of Southeastern Oklahoma Protective Unit. Oklahoma Forest Service. (W.T. Penfound, ed.) Unpubl. manuscript, Univ. Okla. Lib. 53 pp.

Lochmiller, R.L., R.E. Masters and **S.T. McMurry.** 1993. Wildlife stand improvement: effects of midstory vegetation removal and fire on small mammals. Summary of winter 1993 survey. Annual Report. USDA For. Serv. Hot Springs, Arkansas. 15 pp.

Masters, R.E., J.E. Skeen and **J. Whitehead.** 1993. Preliminary fire history of McCurtain County Wilderness Area and implications for Red-cockaded Woodpecker management. *In* Red-cockaded Woodpecker: Recovery, ecology and management. (D.L. Kulhavy, R.G. Hooper, and R. Costa, eds.) Center for Applied Studies, College of Forestry, Stephan F. Austin State Univ., Nacogodoches, Texas.

Mattoon, W.R. 1915. Life history of shortleaf pine. USDA Bull. No. 244. 46 pp.

Montague, W.G., J.C. Neal, J.E. Johnson and D.A. James. 1993. Techniques for excluding Southern Flying Squirrel's from cavities of Red-cockaded Woodpeckers. *In* Red-cockaded Woodpecker: Recovery, ecology and management. (D.L. Kulhavy, R.G. Hooper, and R. Costa, eds.) Center for Applied Studies, College of Forestry, Stephen F. Austin State Univ., Nacogodoches, Texas.

Neal, J.C. and **W.G. Montague.** 1991. Past and present distribution of the Red-cockaded Woodpecker and its habitat in the Ouachita Mountains in Arkansas. Proc. Arkansas Acad. Sci. 45:71-75.

Neal, J.C., W.G. Montague and **D.A. Jones.** 1992. Sequential occupation of cavities by Red-cockaded Woodpeckers and Red-bellied Woodpeckers in the Ouachita National Forest. Proc. Arkansas Acad. Sci. 46:106-108.

Ouachita National Forest. 1990. Final environmental impact statement. Amended land and resource management plan. USDA For. Serv. Hot Springs, Arkansas.

Seagle, S.W., R.A. Lancia, D.A. Adams, M.R. Lennarz and **H.A. Devine.** 1987. Integrating timber and Red-cockaded Woodpecker habitat management. Trans. 52nd N.A. Wildl. and Nat. Resources Conf. 52:41-52.

Smith, K.L. 1986a. Sawmill, the story of cutting the last great virgin forest east of the Rockies. Univ. of Arkansas Press. 246 pp.

Smith, K.L. 1986b. Historical perspective. pp. 1-8, *In* Proceedings of symposium on shortleaf pine ecosystem (P.A. Murphy, ed.) South. For. Exp. Sta., USDA For. Serv., Monticello, Arkansas.

U.S. Fish and **Wildlife Service.** 1985. Red-cockaded Woodpecker recovery plan. U.S. Fish & Wildl Serv. Atlanta. 88 pp.

Waldrop, T.A., D.L. White and **S.M. Jones.** 1992. Fire regimes for pine-grassland communities in the southeastern United States. For. Ecol. Manage. 47:195-210.

Wilson, C.W., R.E. Masters and **G.A. Bukenhofer.** 1995. Effects of midstory vegetation and fire on breeding birds in Red-cockaded Woodpecker clusters. J. Wildl. Manage (In press).

Withgott, J.H., J.C. Neal and **W.G. Montague.** 1993. A technique to deter climbing by rat snakes on cavity trees of Red-cockaded Woodpeckers. *In* Red-cockaded Woodpecker: Recovery, ecology and management. (D.L. Kulhavy, R.G. Hooper and R. Costa, eds.) Center for Applied Studies, College of Forestry, Stephen F. Austin State Univ., Nacogodoches, Texas.

A Fluid Dynamics Model of Data Acquisition and Data Analysis for High-Energy Physics

Charles M. Byrd, Christine A. Byrd, Wilson H. Howe, and W.J. Braithwaite
Department of Physics and Astronomy
University of Arkansas at Little Rock
Little Rock, AR 72204

The current paradigm for accelerator-based high-energy physics experiments involves the design of two distinct detector subsystems for managing data, namely data acquisition and data analysis. In order to establish the design parameters for detector components, the choice of technology for these data management subsystems must be made years in advance. By the time detectors come on-line, hardware will often be obsolete, because the technology choice was made years earlier. The majority of the data analysis will occur off-line, making expensive data storage necessary. Furthermore, the present gap between data acquisition and data analysis would be reduced by having a homogenous software environment throughout the experiment.

The Relativistic Heavy Ion Research Group at the University of Arkansas at Little Rock has developed an alternative archetype for data processing in high-energy physics which makes use of the transputer model to achieve a balance between data communication and data processing. By providing an integrated data acquisition and data analysis environment, the use of transputers allow computing resources to be maximized while minimizing data storage requirements for high-energy physics experiments. By taking advantage of high performance communication hardware developed by GE Corporate Research and Development, a flexible data management system is being designed to provide necessary parameters for detector component development without forcing premature technology choices. The hardware independence of this model insures the experiment can always be operated with state of the art technology. Using a homogenous software environment, this transputer computing model allows a significant portion of the analysis to occur on-line, reducing the volume of data passed to storage systems.

The data streams generated at the Relativistic Heavy Ion Collider (RHIC), Brookhaven and the European Center for Nuclear Research (CERN), Geneva are so enormous that a fundamentally new way of thinking about data acquisition and processing must be developed. The volume of data from the final state particles is so large that it becomes reasonable to use a macroscopic model for what is usually thought of as microscopic. Fluid-dynamics is a near-perfect macroscopic model for data acquisition because it provides a way to quickly obtain consequences to proposed changes. Therefore, to aid in the future development of the algorithms for massively parallel processors, an analogy was drawn between the data flow and fluid flow. In this paper, the fundamental principles of fluid dynamics (Shapiro, 1954) are applied to problems in data acquisition for high-energy physics.

A very simple fluid dynamics model is one which has a control volume M with a mass flow rate in ω_1 and a mass flow rate out ω_2. An Equation for the overall mass balance follows (where $d\theta$ is change in time):

$$\omega_1 - \omega_2 = dM/d\theta,$$
$$\text{or, } \omega_2 - \omega_1 + dM/d\theta = 0.$$

These equations say, simply, that the difference in mass flow rate in and mass flow rate out is equal to a rate of accumulation of mass in the control volume. Usually, one must deal with multiple inputs and outputs in a system such as the one below.

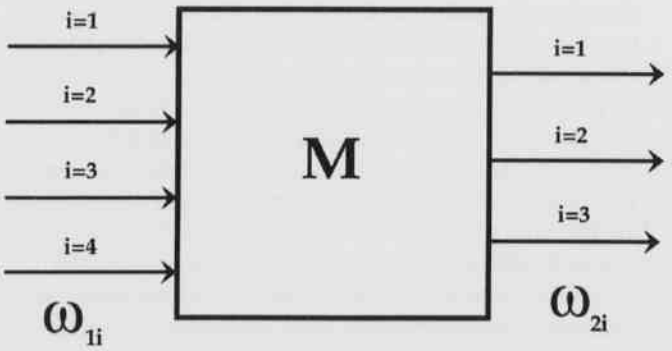

With multiple inputs and outputs the mass balance equations are as follows (subscripts indicate mass balance of each flowing substance):

$$\omega_{2i} - \omega_{1i} + \frac{\partial M_i(\theta)}{\partial \theta} = 0$$

$$X_{ki} = \frac{\omega_{ki}}{\omega} \qquad \text{(for k = 1 or 2)}$$

$$\omega_{2i} X_{2i} - \omega_{1i} X_{1i} + \frac{\partial M_i(\theta)}{\partial \theta} = 0$$

The concentration X_{ki} (k = 1 or 2) is the ratio of the k-th mass flow rate to total flow rate.

The analogy between fluid flow and data flow follows: volume is analogous to memory, mass/sec is analogous to bits/sec, chemical reaction is analogous to data processing, ω_1 (mass in) is analogous to D_1 (data in), ω_2 (mass out) is analogous to D_2 (data out), and $dM/d\theta$ (accumulation of mass) is analogous to dP/dt (accumulation of processed data). Data flow is reduced at each step of the analysis through dP/dt. A large dP/dt results in a proportionately large reduction in ω_2.

The simplest example to model using the principles of fluid dynamics is a two-detector, two-stage data acquisition system. This modeling example is a frequent occurrence in high-energy physics, as the output of two independent systems may be merged to give a unified set of data describing the particle events. This type of paired groupings of data streams may be carried out more than once in modeling the full data acquisition and analysis for the entire system.

An example of merging data streams from a two-detector, two-stage system is found in the track matching effort of the Silicon Vertex Tracker (SVT) and the Time Projection Chamber (TPC) of the STAR Instrument at RHIC. Another example is in the track matching of two vertex TPCs in the NA49 Experiment at CERN. Each example uses a track matching device following the two-detector data streams.

The diagram at the right represents a two-stage system being modeled. Note the analysis software for each detector component (represented by dP/dt) filters out the most interesting events, significantly reducing the outgoing data flow to the track matching device, which in turn filters the data further (also represented by dP/dt).

Using a tangible example of the diagram to the right analysis, particles registered by the SVT and the TPC must be matched by a track matching device. The track matching device must wait for data from both detector components before further processing the data. Since the SVT is a faster device than the TPC, data streams originating from the SVT will reach the track matching device sooner than data streams from the TPC. Thus, in the interest of efficiency, transputers processing elements within the track matching device not currently being used may be reallocated to the TPC by taking advantage of their reconfigurable backplanes. Processor idle time may be minimized under master computer control by this type of dynamic reallocation of elements (Byrd et al., 1993).

There are many advantages to using integrated data acquisition. For instance, data archival costs may be substantially reduced due to prefiltering data used by trigger software. Since interesting data may be extracted by the analysis software at each level, cost of off-line analysis may be significantly reduced, as less archival storage is needed due to prior rejection of the less interesting events.

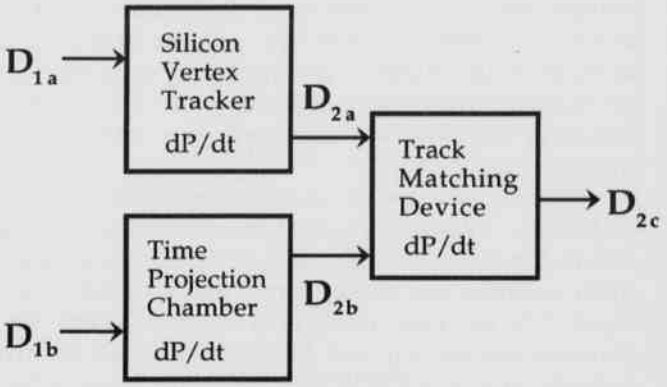

Acknowledgements

This work was supported in part by U.S. Department of Energy and the Arkansas Science and Technology Authority. This work acknowledges the advice and support of the STAR Collaboration at RHIC and of the NA49 collaboration at CERN. The second and third authors acknowledge financial support from the UALR Donaghey Scholars Program.

Literature Cited

Byrd, C.M., C.A. Byrd, D.L. Roetzel and W.J. Braithwaite. 1993. Role of MPP Granularity in Optimizing Monte Carlo Programming. Proceedings of the International Conference on Monte Carlo Simulation in High-Energy and Nuclear Physics. (World Scientific Publ. Co., Singapore) 40-44.

Shapiro, A.H. 1954. The Dynamics and Thermodynamics of Compressible Fluid Flow. Ronald Press Co., New York p. 12-15.

Distributional Records of the Badger (*Taxidea taxus*) in Arkansas

Michael E. Cartwright
Arkansas Game and Fish Commission
P.O. Box 720
Calico Rock, AR 72519

Gary A. Heidt
Department of Biology
University of Arkansas at Little Rock
Little Rock, AR 72204

Hall (The mammals of North America, Wiley-Interscience Press. p. 1012, 1981) and Sealander and Heidt (Arkansas mammals: Their natural history, classification, and distribution. Univ. Arkansas Press. p. 308, 1990) both include the extreme northwestern portion of Arkansas in the distributional range of the badger (*Taxidea taxus*). To date, one specimen from Fayetteville, Washington County, has been documented (Sealander and Heidt, 1990). Reliable sight records have been made in Newton and Franklin counties, and each year one or two badgers from unknown localities are sold annually by Arkansas trappers. We document two additional specimen records.

An adult male badger was trapped by Charles Bonner in January 1983, 2.5 km S of the Ozark Dam (Arkansas River), Franklin County. Land use in this area consists of open pastures and turkey farms interspersed with hardwood. The soil type primarily is sandy-loam and the area contains pocket gophers (*Geomys breviceps*). Burrowing rodents, such as gophers, are major prey items of badgers (Sealander and Heidt, 1990). The presence of pocket gophers also indicates suitable soil for badger activity. This specimen currently is on display at the Arkansas Game and Fish Commission headquarters in Little Rock.

The second specimen was an adult male found as a roadkill on Highway 5 near the community of Optimus, Stone County, by U.S. Forest Service personnel on 25 August 1993. The specimen measured total length - 780mm; tail length - 150; hind foot - 110; and ear - 41. When first examined, an infestation of ticks, along with several scars and healing sores were noted. An examination of the intestinal tract revealed no helminthes or food items; badger hair, however, was present in the lower stomach and upper duodenum. This specimen has been deposited in the Vertebrate Collections at the University of Arkansas at Little Rock.

Optimus is located within the Salem Plateau and the general habitat consists primarily of upland, mixed hardwood-shortleaf pine forest interspersed by pastures. The White River is within 2 km of Optimus. There is one documented record of a gopher from Stone County (vicinity of Newnata), and directly across the river (Izard County) there are several known populations of pocket gophers. Soils along the river and at various locations within the area are shallow and characterized by silt and loam. Badger home ranges have been reported from 200-1700 ha (Lindzey, Badger, *In* Chapman and Feldhammer, eds., Wild mammals of North America, Johns Hopkins Univ. Press. pp. 653-663, 1982); distances potentially within the range of movement from the site where this specimen was found.

Although roadkill records must be evaluated with caution, we believe there is a high degree of probability that this record, although tentative, is valid. Condition and injuries were consistent with a fresh roadkill, and while there have been, to our knowledge, no previous reports of badgers in this area, habitat, soils, and presence of potential prey would indicate that a small population of badgers could be supported.

The badger is an interesting but rare and elusive member of Arkansas' mammalian fauna. More study on its distribution, particularly further confirmation in the Stone County area, is needed.

Ultrasound Assisted Oxidative Cleavage of α-Keto, α-Hydroxy and α-Halo Ketones by Superoxide

Yi hong Cao, A. Toland and D.T.C. Yang*
The University of Arkansas at Little Rock
Department of Chemistry
Little Rock, AR 72204

Potassium superoxide, an oxygen supplier and carbon dioxide scrubber, provided convenient synthetic access to oxidatively cleave α-keto, α-hydroxy, and α-halo ketones to carboxylic acids (Filippo, Jr., J. Org. Chem., 41:1077, 1976). The yields are excellent but the principal disadvantage of this method is the long reaction time required.

We now report that significant improvement in reaction times may be realized by conducting these reactions in the presence of ultrasound (Lindley, Chem. Soc. Rev., 16:275, 1987). Thus, the sonication of camphorquinone with potassium superoxide affords camphoric acid in 85% versus 87% for the same reaction without ultrasound and requires only 1.5 h instead of 24 h. Some other examples are shown in Table 1. In all cases, substantial decreases in reaction times were realized.

In a typical experiment, a dry nitrogen filled 100 mL, three-necked, round-bottomed flask was charged with 18-crown-ether (105 mg, 0.4 mmol), potassium superoxide (284 mg, 4 mmol), d,l-camphorquinone (166 mg, 1 mmol), and dry benzene (25 mL). The flask was submerged in a cold water-bath and the mixture was agitated with ultrasound (Virsonic 300, 400 watt, 20 KHz) for 1.5 hours.

Product isolation was straightforward. The crude product was poured into ice-water (30 mL). The aqueous layer was separated and acidified with 6N hydrochloric acid. The resulting solids were collected and recrystallized from ethanol-water to give 170 mg (85%) of pure camphoric acid. Each product was characterized by m.p., IR, and NMR. These spectra were identical to those of authentic samples.

Table 1.

Substrate	Product	Ultrasound		Thermal (Lit.)	
		Time (h)	Yield %	Time (h)	Yield %
Camphorquinone	Camphoric acid	1.5	85	24	87
Phenanthrenequinone	Diphenic acid	4	63	none	none
2-Chlorocyclohexanone	Adipic acid	2	76	24	60
3-Bromocamphor	Camphoric acid	3	53	24	54
Benzoin	Benzoic acid	1	83	24	98
2-Hydroxycyclohexanone	Adipic acid	3	80	24	69
Ethyl mandelate	Benzoic acid	2.5	85	24	93

Acknowledgements

We thank UALR Faculty Research Fund for partial support of the work.

Status of Endangered Gray Bat (*Myotis grisescens*) Hibernating Populations in Arkansas

Michael J. Harvey
Department of Biology
Tennessee Technological University
Cookeville, TN 38505

Sixteen bat species are endemic to Arkansas. Eight of these are cave bats, i.e., they occupy caves during all or at least part of the year (Harvey, 1986). Three Arkansas cave bat taxa are listed as endangered by both the U.S. Fish and Wildlife Service and the Arkansas Game and Fish Commission. They are *Myotis grisescens*, gray bat; *M. sodalis*, Indiana bat; and *Plecotus townsendii ingens*, Ozark big-eared bat.

I, aided by several individuals, have monitored endangered bat populations in Arkansas annually since the summer of 1978 (Harvey, 1978, 1979, 1984, 1986; Harvey and McDaniel, 1986; Harvey and Barkley, 1990; Harvey et al., 1978, 1979, 1981). The objective of this paper is to report on the current status of gray bat hibernating populations in Arkansas.

The range of the gray bat is concentrated in the cave regions of Arkansas, Missouri, Kentucky, Tennessee, and Alabama, with occasional colonies and individuals found in adjacement states (Barbour and Davis, 1969). The present total population is estimated to number ca. 1,500, 000, of which about 95% hibernate in only eight caves; two in Tennessee, three in Missouri, and one each in Kentucky, Alabama, and Arkansas.

Currently, an estimated 222,000 gray bats hibernate in four Arkansas caves; small hibernating colonies of a few hundred or less are sometimes found in a few additional caves. Although that number is 28,000 less than the 1984 estimate, it is likely that the Arkansas gray bat hibernating population has actually remained relatively stable. Gray bat hibernating colonies, especially larger colonies, are extremely difficult to estimate for several reasons. Bats may be tightly clustered, or scattered. Dense clusters are sometimes several tiers thick, and they often roost on high cave ceilings. The size and configuration of many gray bat caves also adds to the difficulty.

Bonanza Cave, located on Ozark National Forest lands in Baxter County, is one of the eight most important gray bat hibernation caves. The cave was gated in 1975 and regated in 1981 with a more suitable gate. In February 1994 the hibernating population was estimated at 165, 000. Although that number is considerably less than previous estimates of 250,000, other caves in the vicinity have shown significant increases, possibly due to movement from Bonanza Cave. A small cave located only ca. 1 km from Bonanza Cave contained an estimated 25,000 hibernating gray bats in February 1994. Prior to the winter of 1991-92, gray bats were not known to utilize this cave. Previously, usually only a few eastern pipistrelles (*Pipistrellus subflavus*) hibernated in this cave.

Prior to development by the U.S. Forest Service, Blanchard Springs Caverns in Stone County housed a gray bat hibernating colony of 5000-7000 individuals. Construction in the caverns was begun in 1963, and the cave was opened to the public in 1973. By the winter of 1978-79, the hibernating colony decreased to ca. 150 gray bats and reached a low of only 33 bats during the winter of 1985-86. Since that winter, the U.S. Forest Service has limited disturbance at the roost site, located near the natural entrance, and the bat population has increased dramatically. During the last nine winters, the population was estimated as follows: 33, 55, 188, 520, 6200, 8000, 10, 000, 18,800, and 20,000 (February 1994). The summer bachelor colony also increased to an all time high of ca. 42,000 during the summer of 1993.

Cave Mountain Cave, located on Buffalo National River lands in Newton County, houses hibernating colonies of both gray bats and Indiana bats. The greatest number of gray bats reported to hibernate in this cave prior to the winter of 1990-91 was ca. 700 during the winter of 1980-81. During the following winter (1981-82), only ca. 50 gray bats were present. To protect endangered bat colonies from disturbance, the cave was fenced during the summer of 1982 and closed to visitation during the bat hibernation period. Since the cave was fenced, the hibernating gray bat population has gradually increased to an all time high of 16,000 during the winter of 1992-93. During February 1994 the colony was estimated to number 11,700.

Thus, although the hibernating colony at Bonanza Cave may have decreased, significant increases at three other caves have kept the total Arkansas gray bat hibernating population relatively stable over the last several years. Hopefully, continued protection and management will result in removal of the gray bat from the endangered species list.

Acknowledgements

Research resulting in this publication was supported by the Arkansas Game and Fish Commission under provisions of the Federal Aid in Wildlife Restoration Act (Pittman-Robertson Act) and Section 6 of the Endangered Species Act of 1973 as amended (PL 93-205), administered by the U.S. Fish and Wildlife Service, Department of the Interior. Additional support came from the U.S. Forest Service, Ozark National Forest, and National Park Service, Buffalo National River.

Literature Cited

Barbour, R.W. and **W.H. Davis.** 1969. Bats of America. Univ. Press of Kentucky, Lexington. 286 pp.

Harvey, M.J. 1978. Status of the endangered bats *Myotis sodalis, M. grisescens* and *Plecotus townsendii ingens* in the southern Ozarks. Pp. 221-223 *In* Proc. Fifth Int. Bat Res. Conf. (D.E. Wilson and A.L. Gardner, eds.), Texas Tech Press, Lubbock. 434 pp.

Harvey, M.J. 1979. Distribution, status, and ecology of endangered bats of Buffalo National River, Arkansas. Pp. 76-84 (Vol. 8) *In* Proc. Second Conf. on Sci. Res. in the Natl. Parks. 12 Vols.

Harvey, M.J. 1984. Protection of endangered gray bat (*Myotis grisescens*) colonies in Arkansas. Arkansas Acad. Sci. Proc. 38:90-91.

Harvey, M.J. 1986. Arkansas bats: a valuable resource. Arkansas Game and Fish Comm., Little Rock. 48 pp.

Harvey, M.J. and **V.R. McDaniel.** 1986. Population decline of the endangered Indiana bat, *Myotis sodalis*, in Arkansas. Arkansas Acad. Sci. Proc., 40:87-88.

Harvey, M.J. and **S.W. Barkley.** 1990. Management of the Ozark big-eared bat, *Plecotus townsendii ingens*, in Arkansas. Arkansas Acad. Sci. Proc., 44:131-132.

Harvey, M.J., M.L. Kennedy and **V.R. McDaniel.** 1978. Status of the endangered Ozark big-eared bat (*Plecotus townsendii ingens*) in Arkansas. Arkansas Acad. Sci. Proc., 32:89-90.

Harvey, M.J., J.J. Cassidy and **G.G. O'Hagan.** 1979. Status of the endangered bats *Myotis sodalis, M. grisescens* and *Plecotus townsendii ingens* in Arkansas. Arkansas Acad. Sci. Proc., 33:81.

Harvey, M.J., J.J. Cassidy and **G.G. O'Hagan.** 1981. Endangered bats of Arkansas: distribution, status, ecology, and management. Report to Arkansas Game and Fish Commission, U.S. Forest Service, and National Park Service. 137 pp.

The Isolation of *Borrelia burgdorferi* from Infected Laboratory Mice

Lawrence W. Hinck
Department of Biological Sciences
Arkansas State University
State University, AR 72467

Kim K. Simpson
Arkansas Children's Hospital
Little Rock, AR 72202

Sherlita N. Reeves
University of Arkansas for Medical Sciences
Little Rock, AR 72202

Lyme borreliosis is a zoonosis afflicting both humans and domestic animals as well as a wide range of feral animals including a variety of small rodents, rabbits, raccoons, skunks, deer, and ground-feeding birds (Anderson et al., 1983; Anderson et al., 1985; Anderson and Magnerelli, 1984; Bosler et al., 1983; Godsey et al., 1987; Fish and Daniels, 1990; Simpson and Hinck, 1993). In the northeastern United States, where it was discovered and remains highly endemic, the epidemiology is well understood. In the southern states, cases in humans are increasingly reported, yet the vectors, reservoir hosts, and epidemiologic patterns remain less clear (Burgdorfer and Gage, 1987; Cielsielski et al., 1988).

One method commonly employed for studying the distribution in feral hosts has been the cultivation of the etiologic agent, *Borrelia burgdorferi*, from spleen, kidneys and urinary bladder (Anderson et al., 1985; Schwann et al., 1988). Schwann et al. (1988) suggested that cultivation from the urinary bladder might be the most appropriate method for sampling feral rodents since laboratory studies with white mice revealed a 94% rate of infection for that organ. Both live traps and snap traps have been employed for procuring feral animals but definitive data have not been presented to compare the two methods with regard to success rate for cultivation from tissue samples. A preliminary study conducted in our laboratory indicated that the Lyme agent could be cultivated from tissues of laboratory infected white-footed mice (*Peromyscus leucopus*) when held for as long as 8 hours post-mortem at varying temperatures.

The current study was undertaken to better define the conditions of temperature and time post-mortem that would permit realistic expectations for cultivation from trapped rodents. Laboratory white mice were injected intraperitoneally with 0.3 mL of a suspension of *Borrelia burgdorferi*, strain SH-2-82, donated by Dr. Tom Schwann. The spirochetes had been permitted to grow in BSK-II medium (Barbour, 1984; Barbour, 1986; Berger et al., 1985) until a dense growth was observed by dark field microscopy. The mice were divided into five groups with 15 mice per group. Each group was subdivided into three subgroups of five animals per group to be necropsied at zero time, 4 hours, and 8 hours post-mortem. Holding temperatures for the 4-hr and 8-hr groups ranged from 5° C to 25° C. At 4 weeks post-inoculation, the animals were sacrificed by cervical dislocation. To minimize microbial surface contamination, they were denuded with a depilatory, treated with 5.25% hypochlorite for 3 minutes followed by a sterile distilled water rinse, and finally painted with a tincture of iodine. The spleen and urinary bladder of each were aseptically removed and triturated together in 2-mL of BSK-II medium with a sterile Pyrex glass tissue homogenizer. A 1 mL sample of the extract was inoculated into a sterile screw-capped tube containing 6 mL of BSK-II medium. The tubes were incubated at 34° C and examined at weekly intervals for growth by dark field microscopy. Tubes with no growth at 4 weeks were declared negative.

Comparisons with zero time controls (Table 1) indicate that cultivation attempts were equally successful in deceased animals held as long as 8 hours post-mortem at temperatures up to 15° C. At 20° C the recovery rates were reduced to 40% and 20% for the 4-hr and 8-hr groups respectively while the zero time controls provided a rate of 80%. At 25° C no recoveries were recorded at either post-mortem holding time, with the controls producing an 80% recovery once again.

Table 1. Cultivation of *Borrelia burgdorferi* from the spleen and urinary bladder of infected laboratory white mice.

		Recovery Rates at Different Holding Times		
Holding Temperature (Celsius)	Hours:	0	4	8
5		4/5	3/5	4/5
10		3/5	4/5	3/5
15		4/5	3/5	4/5
20		4/5	2/5	1/5
25		4/5	0/5	0/5

The data suggest that snap traps can be utilized with a high probability of providing isolation of *B. burgdorferi* from tissues of infected feral animals when ambient temperatures are fairly cool. The use of snap traps during warmer months would require frequent monitoring so that deceased animals could be removed and necropsied at once. Animals taken during these periods would likely yield better results if live-trapping were employed.

Literature Cited

Anderson, J.F., L.A. Magnarelli, W. Burgdorferi and **A.G. Barbour.** 1983. Spirochetes in *Ixodes dammini* and mammals from Connecticut. Am. J. Trop. Med. Hyg. 32 (4) :818-824.

Anderson, J.F., R.C. Johnson, L.A. Magnerelli and **F.W. Hyde.** 1985. Identification of endemic foci of Lyme disease: isolation of *Borelia burgdorferi* from feral rodents and ticks (*Dermacentor variabilis*). J. Clin. Micro. 22(1) :36-38.

Anderson, J.F. and **L.A. Magnerelli.** 1984. Avian and mammalian hosts for spirochete-infected ticks and insects in a Lyme focus in Connecticut. Yale J. Biol. Med. 57:627-641.

Barbour, A.G. 1984. Isolation and cultivation of Lyme disease spirochetes. Yale J. Biol. Med. 57:521-525.

Barbour, A.G. 1986. Cultivation of *Borrelia*: a historical overview. Zentralbl. Bakt. Mikr. Hyg. A263:11-14.

Berger, B.W., M.H. Kaplan, I.R. Rothenberg and **A.G. Barbour.** 1985. Isolation and characterization of the Lyme disease spirochete from the skin of patients with erythema chronicum migrans. J. Am. Acad. Dermatol. 13:444-449.

Bosler, E.M., J.L. Coleman, J.L. Benach, D.A. Massey, J.P. Hanrahan, W. Burgdorfer and **A.G. Barbour.** 1983. Natural distribution of the *Ixodes dammini* spirochete. Science 220:321-322.

Burgdorfer, W. and **K.L. Gage.** 1987. Susceptibility of the hispid cotton rat (*Sigmodon hispidis*) to the Lyme disease spirochete (*Borrelia burgdorferi*). Am J. Trop. Med. Hyg. 37 (3) :624-628.

Cielsielski, C.A., L.E. Markowitz, R. Horsley, A.W. Hightower, H. Russell and **C.V. Broome.** 1988. The geographic distribution of Lyme disease in the United States. Ann. NY Acad. Sci. 539:283-288.

Fish, D. and **T.J. Daniels.** 1990. The role of medium-sized mammals as reservoir hosts of *Borrelia burgdorferi* in southern New York. J. Wildl. Dis. 26(3) :339-345.

Godsey, M.S., T.E. Amundsen, E.C. Burgess, W. Schell, J.P. Davis, R. Kaslow and **R. Edelmen.** 1987. Lyme disease ecology in Wisconsin: distribution and host preferences of *Ixodes dammini*, and prevalence of anti body to *Borrelia burgdorferi* in small mammals. Am. J. Trop. Med. Hyg. 37 (1) :180-187.

Schwann, T.G., W. Burgdorfer, M.E. Schrumpf and **R.H. Karstens.** 1988. The urinary bladder, a consistent source of *Borrelia burgdorferi* in experimentally infected white-footed mice (*Peromyscus leucopus*). J. Clin. Micro. 26 (5) :893-895.

Simpson, K.K. and **L.W. Hinck.** 1993. The prevalence of *Borrelia burgdorferi*, the Lyme disease spirochete, in ticks and rodents in northeast Arkansas. Proc. Arkansas Acad. Sci. 47 :110-115.

Species of Birds Newly Recorded in Arkansas Since 1985

Douglas A. James
Department of Biological Sciences
University of Arkansas
Fayetteville, AR 72701
Charles Mills
P.O. Box 145
Ogden, AR 71853

Max Parker
2426 S. Main
Malvern, AR 72104
Joseph C. Neal
Poteau Ranger District
USDA Forest Service
P.O. Box 2255
Waldron, AR 72958

The number of bird species recorded in Arkansas has been increasing since early this century due mainly to changing patterns of avian distribution and to progressively increased coverage of the state by devotees to bird study. James and Neal (1986) summarized the results of previous compilations and reported that the first monograph on Arkansas birds (Howell, 1911) listed 242 species for the state. The next monograph (Wheeler, 1924) named 272 species, although as explained in James and Neal (1986) some of these should not have been included. Then Baerg (1931, 1951) published two treatises including 277 and 324 species respectively. The most recent study (James and Neal, 1986) named 366 bird species recorded in the state. Now 14 more have been found increasing the Arkansas list to 380.

In this paper we list the 14 new species and describe the particulars concerning their discovery. In most cases photographs were made, some specimens were obtained, and for each first record a documentation form was completed and placed in the file of Arkansas bird records maintained by the Arkansas Audubon Society (AAS). The forms include the particulars of the sightings and details of the birds seen and are designated by AAS number in the text below. The photographs also are filed with the Audubon Society, often several for each bird, but we name only the photographer(s) whose results provide the primary documentation for the species concerned. All these new Arkansas species were accepted by the committee of the Arkansas Audubon Society that approves unusual bird records for the state.

This annotated list of added species includes 7 water birds, a group that is well known for strong flight and vagrant distributions. The other 7 species are land birds, 4 of which are hummingbirds. Hummingbirds have been increasingly vagrant in recent years. The remaining 3 are 2 dove species that are expanding their ranges and a songbird that characteristically is a wanderer.

Pacific Loon.--(*Gavia pacifica*). There are four records of this species. The first one was found by Bo and Don Verser on the first nursery pond next to Greer's Ferry Lake near the town of Greer's Ferry, Cleburne County, on 25 May 1991 where it remained through 1 June 1991 and was seen by many people. It was in adult winter plumage with a conspicuous chinstrap marking, was documented by AAS form No. 823, and was photographed by Max Parker. The second record, a bird in first winter plumage, was near the dam site in Beaver Lake, Carroll County, on 21 November 1991 where it was seen by Charles Mills (AAS No. 831). The third bird was found by Don Simons on 6 February 1993 on Lake Chicot at Lake Village in Chicot County (AAS 851) and was last seen on 1 April 1993. The final record also was at Lake Chicot found by Don Simons this time on 8 February 1994 where it stayed through 20 February 1994 (AAS No. 856). The chinstrap marking also was well developed in this bird. [This taxon, formerly conspecific with the Arctic Loon, *Gavia arctica* (American Ornithologists' Union, 1983), now has been given species status (American Ornithologists' Union, 1985)].

Yellow-billed Loon.--(*Gavia adamsii*). An individual of this species in immature plumage was discovered by Mike Mlodinow just above the dam site in Beaver Lake, Carroll County, on 19 November 1991 (AAS No. 827). It was also seen on 21 and 30 November by several others and photographed by Max Parker.

Brant.--(*Branta bernicla*). Jeff Wilson found a single Brant on 13 January 1990 at a location east of Turrell, Crittenden County, near the Wapanocca National Wildlife Refuge (AAS No. 785). Charles Mills and Max and Helen Parker were present too and agreed with the identification.

Wilson's Plover.--(*Charadrius wilsonia*). A single bird was found by Nigel Ball on 18 May 1986 at the fish hatchery operated by the Arkansas Game & Fish Commission located just south of Centerton, Benton County. It was seen later by other observers on 21 and 24 May. Photographs were made by Max Parker and the sighting is documented by form AAS No. 675.

Common Black-headed Gull.--(*Larus ridibundus*). There have been two occurrences of this gull. The first (AAS No. 805) was a bird in adult plumage observed by Charles Mills at Millwood Lake, Little River County, on 29

December 1990. It was seen again by many viewers on 2, 5, and 8 January 1991 and photographed by Jeff Wilson. The second bird, in first winter plumage, was found by Don Simons at Lake Chicot, Chicot County, on 8 January 1991 (AAS No. 808).

Lesser Black-backed Gull.--(*Larus fuscus*). A lone bird of this species was first observed by Don Simons on 6 February 1994 on Lake Chicot at Lake Village, Chicot County, and photographed by him (AAS No. 857). The bird, which was in nearly adult plumage, was seen by others on several dates through 18 February.

Royal Tern.--(*Sterna maxima*). The Arkansas County record on 26 August 1950 mentioned in Baerg (1951) was omitted by James and Neal (1986). Also omitted was an old report included in the Audubon Society file describing two Royal Terns sighted by Brooke Meanley on 28 September 1951 at a place know as Tindall's in Arkansas County. More recently, on 14 and 15 June 1986, another individual of this species appeared in Arkansas this time at minnow raising ponds west of Lonoke, Lonoke County, where it was found by Max and Helen Parker and viewed by others (AAS No. 681, photographed by Helen and Max Parker). This female bird was found dead there (shot) on 17 June 1986. A specimen was prepared and deposited in the collection of The University Museum, University of Arkansas at Fayetteville (cat. no. 88-51-1).

Because this species was not included in James and Neal (1986) the three records mentioned here represent an addition to the list of Arkansas birds included in their monograph. Supporting the action taken by Baerg (1951) this returns the Royal Tern to the state list.

Eurasian Collared-Dove.--(*Streptopelia decaocto*). This new species for Arkansas was present in Harrison, Boone County, from 25 June to 1 August 1989 in Martha Milburn's yard (AAS No. 854) where it was photographed by Max Parker. On 17 August it was found dead, feathers plucked and carcass consumed, apparently killed by a predator. The feathers were sent to Roxie Laybourne of the Smithsonian Institution, Washington, D.C., who confirmed that the bird was an Eurasian Collared-Dove.

It has been established (Smith, 1987) that the Eurasian Collard-Dove is a different species from the caged bird available at pet stores known as the Domestic Collared-Dove (*S. 'risoria'*), which is derived from a wild species called the African Collared-Dove (*S. roseogrisea*). This similarity of forms has led to the mistaken belief that the appearance of ringed-doves at various places around the USA has been the result of escapees of the domestic caged variety. In reality, Eurasian Collared-Doves are seldom if ever found caged because dove fanciers are not raising them in captivity (Smith 1987). A rare exception to this situation (Smith 1987) resulted in the establishment of wild Eurasian Collared-Doves in the Bahama Islands after 1974 when a bird breeder's aviary there was ransacked. From there they reached Florida in the late 1970's (Smith, 1987), and by 1991 occurred in all corners of the state (Hengeveld, 1993). There are now numerous outlying records in Georgia, Alabama, and Louisiana (M. Parker, pers. comm.), and this first Arkansas record fits this pattern. This is the same pattern of outlying bridgeheads the European Collared-Dove utilized beginning in the 1920's when it spread outward from its original range in Asia to occupy all of Europe by the 1980's (Hengeveld, 1993). This was stated by Nowak (1971) to be "the most impressive example...of the expansion of an animal species" in his comprehensive treatise on range expansions in animals. The repeat of this phenomenon seems to be in progress in North America and the opportunity now exists to monitor its spread through Arkansas.

The last Check-list of North American Birds (American Ornithologists' Union, 1983) named this species the Ringed Turtle-Dove (*Streptopelia risoria*), but in a recent supplement (American Ornithologists' Union, 1989) it has been changed to Eurasian Collared-Dove (*Streptopelia decaocto*).

White-winged Dove.--(*Zenaida asiatica*). On 8 April 1994, Jean and Jim Niemyer observed a White-winged Dove in their yard in El Dorado, Union County (AAS No. 860). The conspicuous white wing patches and other diagnostic characteristics of the species were noted.

Buff-bellied Hummingbird.--(*Amazilia yucatanensis*). In Searcy, White County, an individual of this species in immature plumage arrived at the hummingbird feeder maintained by T.R. and Doris Garner on 12 November 1992 and stayed through 10 March 1993. It was first identified by Roberta Crabtree, subsequently seen by many others (AAS No. 844), and photographed by Helen and Max Parker.

Magnificant Hummingbird.--(*Eugenes fulgens*). An adult male bird was discovered by Donald and Dolores Harrington on 18 July 1993 at their hummingbird feeder in Arkadelphia, Clark County (AAS No. 850). Although present only one day, its occurrence was verified by other observers and it was photographed by Charles Mills.

Black-chinned Hummingbird.--(*Archilochus alexandri*). There are four records for this species. The first one was an immature male bird in El Dorado, Union County, at Luvois and Shug Shugart's feeder seen between 7 November 1987 and 27 January 1988 by numerous observers (AAS No. 727). The second one was an immature male in North Little Rock, Pulaski County, from 21-27 December 1987 identified by Helen Parker (AAS No. 723) and photographed by Max Parker. The third record was an immature male at a feeder in Little Rock, Pulaski County, from 18 December 1992 through 28 March 1993, seen by many competent observers and photographed by Perk Floyd. It also was trapped, closely inspected, banded

and released by Perk Floyd and Bill Baltosser. The fourth one was in Hope, Hempstead County, at Mrs. Bob Brown's residence from about 26 October 1993 to when last seen on 20 March 1994. It was trapped, banded, and released by Perk Floyd and was photographed by Max Parker.

Anna's Hummingbird.--(*Calypte anna*). Two sightings of this species have been reported. The first was an adult female bird at a hummingbird feeder in Gillett, Arkansas County, from 27-30 January 1988, identified by Helen Parker (AAS No. 726), photographed by Max Parker, and seen by other experienced observers. The second one, found by Donna Adams and viewed by others, also was an adult female but at a feeder in Conway, Faulkner County, from 15 November 1992 through 8 March 1993 (AAS No. 843). It was photographed by Perk Floyd and trapped, closely inspected, banded, and released by Floyd and Bill Baltosser. Baltosser collected a 5th rectrix and 3 magenta gorget feathers that now are kept in the Department of Biology, University of Arkansas at Little Rock.

Northern Wheatear.--(*Oenanthe oenanthe*). This is the only songbird represented in this list. It was found by Helen and Max Parker near Okay Landing at Millwood Lake, Howard County, on 18 October 1990 (AAS No. 799) and seen by many others daily through 21 October. It was photographed by Helen and Max Parker and Jeff Wilson and was representative of the eastern form (*O. o. leucorrhoa*) in first winter plumage.

Literature Cited

American Ornithologists' Union. 1983. Check-list of North American birds, 6th edition. American Ornithologists' Union, Washington, D.C.

American Ornithologists' Union. 1985. Thirty-fifth supplement to the American Ornithologists' Union check-list of North American birds. Auk 102:680-686.

American Ornithologists' Union. 1989. Thirty-seventh supplement to the American Ornithologists' Union check-list of North American birds. Auk 106:532-538.

Baerg, W.J. 1931. Birds of Arkansas. Univ. Arkansas Agric. Exp. Sta., Bull. no. 258, 197 pp.

Baerg. W.J. 1951. Birds of Arkansas. Univ. Arkansas Agric. Exp. Sta., Bull. no. 258 (Rev.), 187 pp.

Hengeveld, R. 1993. What to do about the North American invasion by the Collared Dove? J. Field Ornith. 64:477-489.

Howell, A.H. 1911. Birds of Arkansas. U.S. Dept. Agric., Biol. Surv. Bull. no. 38, 100 pp.

James, D.A. and **J.C. Neal.** 1986. Arkansas birds, their distribution and abundance. Univ. Arkansas Press, Fayetteville, 402 pp.

Nowak, E. 1971. The range expansion of animals and its causes. Zeszty Naukowe 3:1-255.

Smith, P.W. 1987. The Eurasian Collared-Dove arrives in the Americans. Amer. Birds 41:1371-1379.

Wheeler, H.E. 1924. The birds of Arkansas. State Bureau Mines, Manufactures, Agric., Little Rock, 184 pp.

An Effective, Reliable, Inexpensive Cryofixation Device

Lawrence A. Mink and Roger A. Buchanan
Department of Chemistry, Biochemistry and Physics
and Department of Biological Sciences
Arkansas State University
State University, AR 72401

Cryofixation provides a unique method for the preparation of biological specimens that does not introduce the artifacts (chemical substitution, and significant dimensional changes) associated with standard chemical fixation procedures (see Kellenberger et al., 1987). Cryofixation, because of millisecond cooling, produces amorphous (or microcrystalline) ice so that morphological characteristics and elemental location are not modified by ice crystal formation (Van Harreveld and Crowell, 1964; Heuser et al., 1976; Angell and Choi, 1986). Ultrathin cryosections can then be cut from frozen tissue samples and transferred to a liquid nitrogen-cooled cold stage. Elemental analysis of subcellular compartments in these tissue sections can be completed using X-ray microanalysis or electron energy loss spectroscopy in an appropriately configured analytical electron microscope (Buchanan et al., 1993; Leapman et al., 1993). Alternatively, frozen tissue can be prepared by freeze drying or freeze substitution for more conventional transmission or scanning electron microscopy (Buchanan et al., 1988; Landis and Reese, 1983).

We will describe the design, construction, and operation of a cryofixation device that can be produced on a limited budget. Similar commercially produced cryofixation devices are available for approximately $30,000 [one device is available from RMC, Inc. of Tucson, AZ]. We have constructed a very satisfactory similar device in our laboratory for < $4,000, including over $1,000 for the mechanical vacuum pump. We utilized readily available quick-connect vacuum components and a limited amount of machining and welding of the type that is locally available at any machine shop.

Our device (Fig. 1), like some other laboratory and commercial cryofixation devices, consists of a LN_2 (Liquid Nitrogen) cooled cold finger maintained in a vacuum (<10 mTorr). This reduces LN_2 usage and prevents condensation on specimen cooling surface at the cold finger end. Dry pressurized N_2 is used to operate pneumatic valves and cylinders of our device and is introduced to break the vacuum. Electrically operated valves control the N_2 flow.

Commercially available quick-connect vacuum components were used to construct the vacuum chamber. These components include a 6-way quick-connect "T" (ISO #NW40, US 1.5" Series, available from MDC Vacuum Products of Hayward, CA), thermocouple and electrical feed quick-connects, and Al quick-connect blanks that were tapped to accept vacuum gauge, N_2 inlet, cold finger and shutter pneumatic shaft. One of the O-ring metal spacer assemblies was ground flat on one side so that the shutter could slide perpendicular to the "T". The aluminum supporting structure was welded from plate. The copper cold finger was turned on a lathe from electrical purity Cu rod stock (standard 1-1/8" (2.86cm) OD stock). This cold-finger was also bored for the LN_2, tapped for the cooling surface on one end and on the other end for the LN_2 inlet and outlet connections. The replaceable cooling surfaces can be constructed on the lathe from the same (or smaller) Cu rod. Several of the Cu cooling surfaces may then be mounted in tapped holes on a piece of standard 1 by 1" (2.54 by 2.54 cm) steel stock and cheaply ground flat at a local machine shop. Simple power buffing may be used to produce a highly polished cooling surface. These replaceable cooling surfaces can be protected from chemical etching by Au or Pt plating, as are the commercially prepared varieties (RMC, Inc.).

During operation, (Fig. 1), the vacuum-surrounded cold finger cooling surface is first cooled by LN_2 flowing into and out of the cold finger. When the freezing surface is sufficiently cooled (thermocouple attached near the cooling surface), the specimen, after being placed on an aluminum planchet, is affixed using two-sided tape to a foam rubber cube that is then attached to the vertical pneumatic driver rod. The horizontal pneumatically-actuated shutter is then opened in conjunction with the introduction of dry N_2 via an electric valve to break the vacuum. This exposes the cooling surface that is located just above the shutter inside the vacuum chamber. Immediately, the vertical pneumatic cylinder is activated to drive the specimen against the cold surface where it freezes in milliseconds. The pneumatic pressure maintains good thermal contact between the specimen and the cooling surface and prevents bouncing. The foam cube absorbs some of the shock and prevents specimen compression. After freezing, the cryofrozen specimen is grasped with LN_2 cooled tweezers and rapidly transferred to a LN_2 holding container. The shutter is then re-closed (the re-opened vacuum quickly pulls the shutter leak-tight) to limit condensation on the freezing surface.

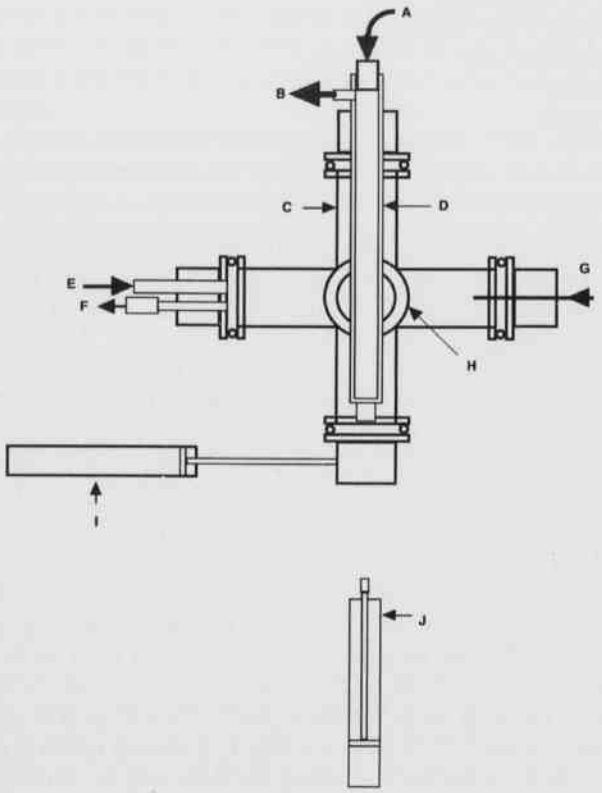

Fig. 1. Arrangement of parts of Cryogenic Fixation Device on a vertical Aluminum plate. Parts: A: LN_2 inlet; B: N_2 & LN_2 outlet; C: 6-way vacuum quick-connect "T"; D: Hollow Copper Cold finger with attached freezing surface; E: Dry N_2 inlet; F: Vacuum gauge; G: Heater-tape power connections; H: fifth (back) and sixth (front) ports for vacuum and thermoccuple, respectively; I: Pneumatic cylinder to open/close shutter; J: Pneumatic cylinder that drives specimen onto freezing surface.

Accumulated ice on the freezing surface is removed by a vacuum-heating cycle: restore vacuum, stop LN_2 flow, heat cold finger end and cooling surface with an electric heat tape while pumping the vacuum. The LN_2 flow is then re-established to re-cool the cold finger and attached cooling surface in preparation for the next specimen.

We expect our cryofixation device to serve many investigators at ASU. We experienced only minor construction problems. First, finding U-bolts and constructing supports to attach and "T" to the A1 frame took longer than expected. Second, positioning of the shutter pneumatic cylinder and the specimen pneumatic cylinder was by eye, not by pre-measure! Third, the length of the Cu cold finger was a trial and adjust procedure. Fourth, the cold hardened the O-ring seal closest to the cold finger causing it to leak. As a result, we redesigned the A1 blank holding the cold finger for maximum thermal resistance and may add a heat tape at the troublesome joint. Finally, should we construct another cryofixation device from scratch, we would use a larger diameter vacuum "T" and a thicker A1 frame.

We would caution all who are considering constructing similar devices that the electro-pneumatic controls should be designed to require two-handed operation because the pneumatic cylinders exert sufficient force to maim careless fingers!

Acknowledgements

Partial funding for this project was provided by ASU and by ASTA grant # 94-B-03.

Literature Cited

Angell, C.A. and **Y. Choi.** 1986. Crystallization and vitrification in the aqueous system. J. Microsc. 141:251-260.

Buchanan, R.A., R.C. Wagner, S.B. Andrews and **J. Frøjkaer-Jensen.** 1988. Effect of section thickness on the morphological characterization of the vesicular system. Microvasc. Res. 35:191-196.

Buchanan, R.A., R.D. Leapman, M.F. O'Connell, T.S. Reese and **S.B. Andrews.** 1993. Biological applications of the field-emission STEM: subcellular structure and analysis in ultrathin tissue cryosections. J. Struct. Biol. 110(3) :244-255.

Heuser, J.E., T.S. Reese and **D.M.D. Landis.** 1976. Preservation of synaptic structure by rapid freezing. Cold Spring Harbor Symp. Quant. Biol. 15:17-24.

Kellenberger, E., E. Carlmalm and **W. Villiger.** 1987. Physics of the preparation and observation of specimens that involve cryoprocedures. *In*: The science of biological specimen preparation for microscopy and microanalysis. (M. Müller, R.P. Becker, A. Boyde and J.J. Wolosewick, Eds.,) Scanning Electron Microscope, Inc., O'Hare, IL. pp 1-20.

Landis, D.M.D. and **T.S. Reese.** 1983. Cytoplasmic organization in cerebellar dendritic spines. J. Cell Biol. 97:1169-1178.

Leapman, R.D., J.A. Hunt, R.A. Buchanan and **S.B. Andrews.** 1993. Measurement of low calcium concentrations in cryosectioned cells by parallel-EELS mapping. Ultramicrosc. 49:225-234.

Van Harreveld and **J. Crowell.** 1964. Electron microscopy after rapid freezing on a metal surface and substitution fixation. Anat. Res. 149:381-386.

Long-Range Dispersal of a Red-cockaded Woodpecker

Warren G. Montague and George A. Bukenhofer
Poteau Ranger District - Ouachita National Forest
USDA Forest Service
P.O. Box 2255
Waldron, AR 72958

The Red-cockaded Woodpecker (*Picoides borealis*) is a federally listed endangered species of limited distribution in Arkansas (James et al., 1981; James and Neal, 1986, 1989) and Oklahoma (Masters et al., 1989). The two populations represented in the shortleaf pine (*Pinus echinata*) forests of the Ouachita Highlands are the Ouachita National Forest (Ouachita NF) population (Neal and Montague, 1991) and the McCurtain County Wilderness Area (McCurtain CWA) population which is managed by the Oklahoma Department of Wildlife Conservation (ODWC, 1991; Kelley et al., 1993). Banding activities necessary to provide information about movements of individual *P. borealis* and relationships between individual *P. borealis* or groups of *P. borealis* began in 1990 on the Ouachita NF and in 1992 in the McCurtain CWA.

A female *P. borealis* was banded as a nestling with a numbered metal band on 14 May 1992 at cluster #109 in the McCurtain CWA. This site (34°18.33'N, 94°42.53'W) is 17.7 km south of Watson, Oklahoma. This woodpecker was recaptured and plastic colored leg bands were attached on 5 November 1992. The 5 November 1992 recapture data was the last time the bird was observed at her natal cavity tree cluster. On 20 August 1993 during routine monitoring activities in compartment 1261/stand 8 (34°48.33'N, 94°10.88'W) of the Ouachita NF, we captured this 15 month-old female where she roosted in a cavity tree cluster with another *P. borealis* pair. She was subsequently observed on 22 November 1993 at a previously inactive cavity tree cluster in compartment 1261/stand 7 (34°48.25'N, 94°11.44'W) 0.9 km northwest of this pair. Extensive resin well work on her roost cavity tree suggested that she had moved into this previously inactive cavity tree cluster well before her presence was detected. This discovery documents a dispersal of 73.6 km for this bird (Fig. 1). All site locations were determined using the global positioning system with an accuracy of +/- 100 m. Sometime prior to 29 December 1993, the female from McCurtain County, Oklahoma, was joined by a male *P. borealis*, which had been released at a site 2.4 km west of this cavity tree cluster on 17 November 1993. He had been captured on the Kisatchie National Forest in Louisiana and was translocated as part of a two-bird group-reinitiation attempt (Montague, unpubl.). This newly formed pair remained together as recently as 3 March 1994.

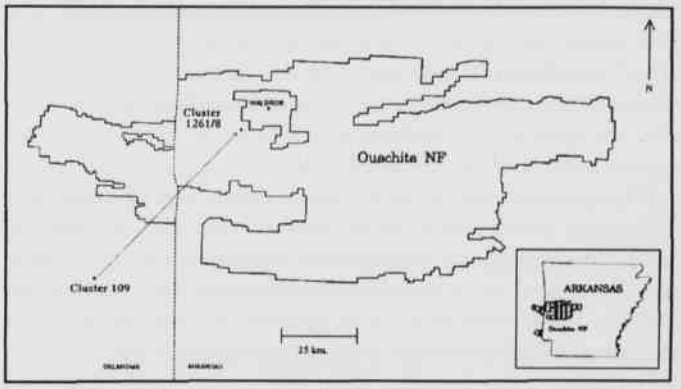

Fig. 1. Seventy-four km dispersal of *P. borealis* from McCurtain County, Oklahoma (cluster 109) to Scott County, Arkansas (Poteau Ranger District cluster 1261/8).

Long distance dispersals of *P. borealis* have been documented in other studies. Such distances include 30.1 km for a male in South Carolina (Jackson, 1990), approximately 80 km for a male in Texas (R.N. Conner, pers. comm.), and 90 km for a female in North Carolina (Walters et al., 1988). Walters (1991) reported maximum dispersal distances of 31.5 km for fledgling females, 21.1 km for fledgling males, and 17.1 km for helper males in the Sandhills of North Carolina. Lay (1973) reported a dispersal of 41.8 km by a helper male in Texas.

Ouachita NF dispersal distances from natal cavity tree clusters of 12.9 km and 15.3 km have been recorded for males, and 8 km, 15.3 km, and 20.2 km have been recorded for females (Ouachita NF unpubl. data). Also documented was a dispersal distance of 13.3 km by a 34-month-old female across the U.S. Highway 71 corridor near Waldron, Arkansas.

The *P. borealis* dispersals we describe here have significant biological and management implications. Dispersal information becomes critical to maintaining sufficient genetic variability within a population (Reed et al., 1988; Haig et al., 1993) and in determining effective population size (Reed et al., 1993). Population viability assessments

of either the Ouachita NF or McCurtain CWA subpopulations necessitate consideration of gene flows from neighboring subpopulations when evaluating potential losses of genetic variability (Reed et al., 1993).

Translocation of individual *P. borealis* identified as surplus to the reproductive needs of their groups of origin is one technique recommended to expedite population growth and to foster increasing genetic variability (Stangel et al., 1992; Haig et al., 1993). Translocations typically involve juvenile females, or juvenile males when at least one helper male would remain with the breeding pair. Such translocations may take place in one of two forms: first, as single-bird augmentations, when single surplus males or females are moved to a cluster with an already established individual of the opposite sex; second, as two-bird group-reinitiations in which male/female pairs of surplus individuals are moved to suitable, unoccupied habitat (Allen et al., 1993).

The occurrence of long distance, natural dispersals of *P. borealis* should help allay fears about the wisdom of future translocations. In this case opportunities to translocate *P. borealis* between the Ouachita NF and McCurtain CWA subpopulations should become a high priority for cooperation between the administering agencies.

Acknowledgements

We thank William Shepherd, John Skeen, Joseph Neal, and Ron Masters for their helpful input concerning various drafts of the manuscript.

Literature Cited

Allen, D.H., K.E. Franzreb and **R.E.F. Escano.** 1993. Efficacy of translocation strategies for Red-cockaded Woodpeckers. Wildl. Soc. Bull. 21:155-159.

Haig, S.M., J.R. Belthoff and **D.H. Allen.** 1993. Population viability analysis for a small population of Red-cockaded Woodpeckers and an evaluation of enhancement strategies. Conservation Biology 7:289-301.

Jackson, J.A. 1990. Intercolony movements of Red-cockaded Woodpeckers in South Carolina. J. Field Ornithol. 61:149-155.

James, D.A., D.L. Hart and **F.L. Burnside.** 1981. Study of the Red-cockaded Woodpecker in Arkansas. Final Report for Ark. Game and Fish Comm., Project E-1-5 (Job II), 143 pp.

James, D.A. and **J.C. Neal.** 1986. Arkansas birds, their distribution and abundance. Univ. of Arkansas Press, Fayetteville. 402 pp.

James, D.A. and **J.C. Neal.** 1989. Update of the status of the Red-cockaded Woodpecker in Arkansas. Final Report to the Ark. Game and Fish Comm. (Proj. E-1). 18 pp.

Kelley, J.F., S.M. Pletschet and **D.M. Leslie, Jr.** 1993. Habitat associations of Red-cockaded Woodpecker cavity trees in an old-growth forest of Oklahoma. J. Wildl. Manage. 57:122-128.

Lay, D.W. 1973. Red-cockaded Woodpecker study. Texas Parks and Wildlife Department. Project W-80-R-16. 33 pp.

Masters, R.E., J.E. Skeen and **J.A. Garner.** 1989. Red-cockaded Woodpecker in Oklahoma: an update of Wood's 1974-77 study. Proc. Okla. Acad. Sci. 69:27-31.

Neal, J.C. and **W.G. Montague.** 1991. Past and present distribution of the Red-cockaded Woodpecker and its habitat in the Ouachita Mountains in Arkansas. Proc. Arkansas Acad. Sci. 45:71-75.

Oklahoma Department of Wildlife Conservation. 1991. McCurtain County Wilderness Area management plan. (Jan. 1991). 39 pp.

Reed, J.M., P.D. Doerr and **J.R. Walters.** 1988. Minimum viable population size of the Red-cockaded Woodpecker. J. Wildl. Manage. 52:385-391.

Reed, J.M., J.R. Walters, T.E. Emigh and **D.E. Seaman.** 1993. Effective population size in Red-cockaded Woodpeckers: population and model differences. Conservation Biology 7:302-308.

Stangel, P.W., M.R. Lennartz and **M.H. Smith.** 1992. Genetic variation and population structure of Red-cockaded Woodpeckers. Conservation Biology 6:283-292.

Walters, J.R. 1991. Application of ecological principles to the management of endangered species: the case of the Red-cockaded Woodpecker. Annu. Rev. Ecol. Syst. 22:505-523.

Walters, J.R., S.K. Hansen, J.H. Carter, III, P.D. Manor and **R.J. Blue.** 1988. Long-distance dispersal of an adult Red-cockaded Woodpecker. Wilson Bull. 100:494-496.

First Record of *Leptodora kindti* in Dardanelle Reservoir and Status of Other Recent Additions to Dardanelle Fauna

John D. Rickett and Robert L. Watson
Department of Biology
University of Arkansas at Little Rock
Little Rock, AR 72204

One of the first reports on the zooplankton in Dardanelle Reservoir, Arkansas, was that of Palko (1970). His list of taxa included the usual rotifers, cladocerans, and copepods. Since 1968 personnel in the Biology Department, University of Arkansas at Little Rock have collected zooplankton samples from the reservoir in association with the construction and operation of Arkansas Power and Light's nuclear generating station (now being operated by Energy Corporation). Rickett and Watson (1983, 1993) reported several genera of rotifers, copepods, and the cladocerans, *Daphnia* sp., *Ceriodaphnia lacustris, C. quadrangula, Bosmina longirostris,* and *Diaphanosoma* sp. We believe this is the first documentation of *Leptodora kindti* in Dardanelle Reservoir and in the main stem of the Arkansas River. Although zooplankton in the Arkansas River have not been exhaustively studied, we feel this record represents a fairly recent range extension from northeast Oklahoma from the Neosho-Grand Rivers drainage basin into the Arkansas River. Researchers at Arkansas Tech University have not documented any large, unusual planktonic organisms in their mid-water trawls for larval fish (C. Gagen, pers. comm.).

Zooplankton samples were taken and handled according to methods described by Rickett and Watson (1992). After a single *L. kindti* was found in a subsample from Station 16 (intake) on 10 June 1993, the remainder of the sample was visually examined in the vial, but no additional specimens were apparent. This specimen was 3.2 mm long and was stained with a 1.0% rose bengal solution and permanently mounted on a standard microscopic slide. None of the samples taken at four other stations on the reservoir contained *Leptodora*.

Leptodora kindti is a large (up to 12 mm long) predatory cladoceran and can usually be seen in a sample without the aid of a microscope. Most reference books (Edmondson 1959; Pennak 1989) state *Leptodora* exhibits only a distribution across northern states, but a search of the available literature (summarized in Table 1) revealed several fairly recent reportings of *Leptodora* in this geographic region. Three hypotheses emerged from these references.

Conner and Bryan (1983) reported that Bryan and colleagues collected *Leptodora* from the lower Mississippi River first in 1973 while conducting an environmental survey for Gulf States Utilities Company, Baton Rouge, LA. They also noted that *Leptodora* was collected from the Atchafalaya River by Binford in 1975 while collecting samples for masters thesis research. Collections began including *Leptodora* shortly after they began sampling for fish larvae and other macroplankton with a large-mouth, 0.505 mm mesh net. Between 1973 and the early 1980s, it was taken at least once a year usually in June and July, but as early as March and as late as November. Specimens from 3-10 mm have been taken, indicating local reproduction; smaller ones were usually taken in late summer and autumn. Population densities ranged from 3-25 per 100 m^3 of water. Citing a paper by Shindler (1969, Jour. Fish. Res. Bd. Can., 26: 1948-1955), they hypothesized that small-mouthed, fine-meshed nets, used almost exclusively for limnological work prior to 1970, were selective against the larger, strong-swimming zooplankters. Still, aside from its ephemeral presence and low densities, it seems probable that a few should have been collected prior to 1970 if it has been present in this geographic region all the while.

Table 1. Recent records of *Leptodora kindti* in the Midwest and South.

Applegate and Mullan (1969)	–north Arkansas, 1967 Bull Shoals Reservoir
Conners and Bryan (1983) Sw. Nat. 28:118	–southeastern Louisiana, 1973 Mississippi River
	–southcentral Louisiana, 1975 Atchafalaya River
Kring et al., (1976)	–southeast Kansas, 1974, 75 Toronto and Fall River Reservoirs
	–southwest Missouri, data unknown Tablerock Reservoir
Holt et al., (1978)	–northeastern Oklahoma, 1975 Grand Lake
	–southeastern Oklahoma, 1975 Lake Texoma
Prophet (1978)	–northcentral Kansas, data unknown Lovewell Reservoir
	–central Kansas, date unknown Lyon County State Lake
Roseberg and Moen (1981)	–southwest Arkansas, 1979 Lake DeGray
Rickett and Watson (1994) Proc. Ark. Acad. Sci.	–westcentral Arkansas, 1993 Dardanelle Reservoir

Kring et al. (1976) reported *Leptodora* from Toronto and Fall River Reservoirs in the Verdigris River basin in southeastern Kansas. Both bodies of water were small with moderately high turbidity, and *Leptodora* was in samples from July 1974 and June, July, and October 1975. It composed less that 1% and less than 0.1% of the zooplankton community in Toronto and Fall River Reservoirs, respectively. Its route of introduction was not known, and they suggested it has been in this area longer than collecting records indicate. Kring et al. (1976) also cited personal communication with R. Anderson indicating *Leptodora* has been collected from Tablerock Reservoir in southwestern Missouri.

Prophet (1978) followed up on the Kring et al. (1976) study and reported *Leptodora* also from Lovewell Reservoir and Lyon County State Lake. In 1976 it was present in some samples between 11 May and 10 October and in all samples between 11 June and 1 October. Prophet (1978) hypothesized the plankter was brought into Kansas with fish stocking activities and was spread locally the same way.

Holt et al. (1978) reported *Leptodora* from the Neosho River, of the Grand River system in southeastern Kansas and northeastern Oklahoma, from Grand Lake itself, and from Lake Texoma on the main stem of the Red River as early as 1975. Samples from several stations in Grand Lake contained *Leptodora*, where it made up 4-5% of the total samples prior to 10 July when it started to decline. It was taken in May in Lake Texoma, in the early afternoon at 5 m depth and near midnight near the surface. *Leptodora* comprised 0.4% of the sample, and size ranged between 1.7 and 8.1 mm, indicating reproduction.

Two previous Arkansas locations for *Leptodora* have been noted. Applegate and Mullan (1969) reported taking a small number (up to 0.16/1) during June, July, and August, 1967 from Bull Shoals Reservoir. Roseberg and Moen (1981) collected *Leptodora* from DeGray Reservoir in 1979 although it was not present during four previous years of intensive collecting of larval fish. Roseberg and Moen (1981) suggested that reservoir construction had increased available habitat for *Leptodora* and, because of its predatory nature, expressed concern for its impact on the overall structure of the zooplankton community in this region. Although hypotheses of its reasons and routes of dispersal did not agree, it is our belief that this reporting represents a natural range extension from the Grand River system in northeast Oklahoma.

Since 1985 we have collected steadily increasing numbers of the estuarine amphipod, *Corophium lacustrae*. In the early 1980s numerous individuals of *Corophium* were collected with artificial substrate samplers (rock baskets and Dendy-type multiplate) in the Arkansas River adjacent to AP&L's White Bluff generating station near Redfield (Bob West, pers. comm.). This genus of euryhaline amphipods is common in sandy shorelines and mud flats along the Texas Gulf Coast where it lives in a tube built of sand grains or small pieces of detritus (Heard, 1982). Collections of *Corophium* in this area indicate a probable natural range extension, not completely unexpected given the historically high salinity of the Arkansas River. However, salinity, as measured by chloride concentration, has declined significantly since the mid-1980s. The fact that *Corophium* is still being collected and in gradually increasing numbers suggests it may be adapting to freshwater.

Since the mid-1980s we have also collected increasing numbers of the attached colonial Entoproct, *Urnatella*. *Urnatella* is easily recognized by its branches or arms that resemble chains of beads. We found most *Urnatella* colonies attached to snail shells and larger pieces of woody detritus. Until our December 1993 samples were taken, it was collected only at Station 16, which was characterized by a virtual absence of soft, finely divided silt. The substrate was composed mostly of hard, gray clay overlain with large pieces of woody debris. There were also localized patches of a non-silty granular material. Pleurocercid snails were also particularly abundant at Station 16, and many entoprocts were attached to snail shells.

We have collected low numbers of the introduced Asiatic clam, *Corbicula fluminea* since 1983, and its numbers have declined slightly in recent years. None of the substrates at our regular sampling stations in Dardanelle (organic muck, silty, sandy, and clay-dominated) were ideal for *Corbicula* colonization. By comparison, Rickett (1989) found *Corbicula* in densities of hundreds per square meter in the upper Saline and Ouachita Rivers in substrate dominated by small rocks and pea gravel and rinsed constantly by flowing water.

Literature Cited

Applegate, R.L. and **J.W. Mullan.** 1969. Ecology of *Daphnia* in Bull shoals Reservoir. U.S. Fish & Wildl. Serv., Bur. Sp. Fish. and Wildl. Res. Rep. 74.

Conner, J.V. and **C.F. Bryan.** 1983. *Leptodora kindti* (Focke) (Crustacea: Cladocera) in southern Louisiana since 1973. Southw. Nat. 28:118-119.

Edmondson, W.T., ed. 1959. Freshwater biology, 2d ed. John Wiley and Sons, New York.

Heard, R. 1982. Guide to the common tidal marsh invertebrates of the northeastern Gulf of Mexico. Miss-Ala Sea Grand Consortium.

Holt, J.R., D.S. White and **A.P. Covich.** 1978. Discovery of *Leptodora kindti* (Focke) (Crustacea: Cladocera) in Oklahoma and Texas. Southw. Nat. 23:686-688.

Kring. L., D. Broaugh, C. Prophet and **T. Mosher.** 1976.

Occurrence of *Leptodora kindti* (Focke) (Crustacea: Cladocera) in Kansas: A new record. Southw. Nat. 21:254-255.

Palko, T.N. 1970. A preliminary study of zooplankton over a six month period on Lake Dardanelle. Proc. Arkansas Acad. Sci. 24:55-61.

Pennak, R.W. 1989. Freshwater invertebrates of the United States, 3rd ed. John Wiley and Sons, New York.

Prophet, C.W. 1978. Observations of *Leptodora kindti* (Focke) (Crustacea: Cladocera) and associated zooplankters in southeastern Kansas lakes. Southw. Nat. 23:168-170.

Rickett, J.D. 1989. Dispersal and abundance of the Asiatic clam, *Corbicula fluminea*, in the upper Saline River, southcentral Arkansas. Poster presented at annual meeting of Amer. Soc. Limn. and Oceanogr., Fairbanks, Alaska.

Rickett, J.D. and **R.L. Watson.** 1983. Zooplankton community structure in Dardanelle Reservoir, Arkansas, 1975-1982. Proc. Arkansas Acad. Sci. 37:65-69.

Rickett, J.D. and **R.L. Watson.** 1992. Zooplankton abundance and diversity in Dardanelle Reservoir, 1981-1990. Proc. Arkansas Acad. Sci. 46:57-60.

Roseberg, R.B. and **T. Moen.** 1981. New record of *Leptodora kindti* (Focke) (Crustacea: Cladocera) in Arkansas. Southw. Nat. 26:74-75.

First Record of the Channel Shiner, *Notropis wickliffi* Trautman, in Arkansas and Comments on the Current River Population of *Notropis volucellus (Cope)*

Henry W. Robison
Department of Biological Sciences
Southern Arkansas University
Magnolia, AR 71753

Thomas M. Buchanan
Department of Biology
Westark Community College
Fort Smith, AR 72901

The channel shiner, *Notropis wickliffi* Trautman, is a poorly known inhabitant of the Ohio, Tennessee, and the Mississippi river drainages. Although originally considered a subspecies of *Notropis volucellus* by Trautman (1931), this form has been regarded more recently as a full species (Robins et al., 1991). Earlier, Robison and Buchanan (1988) had not specifically cited *N. wickliffi* as occurring in Arkansas, but did mention two forms of the unresolved *N. volucellus* complex inhabiting the state. Mayden and Kuhajda (1989) presented evidence from patterns of allozyme variation which corroborated observed patterns of morphological variation and supported a polytypic *N. volucellus* complex rather than a single, panmictic population as implied by earlier taxonomy. In this paper we document and report officially the first records of the occurrence of *N. wickliffi* Trautman in Arkansas.

Originally, Black (1940) reported a single specimen of *Notropis volucellus wickliffi* from the Mississippi River between Barfield and Hickman, Mississippi County, Arkansas collected on 8 August 1939. Recent examination of fishes collected during field trips to the Mississippi River over a decade ago revealed five specimens of the channel shiner, *Notropis wickliffi* Trautman, in two collections from the Mississippi River. The first collection of two specimens of *N. wickliffi* was taken on 14 August 1974 by H. W. Robison and P. H. Robison from the Mississippi River at Barfield Landing, approximately eight miles east of Blytheville, Mississippi County, Arkansas. The second series of three specimens was collected on 11 July 1975 by H. W. Robison and SAU students from the Mississippi River eight miles north of the U.S. Hwy. 82 Greenville Bridge (Sec. 30, R1E, T15S), Chicot County, Arkansas. All five specimens have a large eye and mouth, a pointed dorsal fin, eight anal rays, elevated anterior lateral line scales, a weak predorsal dark streak and a definite postdorsal streak.

Notropis volucellus and *N. wickliffi* are easily confused; however, they may be distinguished from one another on the basis of meristic, morphometric, coloration, and allozyme characters as well as characteristics of the lateralis system and tuberculation (Mayden and Kuhajda, 1989). For workers in Arkansas, the following differentiating characters are provided. Adult *N. wickliffi* differ from sympatric *N. volucellus* in possessing a large eye, bigger mouth, deeper caudal peduncle, and less deepened body (Trautman, 1931). Etnier and Starnes (1994) noted *N. wickliffi* has a less-arched back, a very weak or wanting predorsal blotch (conspicuous in *N. volucellus*), a continuous postdorsal dark streak (absent or not continuous in sympatric *N. volucellus*), and melanophores more evenly distributed over the dorsolateral scales (concentrated near margins in *N. volucellus*). Nuptial tuberculation also differs in the two forms.

B. A. Thompson first called our attention to specimens of a *Notropis volucellus* form in the Current River in the early 1970s. This Current River form in Arkansas is mentioned by Robison and Buchanan (1988) and has remained problematical. J. S. Ramsey in answer to a 1975 HWR inquiry about the Current River form stated that "the large stream form is *Notropis wickliffi* which I feel includes the fish in the Current River" (J. S. Ramsey, pers. comm.). Ramsey further stated "there is no strong evidence suggesting the Current River population is remotely disjunct from the Ohio and upper Mississippi River populations." However, later in 1987 on advice from Ramsey, Robison and Buchanan (1988) referred to all populations of *N. volucellus* in Arkansas as the nominal form.

A recent examination of specimens of *N. volucellus* housed in the Tulane University museum (TU 59687 and TU 65590) and collected in 1969-1970 by B. A. Thompson and R. C. Cashner form the Current River in Randolph County, Arkansas and recent HWR collections revealed two *volucellus*-type morphs in the Current River system. One morph is a small-eyed, slender form while the other is a big-eyed, more robust form. It seems likely that these two morphs are likely referable to *N. volucellus* and *N. wickliffi*, respectively (B. A. Thompson and R. C. Cashner, pers. comm.). Further study of Current River specimens revealed the big-eyed form to have a well-defined postdorsal streak, no conspicuous predorsal blotch and melanophores more evenly distributed over the dorsolateral scales whereas specimens of the smaller

eyed *N. volucellus* in the nearby Black River at Pocahontas, Arkansas (TU 59819) have melanophores more concentrated near the margins of the dorsolateral scales, a rather conspicuous predorsal blotch, and the postdorsal streak is almost absent. On the basis of these morphological and pigmentary differences, we conclude that the large-eyed Current River specimens are *N. wickliffi*, thus establishing this species in the Current River as well as the Mississippi River in Arkansas.

Much work remains to be done on the *Notropis volucellus* complex in Arkansas. The question of whether the Current River specimens actually represent *N. wickliffi* or an undescribed sibling species of the *N. volucellus* complex will require allozyme work in addition to meristic, morphometric, and coloration data if a solution is to be finally forthcoming.

Presently, B. R. Kuhajda, a University of Alabama graduate student, is studying the systematics of the *Notropis volucellus* complex and will have further clarification of the several forms involved in the complex throughout its range.

Thus, in Arkansas the present known distribution of *Nortropis wickliffi* is limited to three sites in the mainstem Mississippi River, several sites in the Current River, and a site on the White River just below U.S. Hwy. 167 at Batesville, Independence County, Arkansas where Mr. Kuhajda (pers. comm.) collected 40 specimens. Until other collections of *N. volucellus* have been analyzed using the characters previously presented, the true distribution of the channel shiner in Arkansas waters will remain ambiguous. In their treatment of Tennessee fishes Etnier and Starnes (1994) report three collections of *N. wickliffi* from the mainstream Mississippi River, all from the Tennessee side of the river.

The addition of the channel shiner to the state ichthyofauna, plus the description this year of the Little River system *Notropis rubellus* form as *Notropis suttkusi* (Humphries and Cashner, 1994), brings to 199 the number of native fish species inhabiting Arkansas waters and 218 the total number of fish species living in Arkansas.

Thanks are extended to B. A. Thompson (Louisiana State University) and R. C. Cashner (University of New Orleans) for discussions on the Current River form throughout the years, W. C. Starnes (Smithsonian Institution) for supplying unpublished information relating to *Notropis volucellus* and *N. wickliffi* in Tennessee, B. C. Kuhajda (University of Alabama) for kindly allowing the use of distributional data and information concerning his study of the *N. volucellus* complex and H. L. Bart, Jr. (Tulane University) for loaning specimens of *N. volucellus* collected form the Current and White Rivers in Arkansas.

Literature Cited

Black, John D. 1940. The distribution of the fishes of Arkansas. Ph.D. Dissertation Univ. Michigan, Ann Arbor. 243 pp.

Etnier, D.A. and **W.C. Starnes.** 1994. Fishes of Tennessee. Univ. Tennessee. Press. Knoxville. 681 p.

Humphries, J.M. and **R.C. Cashner.** 1994. *Notropis suttkusi*, a new cyprinid from the Ouachita Uplands of Oklahoma and Arkansas, with comments on the status of Ozarkian populations of *N. rubellus.* Copeia 1994 (1) : 82-90.

Mayden, R.L. and **B.R. Kuhajda.** 1989. Systematics of *Notropis cahabae*, a new cyprinid fish endemic to the Cahaba River of the Mobile basin. Bull. Alabama Mus. Nat. Hist. No. 9: 16 p.

Robins, C. Richard et. al. (eds.) 1990. A list of common and scientific names of fishes from the United States and Canada. Am. Fish. Soc. Spec. Publ. 20. 183 p.

Robison, H.W. and **T.M. Buchanan.** 1988. Fishes of Arkansas. Univ. Arkansas Press. Fayetteville. 536 p.

Trautman, M.B. 1931. *Notropis volucellus wickliffi*, a new subspecies of cyprinid fish from the Ohio and upper Mississippi rivers. Ohio J. Sci. 31 (6) :468-474.

Food Habits of the Barn Owl (*Tyto alba*) at a Nest Site in Southwest Arkansas

Jonathan L. Westmoreland and Renn Tumlison
Department of Biology
Henderson State University
Arkadelphia, AR 71999-0001
Jim Gann
Logoly State Park
McNeil, AR 71752

The barn owl (*Tyto alba*) is a permanent resident of Arkansas, yet only two studies describe food habits of this raptor in the state. Paige et al. (1979) discussed food habits based on owl pellets collected at a winter roost on the Arkansas State University campus in northeastern Arkansas, and Steward et al. (1988) documented mammalian species recovered monthly at a roost in Hempstead County.

We document foods recovered from a nest site located inside an abandoned farmhouse, located about 1 mile NW of Garland in Miller County. The nest was positioned in the attic above the attic entrance in one of the rooms; pellets fell from the nest and accumulated on the floor below. A total of 203 barn owl pellets was taken from the site. The area over which the owls could forage primarily was an overgrown field, which included marshy areas, situated in the flood plain of the Red River.

The fact that the site had been used by barn owls for several seasons was indicated by the accumulation of pellets on the floor. We collected only those pellets that were fresh and representative of the previous nesting season (pellets were collected on June 17, 1993 after the young fledged from the nest). The pellets were dissolved in water and prey remains were separated. Prey taxa were identified by interpretation of skeletal morphology, dentition, and feather characteristics.

Bilateral skeletal elements were paired according to species and size to establish minimum number of prey items per pellet. A total of 549 prey items (Table 1) was recovered from the pellets. This number is likely an overestimate of the number of larger prey items, because the adult owl often tears apart bodies of larger prey and feeds the parts to the young (Johnsgard, 1988). This was evidenced by the fact that some pellets contained skulls and forelimbs, whereas other pellets contained only hindlimb portions, typically of larger rodents. These composed the majority of the unidentified rodents, thus the unidentified category in our prey list actually consists of the larger rodents found to be common as prey.

Table 1. Food items recovered from 203 Barn Owl pellets collected in Miller County, Arkansas.

Species	Frequency of Occurrence		Percentage of Occurrence	
Small Mammals	252		45.9	
Cryptotis parva		157		28.6
Mus musculus		59		10.7
Reithrodontomys fulvescens		22		4.0
Blarina carolinensis		7		1.3
Reithrodontomys humulis		5		0.9
Reithrodontomys sp.		2		0.4
Medium Mammals	46		8.4	
Microtus pinetorum		35		6.4
Peromyscus sp.		11		2.0
Large Mammals	137		25.0	
Sigmodon hispidus		83		15.1
Oryzomys palustris		46		8.4
Sylvilagus sp.		5		0.9
Rattus norvegicus		2		0.4
Neotoma floridana		1		0.2
Unidentified Rodent	55		10.0	
Birds	55		10.0	
Red-winged Blackbird		19		3.5
Meadowlark		4		0.7
Mourning Dove		3		0.5
House Sparrow		1		0.2
Barn Owl		1		0.2
Unidentified Birds		27		4.9
Amphibians (*Rana* sp.)	2		0.4	
Insects (Grasshoppers)	2		0.4	

Mammalian prey composed 89.3% of the total food remains and was dominated in frequency by the least shrew, *Cryptotis parva*. Rodents associated with human dwellings, such as the house mouse, *Mus musculus*, and the Norway rat, *Rattus norvegicus*, likely reflect foraging around the farm house. Common prey items that inhabit marshes, fields, and woodlands included the marsh rice rat, *Oryzomys palustris*, the hispid cotton rat, *Sigmodon hispidus*, the woodland vole, *Microtus pinetorum*, and the

eastern woodrat, *Neotoma floridana*. The eastern harvest mouse, *Reithrodontomys humulis*, represents a new county record for Miller county. This species has not been trapped frequently in southwestern Arkansas, and only two records exist for it in that part of the state (Steward et al., 1988; Tumlison et al., 1988), the former record resulting from a barn owl pellet study. The diet of the barn owl often provides a better indication of species diversity than does human trapping methods.

We divided the taxonomic categories of mammalian prey items into size classes from the point of view of the owl. We classified as large any prey item that would likely fill the stomach of an owl, and possibly maximize energetic gain with a minimum of energy expenditure. If an owl required several individuals of a taxon to fill the stomach, that species was considered to be a small mammal.

Small mammals were the most common prey type found, with larger mammals, such as *Sigmodon hispidus* and *Oryzomys palustris*, contributing as numerically important foods. The reliance on smaller mammals could be bioenergetically unfavorable to the barn owl, because the net energy gain from a prey item is the difference between the energy content of that prey and the energy expended in capture and consumption. Nesting barn owls should be hunting for the prey items that would yield the most energy to the owl and its young for the least energy expenditure. Hamilton and Neill (1981) demonstrated that barn owls in Texas were specifically selecting larger prey species only during their reproductive periods when energy demands are high. Because their results indicated that smaller prey were more costly and larger prey more optimal for nesting barn owls, the proportion of smaller mammals found in our study may indicate a habitat that would not allow optimal reproduction.

Birds and other prey composed 10.8% of the total items encountered (Table 1), and included red-winged blackbirds (*Agelaius phoeniceus*), a common inhabitant of wetlands, meadowlarks (*Sturnella* sp.), and mourning doves (*Zenadia macroura*). Two grasshoppers and two frogs (*Rana* sp.) also were found. These were identified by comparison with specimens from the Henderson State University Museum of Zoology.

A skull and feathers of a young barn owl in one of the pellets and the remains of two young barn owls on the floor of the nest site provide further evidence that the habitat might have been marginal for reproduction. Most explanations of juvenile owl mortality focus on some form of environmental stress. Siblicidal brood reduction, or lethal aggression among offspring, is attributed to severe weather conditions, nest disturbance, or prey shortage (Mock, 1984; Johnsgard, 1988; Mock et al., 1990). Brood reduction occurs when the habitat used for foraging has not produced adequate energy-efficient prey to permit survival of all young. The killing of one or more offspring by its siblings supposedly eliminates those members of the brood that are unlikely to survive and reproduce, thereby minimizing the parents costs of food delivery to the young (Alcock, 1993). However, it cannot be determined from pellet analysis whether one nestling actually killed and consumed a sibling. Another scenario, also indicative of environmental stress, is that one bird died from starvation, disease, or other causes and subsequently was consumed by a sibling.

Other studies suggest that a habitat incapable of providing for optimal reproductive success would be evidenced by higher numbers of small mammalian prey and increased use of avian prey (Otteni et al., 1972; Hamilton and Neill, 1981; Gubanyi et al., 1992). Their findings of high reproductive success in barn owl nests correlate with a high percentage of larger mammals and a low percentage of birds. Avian prey in our study comprised 10.0% of the total prey items, in contrast to 1.2% (Hamilton and Neill, 1981) and less than 1% (Gubanyi et al., 1992) in studies showing successful reproduction. High frequencies of birds and smaller mammals in our study, coupled with evidence of cannibalism and mortality in the nest, suggest that conditions at the study site are marginal for successful barn owl reproduction.

Literature Cited

Alcock, J. 1993. Animal behavior: an evolutionary approach, 5th ed. Sinauer Assoc., Inc., Sunderland, Mass. 625 pp.

Gubanyi, J.A., R.M. Case and **G. Wingfield.** 1992. Diet and nesting success of barn owls breeding in western Nebraska. Amer. Midl. Nat. 127:224-232.

Hamilton, K.L. and **R.L. Neill.** 1981. Food habits and bioenergetics of a pair of barn owls and owlets. Amer. Midl. Nat. 106:1-9.

Johnsgard, P.A. 1988. North American Owls. Smithsonian Institution Press, Washington. 295 pp.

Mock, D.W. 1984. Siblicidal aggression and resource monopolization in birds. Science 225:731-733.

Mock, D.W., H. Drummond and **C.H. Stinson.** 1990. Avian siblicide. Amer. Sci. 78:438-449.

Otteni, L.C., E.G. Bolen and **C. Cottam.** 1972. Predator-prey relationships and reproduction of the barn owl in southern Texas. Wilson Bull. 84:434-448.

Paige, K.N., C.T. McAllister and **C.R. Tumlison.** 1979. Unusual results from pellet analysis of the American Barn Owl *Tyto alba pratincola* (Bonaparte). Proc. Arkansas Acad. Sci. 33:88-89.

Steward, T.W., J.D. Wilhide, V.R. McDaniel and **D.R. England.** 1988. Mammalian species recovered from a study of barn owl *Tyto alba* pellets from southwestern

Arkansas. Proc. Arkansas Acad. Sci. 42:115-116.
Tumlison, R., V.R. McDaniel and **D.R. England.** 1988. Eastern harvest mouse, *Reithrodontomys humulis*, in Arkansas. Southw. Nat. 33:105-106.

CORRECTION – In the article "New Distributional Records for Arkansas Surgeons" by Thomas M. Buchanan, Henry W. Robison, and Ken Shirley which appeared in volume 47 of the Proceedings of the Arkansas Academy of Science, Page 133 and in the Table of Contents, the Title"...Arkansas Surgeons" should read "...Arkansas Sturgeons".

NOTES

NOTES

PUBLICATION POLICIES AND SUGGESTIONS FOR AUTHORS

The PROCEEDINGS OF THE ARKANSAS ACADEMY OF SCIENCE appears annually. It is the policy of the Arkansas Academy of Science that 1) at least one of the authors of a paper submitted for publication in the PROCEEDINGS must be a member of the Arkansas Academy of Science, 2) that only papers presented at the annual meeting are eligible for publication, and 3) that the manuscript is due at the time of presentation. In accordance with this policy, manuscripts submitted for publication should be given to the section chairman at the time the paper is being presented. Correspondence after this time should be directed to Dr. Stan Trauth, Editor-PAAS, Dept. Biological Sciences, Arkansas State University, State University, AR 72467-0599.

Each submitted paper should contain results of original research, embody sound principles of scientific investigation, and present data in a concise yet clear manner. The COUNCIL OF BIOLOGY EDITORS STYLE MANUAL, published by the American Institute of Biological Sciences, is an example of a convenient and widely consulted guide for scientific writers. Authors should strive for directness and lucidity, achieved by use of the active voice. Special attention should be given to consistency in tense, unambiguous reference of pronouns, and to logically placed modifiers. It is strongly recommended that all authors 1) inspect the existing format for feature articles and general notes in the PROCEEDINGS OF THE ARKANSAS ACADEMY OF SCIENCE and follow that format while drafting their submission, and 2) submit their manuscript to another qualified person for a friendly review to appraise it for clarity, brevity, grammar, and typographical errors.

Preparation of Manuscript

The author should submit three copies of the manuscript, tables, and figures. Manuscripts must be double spaced (preferably typed with a carbon ribboned typewriter) on $8^1/2$ x 11 inch bond paper with at least one inch margins on all sides. Do not staple pages together. Do not hyphenate words on the right-hand margin; do not submit word processed copy printed with justified right-hand margins. Do not submit copy in italics; underline words to be set in italics. If co-authored, designate which author is to receive correspondence and at what address.

An abstract summarizing in concrete terms the methods, findings and implications discussed in the body of the paper must accompany a feature article. The abstract should be completely self-explanatory.

A feature article comprises approximately six or more typewritten pages. A PROCEEDINGS printed page is equal to approximately three and one-half typewritten pages and the author is assessed a PAGE CHARGE (see Procedure section). A separate title page, including authors names and addresses should be included with the manuscript. Feature articles are often divided into the following sections: abstract, introduction, materials and methods, results, discussion, acknowledgements, and literature cited. These sections should be centered. Subheadings should begin at the left-hand margin, but more than one subheading should be avoided.

A general note is usually one to five typewritten pages and rarely utilizes subheadings. A note should have the title at the top of the first page with the body of the paper following. Abstracts are not used for general notes.

Abbreviations: Use of abbreviations and symbols can be ascertained by inspection of recent issues of the PROCEEDINGS. Suggestions for uniformity include the use of numerals before units of measurements (5 m), but nine animals (10 or numbers above, such as 13 animals). Abbreviations must be defined the first time they are used. The metric system of measurements and weights must be employed.

The literature cited section for feature articles should include six or more references; entries should take the following form:

Davis, D. H. S. 1933. Rhythmic activity in the short-tailed vole, *Microtus*. J. Anim. Ecol. 2:232-238.

Hudson, J. W. and **J. A. Rummell**. 1966....

Fleming, T. H. 1969. Population ecology of three species of neotropical rodents. Unpublished Ph.D. dissertation. Univ. Michigan, Ann Arbor, 231 pp.

Jones, I. C. 1957. The adrenal cortex. Cambridge Univ. Press, London, 316 pp.

Wright, P. L. 1966. Observations on the reproductive cycle of the American badger (*Taxidea taxus*). Pp. 27-45, *In* Comparative biology of reproduction in mammals (I. W. Rowlands, ed.) Academic Press, London, xxi + 559 pp.

If fewer than six references are cited in a general note, they should be inserted in text and take these forms: (Jones, The adrenal cortex, Cambridge Univ. Press. p. 210, 1957); (Davis, J. Anim. Ecol., 2:232-238, 1933).

Tables and Illustrations: Tables and figures (line drawings, graphs, or black and white photographs) should not repeat data contained in the text. The author must provide numbers and short legends for illustrations and tables and place reference to each of them in the text. Legends for figures should be typed on a separate piece of paper at the end of the manuscript. Do not run tables in the text. Illustrations must be of sufficient size and clarity to permit reduction to standard page size; ordinarily they should be no larger then twice the size of intended reduction and whenever possible no larger than a manuscript page for ease of handling. Photographs must be printed on glossy paper. Sharp focus and high contrast are essential for good reproduction. Figures and labeling must be of professional quality. Notations identifying author, figure number, and top of print must be made on the back of each illustration. All illustrations must be submitted in duplicate. Tables should be typed with a carbon-ribboned typewriter and in the exact format that the author wishes them to appear in the text. Tables must be of professional quality when submitted. Note preferred placement of figures and tables in the margins of the manuscript.

Review Procedure

Evaluation of a paper submitted to the PROCEEDINGS begins with a critical reading by the Editor. The paper is then submitted to referees for checking of scientific content, originality, and clarity of presentation. Attention to the preceding paragraphs will greatly speed up this process. Judgments as to the acceptability of the paper and suggestions for strengthening it are sent to the author. If the paper is tentatively accepted, the author will rework it, where necessary, and return two copies of the revised manuscript together with the original to the Editor. Usually a time limit for this revision will be requested. If the time limit is not met, the paper may be considered to be withdrawn by the author and rejected for publication. All final decisions concerning the acceptance or rejection of a manuscript are made by the Editor.

When a copy of the proof, original manuscript, and reprint order blanks reach the author, they should be carefully read for errors and omissions. The author should mark corrections on the proof and return both the proof and manuscript to the Editor within 48 hours or the proof will be judged correct. Printing charges accruing from excessive additions to or changes in the proofs must be assumed by the author. Reprint orders are placed with the printer, not the Editor. Page changes are $25/printed page or portion thereof. These changes and excessive printing charges will be billed to the author by the Academy of Science. A page charge will be billed to the author of errata.

ABSTRACT COVERAGE

Each issue of the PROCEEDINGS is sent to several abstracting and review services. The following is a partial list of this coverage.

Abstracts in Anthropology
Abstracts of North America Geology
Biological Abstracts
Chemical Abstracts
Mathematical Reviews
Recent Literature of the Journal of Mammalogy
Science Citation Index
Sport Fishery Abstracts
Wildlife Review
Zoological Record
Review Journal of the Commonwealth Agricultural Bureau

BUSINESS AND SUBSCRIPTION INFORMATION

Remittances and orders for subscriptions and for single copies and changes of address should be sent to Dr. John Rickett, Secretary, Arkansas Academy of Science, Dept. of Biology, University of Arkansas, Little Rock, Little Rock, AR 72204.

Members receive one copy with their undergraduate membership of $5.00, regular membership of $15.00, sustaining membership of $20.00, sponsoring membership of $30.00 or life membership of $200.00. Institutional members and industrial members receive two copies with their membership of $100.00. Library subscription rates for 1989 are $25.00. Copies of most back issues are available. The Secretary should be contacted for prices.

TABLE OF CONTENTS